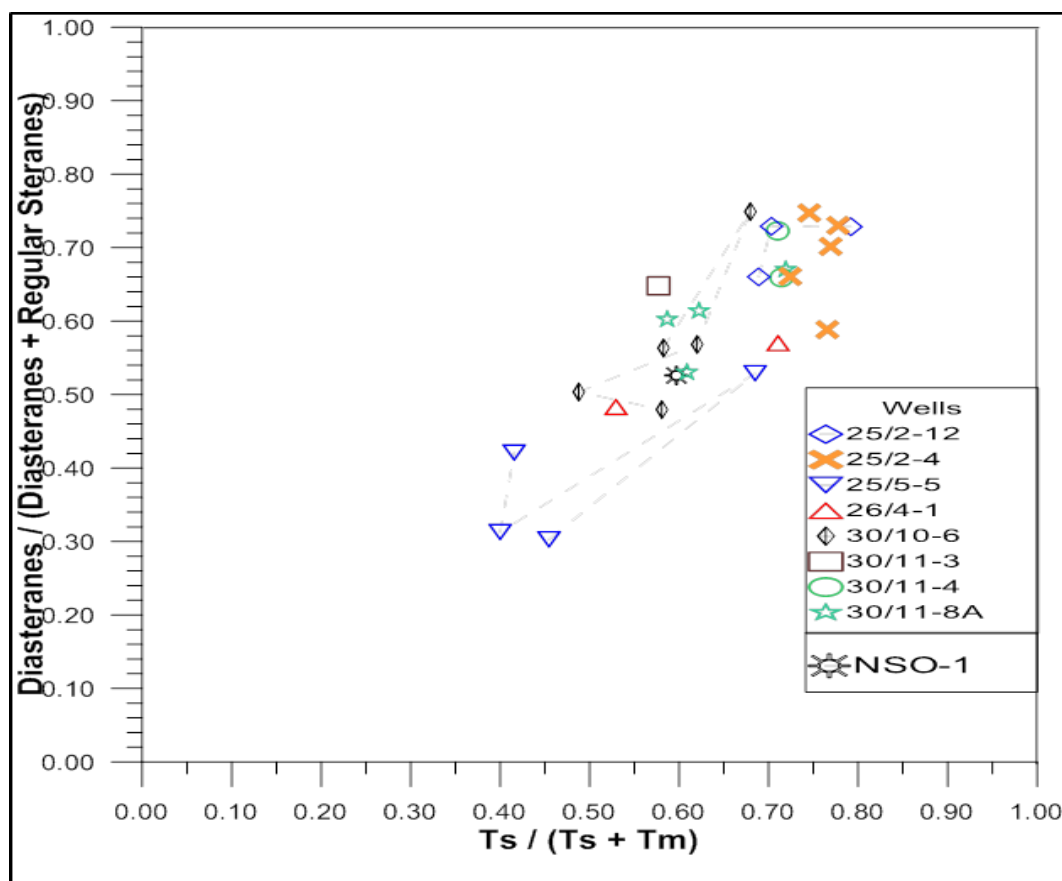


DRY WELLS IN QUADRANT 25, 26 & 30 – GEOCHEMICAL INVESTIGATIONS INTO RESIDUAL OIL & GAS IN DRY WELLS

*Improving “Petroleum System” Understanding by Examination of Residual
Oil and Inclusion Hydrocarbon Gas in Dry Wells*

WAQAS MAQBOOL



UNIVERSITY OF OSLO

FACULTY OF MATHEMATICS AND NATURAL SCIENCES

DRY WELLS IN QUADRANT 25, 26 & 30 – GEOCHEMICAL INVESTIGATIONS INTO RESIDUAL OIL & GAS IN DRY WELLS

*Improving “Petroleum System” Understanding by Examination of Residual Oil and
Inclusion Hydrocarbon Gas in Dry Wells*

WAQAS MAQBOOL



Master Thesis in Geosciences

Discipline: Petroleum Geology and Petroleum Geophysics (PEGG)

Department of Geosciences

Faculty of Mathematics and Natural Sciences

University of Oslo

June, 2014

© **Waqas Maqbool, 2014**

Tutor(s): **Professor Dag A. Karlsen**

This work is published digitally through DUO – Digitale Utgivelser ved UiO

<http://www.duo.uio.no>

It is also catalogued in BIBSYS (<http://www.bibsys.no/english>)

All rights reserved. No part of this publication may be reproduced or transmitted, in any form or by any means, without permission.

Abstract

This thesis represents the findings concerning core samples from 15 examined exploration wells (with a total of 91 samples) on the eastern flank of the Viking Graben, North Sea, that were classified as dry by NPD (meaning no discovery of oil and gas). These samples were studied using geochemical methodology and analytical methods to evaluate if there might exist the remains of migrated oil or gas. Sample selection at NPD was based on apparent coloration or staining of the sandstone cores. The samples were disintegrated manually to yield a sand fraction which was extracted with DCM:MeOH (93:7vol%). The geochemical techniques applied to the bitumen thus produced are, gas chromatography-flame ionization detection (GC-FID), Iatroscan thin layer chromatography-flame ionization detection (TLC-FID) and gas chromatography-mass spectrometry (GC-MS). In addition was the sand fraction crushed in a sling mill to produce gas from inclusions and this was analyzed using GC-FID.

The gas inclusion analysis reveals the presence of palaeo-petroleum migration owing to the higher percentages of wet gas components (C_2+ hydrocarbon species) in the inclusion gas and all samples were examined by this methodology. Variable amounts of C_2+ components were detected, but most samples show in fact C_2+ compositions representative of oil to condensate or wet gas. Thus, most of the samples from the dry wells contain inclusions in authigenic mineral cements which had shown that petroleum did at some time exist in the investigated reservoir sections.

Concerning bitumen extracts, it was found using GC-FID that some wells contained mainly drilling fluid contamination products i.e. diesel or polyethylene glycol and these samples were discarded from more detailed work. Thus, the study was concentrated on samples showing both; a) high C_2+ gas composition and b) also “natural oil”-GC-FID bitumen distributions.

A series of good GC-FID traces could be produced from many of the dry wells samples, and based on steranes and hopane isomerization parameters, it is clear that the bitumen in the reservoir sandstone is allochthonous and not *in-situ* generated. Thus, migrated petroleum was positively identified in the following wells: 25/2-4, 25/2-12, 25/5-5, 26/4-1, 30/10-6, 30/11-3, 30/11-4 and 30/11-8A.

The reservoir bitumen, as assessed by medium range and biomarker maturity parameters, reflects maturities generally in early to peak oil phase of the oil window, and one is struck by the relative uniformity of the data set in terms of organic source rock facies and maturity parameters, albeit the bitumen from the well 30/10-6 shows even higher maturity and reflects characteristics of a condensate. Thus, the dry well samples are generally showing “oil-window” maturities in terms of calculated vitrinite reflectance with values ranging from 0.85% to 1%R_c, and hence point to source rock “kitchens” in deeper parts of the “Petroleum System”. Nonetheless, more detailed analysis is needed to look into the most likely “kitchen-areas” and migration distances to get an improved insight into the overall “Petroleum system” of the investigated regions.

Overall, the bitumen in the dry wells seems to originate from mixed organic sources with clear marine influence, and it is possibly right to conclude on a distal to proximal variation over the “typical for the region” Type II/III Draupne/Kimmeridge Formation source rock facies. The depositional environment, as inferred from isoprenoids to n-alkanes ratios, tends towards clearly anoxic and siliciclastic, i.e. not carbonate source rock facies.

In terms of organic source rock facies and maturity, there exist a close resemblance between the bitumen of the core extracts for the dry wells, and the geochemistry of the petroleum in the producing oil fields, i.e. the Rind and Frøy Discoveries, yet the Rind show even higher maturities and possibly sourced from a Heather type organic facies.

An attempt was made in this thesis to work also with “corrected” ratios of pristane to phytane (corrected for evaporative loss from core extracts) and the extrapolation of n-alkanes (n-C₁₇ and n-C₁₈) and isoprenoids (pristane and phytane) peaks resulted in higher ratios of pristane to phytane, but, except for a slight variation, no significant change in facies and maturity of the samples is observed.

Acknowledgements

I feel instigated from within to extend my steadfast thanks to Almighty Allah whose magnanimous and chivalrous blessings enabled me to perceive and pursue my ambitions and objectives. Special praises to Prophet Muhammad PBUH, who is bellwether for humanity as a whole.

I feel great honor in expressing my avid gratifications to my supervisor Professor Dag Arild Karlsen, under whose dynamic supervision, auspicious and considerate guidance, encouragement and altruistic attitude, I was able to accomplish my work presented in this dissertation.

I also extend my special thanks to Tesfamariam Berhane Abay, Zagros Matapour, Benedikt Lerch and Kristian Backer Owe for their esteemed guidance, suggestions, discussion and professional support throughout my thesis work. I also pay my deepest gratitude to Muhammad Jamil for always being supportive and helpful in my Lab work and allowing me to perform independent lab work under his supervision throughout my thesis work. Without their help I believe my project was incomplete.

Special thanks to my all friends at University of Oslo who will be missed with lunch and coffee breaks.

In the end my whole hearted and incessant gratitude to my loving parents, my brothers and sisters, who always appreciated, encouraged, and helped me during my whole educational career.

Waqas Maqbool.

Table of Contents

1. INTRODUCTION	1
BACKDROP	1
OUTLINE OF THIS STUDY	3
2. GEOLOGICAL FRAMEWORK.....	5
INTRODUCTION	5
REGIONAL TECTONIC FRAMEWORK	6
STRATIGRAPHIC SETTINGS.....	8
PETROLEUM SYSTEM OF THE AREA	11
3. SAMPLE SET, ANALYTICAL METHODS AND PARAMETERS	12
THE SAMPLE SET	12
ANALYTICAL METHODS	17
<i>Introduction.....</i>	<i>17</i>
<i>Gas Chromatography.....</i>	<i>18</i>
<i>Sample preparation and extraction of bitumen</i>	<i>20</i>
<i>Iatroscan – Thin Layer Chromatography-Flame Ionization Detector (TLC-FID).....</i>	<i>20</i>
<i>Gas Chromatography-Flame ionization Detector (GC-FID).....</i>	<i>23</i>
<i>Molecular Sieving – n-alkane removal.....</i>	<i>25</i>
<i>Gas Chromatography-Mass spectrometry (GC-MS).....</i>	<i>26</i>
<i>Gas Analysis from inclusions</i>	<i>28</i>
PETROLEUM GEOCHEMICAL INTERPRETATION PARAMETERS	28
<i>Iatroscan TLC-FID.....</i>	<i>29</i>
<i>GC-FID</i>	<i>30</i>

GC-MS	33
DESCRIPTION OF PARAMETERS	42
<i>Parameters from $m/z = 191$</i>	42
<i>Parameters from $m/z = 217$</i>	43
<i>Parameters from $m/z=218$</i>	44
4. RESULTS	47
ANALYSIS OF HYDROCARBON GASES FROM ENRICHED INCLUSIONS	47
GC-FID	54
CARBON PREFERENCE INDEX	58
GC-MS	60
IATROSCAN TLC-FID	65
5. DISCUSSION	71
COMPOSITION OF HYDROCARBONS	71
<i>Composition on the basis of percentage of gases (C_1 to C_5)</i>	71
<i>Composition on the basis of percentage of saturated and aromatic hydrocarbons and polar compounds</i>	75
ORGANIC FACIES	77
<i>Facies estimation by isoprenoids and n-alkanes</i>	77
<i>Facies estimation by steranes isomers</i>	79
<i>Facies identified by isoprenoids and aromatic hydrocarbons</i>	83
MATURITY	84
<i>Maturity assessment from non-biomarkers</i>	85
<i>Maturity assessment from biomarkers</i>	90
CONCLUSION	96

6. FACIES AND MATURITY COMPARISON OF BITUMEN FROM DRY WELLS WITH THE RIND DISCOVERY AND THE FRØY FIELD	85
ORGANIC FACIES	86
<i>Facies defined by isoprenoids and n-alkanes</i>	<i>86</i>
<i>Facies estimation by sterane isomers</i>	<i>88</i>
MATURITY	89
<i>Maturity assessment from biomarkers</i>	<i>89</i>
CONCLUSION	95
7. COMPARISON OF THE MEASURED VALUES FOR ISOPRENOIDS (PR AND PH) AND N-ALKANES (N-C₁₇ AND N-C₁₈) WITH THE CORRECTED.....	97
8. CONCLUSIVE SUMMARY	102
9. REFERENCES	104
10. APPENDIX	110

1. Introduction

Backdrop

The reservoir core samples from a series of dry wells are obtained from the Norwegian Petroleum Directorate (NPD) and most of them belong to the Frigg area, blocks 25, 26 and 30, on the eastern flank of the Viking Graben, North Sea. The position of wells and geological map of the study area is shown below.

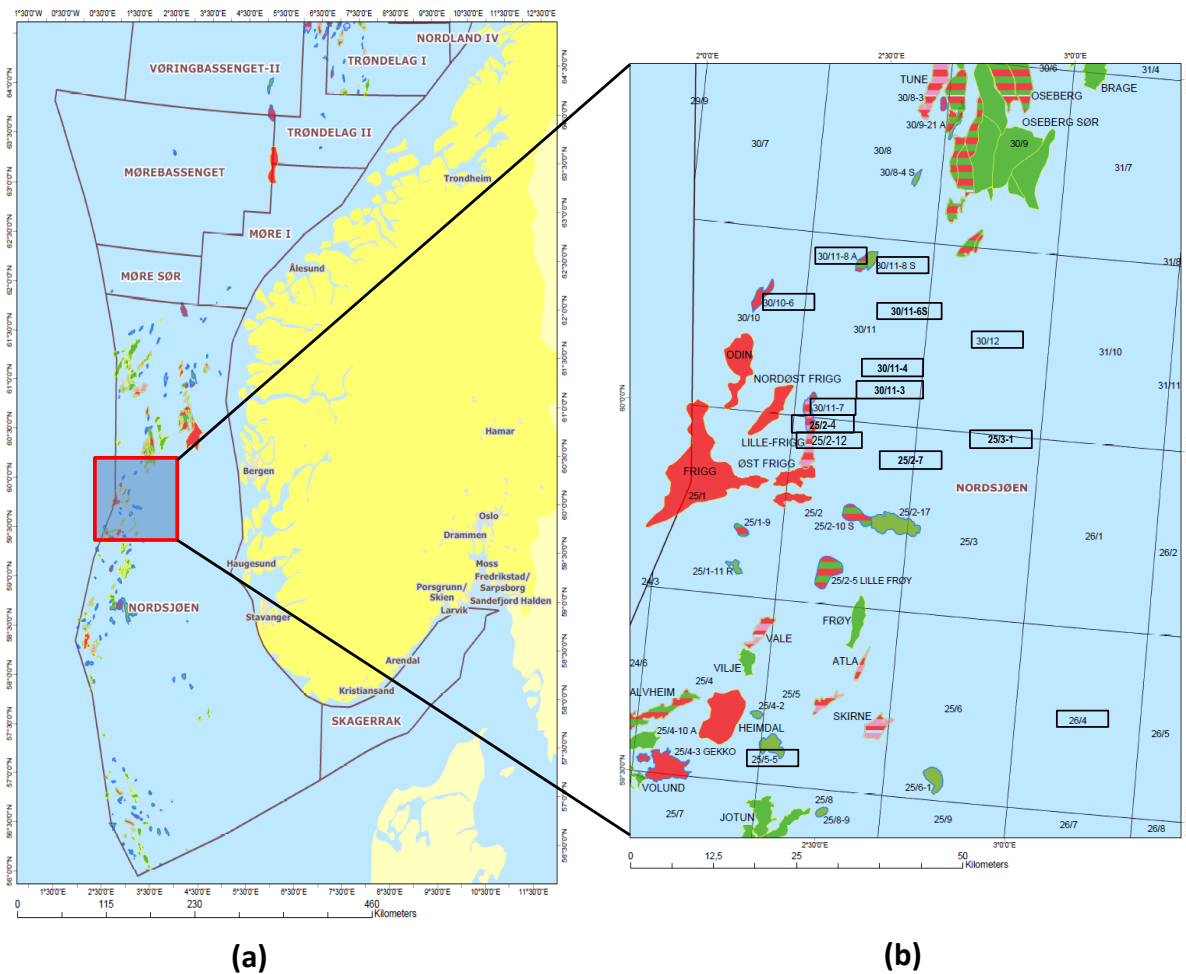


Fig. 1.1. (a) Location of the study area (marked in red box) in the Viking Graben, North Sea. The position of wells is marked in black rectangles in (b), where gas and oil fields are presented in red and green colors respectively (modified from NPD).

Petroleum geochemistry as defined by Hunt (1996) is “the application of chemical principles to the study of origin, migration, accumulation and alteration of petroleum oil and gas and the use of this knowledge in exploring and recovering petroleum”. Organic geochemistry has been aiming on understanding of source rocks, petroleum generation and migration for a number of years (Hunt, 1961; Tissot et al., 1971; Espitalie et al., 1977; Durand, 1980; Leythaeuser et al., 1980), but the focus has greatly deviated towards more practical approach concerning petroleum exploration, appraisal and development (England and Cubitt, 1995). The comparison of current hydrocarbon distribution in the source rocks to the situations in the past, in terms of maturity and facies, tends to develop a better understanding of hydrocarbons generation and migration (Karlsen et al., 1993).

The study of petroleum inclusions in terms of fluorescence and gas bubble size integrated with the gas analysis of trapped gas inclusions (C₁-C₅ hydrocarbons) and geochemical analysis of bitumen sample is rather a new practice to understand petroleum system evolution (Karlsen et al., 1993; Karlsen and Skeie, 2006).

The petroleum inclusion is either gas or oil or a mixture of both that has been trapped during diagenesis. It is believed that inclusions preserve the original composition of hydrocarbons, and if fluid inclusions, characterize the palaeo-petroleum in traps and provide valuable clues for petroleum genesis and migration. Biomarkers are molecules having a base structure inherited from living organisms that are deposited in the sediments with little or no change in their structure (Tissot and Welte, 1984). They may be found in all rocks, sediments, oils and bitumens and usually termed as the fingerprints of source rock. Hydrocarbon compounds constituting petroleum are categorized into three classes:

Alkanes or paraffins – usually normal and branched-chain alkanes (iso-alkanes), *cycloalkanes and naphthalenes* – compounds with ring structures like cyclo-hexane and *aromatics hydrocarbons* – compounds having cyclic structures with double bonds, and all these compound classes are relevant for understanding the origin, source rock facies and maturity of source rocks. It is these compounds this project seeks to look into for the dry wells.

Outline of this study

The purpose of this thesis is to try to characterize any potentially identified and existing hydrocarbon species from dry wells of the study area in terms of palaeo-petroleum generation. A well may be dry in terms of not being a discovery, but it may still have contained oil previously.

Moreover, the purpose is to evaluate the source rock and maturity parameters of the residual oil so that one may infer more about the “Petroleum System” to be explored down-dip of the wells.

To achieve this, the following analytical techniques have been applied such as gas analysis, gas chromatography-flame ionization detection (GC-FID), Iatroscan thin layer chromatography-flame ionization detection (TLC-FID), and gas chromatography-mass spectrometry (GC-MS).

The geochemical analysis methods are used for the following purposes:

- To find any evidence for migrated oil, gas or condensates by analyzing bitumen core extracts and to determine the level of maturity and levels of biodegradation.
- To determine gases (C_1 to C_5) from inclusions in the samples by applying gas analysis technique. This allows measuring the wetness parameters for the gas as this is associated to oil, or condensate or dry gas. An important point is that inclusions cannot be contaminated by the drilling mud, as can residual oil from “dry well” cores.
- To look for detectable n-alkanes signatures in bitumen core samples using GC-FID which is useful in determining the maturity and facies of the source rock for the palaeo-bitumen.
- To evaluate the gross petroleum composition in terms of saturated hydrocarbons, aromatic hydrocarbons and polar compounds by using Iatroscan TLC-FID.
- In the identification and quantification of biomarkers using GC-MS which also determines the facies and maturity of the source rock for the residual bitumen.

Following this introduction, chapter 2 deals with the geological background of the area and chapter 3 includes the sample set and analytical methods. The results are presented in chapter 4 following discussion in the next chapter. A comparison is made between the core samples of the dry wells and the producing oil fields in the Rind Discovery and the Frøy Field on the basis of facies and maturity parameters in chapter 6. This is done to evaluate if the findings of the dry wells show any similarity to these fields and discoveries which have both been studied in detail in previous publications. Chapter 7 is concerned with the assessment of the measured ratios of Pr/n-C₁₇, Ph/n-C₁₈ and Pr/Ph compared to the corrected ones. The summary of conclusions is discussed in the last chapter.

2. Geological Framework

Introduction

The discovery of the Ekofisk Field in 1969 has led to increased demand for hydrocarbon exploration in the North Sea. Due to this fact it is among the best explored continental shelves in the world. The early hydrocarbon discoveries in the central and southern Viking Graben greatly focused the exploration activity towards Jurassic rotated fault blocks along graben margins. A large number of wells have been drilled on the eastern flank of the Viking Graben after the discovery of the Troll Field (1979) in the Horda Platform area (Rønnevik and Hohnsen 1984; Hellem et al., 1986; Gray 1987). The exploration has greatly been concentrated on the syn-rift plays of the Jurassic basins, with some exceptions as Cenomanian to Danian chalk deposits of the Ekofisk field (van den Bark and Thomas, 1980) and Palaeogene sands of the Frigg field (Heritier et al., 1990). But during the last years, the focus has been shifted towards the prospectivity of sands in the post-rift sequences with some discoveries in other different settings as the Agat and the Grane fields, (Gulbrandsen 1987; Shanmugam et al., 1995; Skibeli et al., 1995). About 250 hydrocarbon traps have been found containing recoverable resources totaling of the order of $8000 \times 10^6 \text{ Sm}^3$ of oil-equivalent. Some 70% of these are related to fault blocks; all with Jurassic or older reservoir rocks (Spencer and Larsen, 1990).

This study focuses on selected core samples from a series of dry wells in blocks 25, 26 and 30 (Fig 2.1) to investigate the presence of any migrated hydrocarbon. These so-called dry wells are very close to some known producing oil fields namely Krafla prospect in block 30/11, the Rind Discovery and the Frøy Field in blocks 25/2 and 25/5 respectively.

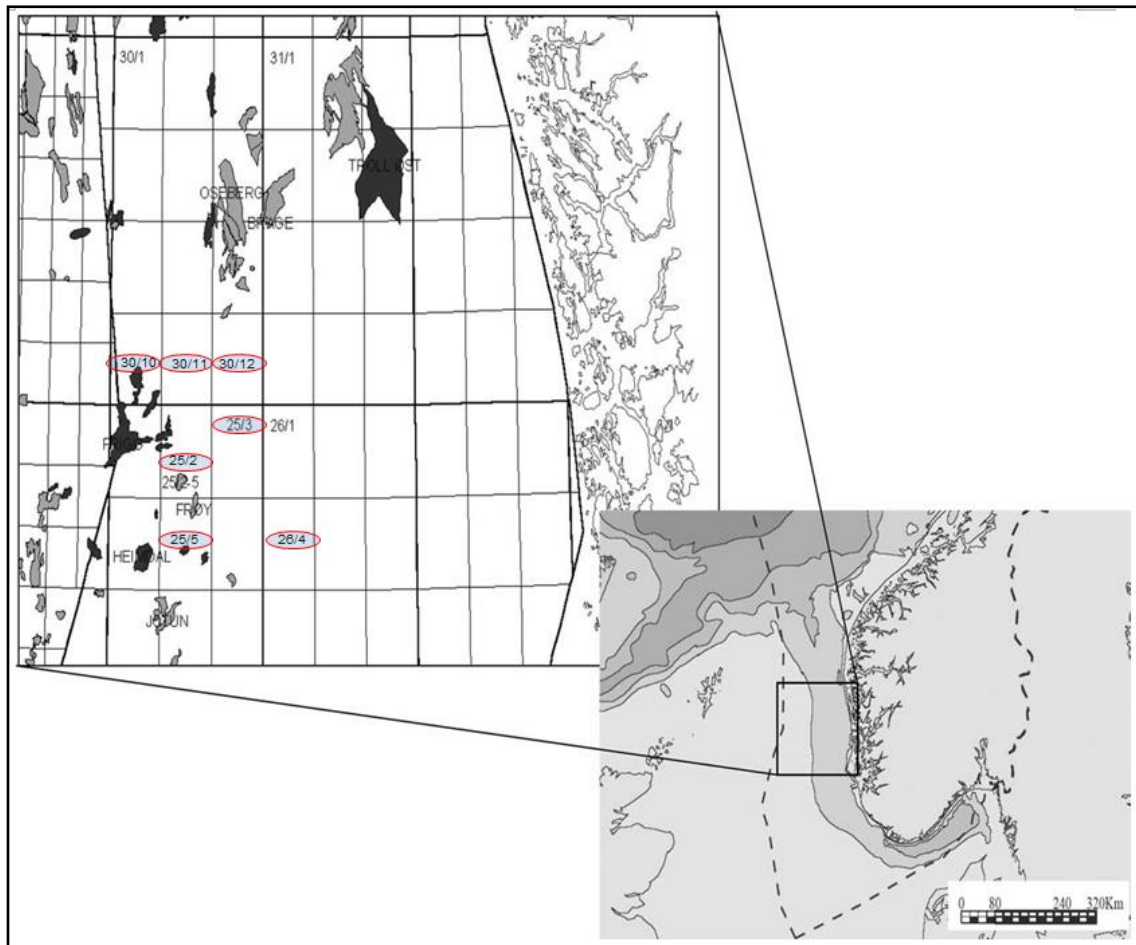
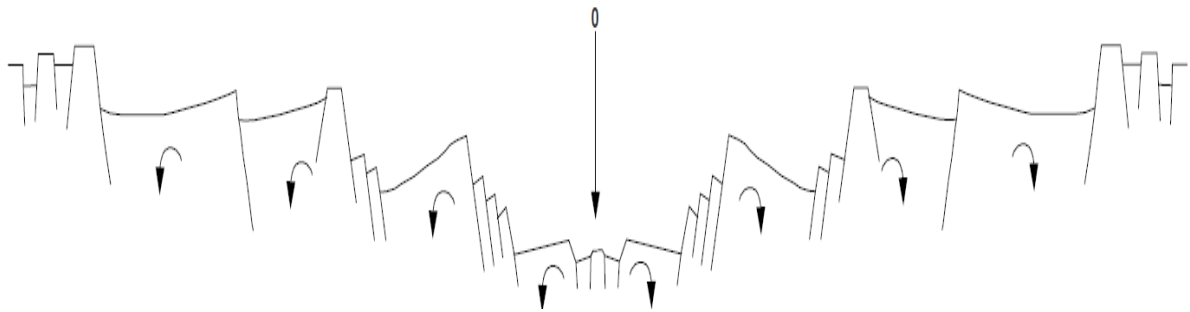


Fig. 2.1 Location map of the study area. The blocks are marked in red ovals (Larter and Rolando, 2005).

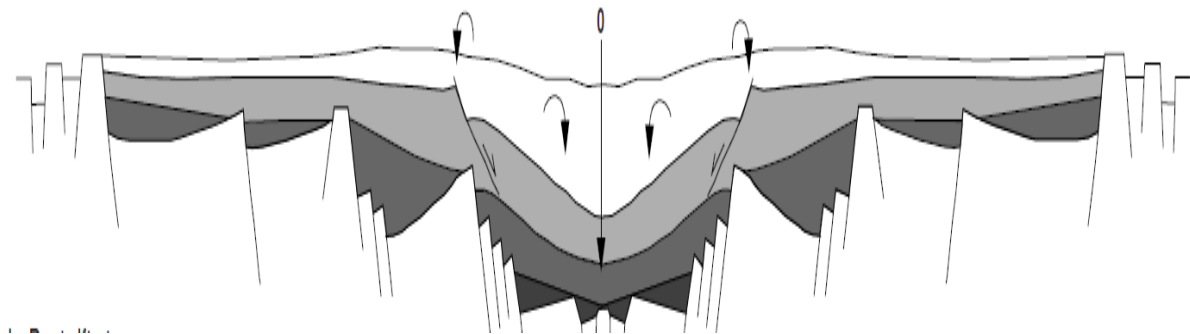
Regional tectonic framework

The northern Viking Graben has gone through multiple rifting phases where the thermal equilibrium is not attained in all extensional episodes. This has greatly affected the style and extent of subsidence between each successive rifting event (Gabrielsen et al., 1990). The tectonics in the North Sea, from late Palaeozoic to Cenozoic, has been subdivided into several rifting phases namely: Devonian-Carboniferous, Permo-Triassic, middle-late Jurassic and late Cretaceous-early Tertiary (Halstead 1975; De'Ath and Schuyleman 1981; Eynon 1981; Gray and Barnes 1981; Hallett 1981; Harding 1983; Whiteman et al., 1975; Zielger 1975, 1978, 1982; Beach et al., 1987; Giltner 1987). The structural history of Devonian-Carboniferous is not very well understood because of lack of data. In spite of considerable uncertainty in the dating of thermal subsidence and crustal stretching/thinning related to

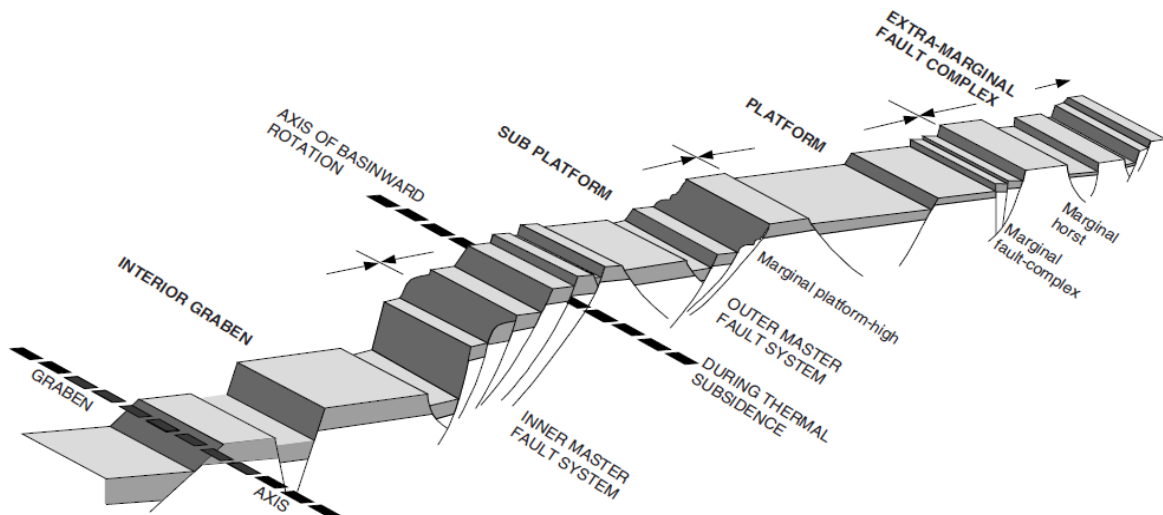
Permo-Triassic rift phase, it has been postulated by many workers (Zielger 1978, 1982; Eynon 1981; Badley et al., 1984, 1985, 1988; Beach et al., 1987; Frost 1987; Giltner 1987; Scott and Rosendahl 1989; Thorne and Watts 1989). The timing of Jurassic-Cretaceous rifting event is however well understood (Zielger 1982; Brown 1984; Giltner 1987; Beach et al., 1987; Badley et al., 1988; Thorne and Watts 1989). According to Christiansson et al., (2000) the rift axis for Permo-Triassic rift is supposed to lie beneath the Horda Platform and middle Jurassic-early Cretaceous rift is centered beneath the Viking Graben. The late Cretaceous-early Tertiary subsidence (Hamar et al., 1980; Beach et al., 1987; Frost 1987) is highly debatable whether it should be considered as a separate extensional event (Badley et al., 1988; Donato and Tully 1981).



a) Syn-rift stage



b) Post-rift stage



c) Rift-basin configuration

Fig. 2.2. Tilting situation for (a) syn-rift, (b) post-rift, and (c) main structural elements of Viking Graben. (Modified from Nøttvedt et al., 1995 and Gabrielsen 1986).

The rift system in the northern North Sea is bounded in the west by the East Shetland Platform and Øygarden Fault Zone (Norwegian Shield) in the east (Fig. 2.2). The sedimentary basins lie within the asymmetric half-grabens and the whole area is characterized by rotated fault blocks.

Stratigraphic settings

Shales are dominant in the upper Cretaceous of the Frigg area with chalky limestone beds of Campanian and Maastrichtian ages. The collapse regarding the Utsira High at the end of Cretaceous has resulted in the inversion of structural relief. The Tertiary of the Frigg area is characterized by the correlative reconstruction of the Shetlands-Orcadian belt on the west, which has resulted in the strong offlap of sediments from west to east. The Palaeocene sediments include mostly clastic material that has been originated in the west and taken into the basin by the action of turbidity currents. This phenomenon has created fan complexes at the foot of the Fladen Group spur and the Shetland escarpment. A new phase of marine sedimentation rich in shaly material, initiated by a major clastic influx, i.e., The Ypresian Frigg sands, started in Eocene. The Oligocene is also marked predominantly by shaly marine sedimentation, however, during the regression in Miocene-Pliocene period sand deposition finally predominated.

The stratigraphic column of the (discovery) well 25/5-5 is typical of the entire field that has been drilled through a (Miocene and Pliocene) sandy section of continental origin. A greenish brown, soft and silty mudstone of middle Oligocene age lies below this section which is underlain by a repetitive soft brown gumbo clay of early Oligocene to middle Eocene age.

Soft, apple-green, pyritic clays followed by silty shales are encountered below 58 m of depth. At 1836 m, the top of Frigg sand of early Eocene age is present which is a gas reservoir. Palaeocene sand is found at a depth of 1976 m, the top of which is marked by palynologic evidence.

A thick shaly section (1322 m) of late Cretaceous age overlies greenish, silty shales with dolomite stringers beneath the Palaeocene sands. Below lie undercompacted dark-gray shales of early Cretaceous age. Kimmeridgian oil shales are found when drilled further down overlain by late Cimmerian unconformity with a strong deep seismic reflector. Below the Kimmeridgian shales, the dark-gray pyritic and calcareous shales (Callovian age) with numerous dolomite stringers in the upper part are present and finally water-bearing Dogger sandstone.

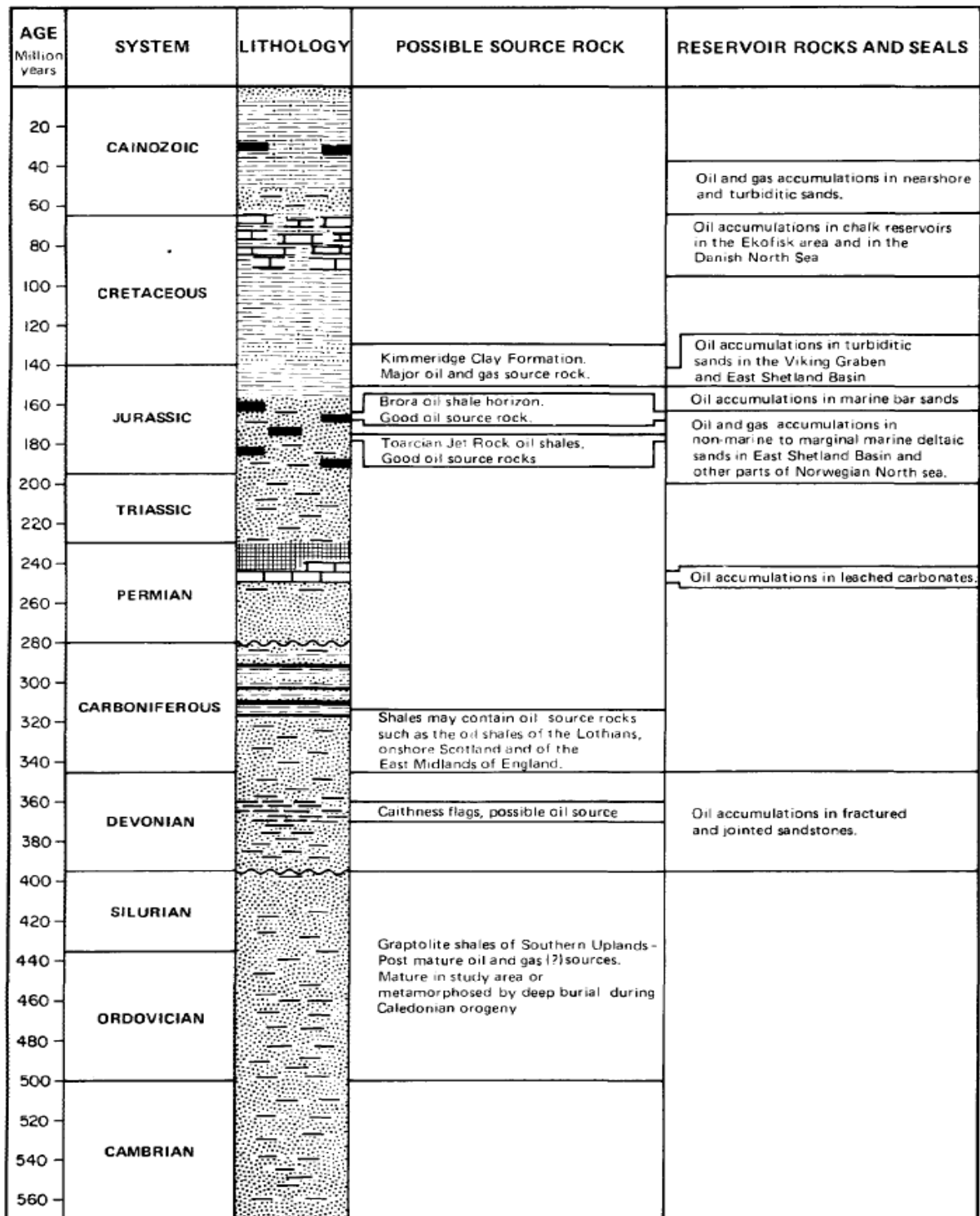


Fig. 2.4. Stratigraphic summary of the petroleum systems in the central and northern North Sea (Cooper and Barnard, 1984).

Petroleum system of the area

Clastic and carbonate sediments, ranging from Cambrian to Recent, dominate in the North Sea and its adjacent areas. The area comprises a number of potential source rocks, however, Jurassic-early Cretaceous sediments are considered to be the major source rocks in central and northern North Sea (Barnard and Cooper, 1981; Ziegler, 1980). Moreover, on the basis of some evidences, early Jurassic rocks are believed to be responsible for some major oil and gas accumulations. This is the case in Frigg field (Heritier, Lossel, and Wathne, 1981) where the late phase of diagenesis resulted in the generation of gas. The present day values for the vitrinite reflectivity of these rocks vary from 1.5 to 1.8.

The reservoir sand is unconsolidated, fine and clean comprising of good characteristics with porosity ranging from 25 to 32% and average permeabilities ranging from 1200 to 1600 md. The structure of the Frigg area resembles the topography of a submarine fan which has been enhanced by the differential compaction of sands and draping and sealed by open-marine shales of Eocene age.

3. Sample Set, Analytical Methods and Parameters

This chapter includes the list of all the samples from a series of dry wells in block 25, 26 and 30 that have undergone geochemical analysis, the analytical techniques applied and their parameters to determine rock type, facies and maturity. The analytical methods, developed tremendously over the last sixty years, are applied for the investigation of organic contents in core extracts and petroleum inclusions. The diagnostic geochemical parameters are used to analyse different properties of samples. The North Sea Oil (NSO-1) sample from the Oseberg field, considered as a standard by Norwegian Petroleum Directorate, has been repeatedly used as reference oil to carry out analytical work.

Figure 3.1 presents a generalized workflow followed in this chapter.

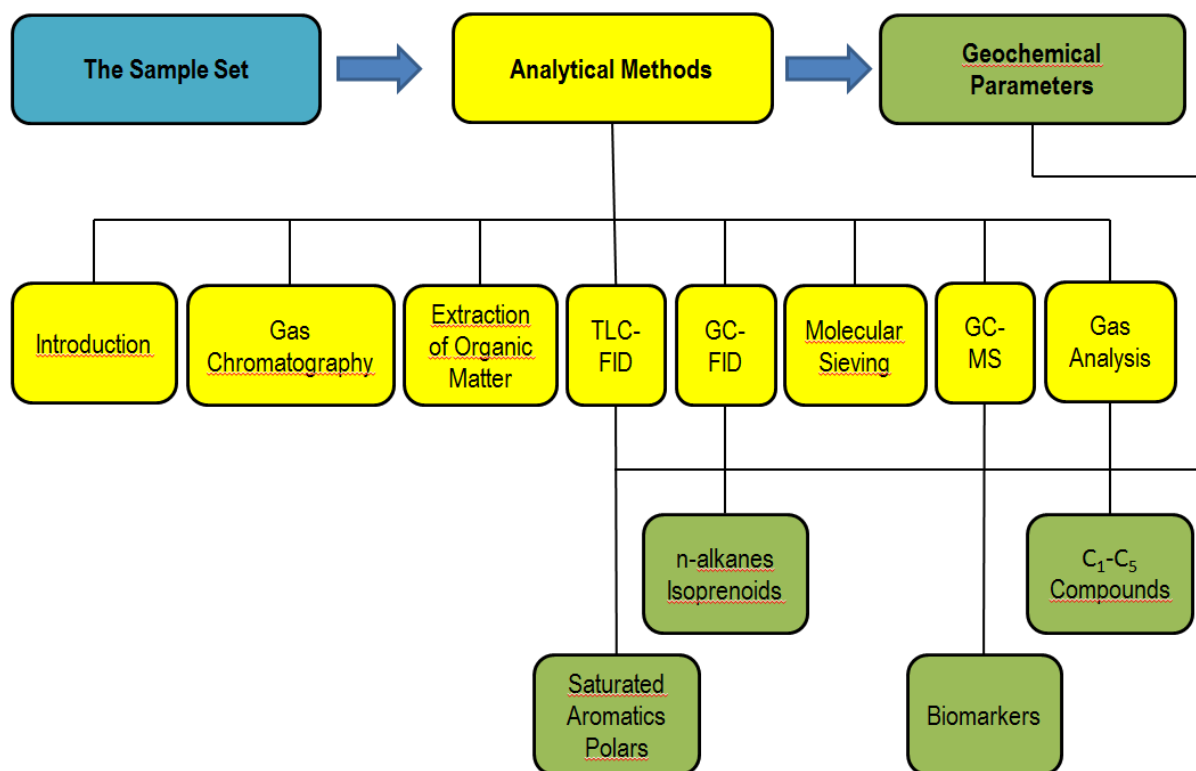


Fig. 3.1. A simple model of the workflow

The Sample Set

The sample set of the study area consists of 91 core samples from fifteen exploratory wells that have previously been declared as dry (table 3.1). The core samples were mostly

reservoir siliciclastic sandstones, however, shales and coals were also encountered at certain depths in few wells. The primary objective of these exploratory wells was to target the Jurassic sandstones with main emphasis on the Vestland and Brent groups. All the samples are listed in table 3.1 with their well, depth, lithology, formation and age description.

Table 3.1. The sample data set of the study area from Viking Graben, North Sea.

No.	Well	Depth (m)	Lithology	Rock Formation	Formation Age
1	25/2-4	3675.0	Sandstone	Hugin Fm	Middle Jurassic
2	25/2-4	3676.0	"	"	"
3	25/2-4	3683.0	"	"	"
4	25/2-4	3684.0	"	"	"
5	25/2-4	3693.0	"	"	"
6	25/2-4	3694.0	"	"	"
7	25/2-7	3437.0	"	Sleipner Fm	"
8	25/2-7	3439.0	"	"	"
9	25/2-12	3698.0	"	Svarte Fm	Late Cretaceous
10	25/2-12	3698.5	"	"	"
11	25/2-12	3706.0	"	"	"
12	25/2-12	3710.0	"	Heather Fm	Middle-late Jurassic
13	25/2-12	3711.0	"	"	"
14	25/3-1	3858.3	"	Dunlin Gp	Early- middle Jurassic
15	25/3-1	3858.8	"	"	"
16	25/3-1	3861.0	"	"	"
17	25/3-1	3861.5	"	"	"
18	25/5-5	2164.5	"	Heimdal Fm	Paleocene
19	25/5-5	2171.5	"	"	"
20	25/5-5	2172.0	"	"	"
21	25/5-5	2173.5	"	"	"
22	26/4-1	2258.7	"	Ty Fm	Early Paleocene
23	26/4-1	2273.5	"	"	"
24	26/4-1	2274.0	"	"	"
25	26/4-1	2274.8	"	"	"
26	26/4-1	2289.2	"	"	"
27	26/4-1	2290.5	"	"	"

28	30/4-1	2742.0	"	Jorsalfare Fm	Late Cretaceous
29	30/4-1	2747.0	"	"	"
30	30/4-1	2749.5	"	"	"
31	30/10-6	4664.0	"	Tarbert Fm	Middle Jurassic
32	30/10-6	4664.5	"	"	"
33	30/10-6	4675.0	"	"	"
34	30/10-6	4675.5	"	"	"
35	30/10-6	4686.0	"	"	"
36	30/10-6	4686.5	"	"	"
37	30/10-6	4691.0	"	"	"
38	30/10-6	4691.5	"	"	"
39	30/10-6	4702.0	"	"	"
40	30/10-6	4702.5	"	"	"
41	30/10-6	4714.2	"	"	"
42	30/10-6	4714.7	"	"	"
43	30/10-6	4962.3	"	"	"
44	30/10-6	4962.8	"	"	"
45	30/11-3	3450.5	Shale interbedded with coal	Hugin Fm	"
46	30/11-3	3457.0	Sandstone	"	"
47	30/11-3	3457.5	"	"	"
48	30/11-3	3468.3	"	"	"
49	30/11-4	3514.5	"	"	"
50	30/11-4	3515.0	"	"	"
51	30/11-4	3515.5	"	"	"
52	30/11-4	3516.0	"	"	"
53	30/11-4	3517.2	"	"	"
54	30/11-4	3526.8	"	"	"
55	30/11-6	3200.5	"	Tarbert Fm	"
56	30/11-6	3203.2	"	"	"
57	30/11-6	3205.0	Coal	"	"
58	30/11-6	3210.3	Sandstone	"	"
59	30/11-6	3210.8	"	"	"
60	30/11-6	3219.5	"	"	"
61	30/11-6	3240.5	"	"	"

62	30/11-6	3249.3	"	"	"
63	30/11-6	3249.8	"	"	"
64	30/11-6	3295.2	"	"	"
65	30/11-6	3295.7	"	"	"
66	30/11-7	3987.5	"	"	"
67	30/11-7	3988.0	"	"	"
68	30/11-7	3988.5	"	"	"
69	30/11-7	3989.2	"	"	"
70	30/11-7	3989.8	"	"	"
71	30/11-7	3990.3	"	"	"
72	30/11-8A	3968.0	"	No further details are available for these wells because they are currently under development.	
73	30/11-8A	3968.5	"		
74	30/11-8A	3986.5	"		
75	30/11-8A	3987.0	"		
76	30/11-8S	3506.1	Sandstone		
77	30/11-8S	3621.5	"		
78	30/11-8S	3622.4	"		
79	30/11-8S	3622.9	"		
80	30/11-8S	3637.4	Sandstone		
81	30/11-8S	3647.2	"		
82	30/11-8S	3651.0	"		
83	30/11-8S	3651.8	"		
84	30/11-8S	3661.5	"		
85	30/11-8S	3666.4	Shale		
86	30/12-1	2905.0	Sandstone	Tarbert Fm	Middle Jurassic
87	30/12-1	2905.5	"	"	"
88	30/12-1	2929.5	"	"	"
89	30/12-1	2930.0	"	"	"
90	30/12-1	2930.5	"	"	"
91	30/12-1	2940.0	Shale interbedded with coal	"	"

The samples were collected from NPD based on coloring and staining of the sandstone cores. A core from well 25/5-5 is shown in the figure (Fig 3.2) below. The sandstone is at certain depth really dark in color which may be due to the consequence of the presence of petroleum.



Fig. 3.2. The figure is showing visible staining in the dry wells.



Fig. 3.3. Figure caption is showing the extracts from the dry wells. The color of extract may represent to some extent the bitumen richness. Generally, the darker the color, the richer the extract. Yellowish color could indicate palaeo-condensate, dark brown color could represent black oil while light brown may indicate lighter oils.

Analytical Methods

The analytical methods which are used to study the various aspects of the samples are discussed in the following manner:

3.2.1 Introduction

3.2.2 Gas Chromatography

3.2.3 Sample preparation and extraction of bitumen

3.2.4 Iatroscan–Thin Layer Chromatography-Flame Ionization Detector (TLC-FID)

3.2.5 Gas Chromatography-Flame ionization Detector (GC-FID)

3.2.6 Molecular Sieving–n-alkane removal

3.2.7 Gas Chromatography-Mass spectrometry (GC-MS)

3.2.8 Gas Analysis

Introduction

The geochemical parameters, indeed, are helpful to analyze the geochemical properties of samples (rock/oil) and divided into two main groups: molecular parameters and bulk parameters. The molecular parameters are associated with the chemical characteristics of either the whole sample or just a specific sample fraction, e.g. Gas Chromatography-Flame Ionization Detector (GC-FID) or Gas Chromatography-Mass Spectrometry (GC-MS). The bulk parameters separate bitumen or oil samples into polar compounds, aromatic and saturated hydrocarbons and illustrate the gross compositional properties of the whole extract/oil. Thin Layer Chromatography-Flame Ionization Detector (TLC-FID) serves the purpose where FID does the quantification and chromatographic separations give the required compound classes.

The samples were subjected to one or more of these analytical procedures in order to investigate the relative amount of bulk petroleum fractions and to determine biomarkers.

Light hydrocarbons may be present in source rocks, however, under normal extraction procedures, they may be usually lost from the rock samples. The hydrocarbons ranging from C₄-C₈ can be analysed in the rock samples by applying various techniques (Schaefer et al., 1978), while they can be directly analysed in oil samples by normal GC-FID applications (Peters et al., 2005). The even lighter hydrocarbons, i.e, C₁-C₄, liberated from inclusions, can

be identified using GC-FID methods and simple preparation techniques (Karlsen et al., 1993).

Gas Chromatography

James and Martin introduced the method of gas chromatography in 1952 (Archer J.P. Martin, 1952). It is an analytical technique that works on the basic principle of separating organic components of a complex mixture into individual molecules based on their volatilities. Hence, only the compounds which can easily vaporize without decomposition are considered suitable for GC analysis. It gives both quantitative and qualitative information for individual organic components in a sample. It is widely utilized because it is relatively non-expensive, fast and easy to use and automate.

The components move through a GC column in gaseous form, either because they are generally gases or heated and vaporized into gaseous state. The compounds partition between the mobile phase (carrier gas and analyte) and the stationary phase (the column) and this differential partitioning allows the compounds to be separated in time and space. The separation is controlled by relative solubility, volatility and adsorption.

The Carrier Gas

The carrier gas, generally referred to as mobile phase, moves the sample from the injector through the column during chromatography. The carrier gas should be inert in order to avoid interaction with the sample being analyzed. Hydrogen, helium and nitrogen are commonly used as carrier gas in gas chromatography. Hydrogen gas is highly explosive in nature and special precautions are required. Helium has a low viscosity at high temperatures which helps to speed up the process of chromatography but is very expensive. It causes very little contamination because it is highly pure. However, nitrogen is a heavy gas which is safe to use and not much expensive. The type of carrier gas affects the efficiency of the column and analysis time, thus the choice of gas determines how fast the substances react with each other, how they move through the column and how swift they are to reach the detector. The transportation of gas from cylinder to chromatograph is controlled by pressure (2-3 bars normal) which is adjustable. This control mechanism ensures the required pressure and flow-speed of the gas to be correct.

Injector and column

The injector is a hollow, heated, glass-lined cylinder where the sample is introduced into the column and vaporized. The temperature of the injector is controlled so that all components in the sample will be vaporized. Usually it is kept at 300°C isothermal temperature. The glass liner is about 4 inches long with internal diameter of 4 mm. The samples are injected, vaporized and transported through the column. Some of the substances with high boiling points are absorbed in the injector and do not flow through the column.

The column is a stationary phase which looks like a spiral and are made up of metal, glass or quartz. Two types of column are known:

1. The packed bed column is completely packed and its stationary phase is in granular form which fills the column completely. These columns are rarely used now-a-days.
2. The open tubular capillary column is usually of a small diameter with organic coating on the inner tube wall. This coating acts as a stationary phase. Substances are allowed to flow through the hole in the center of the column.

The temperature is adjusted and must be high enough for the sample to be vaporized together with the solvent.

Detector

A detector measures the different components that are separated in the column. Concentration-dependent detectors and mass-flow-dependent detectors are the two ways of detecting these components. The two detectors that are widely used are the Thermal Conductivity Detector (TCD) and Flame Ionization Detector (FID). As the analyte passes through the detector, the change in heat occurs which is measured by TCD. This does not destroy the organic components in the process. It gives the least precise measurement and its major drawback is its less dynamic linear range compared to FID. FID on the other hand destroys the sample as it burns the organic compounds and is at least two orders of magnitude more linear than TCD. In spite of the fact that samples are destroyed during the process, FID is still a choice of preference and the most accurate detector.

Sample preparation and extraction of bitumen

The samples were disintegrated carefully by manual crushing into individual grains, treated with chromic acid (3 hours) and ultrasound (10 min) and washed with water to remove any clay or organic matter as well as carbonate from the grains. Disintegration should be done completely in order to open the fractures and occluded spaces for extraction and to retain the inclusions which are prone to destruction during disintegration (Karlsen et al., 1993). These grains were used for gas analysis. Then the extraction of organic contents, like bitumen, from the crushed core samples was done by using a conventional Soxtec system HT 1043. Approximately 5-10 g of the crushed sample in powdered form was filled into pre-extracted cellulose thimbles covered with glass wool. A mixture of dichloromethane and methanol (DCM:MeOH, 93:7 vol%) is used as a solvent to extract the sample. The thimbles were pre-extracted by boiling for 10 minutes and rinsing for 20 minutes. In order to remove any elemental sulphur, copper was added to the solvent which was activated in concentrated nitric acid (HNO₃) and washed with water and solvent (DCM:MeOH, 93:7 vol%). 50ml of the solvent is then heated to 60°C in a stove. Six samples can be extracted at the same time by boiling (1h) and rinsing (2h) in the solvent to extract all the organic contents effectively from the rock samples. The extract was then transferred into 15ml glass vials sealed with Teflon lined plastic corks. It was further concentrated, sieved and treated with other solvents before being used for geochemical analysis, i.e. GC-MS, GC-FID or TLC-FID, depending on the type of analytical method.

Iatroscan – Thin Layer Chromatography-Flame Ionization Detector (TLC-FID)

Thin layer chromatography (TLC) and flame ionization detector (FID), pioneered by Ranny (1987), are integrated in an Iatroscan TLC-FID instrument and used for the geochemical screening of core samples. The instrument used for this technique is actually a silica rod for liquid chromatography and sample application, and FID scanning and quantification of the extract is an electronically integrated process in which the sample is ionized into different components by subjecting it to the flame. Since the extracted sample contains hydrocarbons and non-hydrocarbons (asphaltenes and resins), TLC-FID analysis is used to describe petroleum column heterogeneities in the reservoir by determining the horizontal and vertical distribution of gross petroleum composition in terms of saturated hydrocarbons, aromatic

hydrocarbons and resins/asphaltenes (Karlsen and Larter, 1989). The deviation in FID response is obvious if heteroatoms are present in the organic molecules (Bhullar et al., 2000).

The studied samples have been analysed using Iatroscan MK-5 model instrument coupled with a flame ionization detector (FID). An electronic integrator (Perkin-Elmer LCI-100) is attached to it to calculate the total quantity of different compounds in the extracts. To remove any contaminants from the chromarods and to obtain the constant activity of silica layer, they are subjected to FID. The samples (about 3 μ l each) are then applied to the silica rods, type Chromarods-SIII, with a pore diameter of 60 Å and particle size 5 μ m, on a fixed point near the base of chromarod. Two out of ten rods are used for test run, one with NSO-1 and the other is left blank. The rest are used for samples.

Solvents of different polarity are used to separate the sample into saturated hydrocarbons, aromatic hydrocarbons and polar compounds. The chromarods are developed by placing in normal-hexane for 22 minutes (95% of rod length), dry for 3 minutes and then place in toluene for 13 minutes (65% of rod length). Place the chromarods in oven for 90 seconds (60°C) to remove the solvents and standardizing the samples with larger hydrocarbon fractions ($<C_{15}$). The chromarods are finally placed in Iatroscan instrument with the scanning speed of 30sec/scan, pure grade hydrogen (180ml/min) and air (2.1l/min) supplied by a pump.

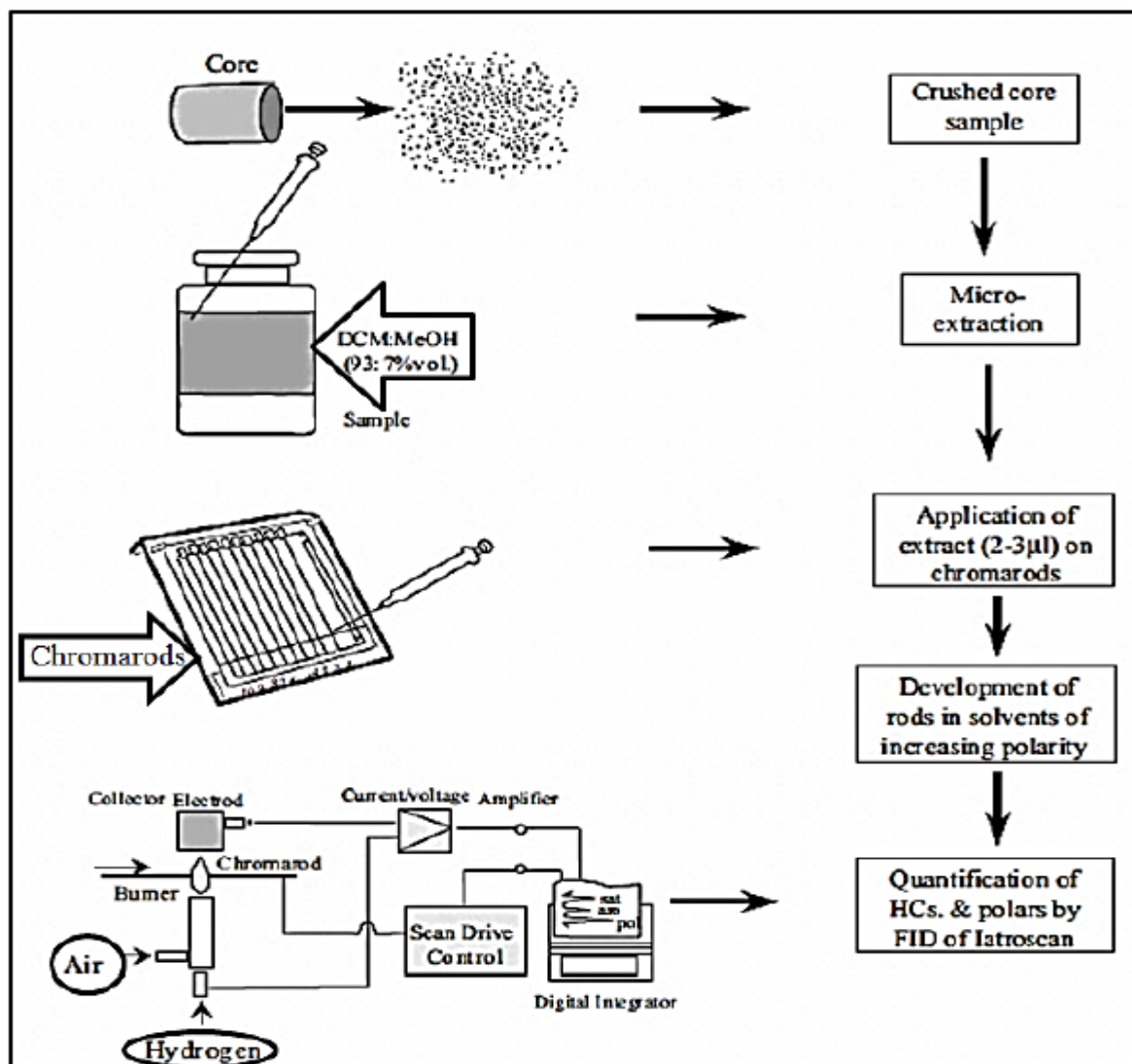


Fig 3.4. Schematic diagram of TLC-FID procedure for micro-extraction of bitumen (Bhullar et al., 2000).

The apparatus for TLC-FID generally consists of the following:

1. A detection system in a FID
2. A digital integrator/recorder with a plotter
3. Other accessories for sample application, extraction and drying of chroma rods

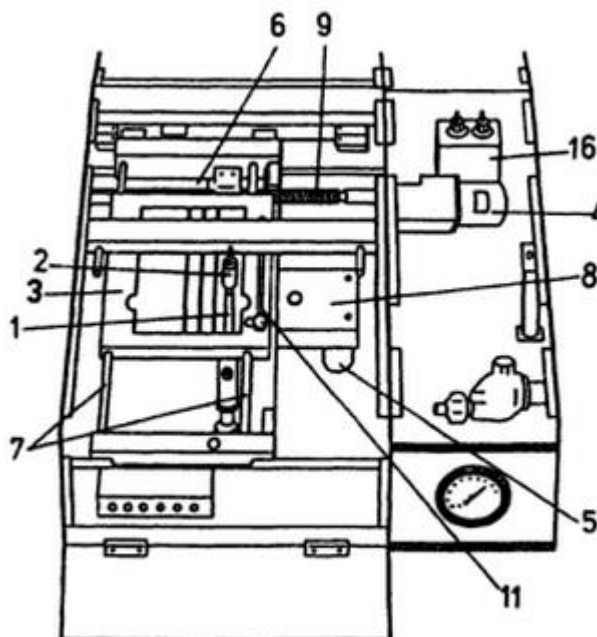


Fig. 3.5. Principal parts of the Interior of TH-10 Mark III series. (1) H₂ burner, (2) FID collector electrode, (3) rod holder, (4) & (5) drive motion, (6) lead screw, (7) & (9) guide rods, (8) screw drive, (11) peak pyrolysis selector, (16) air filter (Ranný, 1987).

Gas Chromatography-Flame ionization Detector (GC-FID)

GC-FID technique helps in the quantification and identification of individually separable components in petroleum such as toluene, hexane, xylene, n-alkanes and isoprenoids etc. The n-alkanes for all core extracts and oils can be analyzed using gas chromatograph with flame ionization detector and nitrogen as a carrier gas (Bhullar et al., 1999). Time and temperature program may vary according to the requirements. The sample is injected and vaporized before entering the chromatographic column where the separation of molecules takes place. A film layer inside the column acts as a stationary phase. The low boiling and high vapour pressure (normally short-chain) molecules travel quickly through the column while it takes much longer time for branched-chain molecules to move through. Helium (He) or nitrogen (N₂) may be used as a carrier gas which are inert and act as a mobile phase. The column is heated from 40°C to 325°C (75min) by a program and kept constant at 325°C for about 20 minutes. Hence the total run takes about 95 minutes. The molecules enter the flame ionization detector as soon as they leave the column and finally the signals are recorded by the computer. Time and temperature are plotted against x-axis and signal intensity (in terms of peaks height equivalent to the relative amount of different components) along y-axis.

GC-FID analysis is carried out in Varian Capillar Gas Chromatography (CP 3800 model) with 25m long Hewlett Packard Ultra II cross-linked Methyl Silicon Gum Column (0.2 mm inner dia) and a film (0.33 μm thick). The temperature of the injector is set to 330°C with initial column temperature of 40°C, 4°C/min gradient and a hold time of 2°C/min. This whole procedure takes about 75 minutes where these parameters are kept constant for further 20 minutes so that the total run is completed in 95 minutes.

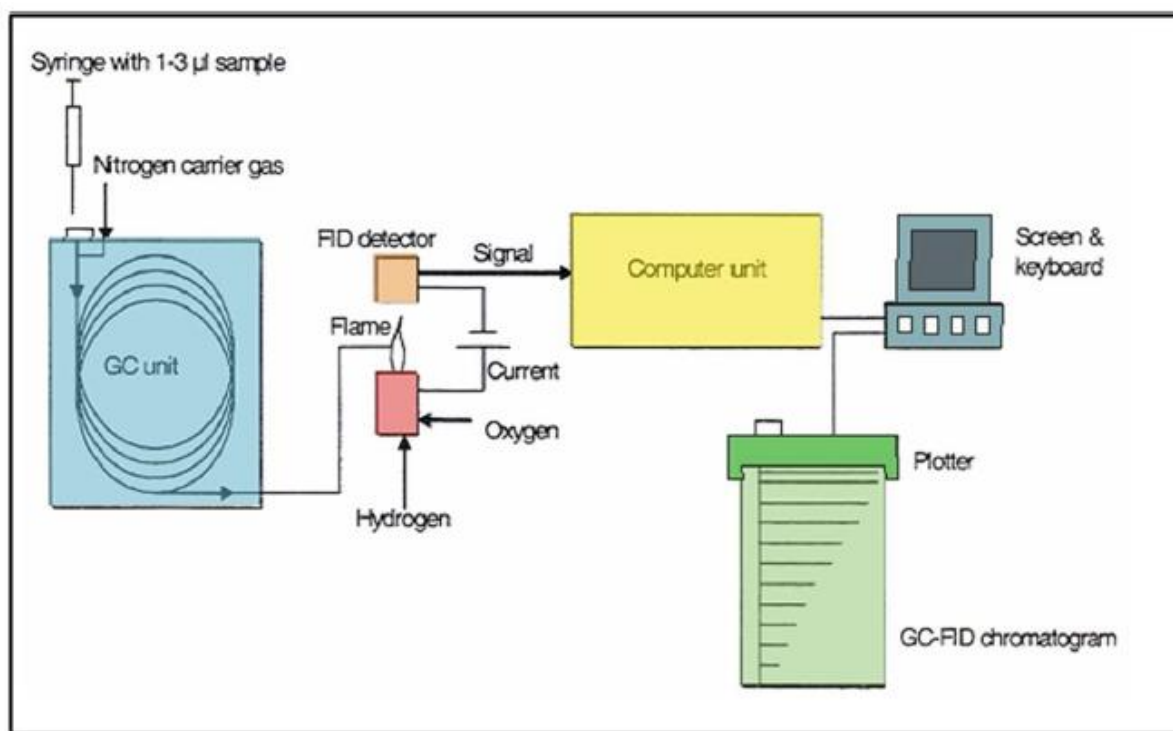


Fig. 3.6. Schematic overview of GC-FID instrument (modified after Pedersen, 2002).

GC-FID is applied to the whole oil, total core extracts or saturated (aromatic) hydrocarbon fractions of bitumen and crude oil. It helps to quantify individual hydrocarbon components and gives information about the source rock type and maturity of the analyzed bitumen/oil. It is also used to distinguish between petroleum contamination and natural background, to map the temporal, vertical and regional extent of contamination and to evaluate the efficacy of biodegradation (Peters et al., 2005). Geochemical screening of the samples can also be determined using GC-FID. Some common geochemical parameters used in GC-FID analysis are:

1. Pristane/Phytane (Pr/Ph)
2. Pristane/n-C₁₇
3. Phytane/n-C₁₈

These compounds as GC-FID parameters are used as facies and maturity indicators and GC-FID chromatograms may also serve as fingerprints for the samples.

GC-FID was carried out on bulk extracts of the studied samples. This helps to acquire information about n-alkanes and isoprenoid distributions and, in some cases, about steranes and terpanes as well. Individual hydrocarbon components were then quantified by measuring the height of the peaks and derived parameters such as Pr/n-C₁₇, Ph/n-C₁₈ and Pr/Ph were used to assess the maturity, organofacies and biodegradation of the extracts.

Molecular Sieving – n-alkane removal

To acquire reliable and accurate results on biomarkers, n-alkanes should be removed preliminary by molecular sieving. Since n-alkanes are straight chain saturated hydrocarbons which interfere with the biomarker signals during GC-MS analysis, molecular sieving makes it possible to keep the signals undisturbed by the elimination of n-alkanes. It also removes the polar compounds from the samples (Pedersen et al., 2006).

The sieve used for this purpose has molecules with channel-like openings (5Å dia), so that the long-chained n-alkanes will fit into these pores and trapped. The molecules larger than the size of the pores cannot enter the openings and will therefore linger in the solution. As a result the sample will be enriched in aromatic fractions and biomarkers and n-alkanes will be depleted fully.

In this study about 0.2 g of molecular sieve (5Å UOP MHS2 – 4120LC silica) is transferred into 15ml glass vial. About 3ml (2-3 drops) of the sample is added to it with the help of pipette. The sample mixture is diluted with cyclo-hexane (2-2.5ml) and stirred thoroughly. It is then centrifuged in a Heraens Sepatech Labofuge H. at 2000 rpm for 3-4 min so that the sieve will settle down. The liquid sample is poured into a new vial with a pipette, the same procedure is repeated again and then it is left for evaporation. When the concentration is reached to the desired level, the sample is transferred to vials using a pipette, specific for GC-MS, and sealed with a teflon-lined cap.

Gas Chromatography-Mass spectrometry (GC-MS)

GC-MS is infact a gas chromatograph (GC) integrated with a mass spectrometer (MS), which helps in the quantification and identification of biomarkers. The former does the compound separation and the later is concerned with the identification of components at a molecular level. The components in a mixture will be separated based on the difference in chemical properties of different molecules in that mixture. The retention time, i.e. the time taken by a molecule to come out of the gas chromatograph, is different for different molecules. As soon as a molecule leaves the gas chromatograph, it enters downstream into a mass spectrometer where it is captured, ionized, accelerated and deflected. It is then detected by a detector attached to mass spectrometer. Each molecule that is ionized by mass spectrometer is detected individually by the detector.

Each molecule has a different charge (z) and mass (m), and mass to charge ratio (m/z) is specific for many molecules of interest, such as biomarkers. Hopanes and triterpanes for example have $m/z = 191$. The detector detects and registers the relative abundance of different ions and m/z value. A PC program is used to record and manage the data. The relative abundance of ions with the selected m/z ratio versus retention time is displayed on the final plot. All n-alkanes are removed prior to the introduction of samples for GC-MS to get stronger biomarker signals.

In the study, a Thermo Scientific Trace 1300 UltraTM GC system in SIM-mode (selected ion monitoring) with 60m long column (0.25mm dia) integrated with TSQ8000 MS is used to determine the composition of samples. The initial temperature of the column is 40°C (1min) which is heated with 20°C/min to raise it to 180°C, and then with 1.7°C/min till it reaches to 310°C where it is kept for 40 minutes.

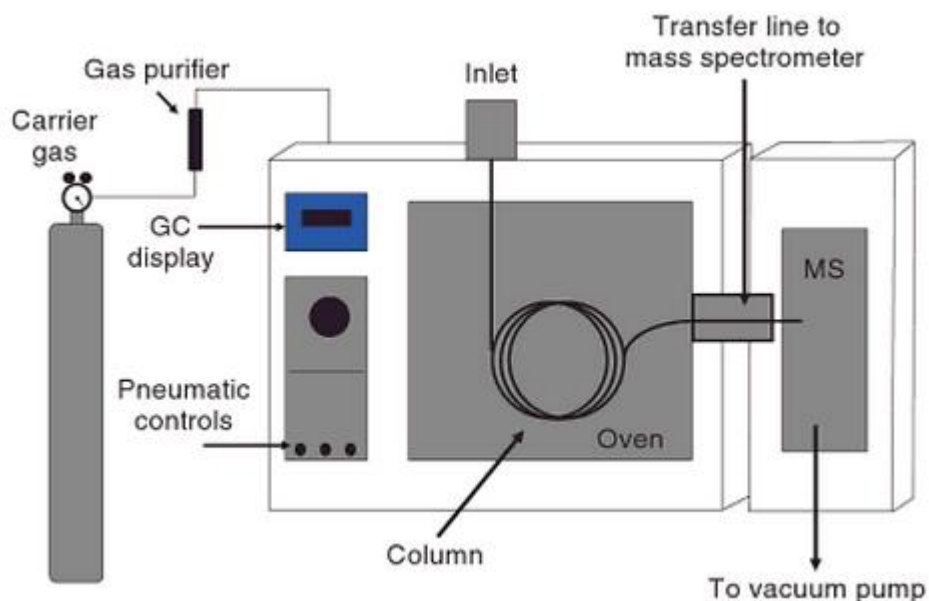


Fig. 3.7. Schematic illustration of a simple GC-MS

The components of a mass spectrograph are kept under a vacuum; the ion source, mass analyzer and detector which are shown in the figure below.

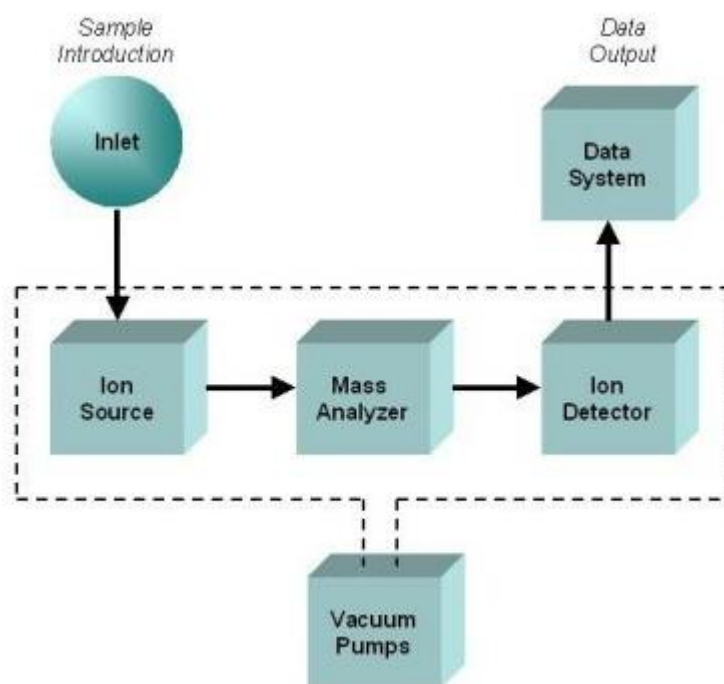


Fig. 3.8. Schematic of a Mass Spectrometer

In the study, GM-MS is used to determine the ions with mass to charge ratio (m/z) of 178, 191, 192, 217, 218, 231 and 253. This gives information about the most common biomarkers, n-alkanes distribution and other related compounds to establish the source, maturity and facies of petroleum.

Gas Analysis from inclusions

The core samples can be examined for inclusion gases by means of gas chromatography. The samples are cleaned and washed prior to gas analysis to avoid any contamination from the drilling mud. The procedure is used to determine the light hydrocarbons (C_1 - C_5) in the samples. Standard gas comprising methane, ethane and propane is run to measure the accuracy of the instrument. The chromatographic trace produced by the standard gas is shown below:

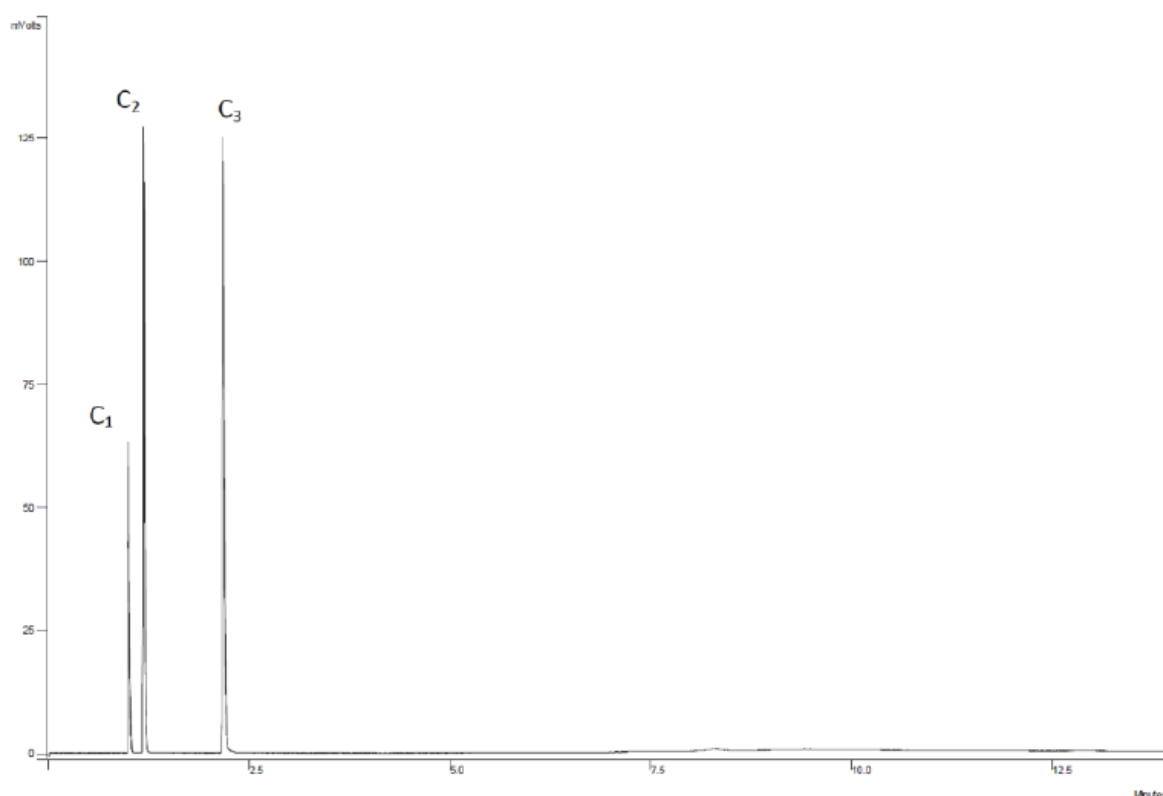


Fig. 3.9. Chromatographic trace of a standard gas run. The concentration of all three gases, i.e, methane, ethane and propane are present in 500ppm concentration.

Petroleum Geochemical Interpretation Parameters

The geochemical techniques discussed above (section 3.2) have various molecular parameters with the help of which the maturity, facies and the degree of biodegradation of the samples from the study area have been determined. These parameters are discussed in the following order:

3.3.1 Iatroscan TLC-FID

3.3.1.1 Saturated and aromatic hydrocarbons and polar compounds

3.3.2 GC-FID

3.2.2.1 Pristane/Phytane

3.2.2.2 Pristane/n-C₁₇ and Phytane/n-C₁₈

3.2.2.3 Carbon Preference Index (CPI) and pattern of n-alkanes peaks

3.3.3 GC-MS

3.3.3.1 Terpanes

3.3.3.2 Sterane

3.3.3.3 Triaromatic Steroids

3.3.3.4 Monoaromatic Steroids

3.3.3.5 Phenanthrene and methyl-phenanthrene

3.3.3.6 Methyl-dibenzothiophene

Iatroscan TLC-FID

Saturated and aromatic hydrocarbons and polar compounds

The extracted bitumen from the core samples are separated into compound classes (saturated hydrocarbons, aromatic hydrocarbons and polar compounds) using Iatroscan TLC-FID technique (section 3.2.4).

The ratio of saturated hydrocarbons to aromatic hydrocarbons (SAT/ARO) defines the source rock maturity and quality (Clayton and Bostick, 1986; Cornford et al., 1983). The ratio generally increases with increasing thermal maturity. However it may also increase in phase-fractionated gas-phase of the petroleum at shallower depths during migration (Østensen, 2005). Polar compounds define either biodegradation or low maturity. The higher the concentration of polar compounds, the lower the maturity of petroleum and condensates and vice versa.



Fig. 3.10. Separation of standard NSO-1 sample into its respective fractions, i.e, SAT = saturated hydrocarbons, ARO = aromatic hydrocarbons and POL = polar compounds.

GC-FID

The GC-FID analysis is done to identify n-alkanes upto C_{40} with the main focus on C_{15+} compounds (Fig 3.11). The distribution of n-alkanes and their ratio with isoprenoids, i.e, Pristane/n- C_{17} and Phytane/n- C_{18} , provide useful information about the source rock maturity and type, depositional facies and biodegradation.

Pristane/Phytane

Pristane and Phytane are a common type of isoprenoid isoalkanes. They have been derived from phytol, according to Tissot and Welte (1978), which is the most abundant source of isoprenoid. Phytol is a side chain of chlorophyll that separates from porphyrine structure during diagenesis after deposition. This relation between pristane and phytane shows a redox potential of source rock as stated by Tissot and Welte (1984). The alteration of phytol into pristane or phytane is determined by the depositional environment. Pristane is formed in oxygen-rich environment where phytol is oxidized to phytanic acid and then decarboxylated to form pristane. However, phytane is formed in anoxic conditions by the simple reduction of phytol. Hence pristane/phytane is a useful tool to determine the depositional environments in terms of oxic and anoxic conditions. The following intervals may help to define them:

$Pr/Ph > 1$ indicates hypersaline or oxidizing environment.

$Pr/Ph < 1$ indicates carbonate, lacustrine or anoxic environment.

$Pr/Ph = 1.3 - 1.7$ indicates marine environment.

$Pr/Ph > 2.5$ indicates marine environment with substantial amount of terrestrial elements.

$Pr/Ph > 3 - 10$ indicates the presence of plentiful woody material in the source rock for oils or the petroleum may have derived from coal.

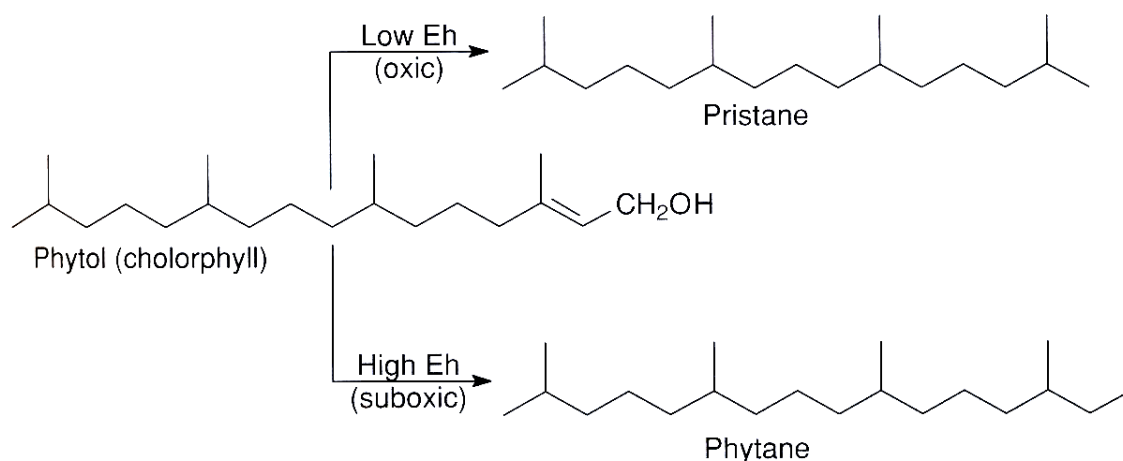


Fig. 3.11. The diagenetic origin of phytane and pristane (Peters et al., 2005)

Phase fractionation may also result in enhanced values that can be found in condensates in normal marine settings (Karlsen et al., 1995; 2004).

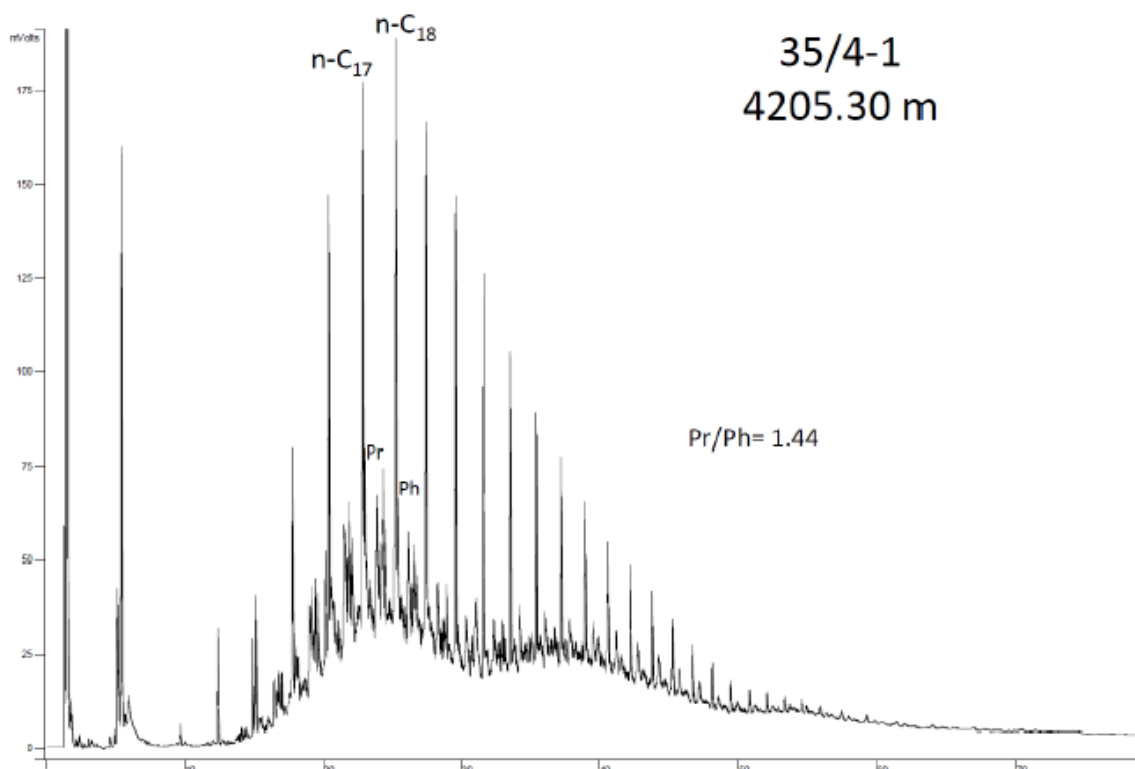


Fig. 3.12. GC-FID chromatogram of extracted bitumen from sandstones from well 35/4-1, 4205.30 m showing n-C₁₇ and n-C₁₈ peaks and isoprenoid pristane and phytane (Karlsen et al., 2006).

The ratio Pr/Ph increases with increasing maturity because phytane, compared to pristane, becomes highly unstable as temperature of the source rock increases.

Pristane/n-C₁₇ and Phytane/n-C₁₈

These ratios help to determine the level of biodegradation, maturation and facies together with other parameters such as bacteria assimilate n-alkanes (Peters and Moldowan, 1993). As maturity increases their value decreases, so they are useful maturity indicators for the organic matter of the same source facies. Isoprenoids are thermally unstable than n-alkanes (Tissot et al., 1971). Since these ratios are highly affected by biodegradation and organic input, great care should be required while interpreting these parameters (Peters and Moldowan, 1993). Lower ratios are indicators of more mature samples since during maturation the isoprenoids break down earlier than n-alkanes. This is because the tertiary carbon-carbon bonds are very less stable than primary and secondary carbon bonds.

Carbon Preference Index (CPI) and pattern of n-alkanes

The carbon preference index measures the ratio of odd to even numbered carbon atoms by weight (Tissot and Welte, 1978) where there is a predominance of molecules with the odd number of carbon atoms. It was first introduced by Bray and Evans in 1961 to determine the thermal maturity of either oil or extract. CPI values considerably below or above 1.0 specify the oil or extract to be thermally immature. However values closer to 1.0 suggest, but not necessarily prove, that the oil or extract is thermally mature (Peters and Moldowan, 1993). Values above 1.0 may indicate a siliciclastic source rock or a lacustrine environment, while values below 1.0 indicate carbonate facies.

$$\text{CPI} = 2(\text{C}_{23} + \text{C}_{25} + \text{C}_{27} + \text{C}_{29}) / [\text{C}_{22} + 2(\text{C}_{24} + \text{C}_{26} + \text{C}_{28}) + \text{C}_{30}]$$

$$\text{OEP (Odd/Even Predominance)} = (\text{C}_{21} + 6\text{C}_{23} + \text{C}_{25}) / (4\text{C}_{22} + 4\text{C}_{24})$$

Chromatograms can be classified on the basis of n-alkane patterns and information about sample facies and maturity can be determined (Peters and Moldowan, 1993). The peak height in oils from the North Sea generally decreases asymptotically with an increase in carbon number which results in a concave curve on chromatogram. The traces from GC-FID may indicate possible biodegradation which can be inferred from the unresolved complex mixture (UCM) rising above the baseline and also by reduction in the peak heights of n-alkanes in the chromatogram (Karlsen et al., 1995). Samples that are heavily biodegraded will have reduced or no pristane, phytane or n-alkanes left to be detected and measured. The

UCMs in oils are considered to be amongst the most complex mixtures of organic compounds (Sutton et al., 2005).

GC-MS

As discussed above the GC-MS technique is applied to identify the ions with mass to charge ratio (m/z) of 178, 191, 192, 198, 217, 218, 231 and 253 (table 3.2). The peaks obtained are further evaluated to determine the maturity and facies parameters as discussed further in this chapter.

Table 3.2. m/z ratios for the generation of chromatograms from GC-MS data.

Ion/Mass ratio (m/z)	Type	Compound class
191	Terpanes	Saturated Hydrocarbons
217	Steranes	
218	Steranes	
231	Triaromatic steroids	Aromatic Hydrocarbons
253	Monoaromatic steroids	
178	Phenanthrene	
192	Methylphenanthrenes	
198	Methyl-dibenzothiophenes	

Terpanes

A group of saturated hydrocarbons that are identifiable on $m/z = 191$ (Fig. 3.13 and table 3.3) are called Terpanes.

Table 3.3. Triterpanes recognizable on $m/z = 191$.

Peak	Stereochemistry	Composition	Compound Name
P		$C_{23}H_{42}$	Tricyclic terpane
Q		$C_{24}H_{44}$	Tricyclic terpane
R	17R+17S	$C_{25}H_{46}$	Tricyclic terpane

S		C ₂₄ H ₄₂	Tetracyclic terpane
U		C ₂₈ H ₄₈	Tricyclic terpane
V		C ₂₉ H ₅₀	Tricyclic terpane
A		C ₂₇	18 α (H)-trisnorneohopane
B		C ₂₇	17 α (H)-trisnorhopane
Z		C ₂₈ H ₄₈	17 α (H), 21 β (H)-bisnorhopane
C		C ₂₉ H ₅₀	17 α (H), 21 β (H)-norhopane
29Ts		C ₂₉	18 α (H)–30-norneohopane
X		C ₃₀ H ₅₂	15 α -methyl-17 α (H)-27-diahopane
D		C ₂₉ H ₅₀	17 β (H), 21 α (H)-30-normoretane
E		C ₃₀ H ₅₂	17 α (H), 21 β (H)-hopane
F		C ₃₀ H ₅₂	17 β (H), 21 α (H)-moretane
G	22S	C ₃₁ H ₅₄	17 α (H), 21 β (H)-22-homohopane
H	22R	C ₃₁ H ₅₄	17 α (H), 21 β (H)-22-homohopane

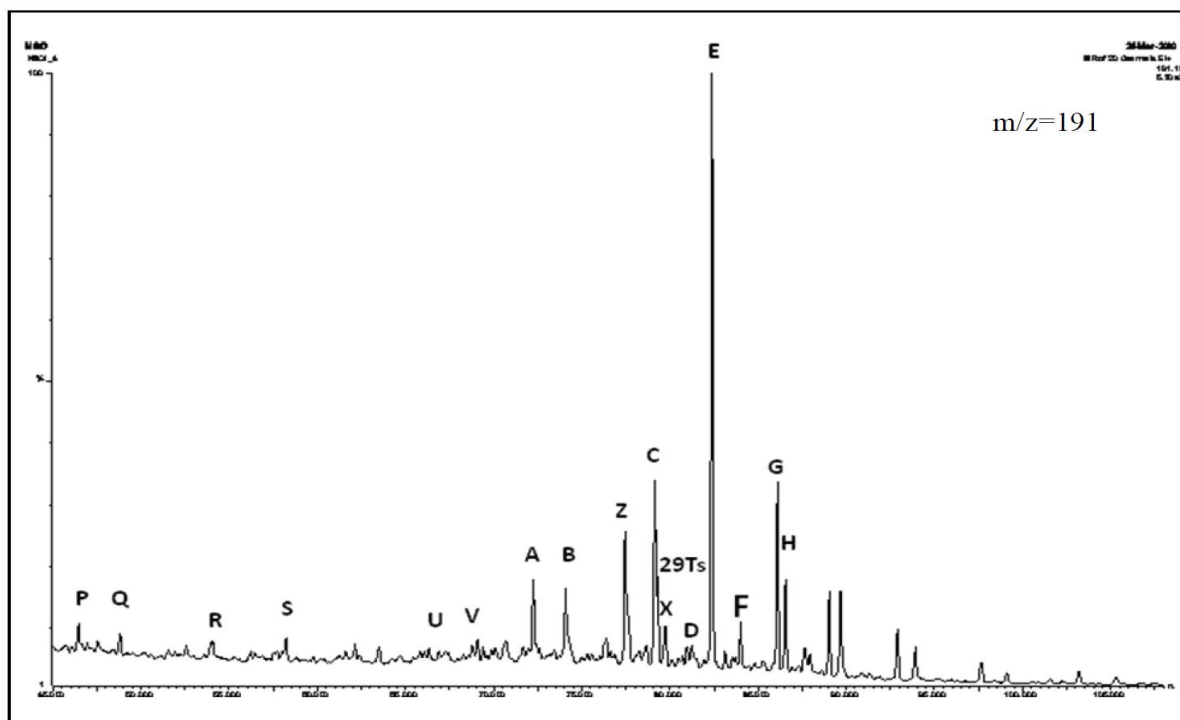


Fig. 3.13. GC-MS chromatogram showing peaks on $m/z = 191$.

Steranes

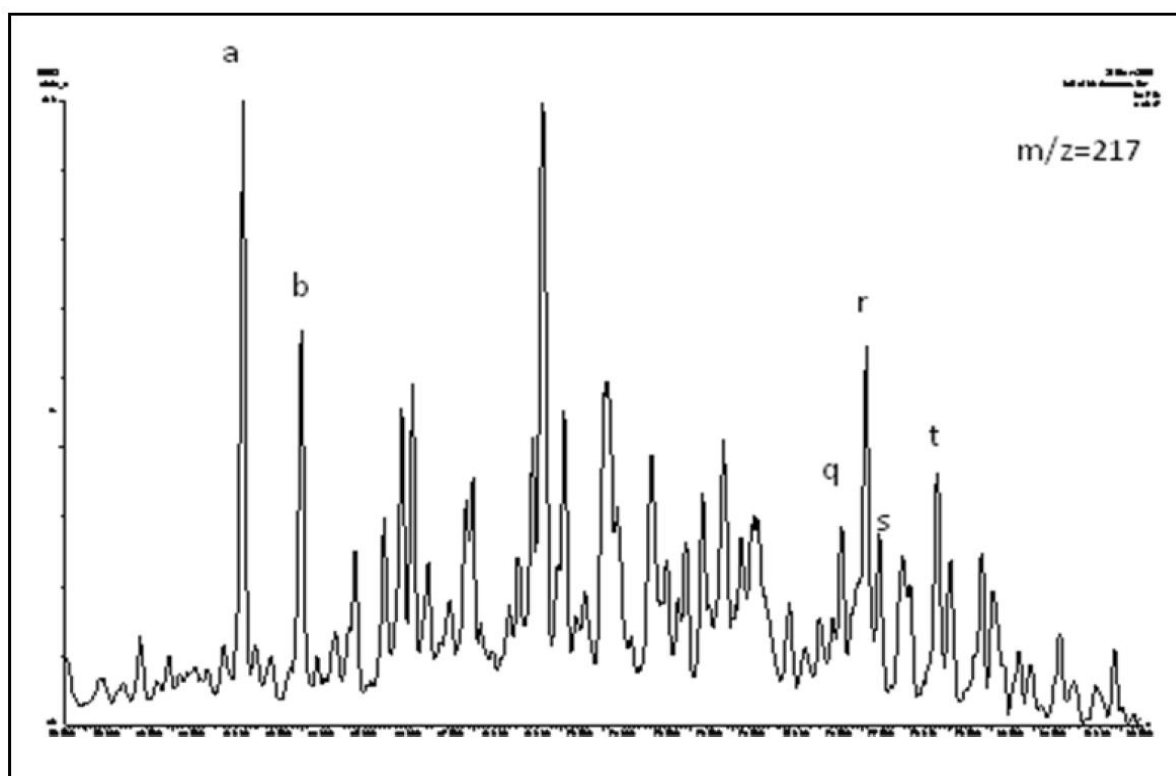
A group of tetracyclic saturated hydrocarbons (one 5-ring and three 6-rings) that are recognizable on $m/z = 217$ (Fig. 3.14) and $m/z = 218$ (Fig. 3.15) are called steranes. The relevant name of the peaks identified on $m/z = 217$ and $m/z = 218$ are shown in tables (3.4) and (3.5) respectively.

Table 3.4. Steranes recognizable on $m/z = 217$ (Weiss et al., 2000).

Peak	Stereochemistry	Composition	Compound name
a	20S	13 β (H), 17 α (H), 20(S)-cholestane (diasterane)	C ₂₇ H ₄₈
b	20R	13 β (H), 17 α (H), 20(R)-cholestane (diasterane)	C ₂₇ H ₄₈
q	20S	24-ethyl-5 α (H), 14 α (H), 17 α (H), 20(S)-cholestane	C ₂₉ H ₅₂
r	20R	24-ethyl-5 α (H), 14 β (H), 17 β (H), 20(R)-cholestane	C ₂₉ H ₅₂
s	20S	24-ethyl-5 α (H), 14 β (H), 17 β (H), 20(S)-cholestane	C ₂₉ H ₅₂
t	20R	24-ethyl-5 α (H), 14 α (H), 17 α (H), 20(R)-cholestane	C ₂₉ H ₅₂

Table 3.5. Steranes recognizable on $m/z = 218$ (Weiss et al., 2000).

Peak	Compound name
i	C ₂₇ regular sterane (5 α (H), 14 β (H), 17 β (H), 20(S)-cholestane)
o	C ₂₈ regular sterane (24-methyl-5 α (H), 14 β (H), 17 β (H), 20(S)-cholestane)
s	C ₂₉ regular sterane (24-ethyl-5 α (H), 14 β (H), 17 β (H), 20(S)-cholestane)

Fig. 3.14. GC-MS Chromatogram showing peaks of steranes on $m/z = 217$ from T5-2 sample.

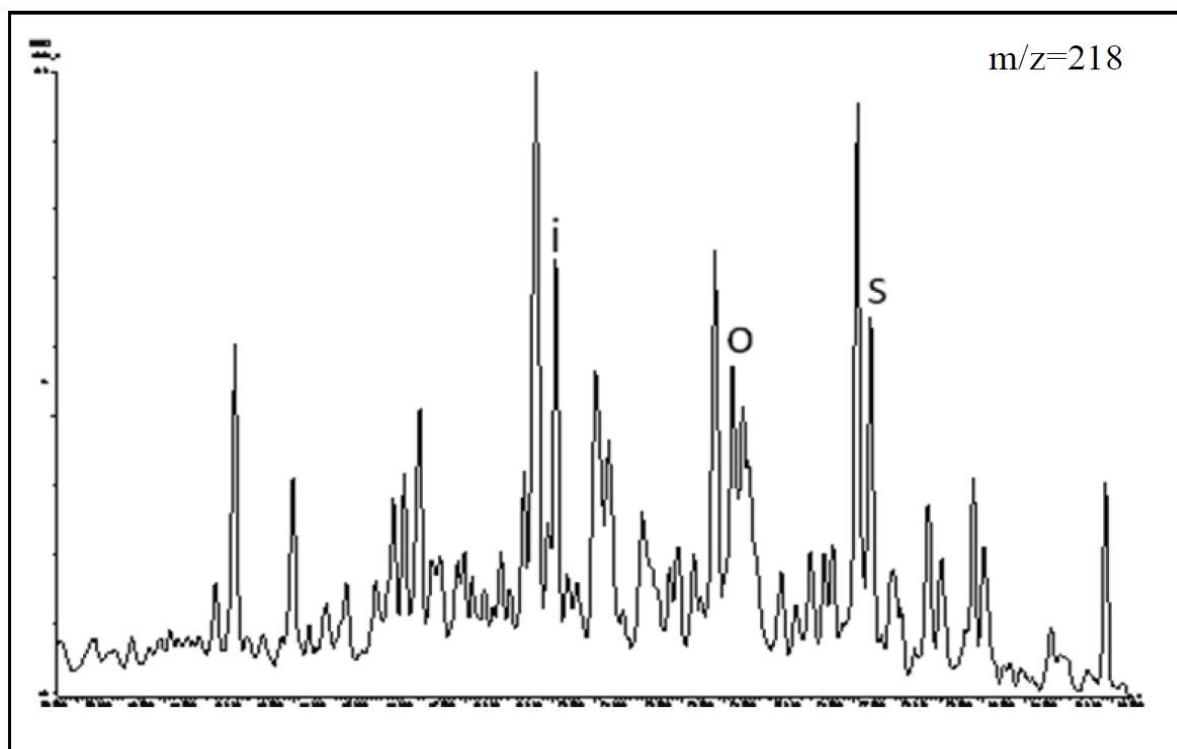


Fig. 3.15. GC-MS Chromatogram showing peaks on $m/z = 231$.

Monoaromatic Steroids

Aromatic hydrocarbons that are identifiable on $m/z = 253$ (Fig. 3.16 and table 3.7) are termed as monoaromatic steroids. They are presumably the precursors of triaromatic steroids and are useful for maturity assessment.

Table 3.7. Monoaromatic steroids recognizable on $m/z = 253$.

Peak	Compound name
H1	C ₂₉ monoaromatic steroid (MA)

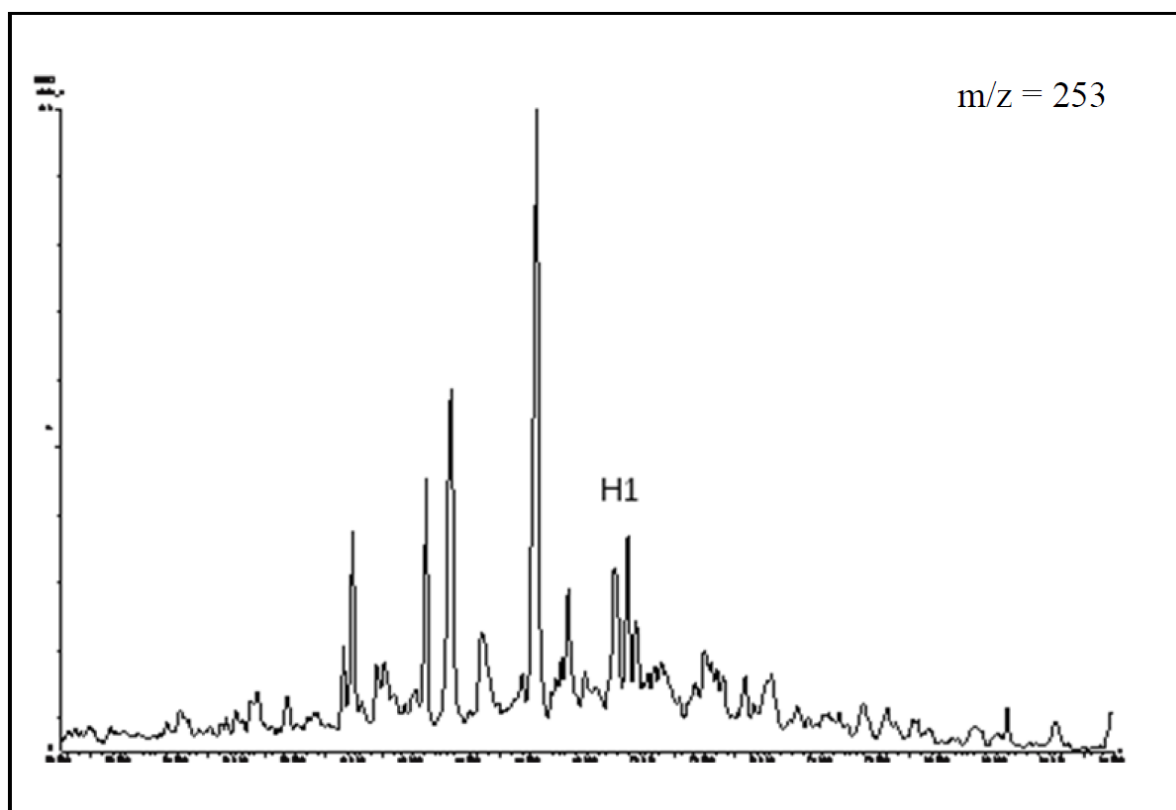


Fig. 3.16. GC-MS Chromatogram showing peaks on $m/z = 253$.

Phenanthrene and methyl-phenanthrene

The aromatic hydrocarbons (C_{14} and C_{15}) identifiable on $m/z = 178$ and 192 (Fig. 3.17 and table 3.8) are termed as phenanthrene and methyl-phenanthrene. They are important medium range maturity parameters.

Table 3.8. Phenanthrene and methyl-phenanthrene on $m/z = 178$ and 192 .

Peak	Compound name
P	Phenanthrene
3-MP	3-methylphenanthrene
2-MP	2-methylphenanthrene
9-MP	9-methylphenanthrene
1-MP	1-methylphenanthrene

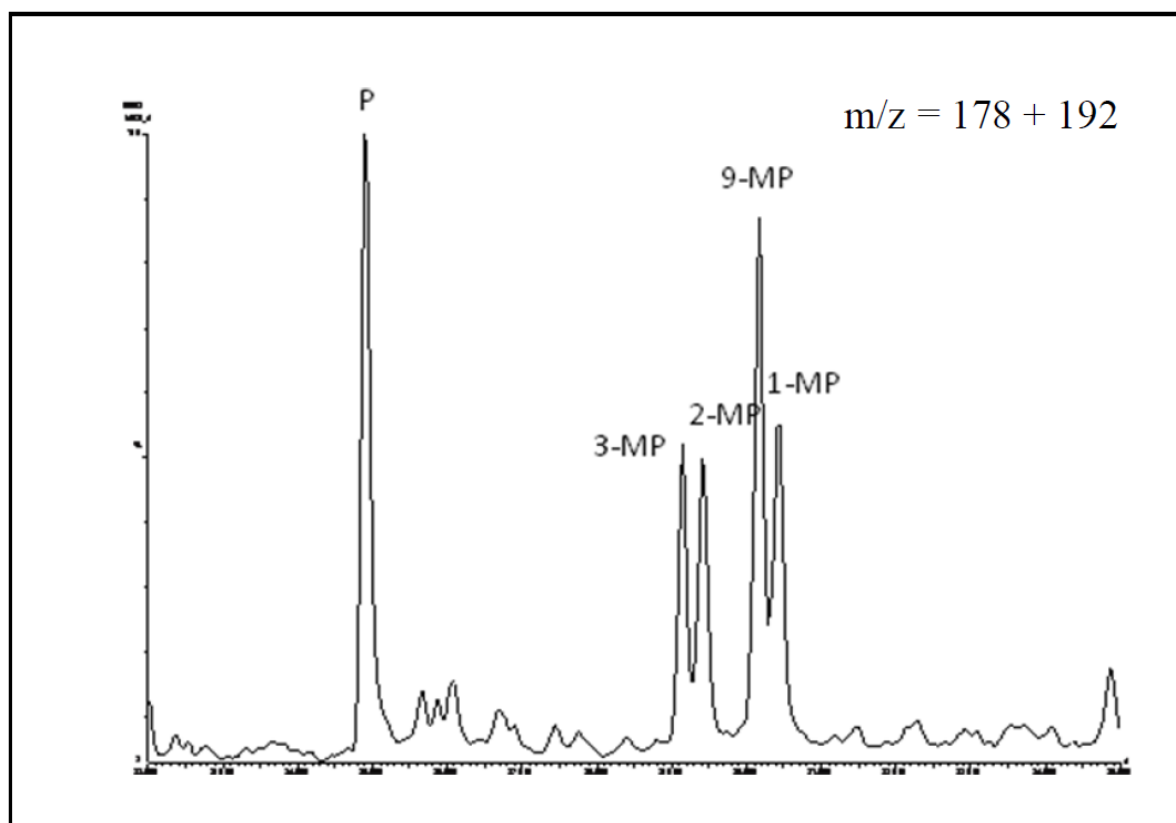


Fig. 3.17. GC-MS chromatogram showing peaks of phenanthrene and methyl-phenanthrene on $m/z = 178$ and 192 .

Methyl-dibenzothiophene

They are (C_{13}) aromatic hydrocarbons with sulphur that are appropriate to the medium range hydrocarbons and are identifiable on $m/z = 198$ (Fig. 3.18 and table 3.9). They are used for estimating maturity, i.e. the relative difference in the peak heights between 4-MDBT and 1-MDBT; the greater the difference the higher the maturity (Peters et al., 2005).

Table 3.9. Methyl-dibenzothiophene aromatic hydrocarbons on $m/z = 198$ (Weiss et al., 2000).

Peak	Compound name
1-MBDT	1-methyldibenzothiophene
4-MBDT	4-methyldibenzothiophene
2+3-MBDT	2+3-methyldibenzothiophene

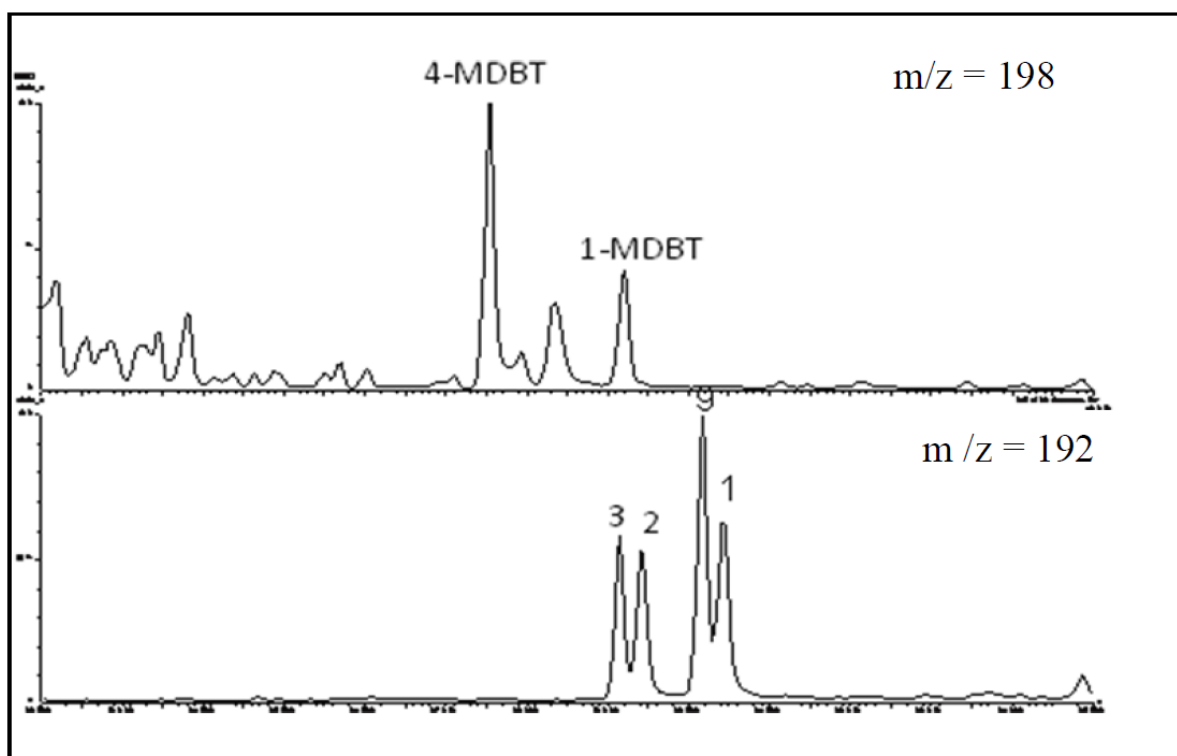


Fig. 3.18. GC-MS chromatograms on $m/z = 198$ and $m/z = 192$.

The peaks described above are representative of certain molecules that can be identified on GC-MS chromatogram. Various parameters can be established by the interpretation of peaks that are summarized in table (3.10) below and values of these parameters were calculated based on peak heights. The calculated parameters are finally used to estimate the depositional facies and maturity of the samples from the study area.

Table 3.10. Different calculated parameters from various peaks of GC-MS chromatograms.

Number	Identification
1	Ts/(Ts+Tm), (<i>Seifert and Moldowan, 1978</i>)
2	Diahopane/(diahopane+normoretane), (<i>Cornford et al., 1986</i>).
3	22S/(22S+22R) of C3117 α (H), 21 β (H)-hopanes (<i>Mackenzie et al., 1980</i>).
4	C30-hopane/(C30-hopane C30-moretane) (<i>Mackenzie et al., 1985</i>).
5	29Ts/(29Ts+norhopane) (<i>Moldowan et al., 1991</i>).
6	Bisnorhopane/(bisnorhopane+norhopane) (<i>Wilhelms and Larter., 1994</i>).
7	C23-C29 tricyclic terpanes/C30 $\alpha\beta$ -hopane (<i>modified from Mello et al., 1988</i>).

8	C24 tetra cyclic terpanes/C30 $\alpha\beta$ -hopane (<i>Mello et al., 1988</i>).
9	Hopane/sterane from the C30 $\alpha\beta$ -hopane and regular C29 sterane (<i>Mackenzie et al., 1984</i>).
10	$\beta\beta/(\beta\beta+\alpha\alpha)$ of C29 (20R+20S) sterane isomer (<i>Mackenzie et al., 1980</i>).
11	20S/(20S+20R) of C29 5 α (H), 14 α (H), 17 α (H) steranes (<i>Mackenzie et al., 1980</i>).
12	Diasterane/(diasterane + regular sterane) (<i>Mackenzie et al., 1985</i>).
13	% C27 of C27+C28+C29 $\beta\beta$ -steranes (<i>Mackenzie et al., 1985</i>).
14	% C28 of C27+C28+C29 $\beta\beta$ -steranes (<i>Mackenzie et al., 1985</i>).
15	% C29 of C27+C28+C29 $\beta\beta$ -steranes (<i>Mackenzie et al., 1985</i>).
16	C20/ (C20+C28) triaromatic steroids (TA) (<i>Mackenzie et al., 1985</i>).
17	C28 TA/(C28TA+C29MA) (<i>Peters and Moldowan., 1993</i>).
18	Methylphenanthrene ratio, MPR (<i>Radke et al., 1982b</i>).
19	Methylphenanthrene index 1, MPI 1 (<i>Radke et al., 1982a</i>).
20	Methylphenanthrene distribution factor (F1 or MPDF) (<i>Kvalheim et al., 1987</i>).
21	Methyldibenzothiophene ratio, MDR (<i>Radke., 1988</i>).
22	Calculated vitrinite reflectivity, $R_m(1)=1.1*\log_{10} MPR+0.95$ (<i>Radke., 1988</i>).
23	Calculated vitrinite reflectivity, $\%R_c=0.6*MPI\ 1+0.4$ (<i>Radke and Welte., 1983</i>).
24	Calculated vitrinite reflectivity, $\%R_o=2.242*MPDF-0.166$ (<i>Kvalheim et al., 1987</i>).
25	Calculated vitrinite reflectivity, $R_m(2)= 0.073*MDR+0.51$ (<i>Radke., 1988</i>).
26	3-methylphenanthrene/4-methyldibenzothiophene (<i>Radke et al., 2001</i>).
27	MDBTs/MPs (<i>Radke et al., 2001</i>).

Description of parameters

The different parameters that can be calculated from m/z ratio are presented in this section (table 3.10).

Parameters from $m/z = 191$

The following parameters can be calculated by the identification of terpanes and triterpanes on the chromatogram with $m/z = 191$:

Parameter 1: $(Ts/(Ts+Tm))$, (peaks A and B)

This parameter is maturity indicator in which the amount of Ts ($C_{27}18\alpha(H)$ -trisorneohopane) increases with increasing maturity relative to Tm ($C_{27}17\alpha(H)$ -trisnorhopane). The maximum value for this ratio is 1.0 and is best appropriate for immature, mature and over-mature oils (Peters and Moldowan, 1993). The ratio decreases during maturation at quite later stages ($>0.9\%$ Ro) (Waples and Machihara, 1991).

Parameter 2: $(Diahopane/(diahopane + normoretane))$, (peaks X and D)

Peters and Moldowan (1993) have suggested a relation between maturity and this parameter where high values indicate high maturity.

Parameter 3: $22S/(22S + 22R)$ of $C_{31} 17\alpha (H)$, $21\beta (H)$ -hopanes (peaks G and H)

The S and R isomers of $C_{31} 17\alpha (H)$, $21\beta (H)$ -hopanes have a different behavior with maturation. The stability of 22S is quite high comparative to 22R which increases the ratio during maturation. The maximum value for this parameter is 0.6 (Peters and Moldowan, 1993) and it can be used for early mature to immature petroleum in the oil window.

Parameter 4: C_{30} -hopane/ $(C_{30}$ -hopane + C_{30} -moretane), (peaks E and F)

The ratio increases with increasing maturity due to the high thermal stability of C_{30} -hopane. The application of this ratio is limited to immature samples and extracts because C_{30} -moretane is lost at relatively low maturity.

Parameter 5: $29Ts/(29Ts + norhopane)$, (peaks 29Ts and C)

Moldowan et al., (1991) introduced this parameter for assessing maturity of samples. The ratio increases with increasing thermal maturity due to higher stability of 29Ts.

Parameter 6: $Bisnorhopane/(bisnorhopane + norhopane)$, (peaks Z and C)

Peters and Moldowan (1993) suggested bisnorhopane as indicative of anoxic environments. An increase in maturity results in the reduced amount of bisnorhopane in the oil window while the peak of norhopane rises on the contrary.

Parameter 7: C_{23} - C_{29} tricyclic terpanes/ C_{30} $\alpha\beta$ -hopane, (peaks P,Q,R,T,U,V and E)

Maturity increases as the amount of C_{23} - C_{29} tricyclic terpanes increase. The parameter is highly influenced by evaporative and phase fractionation and considered valid in the whole oil window (Karlsen et al., 1995).

Parameter 8: C_{24} tetracyclic terpanes/ C_{30} $\alpha\beta$ -hopane, (peaks S and E)

With an increase in thermal maturity, the amount of C_{24} tetracyclic terpanes increases relative to C_{30} $\alpha\beta$ -hopane (Peters and Moldowan, 1993).

Parameter 9: hopane/sterane, (peaks E, q, r, s and t)

This is a facies parameter obtained from $m/z = 191$ and 217 chromatograms. The origin of hopanes is mainly related to bacteria while steranes are originated from higher plants and algae. Higher ratios indicate bacterially reworked organic matter and bacteria rich facies (Peters and Moldowan, 1993). Moreover, hopanes are thermally less stable than steranes.

Parameters from $m/z = 217$

By identifying six isomers of diacholestanes and ethyl-cholestanes, it is possible to calculate the following parameters from $m/z = 217$ chromatogram.

Parameter 10: $\beta\beta/(\beta\beta+\alpha\alpha)$ of the C_{29} (20R + 20S) sterane isomers, (peaks q, r, s and t)

The $\beta\beta$ -isomer tends to increase with increasing maturity as compare to $\alpha\alpha$ -isomer. The maximum equilibrium ratio for this parameter is 0.7 (Peters and Moldowan, 1993) and it is highly affected by the mineralogy of rocks.

Parameter 11: $20S/(20S + 20R)$ of the C_{29} 5α (H), 14α (H), 17α (H) sterane isomers, (peaks q, r, s and t)

During maturation the 20R isomer is converted into 20S isomer and in the middle of the oil window, equilibrium is reached at about 0.52– 0.55 (Seifert and Moldowan, 1986). Facies, biodegradation and weathering can also affect this parameter. The maximum equilibrium ratio for this parameter is 0.55 (Peters and Moldowan, 1993).

Parameter 12: Diasteranes/(diasteranes+regular steranes), (peaks a, b, q, r, s and t).

The amount of diasteranes increase relative to the regular steranes with increasing thermal maturity. The parameter is applicable within the whole oil window and the maximum ratio is

1.0. Oils from clastic source rocks may have higher ratios than oils from carbonate source rocks (Peters and Moldowan, 1993). Presence of diasteranes gives indication of siliciclastic source rock.

Parameters from $m/z=218$

Parameters 13, 14 and 15: correspond to peaks i, o and s respectively and represent the relative percentages of the C_{27} , C_{28} and C_{29} $\beta\beta$ -steranes. The calculated percentages of these three peaks are often used as organic facies indicator when plotted in a ternary diagram (Huang and Meinschein, 1979; Moldowan et al., 1985).

3.4.4. Parameters from $m/z = 231$ & 253

It is possible to calculate the following parameters from the $m/z = 231$ and $m/z = 253$ chromatograms:

Parameter 16: $C_{20}/(C_{20}+C_{28})$ triaromatic steroids (TA), (peaks a1 and g1).

The amount of C_{20} increases relative to C_{28} during maturation. The parameter is valid in the whole oil window but is very prone to phase fractionation (Karlsen et al., 1995). Maximum ratio is 1.0 (Peters and Moldowan, 1993).

Parameter 17: $C_{28}TA/(C_{28}TA + C_{29}MA)$, (peaks g1 and H1).

The monoaromatics (MA) are rearranged to triaromatics (TA) during thermal maturation. The ratio between these two molecules can be used to estimate phase fractionation and maturity. This parameter is effective to peak oil generation. Maximum ratio is 1.0 (Peters and Moldowan, 1993).

3.4.5 Parameters from $m/z=198$ and 192

Tricyclic aromatic hydrocarbons that can be identified from $m/z = 178$, 192 and $m/z = 198$, 192 chromatograms are employed in the parameters given below. The calculation can be made from the amount of four isomers of methylphenanthrene and the phenanthrene. The location of methyl group ($-CH_3$) is assigned by a number. 3-MP and 2-MP are the most thermally stable isomers. During maturation, 1-MP and 9-MP isomers will be more rapidly depleted.

Parameter 18: Methyl phenanthrene ratio (MPR), (peaks 1 and 2)

It is a maturity indicator and can be estimated as:

$$MPR = 2-MP/1-MP$$

Parameter 19: Methyl phenanthrene index 1 (MPI 1), (peaks P, 1, 2, 3 and 9)

It is also a maturity parameter that can be calculate as:

$$\text{MPI } 1 = 1, 5(3\text{-MP} + 2\text{-MP}) / (P + 9\text{-MP} + 1\text{-MP})$$

Parameter 20: Methyl phenanthrene distribution factor (F1 or MPDF), (peaks 1, 2, 3 and 9).

Also a maturity parameter and estimated as:

$$\text{MPDF} = (3\text{-MP} + 2\text{-MP}) / (3\text{-MP} + 2\text{-MP} + 1\text{-MP} + 9\text{-MP})$$

Parameter 21: Methyl dibenzothiophene ratio, MDR, (peaks 4 and 1)

This is an important facies and maturity indication parameter where MDR represents the peaks 4-MDBT and 1-MDBT on $m/z=198$. It can be estimated using the relation below:

$$\text{MDR} = 4\text{-MDBT} / 1\text{-MDBT} \text{ (Radke, 1988).}$$

The relationship between the two isomers of methyl dibenzothiophene, 4-MDBT and 1-MDBT defines this parameter. Thermal stability of 4-MDBT isomer is higher. As thiophene structure contains a sulphur atom in it, the amount of MDBT in oils may indicate the sulphur contents in the oil/source rock. Based on the measurements of phenanthrene, methyl-phenanthrenes and methyl-dibenzothiophene, vitrinite reflectance can be calculated.

Parameter 22, 23, 24 and 25: (measure of Vitrinite reflectivity)

These parameters are used to calculate the vitrinite reflectivity from the following parameters:

Parameter 22 (calculated from parameter 18): $R_{m(1)} = 1.1 * \log_{10} \text{MPR} + 0.95$

Parameter 23 (calculated from parameter 19) $\%R_c = 0.6 * \text{MPI } 1 + 0.4$

Parameter 24 (calculated from parameter 20) $\%R_o = 2.242 * \text{MPDF} - 0.166$

Parameter 25 (calculated from parameter 21) $R_{m(2)} = 0.073 * \text{MDR} + 0.51$

Parameter 26: 3-methyl phenanthrene/4-methyl dibenzothiophene, (peaks 3 and 4).

This parameter, alongwith other parameters as Pr/Ph, is applied to indicate different types of organic facies, e.g. shales and carbonates (Hughes et al., 1995; Radke, 1988). The relative amount of sulphur in the source rock can also be identified (Radke, 1988).

Parameter 27: MDBTs/MPs

It is a facies parameter that can be calculated from peaks 1, 2, 3, 4 and 9 on $m/z = 178$ and 192 and peaks 1, 2+3 and 4 on $m/z = 192$ chromatograms. Values above and below 1 indicate carbonate and shale facies respectively.

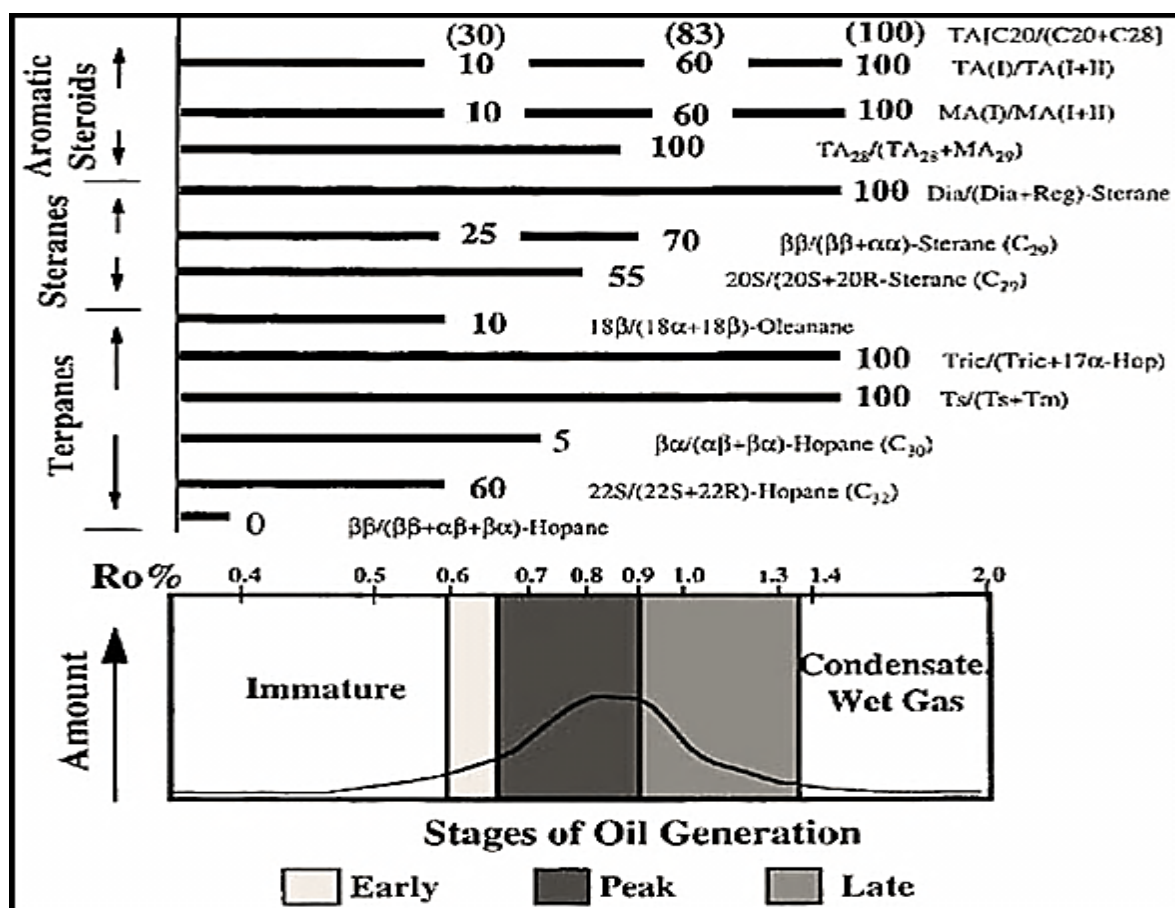


Fig. 3.19. Different maturity parameters for biomarkers and corresponding ranges within the oil window (from Peters and Moldowan, 1993).

4. Results

The results obtained from the geochemical analysis of the sample set are presented in this chapter with discussions in the next chapter. The discussion includes the presentation of the findings with the help of various cross plots, bar charts and diagrams with references from the literature. The results are presented in the following manner:

4.1 Analysis of hydrocarbon gases from enriched inclusions

4.2 GC-FID of core extracts

4.3 Carbon Preference Index (CPI)

4.4 GC-MS of core extracts

4.5 Iatroscan TLC-FID of core extracts

Analysis of hydrocarbon gases from enriched Inclusions

The core samples from the selected dry wells of the northern North Sea are inspected for inclusion gases study using gas chromatography. The main focus of this study is in particular the identification of methane to pentane (C_1 to C_5) hydrocarbon compounds. The disintegrated sandstone samples are cleaned and washed prior to analysis in order to avoid any contamination from drilling mud. The wells are presented in tables 4.1 to 4.10 along with the results in percentage composition of C_1 to C_5 hydrocarbon compounds. The chromatograms are presented in appendix A to assist in understanding the results.

4.1.1 Well 25/2-4

This is a reference well for the Drake formation lying on the eastern flank of the Viking Graben. According to the geochemical information on the NPD fact pages, water based mud was used for drilling from a depth of 136m to 4360m. The percentage of C_{2+} generally increases with increasing depth. The lowest value observed for C_{2+} is 32.3% at a depth of 3693.0m and the highest percentage is 46.3% at 3684.0m depth, hence the average

percentage is 37.9%. The ratio of iso-butane to normal-butane lies in a range of 0.4 to 0.5 and 0.67 to 0.82 for iso-pentane to normal-pentane ratio. Hence both ratios reflect values of less than unity.

Table 4.1. The composition of hydrocarbon species from inclusions for dry well 25/2-4. Ratios of butane and pentane isomers are also presented.

No.	Well	Depth (m)	Weight (g)	C ₁ %	i-C ₄ /n-C ₄	i-C ₅ /n-C ₅	C ₂ +	C ₁ /C ₂ +C ₃
1	25/2-4	3675.0	2.62	65.38	0.50	0.67	34.62	2.81
2	25/2-4	3676.0	2.51	63.28	0.44	0.80	36.72	2.68
3	25/2-4	3683.0	2.69	56.00	0.40	0.73	44.00	2.12
4	25/2-4	3684.0	2.64	53.75	0.43	0.75	43.25	2.15
5	25/2-4	3693.0	3.10	67.71	0.44	0.73	32.29	3.04
6	25/2-4	3694.0	3.16	66.52	0.45	0.82	33.48	2.90

4.1.2 Well 25/2-12

This is an appraisal well drilled on the crest of NNE-SSW trending westward tilting Jurassic fault block, the northern extension of which was drilled in 1975 by well 25/2-4. It has been drilled using water based mud and encountered severe drilling problems (NPD factpages, 2014). The value of C₂+ at a depth of 3698.0m is recorded to be 41.7% and 48.3% at 3710m, the average being 45% (table 4.2). The ratios of iso-butane to n-butane and iso-pentane to n-pentane are less than unity and i-C₅/n-C₅ values are very close to unity.

Table 4.2. The composition of hydrocarbon species from inclusions for dry well 25/2-12. The ratios of butane and pentane isomers are also presented.

No.	Well	Depth (m)	Weight (g)	C ₁ %	i-C ₄ /n-C ₄	i-C ₅ /n-C ₅	C ₂ +	C ₁ /C ₂ +C ₃
1	25/2-12	3698.0	4.63	58.23	0.42	0.92	41.68	2.20
2	25/2-12	3710.0	5.00	51.71	0.42	0.89	48.29	2.14

4.1.3 Well 25/3-1

This is a wildcat well drilled at Utsira High to target a narrow NNW-SSE trending horst structure. The key purpose of the well was to test the hydrocarbon potential of the sandstones

in Vestland Group and Statfjord Formation. Water based mud was used from a depth of 909m to 3871.0m during drilling (NPD factpages, 2014). There is a significant variation in the percentage of C_2+ hydrocarbons with depth. The lowest value recorded is 16.6% at a depth of 3861.0m and 29.8% at 3858.8m (table 4.3). The average is therefore 22.8%. The ratios of iso-butane to normal-butane and iso-pentane to normal-pentane are in general increasing with depth where the values for $i-C_4/n-C_4$ range from 0.6 to 1.0% and for $i-C_5/n-C_5$ lies between 0.8 to 1.5%.

Table 4.3. The composition of hydrocarbon species from inclusions for dry well 25/3-1. The ratios of butane and pentane isomers are also presented.

No.	Well	Depth (m)	Weight (g)	$C_1\%$	$i-C_4/n-C_4$	$i-C_5/n-C_5$	C_2+	C_1/C_2+C_3
1	25/3-1	3858.3	5.40	76.20	0.63	0.92	23.80	7.92
2	25/3-1	3858.8	5.96	70.23	0.71	1.11	29.77	6.16
3	25/3-1	3861.0	4.81	83.42	0.70	0.75	16.58	10.06
4	25/3-1	3861.5	5.52	78.98	1.00	1.46	21.02	20.93

4.1.4 Well 30/10-6

The exploration well, 30/10-6, lies approximately 10 km north of the Odin Field in the central part of the block 30/10. The purpose of the well has been to explore the hydrocarbon potential in the Middle Jurassic Brent Group. The well is drilled to a depth of 5250m using water based mud. The percentage of C_2+ hydrocarbons in this well seems to be very low compared to the samples from all other wells with value as low as 6.43% at a depth of 4714.7m (table 4.4). There is a general decreasing trend of C_2+ with depth. The ratios of $i-C_4/n-C_4$ and $i-C_5/n-C_5$ also reflect very high values even greater than unity, however, pentane peaks are not detected by GC for most of the samples.

Table 4.4. The composition of hydrocarbon species from inclusions for dry well 30/10-6. The ratios of butane and pentane isomers are also presented.

No.	Well	Depth (m)	Weight (g)	C ₁ %	i-C ₄ /n-C ₄	i-C ₅ /n-C ₅	C ₂ +	C ₁ /C ₂ +C ₃
1	30/10-6	4691.5	4.46	85.71	0.80	2.00	14.29	7.71
2	30/10-6	4714.2	4.41	91.38	1.25	ND	8.62	15.14
3	30/10-6	4714.7	4.65	93.57	1.00	ND	6.43	17.78

4.1.5 Well 30/11-4

Water based drilling mud was used for this exploratory wildcat well to estimate the hydrocarbon potential of the Lower Jurassic Statfjord Formation (NPD factpages, 2014). The values are essentially, on average, close to 30% for C₂+ hydrocarbons. The ratio i-C₄/n-C₄ represents slightly higher values than 0.5. The i-C₅/n-C₅ ratio show values higher than unity, yet in some samples the pentanes are not detected.

Table 4.5. The composition of hydrocarbon species from inclusions for dry well 30/11-4. The ratios of butane and pentane isomers are also presented.

No.	Well	Depth (m)	Weight (g)	C ₁ %	i-C ₄ /n-C ₄	i-C ₅ /n-C ₅	C ₂ +	C ₁ /C ₂ +C ₃
1	30/11-4	3514.5	4.73	65.18	0.54	1.60	34.82	2.75
2	30/11-4	3515.0	4.90	67.12	0.55	1.40	32.88	2.98
3	30/11-4	3515.5	5.00	69.55	0.60	ND	30.45	2.95
4	30/11-4	3516.0	5.00	67.03	0.61	0.75	32.97	2.67
5	30/11-4	3517.2	5.00	67.07	0.50	1.60	32.93	2.98
6	30/11-4	3526.8	4.76	76.46	0.62	ND	23.54	4.51

4.1.6 Well 30/11-6

The wildcat well 30/11-6 has been drilled using seawater and pills of bentonite spud mud down to 1415m and with Glydril KCL/polymer mud from 1415m to the total depth (NPD factpages, 2014). There is a considerable variation in the percentages of C₂+ hydrocarbons (table 4.6) with values even as high as 99.4% and 87.3% at depths of 3205.0m and 3210.3m,

respectively (table 4.6). This huge uncertainty in the values may reflect contaminations in the drilling mud or even shale fragments that could not be effectively removed. The ratio of butane isomers (i-C₄/n-C₄) for most of the samples range from 0.36 to 0.73 except for one sample at depth 3249.3m, where it is very close to unity. The ratio of pentane isomers (i-C₅/n-C₅) at relatively shallower depths (3205.0m-3240.5m) is higher than unity, in contrast, the average value at greater depths is 0.67.

Table 4.6. The composition of hydrocarbon species from inclusions for dry well 30/11-6. The ratios of butane and pentane isomers are also presented.

No.	Well	Depth (m)	Weight (g)	C ₁ %	i-C ₄ /n-C ₄	i-C ₅ /n-C ₅	C ₂ +	C ₁ /C ₂ +C ₃
1	30/11-6	3200.5	4.08	81.52	0.62	ND	18.48	6.38
2	30/11-6	3203.2	5.00	84.75	0.60	ND	15.25	7.89
3	30/11-6	3205.0	5.00	0.62	0.73	1.50	99.39	0.007
4	30/11-6	3210.3	5.00	12.74	0.36	1.58	87.26	0.23
5	30/11-6	3210.8	5.00	52.26	0.43	1.41	47.74	2.26
6	30/11-6	3219.5	3.70	70.62	0.62	1.43	29.38	4.58
7	30/11-6	3240.5	5.00	70.80	0.55	1.08	29.20	5.60
8	30/11-6	3249.3	5.00	77.52	0.93	ND	22.48	5.00
9	30/11-6	3249.8	5.00	76.66	0.71	0.63	23.34	5.38
10	30/11-6	3295.2	5.00	84.17	0.73	0.71	15.83	11.0
11	30/11-6	3295.7	5.00	85.33	0.63	0.67	14.67	10.0

4.1.7 Well 30/11-7

The well was drilled in the Jorsalfare Formation using Versatec oil based mud until the total depth (NPD factpages, 2014). The average value of C₂+ is approximately 32% for the samples. The ratio of butane isomers is very close to the equilibrium value, i.e. 0.5 while it is nearly unity for pentane isomers.

Table 4.7. The composition of hydrocarbon species from inclusions for dry well 30/11-7. The ratios of butane and pentane isomers are also presented.

No.	Well	Depth (m)	Weight (g)	C ₁ %	i-C ₄ /n-C ₄	i-C ₅ /n-C ₅	C ₂ +	C ₁ /C ₂ +C ₃
1	30/11-7	3987.5	5.00	67.56	0.45	1.00	32.44	3.24
2	30/11-7	3988.0	5.00	67.25	0.57	0.90	32.75	3.15
3	30/11-7	3988.5	5.00	69.07	0.53	0.90	30.93	3.44
4	30/11-7	3989.2	5.00	70.20	0.56	0.80	29.80	3.57
5	30/11-7	3989.8	5.00	67.56	0.50	0.85	32.44	3.42
6	30/11-7	3990.3	5.00	68.88	0.53	0.90	31.12	3.42

4.1.8 Well 30/11-8A

This is a sidetrack well for 30/11-8S in the Fensal Sub-basin between the Oseberg and Frigg fields in the North Sea drilled with XP-07 OBM from kick-off to the total depth (NPD factpages, 2014). The percentage composition of C₂+ compounds for the samples at relatively shallow depth is 36.4% and approximately 23% for the samples at greater depth (table 4.8). The average ratio of butane isomers is 0.61, which is slightly higher yet closer to the equilibrium value of 0.45-0.55. The value of unity is likely to be for the samples at shallower depth in terms of pentane isomers which is not detected in the samples at greater depth.

Table 4.8. The composition of hydrocarbon species from inclusions for dry well 30/11-8A. The ratios of butane and pentane isomers are also presented.

No.	Well	Depth (m)	Weight (g)	C ₁ %	i-C ₄ /n-C ₄	i-C ₅ /n-C ₅	C ₂ +	C ₁ /C ₂ +C ₃
1	30/11-8A	3968.0	5.00	63.58	0.58	1.00	36.42	2.72
2	30/11-8A	3968.5	5.00	63.58	0.60	0.92	36.42	2.75
3	30/11-8A	3986.5	5.00	76.40	0.58	ND	23.60	4.39
4	30/11-8A	3987.0	5.00	77.24	0.69	ND	22.76	4.51

4.1.9 Well 30/11-8S

This well is located in block 30/11 at a distance of about 26 km south of the Oseberg Field and generally known as the Krafla prospect. This well was sidetracked from well 30/11-8A and drilled using XP-07 OBM from kick-off to the total depth (NPD factpages, 2014). A general increasing trend in C₂₊ percentage composition is observed with depth. The lowest percentage, i.e. 11.11, is seen in the sample at depth 3637.4 m and unusual high percentage value is observed in the sample at the greatest depth, 3666.4 m (table 4.9).

The pentane isomers have essentially higher ratio than butane isomers. The lowest ratio for butane isomers is calculated to be 0.35 at 3666.4 m which is certainly very low.

Table 4.9. The composition of hydrocarbon species from inclusions for dry well 30/11-8S. The ratios of butane and pentane isomers are also presented.

No.	Well	Depth (m)	Weight (g)	C ₁ %	i-C ₄ /n-C ₄	i-C ₅ /n-C ₅	C ₂ +	C ₁ /C ₂ +C ₃
1	30/11-8S	3506.1	3.56	83.44	0.83	ND	16.56	8.86
2	30/11-8S	3621.5	5.00	80.11	0.50	1.00	19.89	7.35
3	30/11-8S	3622.4	5.00	73.90	0.45	0.77	26.10	5.56
4	30/11-8S	3622.9	5.00	73.04	0.38	0.69	26.96	5.42
5	30/11-8S	3637.4	2.96	88.89	ND	ND	11.11	8.00
6	30/11-8S	3661.5	5.00	87.39	0.78	ND	12.61	11.19
7	30/11-8S	3666.4	4.80	2.97	0.35	1.13	97.03	0.05

4.1.10 Well 30/12-1

Exploration well 30/12-1 was drilled with seawater and bentonite down to a depth of 1130 m and with ANCO 2000 from 1130 m to the total depth. The average percentage composition of C₂₊ compounds is about 25% with a generally increasing trend with depth. The value of i-C₄/n-C₄ lies around unity and is even higher than unity for pentane isomers.

Table 4.10. The composition of hydrocarbon species from inclusions for dry well 30/12-1. The ratios of butane and pentane isomers are also presented.

No.	Well	Depth (m)	Weight (g)	C ₁ %	i-C ₄ /n-C ₄	i-C ₅ /n-C ₅	C ₂ +	C ₁ /C ₂ +C ₃
1	30/12-1	2905.0	4.10	78.68	0.83	ND	21.32	5.46
2	30/12-1	2905.5	4.39	79.66	0.86	ND	20.34	6.18
3	30/12-1	2929.5	3.89	72.40	1.06	1.40	27.60	5.44
4	30/12-1	2930.0	4.35	71.96	0.82	1.10	28.04	4.75
5	30/12-1	2930.5	4.74	72.31	0.94	1.50	27.69	5.32

GC-FID

The extracts from the core samples of the dry wells have been prepared for geochemical analysis using GC-FID as described in chapter 3 (section 3.2.5). This helps in determining n-alkane and isoprenoid distribution patterns and provides additional information about the source rock facies and maturity of the samples (Peters and Moldowan, 1993). This is very important for evaluating the source rock facies and to identify the maturity of the migrated oil in these dry wells for better understanding of the “Petroleum System”. The GC-FID traces may essentially indicate the degree of biodegradation for which the unresolved complex mixture (UCM) will be significant and also n-alkane concentrations have been reduced. The North Sea Oil (NSO-1) has been used as a reference sample to ensure accuracy and measure the response factor of n-alkanes. The peak heights in NSO-1 decrease asymptotically with increasing carbon number, thus creating a concave curve on the chromatogram. The parameters calculated from GC-FID chromatograms are shown in table 4.11 and chromatograms are presented in appendix B.

The samples are shortlisted on the basis of GC-FID results. Hence the wells with samples which have shown nothing else than drilling mud are therefore not presented and discussed further. A type sample from all such wells is presented in appendix B.

4.2.1 Well 25/2-4

The samples representing well 25/2-4 from a depth of 3675.0m to 3694.0m show pristane to phytane ratio (Pr/Ph) in a generally increasing trend, i.e. from 1.1 to 2 (table 4.11). The ratio

of pristane to n-C₁₇ (Pr/n-C₁₇) is in a range of 0.5 to 0.6 while it is constant throughout the depth for phytane to n-C₁₈ (Ph/n-C₁₈) with a value of 0.3.

4.2.2 Well 25/2-12

The values for Pr/Ph from a depth of 3698.0m to 3711.0m for the well 25/2-12 lies within a range of 1.7 to 2.0 (table 4.11). The value for Ph/n-C₁₈ is 0.3 which is constant throughout the well at all depths. The ratio of pristane to n-C₁₇ is also constant for all the extracts with a value of 0.7, except for an extract at depth 3706.0m where it is 0.8.

4.2.3 Well 25/5-5

The extracts from the well 25/5-5, ranging in depths from 2164.5m to 2173.5m, have average values of 0.7, 0.55 and 0.8 for Pr/Ph, Pr/n-C₁₇ and Ph/n-C₁₈, respectively (table 4.11).

4.2.4 Well 26/4-1

This well shows a huge variation in Pr/Ph values ranging from 0.9 to 2.5 from a depth of 2258.7m to 2290.5m (table 4.11). The values are 0.5 to unity for Pr/n-C₁₇ ratio and 0.3 to unity for Ph/n-C₁₈.

4.2.5 Well 30/10-6

A huge variation in Pr/Ph values can be seen in this well where the lowest value recorded is 0.9 for the sample at 4686.5m, and 4.6 is the highest value detected at 4664.5m, which is an outlier in the sample set (table 4.11). The values of Pr/n-C₁₇ and Ph/n-C₁₈ vary from 0.3 to 1.3 and 0.2 to 0.6, respectively.

4.2.6 Well 30/11-3

The samples selected from the depth 3450.5m to 3468.3m for this well show variation in the ratios for Pr/Ph ranging from 1.4 to 3.4, Pr/n-C₁₇ ranging from 0.6 to 1.3 and Ph/n-C₁₈ ranging from 0.3 to 0.5.

4.2.7 Well 30/11-4

The chromatograms that have been produced by GC-FID from the extracts of this well show values of Pr/Ph that vary from 0.7 to 2.8 for Pr/Ph, 0.3 to 0.9 for Ph/n-C₁₈ and 0.7 on average for Pr/n-C₁₇ (table 4.11).

4.2.8 Well 30/11-8A

The ratio varies from 2.6 to 3.6 for Pr/Ph, 0.6 on average for Pr/n-C₁₇ and 0.2 for Ph/n-C₁₈.

Table 4.11. The results from GC-FID analysis showing the ratios of isoprenoids and n-alkanes for dry well samples.

No.	Well	Depth (m)	Pr/Ph	Pr/n-C ₁₇	Ph/n-C ₁₈
1	25/2-4	3675.0	1.1	0.5	0.3
2	25/2-4	3676.0	1.2	0.6	0.3
3	25/2-4	3683.0	1.2	0.5	0.3
4	25/2-4	3693.0	2.0	0.6	0.3
5	25/2-4	3694.0	1.7	0.6	0.3
6	25/2-12	3698.0	2.0	0.7	0.3
7	25/2-12	3698.5	1.7	0.7	0.3
8	25/2-12	3706.0	1.7	0.8	0.3
9	25/2-12	3710.0	2.0	0.7	0.3
10	25/2-12	3711.0	2.0	0.7	0.3
11	25/5-5	2164.5	0.7	0.5	0.8
12	25/5-5	2171.5	0.6	0.5	0.7
13	25/5-5	2172.0	0.7	0.6	0.8
14	25/5-5	2173.5	0.7	0.6	0.8
15	26/4-1	2258.7	1.1	0.5	0.6
16	26/4-1	2273.5	1.2	0.6	0.3
17	26/4-1	2274.0	0.9	1.0	1.0
18	26/4-1	2274.8	2.0	0.6	0.7

19	26/4-1	2290.5	2.5	0.7	0.5
20	30/10-6	4664.0	1.1	0.5	0.3
21	30/10-6	4664.5	4.6	0.5	0.2
22	30/10-6	4675.0	2.3	0.5	0.4
23	30/10-6	4675.5	2.4	0.6	0.4
24	30/10-6	4686.0	1.7	0.5	0.4
25	30/10-6	4686.5	0.9	0.7	0.6
26	30/10-6	4691.0	1.5	1.0	0.4
27	30/10-6	4691.5	2.3	0.4	0.3
28	30/10-6	4702.0	1.3	0.9	0.4
29	30/10-6	4702.5	1.7	1.3	0.5
30	30/10-6	4714.2	1.2	0.9	0.4
31	30/10-6	4714.7	2.3	0.3	0.2
32	30/10-6	4962.3	1.9	0.5	0.5
33	30/10-6	4962.8	1.7	0.5	0.5
34	30/11-3	3450.5	1.4	1.3	0.5
35	30/11-3	3457.0	2.0	0.9	0.3
36	30/11-3	3457.5	1.7	0.8	0.3
37	30/11-3	3468.3	3.4	0.6	0.4
38	30/11-4	3514.5	1.0	0.7	0.5
39	30/11-4	3515.0	1.0	0.6	0.4
40	30/11-4	3515.5	1.2	0.6	0.3
41	30/11-4	3516.0	0.7	0.8	0.9
42	30/11-4	3517.2	1.2	0.7	0.3
43	30/11-4	3526.8	2.8	0.8	0.3
44	30/11-8A	3968.0	2.6	0.6	0.2

45	30/11-8A	3968.5	3.6	0.6	0.2
46	30/11-8A	3986.5	3.6	0.5	0.2
47	30/11-8A	3987.0	2.8	0.7	0.3
48	NSO-1		1.5	0.8	0.6

Carbon Preference Index

CPI is used to study the odd-carbon numbers predominance from the selected chromatograms of the dry wells that have well developed peaks of normal alkanes. Two values for CPI, referred to as CPI-1 and CPI-2, are used to determine the maturity of the samples bearing in mind that the ratio will asymptotically approach unity at a source rock maturity of c. 0.9 %Rc (Peters et al., 2005). The values lie in a range of 0.6 to 1.1 which, for most of the samples, are very close to unity (table 4.12). Values less than unity may reflect carbonate in the source rock, while values greater than unity reflect siliciclastic source rocks. Besides, these values determine thermally mature samples (Peters et al., 2005).

Table 4.12. CPI values for the selected dry well samples.

No.	Well	Depth (m)	CPI-1	CPI-2
1	25/2-4	3675.0	1.0	1.1
2	25/2-4	3676.0	1.0	1.0
3	25/2-4	3683.0	1.0	1.0
4	25/2-4	3693.0	1.0	1.0
5	25/2-4	3694.0	1.0	1.0
6	25/2-12	3698.0	1.0	1.1
7	25/2-12	3698.5	1.0	1.0
8	25/2-12	3706.0	1.0	1.0
9	25/2-12	3710.0	1.0	1.0
10	25/2-12	3711.0	1.0	1.0
11	25/5-5	2164.5	0.9	1.0

12	25/5-5	2171.5	0.9	0.9
13	25/5-5	2172.0	0.9	1.0
14	25/5-5	2173.5	1.0	1.0
15	26/4-1	2258.7	0.9	0.9
16	26/4-1	2273.5	1.0	1.1
17	26/4-1	2274.0	0.8	0.9
18	26/4-1	2274.8	0.9	0.9
19	26/4-1	2290.5	1.1	0.6
20	30/10-6	4664.5	1.0	1.0
21	30/10-6	4675.0	1.0	0.9
22	30/10-6	4675.5	1.0	1.0
23	30/10-6	4686.0	0.9	1.1
24	30/10-6	4691.5	1.1	---
25	30/10-6	4714.7	1.0	1.0
26	30/10-6	4962.3	0.7	---
27	30/10-6	4962.8	0.8	0.7
28	30/11-3	3457.0	1.1	1.1
29	30/11-3	3457.5	1.0	1.0
30	30/11-4	3514.5	1.1	1.0
31	30/11-4	3515.0	1.1	1.1
32	30/11-4	3515.5	1.0	1.1
33	30/11-4	3516.0	1.8	---
34	30/11-4	3517.2	1.1	1.0
35	30/11-4	3526.8	1.0	1.0
36	30/11-8A	3968.0	1.0	1.1
37	30/11-8A	3968.5	1.0	1.1

38	30/11-8A	3986.5	1.0	1.0
39	30/11-8A	3987.0	1.0	1.0
40	NSO-1		1.0	0.6

GC-MS

GC-MS is used to identify biomarkers, the compounds of higher molecular weight, by the technique discussed in chapter 3 (section 3.2.7), which makes it possible to study the compounds in the complex mixture of petroleum even if present in only very low concentrations. Besides biomarkers, methyl dibenzothiophenes and phenanthrene compounds are also studied using the same technique. Several facies and maturity parameters have been calculated based on the peaks identified on GC-MS chromatograms, and these have previously been described in chapter 3. The calculated values for these parameters are given in table 4.13 and chromatograms are presented in appendix C.

4.43.1 Well 25/2-4

The samples from this well show an increasing trend with depth in terms of $Ts/(Ts+Tm)$, diahopane/(diahopane+normoretane) and $29Ts/(29Ts+norhopane)$ parameters resulting in values from 0.60 to 0.77, 0.64 to 0.90 and 0.32 to 0.45 respectively. Conversely, the ratio decreases with depth for hopane/sterane and the values range from 2.46 to 1.29. The maturity parameter $C_{20}/C_{20}+C_{28}$ has a low ratio at depth 3675.0m and abruptly increases with depth with an average ratio of 0.81. The parameters defining the calculated vitrinite reflectance have average values less than unity (see table 4.13).

4.4.2 Well 25/2-12

Unlike well 25/2-4, the ratios of $Ts/(Ts+Tm)$, diahopane/(diahopane+normoretane) and $29Ts/(29Ts+norhopane)$ in this well decrease with depth while diasterane/(diasterane+regular steranes) ratios remain constant throughout the well (table 4.13). The parameters for vitrinite reflectance still remain less than unity for all the samples. The maturity parameter $C_{20}/C_{20}+C_{28}$ varies from 0.77 to 0.85 and decreases with depth.

4.4.3 Well 25/5-5

The ratio of $Ts/(Ts+Tm)$ lies between 0.40 and 0.69 while diahopane/(diahopane+norhopane) ratio varies from 0.50 to 0.88. The vitrinite reflectivity parameters lie in most of the samples close to unity. A very minor variation in the ratios of hopane to sterane and $29Ts/(29Ts+norhopane)$ is observed and the values range from 1.60 to 2.08 and 0.27 to 0.39 respectively (see table 4.13).

4.4.4 Well 26/4-1

There is in this well considerable variation in methyl phenanthrene index (MPI) values which range from 0.04 to 0.70. All other parameters show only minor variation. The values lie in a range of 0.57–0.73, 0.21–0.28 and 1.41–1.45 for diahopane/(diahopane+normoretane), $29Ts/(29Ts+norhopane)$ and hopane to steranes ratios respectively, decreasing with depth. However, the ratio increases with depth for $Ts/(Ts+Tm)$ and diasteranes/(diasteranes+regular steranes), ranging in values from 0.42 to 0.53 and 0.42 to 0.48 respectively. The parameters for calculated vitrinite reflectance have values less than unity (see table 4.13).

4.4.5 Well 30/10-6

The ratio of $Ts/(Ts+Tm)$ decreases with depth and have values of 0.49–0.71 and the ratio varies from 0.45 to 0.85 for diahopane/(diahopane+normoretane). The minimum values are observed in this well for the $29Ts/(29Ts+norhopane)$ ratio that lies between 0.15 and 0.39. $C_{20}/C_{20}+C_{28}$ ratios vary from 0.38 to 0.66 and the values for calculated vitrinite reflectance, in most of the samples, is higher than unity approaching to 1.75 %Rb (see table 4.13).

4.4.6 Well 30/11-3

Only one sample from this well has GC-MS amendable results with moderate values for the parameters. The ratios of $Ts/(Ts+Tm)$ and diahopane/(diahopane+normoretane) are 0.58 and 0.44, respectively, while $29Ts/(29Ts+norhopane)$ is 0.15, which is the lowest value compared to the samples from other wells. The calculated vitrinite reflectance lies between 0.51 and 1.39%Rc (see table 4.13).

4.4.7 Well 30/11-4

The ratios of $Ts/(Ts+Tm)$ and diahopane/(diahopane+normoretane) increase with depth and the values are 0.58–0.71 and 0.67–0.83 respectively. The ratio of $29Ts/(29Ts+norhopane)$ varies from 0.36 to 0.43 and 1.44 to 2.15 for hopane to steranes. The values of calculated vitrinite reflectance for all samples are close to unity (see table 4.13).

4.4.8 Well 30/11-8A

There is a slight variation in $Ts/(Ts+Tm)$, diahopane/(diahopane+normoretane) and $29Ts/(29Ts+norhopane)$ ratios corresponding to the values 0.61–0.72, 0.70–0.83 and 0.27–0.33 respectively. The hopane to sterane ratio generally increases with depth and varies from 1.24 to 1.53 while the values for maturity parameter, $C_{20}/C_{20}+C_{28}$, lie between 0.78 and 0.88. The values for the calculated vitrinite reflectance are either close to or equal to unity (see table 4.13).

Table 4. 13. Biomarker parameters calculated from GC-MS chromatograms (see table 3.10 for the description of parameters) of the dry wells

No.	Well	Depth (m)	1	2	3	4	5	6	7	8	9	10	11	12	13	14	15	16	17	18	19	20	21	22	23	24	25	26	27
1	25/2-4	3675.0	0,60	0,64	0,55	0,89	0,32	0,31	0,32	0,03	2,46	0,54	0,43	0,53	33	35	32	0,43	0,80	0,85	1,15	0,43	2,63	0,87	1,09	0,80	0,70	1,88	0,41
2	25/2-4	3676.0	0,77	0,87	0,61	0,93	0,43	0,16	1,20	0,13	1,29	0,60	0,46	0,70	39	26	35	0,80	0,61	0,85	0,24	0,41	5,07	0,87	0,54	0,75	0,88	4,45	0,14
3	25/2-4	3683.0	0,72	0,80	0,53	0,92	0,45	0,16	1,28	0,18	1,39	0,65	0,50	0,66	38	29	33	0,80	0,59	0,98	0,86	0,43	5,85	0,94	0,92	0,81	0,94	3,88	0,16
4	25/2-4	3684.0	0,77	0,90	0,61	0,92	0,42	0,22	1,27	0,17	1,37	0,60	0,53	0,59	39	26	35	0,80	0,60	0,79	0,36	0,38	4,47	0,84	0,62	0,69	0,84	4,29	0,13
5	25/2-4	3694.0	0,75	0,86	0,60	0,92	0,45	0,19	1,06	0,17	1,79	0,61	0,50	0,75	38	26	35	0,83	0,54	0,82	0,89	0,40	4,75	0,86	0,93	0,74	0,86	3,80	0,16
6	25/2-12	3698.0	0,78	0,90	0,65	0,92	0,44	0,14	1,06	0,11	1,44	0,65	0,52	0,73	34	29	36	0,85	0,62	0,92	0,97	0,44	6,33	0,91	0,98	0,82	0,97	3,33	0,18
7	25/2-12	3698.5	0,79	0,86	0,59	0,90	0,42	0,17	1,66	0,17	0,94	0,67	0,54	0,73	27	34	40	0,77	0,62	0,89	0,52	0,41	5,43	0,89	0,71	0,76	0,91	3,67	0,17
8	25/2-12	3711.0	0,70	0,78	0,54	0,90	0,37	0,14	1,73	0,23	1,71	0,62	0,53	0,73	29	31	41	0,77	0,53	0,93	0,49	0,42	4,75	0,91	0,69	0,78	0,86	4,62	0,14
9	25/5-5	2164.5	0,69	0,88	0,58	0,92	0,39	0,20	1,14	0,12	1,60	0,65	0,51	0,66	33	25	42	0,72	0,64	0,85	0,56	0,40	4,47	0,87	0,73	0,73	0,84	4,29	0,14
10	25/5-5	2171.5	0,45	0,55	0,56	0,93	0,27	0,33	0,37	0,03	2,01	0,56	0,39	0,30	38	28	34	0,25	0,89	0,83	0,82	0,38	1,03	0,86	0,89	0,69	0,59	0,68	1,41
11	25/5-5	2172.0	0,68	0,84	0,58	0,92	0,32	0,09	0,52	0,04	2,08	0,61	0,50	0,53	34	25	41	0,69	0,68	1,02	0,96	0,43	5,92	0,96	0,98	0,80	0,94	4,74	0,12
12	25/5-5	2173.5	0,40	0,50	0,58	0,93	0,28	0,29	0,38	0,03	1,98	0,55	0,34	0,31	34	30	36	0,26	0,87	0,76	0,31	0,36	0,97	0,82	0,59	0,65	0,58	0,71	1,33
13	26/4-1	2258.7	0,42	0,73	0,66	0,96	0,28	0,33	0,69	0,07	1,45	0,61	0,45	0,42	41	28	31	0,45	0,73	0,81	0,70	0,39	1,17	0,85	0,82	0,71	0,60	0,65	1,47
14	26/4-1	2273.5	0,53	0,57	0,61	0,91	0,21	0,27	1,10	0,10	1,41	0,53	0,40	0,48	39	25	36	0,49	0,69	0,80	0,04	0,41	1,54	0,84	0,42	0,75	0,62	1,21	0,75
15	30/10-6	4664.0	0,71	0,85	0,63	0,94	0,39	0,15	0,52	0,05	1,88	0,63	0,50	0,57	40	23	38	0,65	0,72	0,94	1,22	0,45	6,33	0,92	1,13	0,84	0,97	4,80	0,13
16	30/10-6	4664.5	0,61	0,45	---	1,00	0,23	0,13	4,11	0,33	0,84	0,63	0,56	0,68	41	33	27	0,58	0,33	3,04	0,06	0,71	5,43	1,48	0,43	1,43	0,91	5,32	0,19
17	30/10-6	4675.0	0,58	0,47	0,58	0,90	0,16	0,10	2,95	0,35	1,11	0,57	0,41	0,56	49	25	26	0,64	0,23	3,00	2,25	0,71	5,07	1,47	1,75	1,42	0,88	4,81	0,21
18	30/10-6	4675.5	0,68	0,45	0,64	0,91	0,18	0,08	6,91	0,65	0,96	0,56	0,47	0,75	47	29	23	0,66	0,33	2,62	0,27	0,69	5,85	1,41	0,56	1,39	0,94	3,60	0,27
19	30/10-6	4686.0	0,62	0,55	0,62	0,92	0,15	0,10	3,55	0,33	1,09	0,58	0,47	0,57	46	20	34	0,38	0,50	2,92	0,74	0,72	6,33	1,46	0,85	1,45	0,97	4,76	0,22
20	30/10-6	4691.5	0,49	0,67	0,57	0,90	0,16	0,13	2,10	0,18	1,28	0,56	0,46	0,50	38	30	32	0,57	0,63	2,11	1,03	0,64	4,75	1,31	1,02	1,27	0,86	3,16	0,29

21	30/11-3	3457.5	0,58	0,44	0,65	0,92	0,15	0,11	2,14	0,29	1,29	0,54	0,43	0,48	34	26	40	0,55	0,41	2,54	0,19	0,67	5,07	1,39	0,51	1,32	0,88	3,92	0,11
22	30/11-4	3515.0	0,58	0,67	0,60	0,91	0,36	0,19	0,89	0,15	2,15	0,64	0,46	0,65	39	23	38	0,67	0,56	0,84	0,95	0,41	4,17	0,86	0,97	0,75	0,81	5,48	0,05
23	30/11-4	3526.8	0,71	0,83	0,62	0,91	0,43	0,14	0,96	0,11	1,44	0,61	0,57	0,66	40	24	36	0,83	0,59	0,98	0,75	0,42	5,07	0,94	0,85	0,78	0,88	6,07	0,04
24	30/11-8A	3968.0	0,71	0,83	0,62	0,87	0,31	0,11	2,27	0,29	1,24	0,57	0,56	0,72	44	21	34	0,88	0,32	1,05	0,58	0,45	6,91	0,97	0,75	0,83	1,01	6,11	0,04
25	30/11-8A	3968.5	0,61	0,73	0,54	0,91	0,27	0,11	1,43	0,16	1,46	0,61	0,43	0,53	36	25	39	0,85	0,29	1,05	0,86	0,47	5,43	0,97	0,91	0,89	0,91	4,13	0,08
26	30/11-8A	3986.5	0,62	0,70	0,61	0,92	0,33	0,14	1,75	0,14	1,53	0,61	0,39	0,61	37	24	38	0,78	0,58	1,00	0,12	0,46	4,69	0,95	0,47	0,85	0,85	3,59	0,09
27	30/11-8A	3987.0	0,72	0,80	0,54	0,90	0,27	0,13	2,16	0,17	1,42	0,58	0,46	0,67	36	27	37	0,84	0,53	0,95	1,02	0,44	5,00	0,93	1,01	0,82	0,88	3,16	0,09
28	NSO-1		0,59	0,73	0,52	0,91	0,25	0,10	1,70	0,17	1,33	0,63	0,49	0,60	34	25	41	0,85	0,40	1,07	0,71	0,46	5,85	0,98	0,82	0,86	0,94	3,72	0,08

Iatroscan TLC-FID

As suggested by Karlsen and Larter (1989, 1991) the gross composition and the relative percentages of saturated and aromatic hydrocarbons and polar compounds can effectively be determined in a reservoir by Iatroscan TLC-FID. The results of the Iatroscan analysis for all the extracts are given in table 4.14 and the chromatograms are presented in appendix D.

4.5.1 Well 25/2-4

The percentage composition of saturated hydrocarbons in this well is more than 50% with a maximum value of 62.1%. The composition varies from 25% to 44.8% for polars whereas aromatic hydrocarbons show percentages less than 13% (see table 4.14). The extract yield ranges from 3.11 to 4.61 mg/g rock.

4.5.2 Well 25/2-12

The saturated hydrocarbons are dominant in percentage with values ranging from 53.3% to 64.2% whereas polar compounds vary from 26.2% to 44.7%. Aromatic hydrocarbons are less than 10% with a minimum percentage value of 1.9% which in general decreases with depth. The extract yield lies in between 1.16 and 2.48 mg/g rock and decreases with depth (see table 4.14).

4.5.3 Well 25/5-5

The percentage of polar compounds varies from 28.3% to 46.4% and generally decreases with depth. The average percentage for saturated hydrocarbons is 31% and varies from 20.7% to 42.7% for aromatic hydrocarbons. The samples from this well have produced the highest amount of extract ranging from 40 to 46.9 mg/g rock (see table 4.14).

4.5.4 Well 26/4-1

The polar compounds show dominance in percentage composition in this well. The values are in a range of 32.5% to 85.2% for polars, 12.8% to 37.1% for saturated hydrocarbons and 1.3 to 35% for aromatic hydrocarbons. The total extractable organic matter is estimated to be 0.14-0.73 mg/g rock and is the second lowest among all the samples (see table 4.14).

4.5.5 Well 30/10-6

The fraction of saturated hydrocarbons in this well is relatively low at shallower depths, i.e. from 4664.0m to 4702.0m, and increases drastically at greater depths. The case is reverse for polar compounds. There is a significant variation in the percentages of aromatic hydrocarbons with values as low as 1.0 % to a maximum of 45.3%. The samples from this well have produced the lowest amount of extract yield ranging from 0.22 to 0.59 mg/g rock (see table 4.14).

4.5.6 Well 30/11-3

The percentages vary significantly for all three fractions in this well. The values correspond to 15.5–64.9%, 0.5–46.2% and 25.0–83.5% for saturated hydrocarbons, aromatic hydrocarbons and polar compounds respectively. The amount of extractable organic matter decreases with depth and ranges from 0.21 to 5 mg/g rock (see table 4.14).

4.5.7 Well 30/11-4

The fraction of saturated hydrocarbons varies in percentage from 32.4% to 45.0% and 40.7% to 59.8% for polar compounds. The percentage for aromatic hydrocarbons is less than 15% where 1.3% is the minimum for the sample at depth 3526.8m. The extract yield ranges from 1.3 to 4.53 mg/g rock (see table 4.14).

4.5.8 Well 30/11-8A

The saturated hydrocarbons have an average percentage of 60% in this well with clear dominance. The percentage values for polar compounds vary from 26.2% to 38.8% while they are less than 10% for aromatic hydrocarbons. The extract yield tends to be uniform with depth and ranges from 1.78 to 2.01 mg/g rock (see table 4.14).

Table 4.14. Iatroscan results for the dry well samples from the North Sea showing the relative fraction of all the compounds and the content of hydrocarbons (saturated and aromatic) and non-hydrocarbons (polars) in mg/g of rock.

No	Well	Depth	Weight (g)	Total vol. (ml)	Vol. used (ul)	Area			Extract concentration (mg/ml)				Extract concentration (%)				Extract yield (mg/g rock)				SAT/ARO
						SAT	ARO	POL	SAT	ARO	POL	TOTAL	SAT	ARO	POL	TOTAL	SAT	ARO	POL	TOTAL	
1	25/2-4	3675.0	7	10	3	5488	642	9102	1.11	0.12	1.00	2.23	49.8	5.4	44.8	100	1.59	0.17	1.43	3.19	9,22
2	25/2-4	3676.0	7	10	3	5627	810	8059	1.14	0.15	0.88	2.18	52.4	7.0	40.6	100	1.63	0.22	1.26	3.11	7,49
3	25/2-4	3683.0	7	10	3	9224	1818	8591	1.87	0.34	0.94	3.15	59.2	10.9	29.9	100	2.67	0.49	1.35	4.50	5,43
4	25/2-4	3684.0	7	10	3	9907	2209	7357	2.01	0.42	0.81	3.23	62.1	12.9	25.0	100	2.86	0.59	1.15	4.61	4,81
5	25/2-4	3693.0	7	10	3	8829	938	10177	1.79	0.18	1.12	3.08	58.0	5.7	36.2	100	2.55	0.25	1.59	4.40	10,18
6	25/2-4	3694.0	7	10	3	6880	574	8610	1.39	0.11	0.94	2.44	57.0	4.4	38.6	100	1.99	0.15	1.35	3.49	12,95
7	25/2-12	3698.0	7	10	3	5250	501	5303	1.06	0.09	0.58	1.74	61.1	5.4	33.4	100	1.52	0.13	0.83	2.48	11,31
8	25/2-12	3698.5	7	10	3	4639	746	3499	0.94	0.14	0.38	1.46	64.2	9.6	26.2	100	1.34	0.20	0.55	2.09	6,69
9	25/2-12	3706.0	7	10	3	2931	114	3547	0.59	0.02	0.39	1.00	59.1	2.1	38.8	100	0.85	0.03	0.56	1.43	28,14
10	25/2-12	3710.0	7	10	3	2177	90	3370	0.44	0.02	0.37	0.83	53.3	2.0	44.7	100	0.63	0.02	0.53	1.18	26,65
11	25/2-12	3711.0	7	10	3	2155	84	3275	0.44	0.02	0.36	0.81	53.8	1.9	44.3	100	0.62	0.02	0.51	1.16	28,32

12	25/5-5	2164.5	7	10	3	53461	36110	138833	10.82	6.80	15.2	32.84	32.9	20.7	46.4	100	15.46	9.71	21.75	46.92	1,59
13	25/5-5	2171.5	7	10	3	46122	72951	83167	9.34	13.73	9.12	32.19	29.0	42.7	28.3	100	13.34	19.62	13.03	45.98	0,68
14	25/5-5	2172.0	7	10	3	38965	63324	74599	7.89	11.92	8.18	27.99	28.2	42.6	29.2	100	11.27	17.03	11.69	39.98	0,66
15	25/5-5	2173.5	7	10	3	45987	55810	74615	9.31	10.51	8.18	28.00	33.2	37.5	29.2	100	13.30	15.01	11.69	40.00	0,89
16	26/4-1	2258.7	7	10	3	143	84	1648	0.03	0.02	0.18	0.23	12.8	7.0	80.1	100	0.04	0.02	0.26	0.32	1,83
17	26/4-1	2273.5	7	10	3	398	179	1609	0.08	0.03	0.18	0.29	27.7	11.6	60.7	100	0.12	0.05	0.25	0.42	2,39
18	26/4-1	2274.0	7	10	3	805	932	1484	0.16	0.18	0.16	0.50	32.5	35.0	32.5	100	0.23	0.25	0.23	0.72	0,93
19	26/4-1	2274.8	7	10	3	76	8	885	0.02	0.00	0.10	0.11	13.5	1.3	85.2	100	0.02	0.00	0.14	0.16	10,38
20	26/4-1	2289.2	7	10	3	129	0	652	0.03	0.00	0.07	0.10	26.8	0.0	73.2	100	0.04	0.00	0.10	0.14	---
21	26/4-1	2290.5	7	10	3	938	271	2474	0.19	0.05	0.27	0.51	37.1	10.0	53.0	100	0.27	0.07	0.39	0.73	3,71
22	30/10-6	4664.0	7	10	3	156	493	732	0.03	0.09	0.08	0.20	15.4	45.3	39.2	100	0.05	0.13	0.11	0.29	0,34
23	30/10-6	4664.5	7	10	3	190	321	2431	0.04	0.06	0.27	0.37	10.5	16.5	72.9	100	0.05	0.09	0.38	0.52	0,64
24	30/10-6	4675.0	7	10	3	61	765	2324	0.01	0.14	0.25	0.41	3.0	35.0	62.0	100	0.02	0.21	0.36	0.59	0,09
25	30/10-6	4675.5	7	10	3	120	203	913	0.02	0.04	0.10	0.16	14.9	23.5	61.6	100	0.03	0.05	0.14	0.23	0,63
26	30/10-6	4686.0	7	10	3	173	324	549	0.04	0.06	0.06	0.16	22.4	39.0	38.5	100	0.05	0.09	0.09	0.22	0,57
27	30/10-6	4686.5	7	10	3	66	574	1304	0.01	0.11	0.14	0.26	5.1	40.9	54.1	100	0.02	0.15	0.20	0.38	0,12

28	30/10-6	4691.0	7	10	3	24	435	959	0.00	0.08	0.11	0.19	2.5	42.7	54.8	100	0.01	0.12	0.15	0.27	0,06
29	30/10-6	4691.5	7	10	3	315	18	2381	0.06	0.00	0.26	0.33	19.4	1.0	79.5	100	0.09	0.00	0.37	0.47	19,40
30	30/10-6	4702.0	7	10	3	133	36	2157	0.03	0.01	0.24	0.27	10.0	2.5	87.5	100	0.04	0.01	0.34	0.39	4,00
31	30/10-6	4702.5	7	10	3	756	192	898	0.15	0.04	0.10	0.29	53.2	12.6	34.2	100	0.22	0.05	0.14	0.41	4,22
32	30/10-6	4714.7	7	10	3	504	30	404	0.10	0.01	0.04	0.15	67.1	3.7	29.2	100	0.15	0.01	0.06	0.22	18,14
33	30/10-6	4962.3	7	10	3	1131	0	1033	0.23	0.00	0.11	0.34	66.9	0.0	33.1	100	0.33	0.00	0.16	0.49	---
34	30/11-3	3450.5	7	10	3	2676	8589	12236	0.54	1.62	1.34	3.50	15.5	46.2	38.3	100	0.77	2.31	1.92	5.00	0,34
35	30/11-3	3457.0	7	10	3	2552	427	1812	0.52	0.08	0.20	0.80	64.9	10.1	25.0	100	0.74	0.11	0.28	1.14	6,43
36	30/11-3	3457.5	7	10	3	2307	412	2203	0.47	0.08	0.24	0.79	59.4	9.9	30.7	100	0.67	0.11	0.35	1.12	6,00
37	30/11-3	3468.3	7	10	3	117	4	1126	0.02	0.00	0.12	0.15	16.0	0.5	83.5	100	0.03	0.00	0.18	0.21	32,00
38	30/11-4	3514.5	7	10	3	1650	429	5621	0.33	0.08	0.62	1.03	32.4	7.8	59.8	100	0.48	0.12	0.88	1.47	4,15
39	30/11-4	3515.0	7	10	3	1562	304	4902	0.32	0.06	0.54	0.91	34.7	6.3	59.0	100	0.45	0.08	0.77	1.30	5,51
40	30/11-4	3515.5	7	10	3	6505	2312	11964	1.32	0.44	1.31	3.06	43.0	14.2	42.8	100	1.88	0.62	1.87	4.38	3,03
41	30/11-4	3516.0	7	10	3	7053	2401	11768	1.43	0.45	1.29	3.17	45.0	14.3	40.7	100	2.04	0.65	1.84	4.53	3,15
42	30/11-4	3517.2	7	10	3	2228	418	4815	0.45	0.08	0.53	1.06	42.6	7.4	49.9	100	0.64	0.11	0.75	1.51	5,76
43	30/11-4	3526.8	7	10	3	3159	113	8564	0.64	0.02	0.94	1.60	40.0	1.3	58.7	100	0.91	0.03	1.34	2.29	30,77

44	30/11-8A	3968.0	7	10	3	3295	242	6362	0.67	0.05	0.70	1.41	57.0	4.4	38.6	100	0.95	0.07	1.00	2.01	12,95
45	30/11-8A	3968.5	7	10	3	3359	0	5234	0.68	0.00	0.57	1.25	61.1	5.4	33.4	100	0.97	0.00	0.82	1.79	11,31
46	30/11-8A	3986.5	7	10	3	2507	215	6336	0.51	0.04	0.69	1.24	64.2	9.6	26.2	100	0.72	0.06	0.99	1.78	6,69
47	30/11-8A	3987.0	7	10	3	3276	0	6735	0.66	0.00	0.74	1.40	59.1	2.1	38.8	100	0.95	0.00	1.06	2.00	28,14

5. Discussion

The results that were presented in the preceding chapter will be discussed here in detail in terms of maturity, organic facies and compositional heterogeneities. The discussion includes the representation of the findings with the help of different cross plots, bar charts and diagrams with references from the literature. The issues of major concern will be further discussed in conclusions.

The outline of the discussion is as follows:

5.1 Composition of hydrocarbons

5.2 Organic facies

5.3 Maturity

5.4 Conclusion

Composition of hydrocarbons

The gross composition of hydrocarbons is estimated for all the samples based on the results of gas analysis and Iatroscan TLC-FID and is done to assist in differentiatinal drilling mud from migrated petroleum and also in-situ generated hydrocarbon products. The gross composition, in terms of gases extracted from the core samples, is the percentage of methane (C₁) to pentane (C₅) hydrocarbons while for the core extracts it refers to the percentage amount of saturated and aromatic hydrocarbons and polar compounds and also absolute amounts of extracted bitumen.

Composition on the basis of percentage of gases (C₁ to C₅)

The type of kerogen and maturity has a strong influence on the percentage composition of gases (Whiticar, 1994). The percentage of C₂+ compounds determines whether the gas is biogenic or thermogenic. Biogenic gas, generally pure methane, is believed to be formed by methanogenic bacteria by fermentation process or CO₂ reduction at temperature less than

50°C where the percentage of C_{2+} compounds is less than 1 (Whiticar, 1994). C_{2+} compounds are produced by the thermal cracking of complex or heavy hydrocarbons and are called oil associated gases. The percentage of higher boiling compounds (C_{2+}) is sufficiently increased with increasing maturity, reaching about 20-25% in the oil window (Whiticar, 1994).

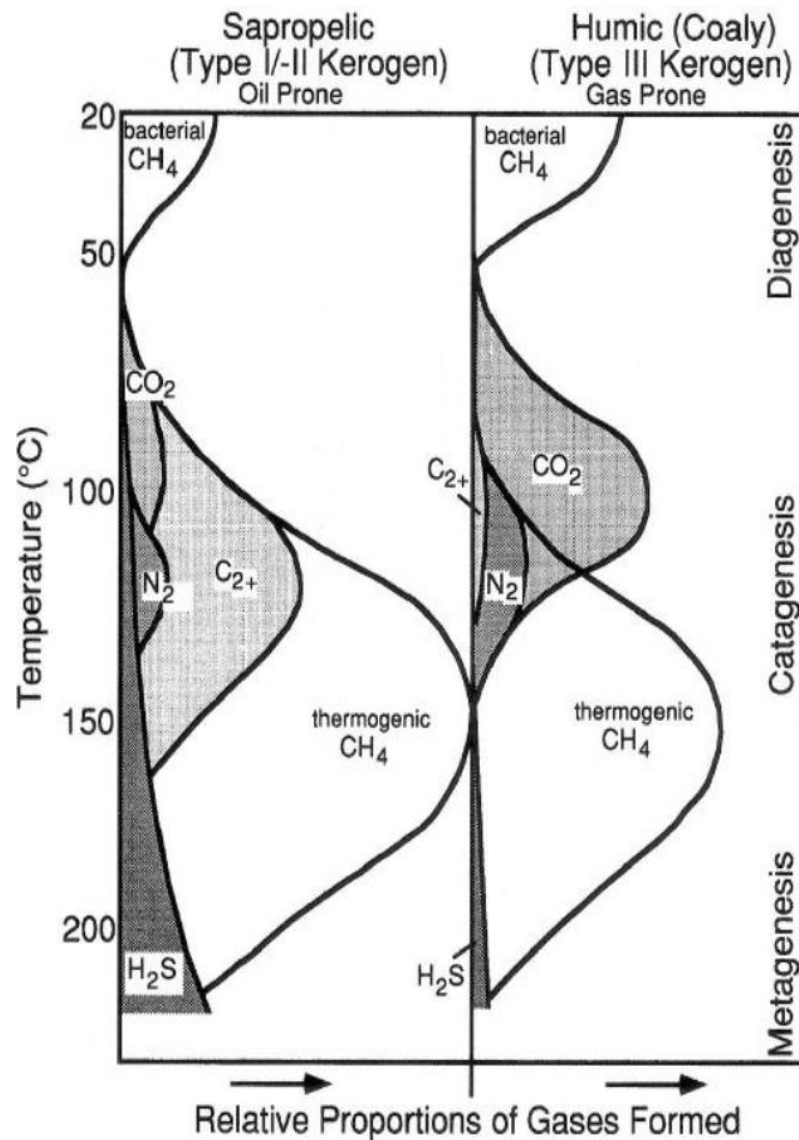


Fig. 5.1. Diagram showing the relative proportions of natural gases generated from different types of kerogen, i.e. sapropelic (type I and type II) and humic (3) (From Hunt, 1979).

Thus, the percentage of wet gases (C_2-C_5) is usually higher than 5% of the total hydrocarbons generated from a source and represents wet gas existence provided $\Sigma C_{2+} > 5$ (Floodgate and Judd, 1992) while the values lying in a range of 12-15% represents condensate associated gases (Schoell, 1983). On contrary, the percentage of ΣC_{2+} less than

5% indicates dry gases which are generated at low thermal maturity (Hunt, 1979; Whiticar, 1994). The results from gas analysis indicate the percentage of C_2+ hydrocarbons, in most of the core samples, to be between 20-40% referring them to be wet/oil associated (Fig 5.2). This rich gas was generated together with oil and oil did exist in the trap at some time.

A few samples from the well 25/3-1 represent values less than 20% but still higher than 15%, which gives indication of light oil and not even condensate. However, the samples from the well 30/10-6 show distinct characteristics of a condensate, which is also evident in fig 5.3, where the values of C_2+ hydrocarbons are between 5 to 15%. The ratio of iso-butane to n-butane is less than unity for almost all of the samples except some samples from the well 30/10-6 where it exceeds the value of one. According to Horstad and Larter (1977), this increase in the butane isomers ratio may indicate the transformation processes like biodegradation or gas fractionation.

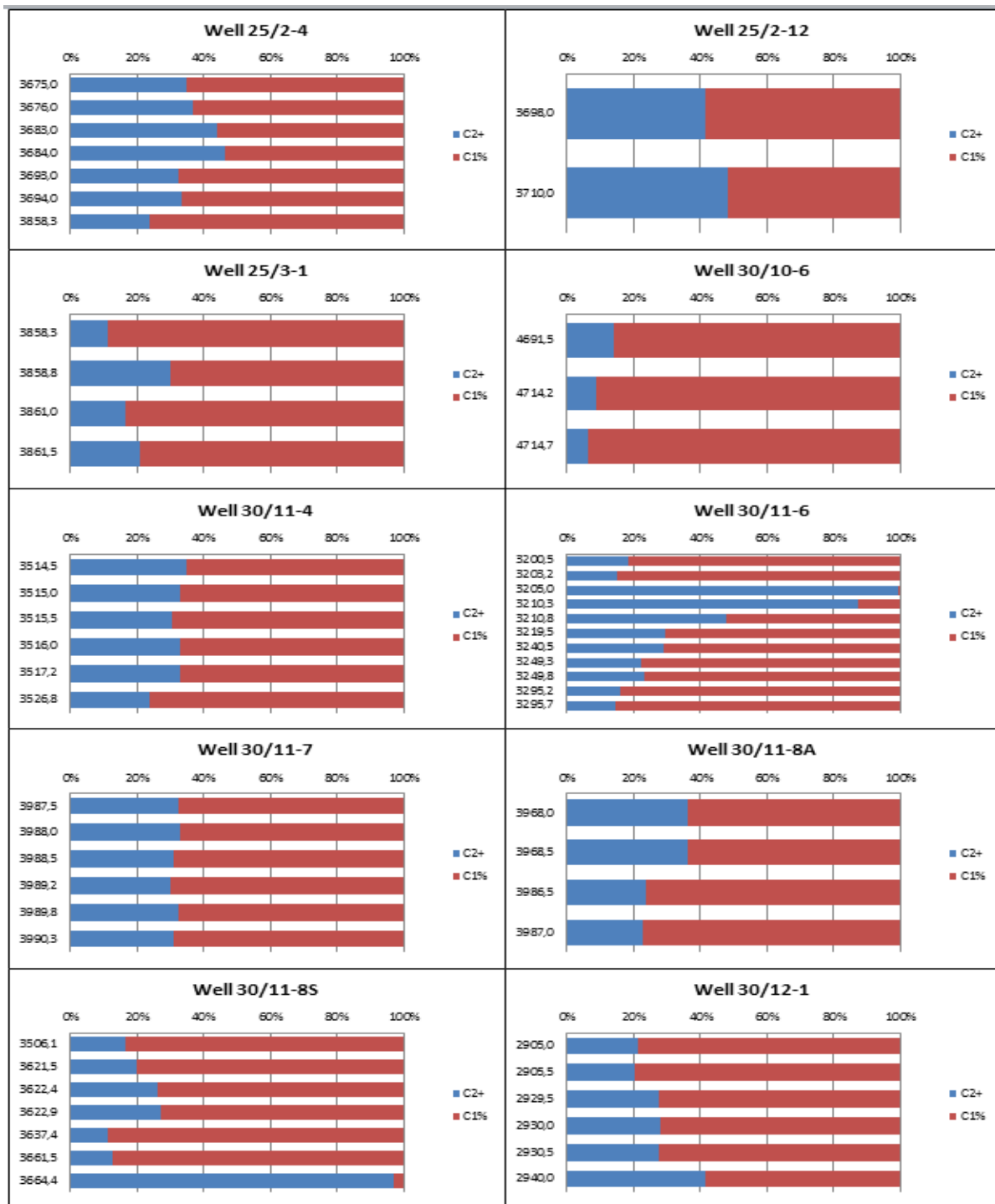


Fig. 5.2. Bar charts showing the percentage of methane against the wet components (C₂+) along x-axis and depth (m) along y-axis. It is necessarily suggesting that the petroleum phase was most likely condensate to oil at the time of inclusion formation in all these wells which today are dry.

In short, all the samples are supposed to contain oil and are clearly wetter than a condensate as shown in the wetness diagram below.

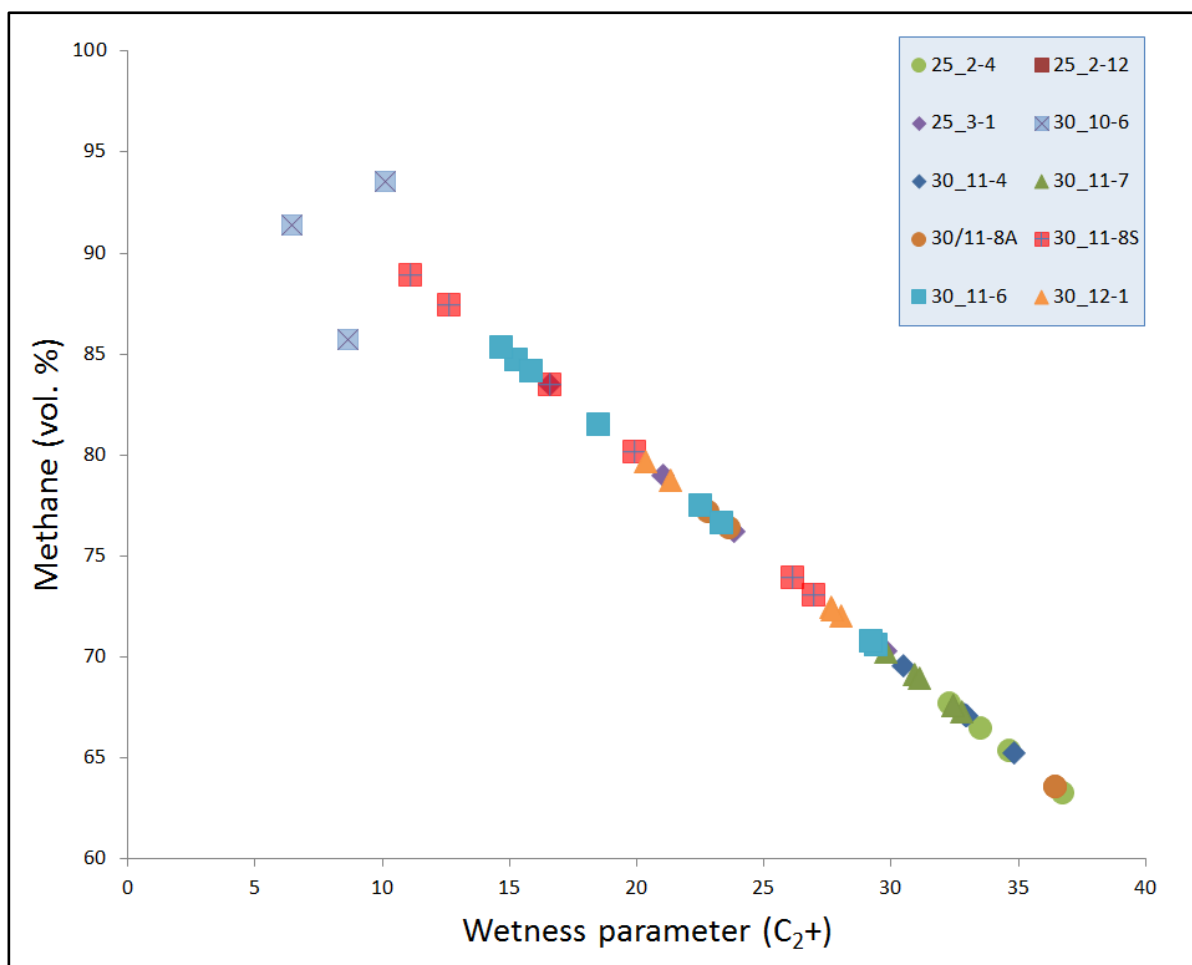


Fig. 5.3. Cross plot showing the wetness parameter (C_2+) along x-axis and volume percentage of methane along y-axis. Surprisingly most of the samples from the dry wells are oil-wet, however a few samples are also condensate wet.

Composition on the basis of percentage of saturated and aromatic hydrocarbons and polar compounds

The results from Iatroscan TLC-FID analysis of core extracts show a pronounced variation in the composition in terms of saturated and aromatic hydrocarbons and also polar compounds for various wells. The average percentage of saturated hydrocarbons and polar compounds for the samples from block 25/2 is 56% and 35% respectively whereas aromatic hydrocarbons show generally lower values ranging from 2 to 12% (Fig 5.4). On the contrary, the polar compounds (resins plus asphaltenes) dominate in the samples from blocks 26/4, 30/10 and 30/11 with values higher than 50% and in some samples even reaching values of around 80%. However the values are uniform for well 25/5-5 with almost equal percentages of saturated and aromatic hydrocarbons and polar compounds. The percentage of aromatic

hydrocarbons is higher than 30% reaching upto 40% in the samples from well 25/5-5 and some samples from well 30/10-6.

The amount of low molecular weight hydrocarbons, i.e. below C_{15} , is generally increased during thermal alteration. The percentage of aromatic hydrocarbons in the crude oils is decreased with increasing maturity hence reflecting the maturity of oils (Tissot and Welte, 1984). Since the saturated fractions tend to alter less with increasing thermal maturity (Tissot and Welte, 1984), the discussion with respect to maturity is more focused on the proportion of aromatic hydrocarbons. The samples from the well 30/11-8A show the highest maturity followed by the samples of well 25/2-12 in terms of their lowest aromatic content.

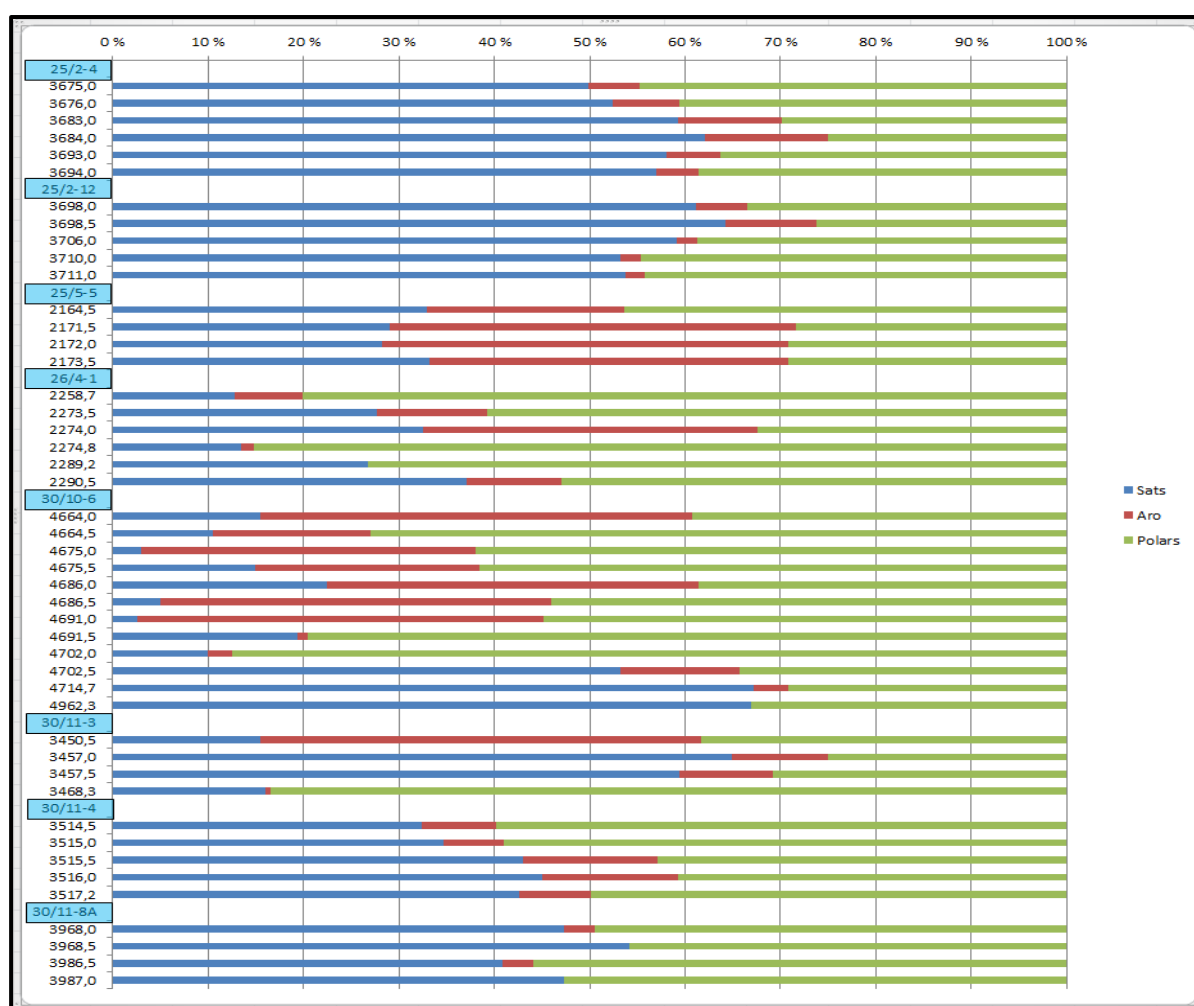


Fig. 5.4. Bar chart showing the percentage composition of saturated (Sats), aromatic (Aro) and polar compounds based on Iatroscan results. The comparatively high percentages of polar compounds in some wells may probably suggest the palaeo-petroleum migration, and also intra-reservoir modifications like biodegradation which increases the amount of polar compounds. Note that biodegradation may have occurred when the well was much more shallow.

Organic Facies

Organic facies as defined by (Hunt, 1996) are the mappable subdivisions of stratigraphic units distinguished from the adjacent subdivisions by the character of their organic matter. To infer the depositional environment, organic source input and the relationship between the samples, biomarker and non-biomarker parameters together can serve as an effective tool (Peters and Moldowan, 1993). The difference in the amount and type of the hydrocarbons depends upon the organic input source.

Facies estimation by isoprenoids and n-alkanes

The ratios of isoprenoids to n-alkanes, i.e. Pr/n-C₁₇ and Ph/n-C₁₈, may prove to be useful in order to predict the depositional environment of source rocks (Peters and Moldowan, 1993). They may also be helpful to determine the type of kerogen, oxic/anoxic conditions and maturity. Most of the samples from the dry wells have high maturity and originated from type II kerogen (Fig 5.5), however some samples from wells 25/5-5 and 26/4-1 show low maturity. Moreover, as inferred from the facies diagram (Fig 5.6), the samples from the dry wells have originated from mixed organic sources with more marine influence which is normal for transitional environments. Since these ratios are greatly influenced by both maturity and facies (Peters and Moldowan, 1993), it is important to assess whether source facies or maturity have had the greater influence on the samples.

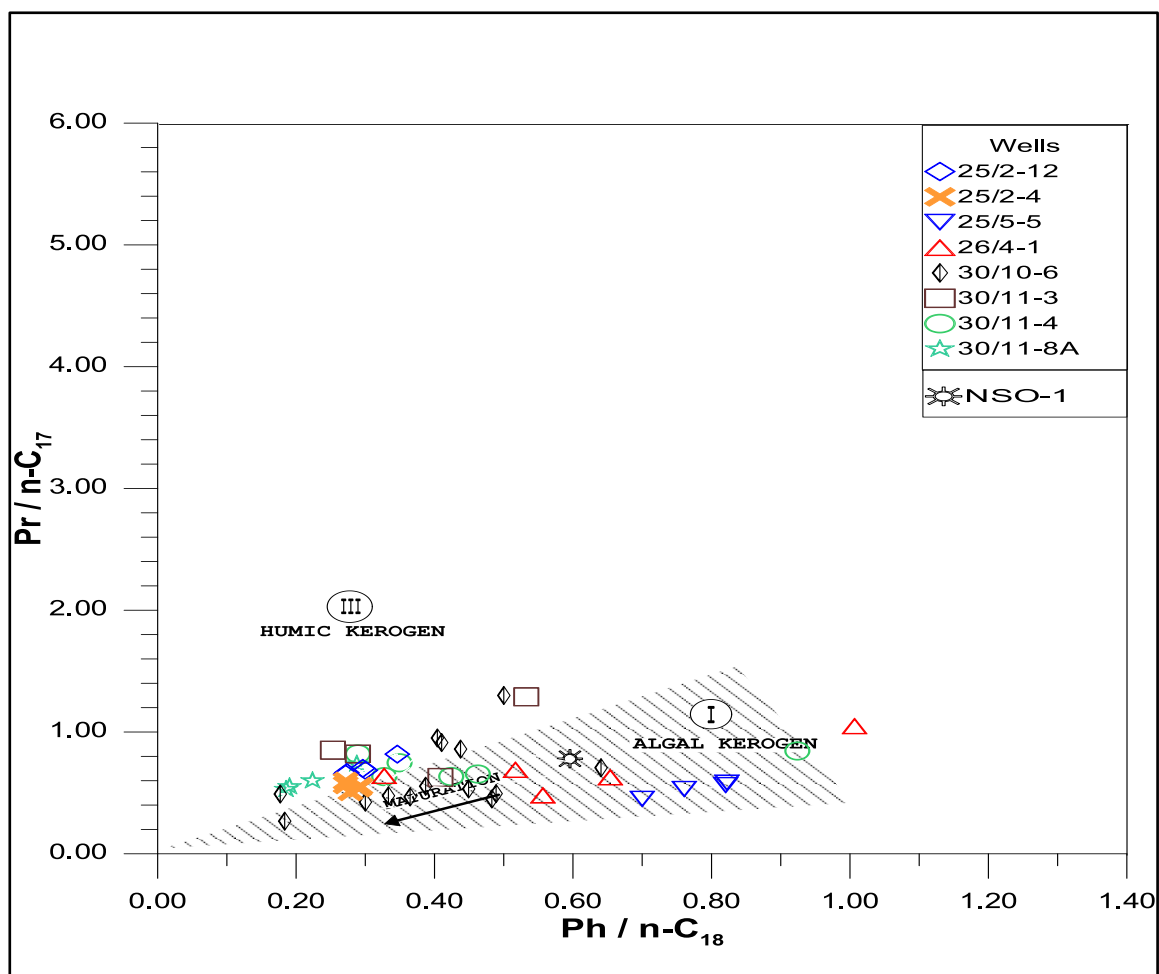


Fig. 5.5. A plot of $Pr/n-C_{17}$ along y-axis and $Ph/n-C_{18}$ along x-axis (modified from Connan and Casson, 1980) to determine the type of kerogen. The data is nicely grouped together with some spread indicating variable maturity and generally type II kerogen. The NSO (Oseberg oil) sourced from the Draupne Formation is shown for comparison.

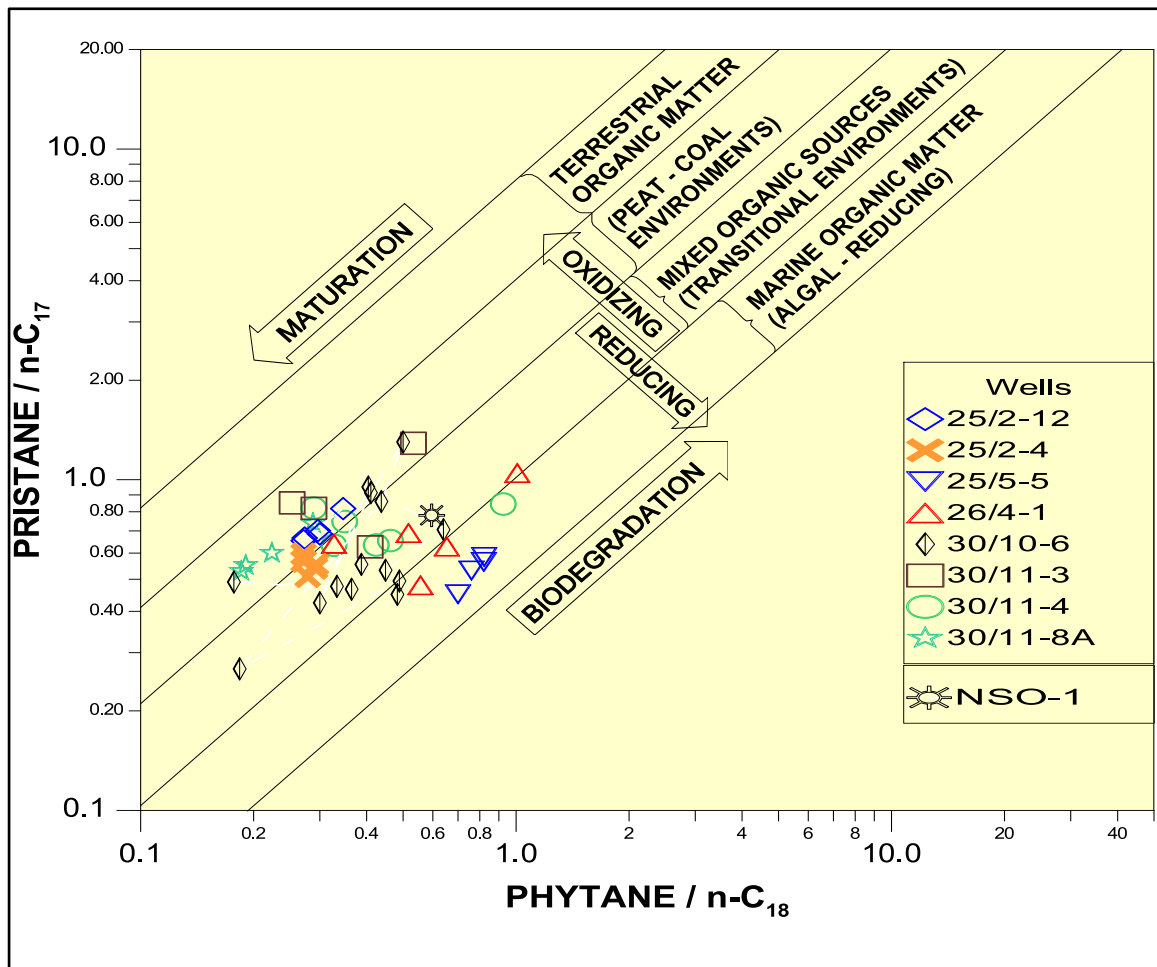


Fig. 5.6. Facies diagram proposed by Shanmugam (1985) to describe the maturity and relative changes in facies. The data suggests mixed marine source facies for the dry wells and may indicate that the source rocks for the bitumen could represent more proximal to distal variation or even more dysoxic conditions than typical for e.g. the NSO-1 oil from the Draupne source rock at Oseberg.

Facies estimation by steranes isomers

The percentages of C_{27} , C_{28} and C_{29} steranes are useful biomarker facies parameters to depict the environment of deposition. They are plotted in a bar chart (Fig 5.7) and ternary diagram (Fig 5.8) where the divisions in the triangle represent the type of depositional environment or source of hydrocarbons. The abundance of C_{29} steranes states higher plants as a source of organic matter while lacustrine environment refers to high concentrations of C_{28} isomers (Shanmugam, 1985).

All the samples from the dry wells are concentrated in the center of ternary diagram which certainly could indicate mixed marine environment conditions with marine source rock facies. Though some samples from the well 25/2-12 are also showing estuarine influence.

The validity of ternary diagram is debated and the identification of source rock facies based entirely on steranes distribution is not suggested (Moldowan et al., 1985). However, it is still widely used and continues to provide effective source rock discrimination. The data for the bar chart is given in table 5.1 and the distribution of all three sterane isomers are demonstrated in the bar chart.

Table 5.1. The sample data for C₂₇, C₂₈ and C₂₉ steranes.

No.	Well	Depth (m)	%C ₂₇	%C ₂₈	%C ₂₉
1	-----				
2	NSO-1		33	35	32
3	25/2-4	3675.0	39	26	35
4	25/2-4	3676.0	38	29	33
5	25/2-4	3683.0	39	26	35
6	25/2-4	3684.0	38	26	35
7	25/2-4	3694.0	34	29	36
8	25/2-12	3698.0	27	34	40
9	25/2-12	3698.5	29	31	41
10	25/2-12	3711.0	33	25	42
11	25/5-5	2164.5	38	28	34
12	25/5-5	2171.5	34	25	41
13	25/5-5	2172.0	34	30	36
14	25/5-5	2173.5	41	28	31
15	26/4-1	2258.7	39	25	36
16	26/4-1	2273.5	40	23	38

17	30/10-6	4664.5	49	25	26
18	30/10-6	4675.0	47	29	23
19	30/10-6	4675.5	46	20	34
20	30/10-6	4686.0	38	30	32
21	30/10-6	4691.5	34	26	40
22	30/11-3	3457.5	39	23	38
23	30/11-4	3515.0	40	24	36
24	30/11-4	3526.8	44	21	34
25	30/11-8A	3968.0	36	25	39
26	30/11-8A	3968.5	37	24	38
27	30/11-8A	3986.5	36	27	37
28	30/11-8A	3987.0	34	25	41
29	-----				

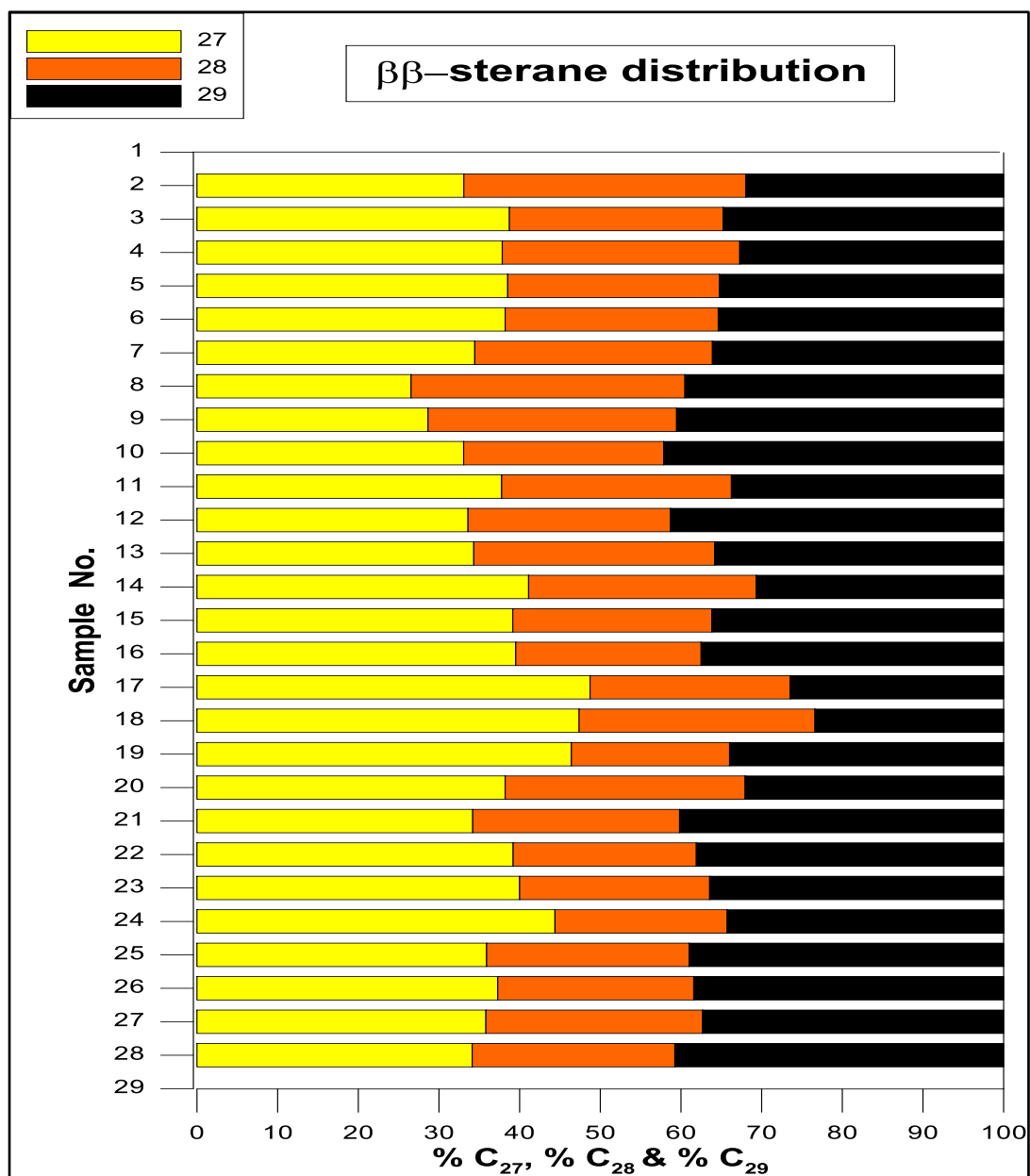


Fig. 5.7. Bar chart showing the distribution of C₂₇, C₂₈ and C₂₉ sterane isomers (see table 5.1 for details).

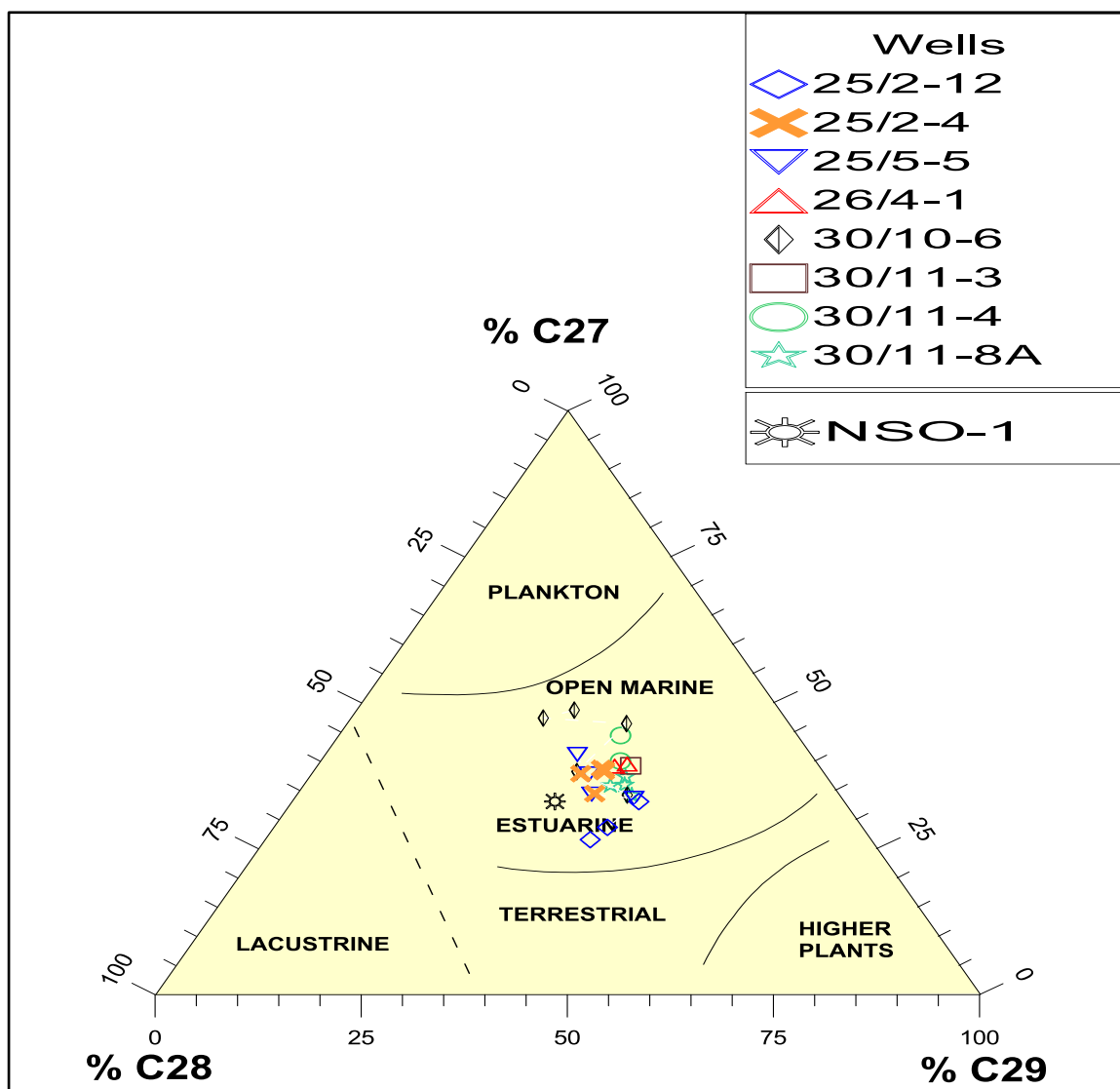


Fig. 5.8. The percentage distribution of steranes (C_{27} , C_{28} & C_{29}) to predict organic facies of the source rock for the residual bitumens. All the samples are essentially reflecting the marine window with same source rock facies, but with more variability than for the oils sourced from distal marine type II source rocks which plot more dead-center (cf. Karlsen et al., 1993).

Facies identified by isoprenoids and aromatic hydrocarbons

The distribution of source rock facies can be identified by the ratios of isoprenoids (Pr/Ph) and methylphenanthrenes, i.e. MDBT/MPHEN. Methyl dibenzothiophene and methylphenanthrene are important medium range maturity parameters. Most of the samples from the dry wells are lying in Zone 3 showing marine/lacustrine environment (Fig 5.9).

Some samples from the well 25/5-5 are though showing a slight bend towards sulphate-rich conditions. This variation in environmental conditions from sulphate-poor to sulphate-rich may reflect the effect of maturity.

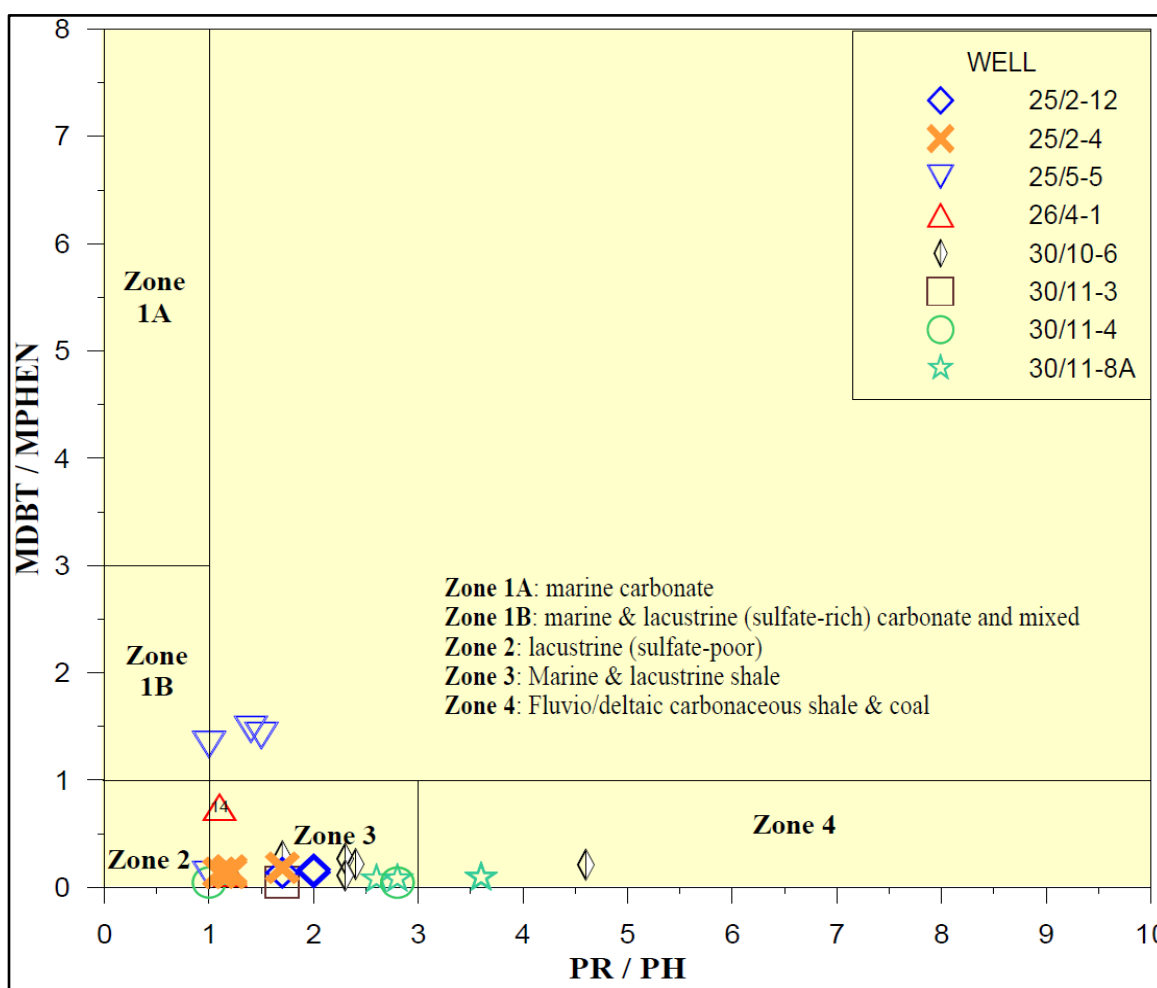


Fig. 5.9. Cross plot showing ratios of isoprenoids along the x-axis and aromatic hydrocarbons along the y-axis (modified from Hughes et al., 1995) where most of the samples lie in Zone 3 reflecting marine environment.

Maturity

The term maturity refers to the degree of heat experienced by a source rock until the petroleum is expelled from it. It generally increases with depth and the depth at which the petroleum source rock generates and expels oil is termed as oil window. As suggested by Hunt in 1996, the oil window corresponds to a depth of 2 to 5 km within a temperature range of 60°C to 160°C where the geothermal gradient is supposed to be 30-35°C and most oils are found to be expelled only at maturities of c. 0.85% and higher (Karlsen et al., 1993).

The organic matter is immature, mature or post mature depending on its relation to the oil window (Tissot and Welte, 1984). Immature organic matter is altered physically, chemically and biologically due to the effect of diagenesis without the involvement of temperature. Mature organic matter is however affected by catagenesis which is a thermal process within a temperature range between diagenesis and metagenesis. Post mature oil is heated at very high temperatures such that it is reduced to a hydrogen-poor residue and left with the capability to generate only gases.

The maturity of the dry well samples has been investigated on the basis of various biomarker and non-biomarker parameters, the integration of which, as suggested by Peters and Moldowan (1993), is typically required to assess the thermal maturity of the source rock responsible for generating oil and gas. These parameters, in general, will reflect the maturity of the samples, even though several of these parameters are influenced by migration histories, different source rock facies, biodegradation, fractionation and degree of intra-reservoir mixing, gas stripping or water washing (Karlsen et al., 1993).

Maturity assessment from non-biomarkers

The ratios of isoprenoid to n-alkanes, CPI values, aromatic hydrocarbons and their associated calculated vitrinite reflectances will be discussed in this section to explain the maturity of the dry wells.

With increasing thermal maturity the ratios of isoprenoids to n-alkanes decrease due to the fact that the amount of normal alkanes is increased in the petroleum during thermal cracking (Tissot et al., 1971). There is lower bond strength among the carbon atoms in isoprenoids and isoprenoids are therefore less stable than n-alkanes. The ratios are quite helpful in grading the thermal maturity of non-biodegraded oils and bitumens. However, these are greatly influenced by the secondary processes like biodegradation and organic matter input (Alexander et al., 1981b). From the data in figure 5.6, it is concluded that the dry wells are all fully mature and are almost in the same maturity range except some samples from well 30/10-6 which are showing relatively higher maturity.

The second maturity parameter evaluated is the carbon preference index (CPI) for which the ratio will asymptotically approach unity (Peters et al., 2005). Values significantly higher

than unity indicate siliciclastic source rocks (shales) while lower values reflect a carbonate source rock or high amounts of carbonate in the source rock. Sometimes we observe a CPI value at the heavy end of the alkane spectra only as the CPI is already lost at the lighter end. This is due to the dilution of the shorter n-alkanes by newly cracked n-alkanes. This can be the reason for the variation in the values between CPI-1 and CPI-2. The values for most of the samples fall in a range of unity, i.e. 1.0 to 1.1, which are certainly indicating mature source rock samples (Fig 5.10) and a maturity in the range of about 0.9%Rc or higher.

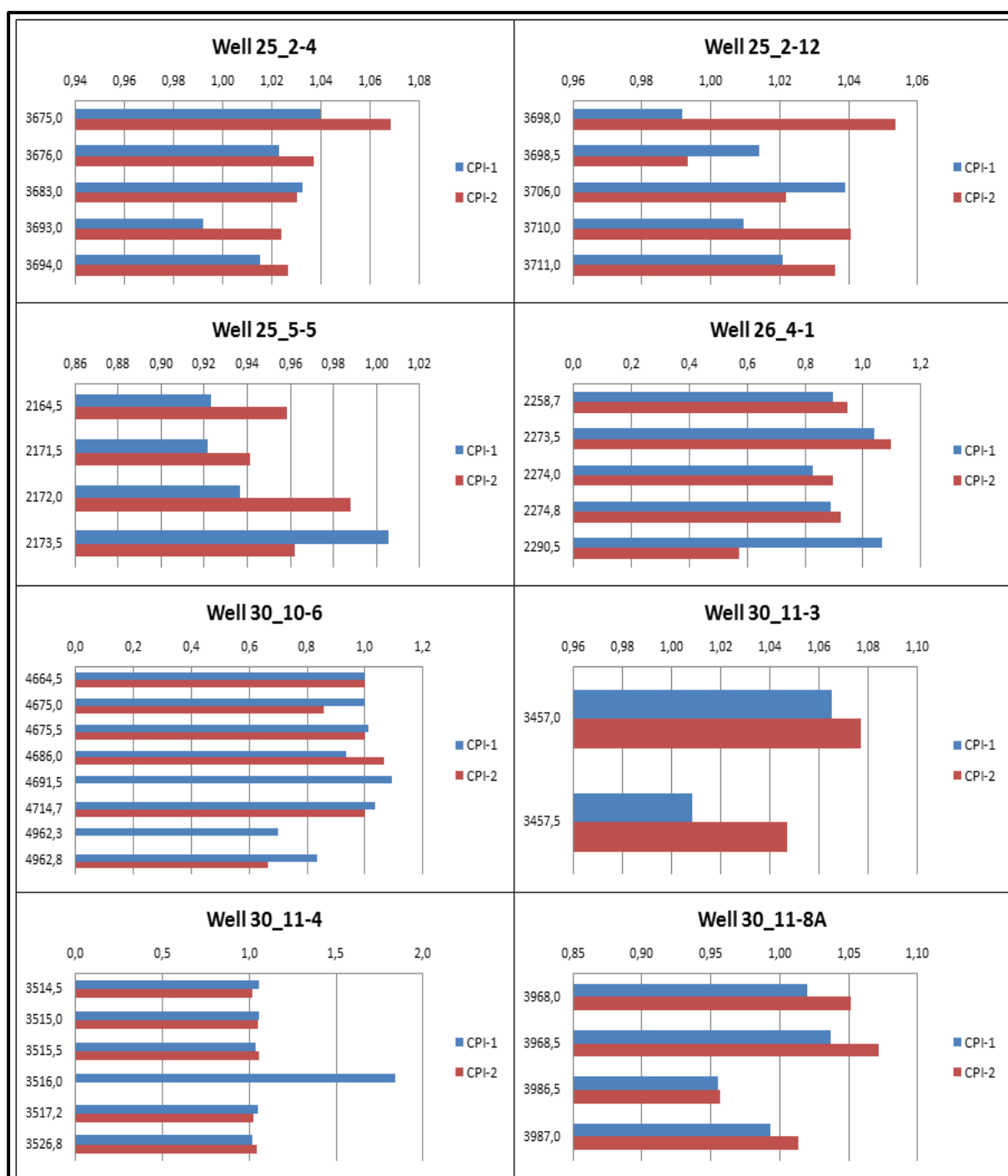


Fig. 5.10. The bar charts demonstrating the CPI values approaching unity and depicting mature samples which could certainly be sourced from siliciclastic source rocks. CPI-1 and CPI-2 are plotted along x-axis and depth (m) is plotted on the y-axis. The residual petroleum or bitumens are certainly mature for CPI-1 which reflect C_{22} to C_{24} range and is often higher for CPI-2 (see text for discussion).

The values for vitrinite reflectances have been calculated based on the measurements of medium range aromatic maturity parameters such as methylphenanthrenes and methyldibenzothiophenes. Both these parameters describe maturity, but in a variable range

of oil window (Karlsen and Skeie, 2006). Methylphenanthrenes characterize generally the higher end of the oil window while methyldibenzothiophenes are limited to the earlier part and are generally more correctly reflecting maturities in the early phase of the oil window (Karlsen et al., 1995).

Thus the parameter 25 of the calculated vitrinite reflectance, the sulphur aromatics, reflects better maturity for marine source rocks at the early stages of the oil window. This is due to the lower stability of sulphur molecules (thiophene ring) that makes it more labile. It seems that most of the oils started to expel effectively around an average value of 0.85%Rc and this is similar to Haltenbanken samples as observed by Karlsen et al., (1995).

If the maturity assessment is based on methylphenanthrenes, i.e. parameters 23, 24 and 25, it is evident that the values are more or less inclined towards 1%Rc (Fig 5.11) which could reflect progressive infill of the structure with more mature oil in the lower sections.

The samples from the well 30/10-6 are reflecting a higher maturity than all other samples in terms of phenanthrenes, approaching a value of 1.4%Rc, yet the sulphur aromatics are uniform around an average value of 0.85%Rc. This discrepancy is most likely caused by the quality of vitrinite precursors in the source rock of which the phenanthrenes have been originated, i.e. it is possible that some of the vitrinite in the source rock kerogen was partly oxidized or resedimented.

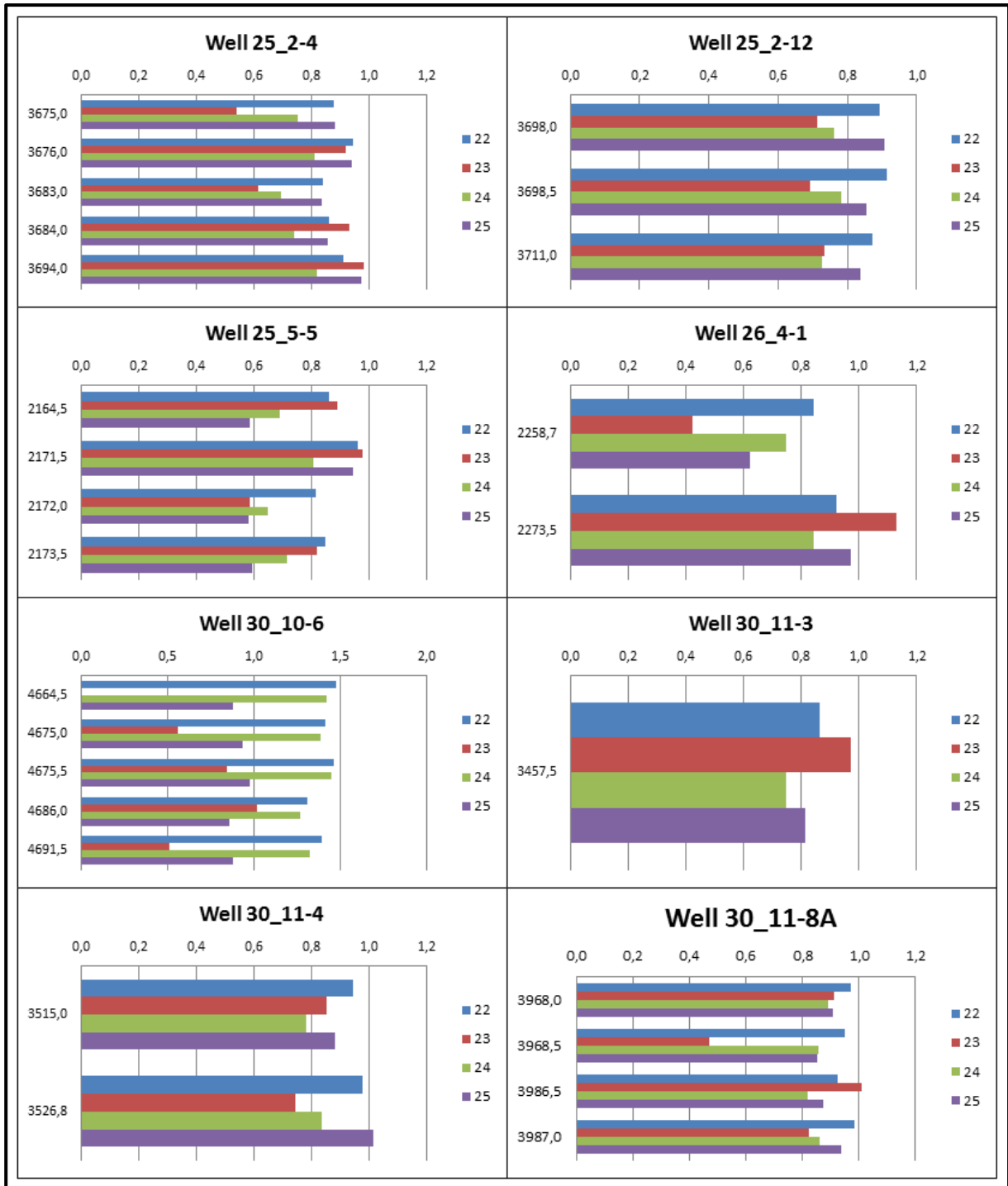


Fig. 5.11. Bar charts showing the calculated vitrinite reflectance of medium range parameters along the x-axis and depth (m) along the y-axis reflecting peak oil window which means that the bitumen from these wells was generated at maturities ranging from c. 0.85%R_c to c. 1%R_c with even higher maturities from well 30/10-6. The similarity observed between parameters 22 and 24 may be due to the application of similar isomer pairs. (22 = $R_{m(1)} = 1.1 \cdot \log_{10} \text{MPR} + 0.95$, 23 = $\%R_c = 0.6 \cdot \text{MPI} + 0.4$, 24 = $\%R_o = 2.242 \cdot \text{MPDF} - 0.166$, 25 = $R_{m(2)} = 0.073 \cdot \text{MDR} + 0.51$).

Maturity assessment from biomarkers

The heavier portion of petroleum holds long chain biomarkers whose maturity, in some cases, may differ from medium range parameters (Karlsen et al., 2004). The reduced concentrations of biomarkers are either due to increased maturity (Mackenzie et al., 1985) or phase fractionation (Karlsen and Skeie, 2006). Some of the most commonly used thermal maturity parameters are saturated and aromatic biomarker compounds which may result from either thermal cracking (including aromatization) or isomerization. The approximate ranges of these parameters in correspondence with the stages of oil generation and vitrinite reflectivity have been described in fig 3.18.

20S/20S+20R and $\beta\beta/(\beta\beta+\alpha\alpha)$ of C₂₉ steranes

The relationship between two maturity parameters 20S/20S+20R and $\beta\beta/(\beta\beta+\alpha\alpha)$ of C₂₉ steranes is shown in figure 5.12. 20S/20S+20R shows the maximum value of 0.55 around maturity of Rc=0.9% whereas $\beta\beta/(\beta\beta+\alpha\alpha)$ reaches a maximum value of 0.7 around maturity of Rc=0.9% (Peters and Moldowan, 1993; Peters et al., 2005). The parameter 20S/20S+20R is considered best for the petroleum sourced from marine siliciclastic source rocks (Peters et al., 2005).

The values for 20S/20S+20R and $\beta\beta/(\beta\beta+\alpha\alpha)$ of C₂₉ steranes are 0.34 to 0.57 and 0.53 to 0.67 respectively for the whole sample set where slightly higher values for 20S/20S+20R than the proposed range could possibly be due to the partial biodegradation of C₂₉ $\alpha\alpha\alpha$ R-steranes (Hunt, 1996; Peters et al., 2005). Moreover, the data in the cross plot is showing a linear relationship between both parameters which is indicating high maturity of the samples and uniformity in organic source rock facies.

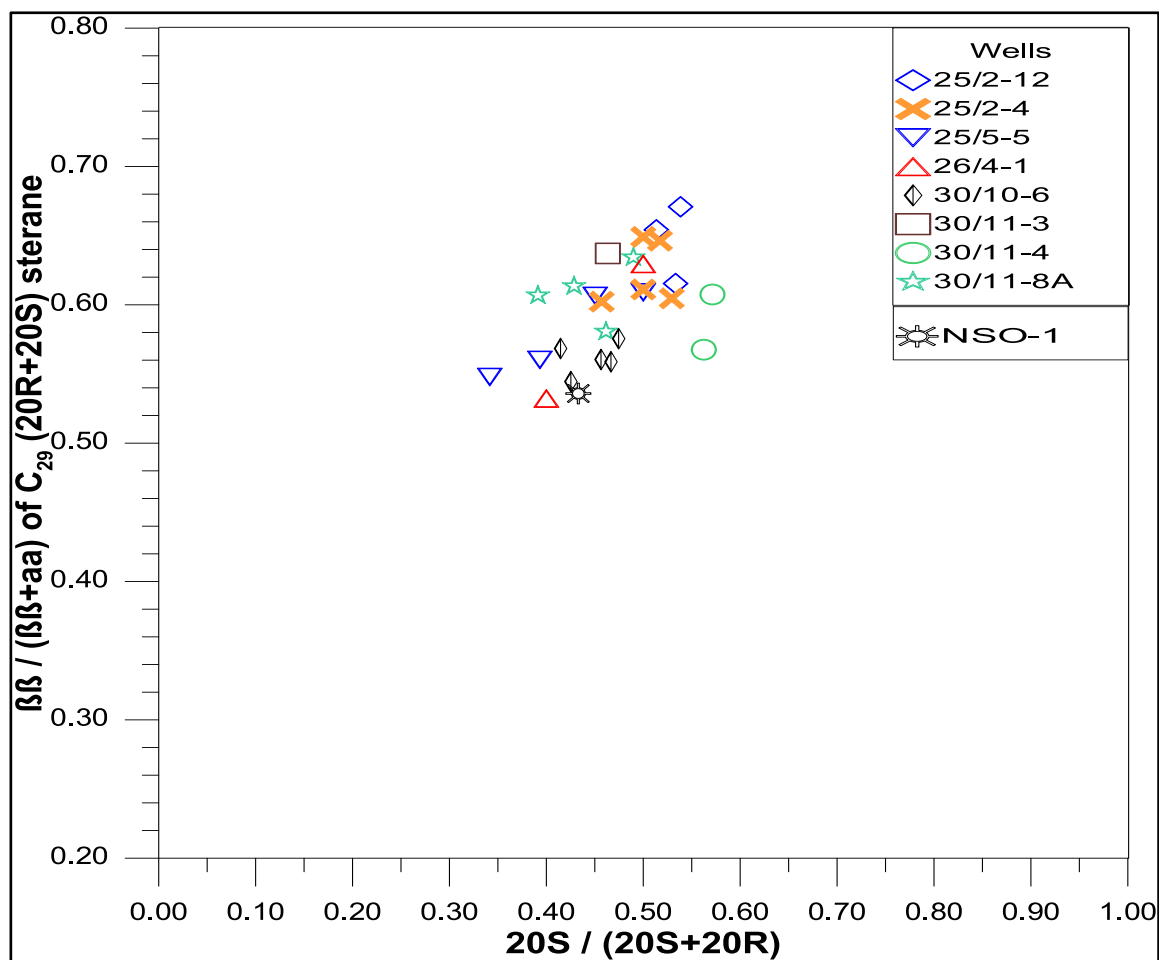


Fig. 5.12. Cross plot of maturity parameters $20S/20S+20R$ and $\beta\beta/\beta\beta+\alpha\alpha$ (Modified after Seifert and Moldowan, 1986) showing tendency for a linear relationship and representing that all bitumen samples have a maturity of at least 0.85%Rc-0.9%Rc and this is generally higher than for the NSO-1 oil from the Oseberg.

22S/22S+22R and MPDF

The equilibrium value for the hopanes ($22S/22S+22R$) is between 0.57 to 0.62 (Seifert and Moldowan, 1986) and this is reached already at a maturity of Rc=0.6% which shows that the residual oils have been migrated and not in-situ generated. This ratio does not increase with higher maturities. The values vary from 0.52 to 0.66 which indicates that most of the samples from the dry wells are in the peak oil window. The methylphenanthrene distribution factor is calculated from 4 isomers of methylphenanthrene, i.e. 3-, 2-, 9- and 1-MP, and it determines the aromatic maturity of the extracts. Samples from the well 30/10-6 are showing higher maturity while all other samples are essentially showing uniform maturity distribution in terms of hopanes (Fig 5.13).

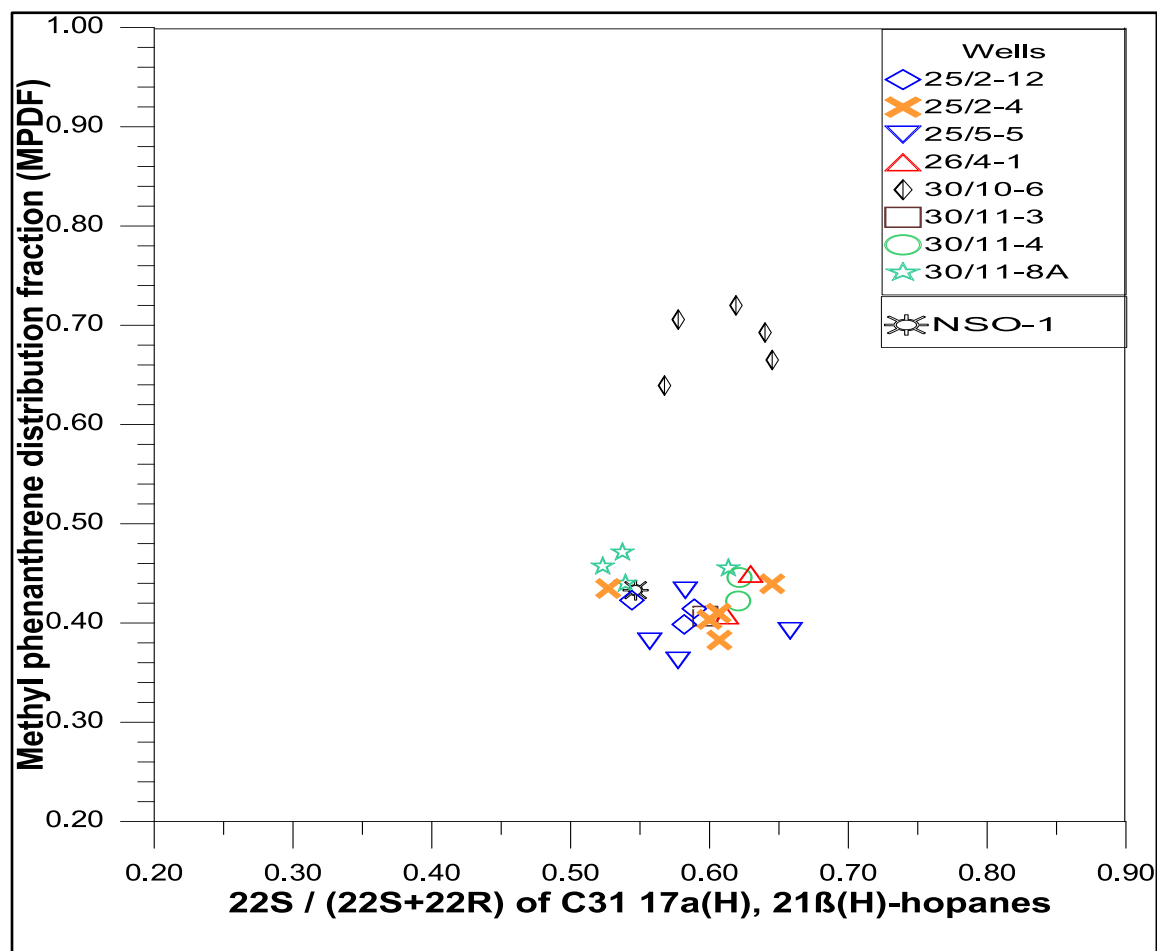


Fig. 5.13. A cross plot of medium range HC parameter (y-axis) against biomarker range parameter (x-axis). Bitumen from well 30/10-6 shows a higher maturity than the other samples.

20S/20S+20R and 22S/22S+22R

Both these parameters define the degree of isomerization of respectively steranes and hopanes and are for reservoir studies mainly used to show that bitumen is allochthonous (migrated) and not in-situ generated. A relationship between them is shown in a cross plot (Fig 5.14). The equilibrium values for both parameters are discussed earlier. It is clear that the data in the cross plot is clustered together (almost circular) which is essentially reflecting that both the steranes and hopanes are fully isomerized. Hence, reflecting the source rock of the residual oils to have been expelled from a mature source rock and not from in-situ organic matter in the reservoir.

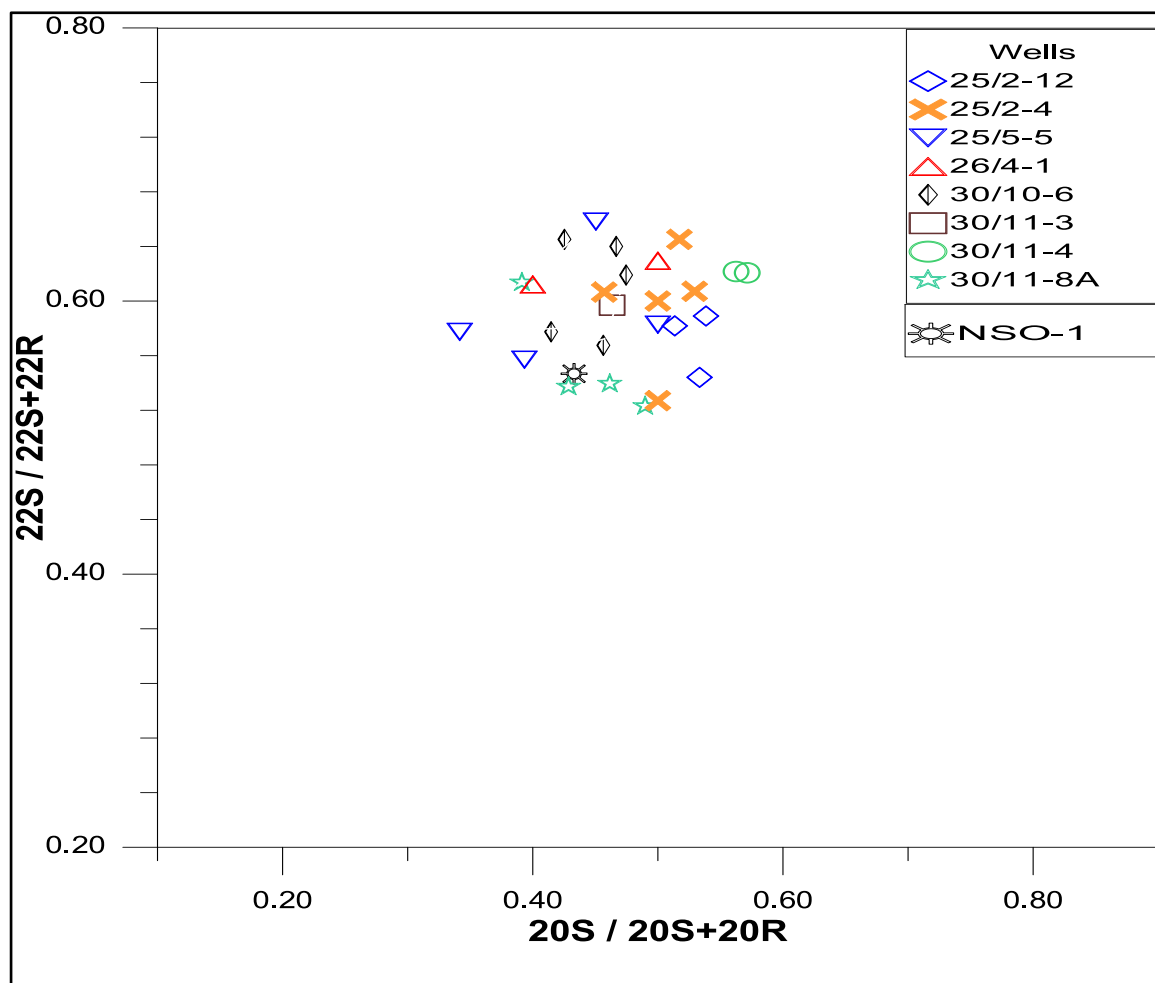


Fig. 5.14. Cross plot demonstrating that the bitumen from the dry wells based on hopanes and steranes isomerization parameters are fully isomerized.

C_{24} tetracyclic terpanes/ C_{30} $\alpha\beta$ -hopane and C_{23} - C_{29} tricyclic terpanes/ C_{30} $\alpha\beta$ -hopane

Both these parameters are highly affected by phase fractionation, yet there exist a strong maturity relation between them which can be used to interpret the degree of maturation. As suggested by Karlsen and Skeie (2006), the vertical migration of petroleum results in phase separation which may cause variation in the composition of petroleum. One such variation is the enrichment of tricyclic terpanes in the petroleum which have high GOR.

The data in the cross plot (Fig 5.13) is showing a linear relationship between the samples and high maturities. The even higher values for the well 30/10-6 could indicate more condensate type facies which contain shorter molecules than the longer ones.

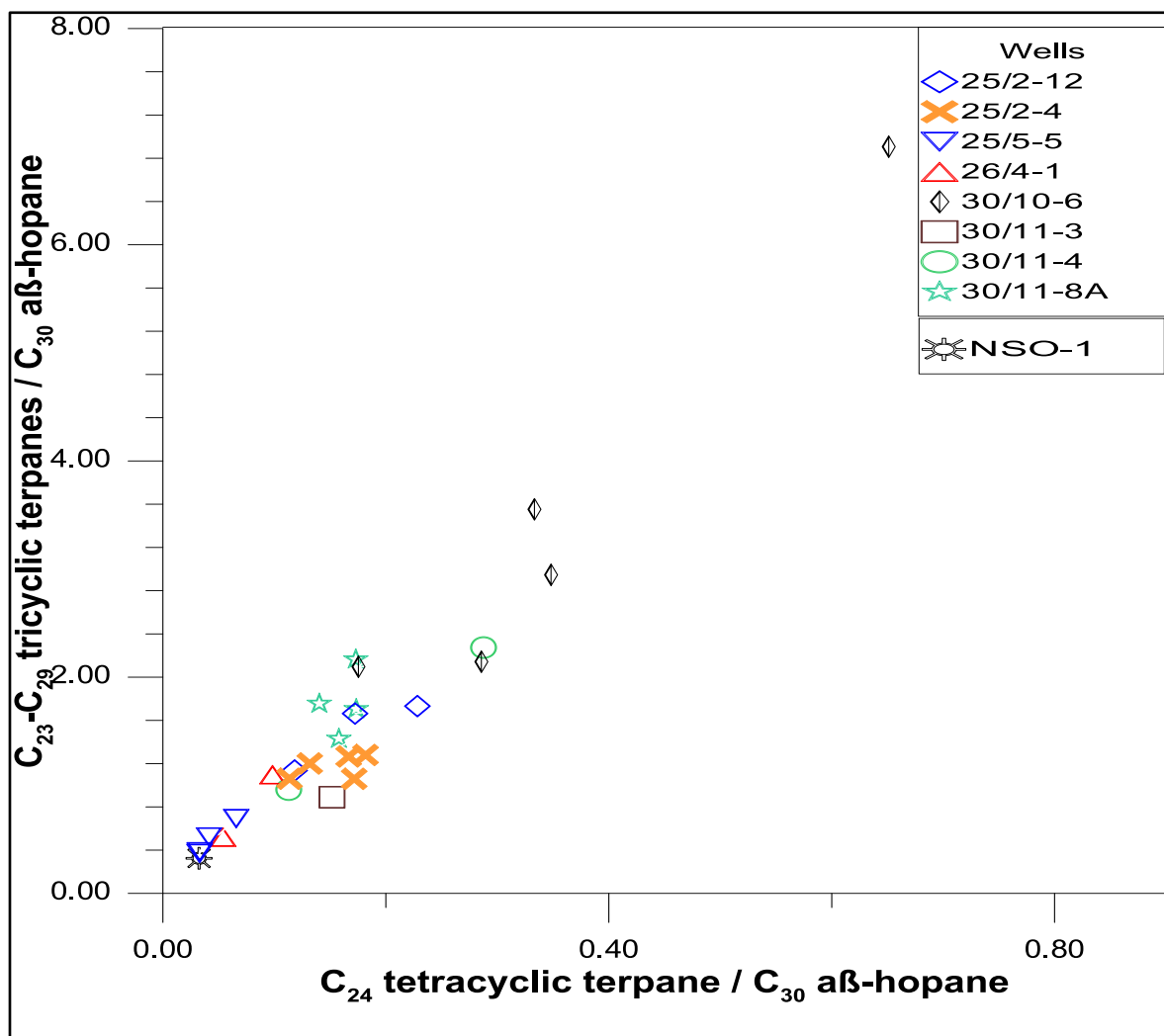


Fig. 5.13. The cross plot is showing relationship between two biomarker maturity parameters, i.e. tetracyclic and tricyclic terpanes and hopanes. The data in it is suggestive of sourcing from uniformly the same source rock facies.

Ts/Ts+Tm and Diasteranes/Diasteranes+Regular Steranes

Both are typical classic maturity and facies parameters where the diasteranes ratio is not much affected by phase fractionation and GOR. However, it may be affected by siliciclastic versus carbonate source rock facies. Oils sourced from carbonate source rocks have generally lower ratios for the diasterane parameter than oils sourced from clastic source rocks (Peters and Moldowan, 1993). Ts/Ts+Tm can also be influenced by source facies. The data in the cross plot (Fig 5.14) is showing high maturities for the samples and a linear relationship and this supports that the potential facies effect on these parameters is absent, i.e. the reservoir bitumen is of generally speaking the same organic source rock facies.

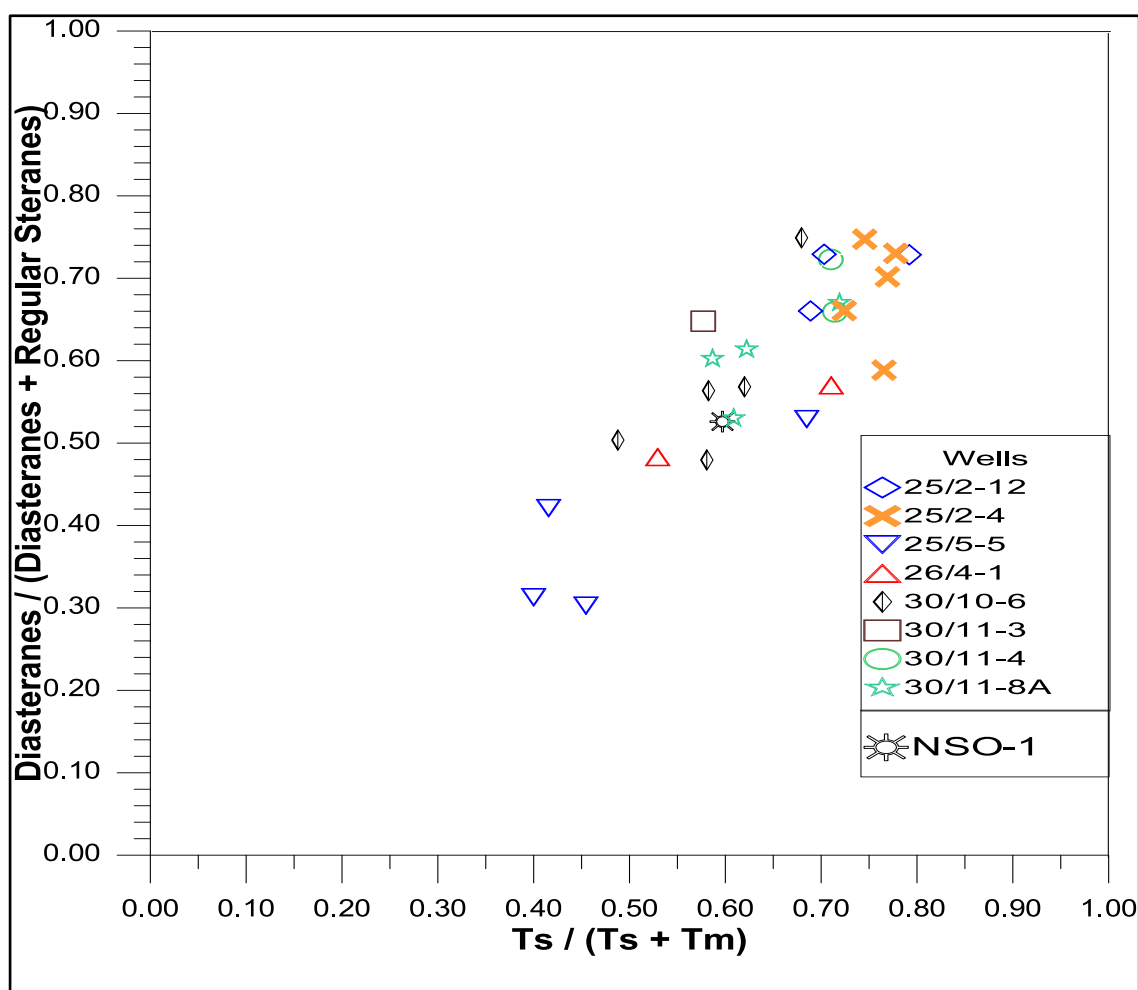


Fig. 5.14. A cross plot of facies and maturity parameters with $Ts/Ts+Tm$ along the x-axis and diasteranes/diasteranes+regular steranes along the y-axis determining the maturity of bitumens in the dry well samples. Both parameters may be affected by organic facies. High maturities are indicated for generally but to different degree and for independent organic facies reasons. Thus, the linearity does not support that more than one type of source rock formation is responsible for the migrated bitumen.

$Ts/Ts+Tm$ and $29Ts/29Ts+norhopane$

$29Ts/29Ts+norhopane$ is considered to be a maturity parameter with no influence of phase fractionation, while $Ts/Ts+Tm$ is known to be influenced by organic facies and also by phase fractionation, i.e. the GOR of the entrapped palaeo-petroleum. The lack of linearity in the data (Fig 5.15) could be indicative of different source rock facies related to the consequence of organic facies effect on $Ts/Ts+Tm$ parameter.

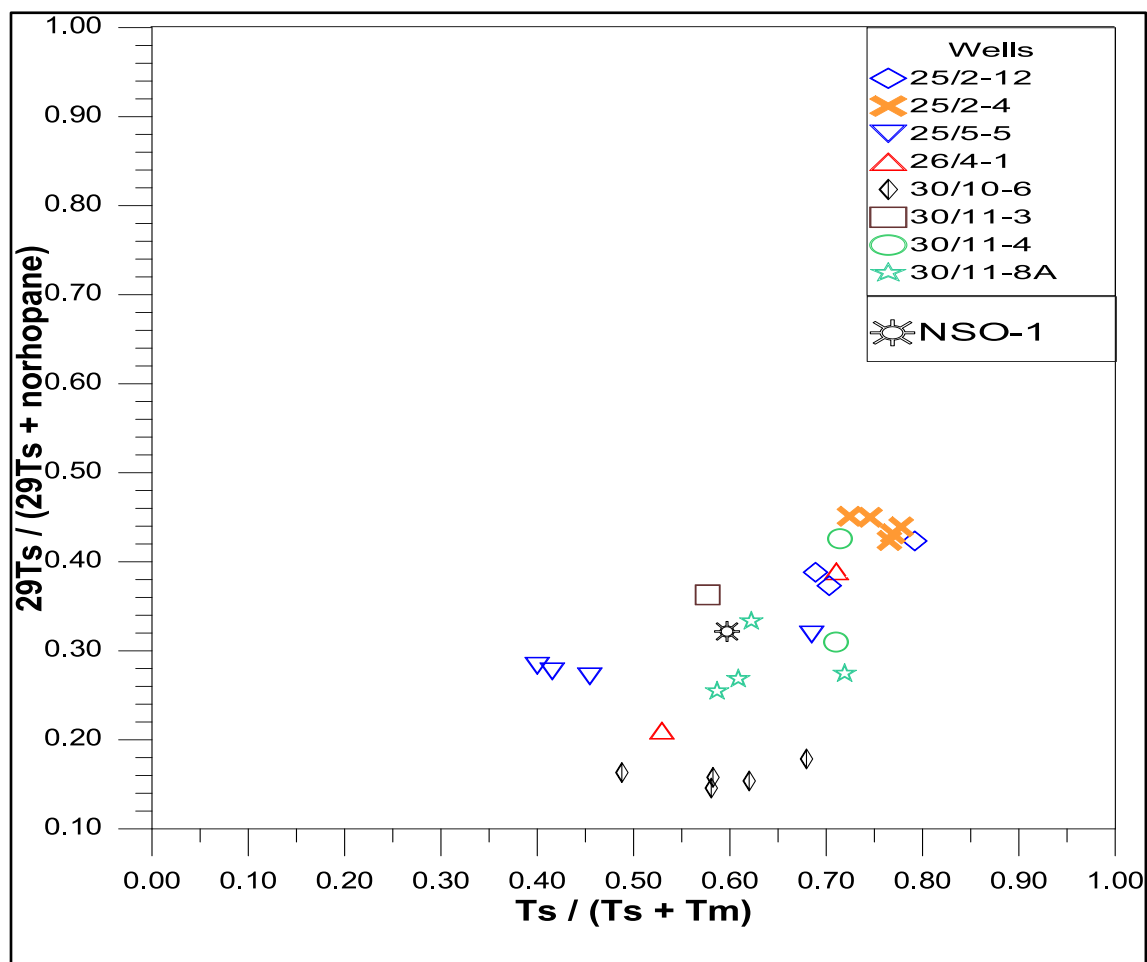


Fig. 5.15. The cross plot of $Ts/Ts+Tm$ plotted along the x-axis and $29Ts/29Ts+norhopane$ along the y-axis indicating mainly maturity. The former which can be affected by organic facies and phase fractionation with the $29Ts$ parameter not being sensitive to neither phase fractionation nor organic facies (see text for discussion).

Conclusion

The reservoir core samples from a series of dry wells located on the eastern flank of the Viking Graben have been geochemically analyzed using different analytical techniques, i.e. gas analysis from inclusions, GC-FID, GC-MS and Iatroscan TLC-FID. The results lead to the following conclusions:

- There is clear evidence for the presence of migrated petroleum in these dry wells as reflected by the Iatroscan analysis. These so-called dry wells contain free hydrocarbons to be extracted and the composition of such hydrocarbons as well as the maturity and organic facies parameters show irrefutably that the bitumen is migrated palaeo-oil.

- The wetness parameters of gas liberated from inclusions based on the percentage of C₂+ compounds reveal that all the samples are either oil-wet or condensate-wet suggesting higher maturities, i.e. oil-window maturities. The samples from well 30/10-6 reflect clear characteristics of condensate wet gas origin, and this goes along with generally high scores on the maturity parameters in this well.
- The depositional environment as inferred from isoprenoids, steranes and n-alkanes is more likely open marine with very little terrestrial input and the bitumen in the wells is considered to be sourced from algal type II kerogen.
- The samples are highly mature based on the vitrinite reflectances of non-biomarker maturity parameters (methylphenanthrenes and methyldibenzothiophenes) with values more than 0.8%R_c. Moreover, the samples show yet higher maturities based on the evaluation from biomarker maturity parameters reflecting origins from mature source rock kitchen.

6. Facies and maturity comparison of bitumen from dry wells with the Rind discovery and the Frøy field

The Rind Discovery and the Frøy Field are located in blocks 25/2 and 25/5 respectively on the Norwegian continental shelf. The approximate distance between these two fields is 7 km (Fig. 5.1). All the wells in both fields penetrate the Tarbert and Ness formations except well 25/5-2 and 25/2-15R2 in the Frøy and Rind, respectively, which are drilled down to the Tarbert Formation.

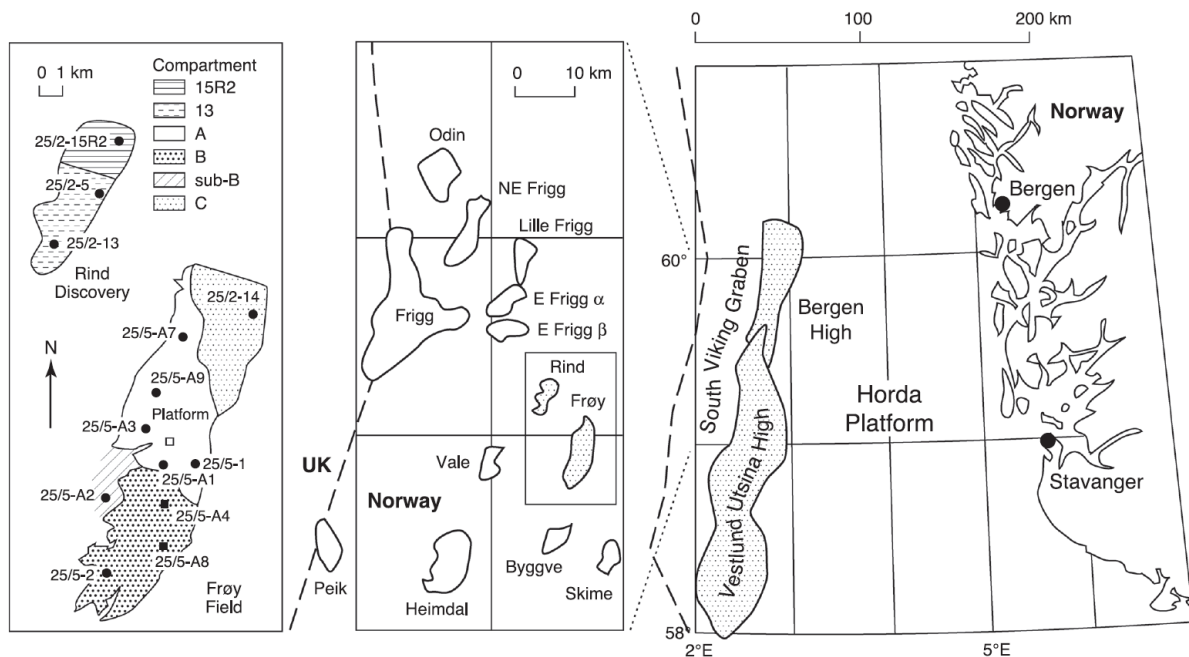


Fig. 5.1. Map representing the main structural elements in the Frigg area. The well locations alongwith the main structural compartments of the Frøy Field and Rind Discovery are also shown (Bhullar et al., 2003).

The main Rind structure is penetrated by two wells, 25/2-5 and 25/2-13, which contains gas/condensate, oil and water as mobile phases. The other well, 25/2-15R2, is drilled across a major fault, located northeast of the Rind Discovery, which contains only residual oil present in the Statfjord Formation and Brent Group (cf. Bhullar et al., 1999b). The oils encountered in the Rind discovery show a significant variation from the fluids found in the Frøy field. The clear differences in maturity between the oils of the Frøy indicate that the most mature oils are present at the crest of the reservoir and lower maturity oils are encountered towards the flanks. A clearly distinguishable and individual petroleum population exists for both fields in

terms of facies and maturity biomarker parameters of DST oils and core extracts (Bhullar et al., 2003). The source rock for the Rind Discovery is the Heather Formation which was deposited under less anoxic environment and is more terrestrially influenced (cf. Thomas et al., 1985). The most likely source rock candidates for the oils in the Frøy Field are considered to be the Draupne Formation.

Several maturity and facies parameters are used in different cross plots to show a comparison between the core extracts of dry wells, and the DST oils and core extracts from the Rind Discovery and the Frøy Field. These diagrams are discussed below.

Organic Facies

Facies defined by isoprenoids and n-alkanes

The facies parameters including ratios of isoprenoids (Pr and Ph) to n-alkanes have been used to define the environment of deposition for the dry wells and producing oil fields. Figures 5.2 and 5.3 clearly show that almost all the samples from the dry wells lie in the same maturity range as outlined by the Rind and the Frøy fields, yet Rind is showing even higher maturity. Thus, overall they all seem to lie in the same range as the producing oil fields showing expulsion of oil from mature source rock kitchens of the same general maturity as for the Rind and the Frøy. In terms of organic facies, the dry wells at the most show a mixed marine environment except well 25/5-5, while Rind samples are possibly slightly more terrestrially influenced and from a less anoxic source rock environment (Fig 5.2).

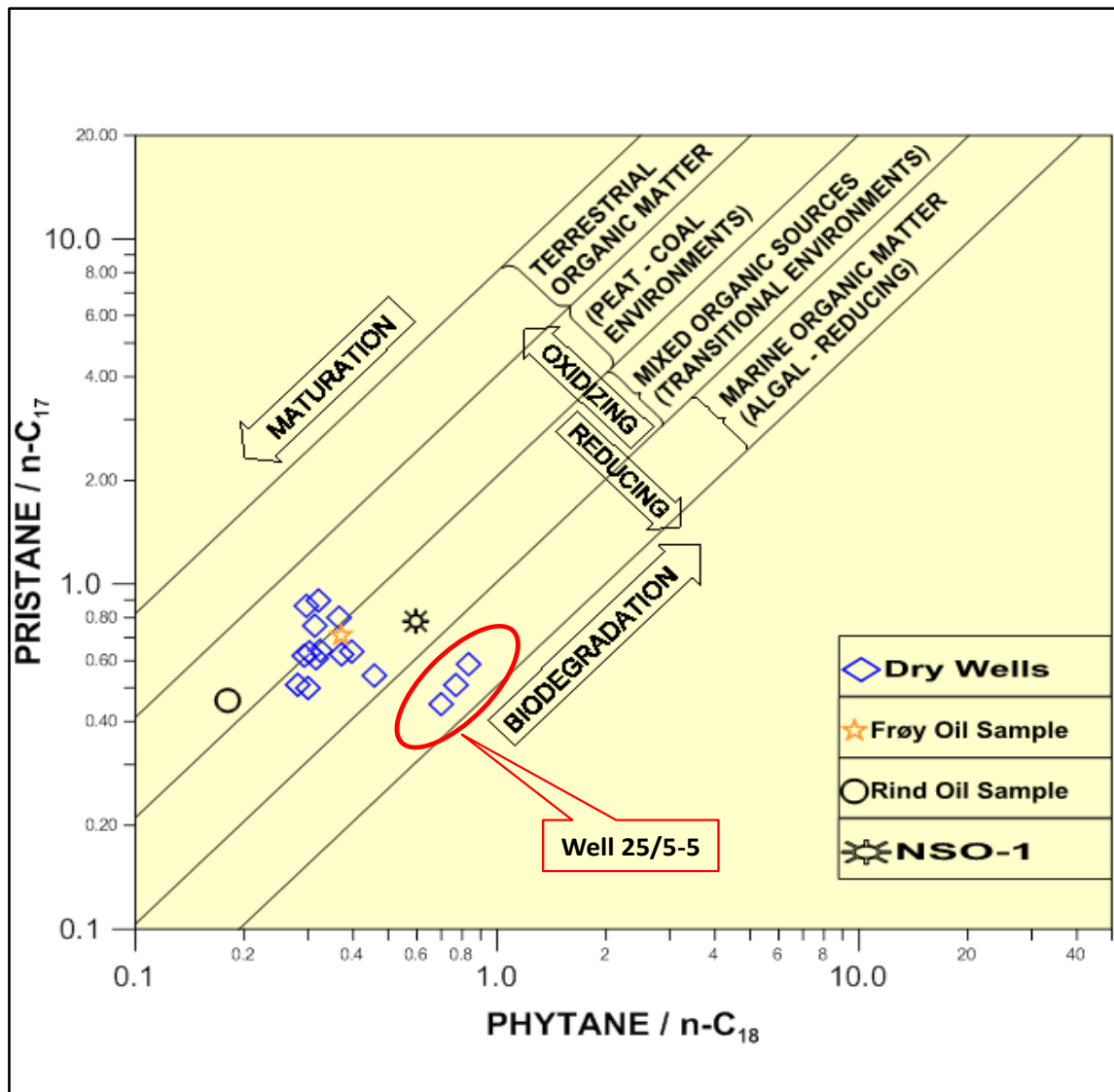


Fig. 5.2. Facies diagram proposed by Shanmugam (1985) to define the relative changes in facies. It is suggesting that essentially all the dry well samples lie within the same maturity range with even slightly higher maturity for the Rind oil sample. In terms of organic facies this is for most of the dry wells inferred to be similar to that of the Frøy, i.e. a Draupne source rock facies, apart from 25/5-5 which is more terrestrial.

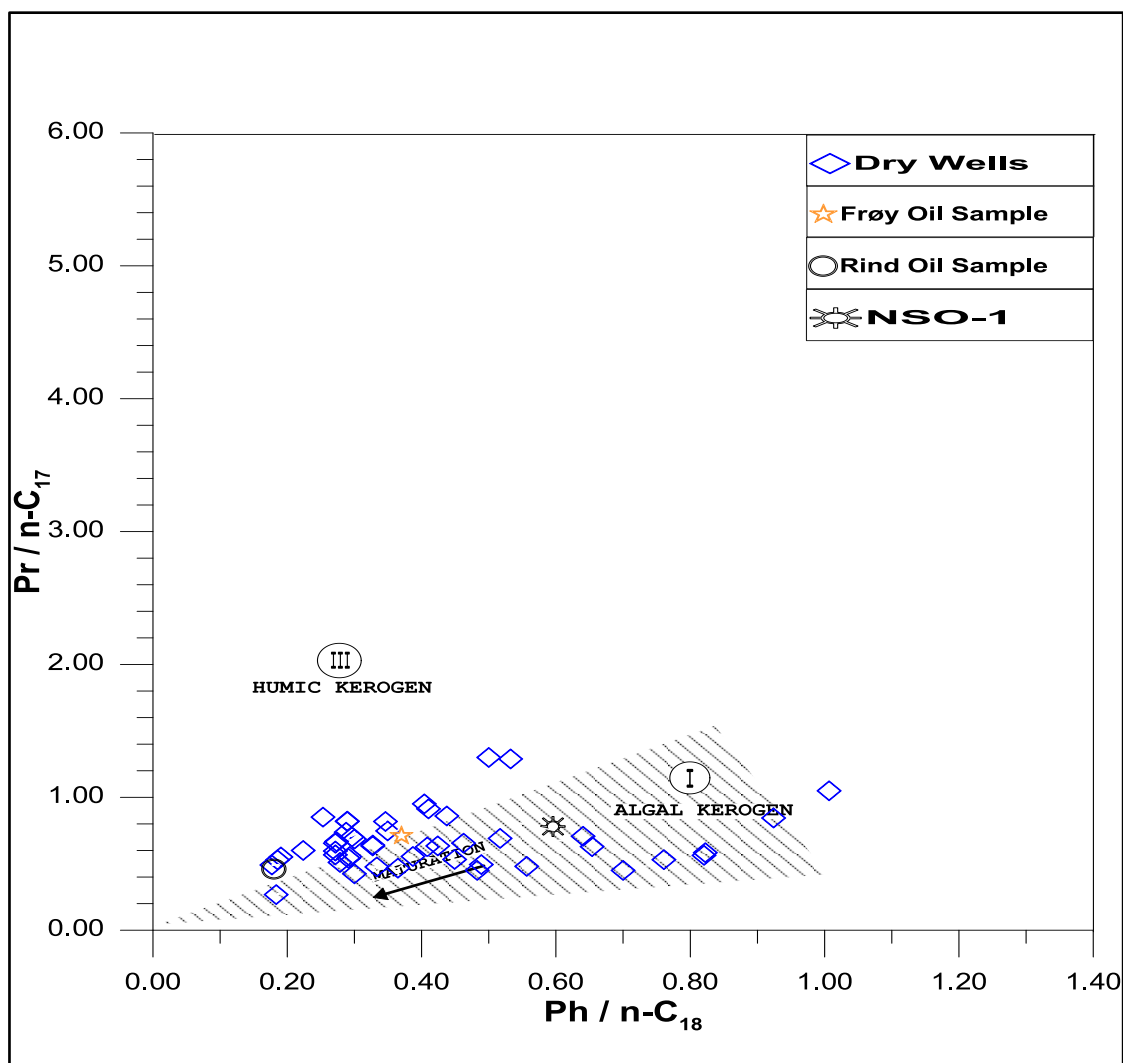


Fig. 5.3 The diagram is demonstrating that the extracts from the dry wells are grouped closely together and the maturity signature is identical to both oil fields. Although some samples from the wells 25/5-5 and 26/4-1 show lower maturity.

Facies estimation by sterane isomers

The core samples data from the dry wells is plotted in the ternary diagram in association with the core samples and DST oils from the Rind Discovery and the Frøy Field (Fig 5.4). They are all falling nearly in the same part of the diagram signifying closeness in terms of organic facies and maturity.

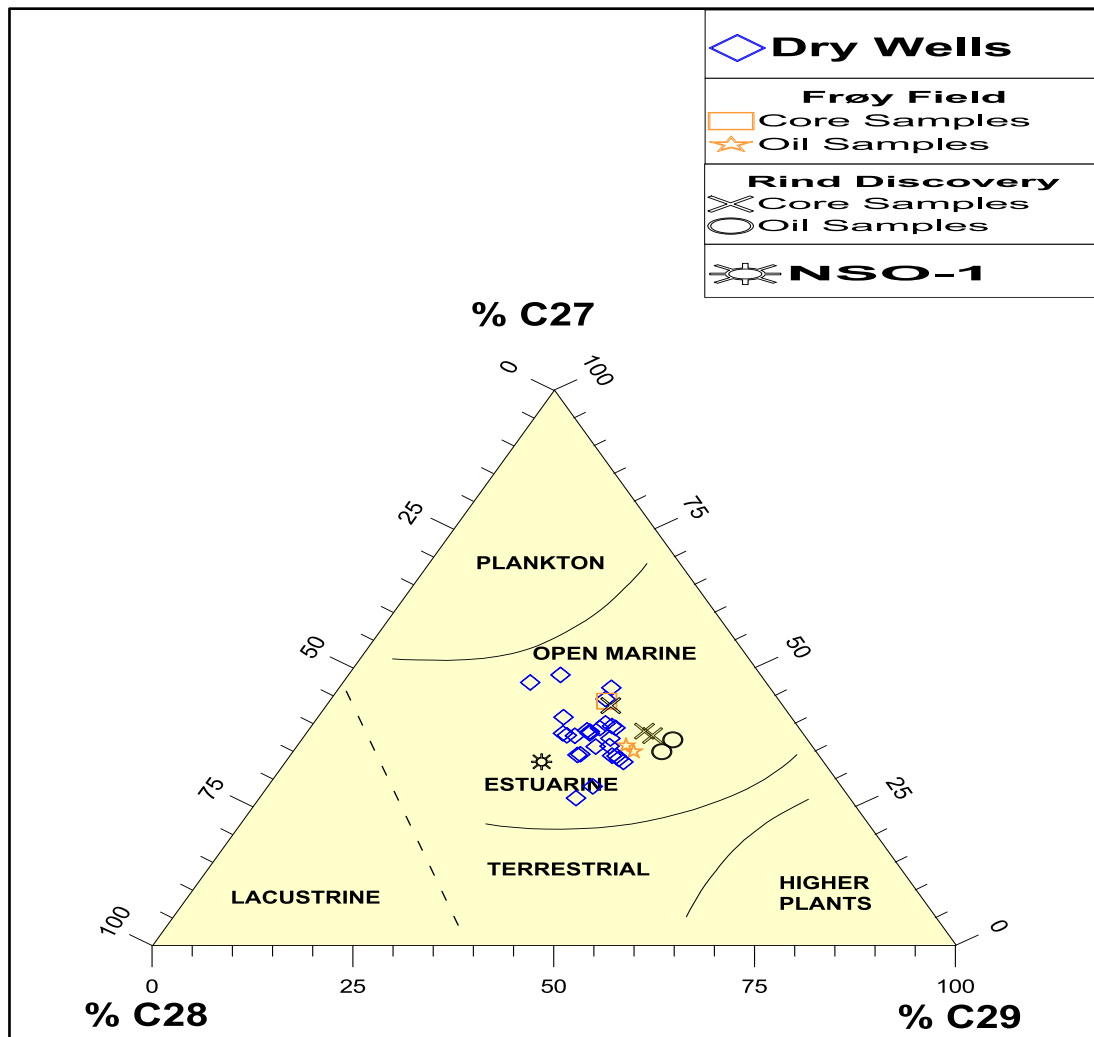


Fig. 5.4. Ternary diagram showing the distribution of steranes (C_{27} , C_{28} and C_{29}) used to determine the organic source rock facies of oils. All the samples from the dry wells, the Rind and the Frøy fields are plotted in a general region with dry wells essentially indicating mixed marine environment and marine source rocks, however, some are likely reflecting closeness proximity to the coastline. Thus, it is concluded that the dry wells contain oil sourced basically from the same source rock facies as the Rind and the Frøy.

Maturity

Maturity assessment from biomarkers

The extracts from the dry wells are compared with the oil and core samples of the Rind Discovery and the Frøy Field in terms of biomarker maturity parameters. There seems to be a clear match in the maturity and facies signatures between the dry wells and both oil fields. However, some samples from the well 30/10-6 has shown even higher maturity. The parameters are demonstrated in cross plots and discussed below.

Ts/Ts+Tm vs 29Ts/29Ts+norhopane

The data in the cross plot is showing a clear linear trend which may be indicative of the same source rock facies feeding the reservoir. Furthermore, the dry wells show a fair similarity in maturity to the oil fields.

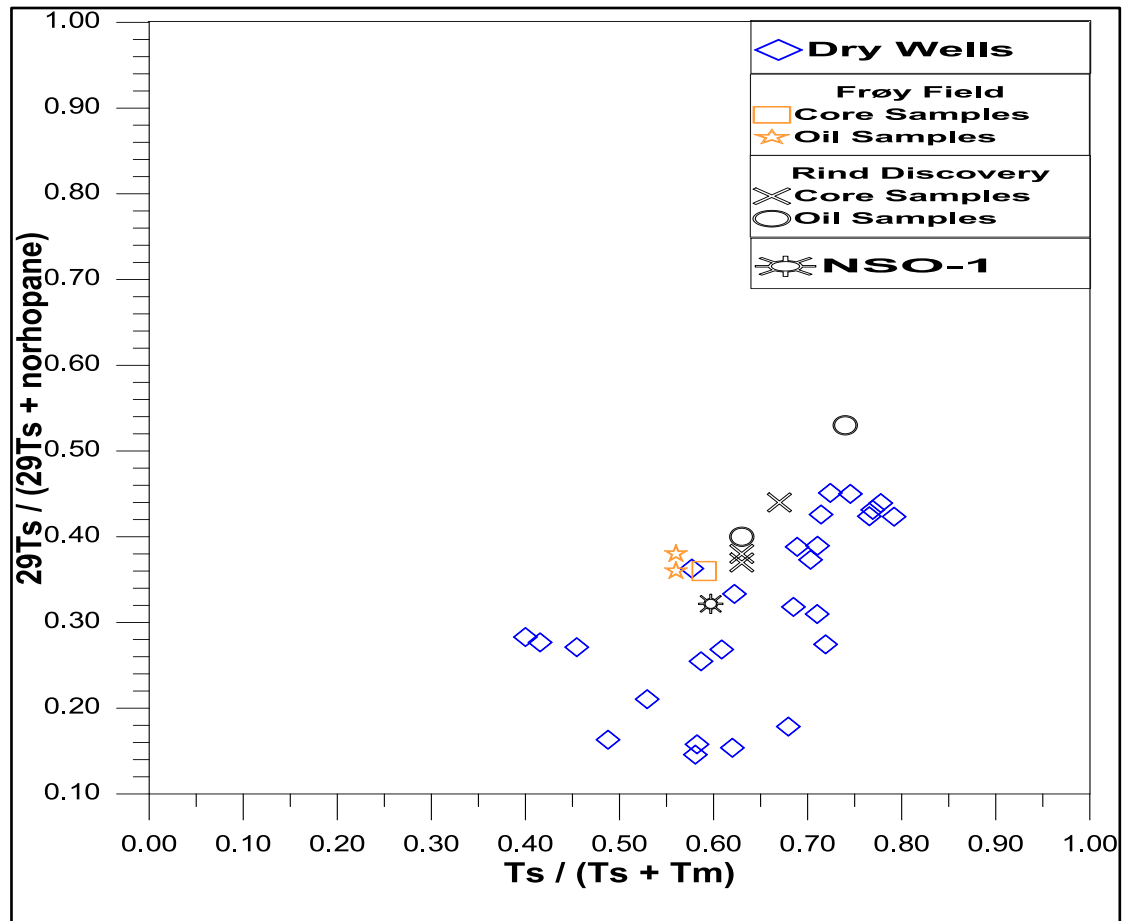


Fig. 5.5. The cross-plot of two maturity parameters of which $Ts/Ts+Tm$ is somewhat sensitive to organic facies whereas the $29Ts$ parameter is not, nor affected by phase fractionation. The maturity of dry wells closely resembles the petroleum in the Frøy and the Rind fields, but with lower and somewhat higher maturity.

Ts/Ts+Tm vs diasteranes/diasteranes+regular steranes

The sterane parameter is a very important maturity and facies parameter as it is less affected by phase fractionation and GOR. On the contrary, $Ts/Ts+Tm$ is influenced by organic facies. The relation, for the sample set, between these two parameters is shown in the figure below. The sample distribution is reflecting a broad 45 degree sloping trend indicating that the

bitumen from the dry wells span the same general maturity range as the Rind and the Frøy, with also bitumen of slightly lower and slightly higher maturity.

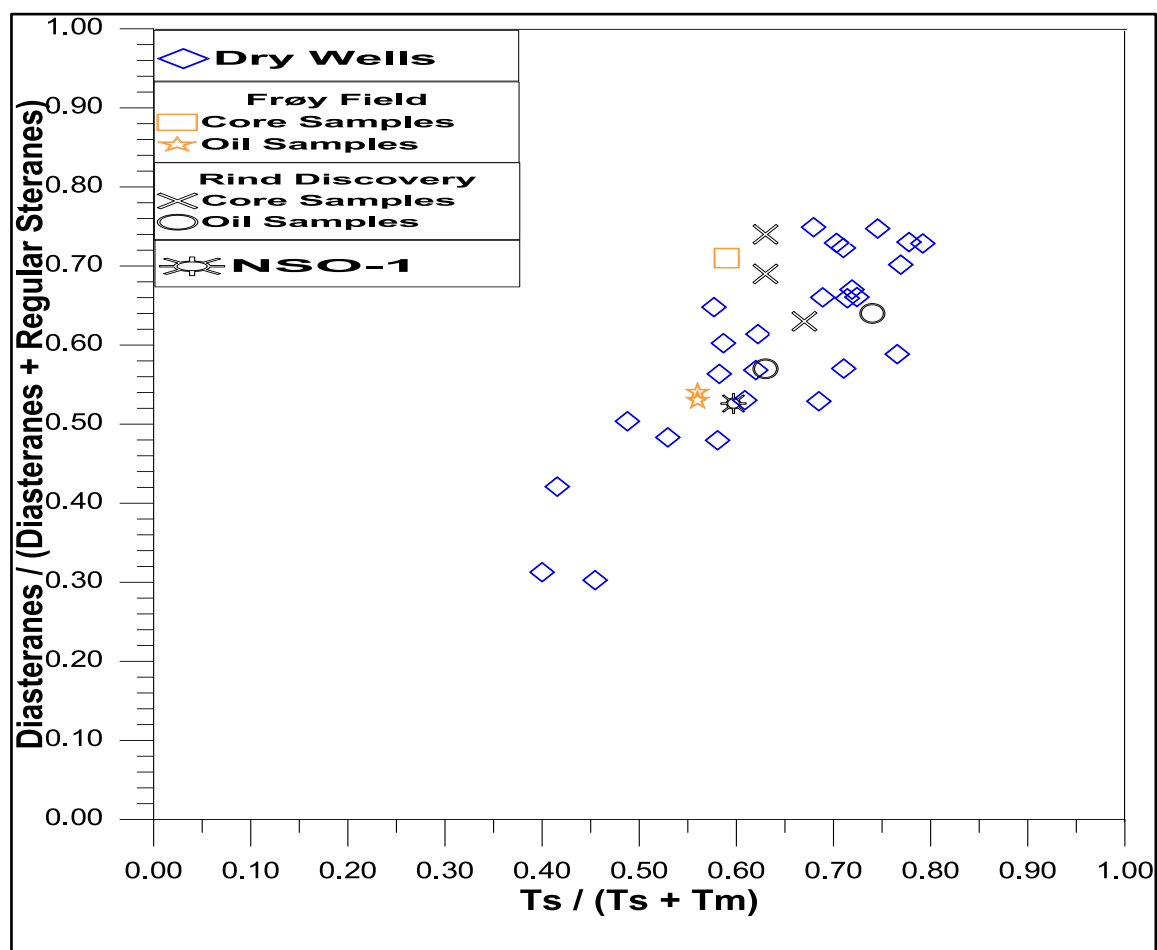


Fig. 5.6. The maturity cross plot showing a linear relation for the data set from the dry wells and the Frøy and Rind fields. Most of the samples from the dry wells have very high maturity similar to the Rind Discovery which is even higher in maturity than the Frøy Field.

20S/20S+20R vs $\beta\beta/\beta\beta+\alpha\alpha$ steranes

The data in the cross plot is showing the same maturity signatures for the dry wells as the Frøy and the Rind fields and are clustered very close together.

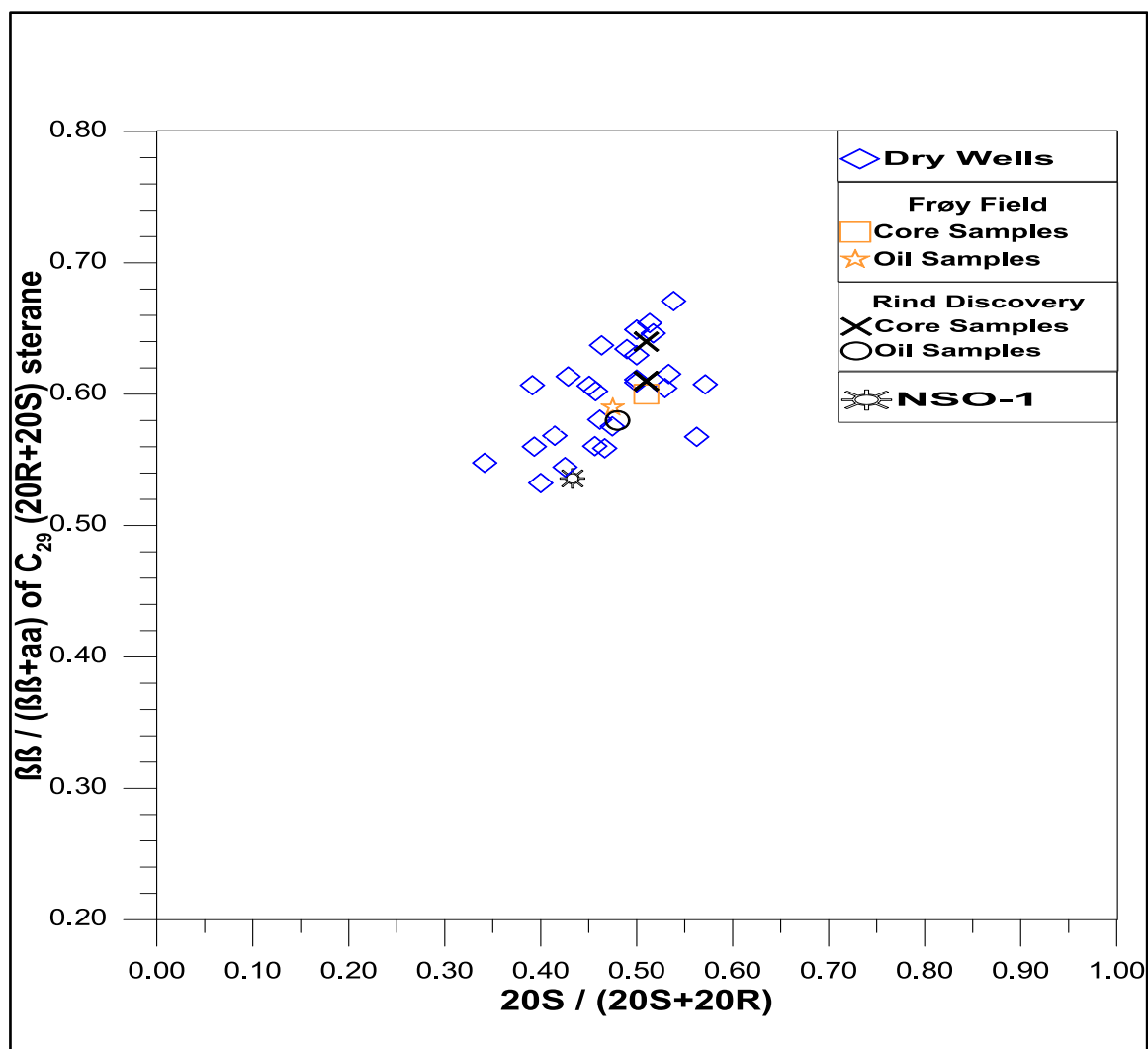


Fig. 5.7. The cross plot of 20S/20S+20R on the x-axis and $\beta\beta/\beta\beta+aa$ on the y-axis which is essentially demonstrating that all the samples from the dry wells lie in the general maturity range of the producing oil fields.

Medium range HC parameters (MPDF) vs biomarker range parameters (C_{31})

The cross plot is showing that the extracts from most of the dry wells have the same general maturity as the Rind and the Frøy field and most bitumes are therefore singular and uniformly migrated oils, yet samples from well 30/10-6 show high maturity in terms of medium range hydrocarbon parameters, i.e. MPDF. Still it is lying in the same general trend as for other samples in association with biomarker range parameters, which means that it could be a medium mature oil and more mature later arriving condensate.

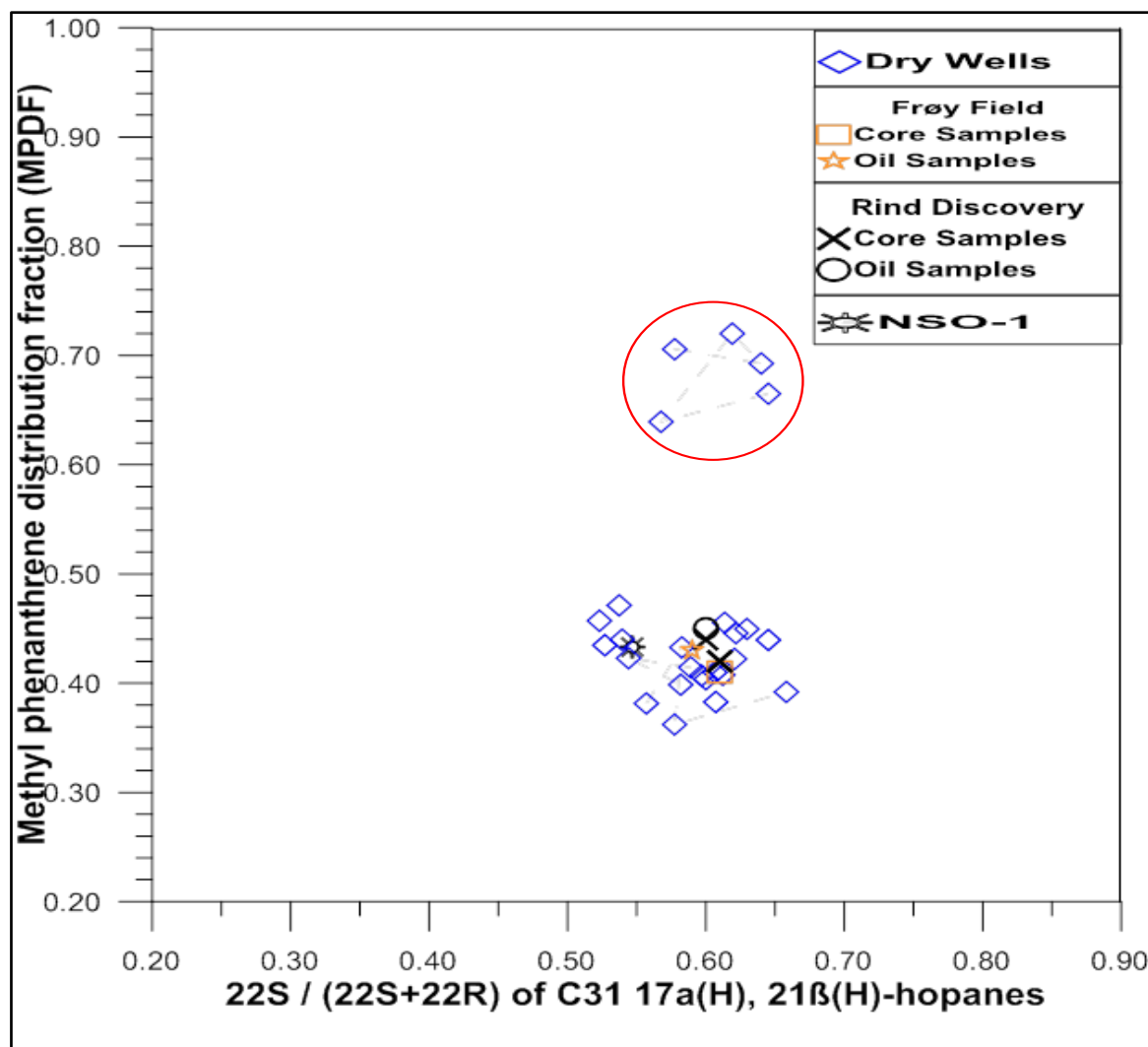


Fig. 5.8. Cross plot showing data with a biomarker range parameter along x-axis and a medium range HC parameter along y-axis. The samples from well 30/10-6 (marked in red circle) are showing higher maturity than the other samples (see text for discussion).

Hopane and Sterane isomerization parameters

A relation between hopane and sterane isomerization parameters is demonstrated in this cross plot to define the maturation level of the dry wells in relation to the oil fields. It is obvious from the figure that essentially all the samples are clustered very close to the Rind and the Frøy samples and that they are fully isomerized and of the same general maturity as the petroleum in the Rind and Frøy.

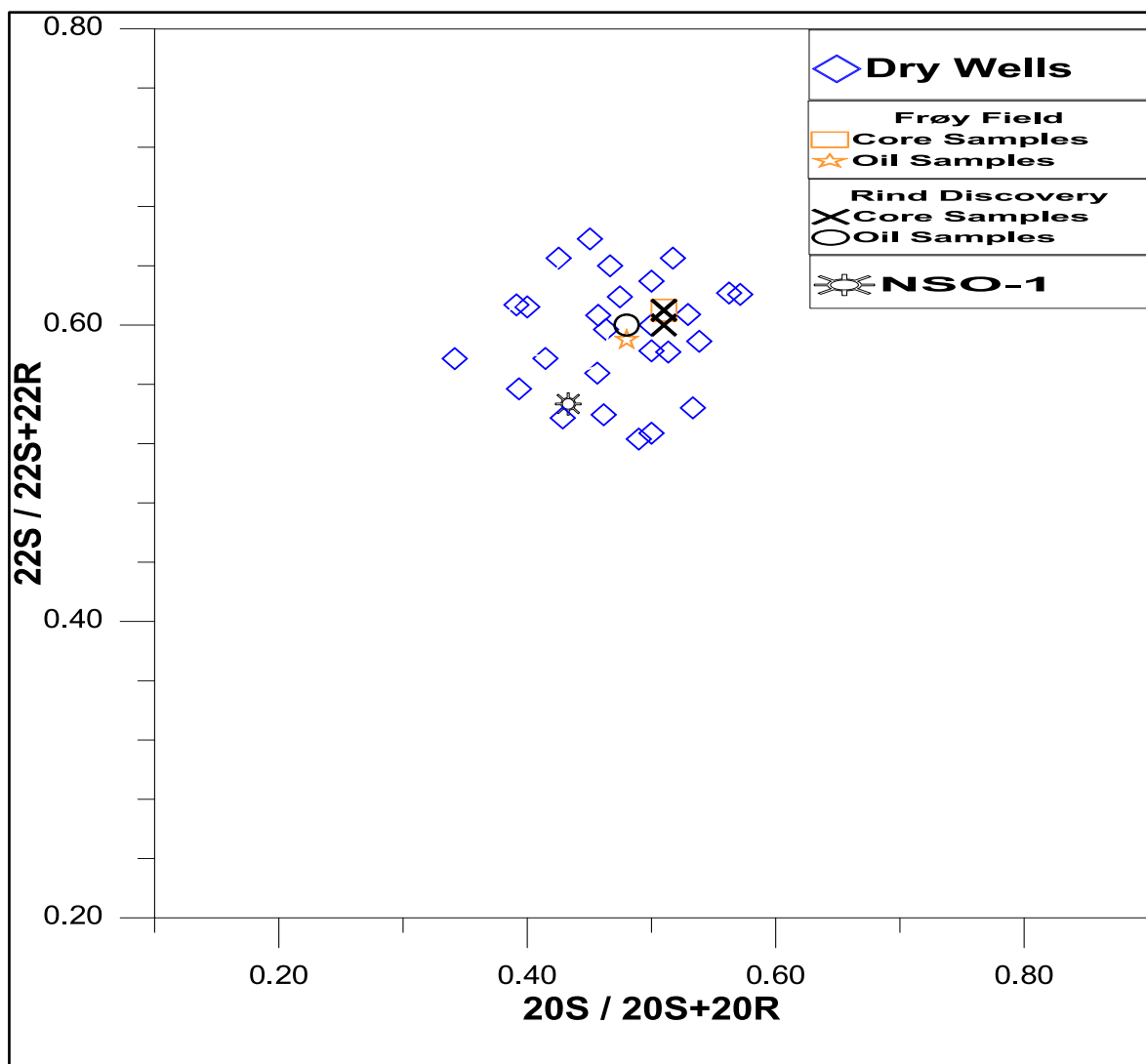


Fig. 5.9. Cross plot showing a relation between hopane and sterane parameters in which $20S/20S+20R$ is plotted along x-axis and $22S/22S+22R$ is plotted along y-axis. Both these parameters show that all samples are uniformly mature, i.e. oils from the Frøy and the Rind and bitumen from the dry wells.

C_{24} Tetracyclic terpane/ C_{30} hopane vs C_{23} - C_{29} tricyclic terpanes/ C_{30} hopane

Both parameters shown in the cross plot are facies and maturity parameters. It is obvious that the Rind has high maturity compared to most of the extracts from the dry wells and the Frøy field, yet a sample from the dry well 30/10-6 is showing high maturity. Thus, it may be an indication of a condensate. Overall all the samples are essentially plotted in the same region which certainly could indicate that the source of facies is more or less the same and represent for the bitumen samples the single petroleum migration event.

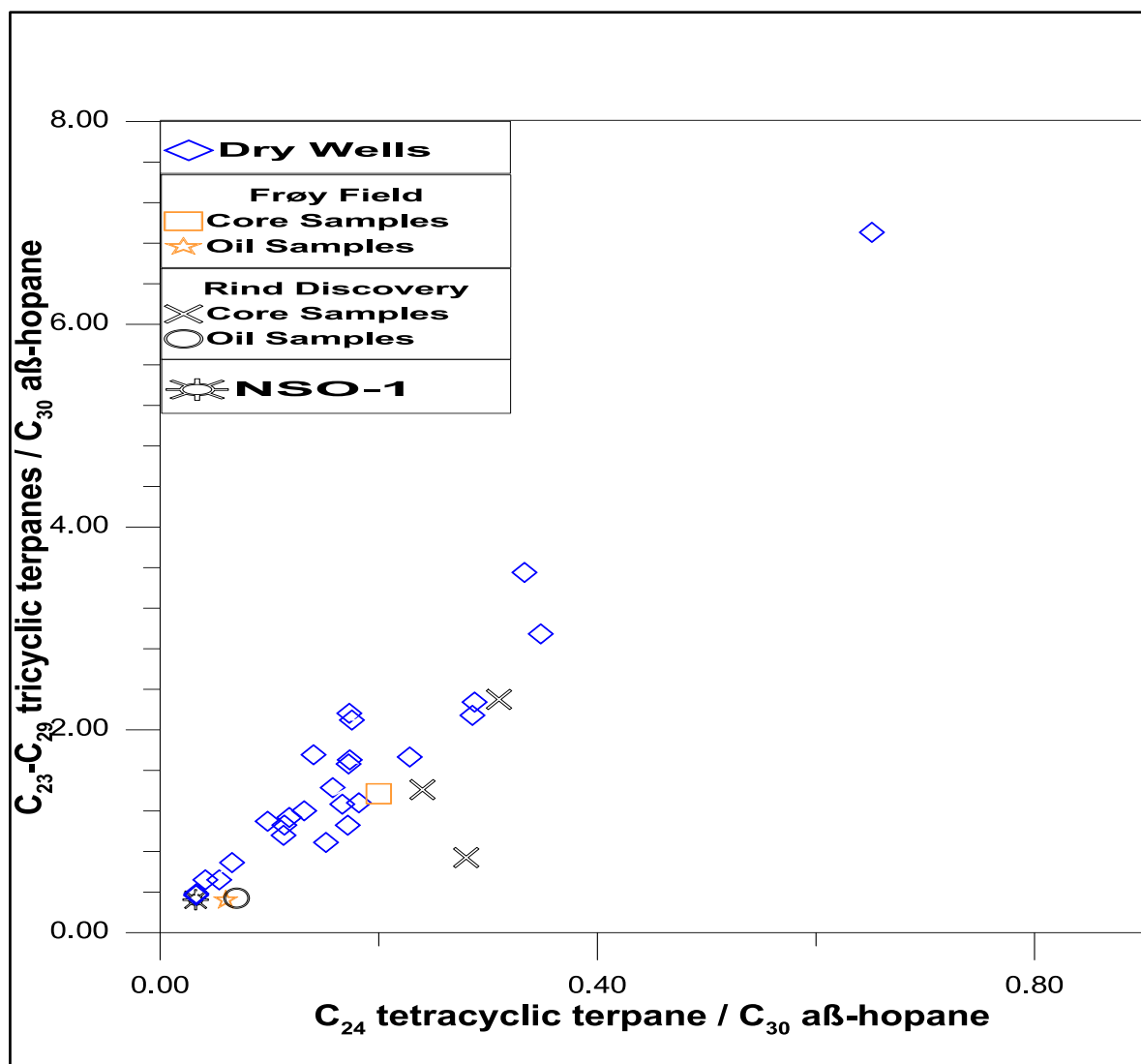


Fig. 5.10. Cross plot showing comparison of data between the dry wells and producing oil fields, the Rind and the Frøy, with tetracyclic terpanes to hopane ratio along the x-axis and tricyclic terpanes to hopane ratio along the y-axis.

Conclusion

The comparison, based on facies and maturity parameters, reveals that most of the samples from the dry wells show strong correspondence to the known producing fields, the Rind Discovery and the Frøy Field. The depositional environment tends to be mixed marine for the dry wells while the Rind and Frøy fields show terrestrial characteristics with rich oxic conditions. The source rocks which were feeding the reservoirs in the dry wells may therefore have been a Kimmeridgean equivalent which are identical for the Rind and the Frøy fields. Maturity assessment on the basis of biomarker and aromatic hydrocarbons show resemblance

with the maturity signatures from the Frøy and Rind fields, yet Rind has even higher maturity than the Frøy Field and dry wells except 30/10-6.

7. Comparison of the measured values for isoprenoids (Pr and Ph) and n-alkanes (n-C₁₇ and n-C₁₈) with the corrected

In geochemical terms, the oil that has lost much of its lighter end hydrocarbons is called a residual oil. The residual oil is hard to displace from a reservoir since it becomes immobile due to the loss of the lighter hydrocarbon fractions. The lighter hydrocarbons may be lost from the extract during core retrieval, sample handling, biodegradation and storage. This adversely affects the results of GC-FID analysis as some peaks are not representatively showing upon GC-FID chromatograms (Fig 7.1) which may mislead in determining the facies and maturity of the core samples.

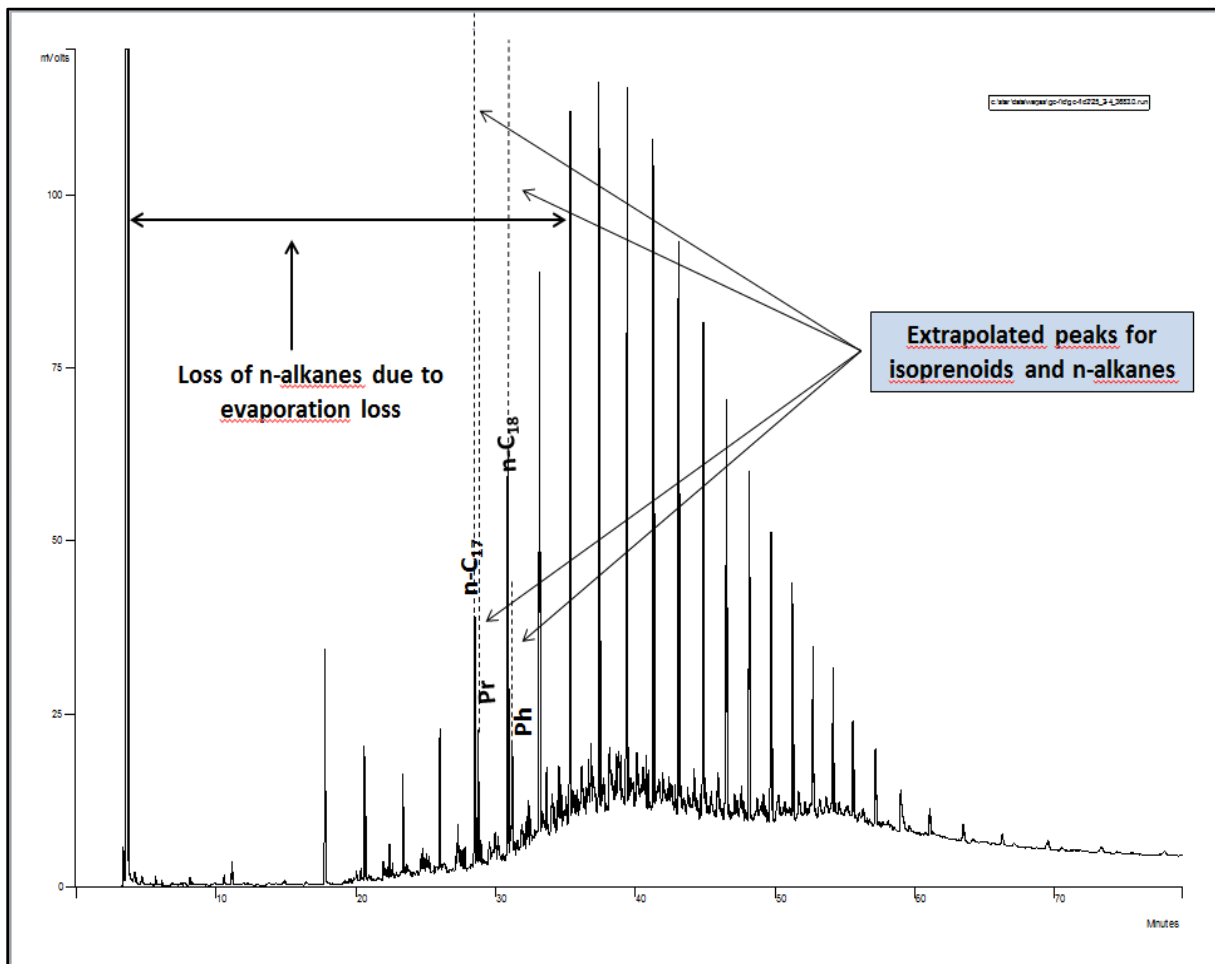


Fig. 7.1. The figure is showing the loss of n-alkanes due to evaporation and the extrapolated peaks for isoprenoids and n-alkanes.

It is therefore necessary to extrapolate the isoprenoids (pristane and phytane) and n-alkanes (n-C₁₇ and n-C₁₈) peaks to evaluate effectively the maturity and source rock facies. Basically

this is done by extending or lacking-up the peaks to the normal n-alkane envelope as shown in figure 7.1. The corrected values for pristane to phytane ratio are listed in the table below which clearly shows an increase in the isoprenoid ratio. The chromatograms with extrapolated peaks are presented in appendix B.

Table 7.1. Showing the corrected values after extrapolation for the isoprenoid and n-alkane peaks.

No.	Well	Depth (m)	Pr/Ph (Before)	Pr/Ph (After)	Pr/n-C ₁₇	Ph/n-C ₁₈
1	25/2-4	3675.0	1.1	1.8	0.5	0.3
2	25/2-4	3676.0	1.2	1.8	0.6	0.4
3	25/2-4	3683.0	1.2	1.9	0.5	0.3
4	25/2-12	3698.0	2.0	2.5	0.6	0.3
5	25/2-12	3698.5	1.7	2.2	0.6	0.3
6	25/2-12	3706.0	1.7	2.5	0.8	0.3
7	25/5-5	2171.5	0.6	0.7	0.4	0.7
8	25/5-5	2172.0	0.7	0.7	0.5	0.8
9	25/5-5	2173.5	0.7	0.7	0.6	0.8
10	26/4-1	2273.5	1.2	2.1	0.6	0.3
11	30/11-3	3457.0	2.0	3.2	0.9	0.3
12	30/11-3	3457.5	1.7	3.1	0.9	0.3
13	30/11-4	3514.5	1.0	1.3	0.5	0.5
14	30/11-4	3515.0	1.0	1.8	0.6	0.4
15	30/11-4	3515.5	1.2	2.1	0.6	0.3
16	30/11-4	3517.2	1.2	2.3	0.8	0.4

Based on this, facies and maturity diagrams are generated to develop a basis for comparison between the measured and corrected peak values. There is infact no considerable variation seen in maturity and facies overall except for a minor shift in the positions of some samples. Thus, while the Pr/Ph value is modified, the Pr/n-C₁₇ and Ph/n-C₁₈ ratios do not change markedly the positions of the samples in the characterization diagrams.

In figure 7.3, samples from the well 30/11-4 tend to show terrestrial influence which were previously been seen more influenced by marine environment. Similarly samples from most of the wells including 30/11-4, 30/11-3, 26/4-1 and 25/5-5 show variation in the position along x-axis (Fig 7.4). The concentration of most of the samples entirely in zone 3, after peaks being extrapolated, corresponds to higher values of pristane to phytane ratios with samples from well 30/11-3 showing more terrestrial influence.

It should be noted that no major difference in facies and maturity of the samples has been identified for the extrapolated peaks. The samples still reflect the marine source rock facies with little or no terrestrial influence.

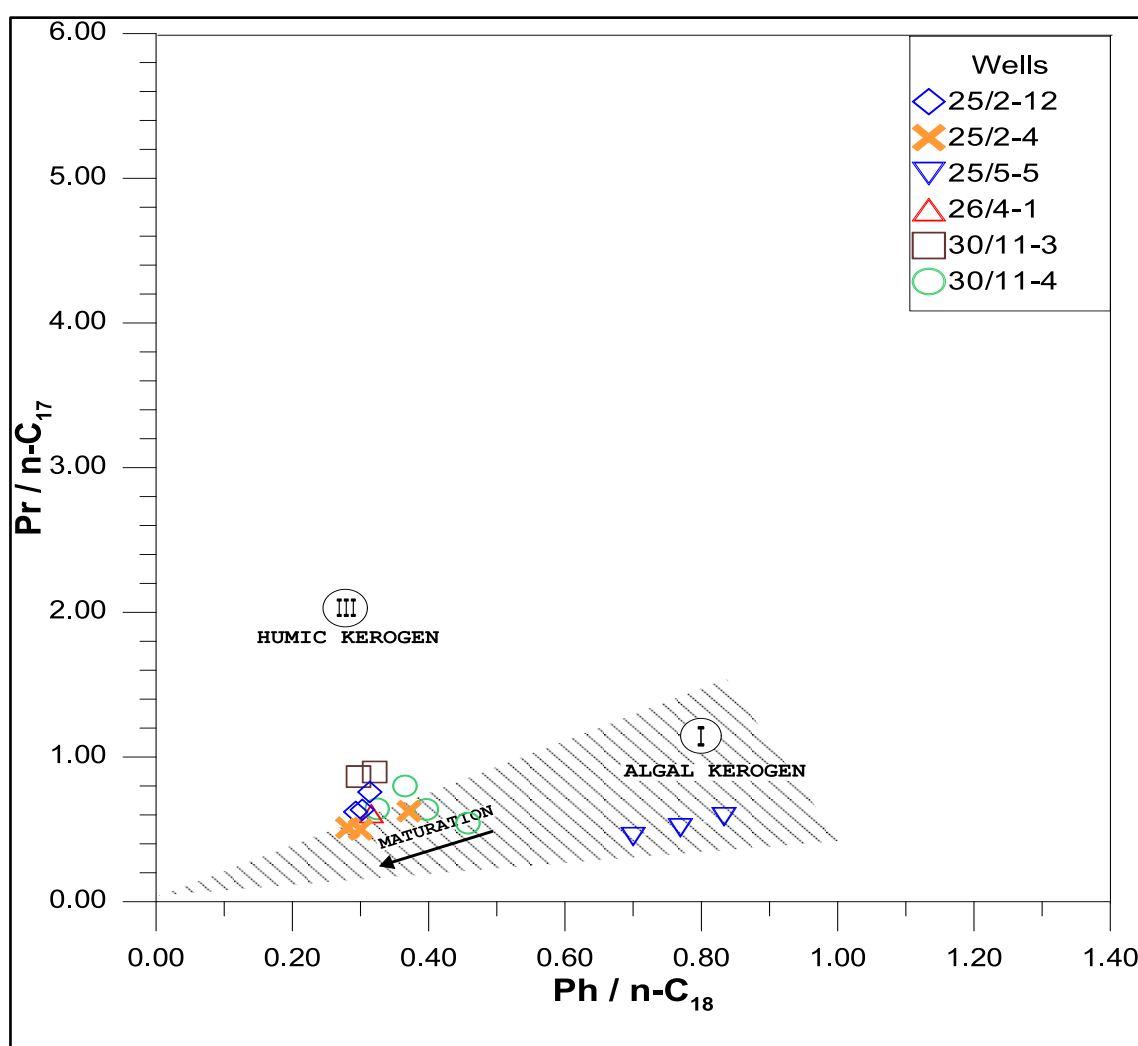


Fig. 7.2. The cross plot showing the ratios of isoprenoid to n-alkanes for the extrapolated peaks where $Pr/n-C_{18}$ is plotted on the x-axis and $Ph/n-C_{17}$ is plotted on the y-axis.

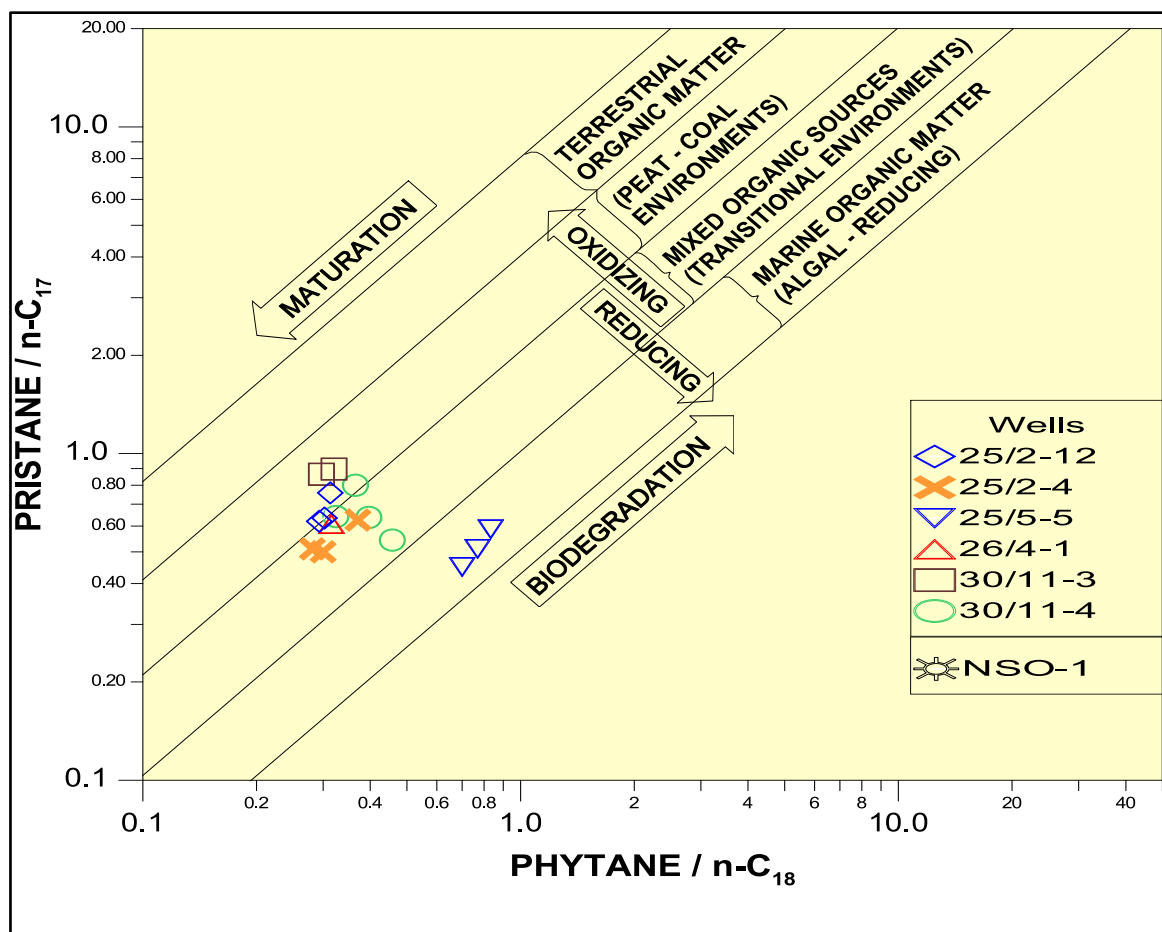


Fig. 7.3. Facies diagram based on the ratios of isoprenoids to n-alkanes (From Shanmugam, 1985). All samples represent palaeo-oil from basically a type II source rock of medium maturity.

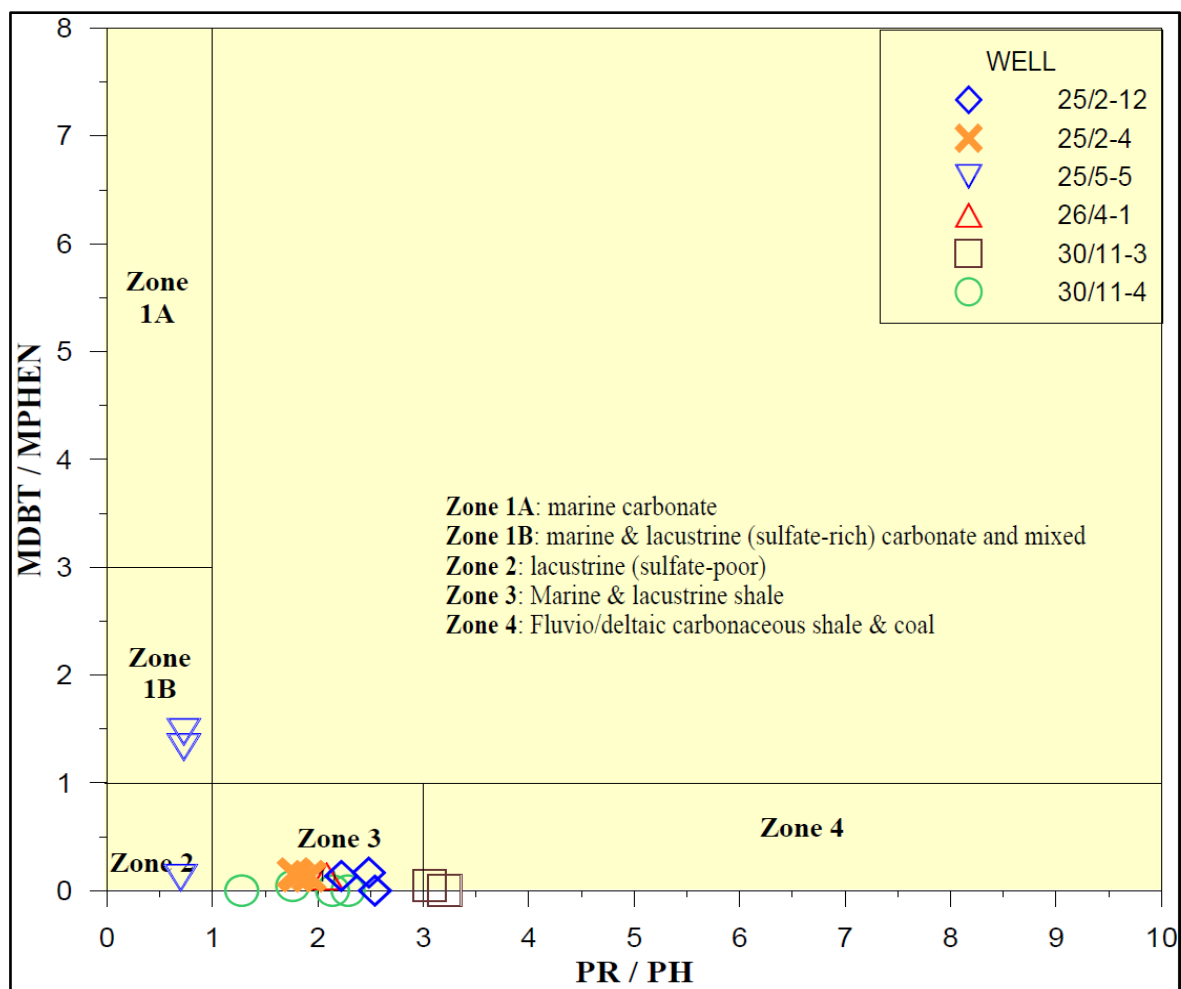


Fig. 7.4. Corrected Pr/Ph values are plotted in the facies diagram from Hughes et al., (1995) and we note that the Pr/Ph values are now generally higher.

8. Conclusive Summary

Conclusions are organized in two parts: Part one concern the geochemical analysis of the dry well samples and the discussion of the findings concerning gas from inclusions and bitumen, including the gas wetness and the maturity and facies of the residual oil. Part two concerns comparison between the bitumen facies and maturity parameters within a regional context of producing oil and DST samples from nearby Frøy and Rind. In addition is there an evaluation of the usefulness of using corrected and extrapolated isoprenoids and n-alkanes peaks in relation to non-corrected parameters when dealing with partly evaporated reservoir core bitumen.

Organic geochemical characterization of 91 core extracts from 15 exploration wells in the Viking Graben, North Sea reveals the presence of migrated palaeo-oil in a surprising number of the dry wells, suggesting clearly that dry wells do not constitute proof of lack of generation, nor migration and entrapment of oil and gas. Thus, “absence of proof” in terms of no discoveries constitutes in no way “proof of absence” – in this case of prolific and generative source rocks and generative and expelling “Petroleum Machineries”. This is obviously important concerning exploration in the general region which may, otherwise be considered a “dry-hole-region”.

In more detail it is clear that the higher percentages of wet gas components in the inclusion gas shows that petroleum, and often oil, did exist at some time in a number of these wells e.g. 25/2-4, 25/2-12, 25/3-1, 30/10-6, 30/11-4, 30/11-6, 30/11-7, 30/11-8A, 30/11-8S and 30/12-1. As inclusions are closed, these cannot become contaminated by drilling fluid products. Moreover, hopane and sterane isomerization parameters from bitumen core extracts support an allochthonous origin of the presented data and most bitumen samples show maturity in the range of 0.85-1%Rc. Thus, the dry well samples include bitumen of obvious allochthonous origins and reflect medium to high oil-window maturities.

Thus based on medium range and biomarker maturity parameters, it is concluded that wells 25/2-4, 25/2-12, 25/5-5, 26/4-1, 30/10-6, 30/11-3, 30/11-4 and 30/11-8A contain residual bitumen within the medium to peak phase of the oil window, yet bitumen from well 30/10-6 is an outlier with even higher maturity than the other samples. The bitumen from the dry wells is

found to be sourced from mixed “Type II/III organic source rock facies with obvious similarities to the general Mandal Fm of the region, which was deposited under variable distal/proximal marine and anoxic conditions.

The geochemistry of bitumen from dry wells compared to oils and core samples of the Rind and the Frøy fields (literature data) shows much more similarities than differences in terms of source rock facies and maturities, yet the oil and bitumen from Rind has even higher maturities, and possibly also contributions from a Heathers source rock facies not recorded among the dry wells.

An evaluation of a simple and straight forward “correction method” for n-alkanes and isoprenoids lost due to evaporation from core samples, was undertaken. In this method partly evaporated compounds in the C18 to C20 range were manually “backed-up” the assumed original n-alkane profile, evaluated from the C22-C30 n-alkane profile, and these corrected ratios of Pr/Ph, Pr/n-C₁₇ and Ph/n-C₁₈ were compared to the non-corrected and directly measured parameters, as done by most service laboratories. A substantial increase in the pristane to phytane ratio (Pr/Ph) is observed which could influence facies assessments, however, no significant change was observed in the logarithmic Pr/n-C₁₇ versus Ph/n-C₁₈ diagrams (Connan & Cassou/Shanmugam diagrams), and the facies and the maturity of the samples seem in such diagrams to be similar for both corrected and non-corrected data, but could possibly be improved with more detailed knowledge about the actual vapor pressures of the isoprenoids and the n-alkanes.

The findings of this thesis suggests that the region with the dry wells may indeed be more productive than possibly assumed, as the data of this thesis constitutes proof of generation of oil in down-dip source rock basins. The reasons why the wells penetrated dry structures is not dealt with in this thesis but can include wells placed too far on the flank of the structure, tectonic tilting of the structures or simply dismigration due to leaking cap rock or fault-seal breaching.

9. References

- ALEXANDER, R., KAGI, R. & WOODHOUSE, G. 1981. Geochemical correlation of Windalia oil and extracts of Winning Group (Cretaceous) potential source rocks, Barrow Subbasin, Western Australia. *AAPG Bulletin*, 65, 235-250.
- ALEXANDER, R., KAGI, R. I. & WOODHOUSE, G. W. 1981. Factors influencing the evolution of petroleum aromatics from an immature crude oil during pyrolysis on a shale matrix. *Journal of Analytical and Applied Pyrolysis*, 3, 59-70.
- BHULLAR, A., DI PRIMIO, R., KARLSEN, D. A. & GUSTIN, D.-P. 2003. AAPG/Datapages Discovery Series No. 7: Multidimensional Basin Modeling, Chapter 9: Determination of the Timing of Petroleum System Events Using Petroleum Geochemical, Fluid Inclusion, and PVT Data: An Example from the Rind Discovery and Froy Field, Norwegian North Sea.
- BHULLAR, A., KARLSEN, D., HOLM, K., BACKER-OWE, K. & LE TRAN, K. 1998. Petroleum geochemistry of the Frøy field and Rind discovery, Norwegian Continental Shelf. Implications for reservoir characterization, compartmentalization and basin scale hydrocarbon migration patterns in the region. *Organic geochemistry*, 29, 735-768.
- BHULLAR, A. G., KARLSEN, D. A., BACKER-OWE, K., SELAND, R. T. & LE TRAN, K. 1999. Dating reservoir filling—A case history from the North Sea. *Marine and Petroleum Geology*, 16, 581-603.
- CHRISTIANSSON, P., FALEIDE, J. & BERGE, A. 2000. Crustal structure in the northern North Sea: an integrated geophysical study. *SPECIAL PUBLICATION-GEOLOGICAL SOCIETY OF LONDON*, 167, 15-40.
- CLAYTON, J. & BOSTICK, N. 1986. Temperature effects on kerogen and on molecular and isotopic composition of organic matter in Pierre Shale near an igneous dike. *Organic geochemistry*, 10, 135-143.
- COOPER, B. & BARNARD, P. 1984. Source rocks and oils of the central and northern North Sea.

- CORNFORD, C., MORROW, J., TURRINGTON, A., MILES, J. & BROOKS, J. 1983. Some geological controls on oil composition in the UK North Sea. *Geological Society, London, Special Publications*, 12, 175-194.
- CUBITT, J. M. & ENGLAND, W. A. 1995. *The geochemistry of reservoirs*, Geological Society.
- DAHL, B. & SPEERS G.C. (1986). Geochemical characterization of a tar mat in the Oseberg Field Norwegian sector, North Sea. In *Advances in Organic Geochemistry 1985* (Edited by Leythaeuser D. and Rullkotter J.). *Org. Geoche.* 10, 547-558 Pergamon Press, Oxford.
- GABRIELSEN, R. 1986. Structural elements in graben systems and their influence on hydrocarbon trap types. *Habitat of hydrocarbons on the Norwegian Continental Shelf*, 55-60.
- GABRIELSEN, R., FÆRSETH, R., STEEL, R., IDIL, S. & KLØVJAN, O. 1990. Architectural styles of basin fill in the northern Viking Graben. *Tectonic Evolution of the North Sea Rifts*. Clarendon Press, Oxford, 158-179.
- GABRIELSEN, R., FÆRSETH, R., STEEL, R., IDIL, S. & KLØVJAN, O. 1990. Architectural styles of basin fill in the northern Viking Graben. *Tectonic Evolution of the North Sea Rifts*. Clarendon Press, Oxford, 158-179.
- GABRIELSEN, R. H., KYRKJEBØ, R., FALEIDE, J. I., FJELDSKAAR, W. & KJENNERUD, T. 2001. The Cretaceous post-rift basin configuration of the northern North Sea. *Petroleum Geoscience*, 7, 137-154.
- HAGEMANN, H. & HOLLERBACH, A. 1986. The fluorescence behaviour of crude oils with respect to their thermal maturation and degradation. *Organic Geochemistry*, 10, 473-480.
- HERITIER, F., LOSSEL, P. & WATHNE, E. 1980. Frigg Field--Large Submarine-Fan Trap in Lower Eocene Rocks of the Viking Graben, North Sea.

- HUGHES, W. B., HOLBA, A. G. & DZOU, L. I. 1995. The ratios of dibenzothiophene to phenanthrene and pristane to phytane as indicators of depositional environment and lithology of petroleum source rocks. *Geochimica et Cosmochimica Acta*, 59, 3581-3598.
- HUNT, J. 1996. Petroleum geology and geochemistry. *Freeman and Company, New York*, 743.
- JUSTWAN, H., DAHL, B., ISAKEN, G. H., & MEISINGSET, I. (2005). Late to Middle Jurassic source facies and quality variations, South Viking Graben, North Sea. *Journal of Petroleum Geology*, 28(3), 241-268.
- JUSTWAN, H., MEISINGSET, I., DAHL, B., & ISAKSEN, G. H. (2006). Geothermal history and petroleum generation in the Norwegian South Viking Graben revealed by pseudo-3D basin modelling. *Marine and Petroleum Geology*, 23(8), 791-819.
- JUSTWAN, H., DAHL, B., & ISAKSEN, G. H. (2006). Geochemical characterisation and genetic origin of oils and condensates in the South Viking Graben, Norway. *Marine and Petroleum Geology*, 23(2), 213-239.
- KARLSEN, D., NYLAND, B., FLOOD, B., OHM, S., BREKKE, T., OLSEN, S. & BACKER-OWE, K. 1995. Petroleum geochemistry of the Haltenbanken, Norwegian continental shelf. *Geological Society, London, Special Publications*, 86, 203-256.
- KARLSEN, D. & SKEIE, J. 2006. Petroleum migration, faults and overpressure, Part I: calibrating basin modelling using petroleum in traps—a review. *Journal of Petroleum Geology*, 29, 227-256.
- KARLSEN, D. A., NEDKVITNE, T., LARTER, S. R. & BJØRLYKKE, K. 1993. Hydrocarbon composition of authigenic inclusions: application to elucidation of petroleum reservoir filling history. *Geochimica et Cosmochimica Acta*, 57, 3641-3659.
- KARLSEN, D. A., SKEIE, J. E., BACKER-OWE, K., BJØRLYKKE, K., OLSTAD, R., BERGE, K., CECCHI, M., VIK, E. & SCHAEFER, R. G. 2004. Petroleum migration, faults and overpressure. Part II. Case history: the Haltenbanken Petroleum Province, offshore Norway. *Geological Society, London, Special Publications*, 237, 305-372.

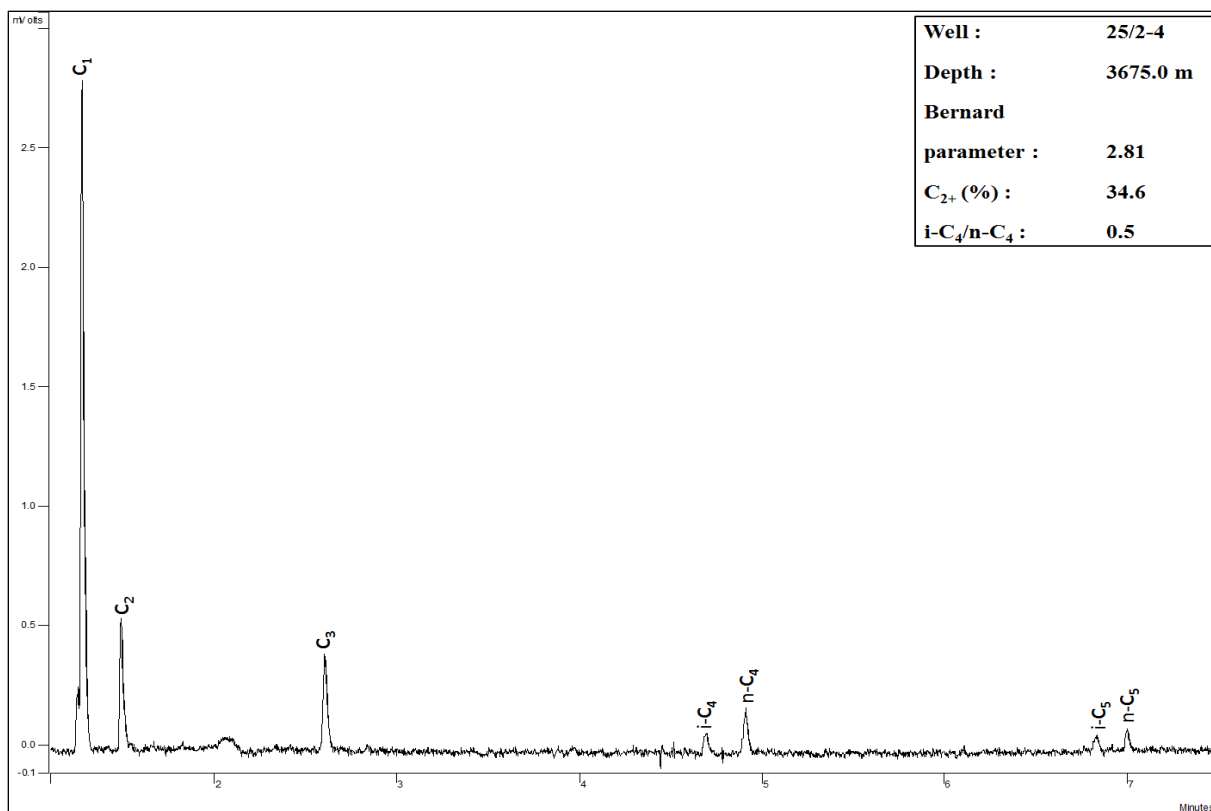
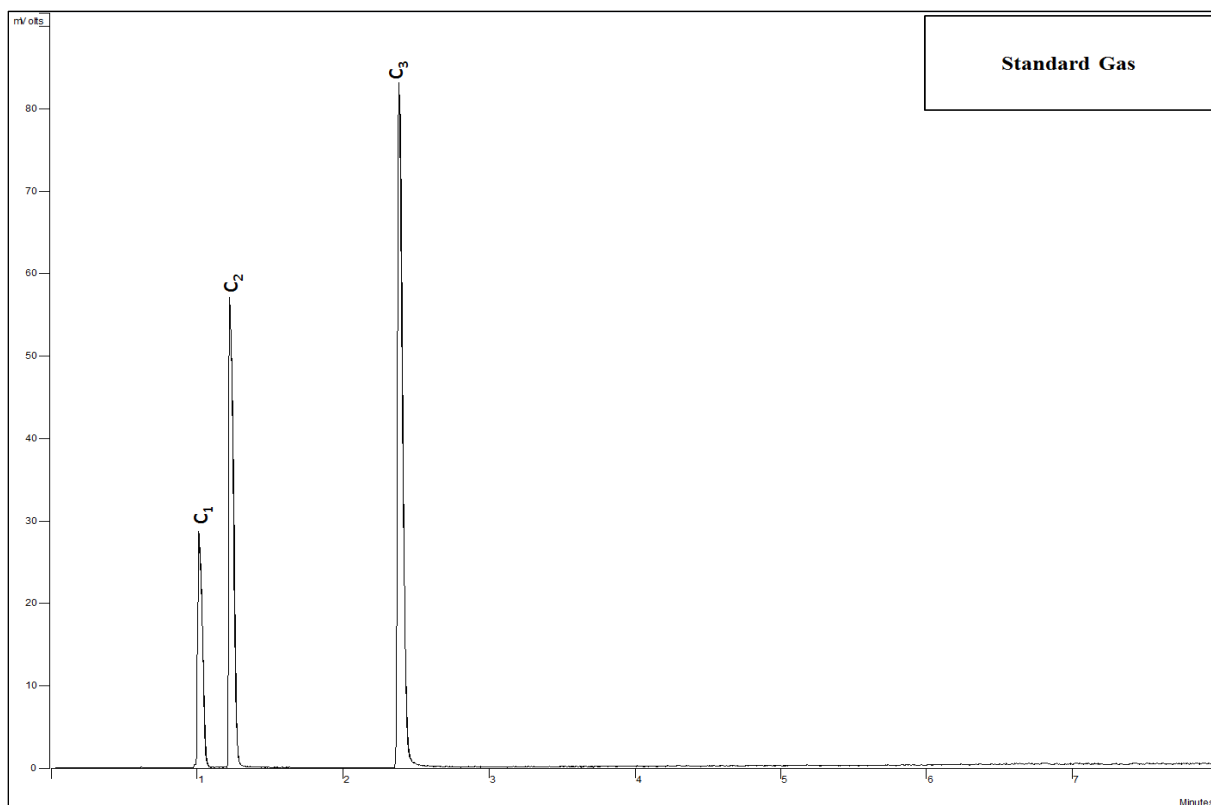
- LARTER, S. & DI PRIMIO, R. 2005. Effects of biodegradation on oil and gas field PVT properties and the origin of oil rimmed gas accumulations. *Organic Geochemistry*, 36, 299-310.
- MACKENZIE, A., RULLKOTTER, J., WELTE, D. & MANKIEWICZ, P. 1985. Reconstruction of Oil Formation and Accumulation in North Slope, Alaska, Using Quantitative Gas Chromatography-Mass Spectrometry: SOURCE ROCK EVALUATION INCLUDING ISOTOPES AND BIOMARKERS.
- MARTIN, A. J. P. 1953. *The development of partition chromatography*, Norstedt.
- MOLDOWAN, J. M., FAGO, F. J., CARLSON, R. M., YOUNG, D. C., CLARDY, J., SCHOELL, M., PILLINGER, C. T. & WATT, D. S. 1991. Rearranged hopanes in sediments and petroleum. *Geochimica et Cosmochimica Acta*, 55, 3333-3353.
- NOTTVEDT, A., GABRIELSEN, R. & STEEL, R. 1995. Tectonostratigraphy and sedimentary architecture of rift basins, with reference to the northern North Sea. *Marine and Petroleum Geology*, 12, 881-901.
- PEDERSEN, J. H., KARLSEN, D. A., BACKER-OWE, K., LIE, J. E. & BRUNSTAD, H. 2006. The geochemistry of two unusual oils from the Norwegian North Sea: implications for new source rock and play scenario. *Petroleum Geoscience*, 12, 85-96.
- PETERS, K. E. & MOLDOWAN, J. M. 1993. *The biomarker guide: interpreting molecular fossils in petroleum and ancient sediments*, Prentice Hall Englewood Cliffs, NJ.
- PETERS, K. E., WALTERS, C. C. & MOLDOWAN, J. M. 2005. *The biomarker guide: Biomarkers and isotopes in the environment and human history*, Cambridge University Press.
- PHILP, R. 1985. Petroleum Formation and Occurrence. *Eos, Transactions American Geophysical Union*, 66, 643-644.
- RADKE, M. 1988. Application of aromatic compounds as maturity indicators in source rocks and crude oils. *Marine and Petroleum Geology*, 5, 224-236.

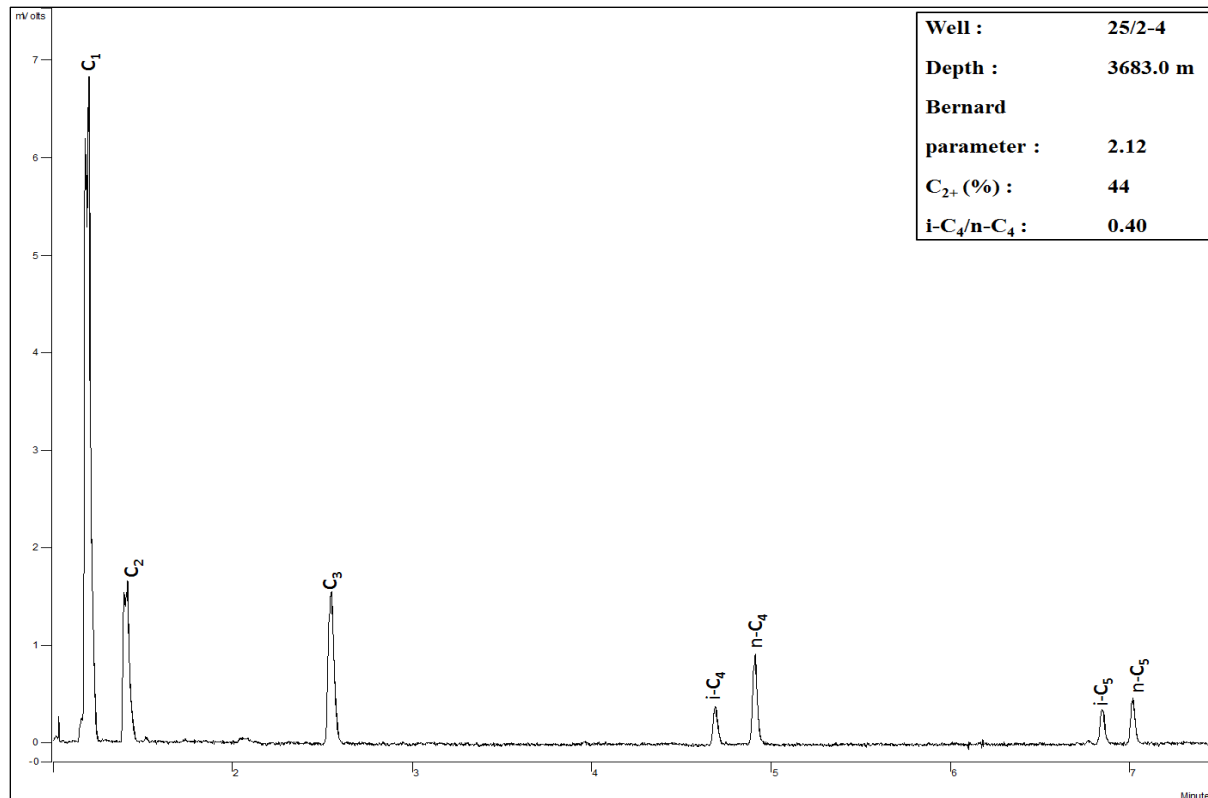
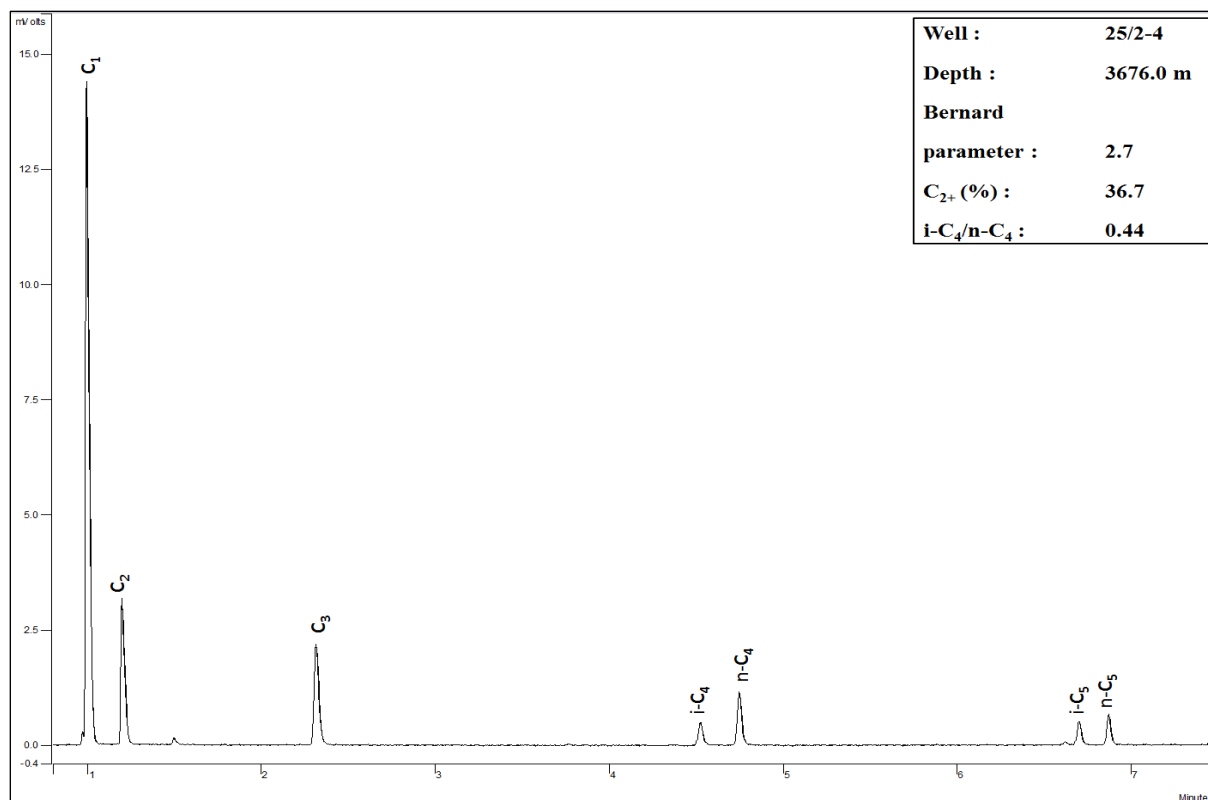
- RANNÝ, M. 1987. *Thin-layer chromatography with flame ionization detection*, Springer.
- SCHOELL, M. 1983. Genetic characterization of natural gases. *AAPG bulletin*, 67, 2225-2238.
- SHANMUGAM, G. 1985. Significance of coniferous rain forests and related organic matter in generating commercial quantities of oil, Gippsland Basin, Australia. *AAPG Bulletin*, 69, 1241-1254.
- SPENCER, A. & LARSEN, V. 1990. Fault traps in the northern North Sea. *Geological Society, London, Special Publications*, 55, 281-298.
- SUTTON, P., LEWIS, C. & ROWLAND, S. 2005. Isolation of individual hydrocarbons from the unresolved complex hydrocarbon mixture of a biodegraded crude oil using preparative capillary gas chromatography. *Organic Geochemistry*, 36, 963-970.
- TISSOT, B., CALIFET-DEBYSER, Y., DEROO, G. & OUDIN, J. 1971. Origin and evolution of hydrocarbons in early Toarcian shales, Paris Basin, France. *AAPG Bulletin*, 55, 2177-2193.
- TISSOT, B. P. & WELTE, D. H. 1978. Petroleum formation and occurrence: a new approach to oil and gas exploration.
- WALDERHAUG, O. 1994. Precipitation rates for quartz cement in sandstones determined by fluid-inclusion microthermometry and temperature-history modeling. *Journal of Sedimentary Research*, 64.
- WAPLES, D. W. & MACHIHARIA, T. 1991. Biomarkers for geologists.
- WEISS, H., WILHELMS, A., MILLS, N., SCOTCHMER, J., HALL, P., LIND, K. & BREKKE, T. 2000. NIGOGA—The Norwegian industry guide to organic geochemical analyses. *Norsk Hydro, Statoil, Geolab Nor, SINTEF Petroleum Research and the Norwegian Petroleum Directorate*.
- WHITICAR, M. J. 1994. Correlation of natural gases with their sources. *MEMOIRS-AMERICAN ASSOCIATION OF PETROLEUM GEOLOGISTS*, 261-261.

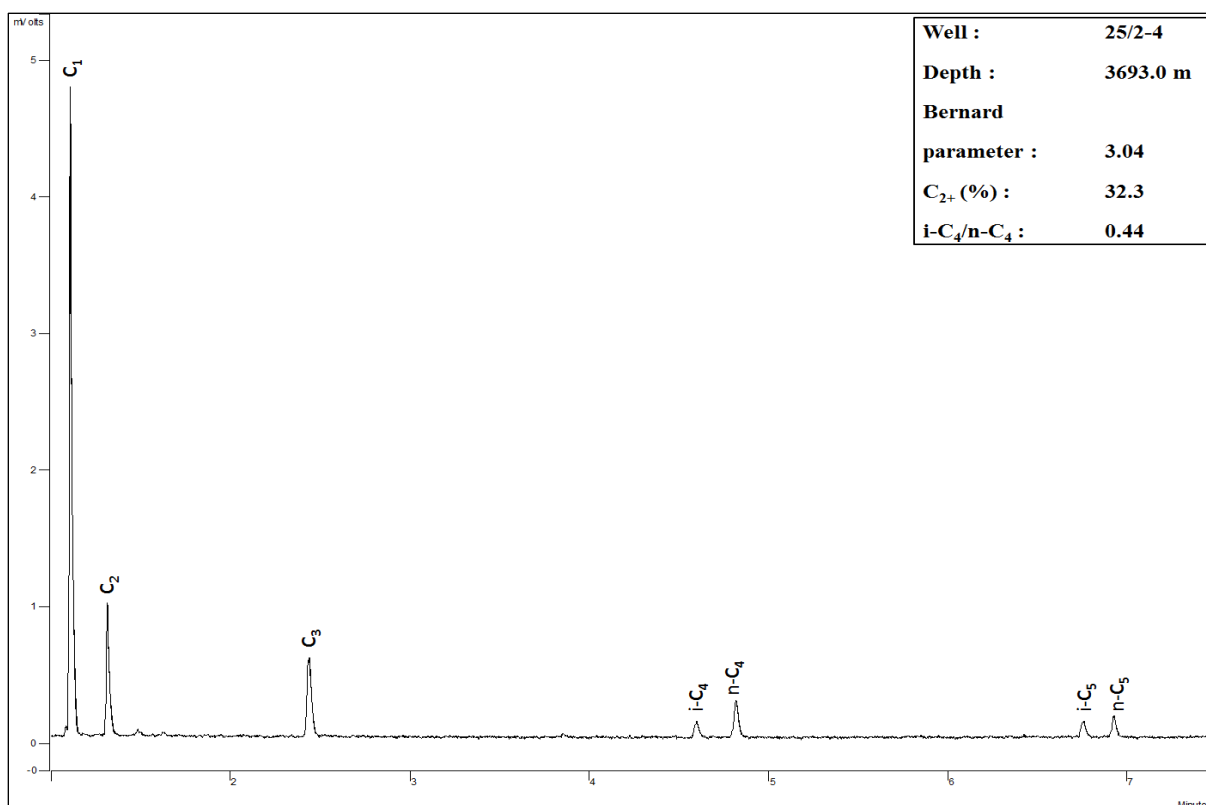
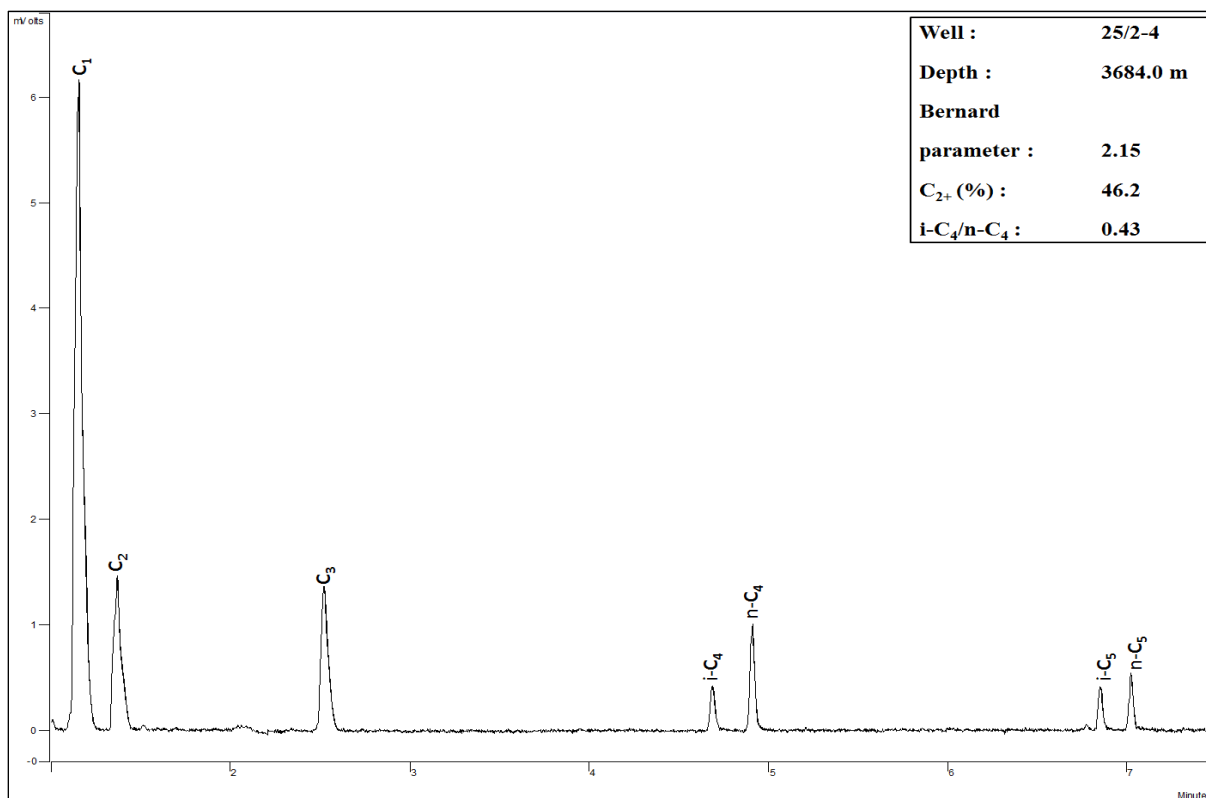
ØSTENSEN, M. 2005. A geochemical assessment of petroleum from underground oil storage caverns in relation to petroleum from natural reservoirs offshore Norway.

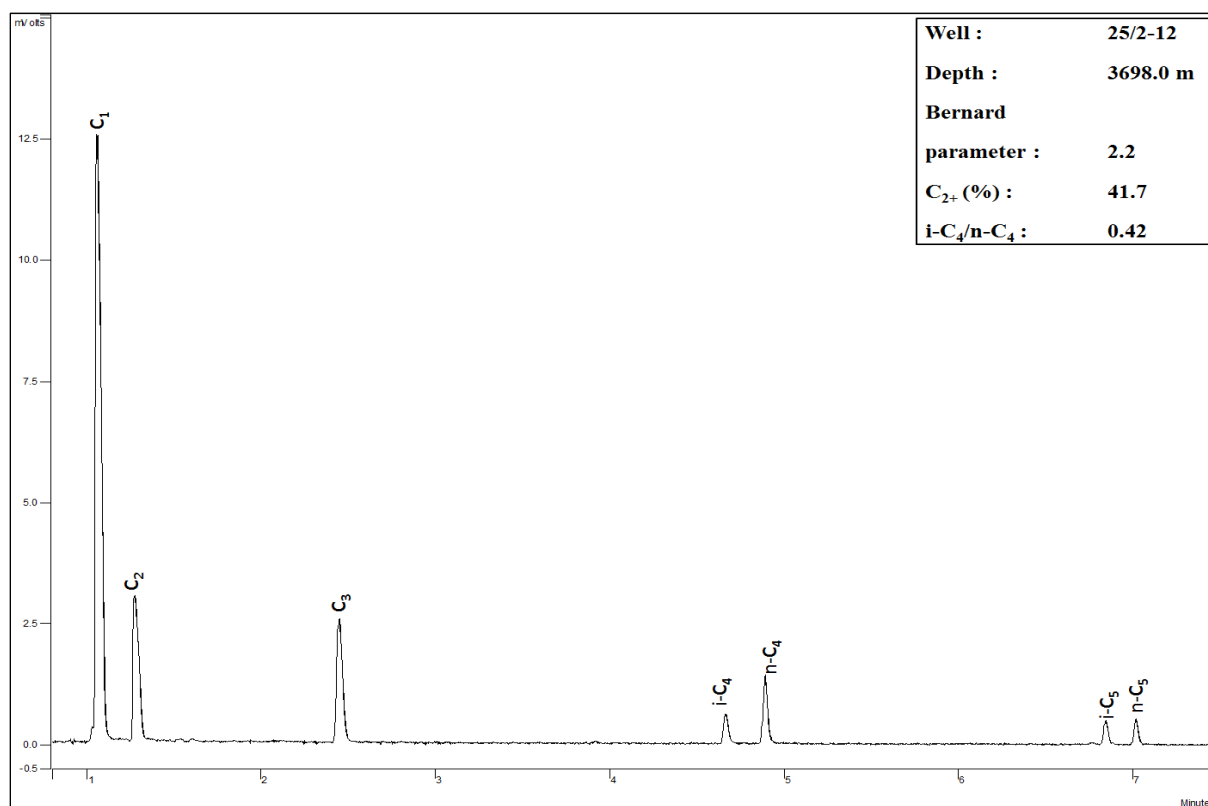
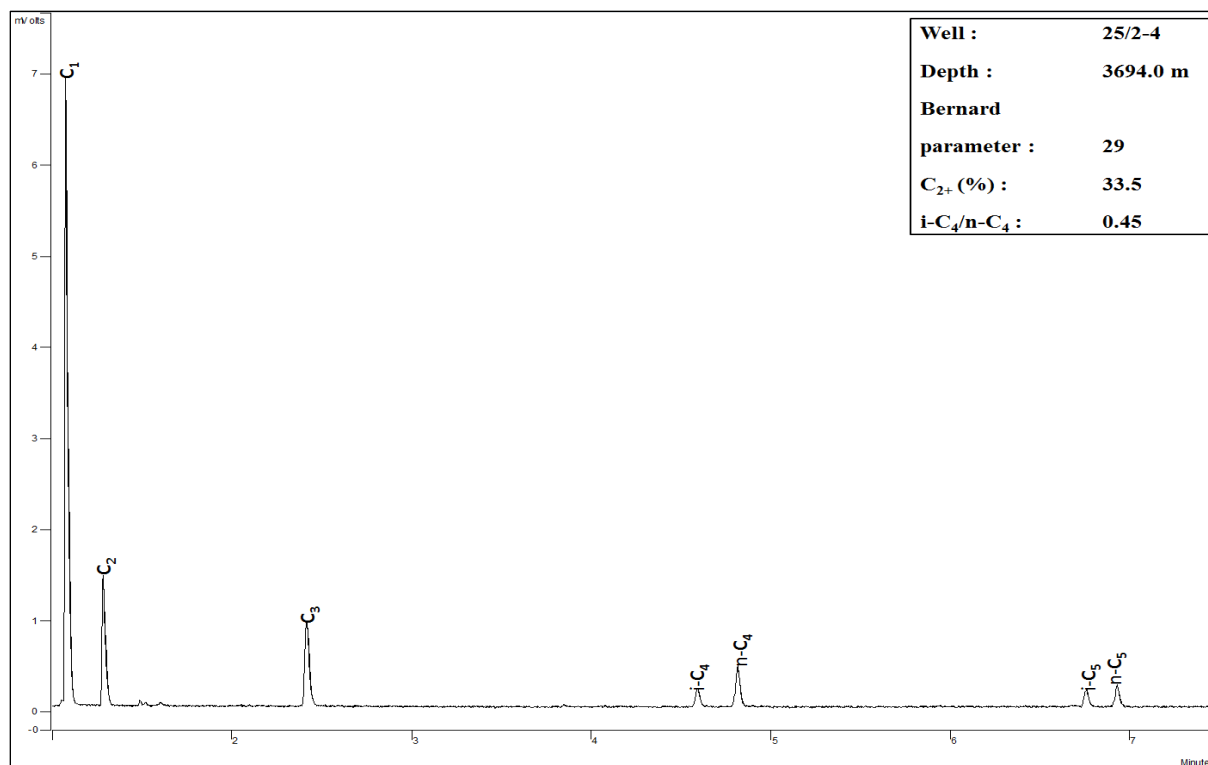
10.Appendix

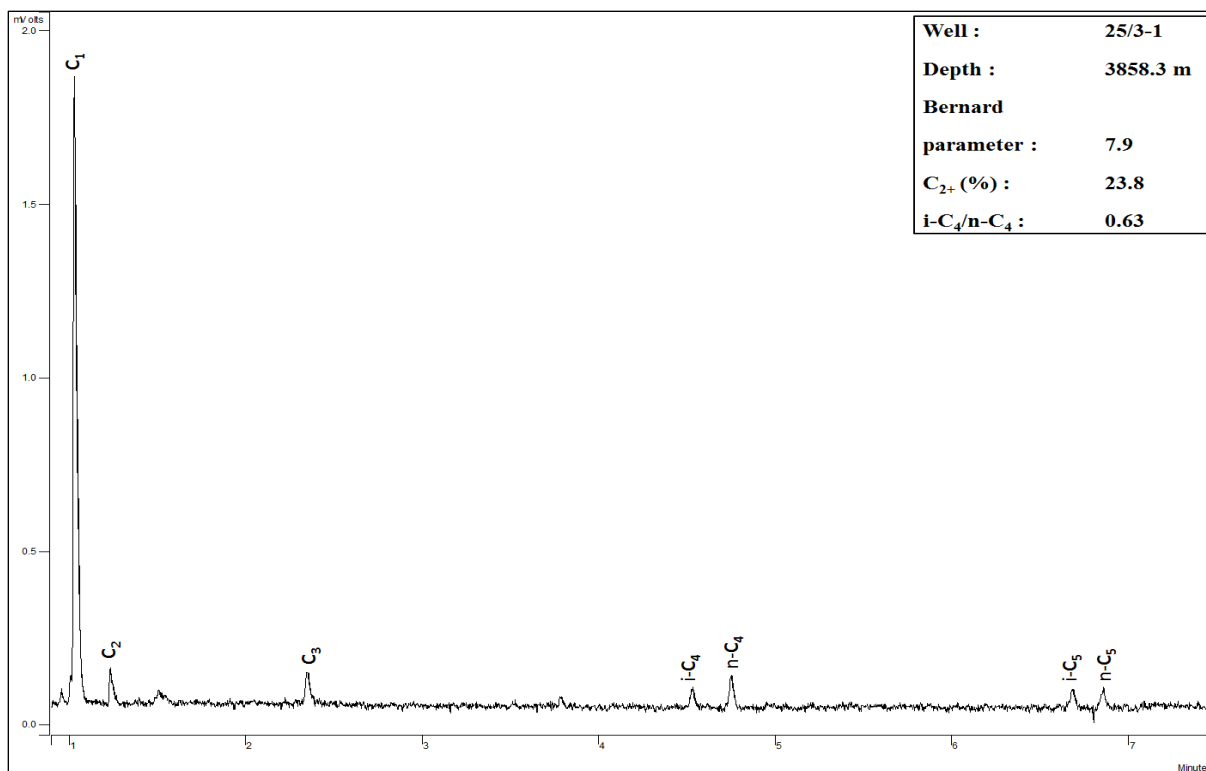
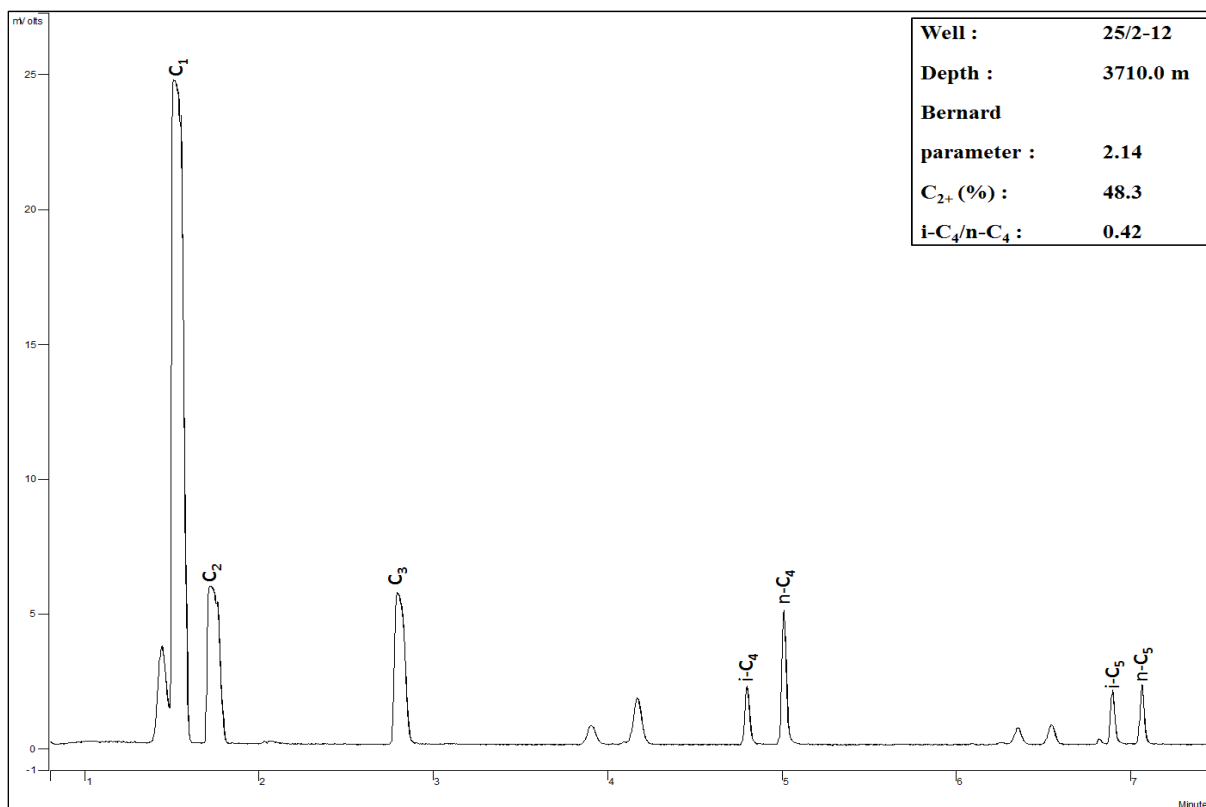
Appendix A (Gas Analysis Chromatograms)

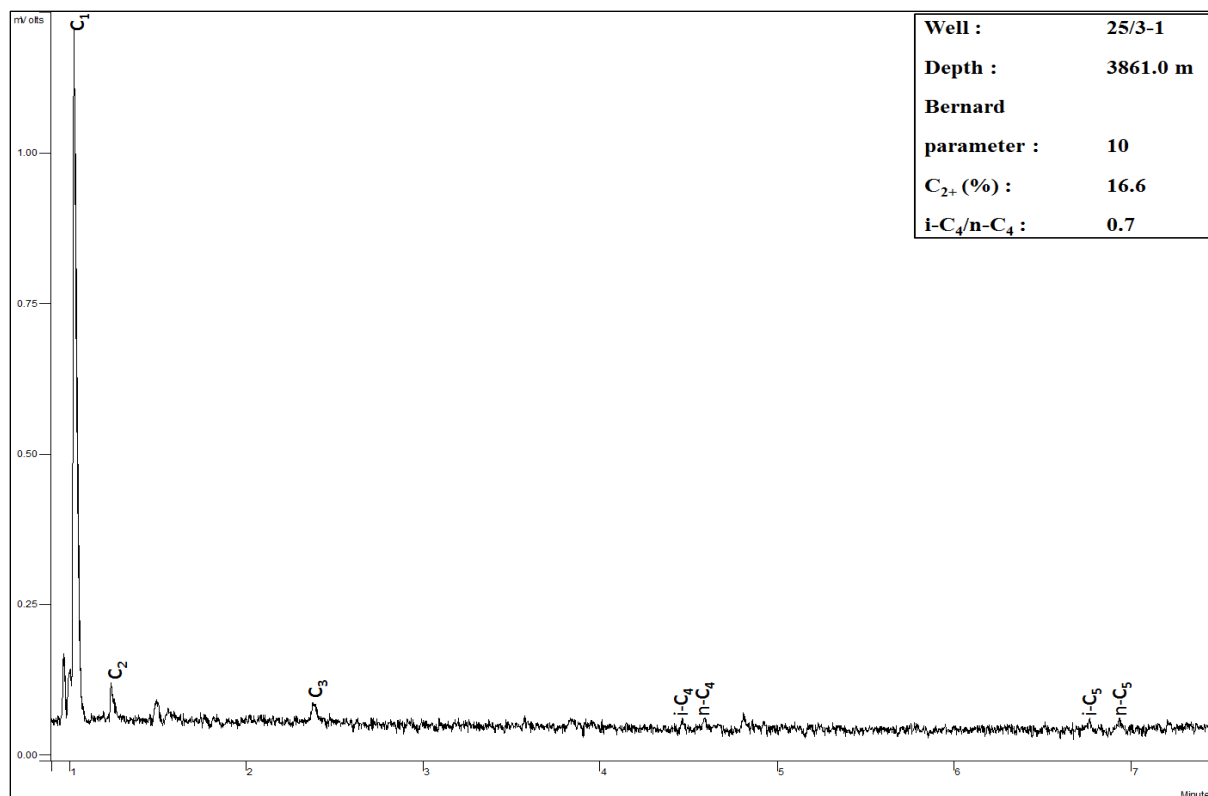
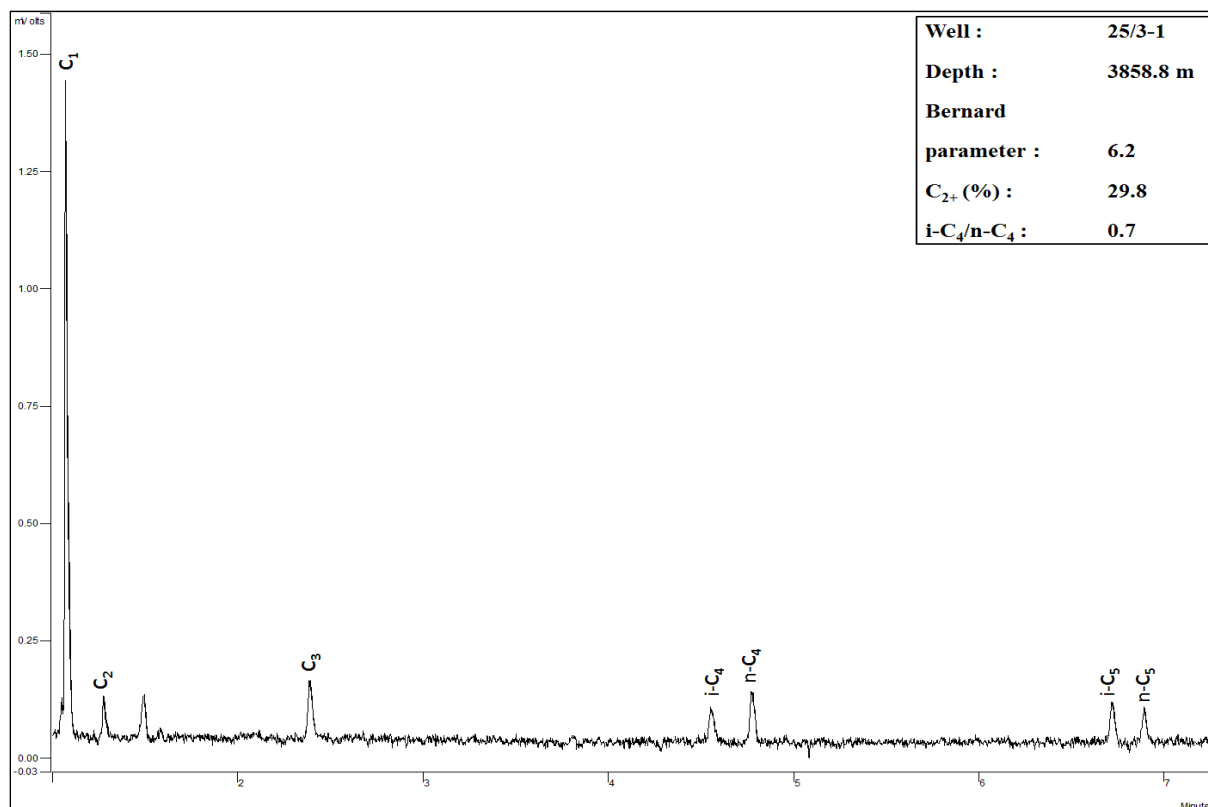


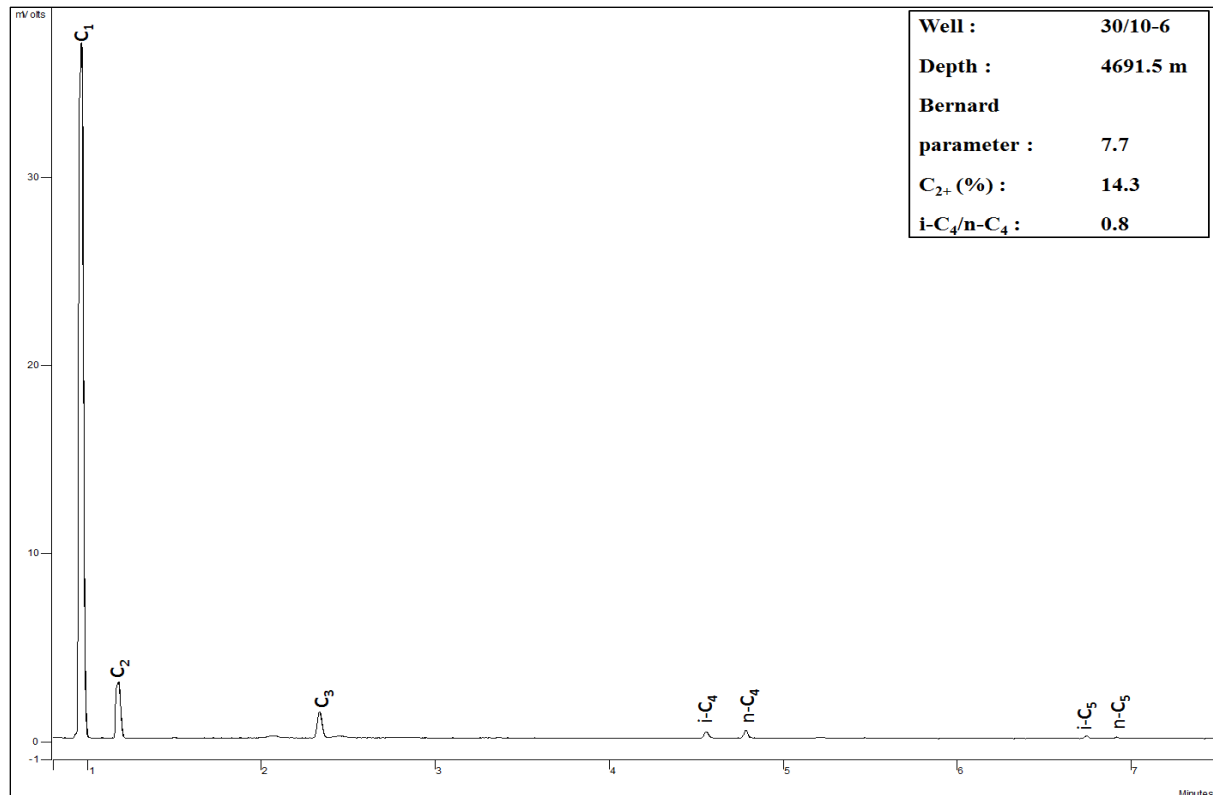
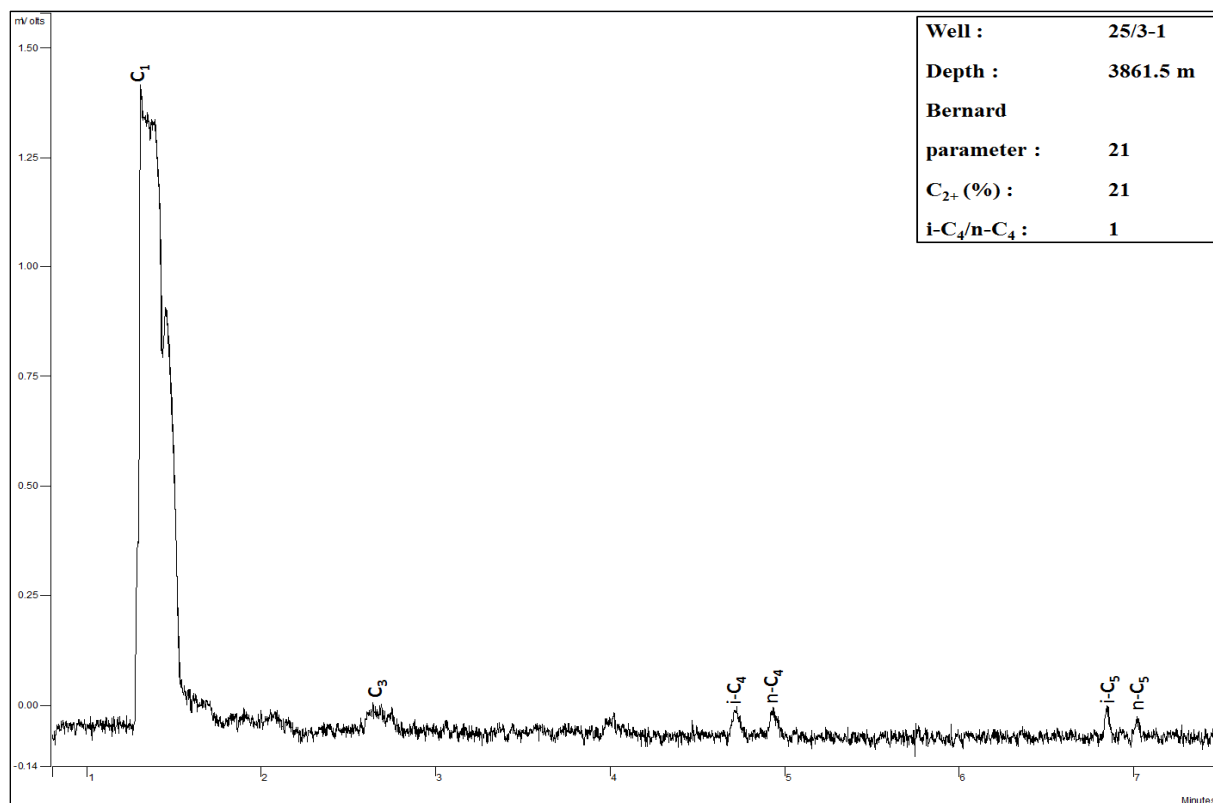


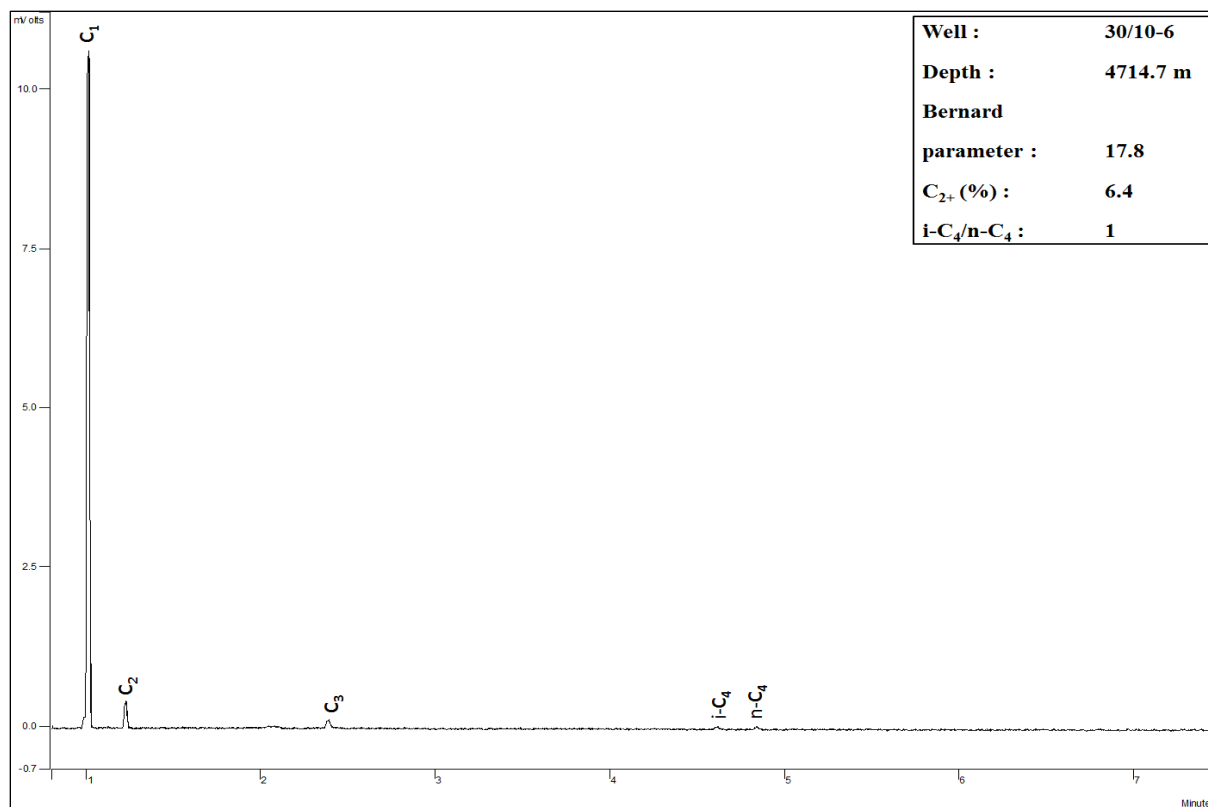
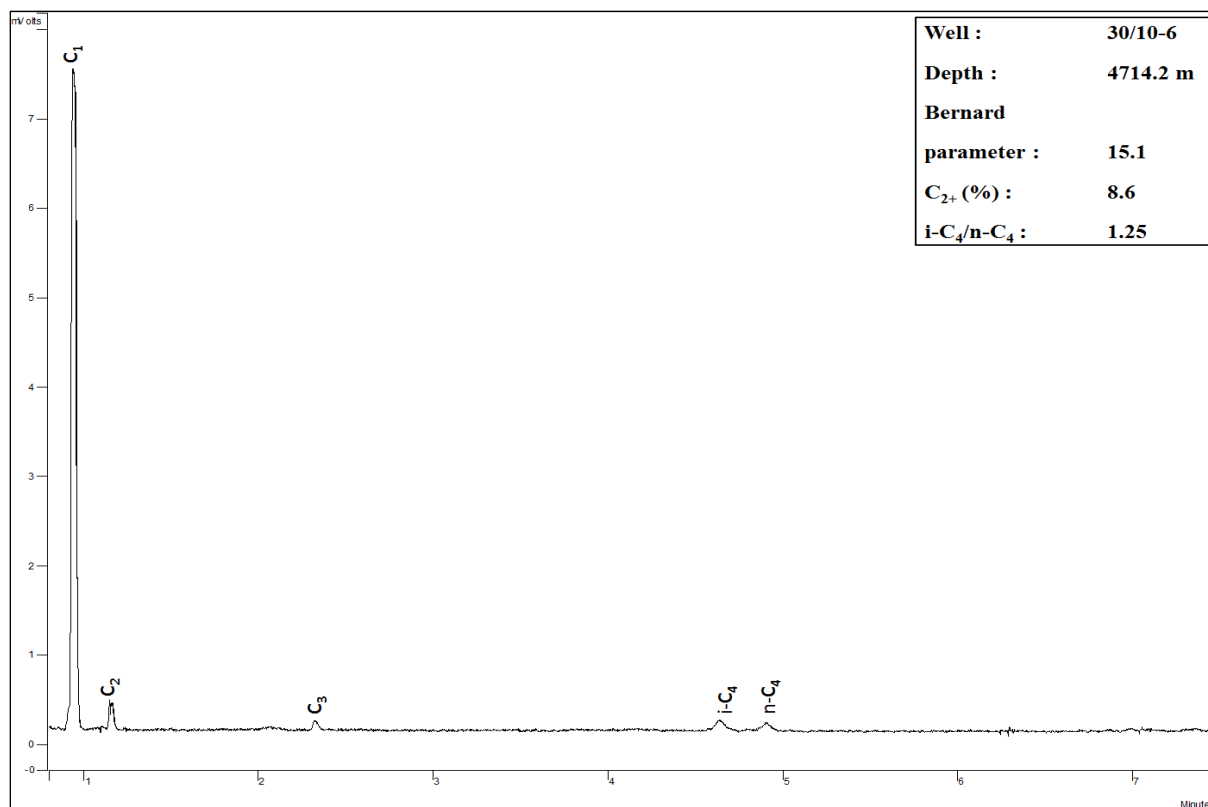


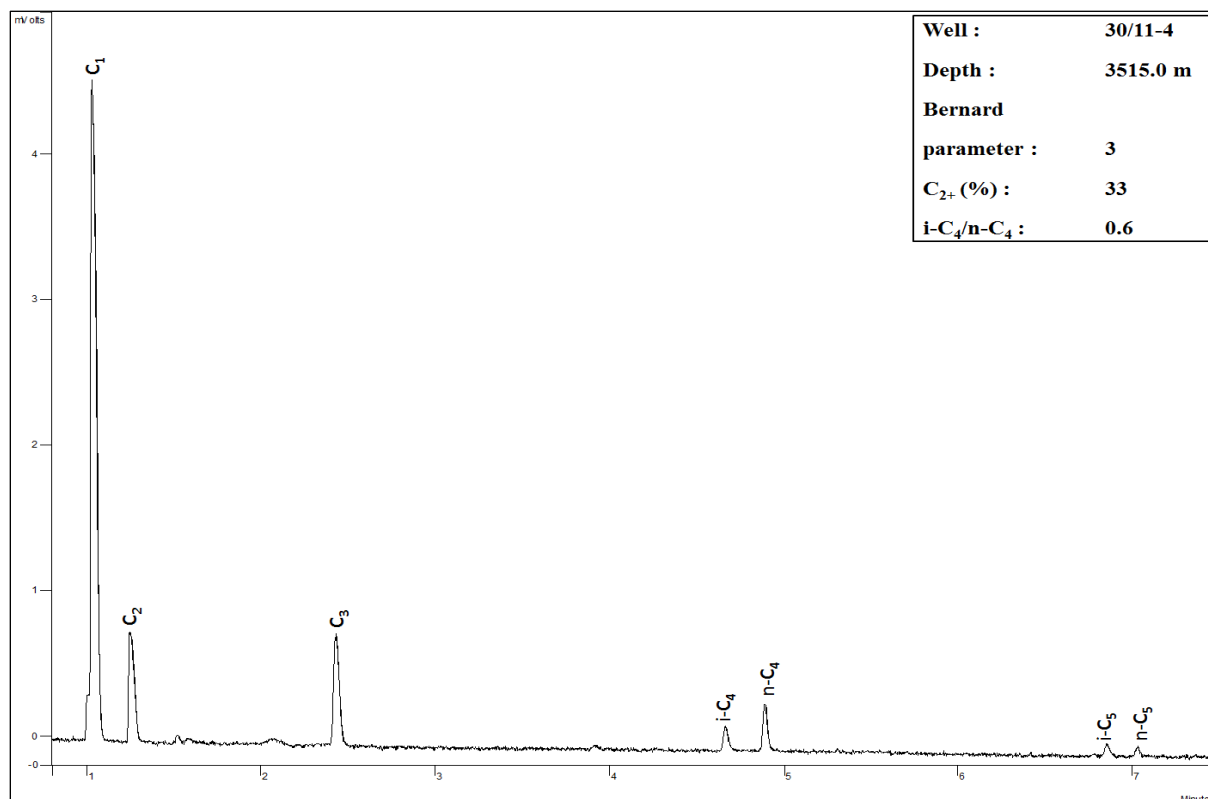
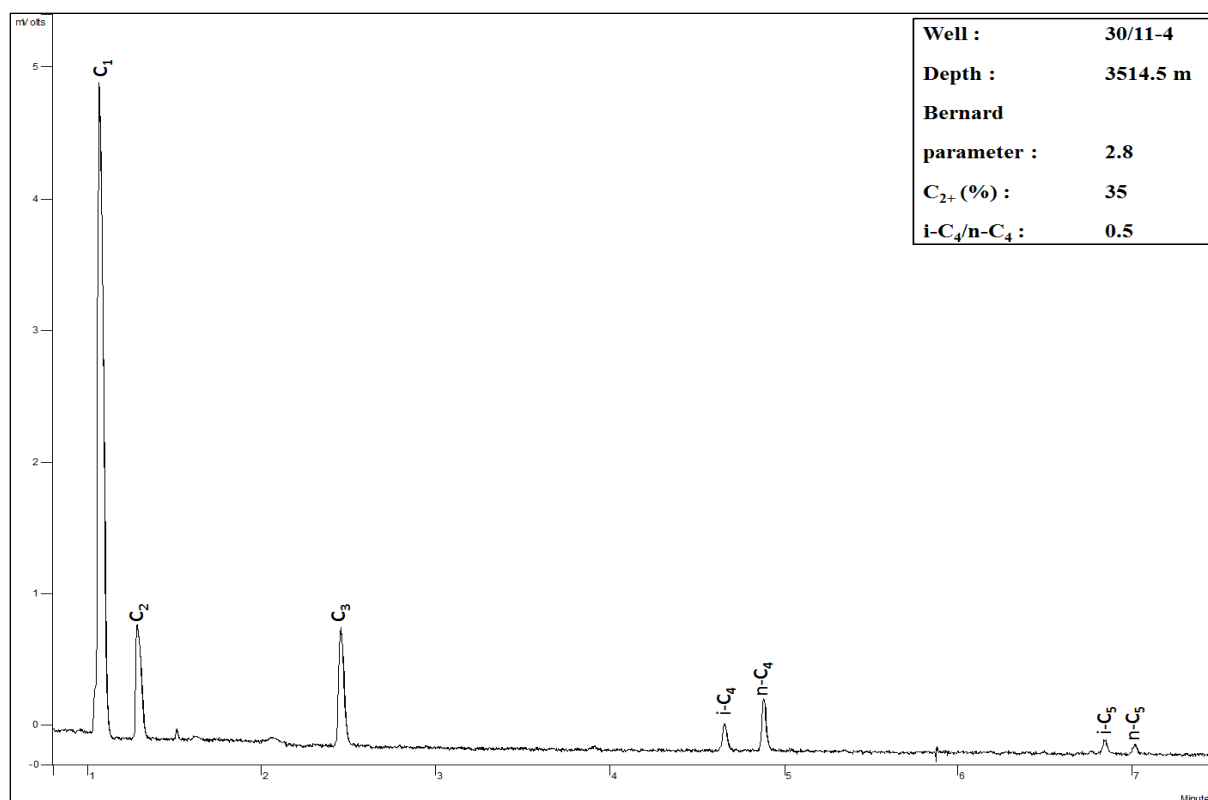


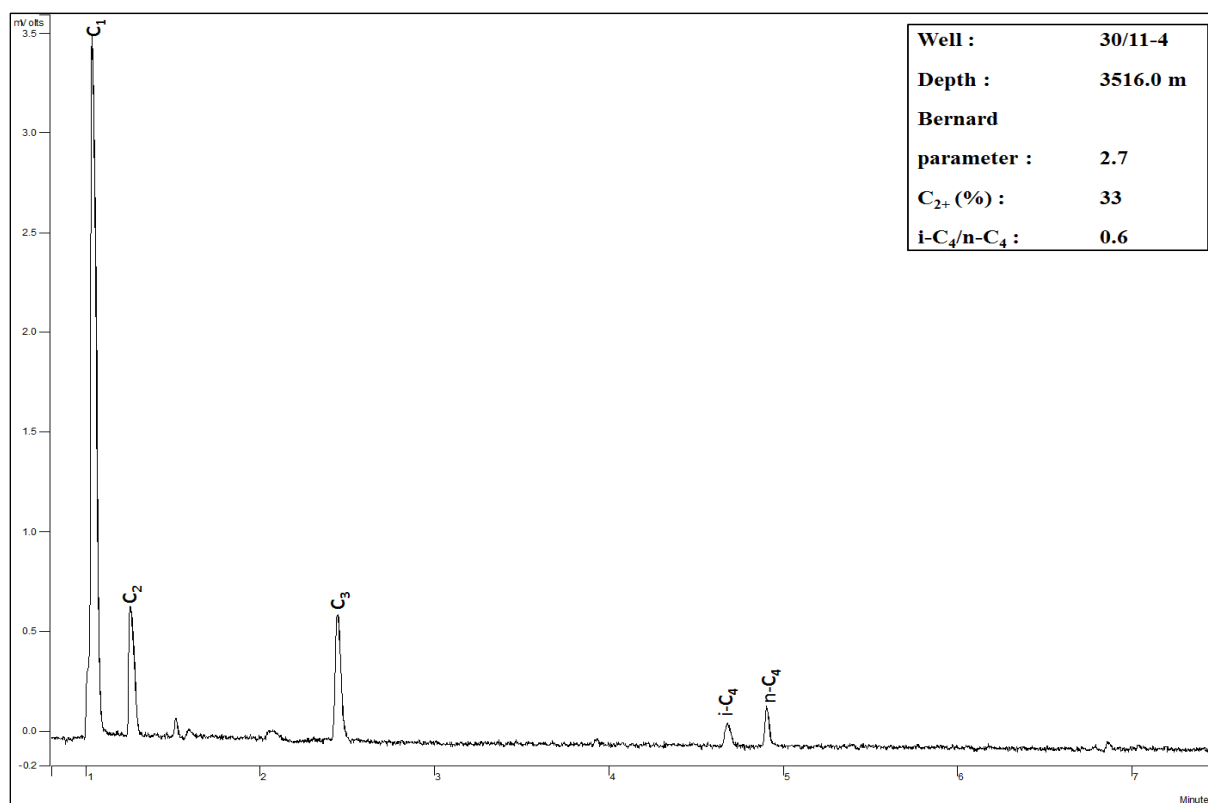
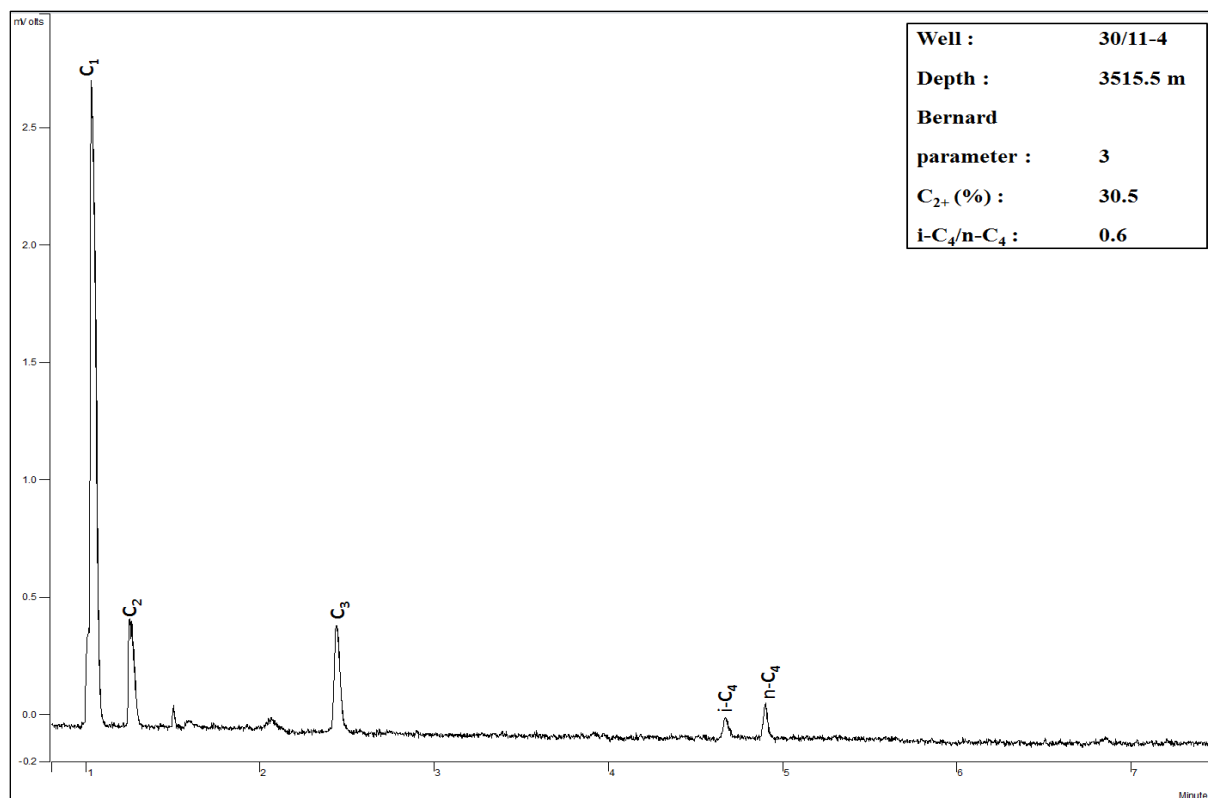


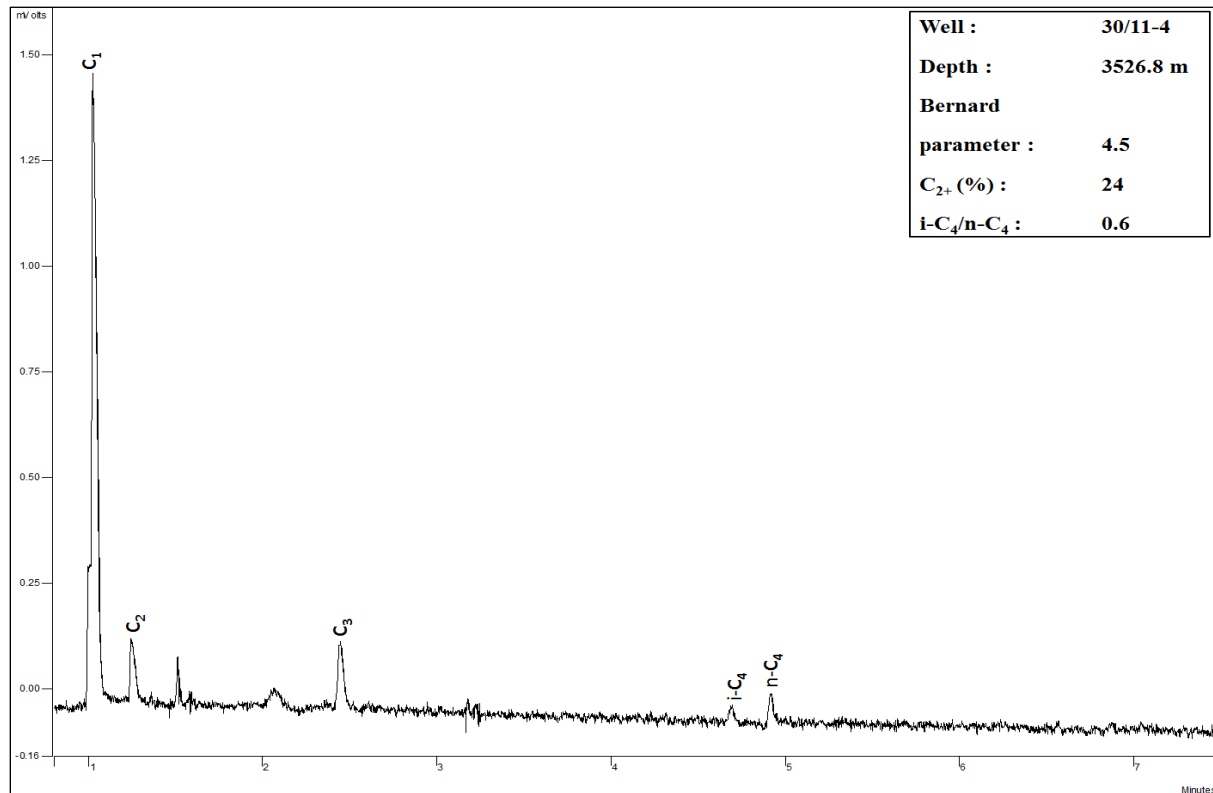
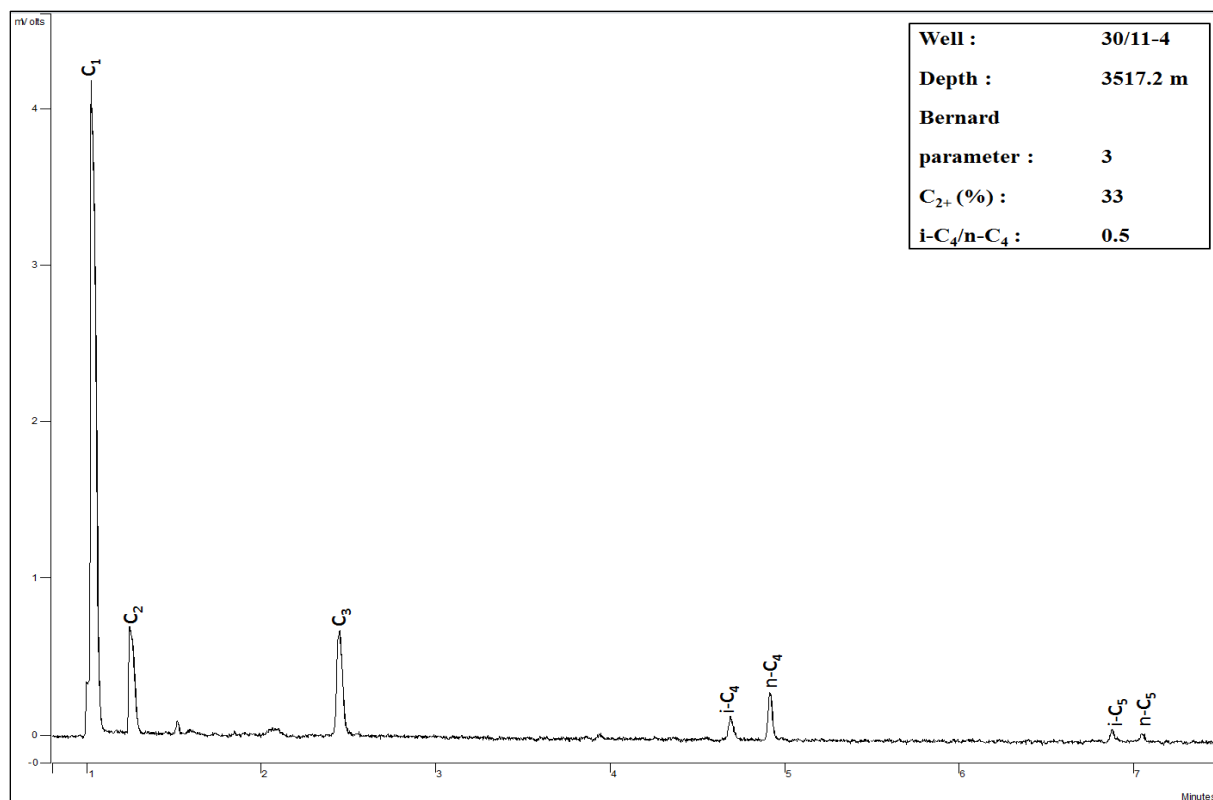


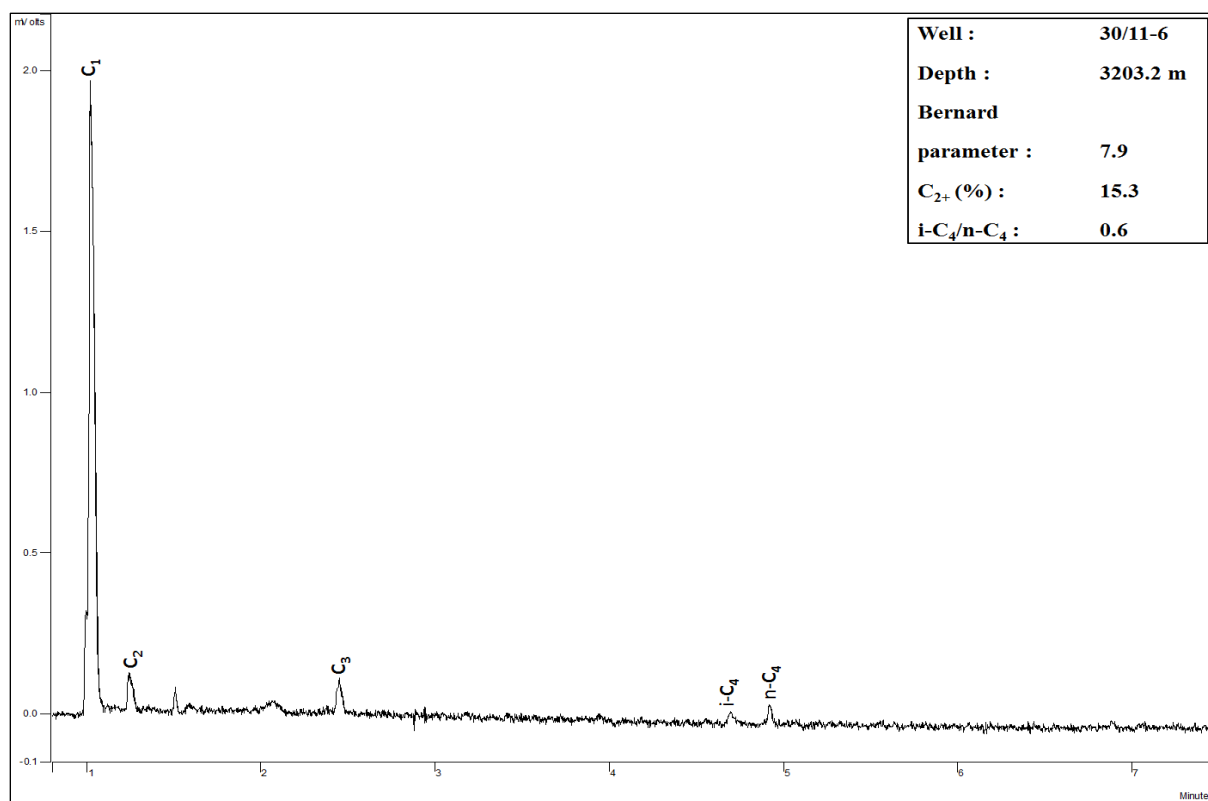
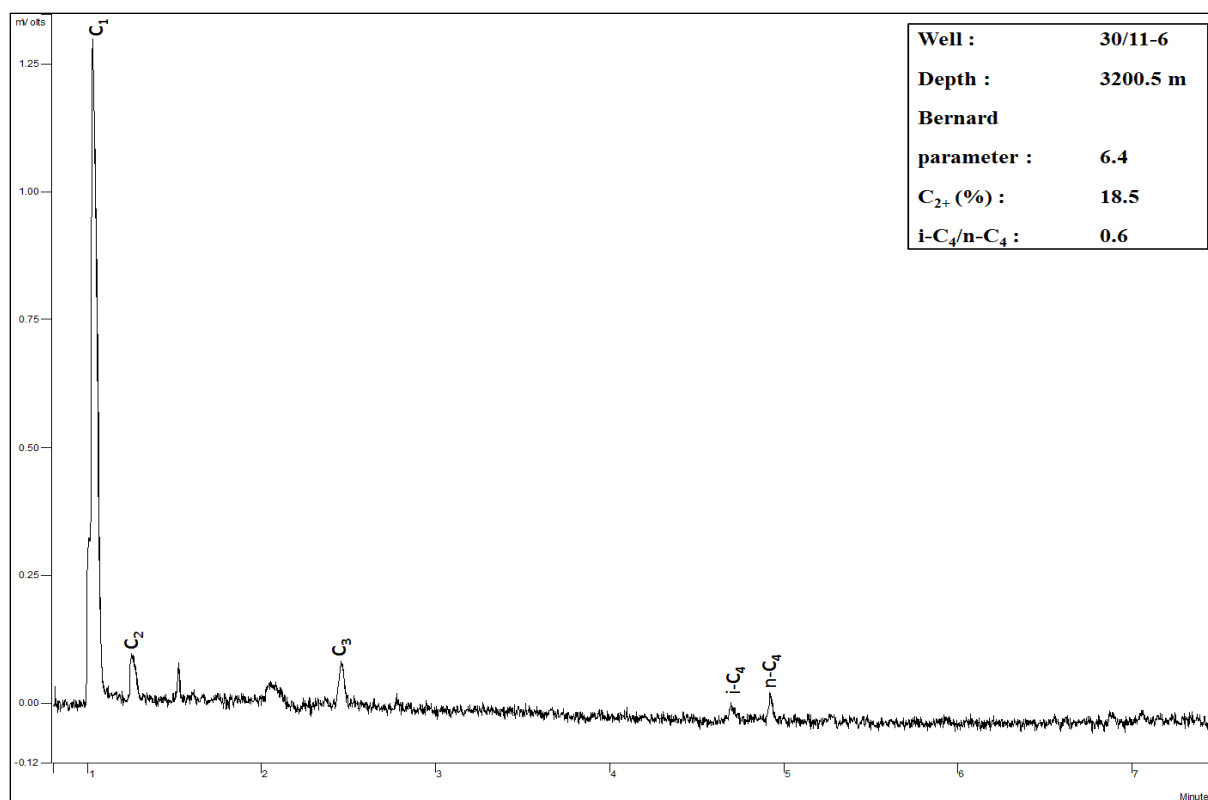


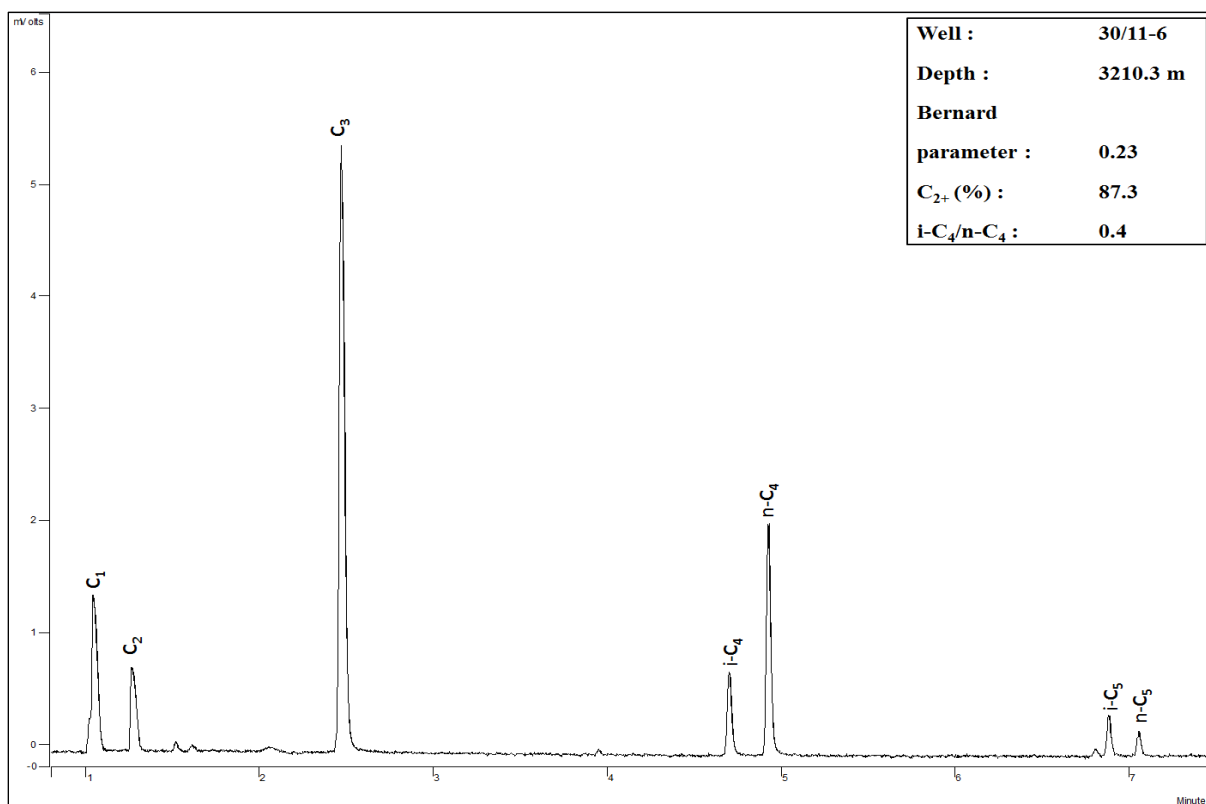
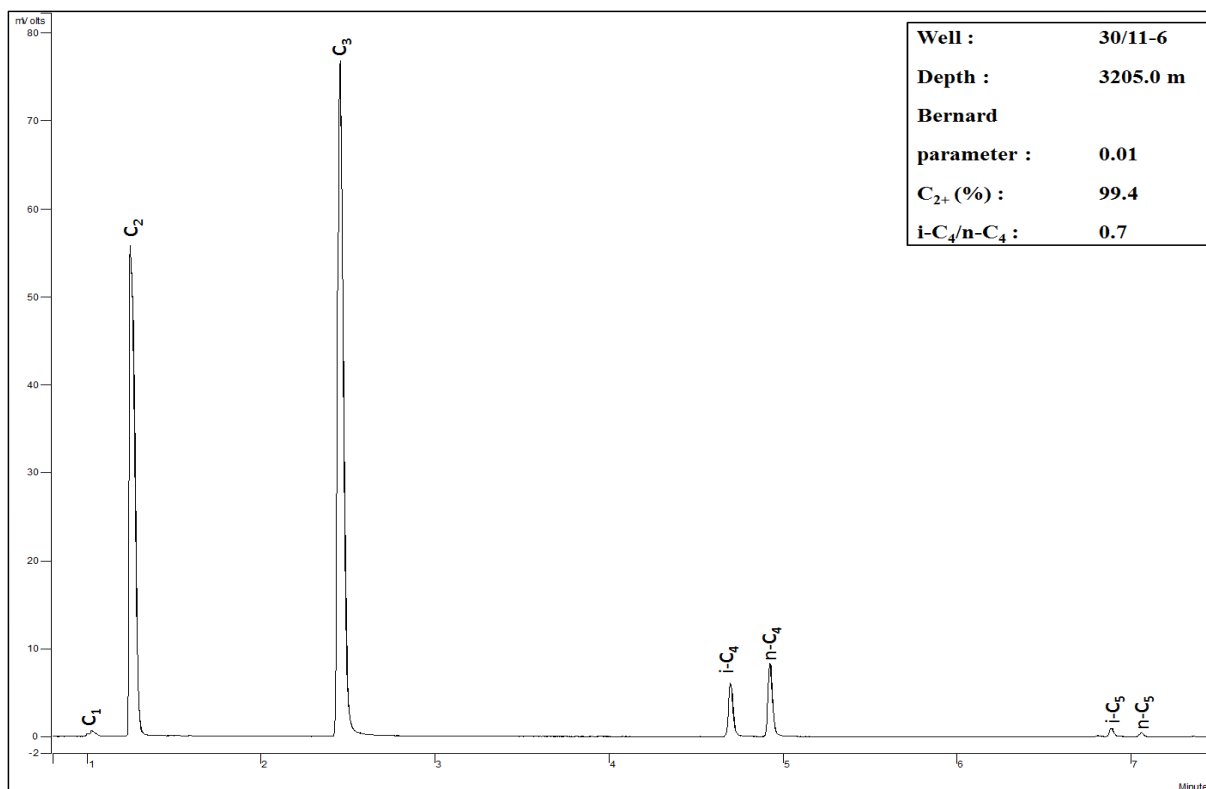


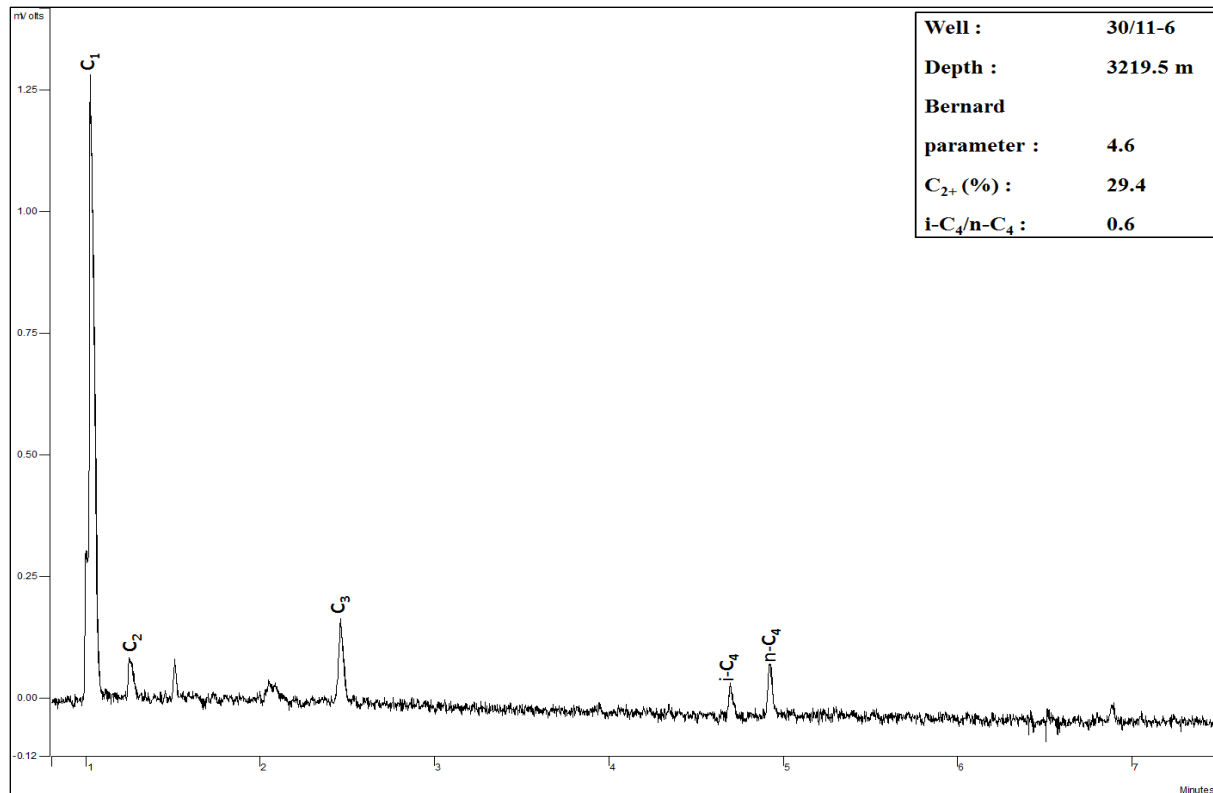
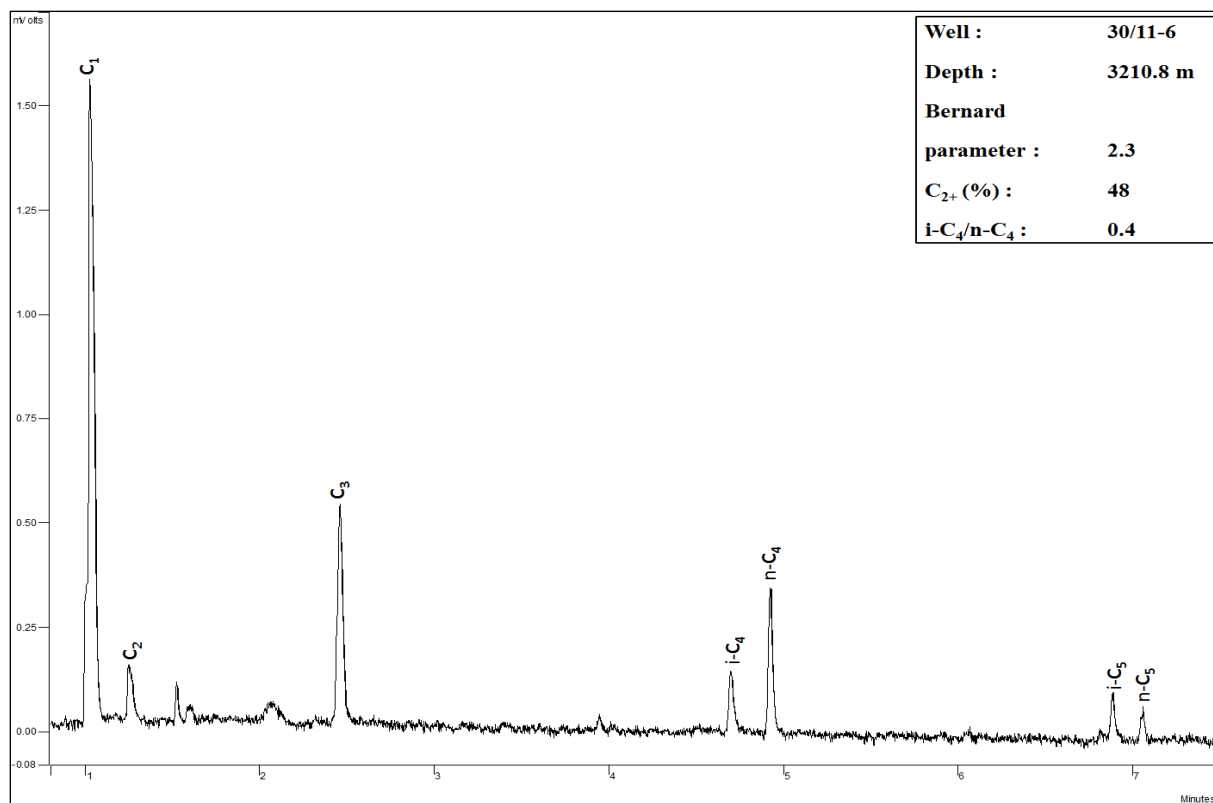


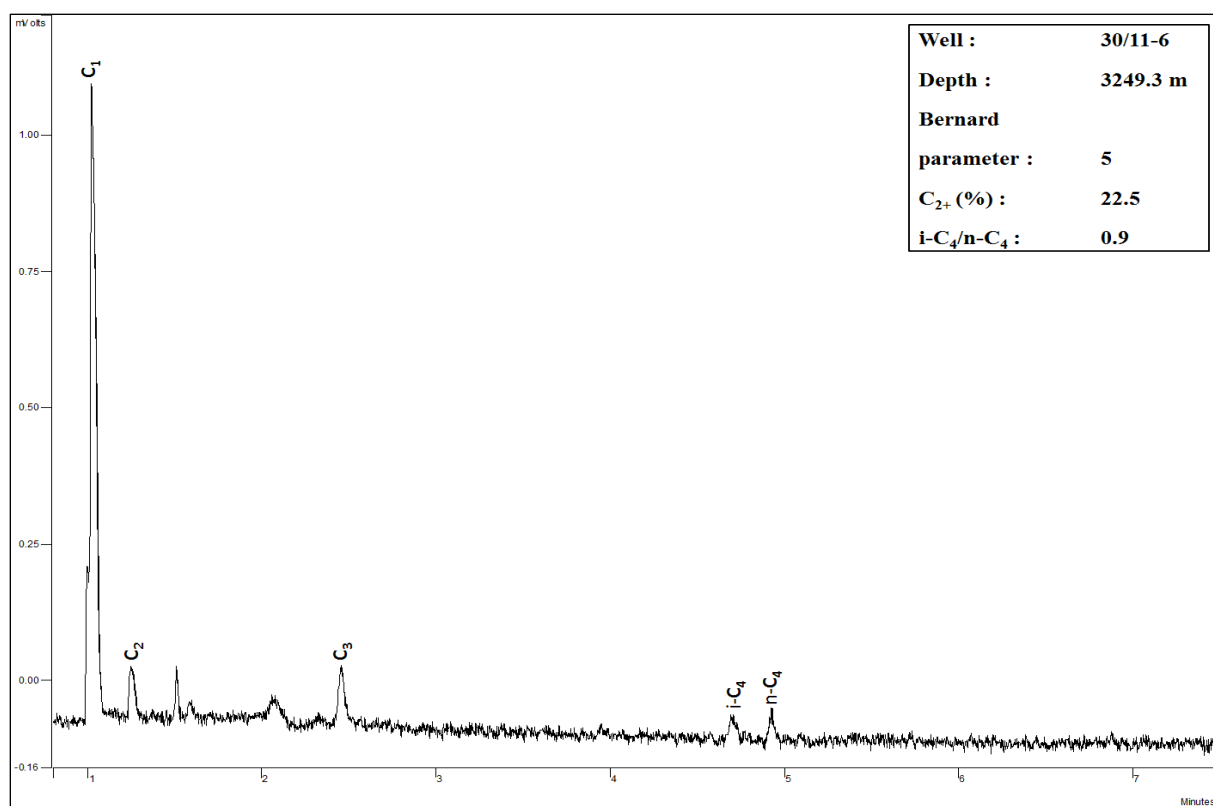
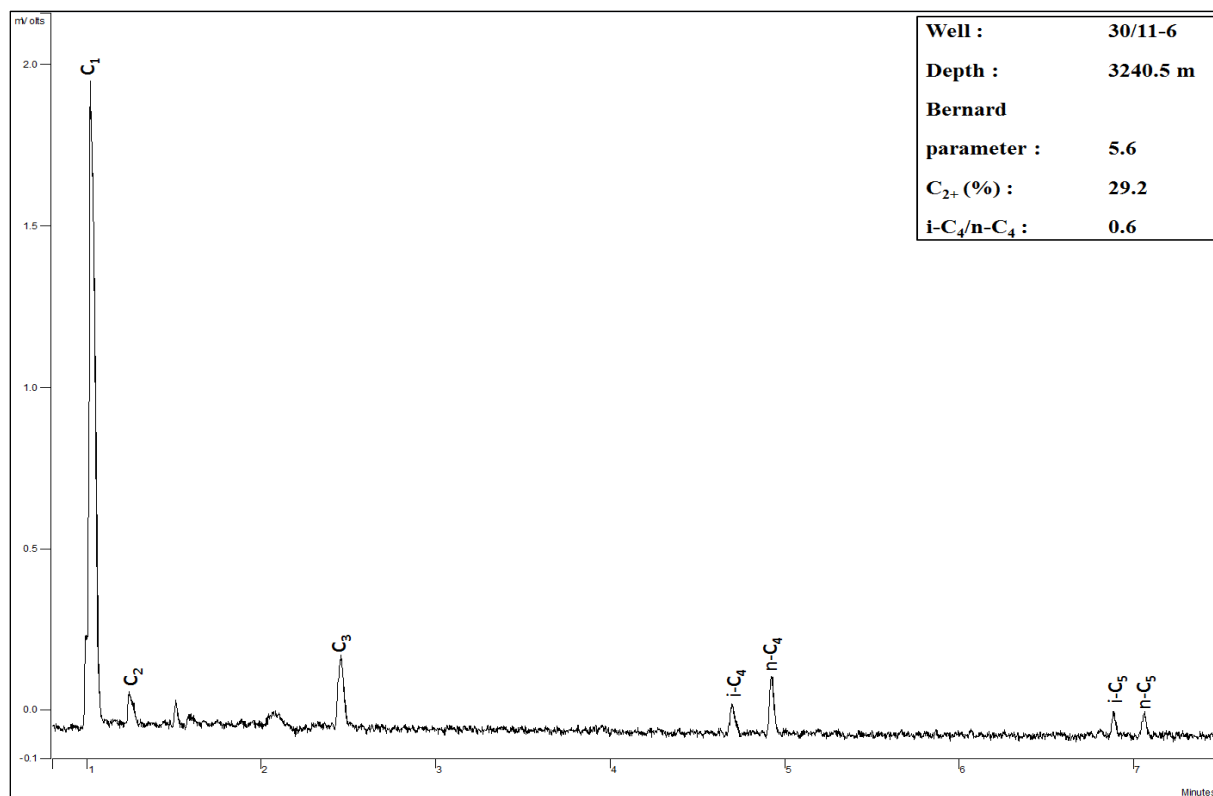


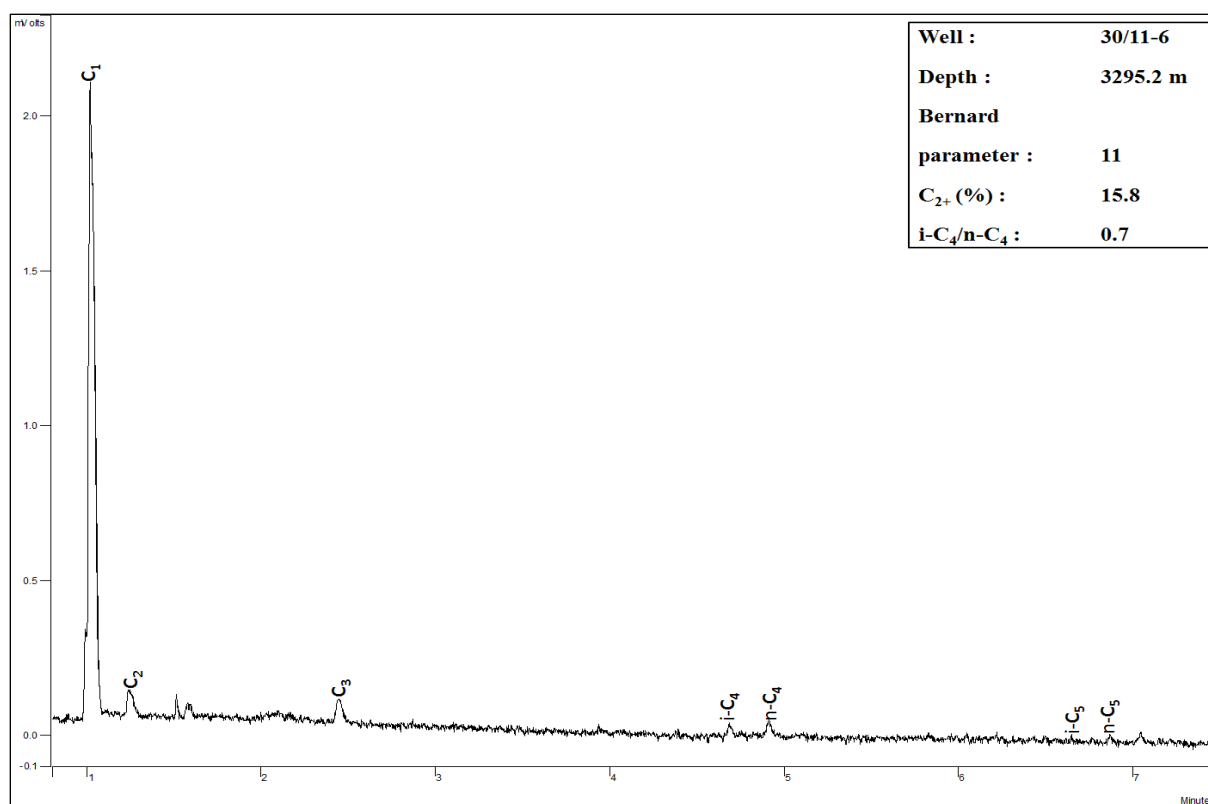
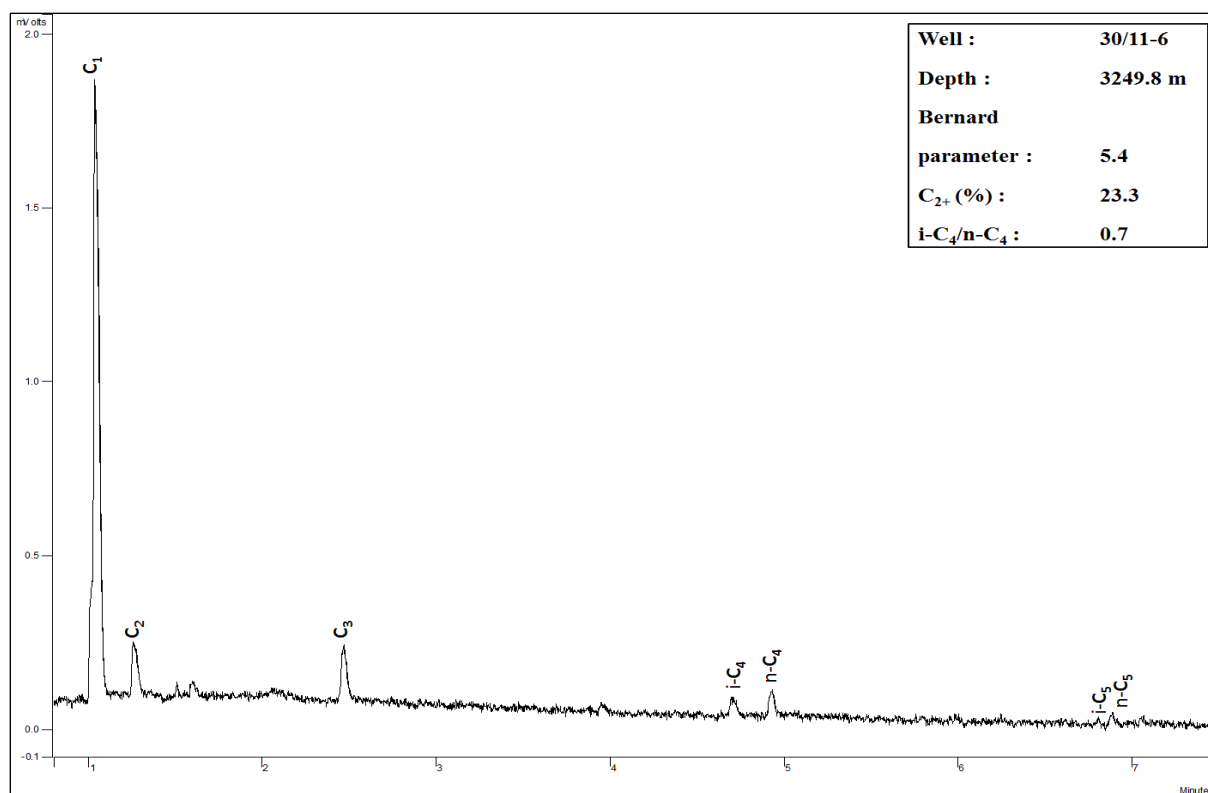


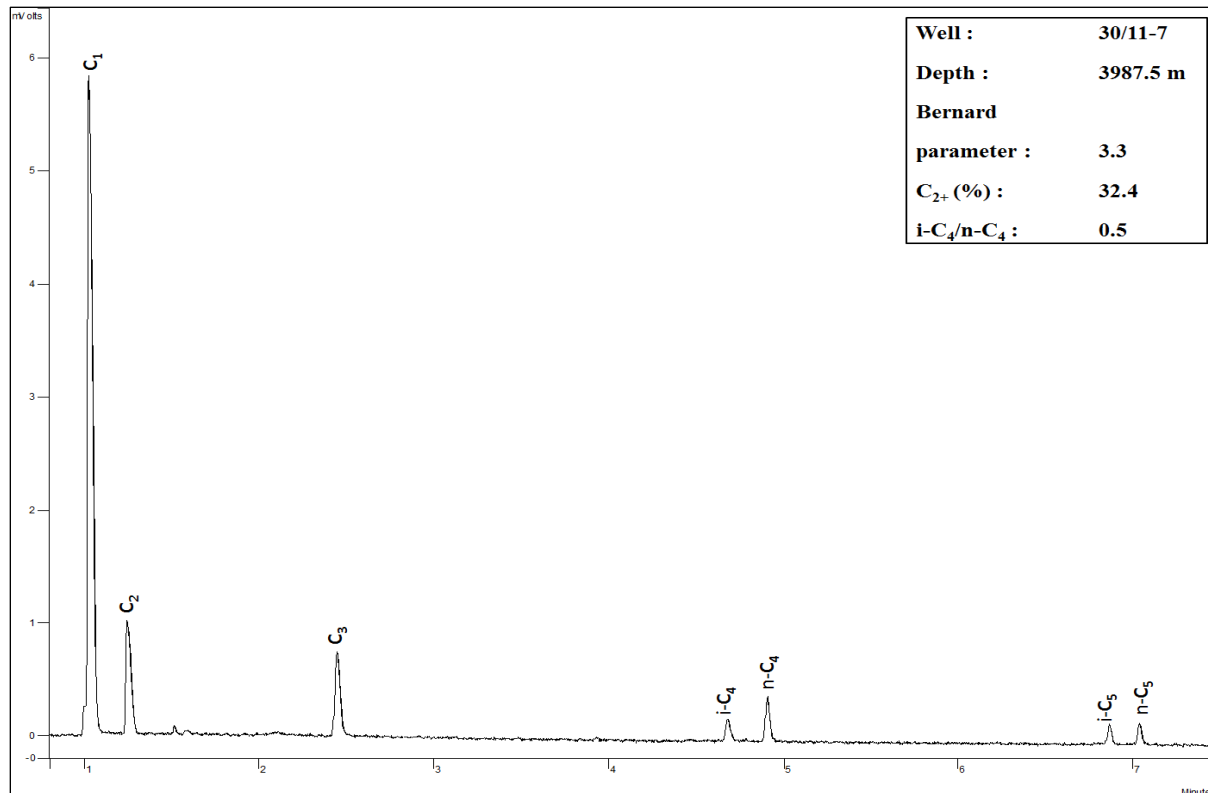
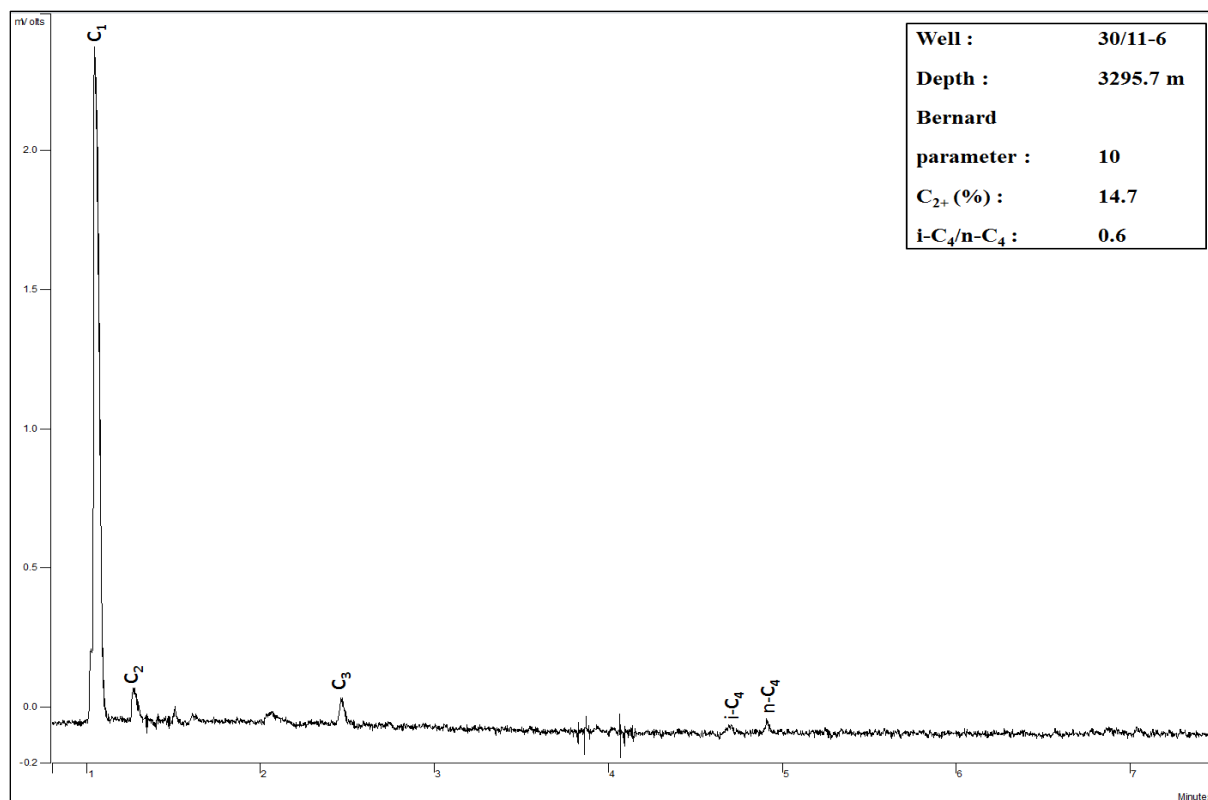


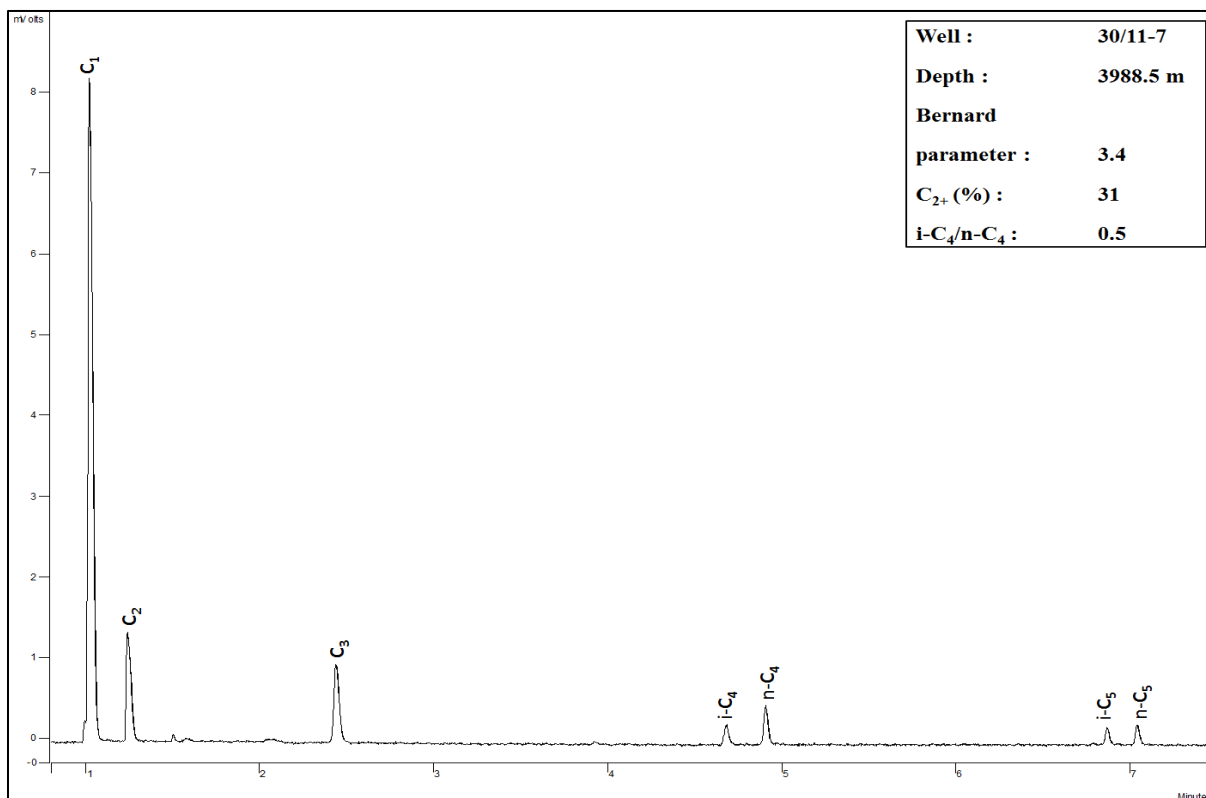
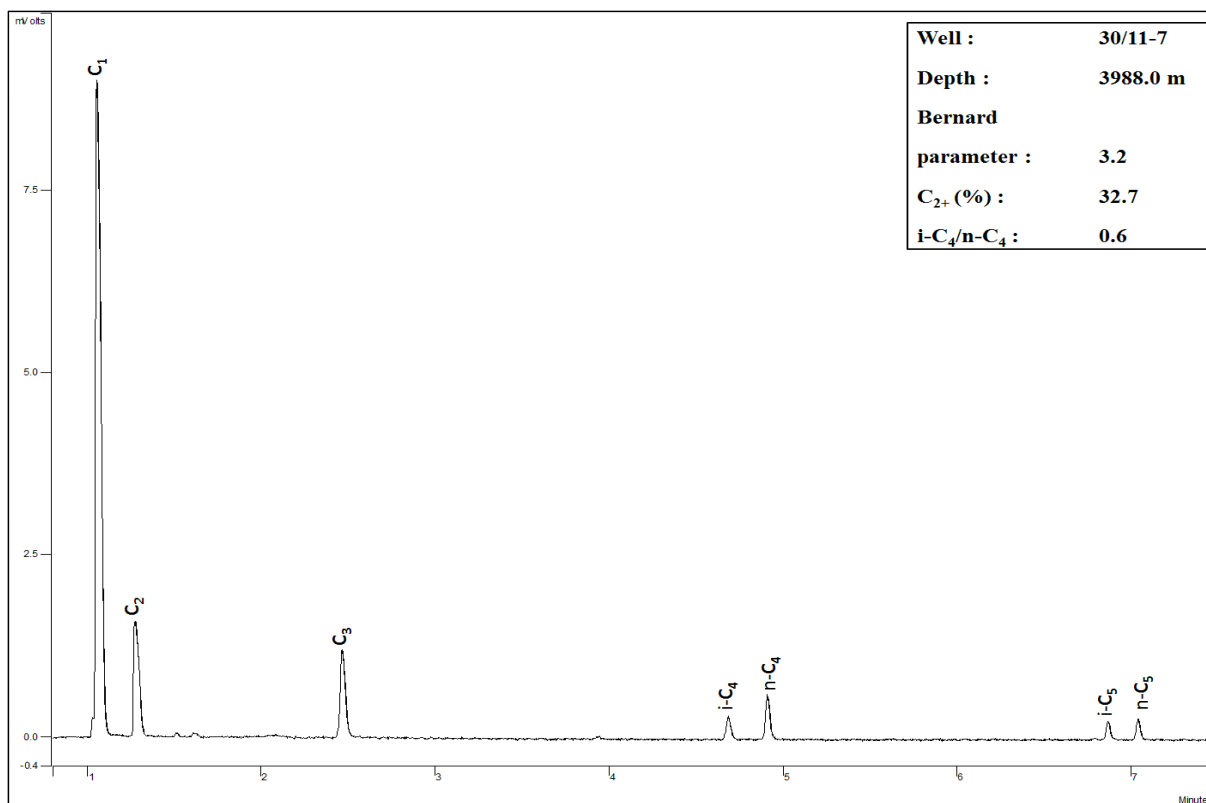


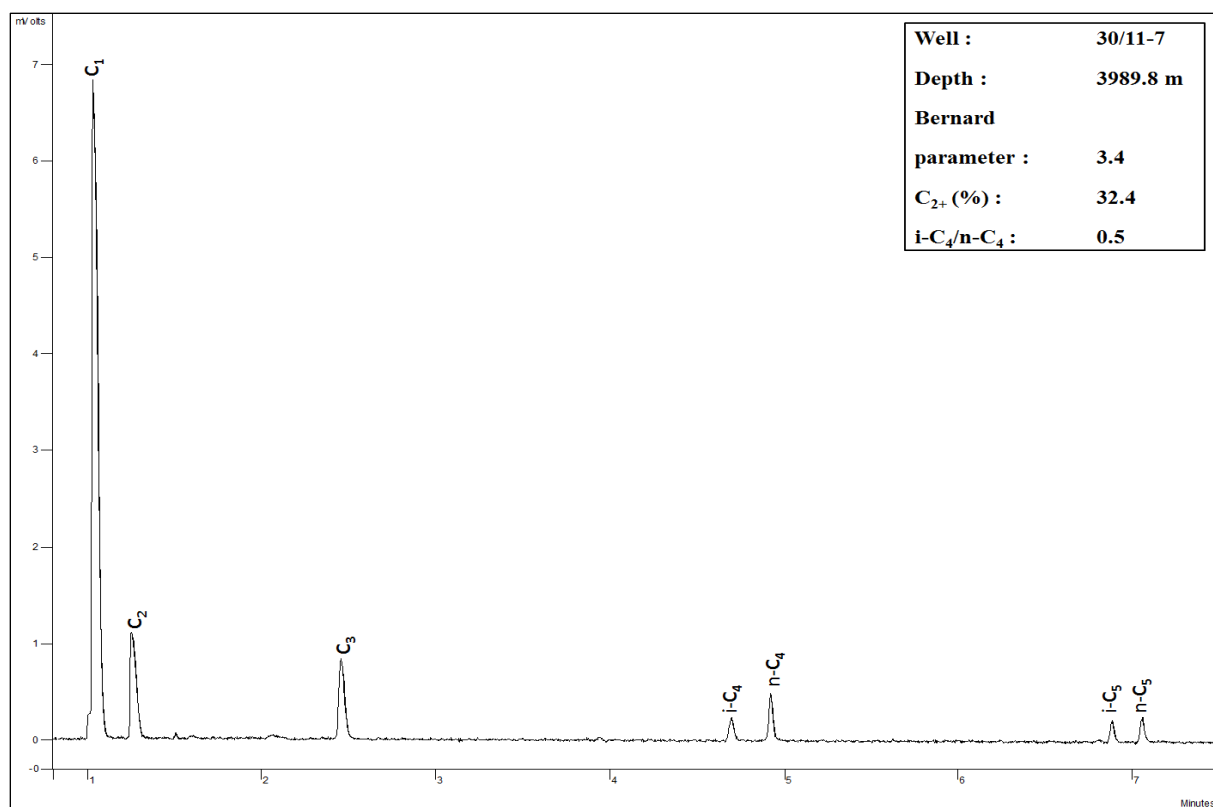
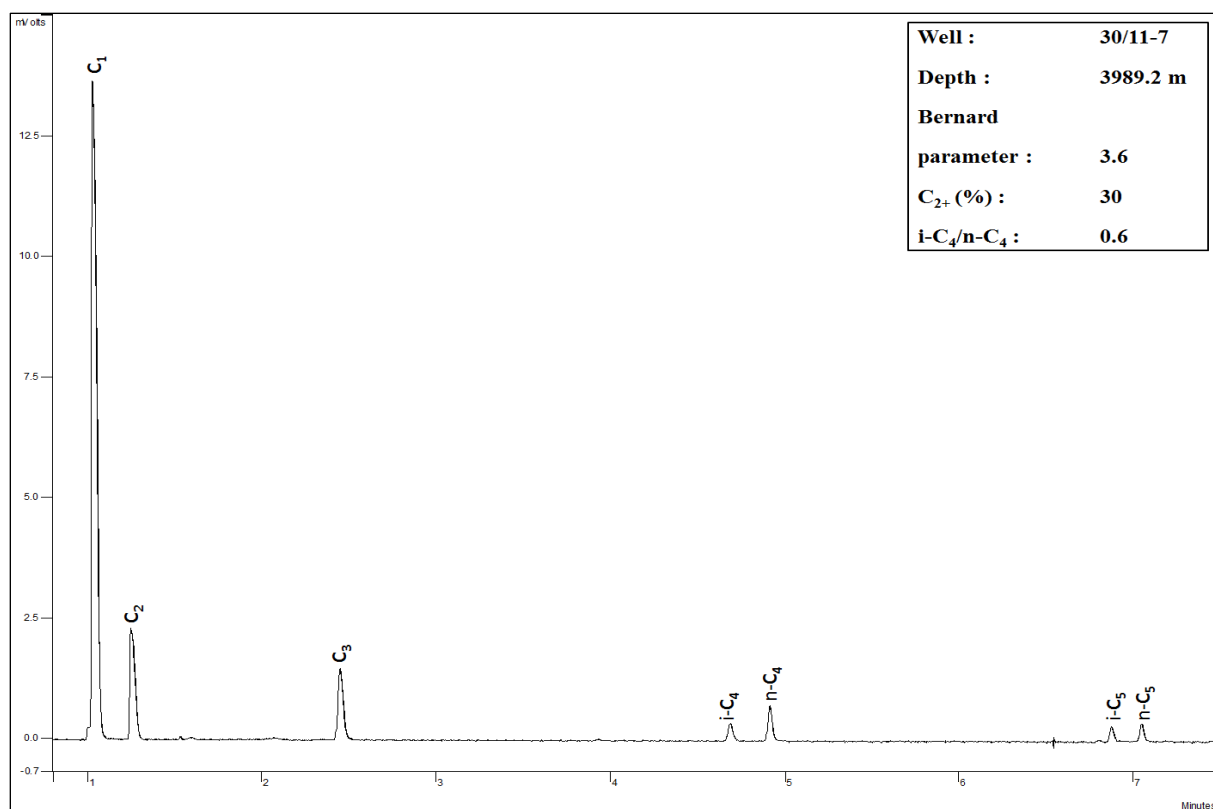


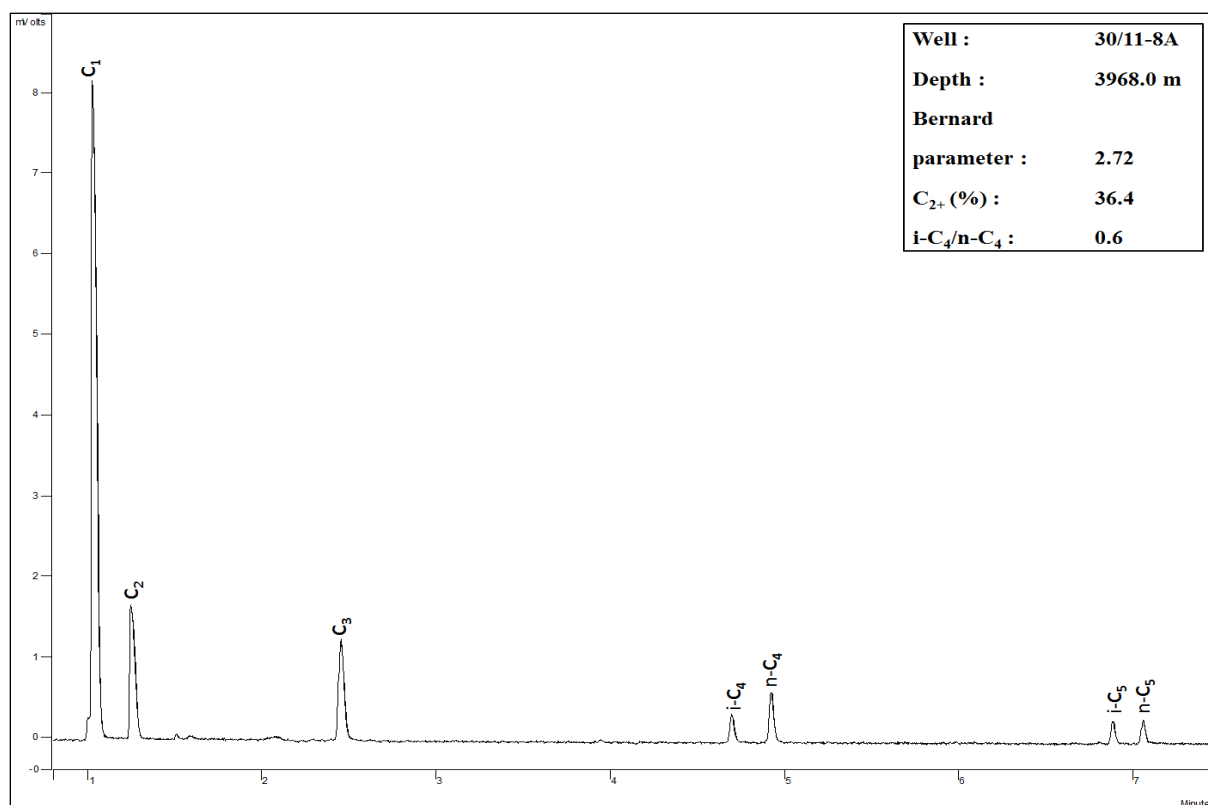
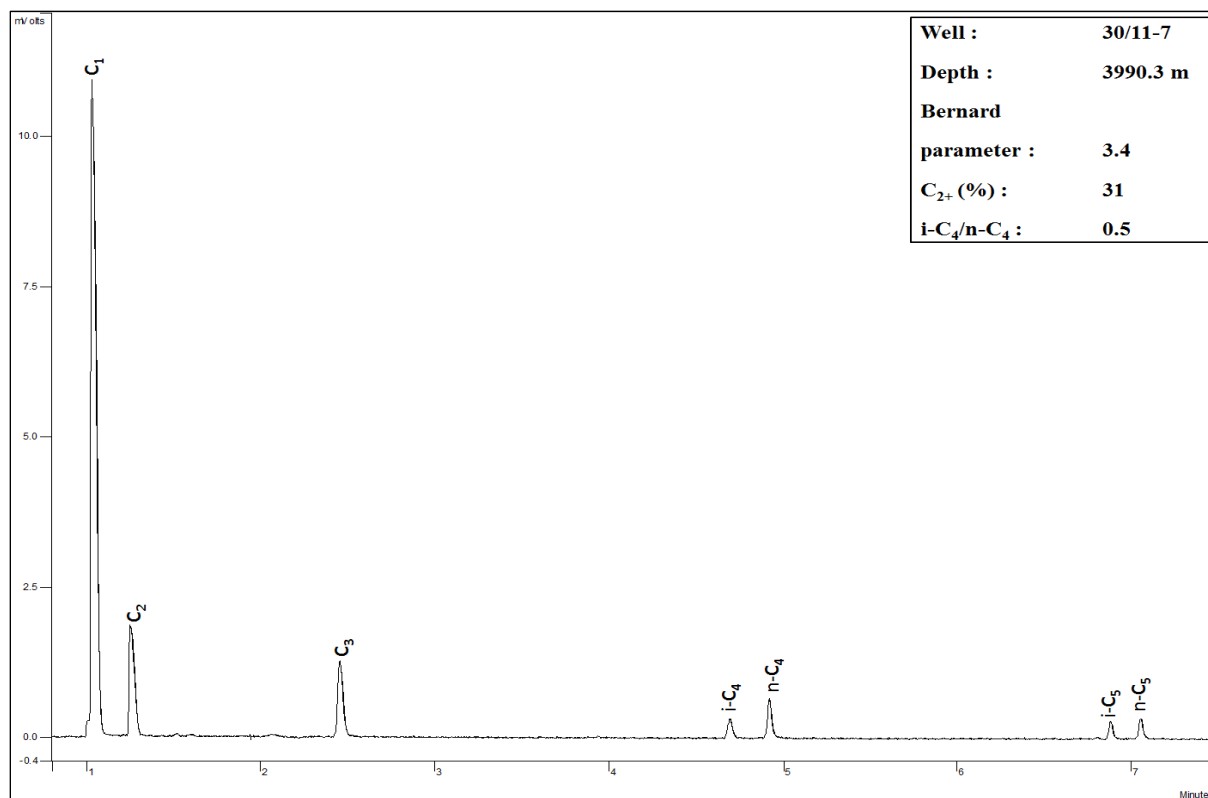


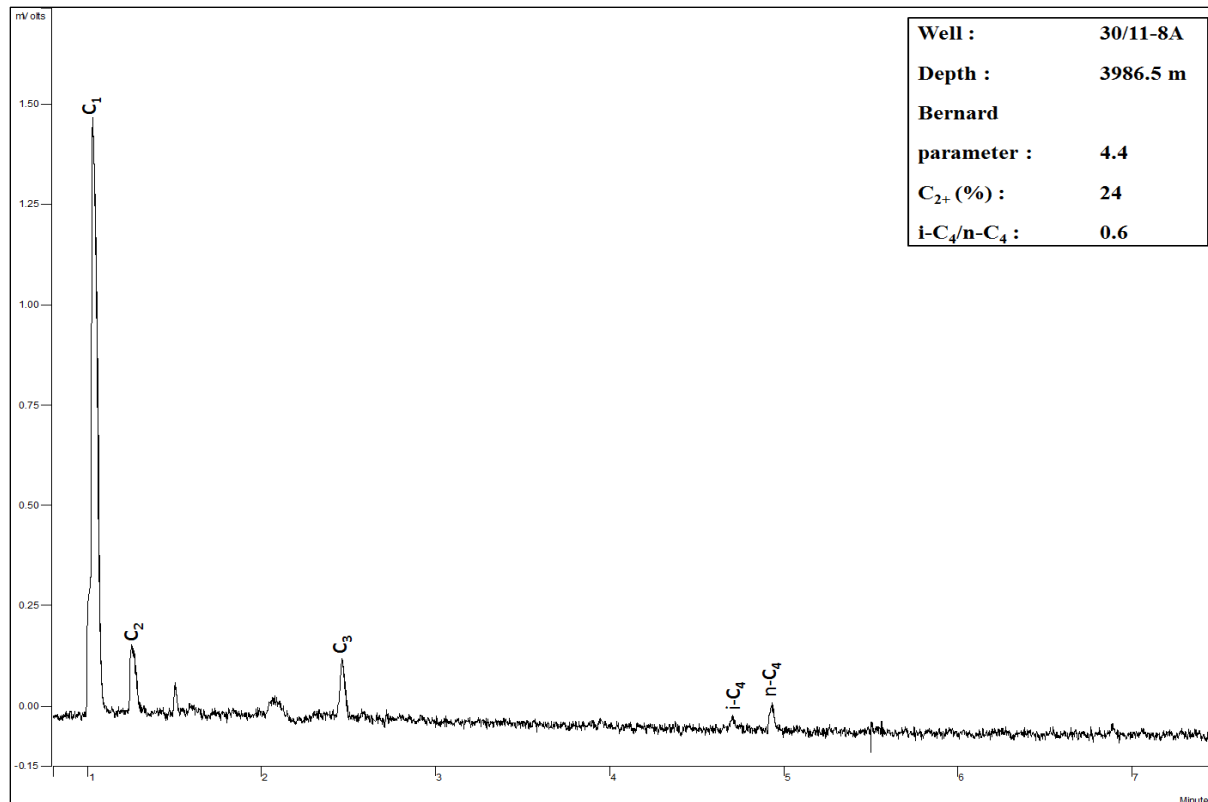
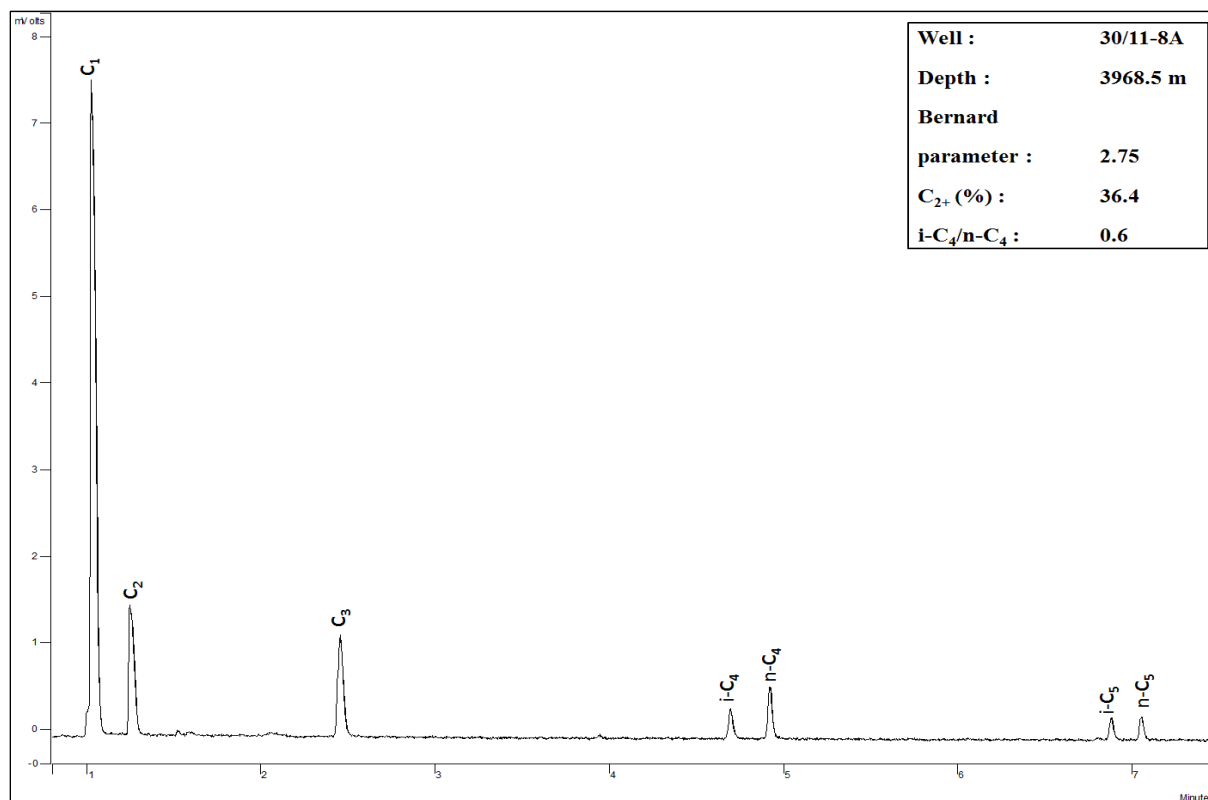


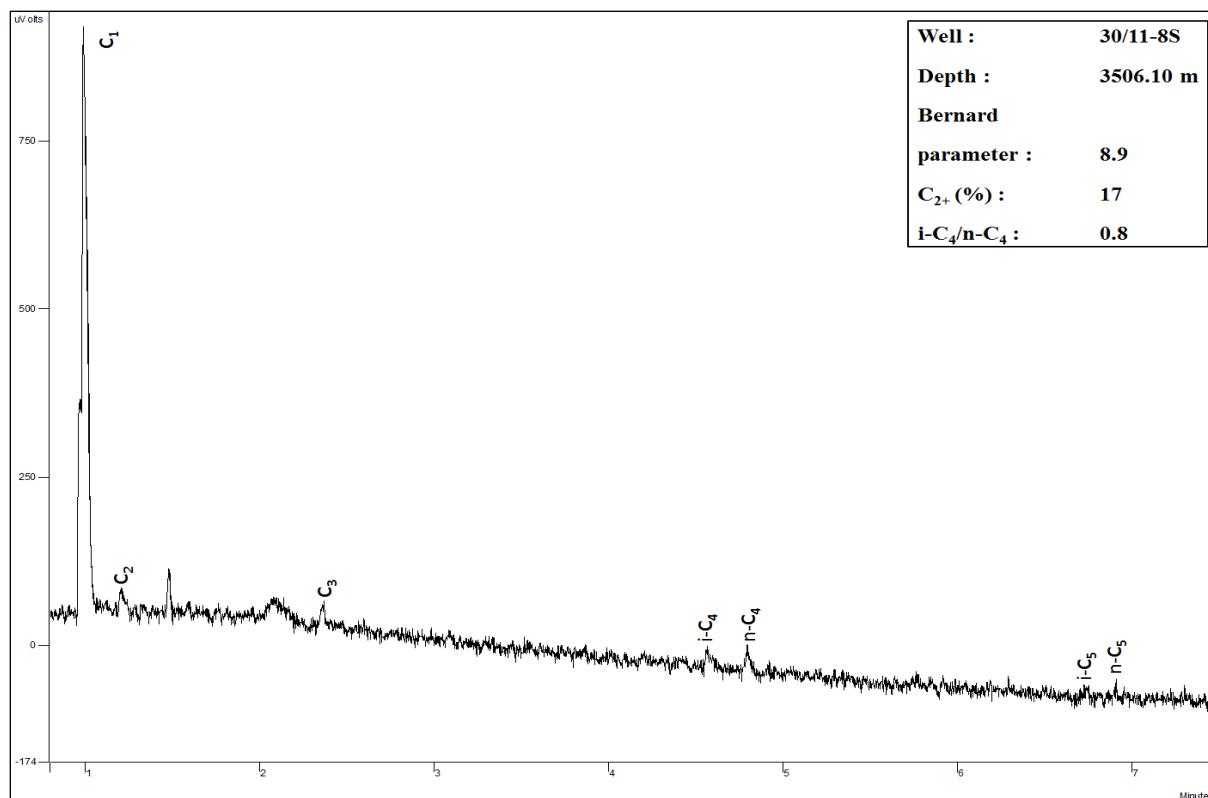
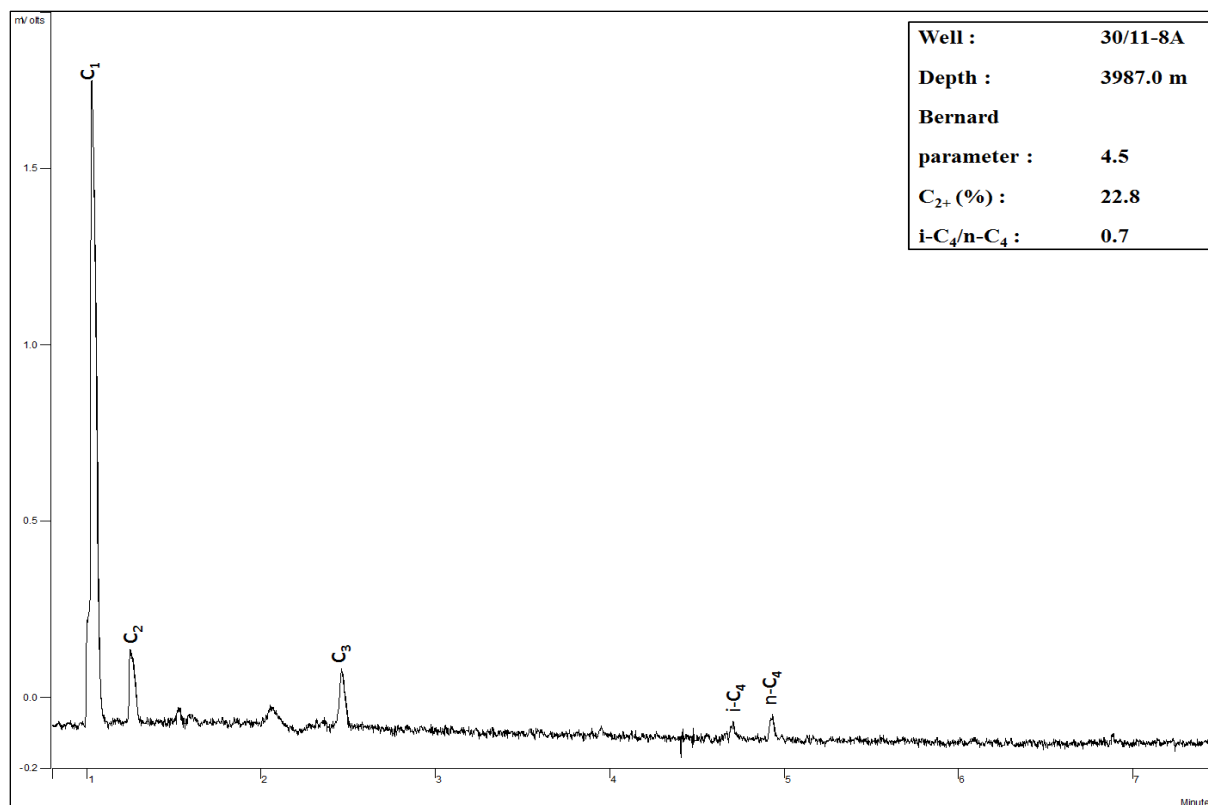


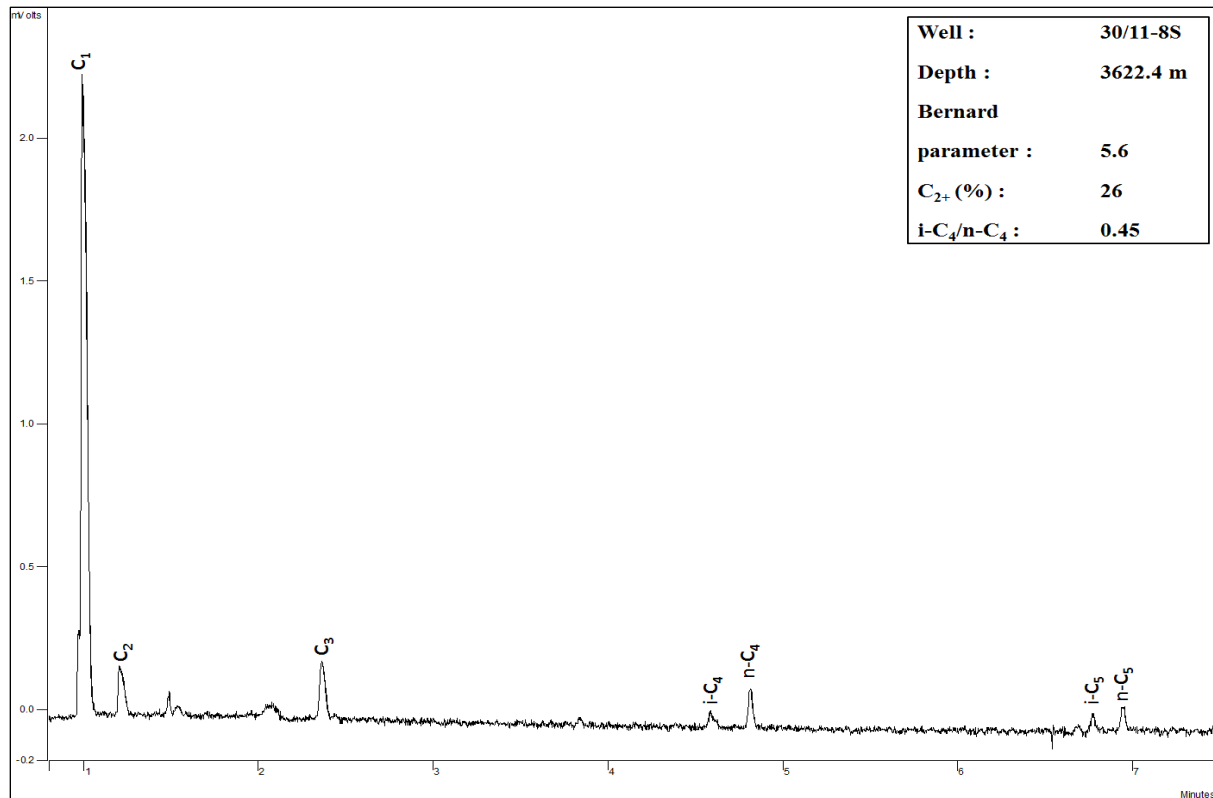
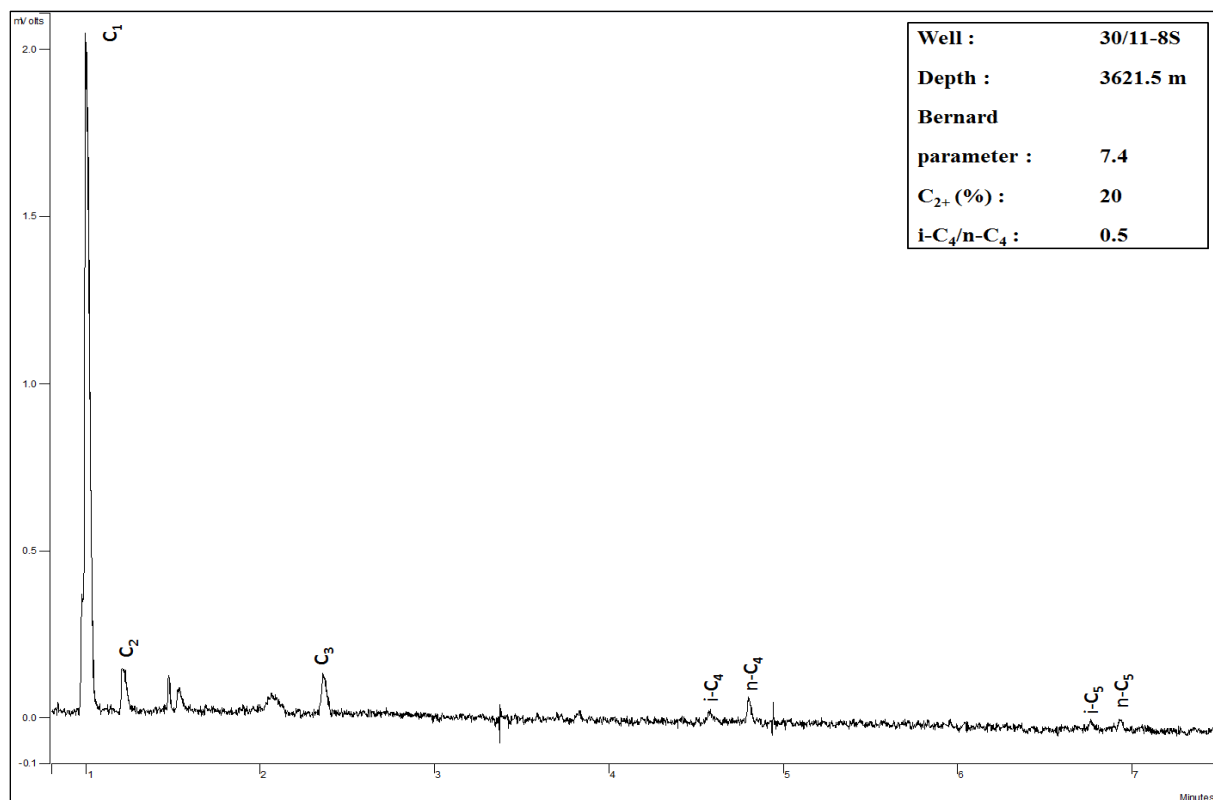


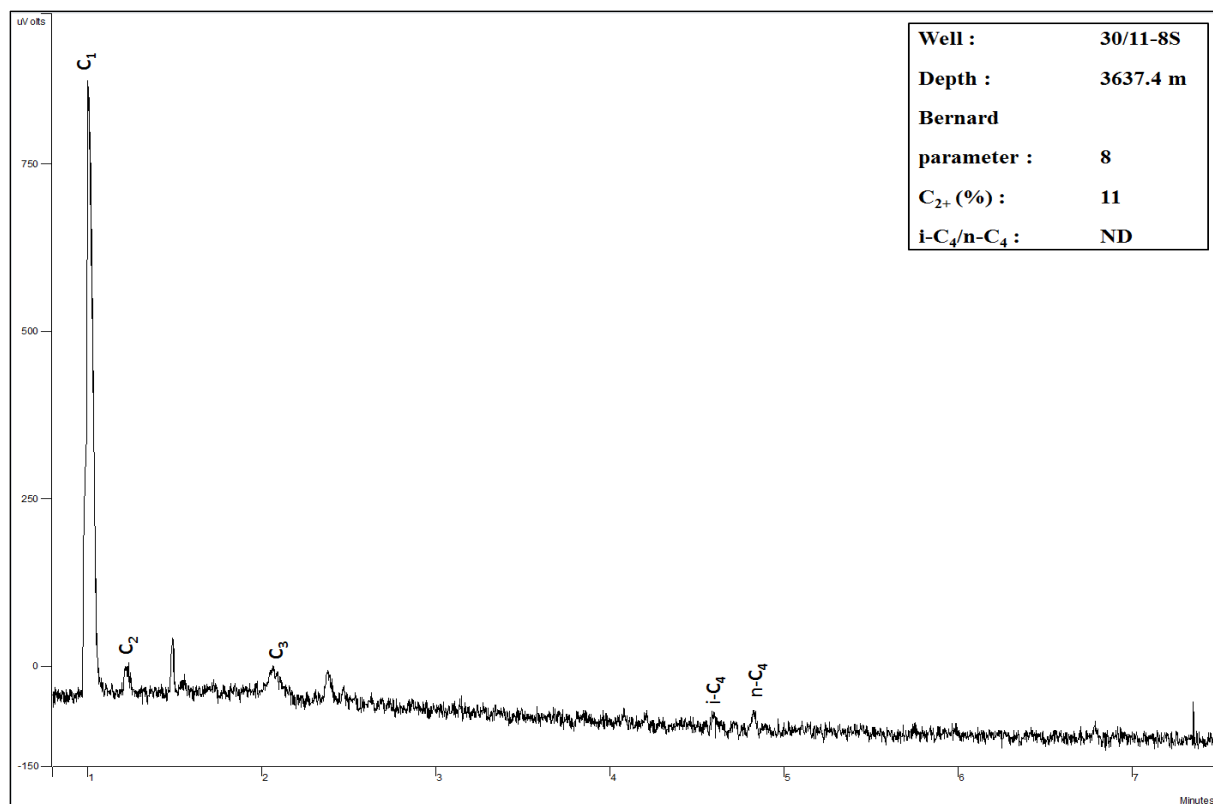
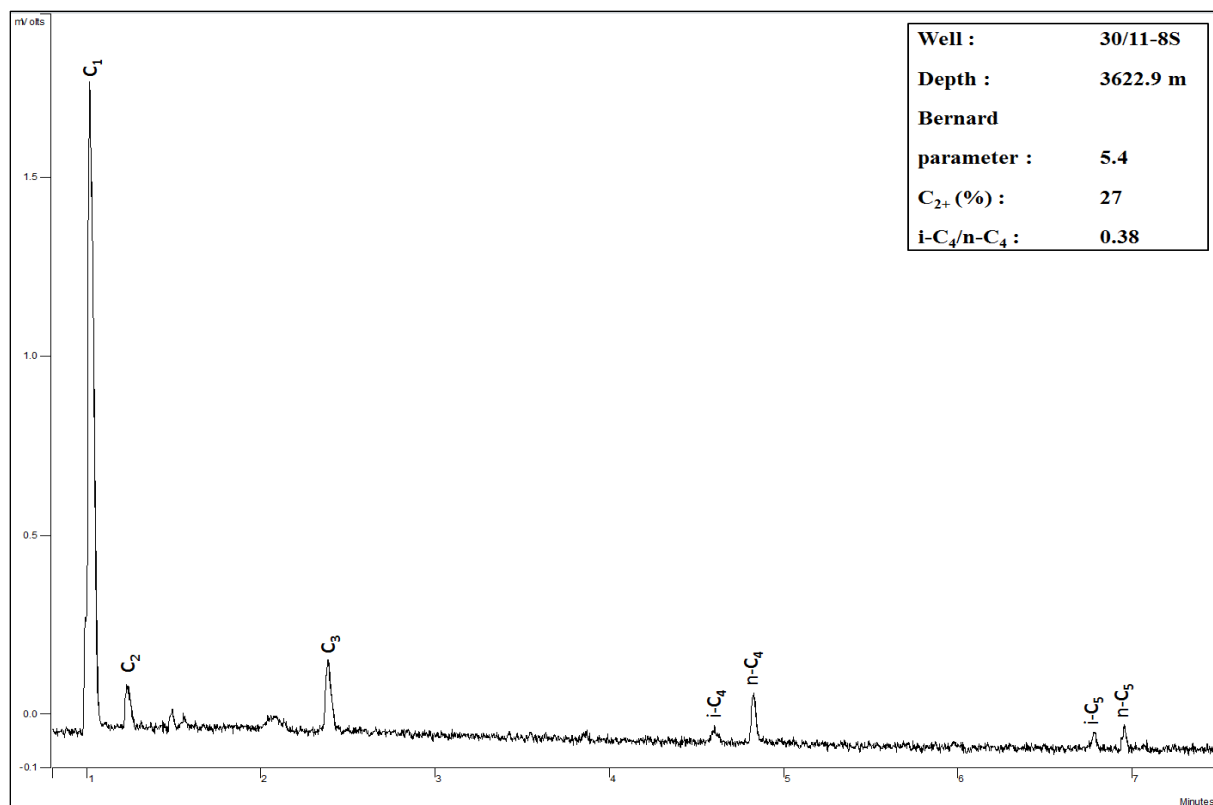


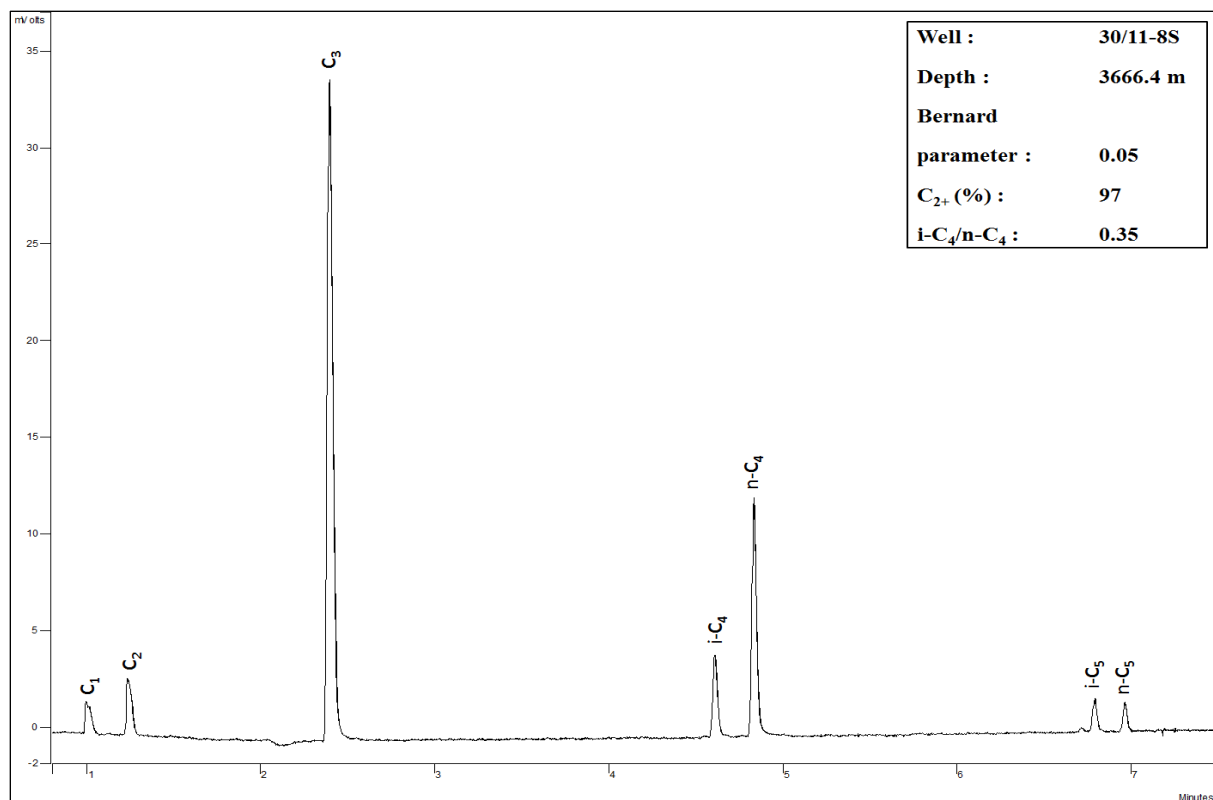
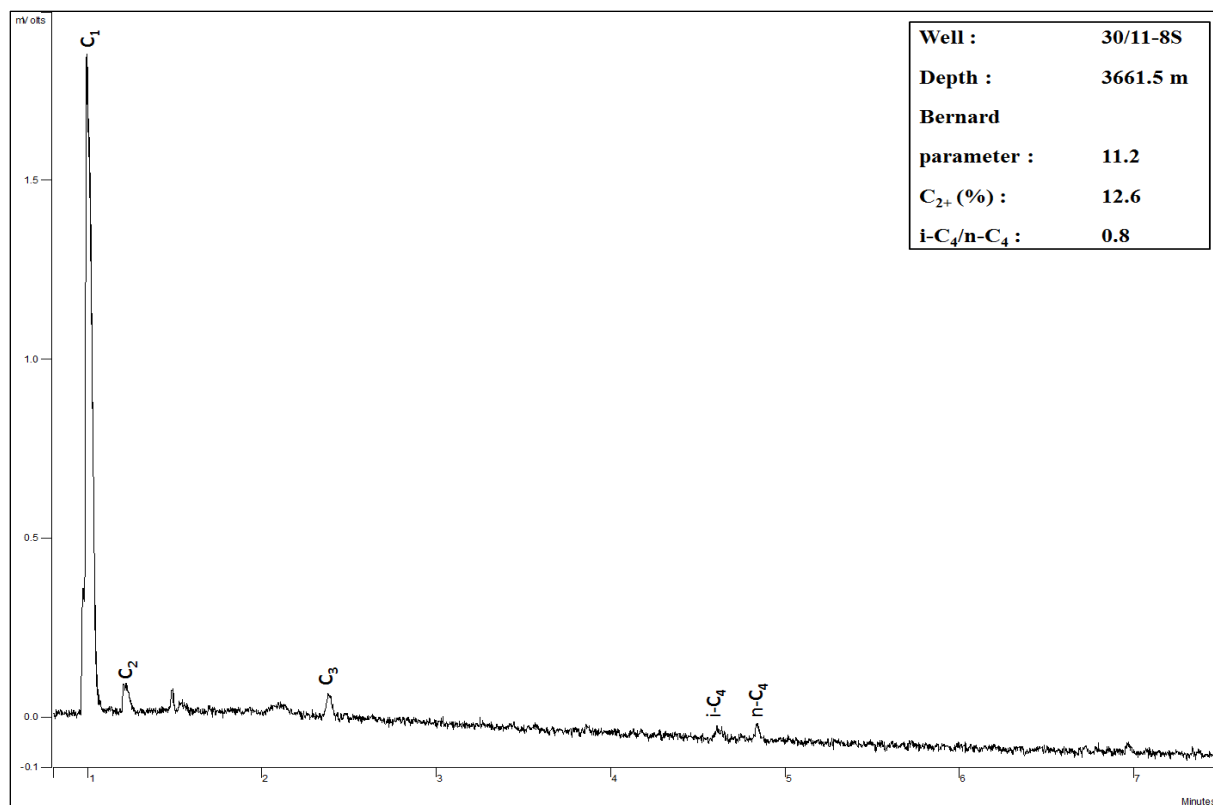


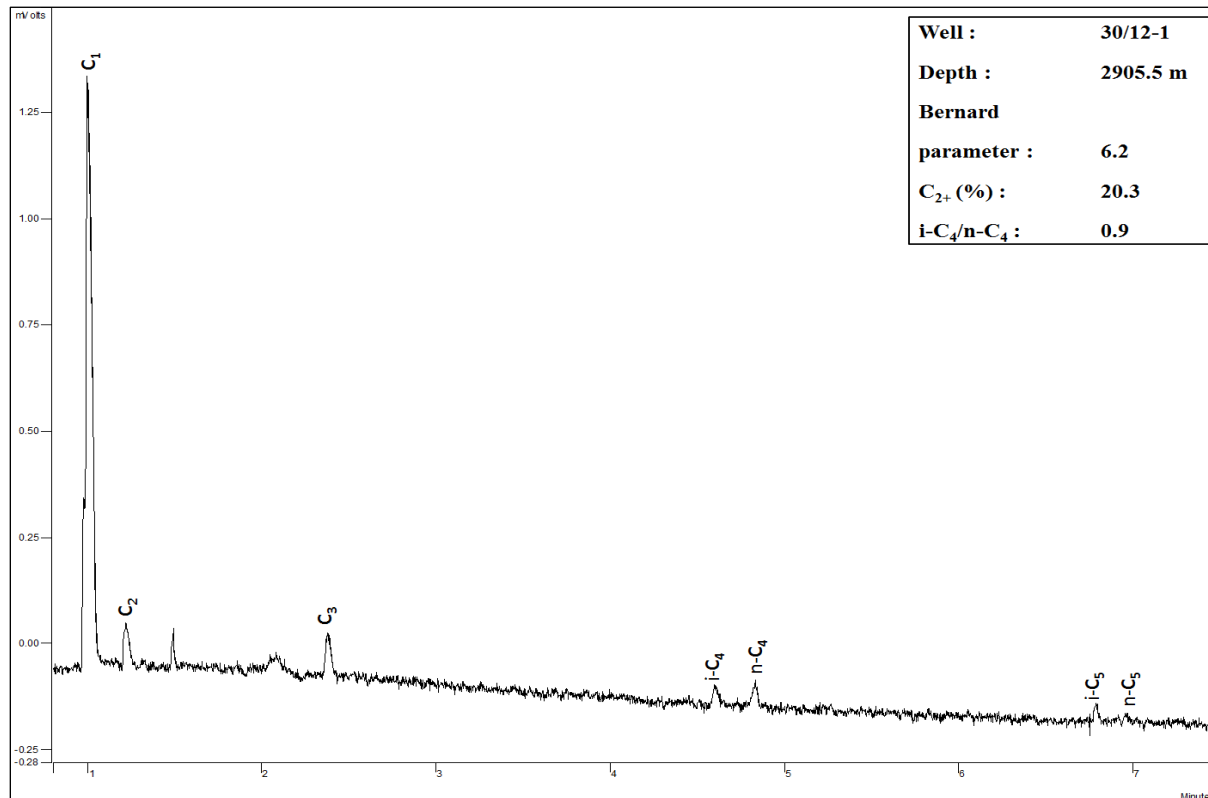
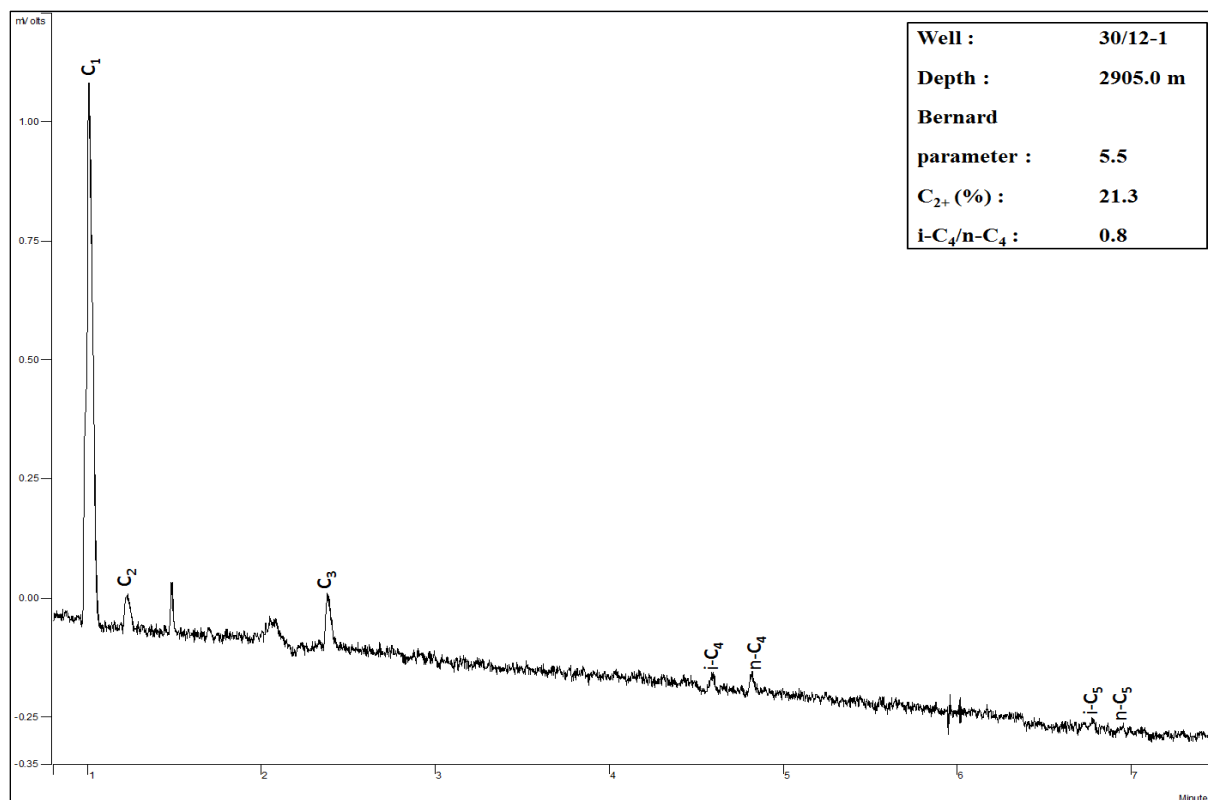


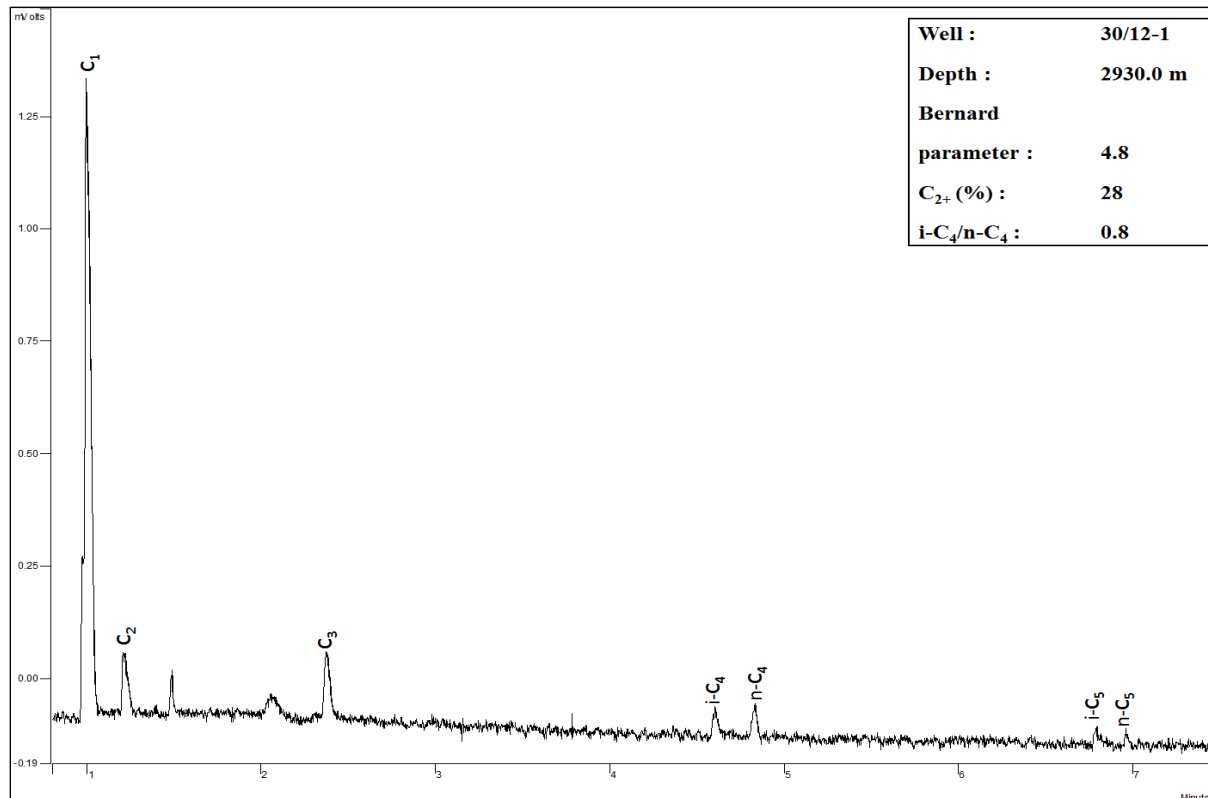
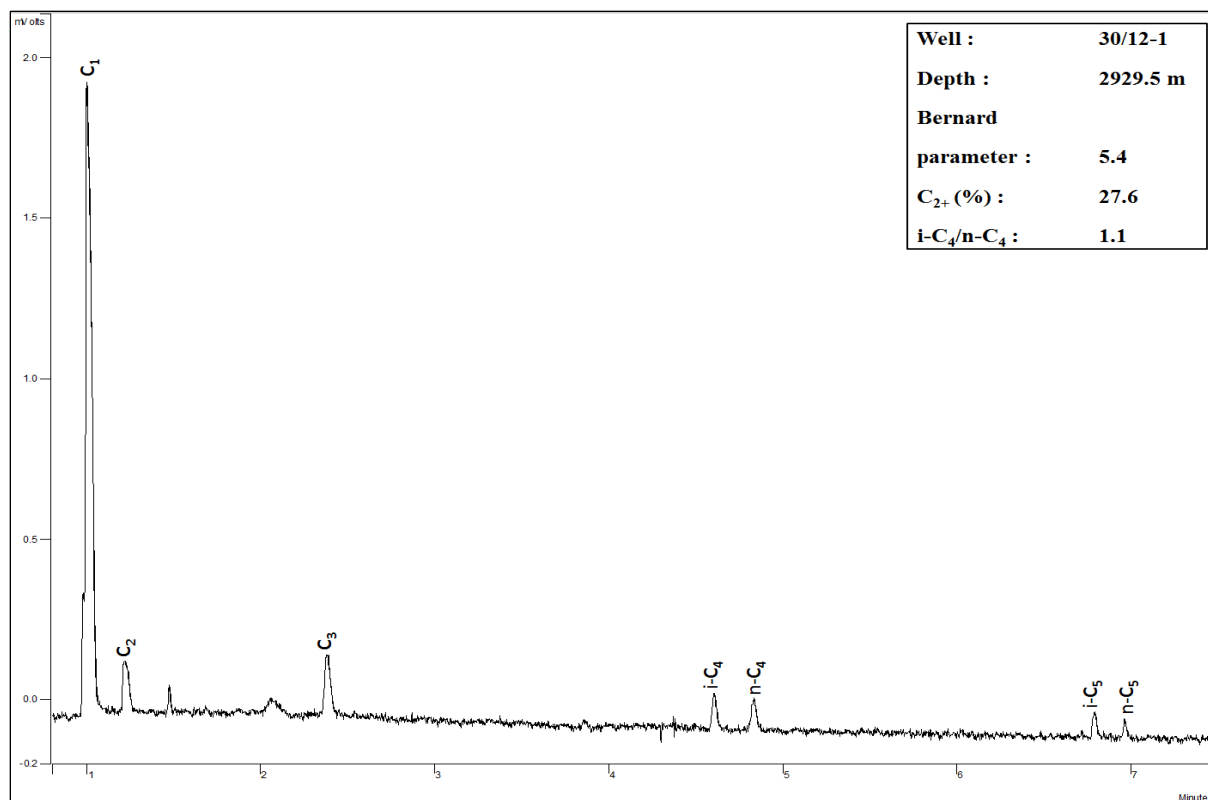


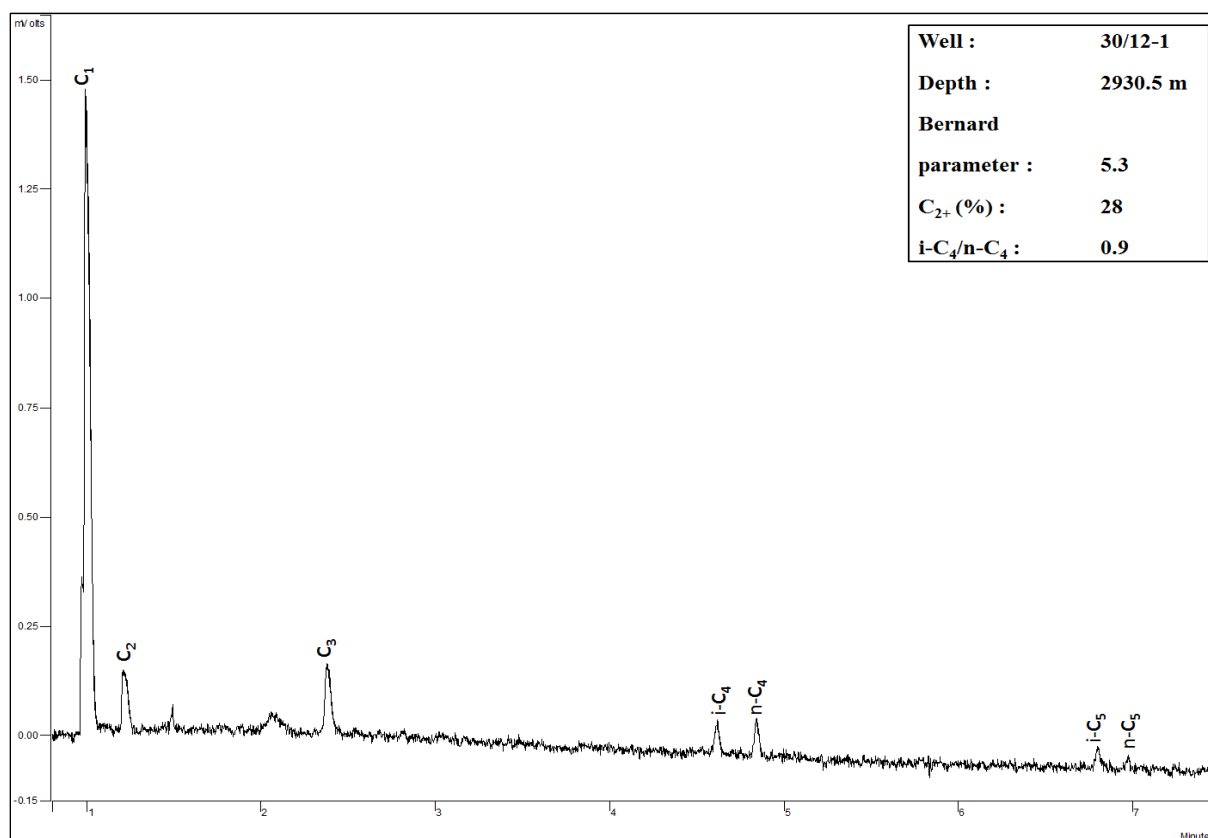




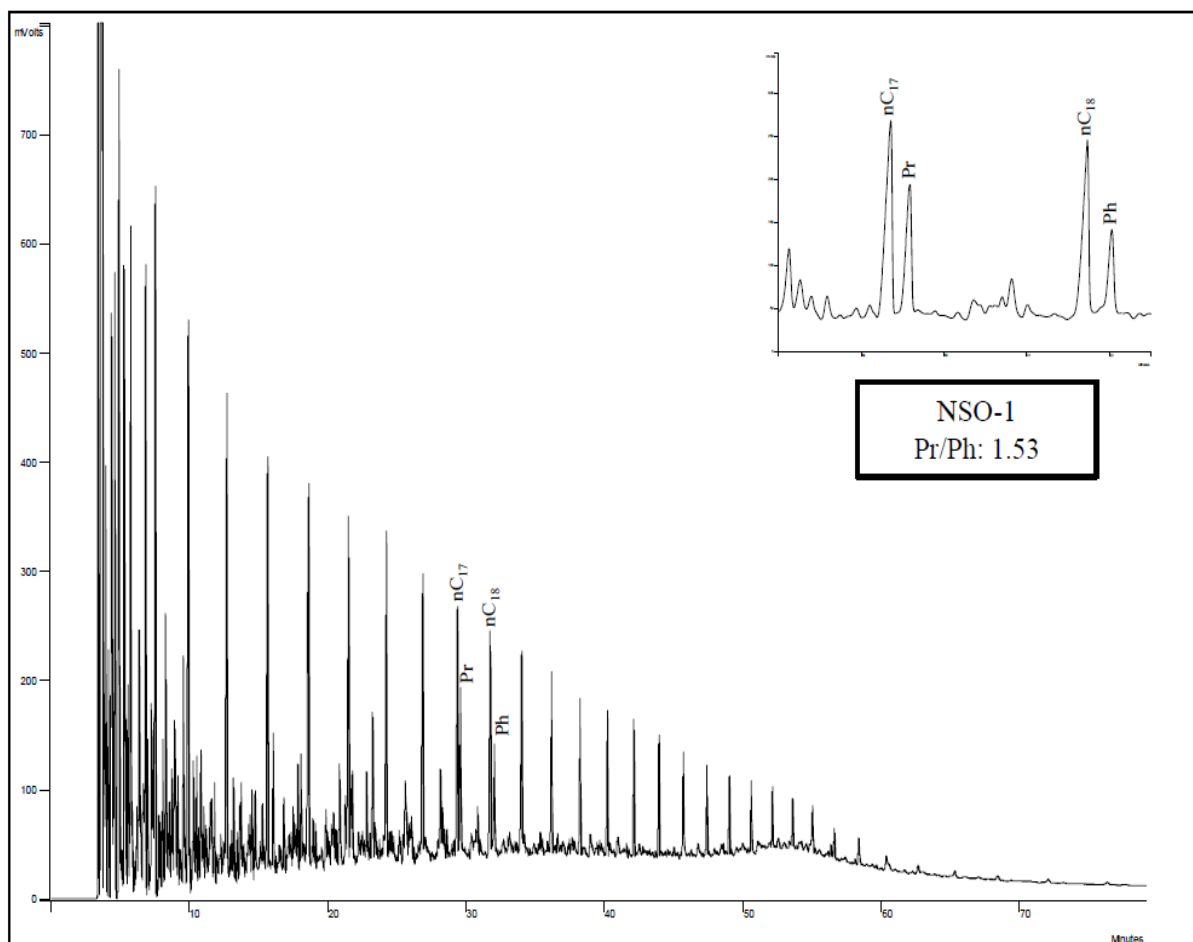


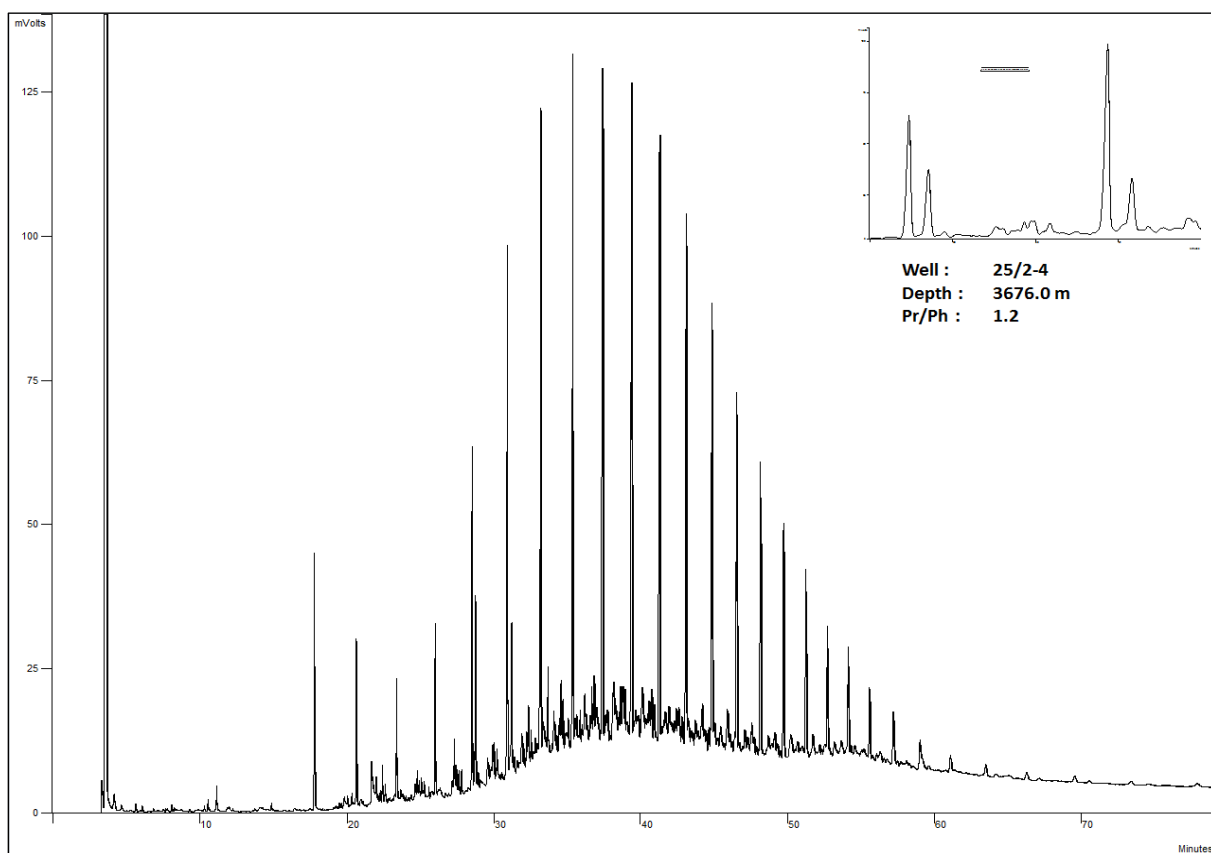
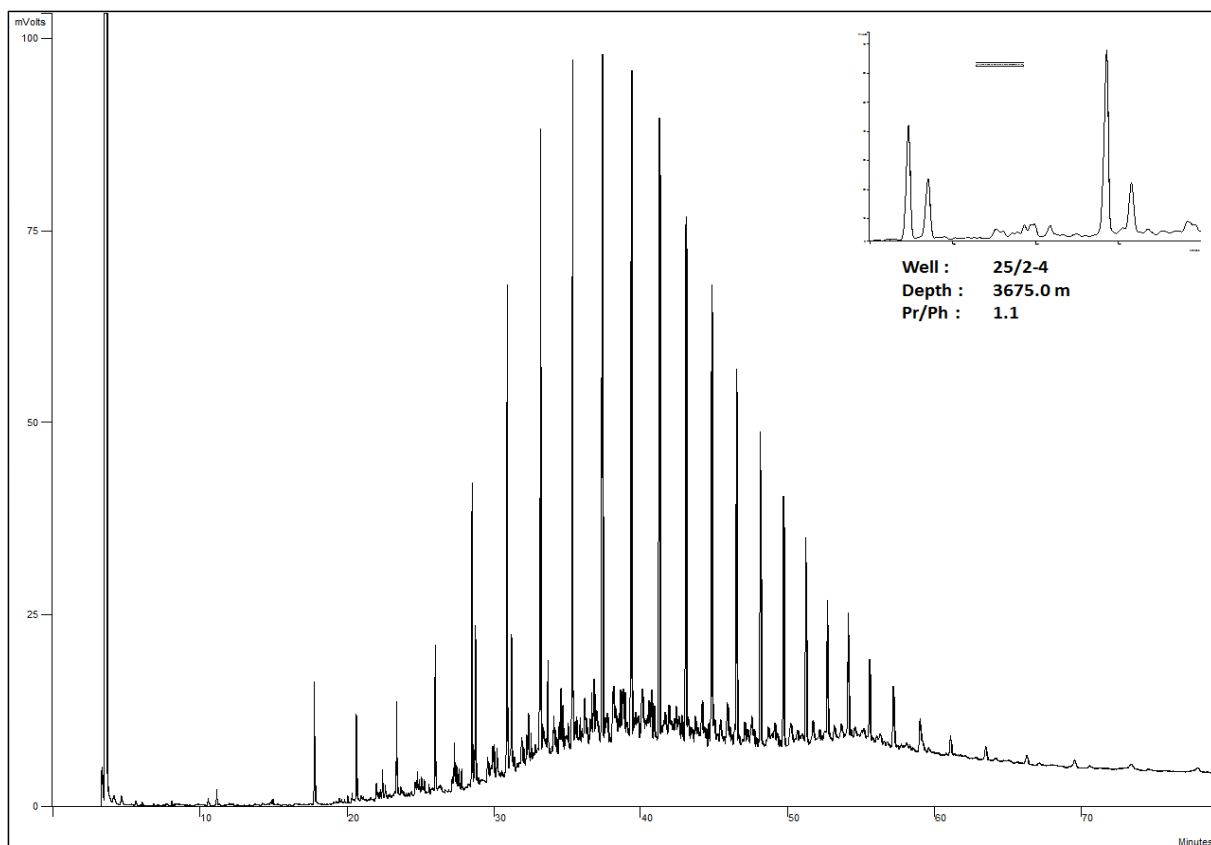


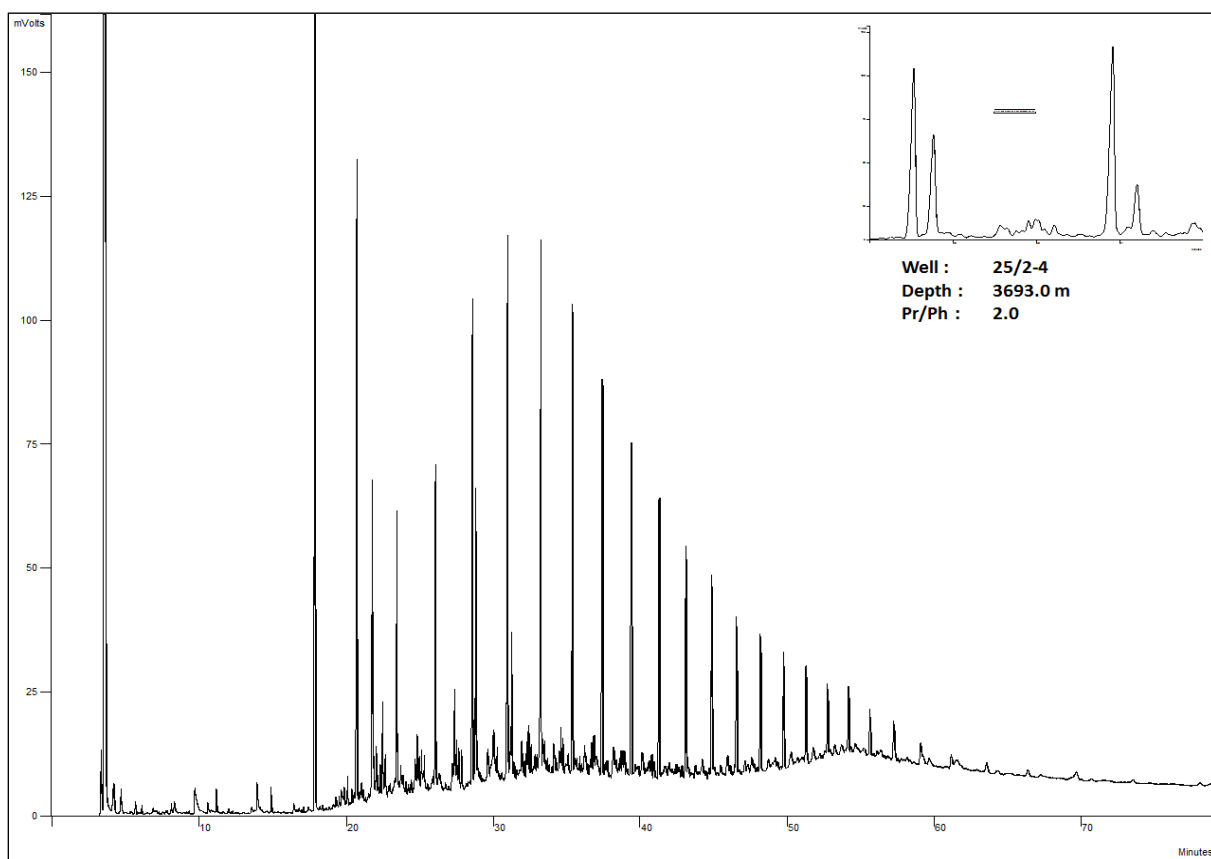
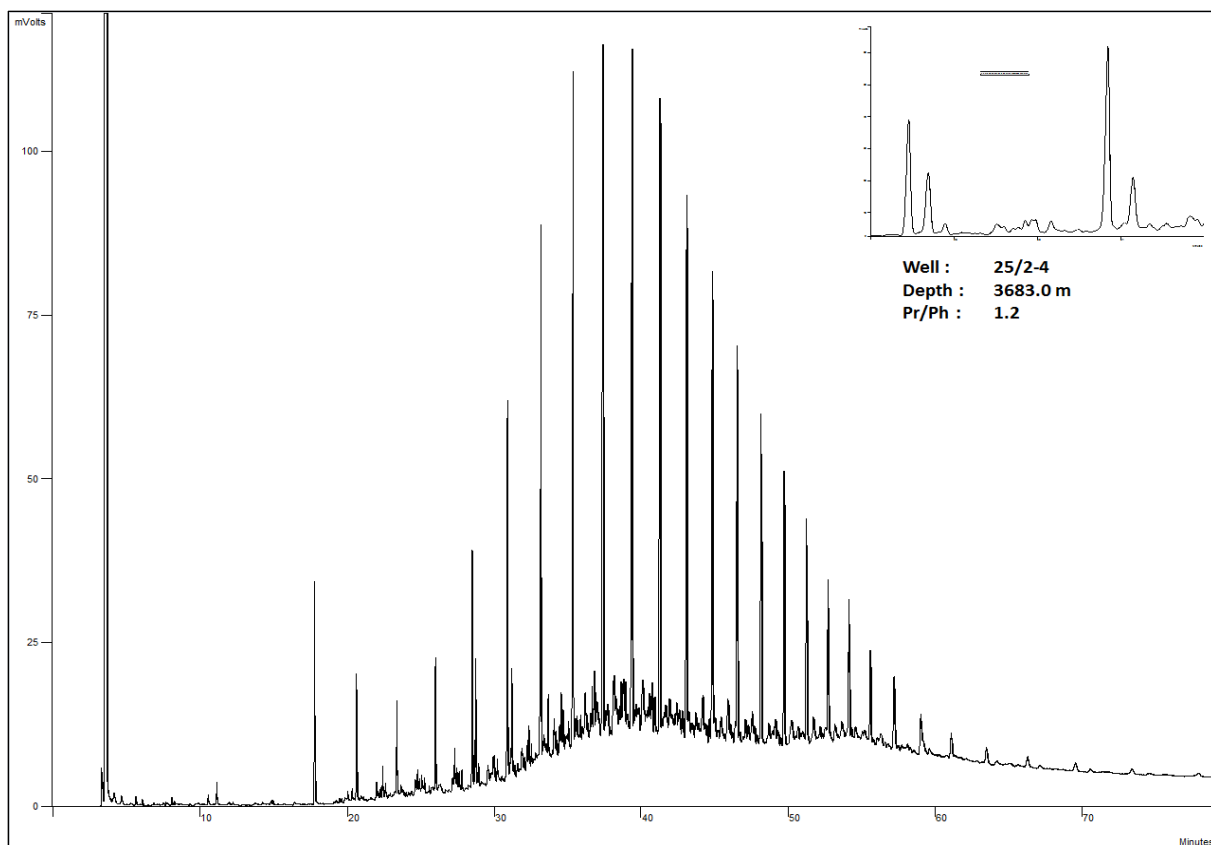


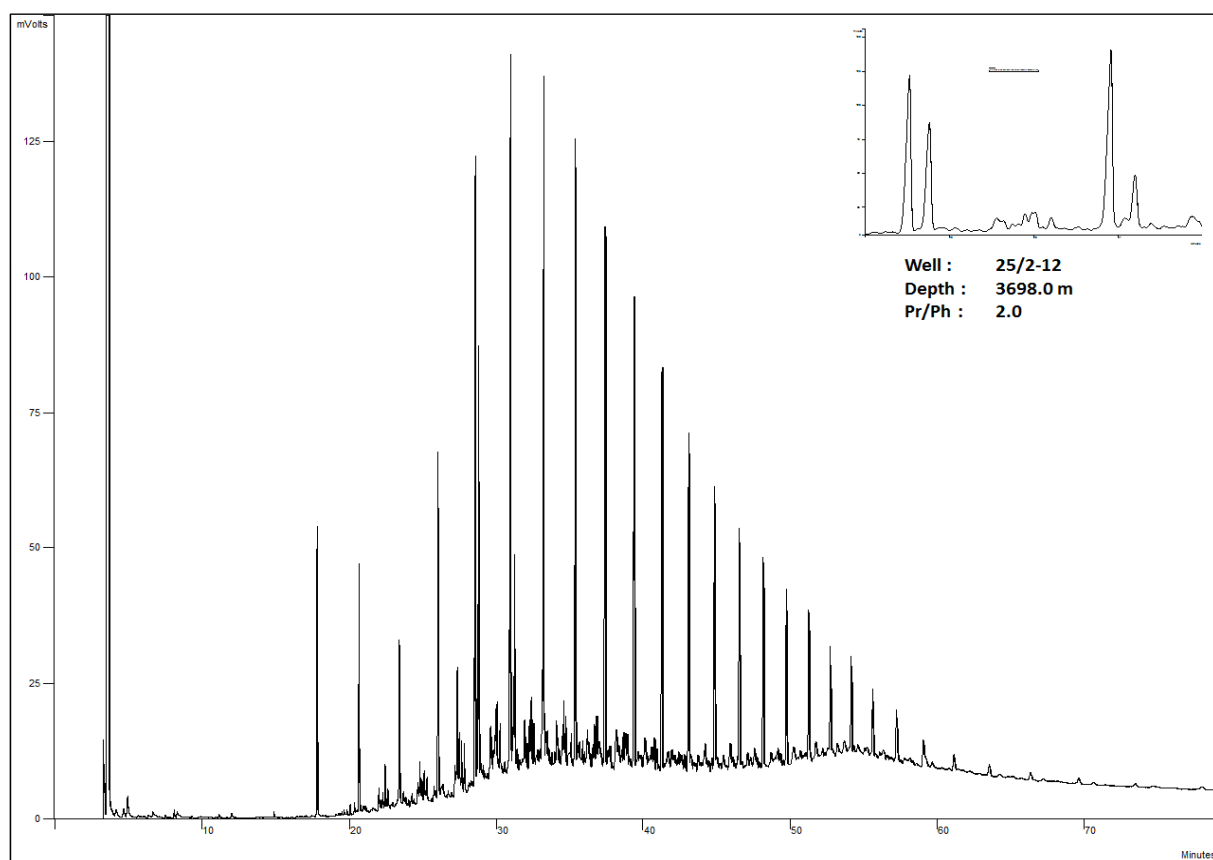
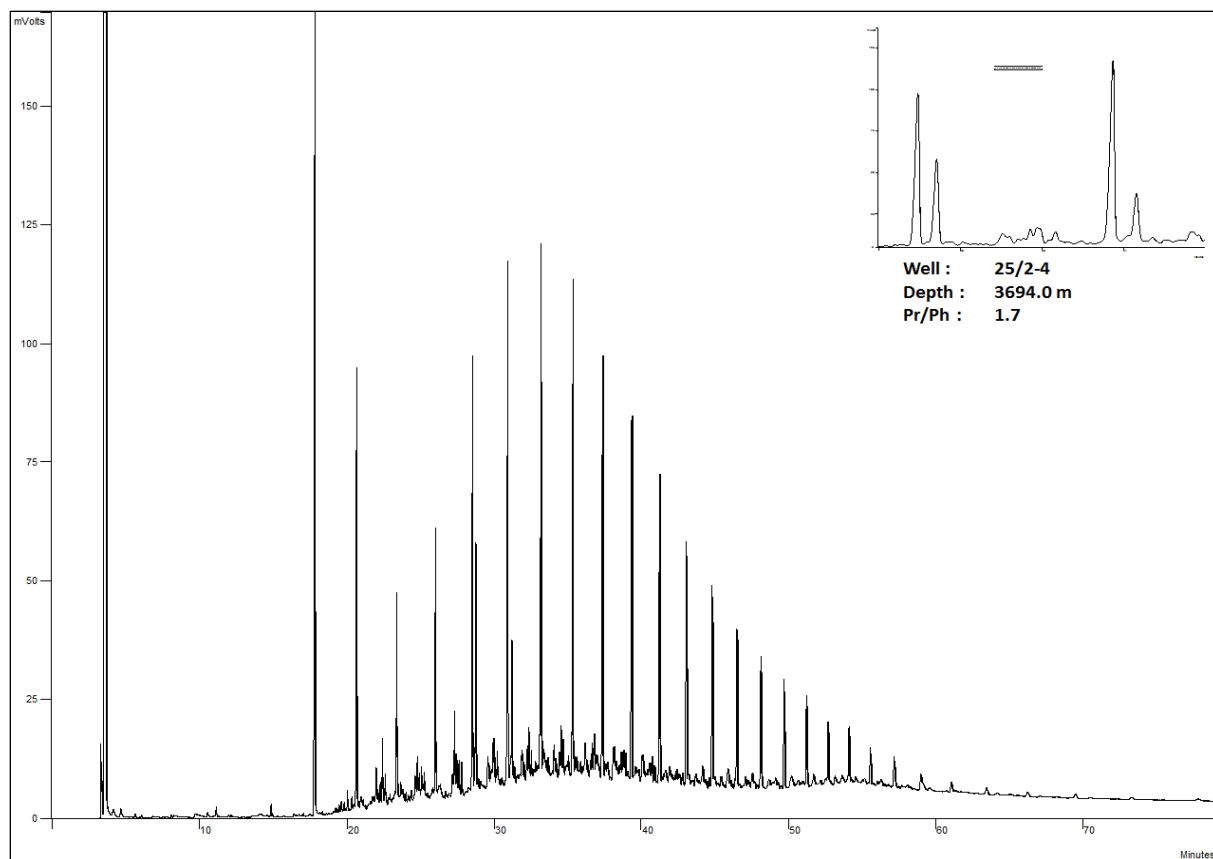


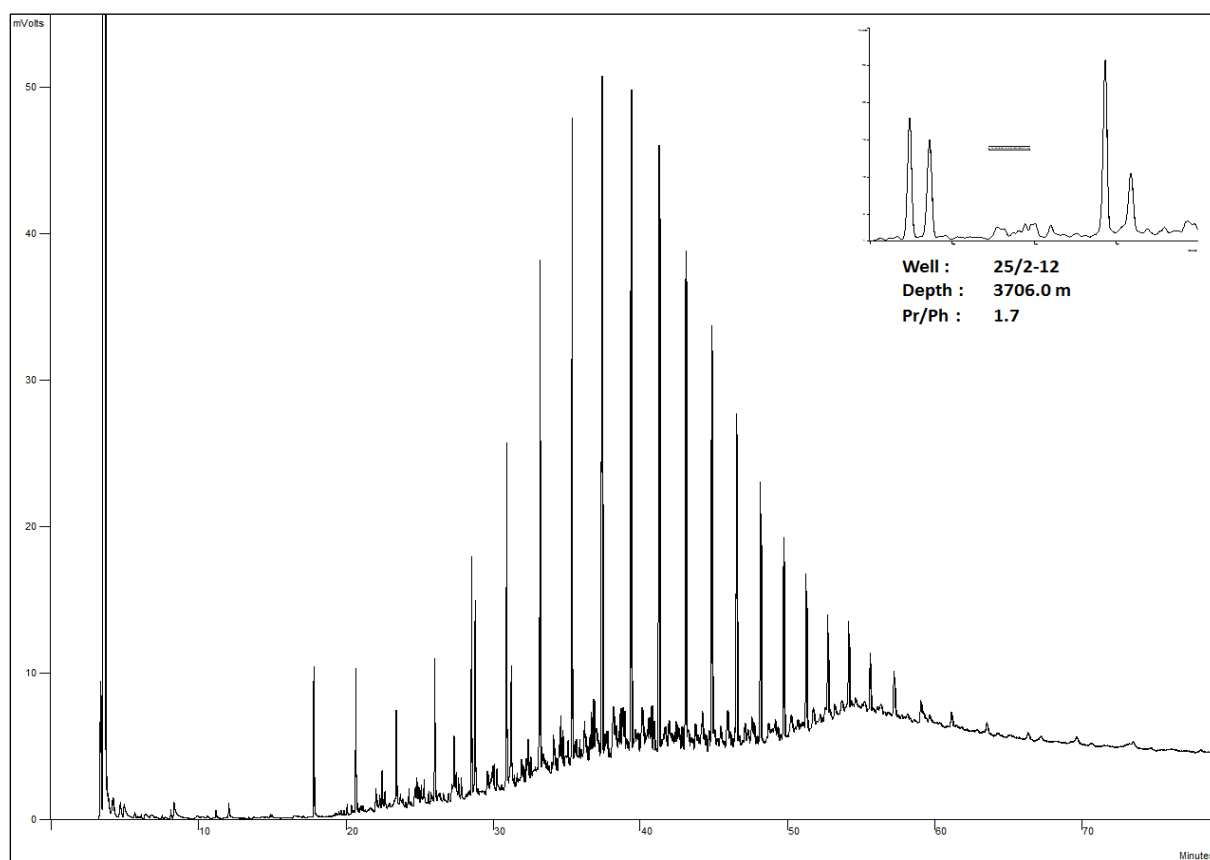
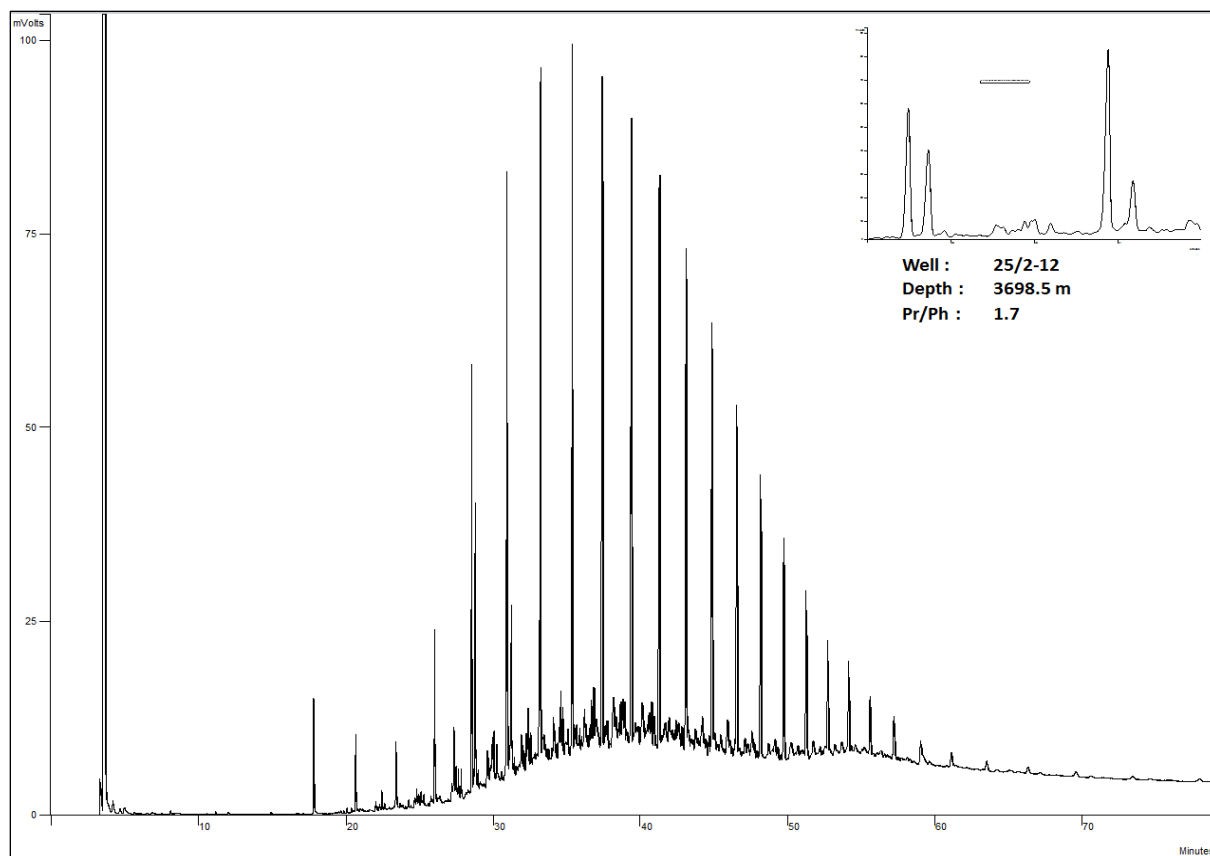
Appendix B (GC-FID Chromatograms)

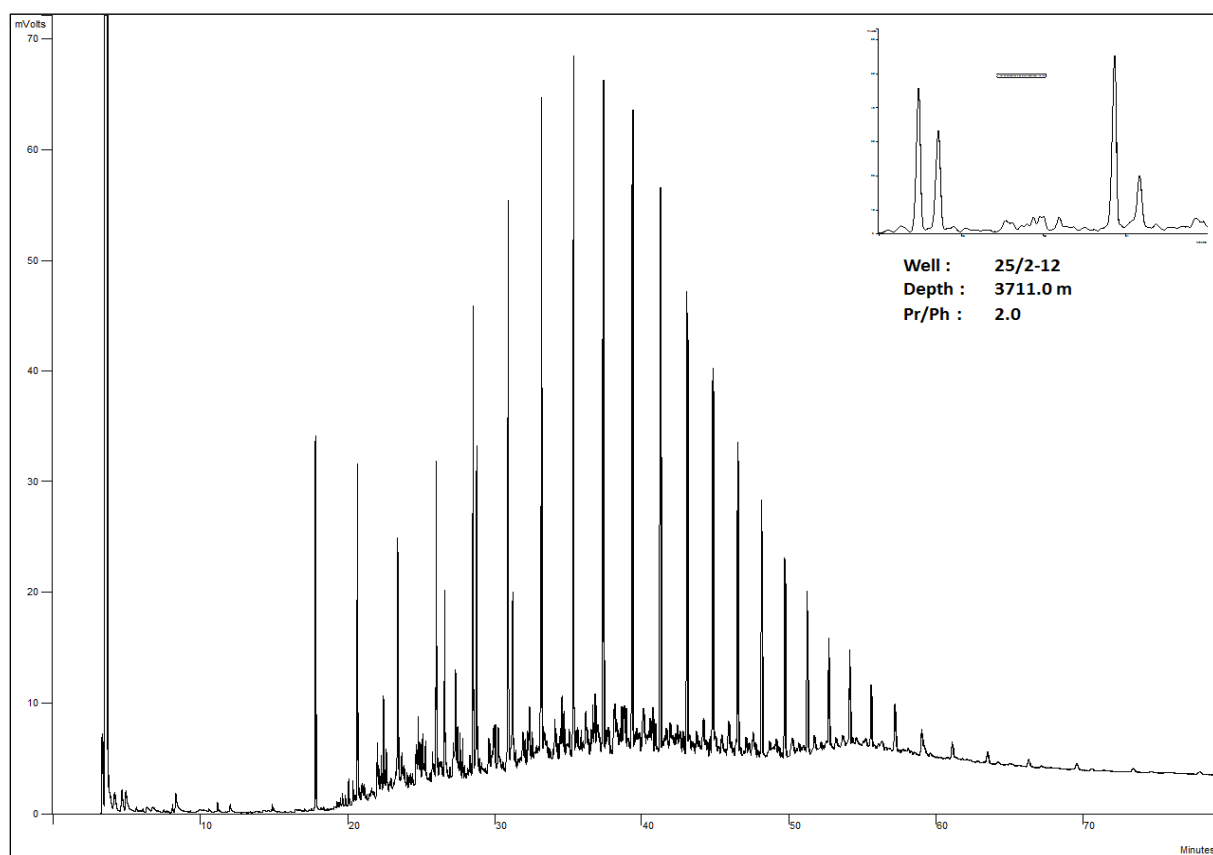
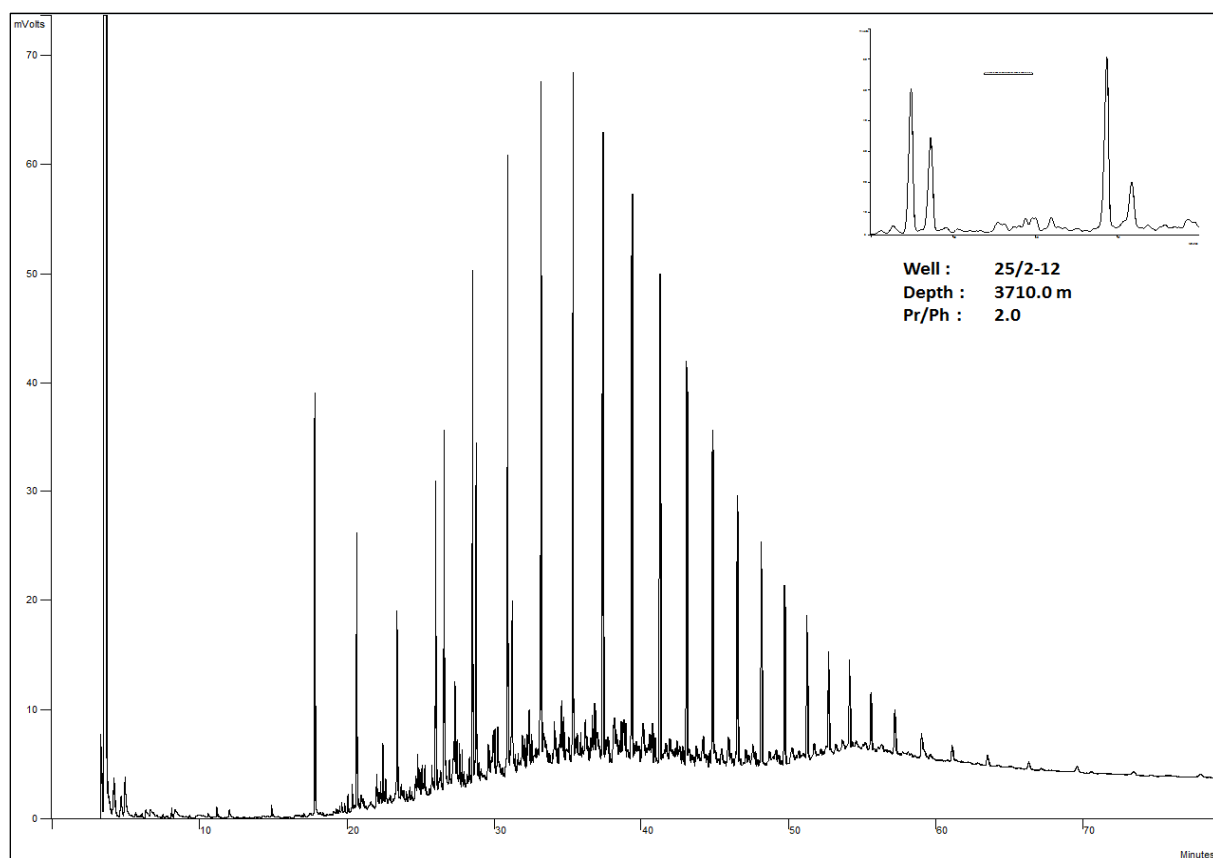


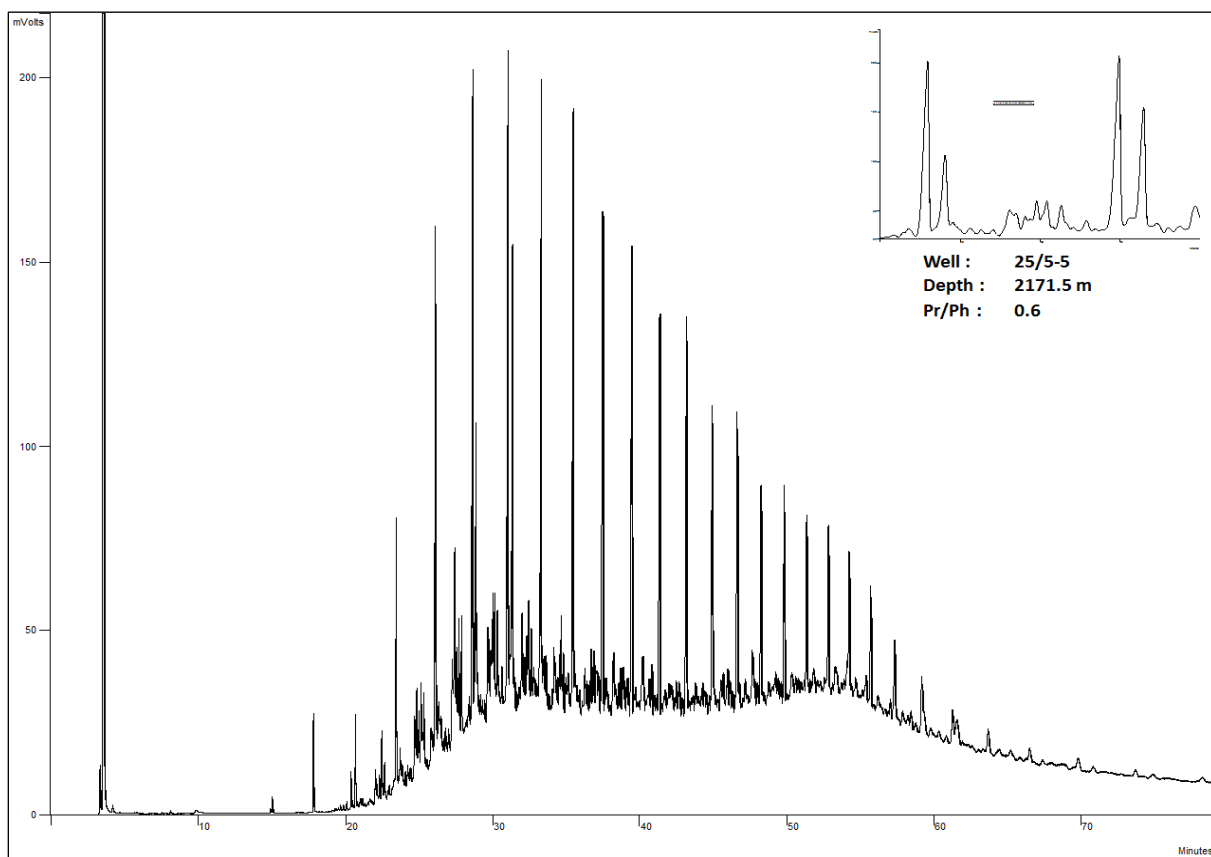
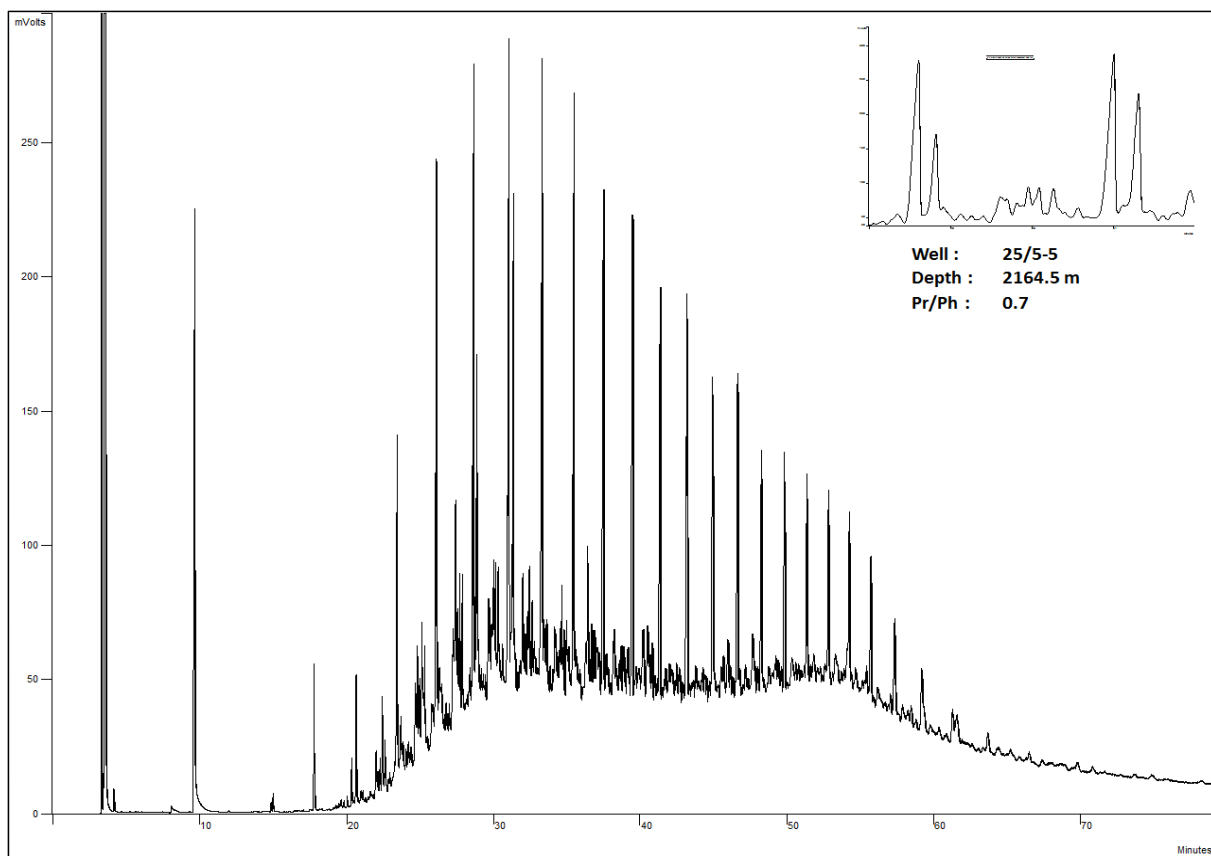


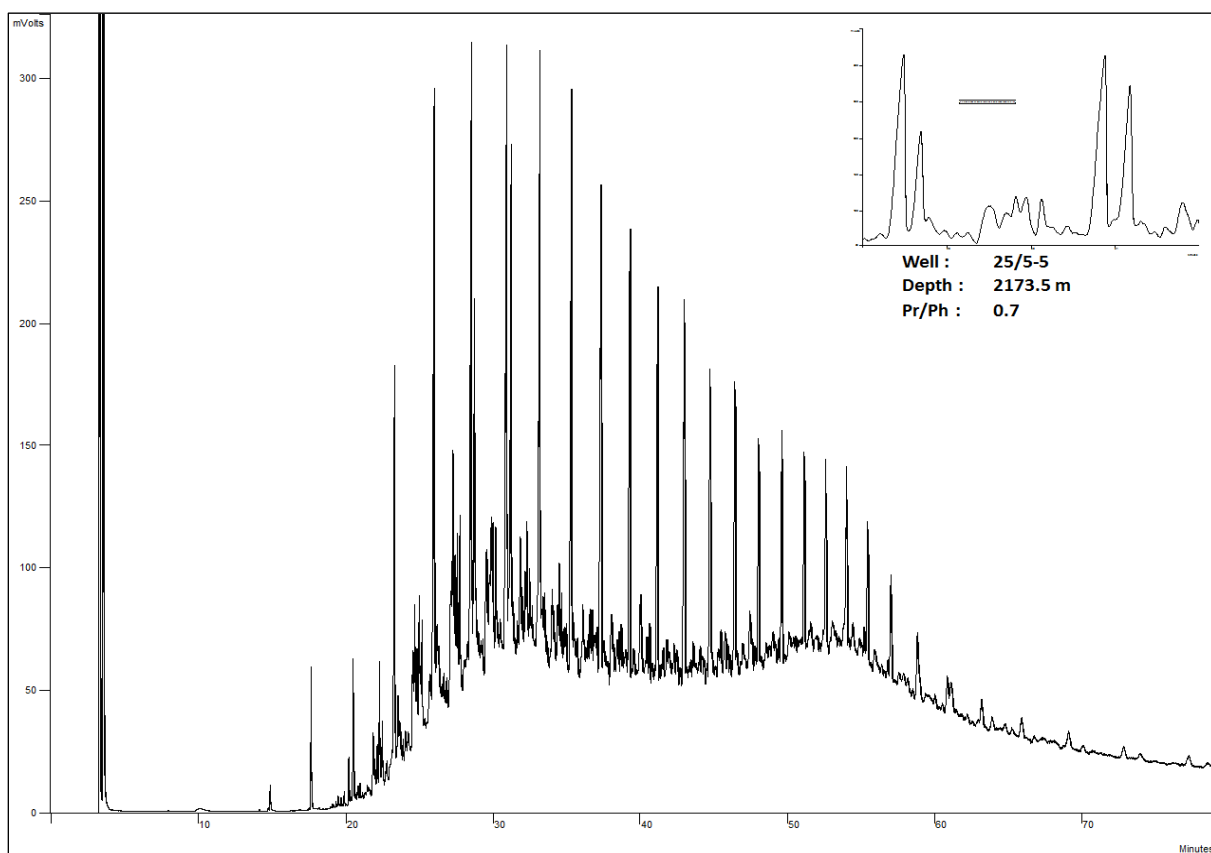
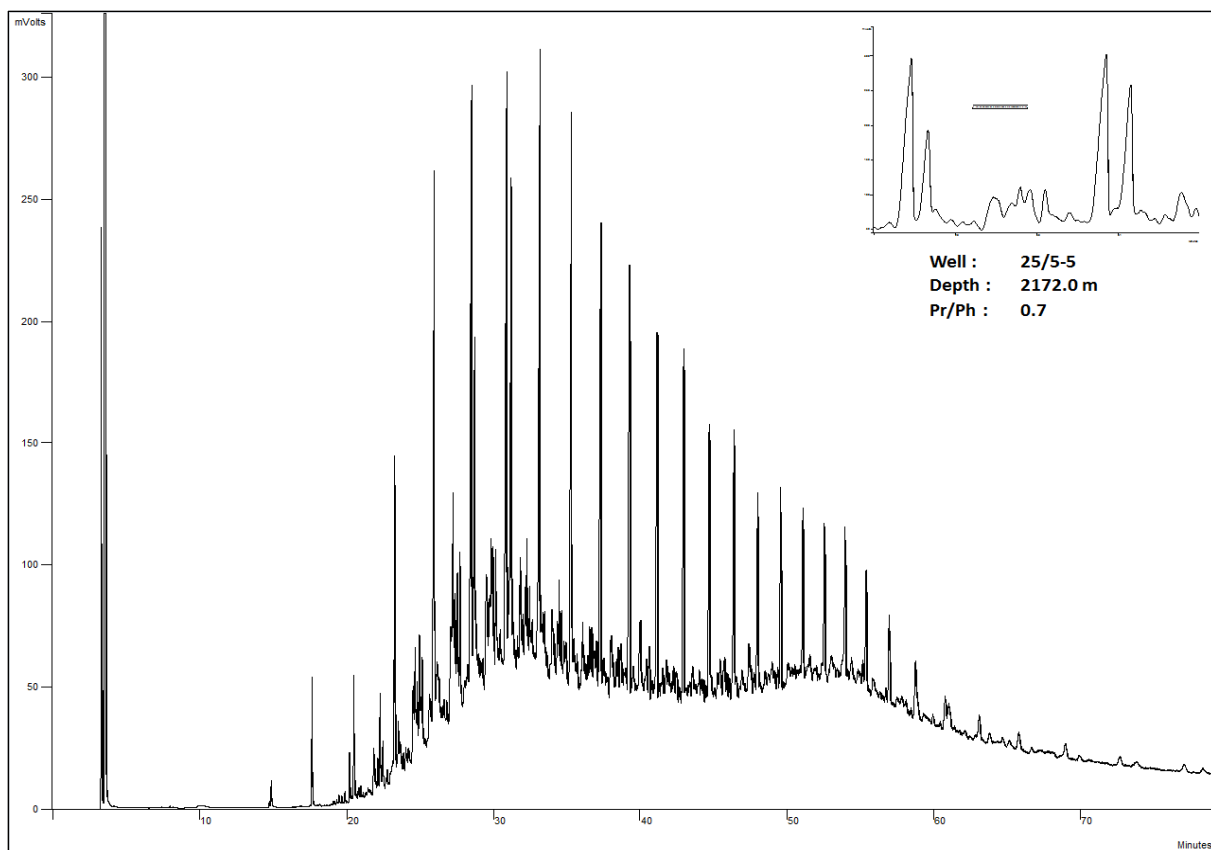


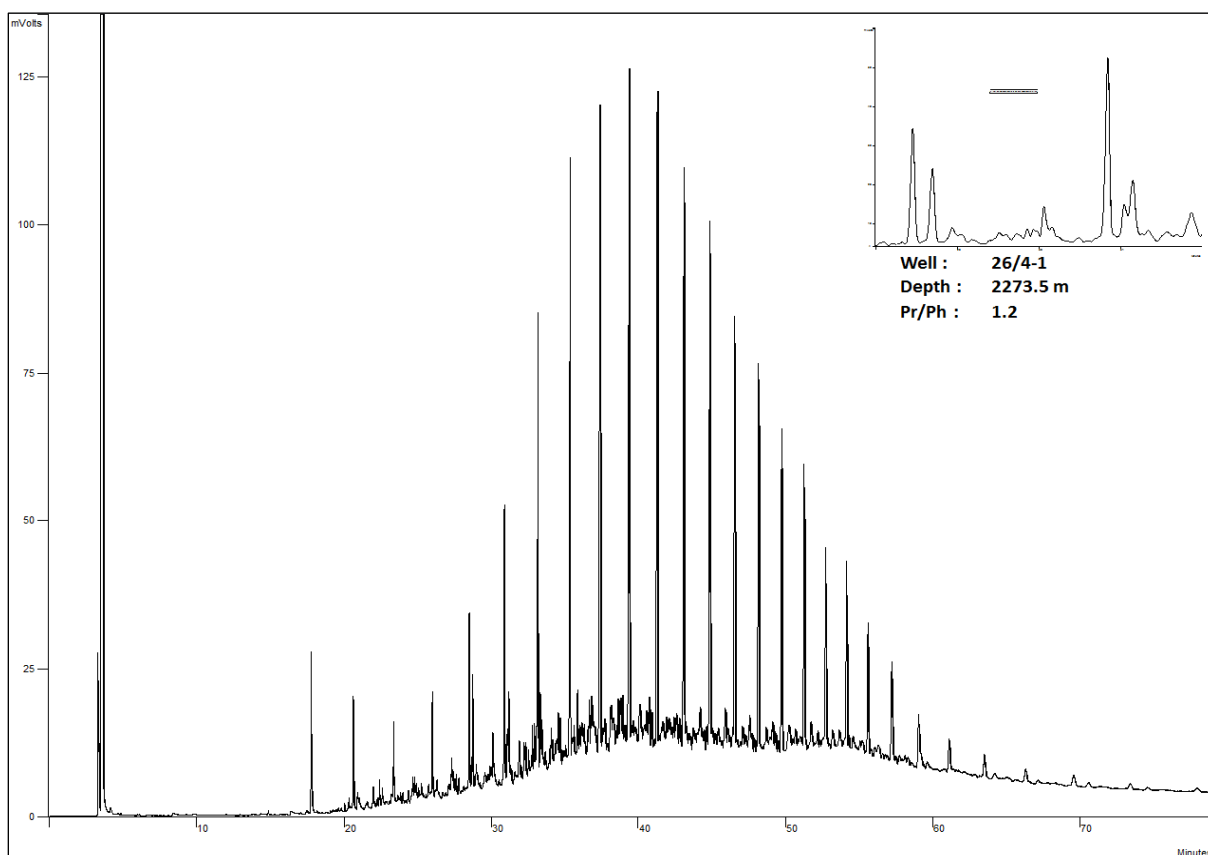
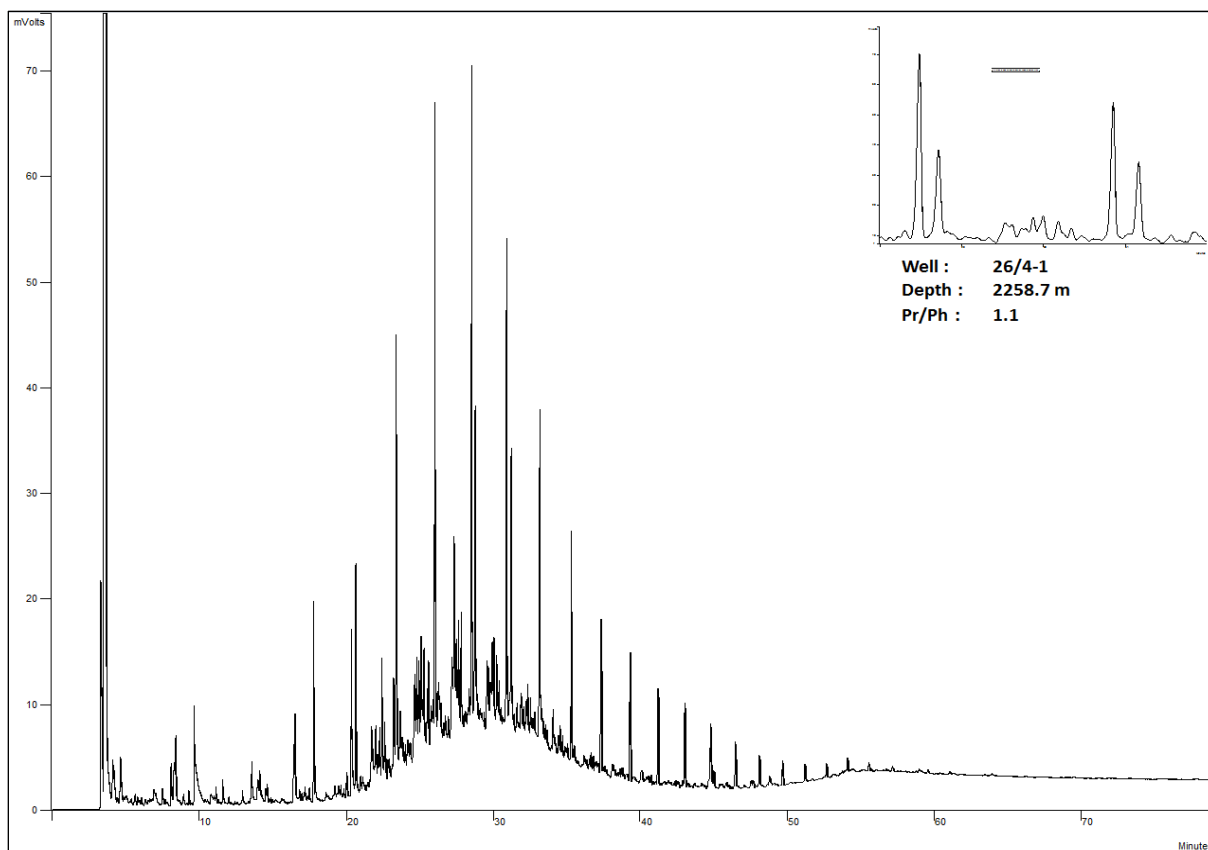


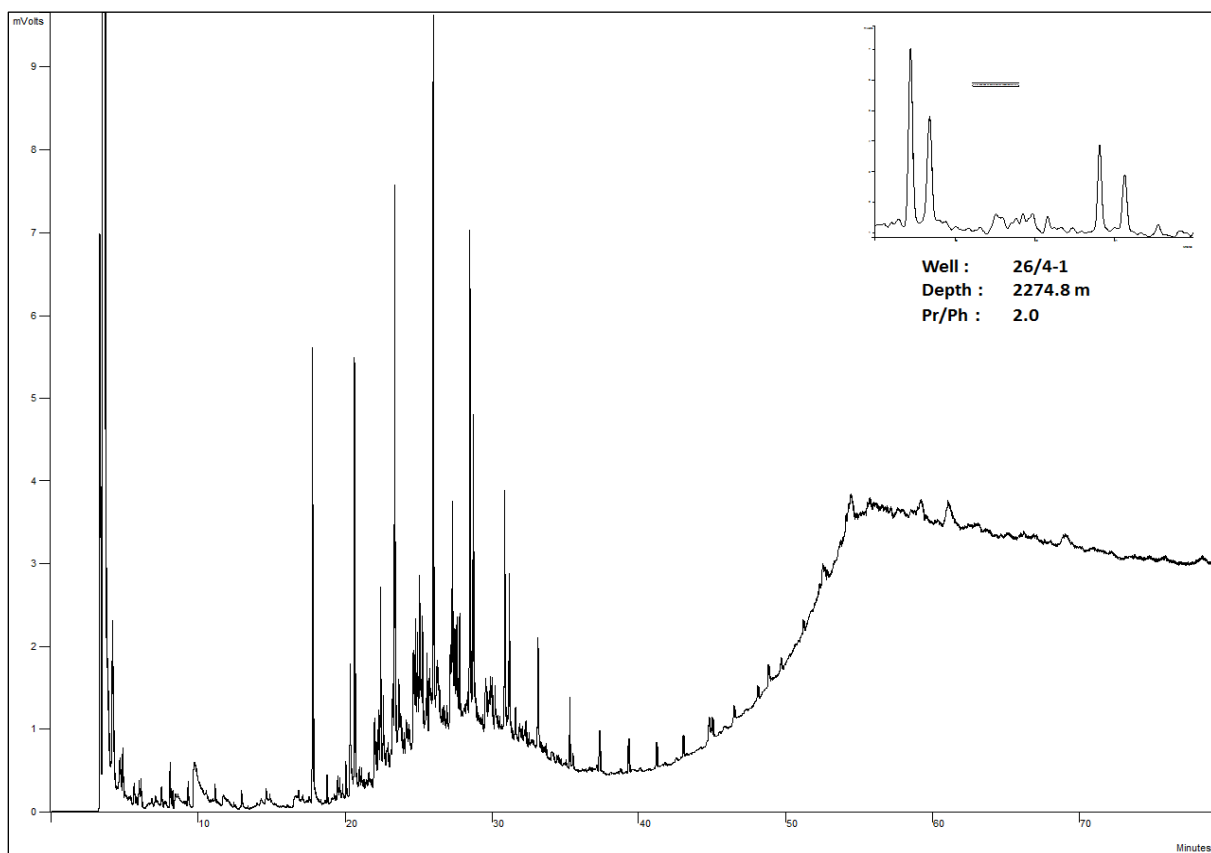
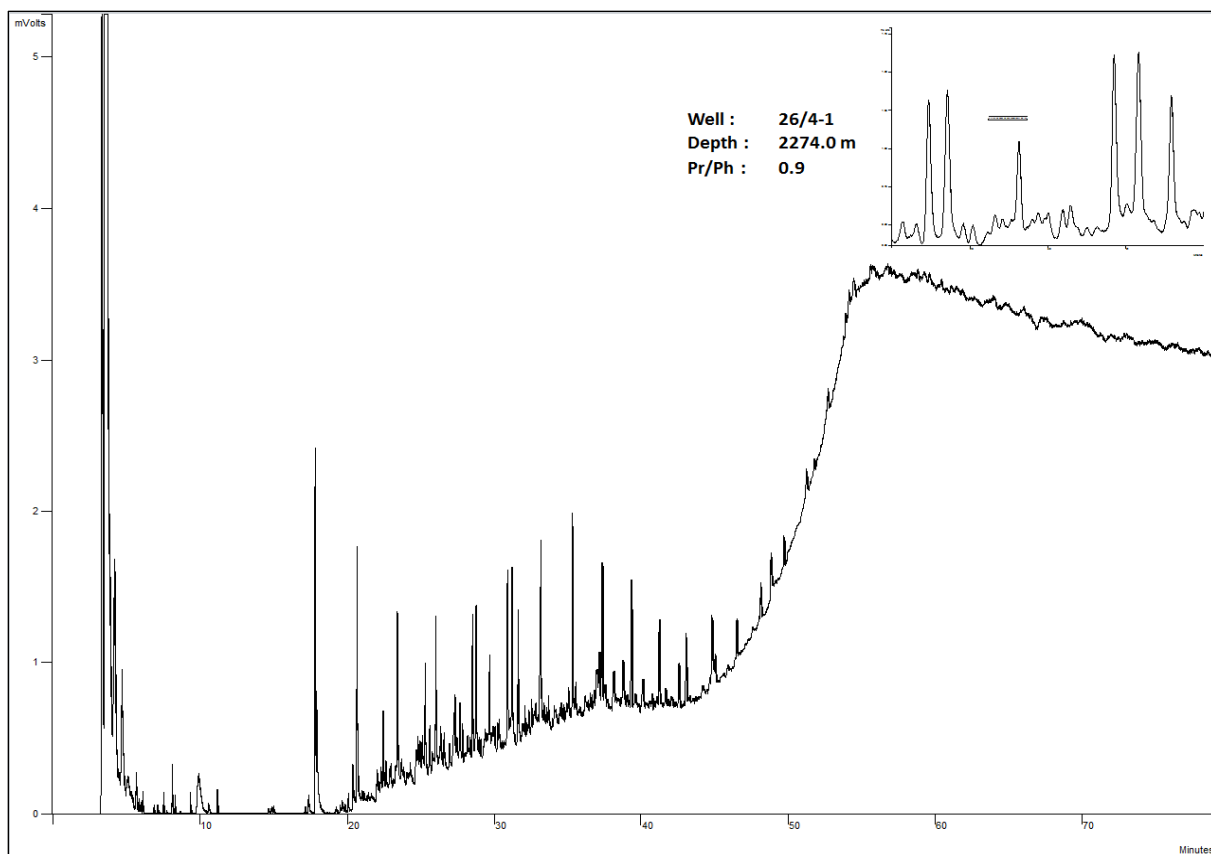


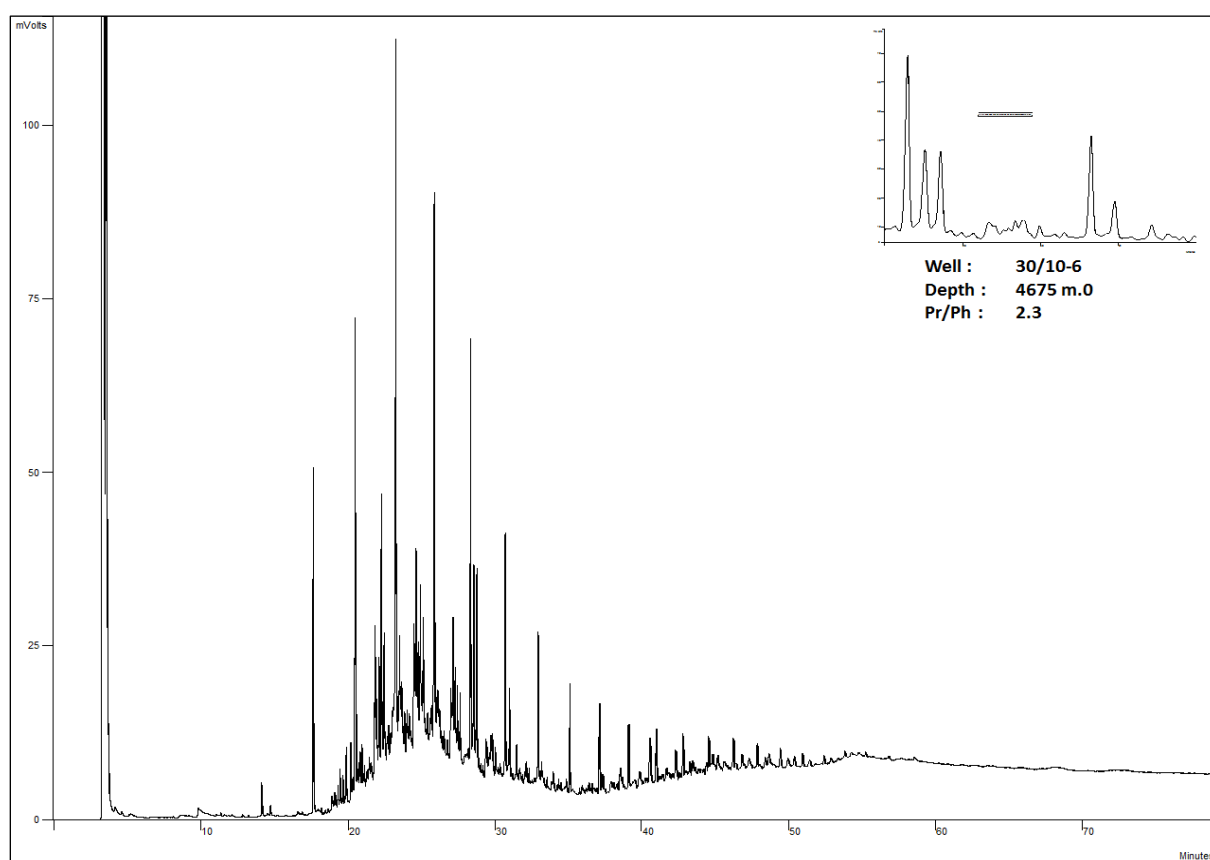
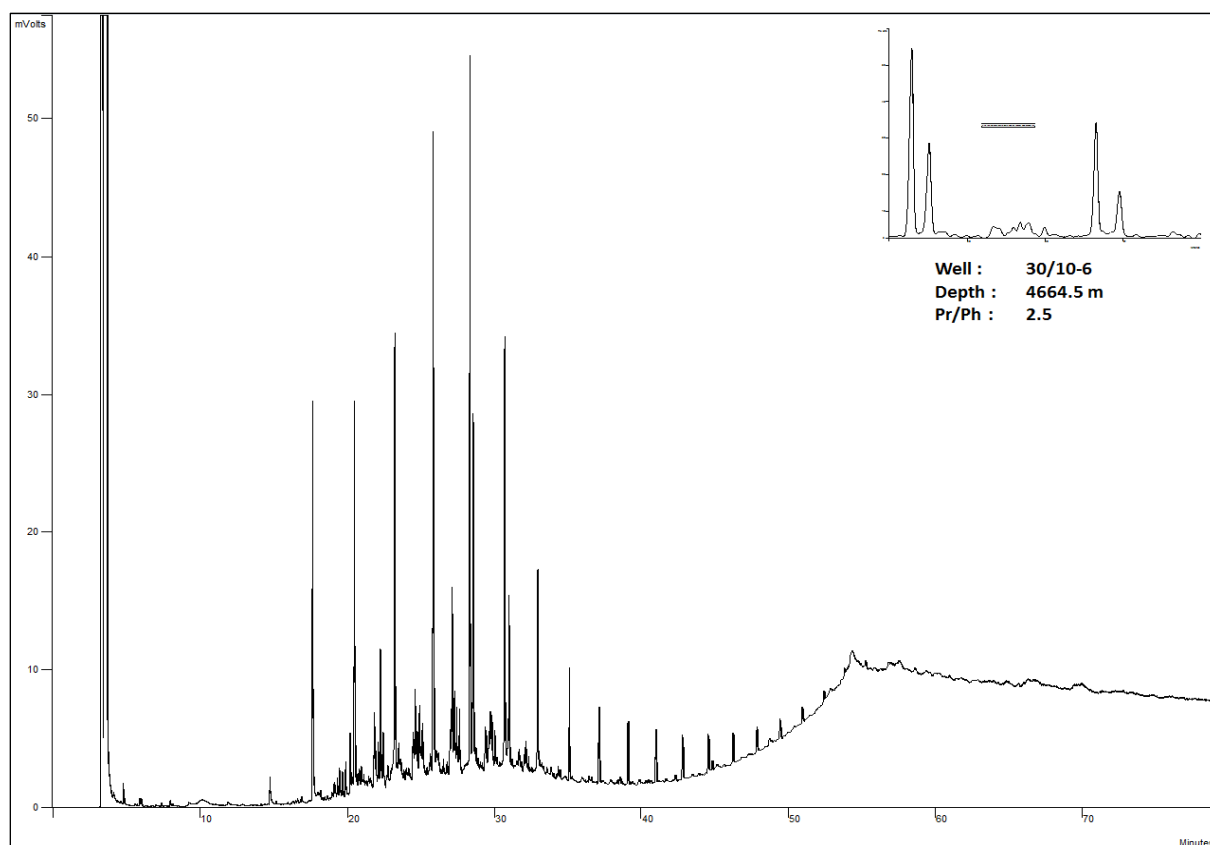


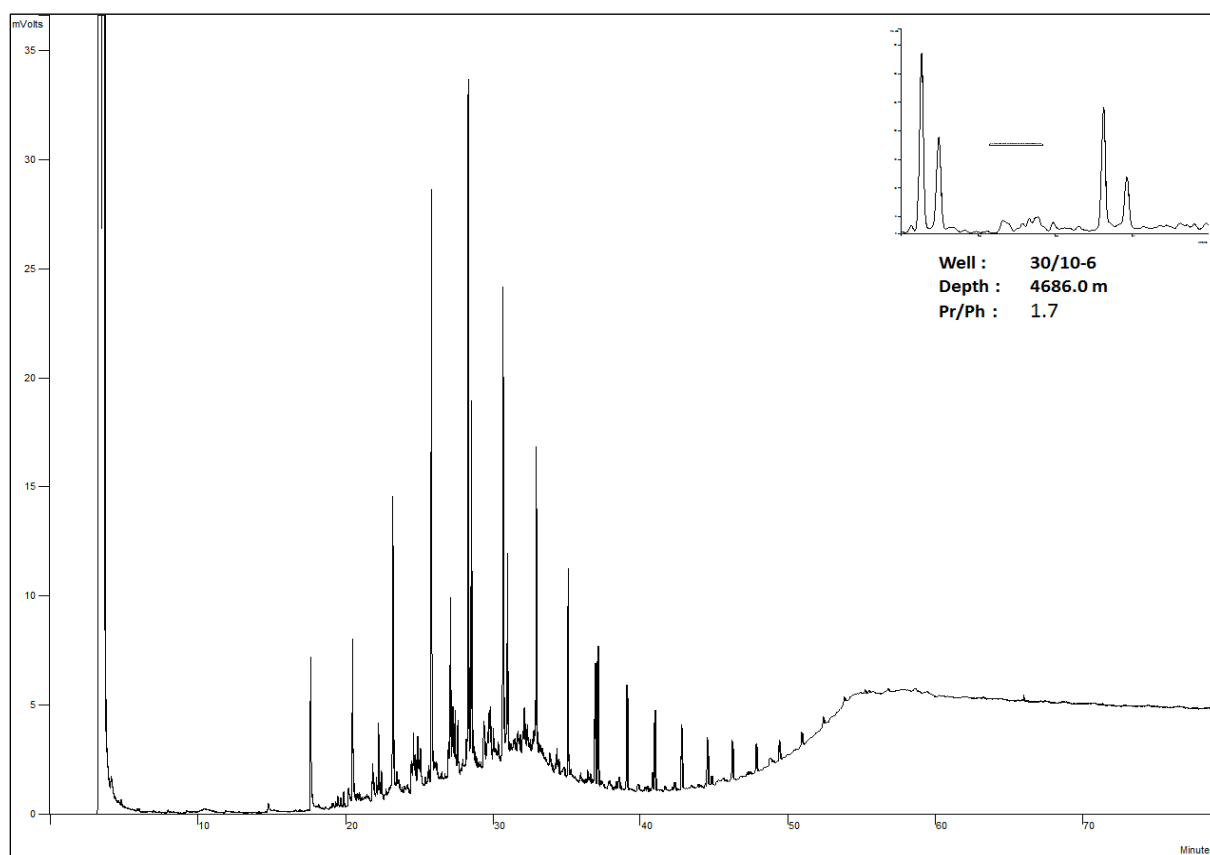
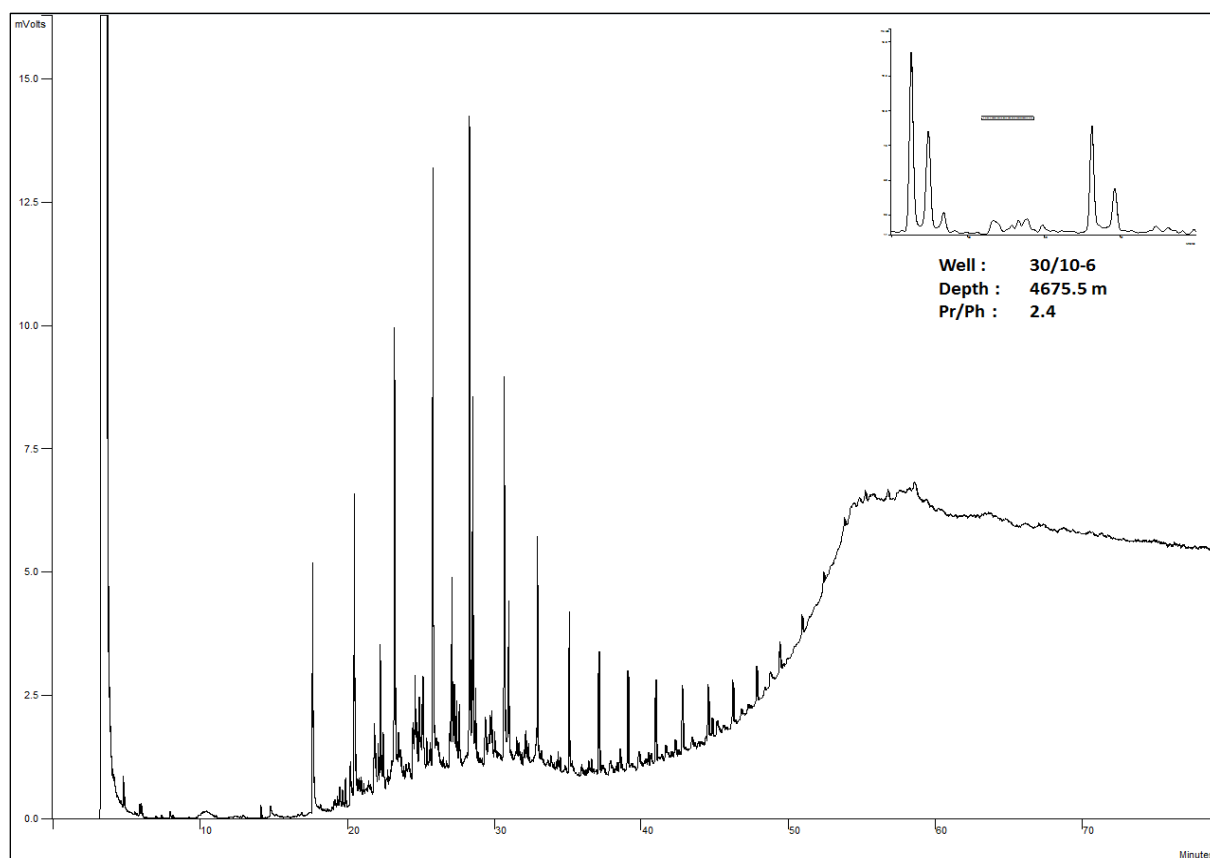


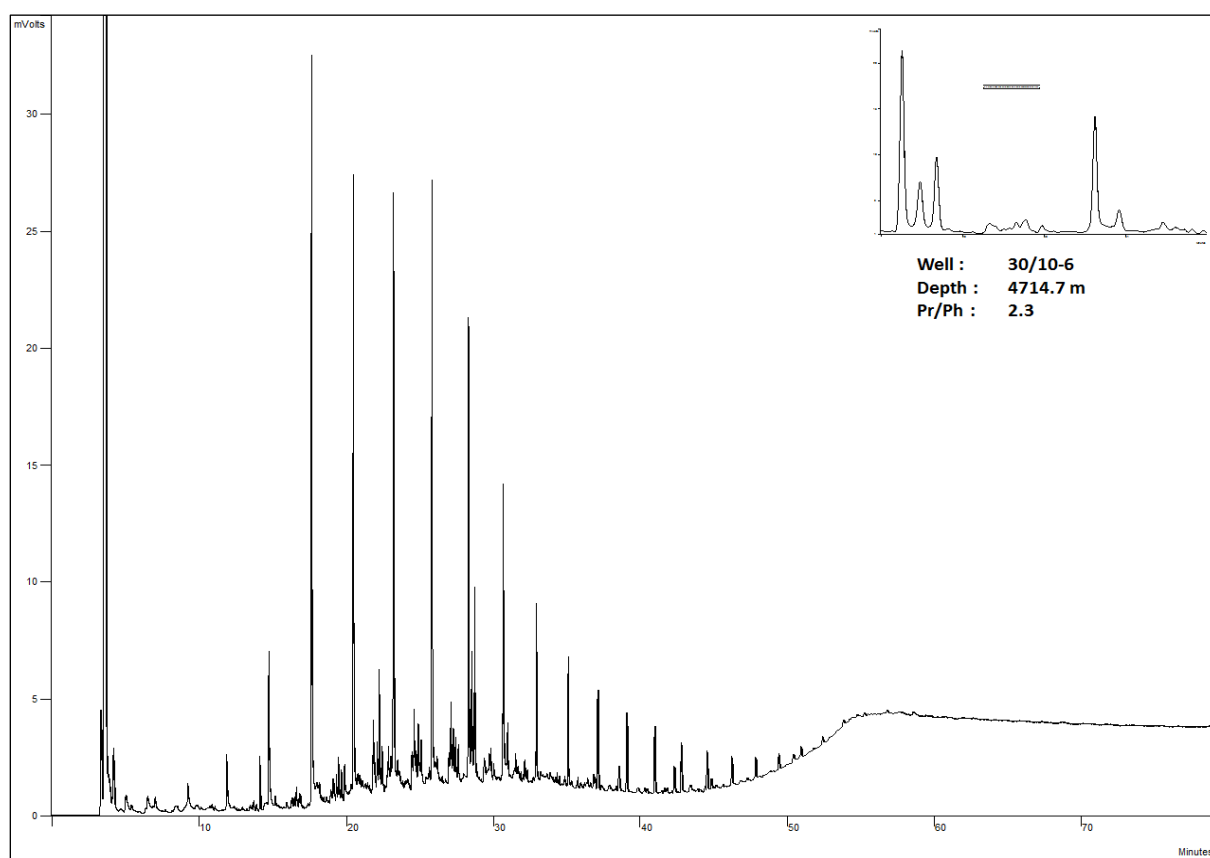
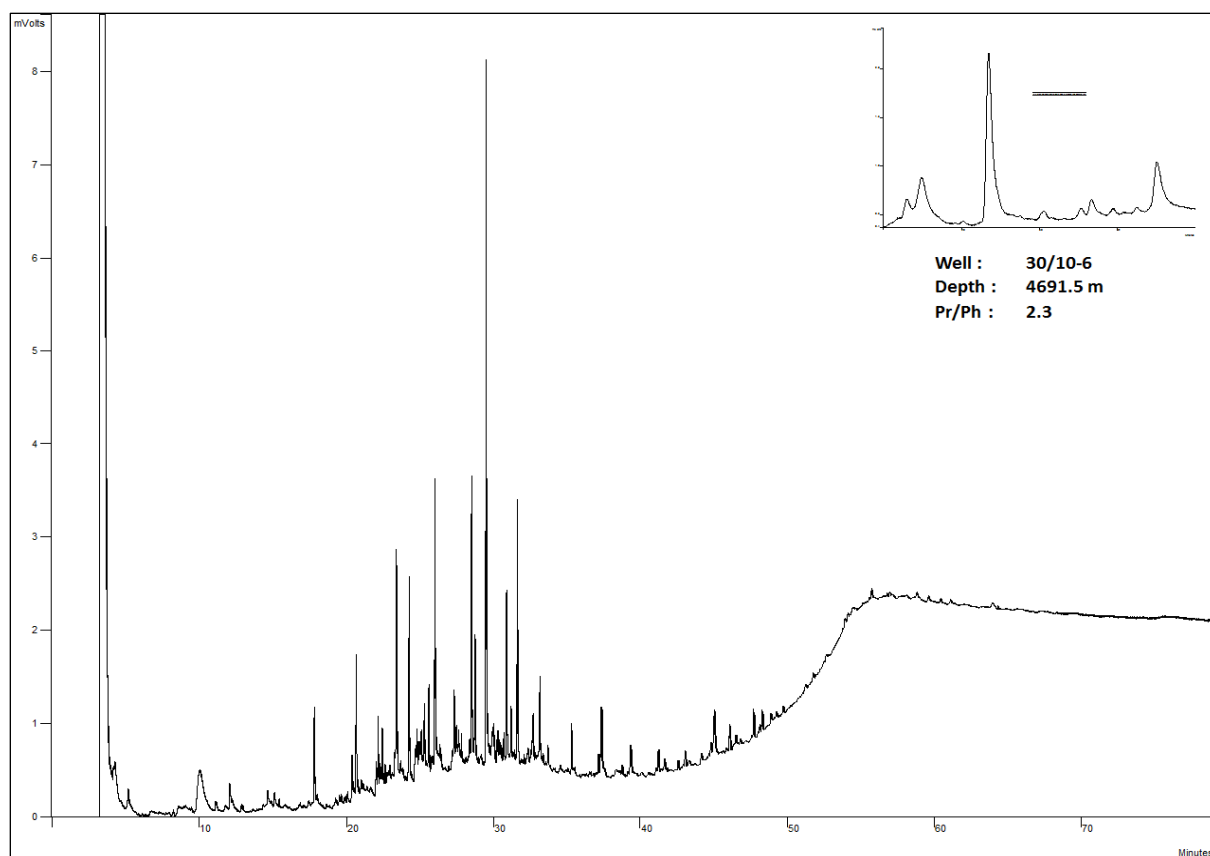


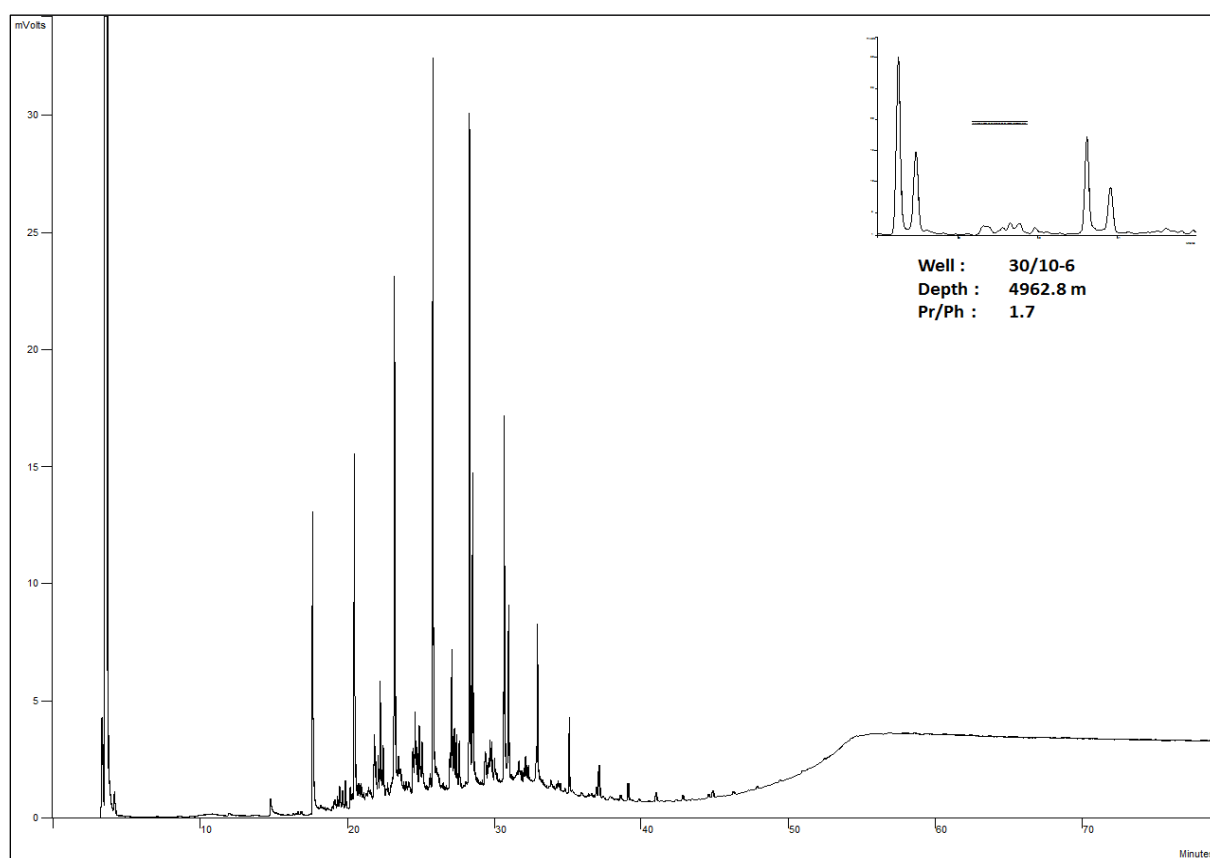
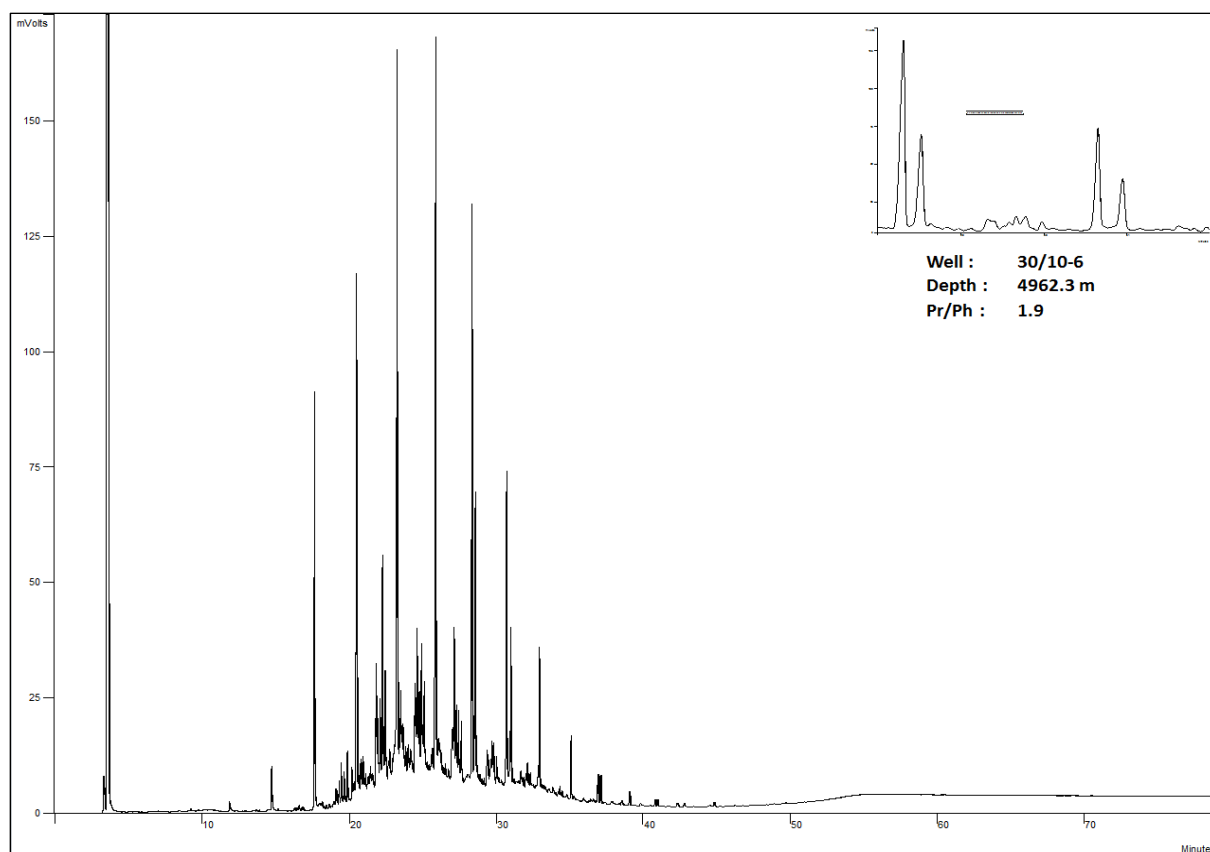


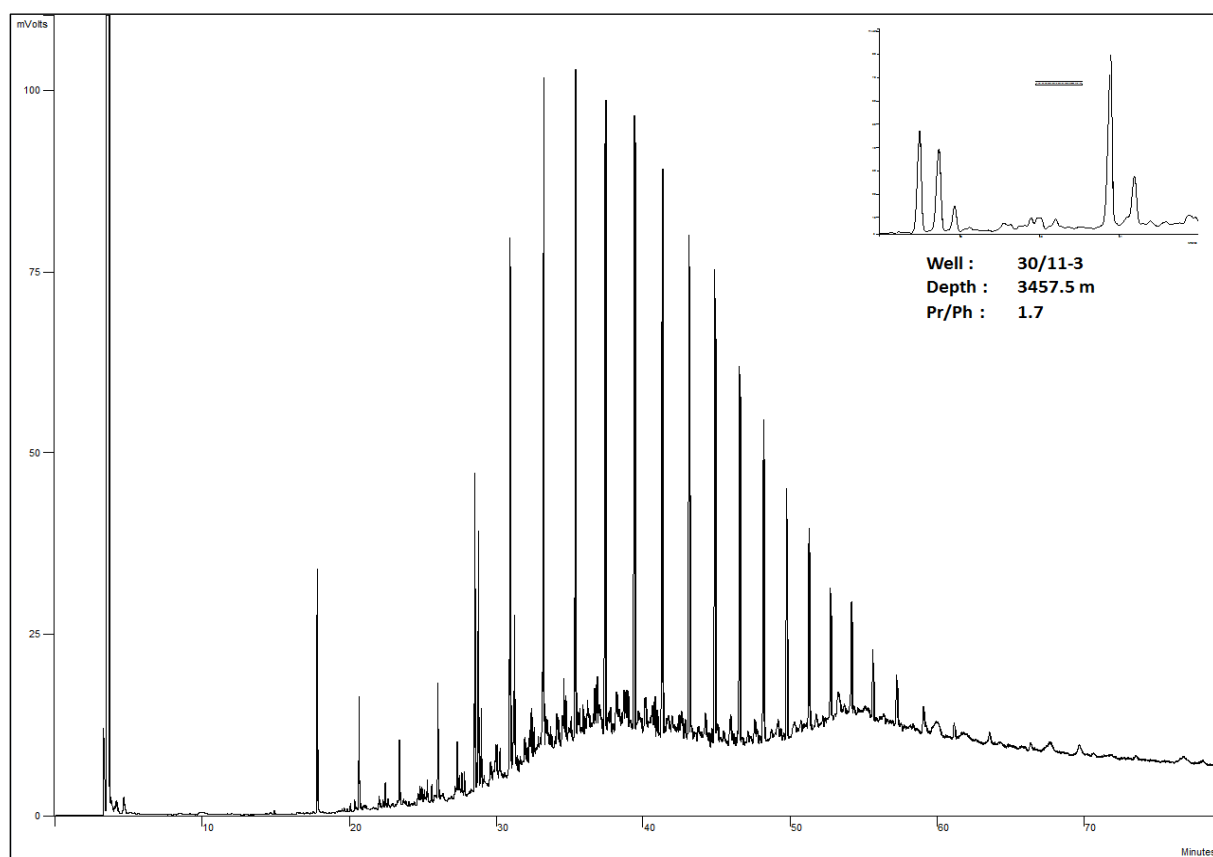
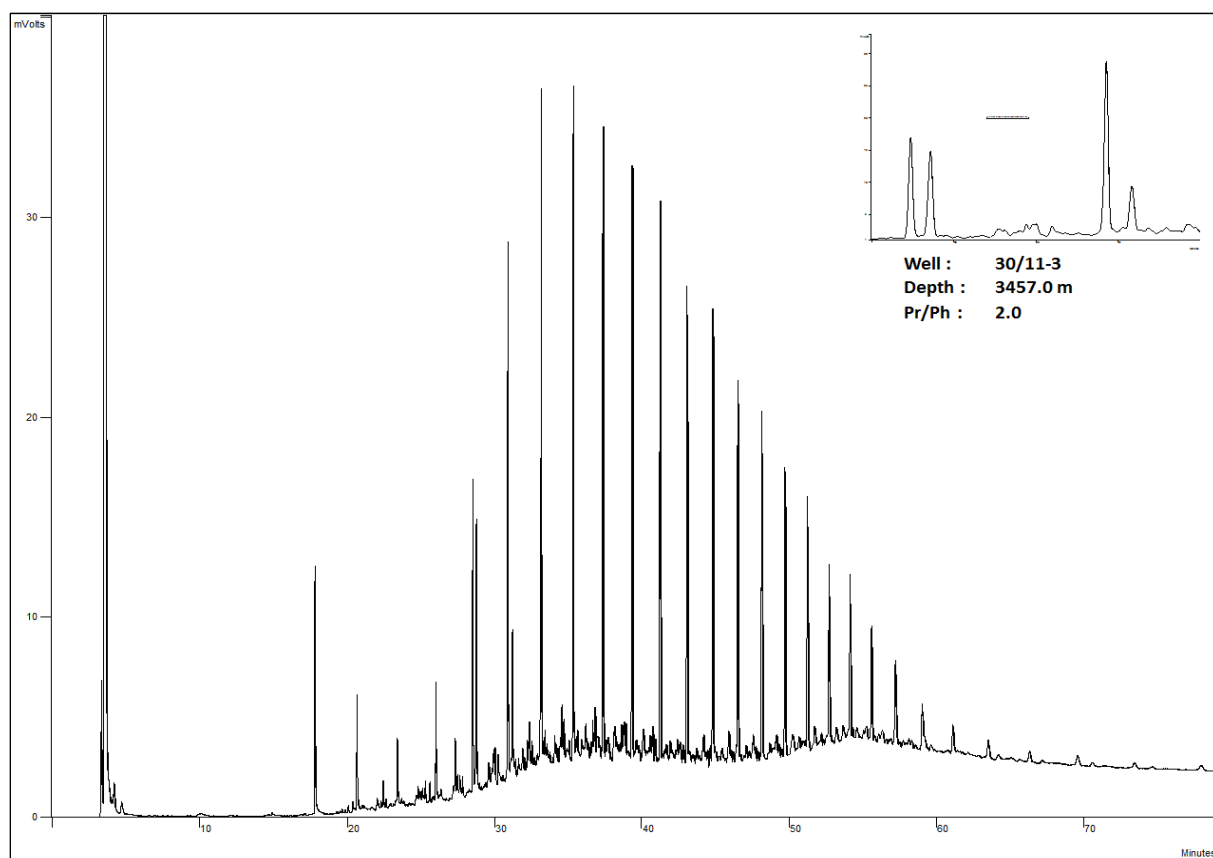


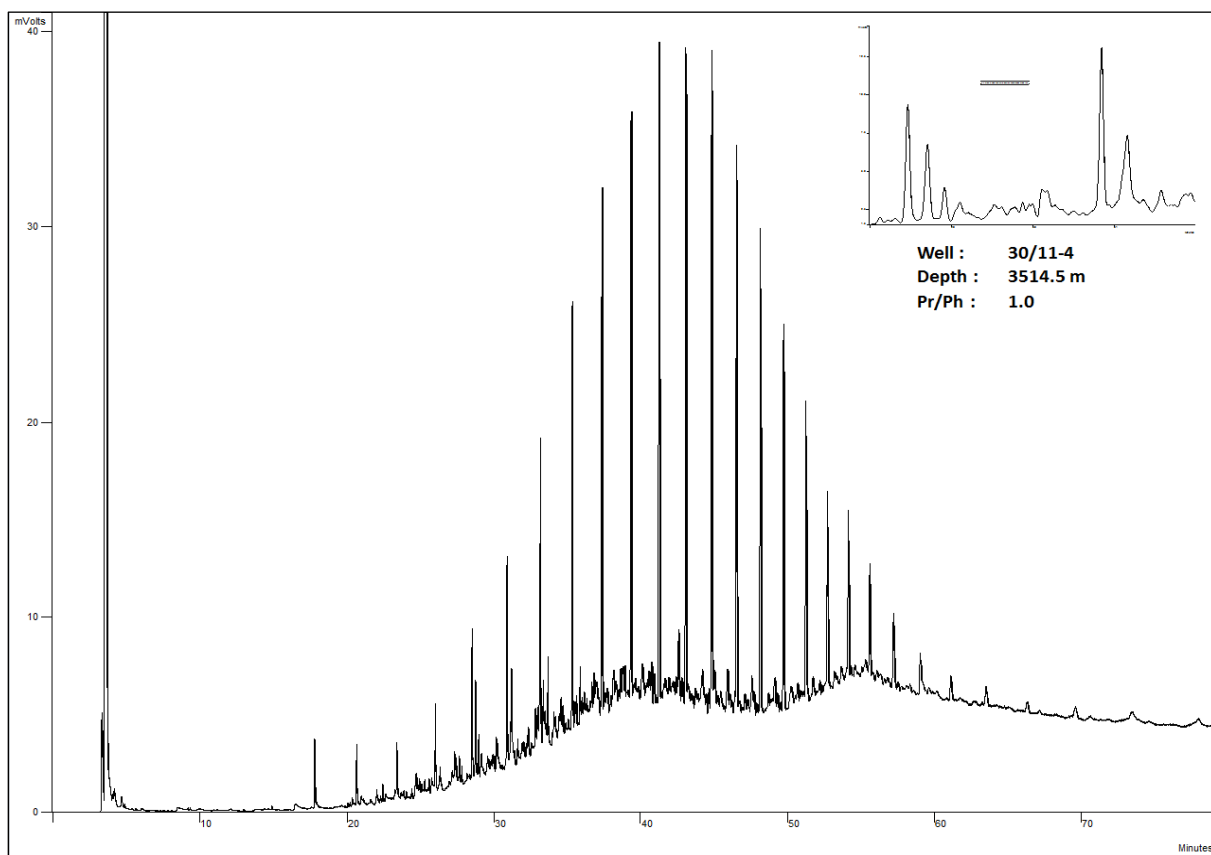
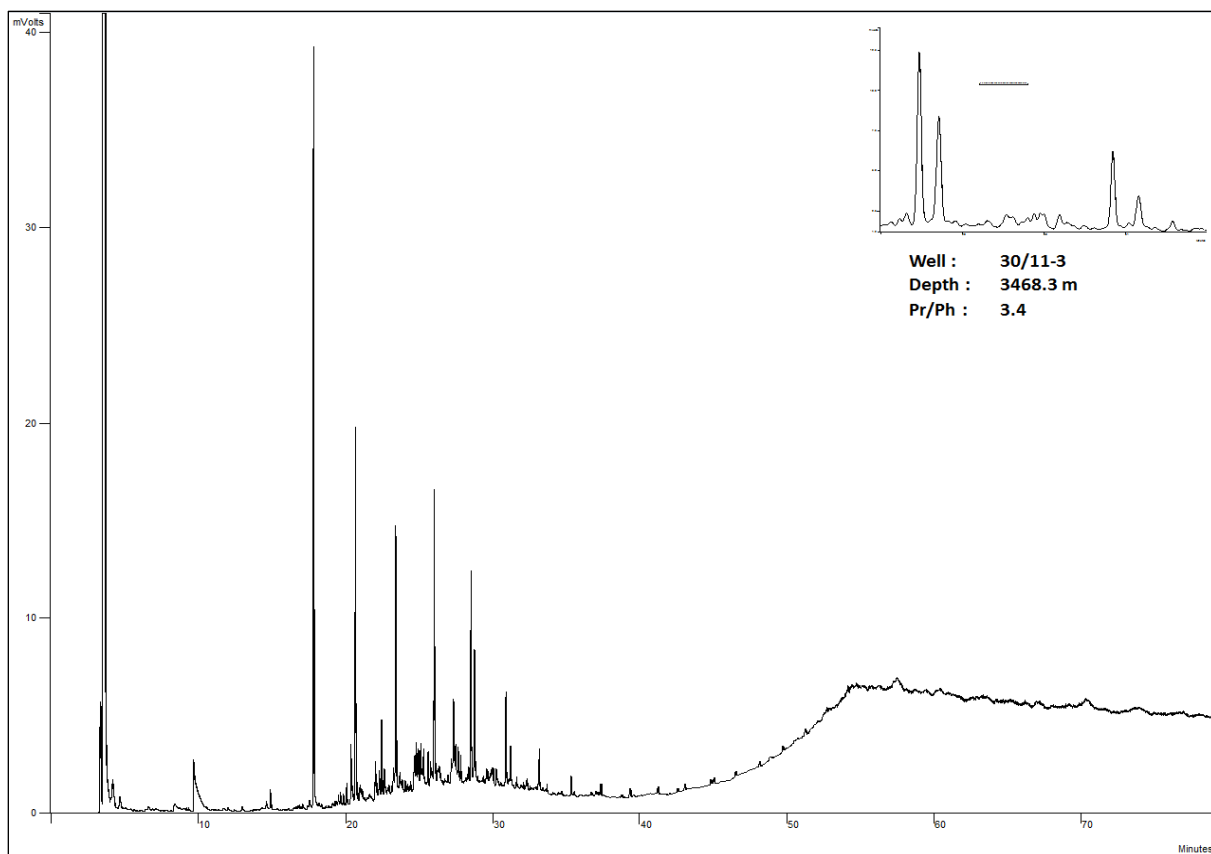


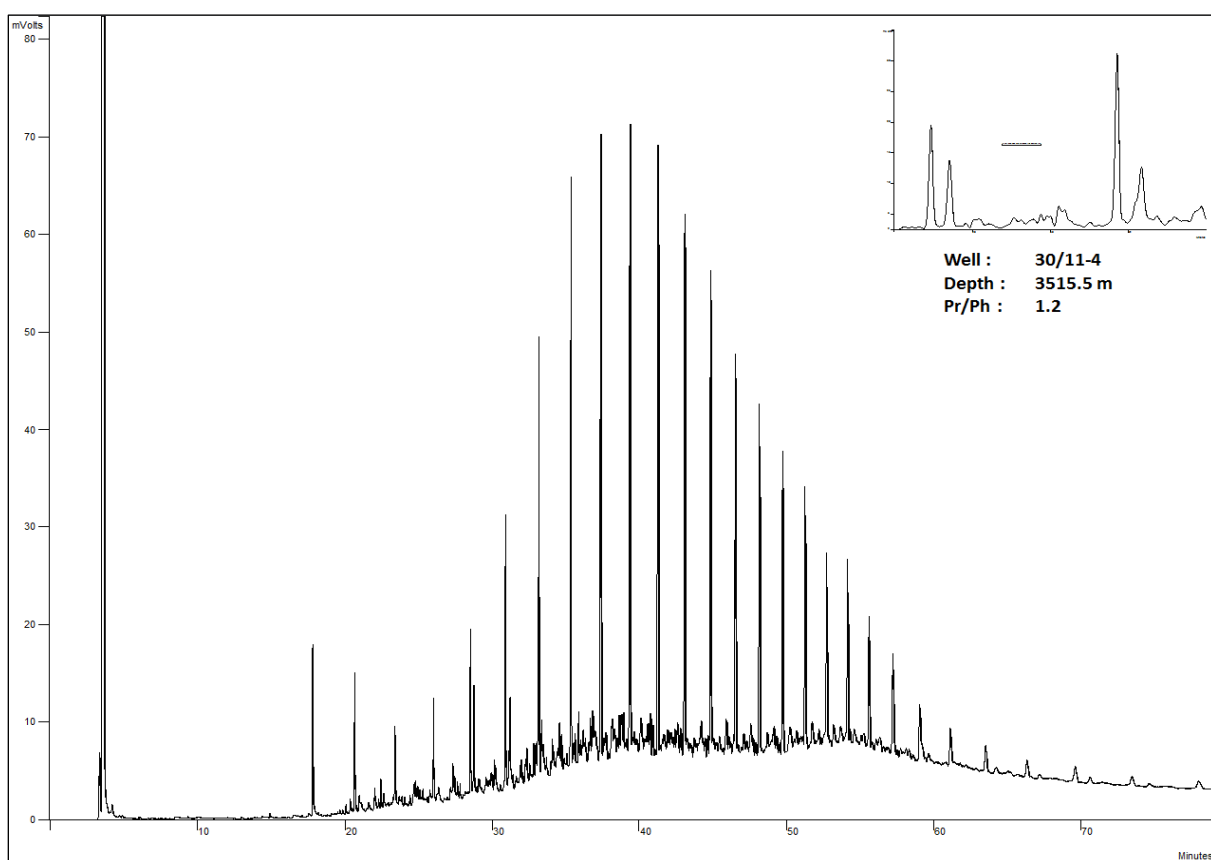
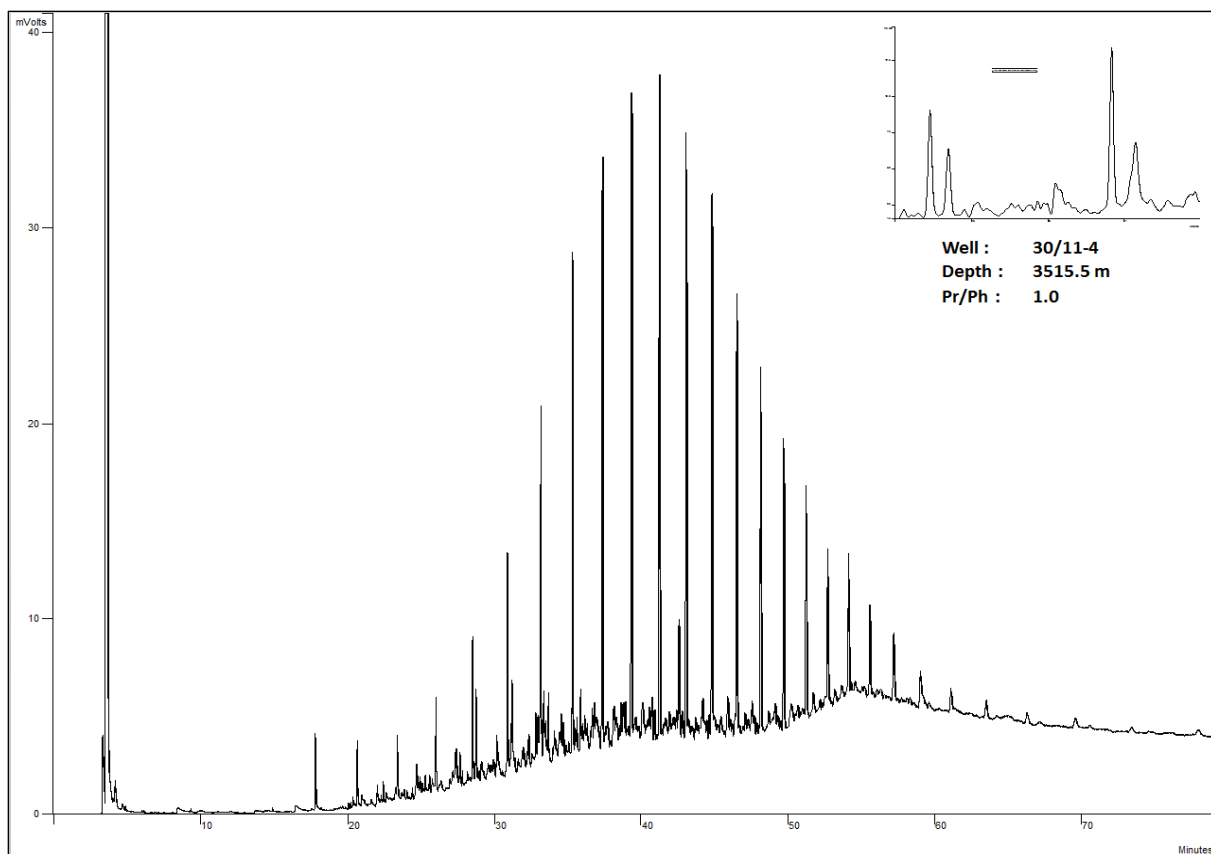


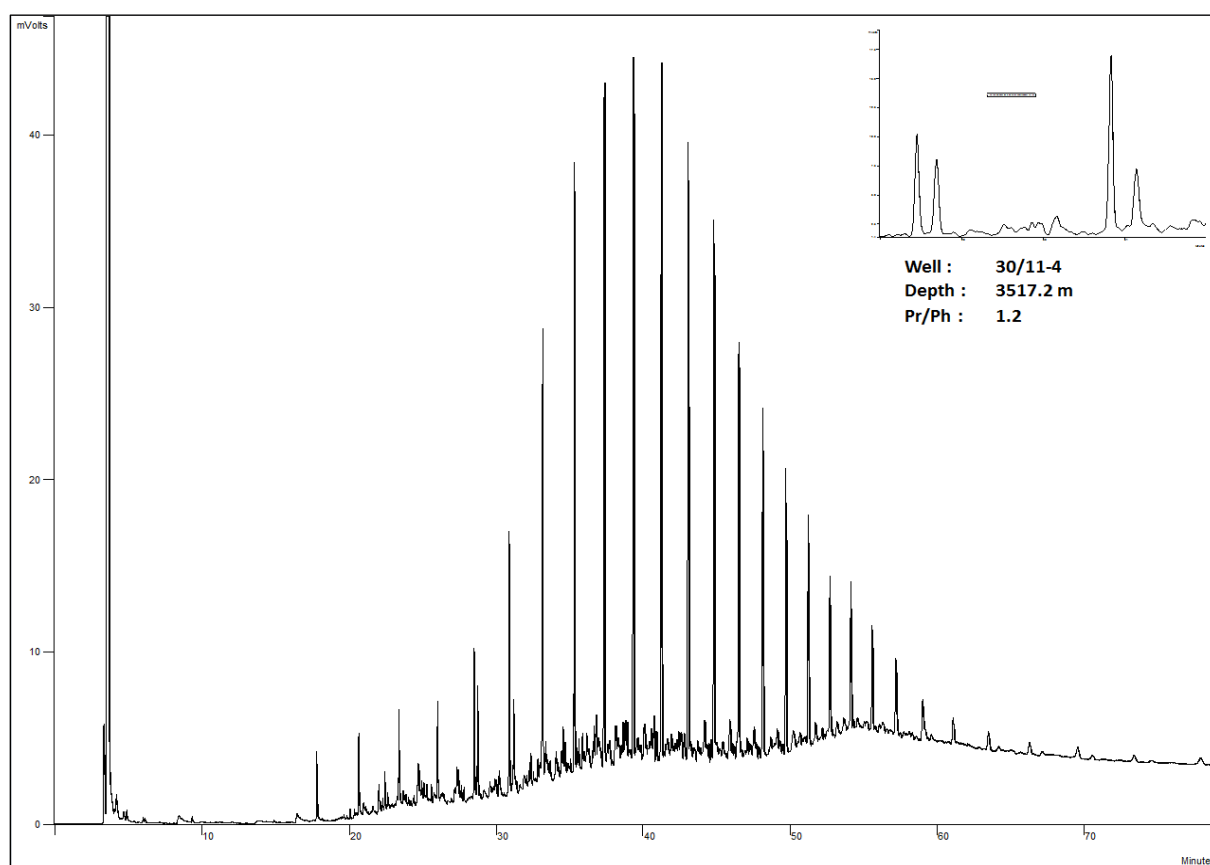
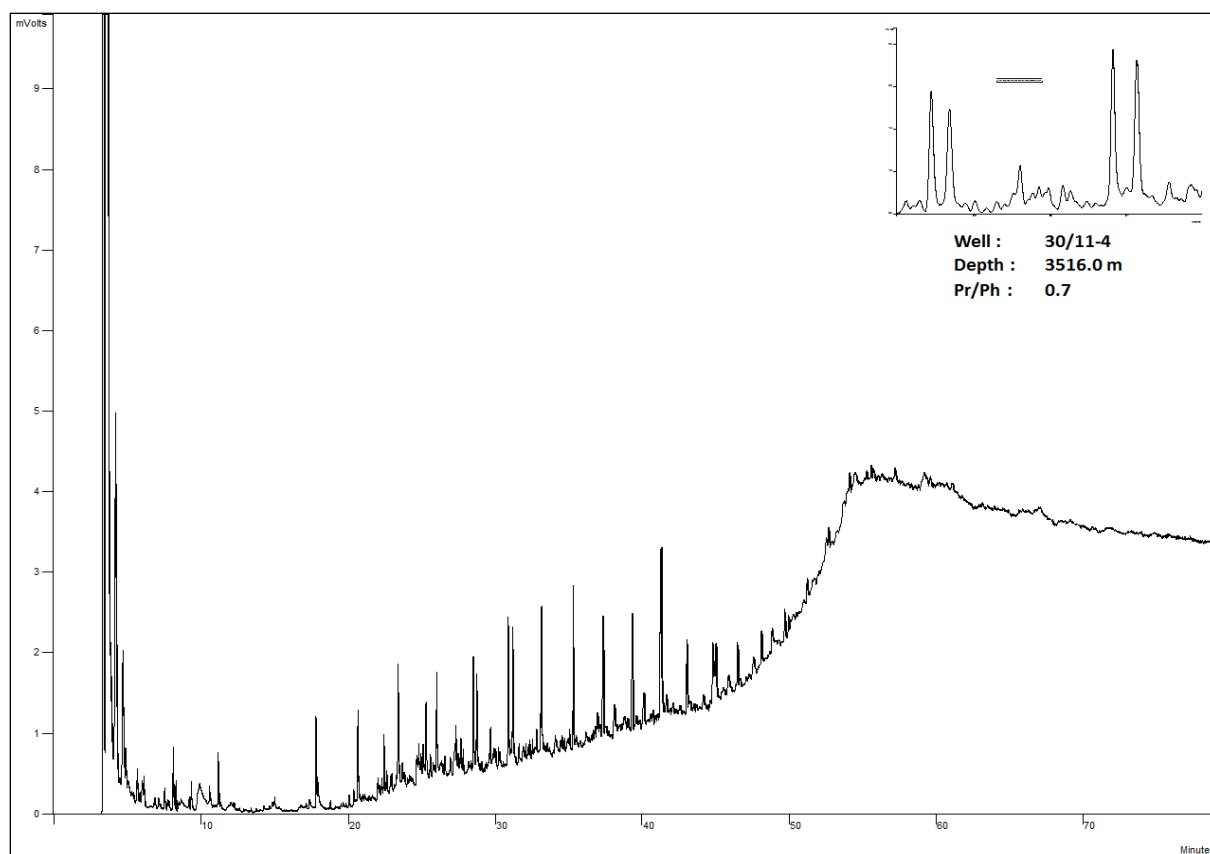


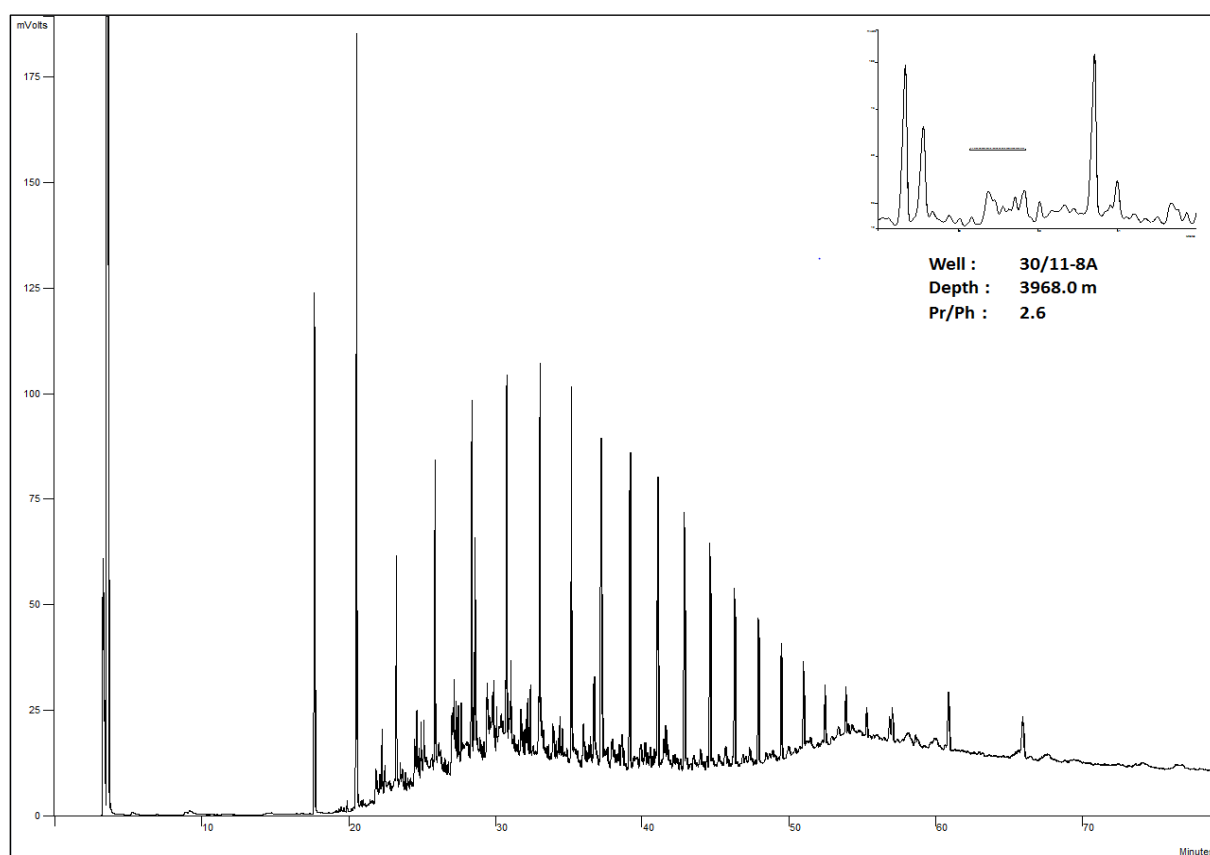
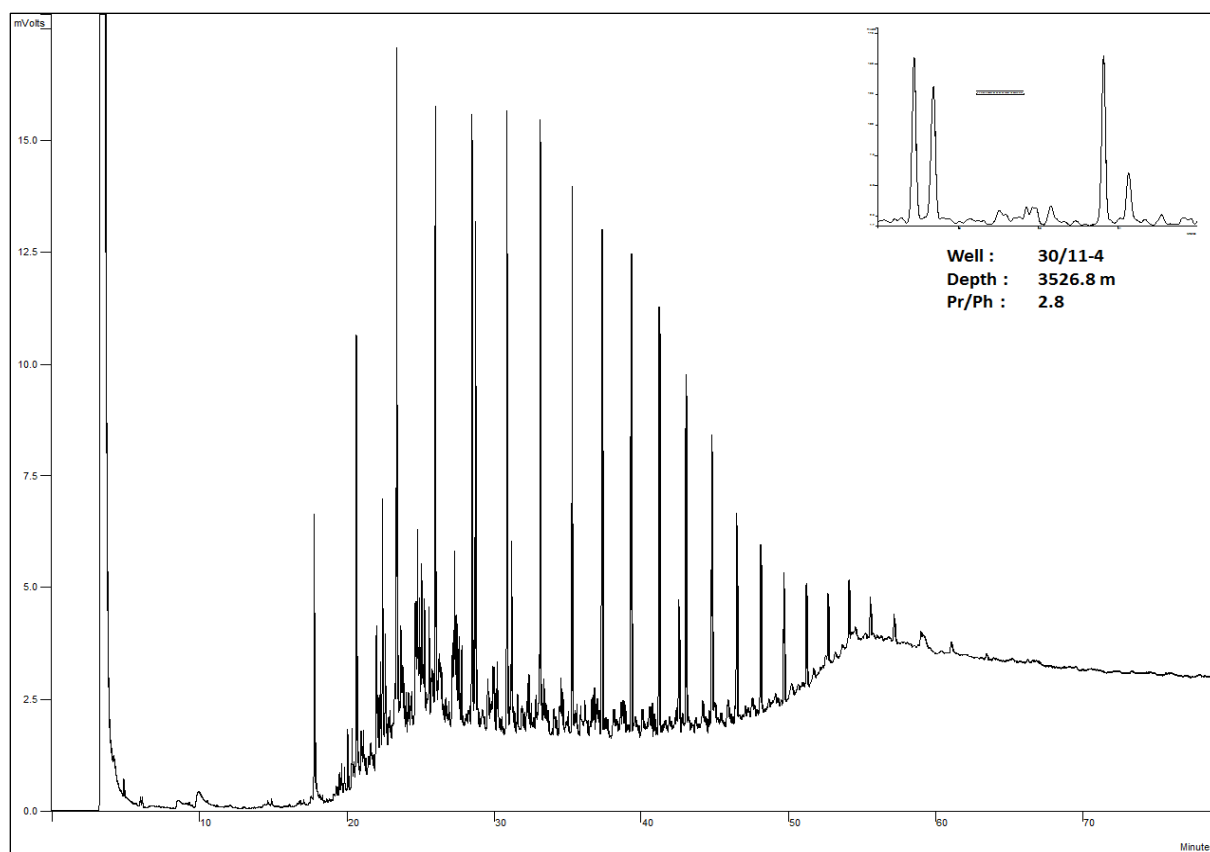


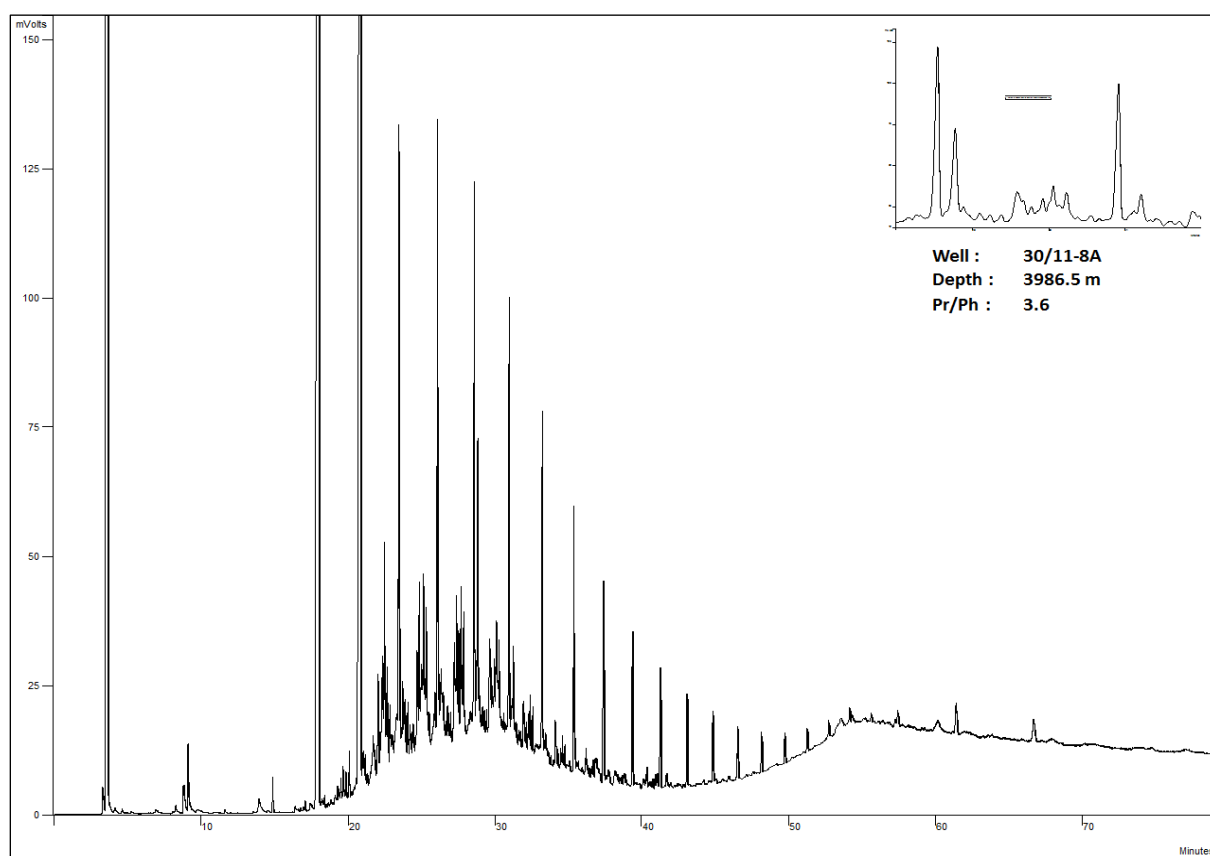
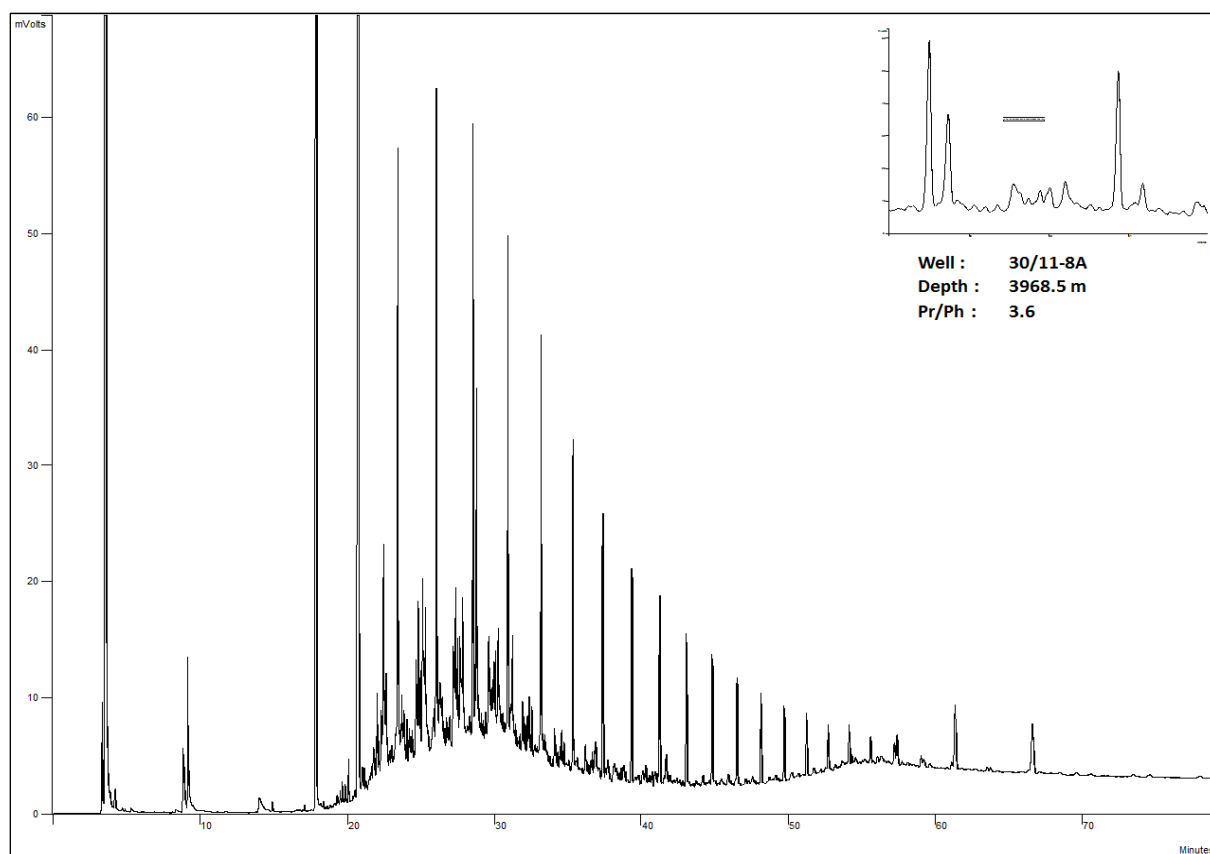


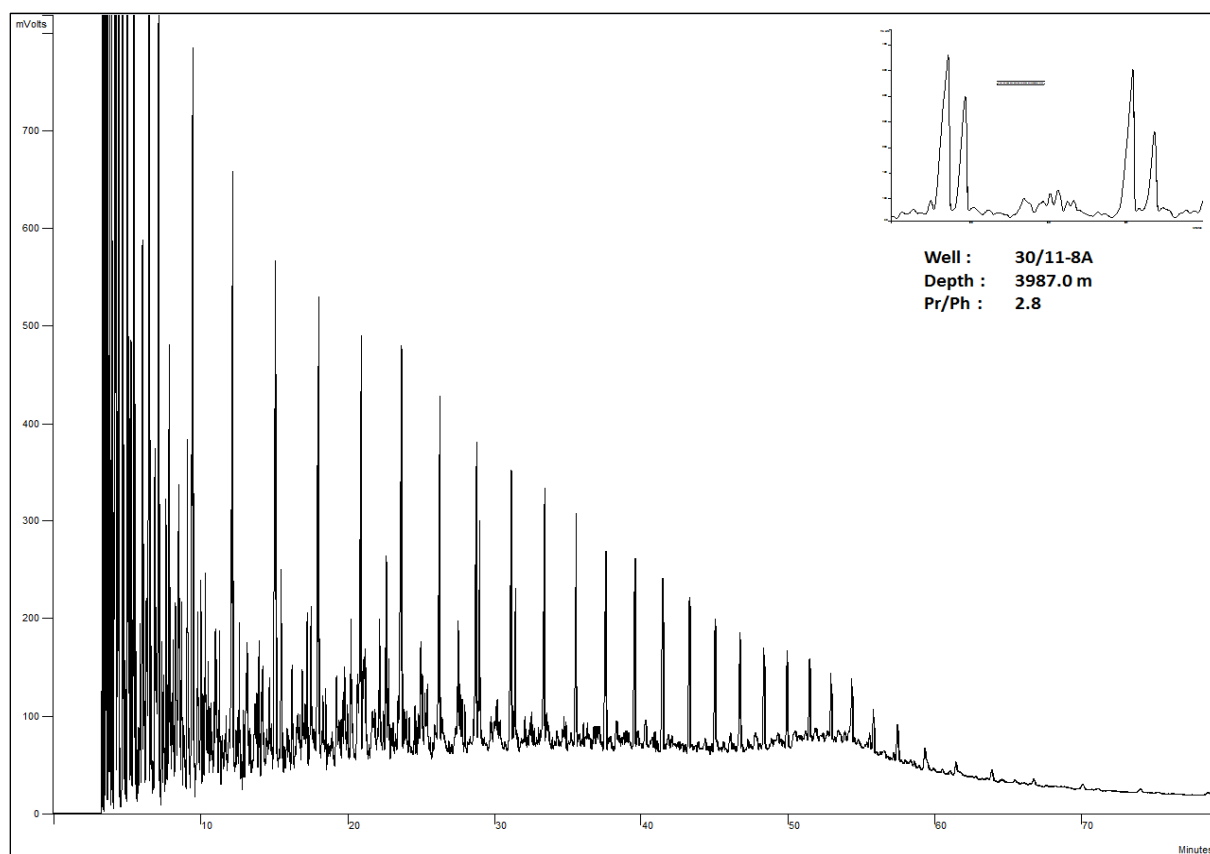




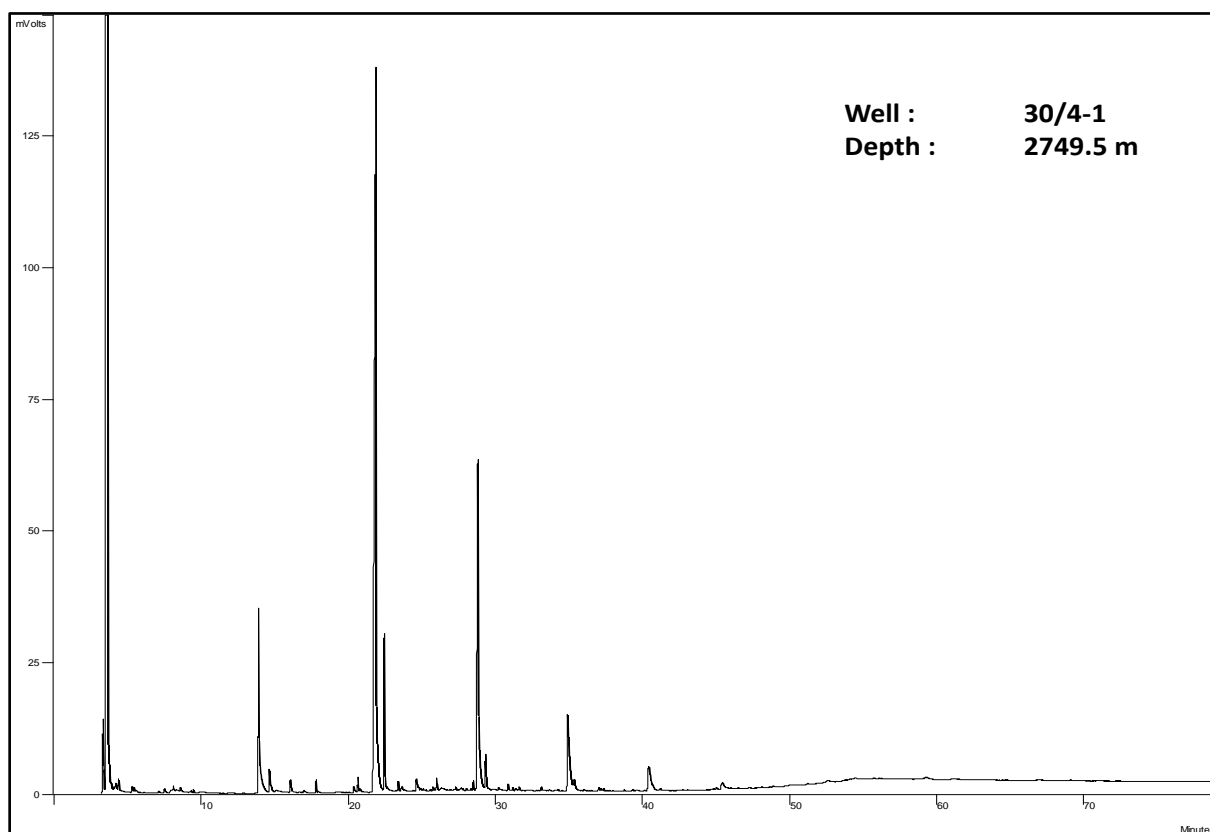
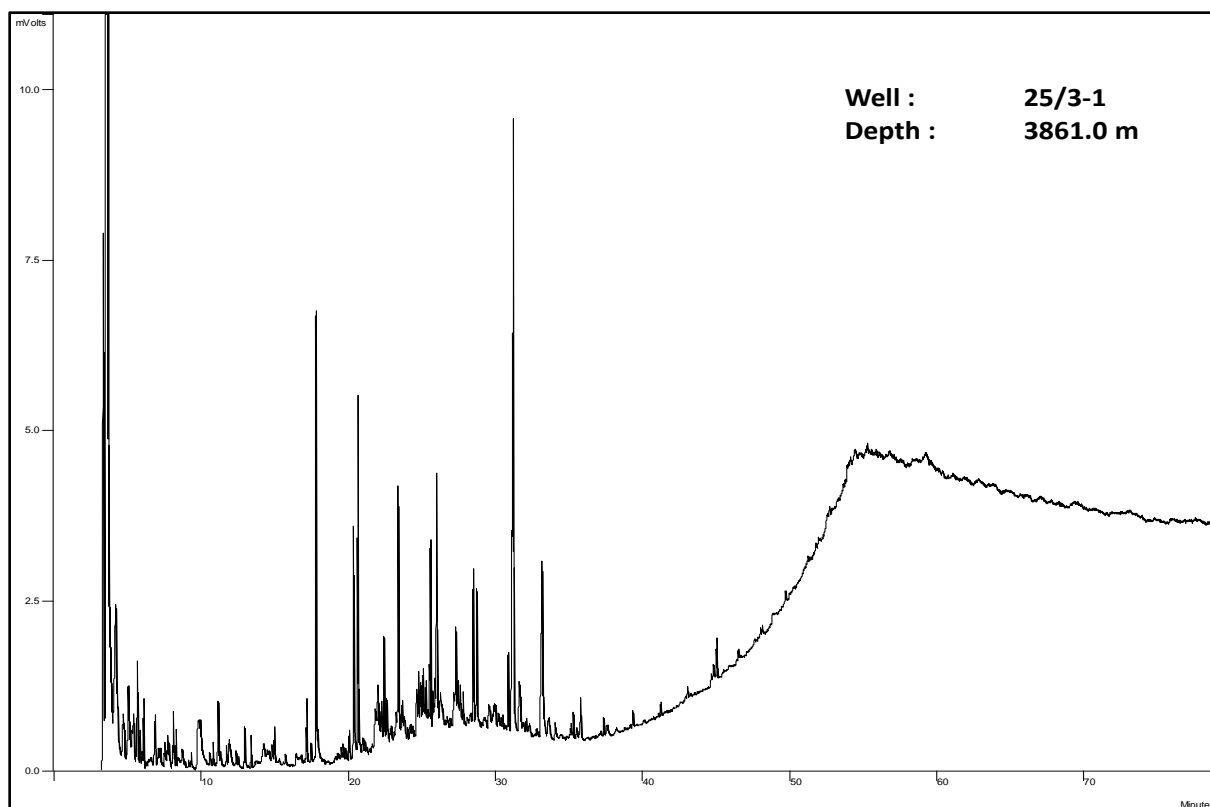


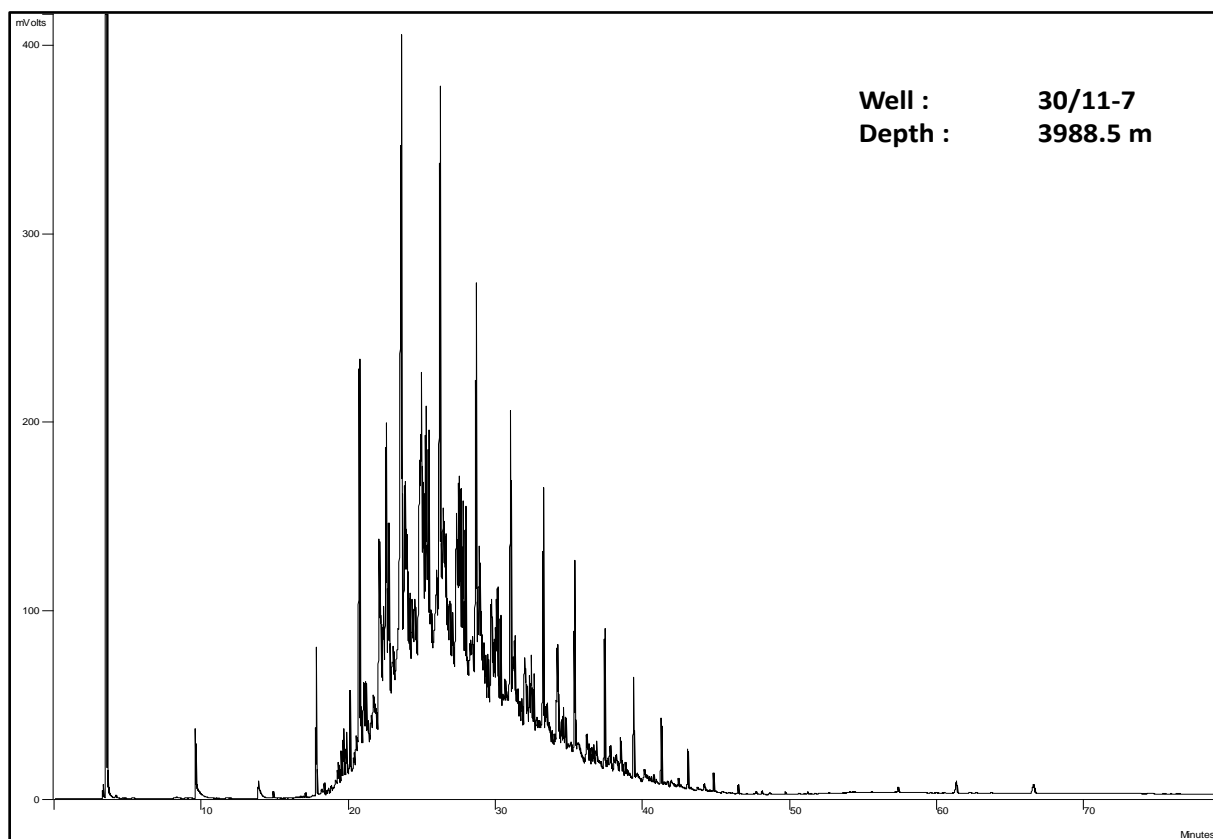
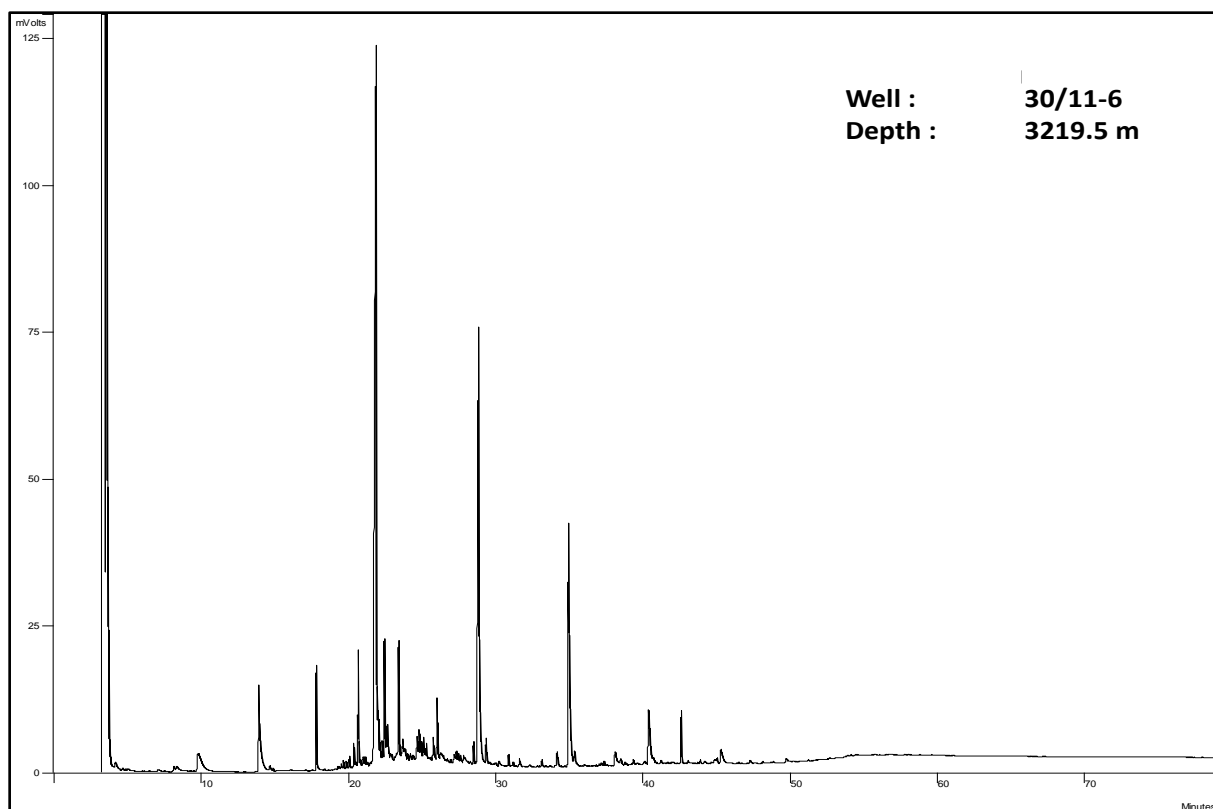


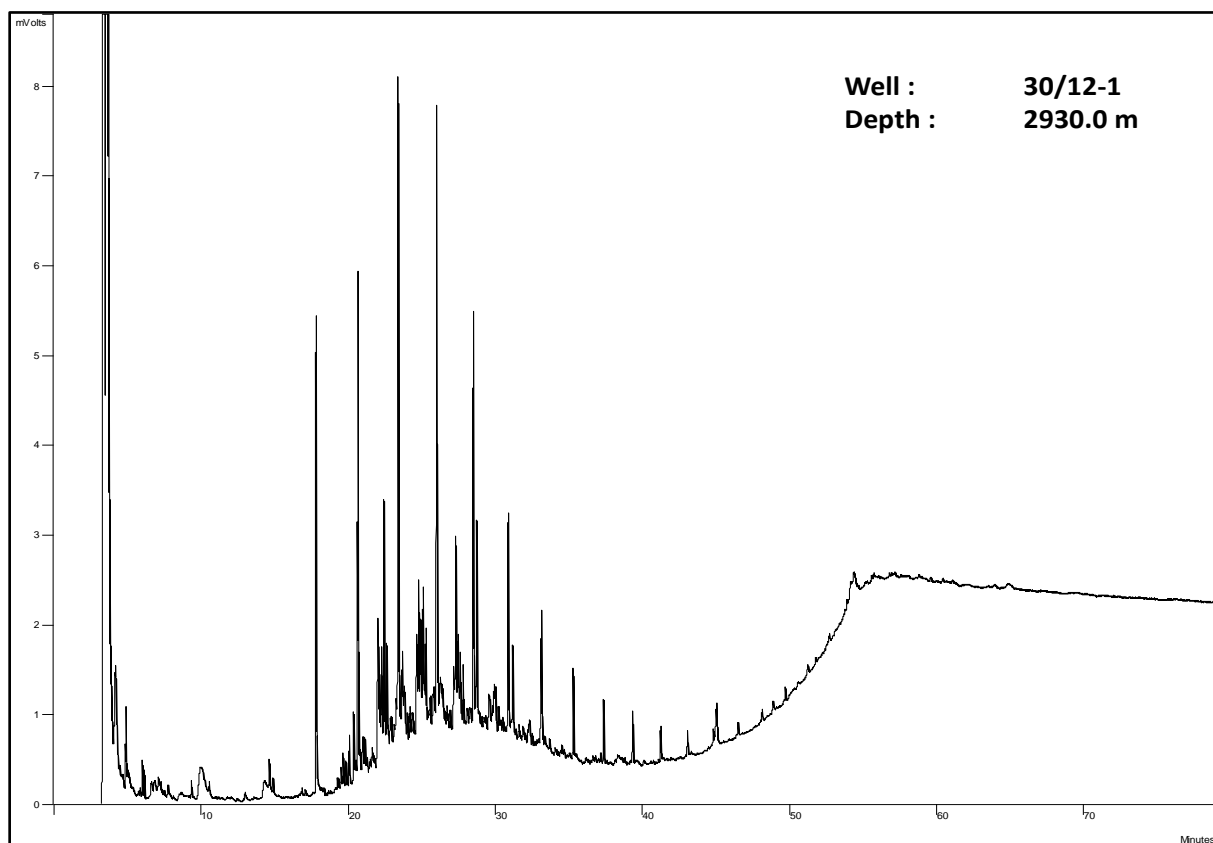
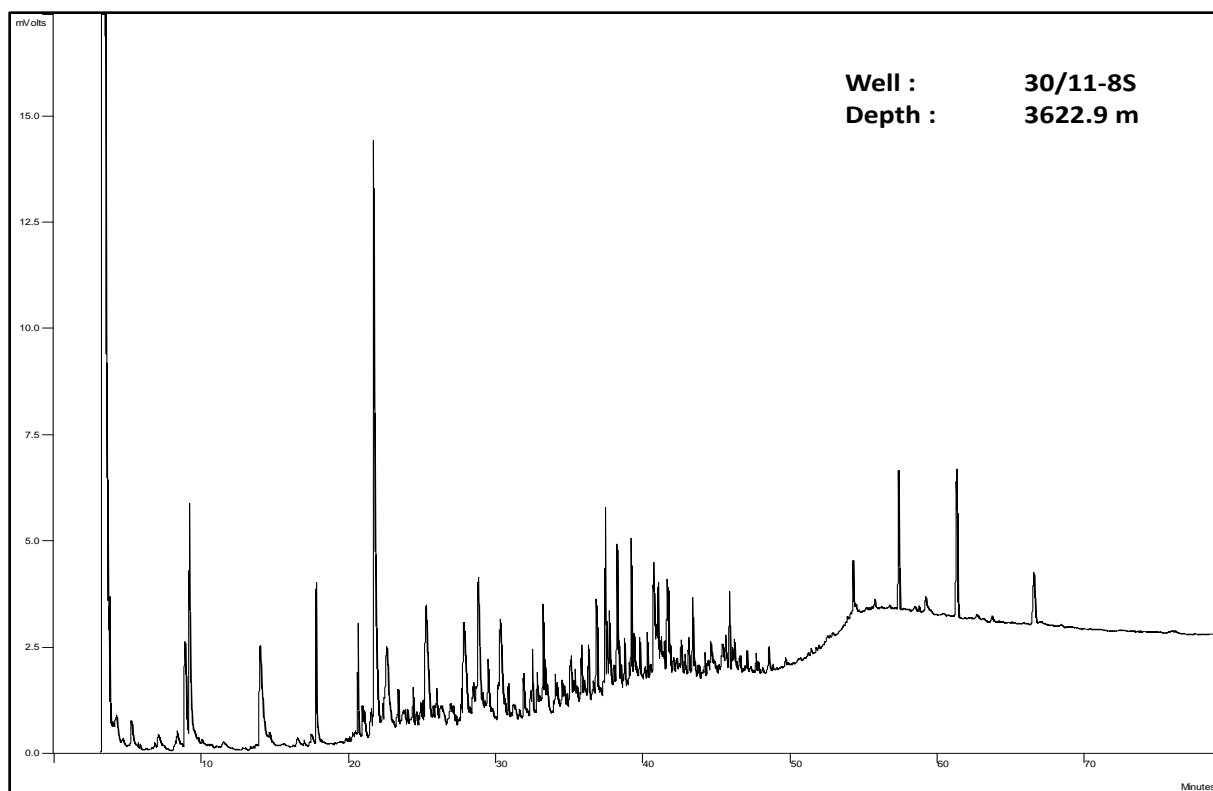




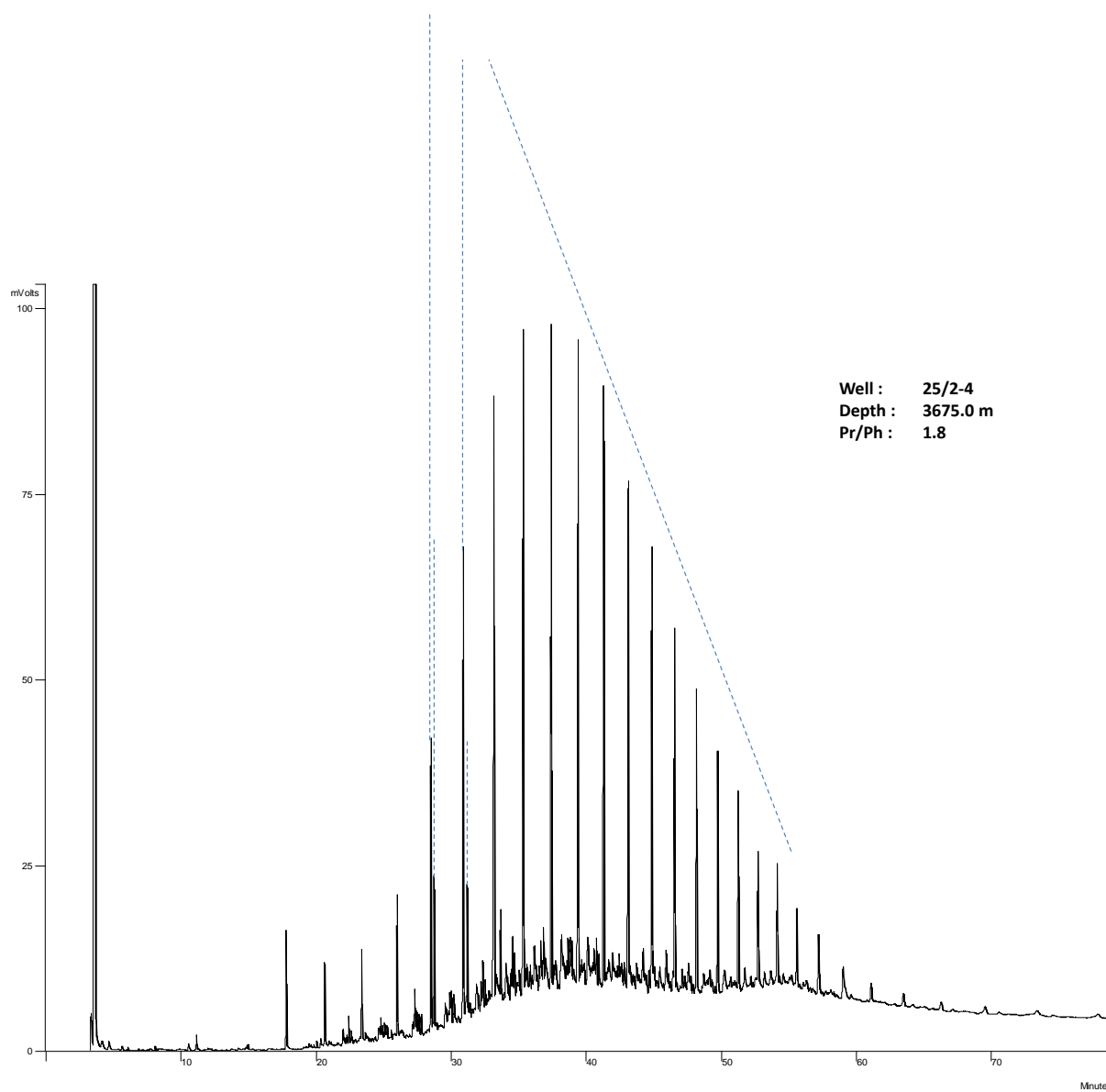
GC-FID Chromatograms of the samples with diesel mud contamination

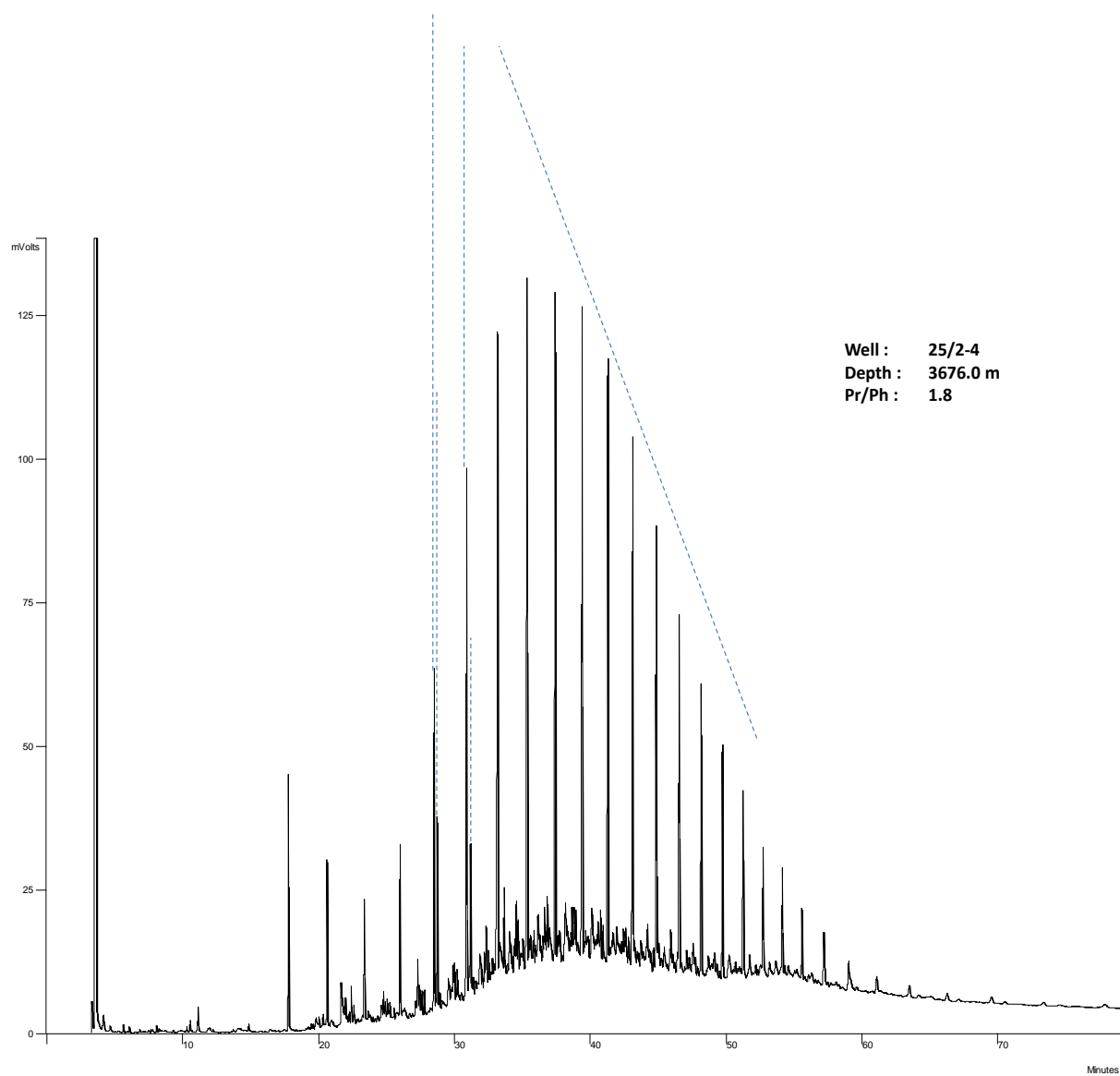


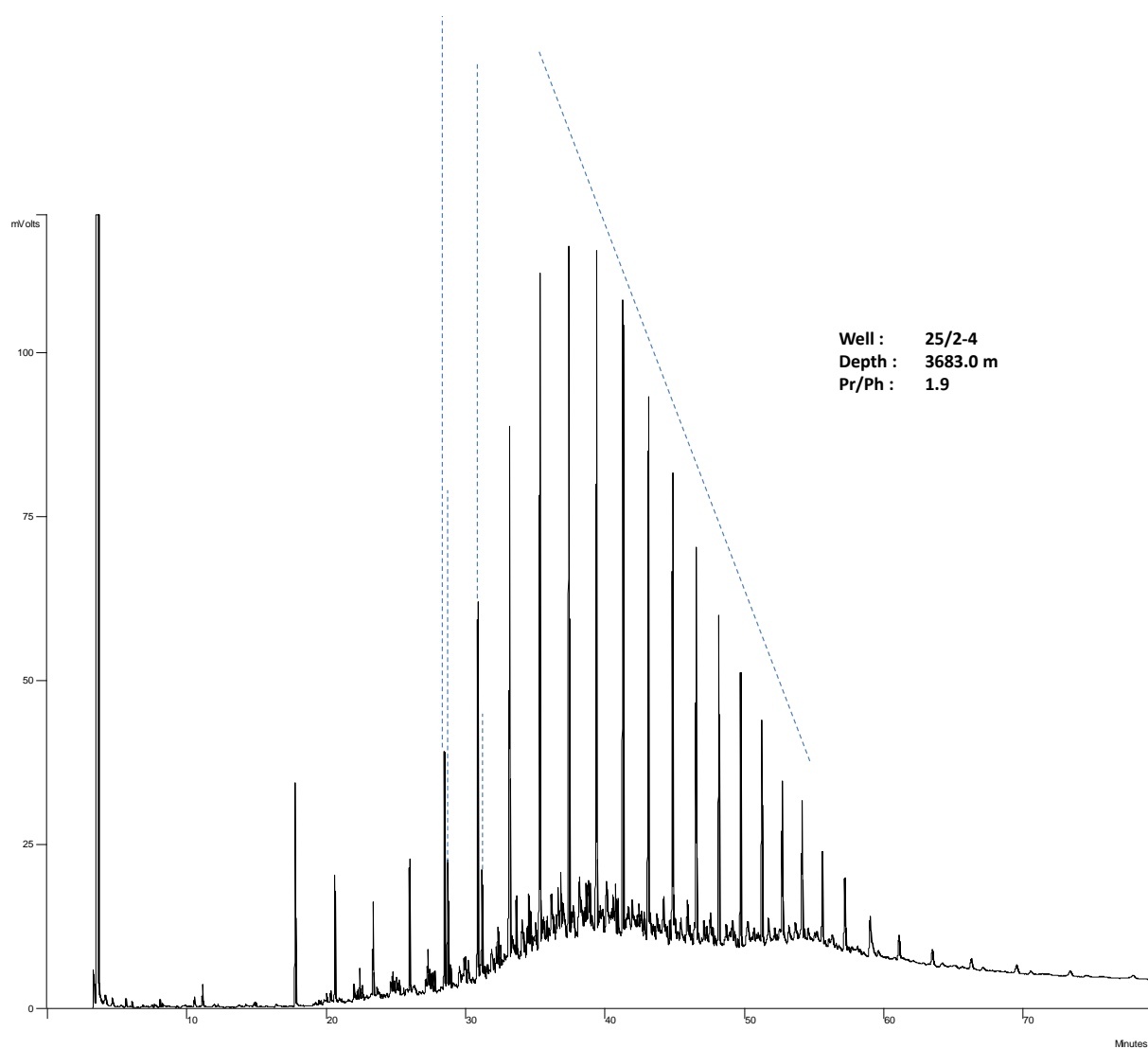


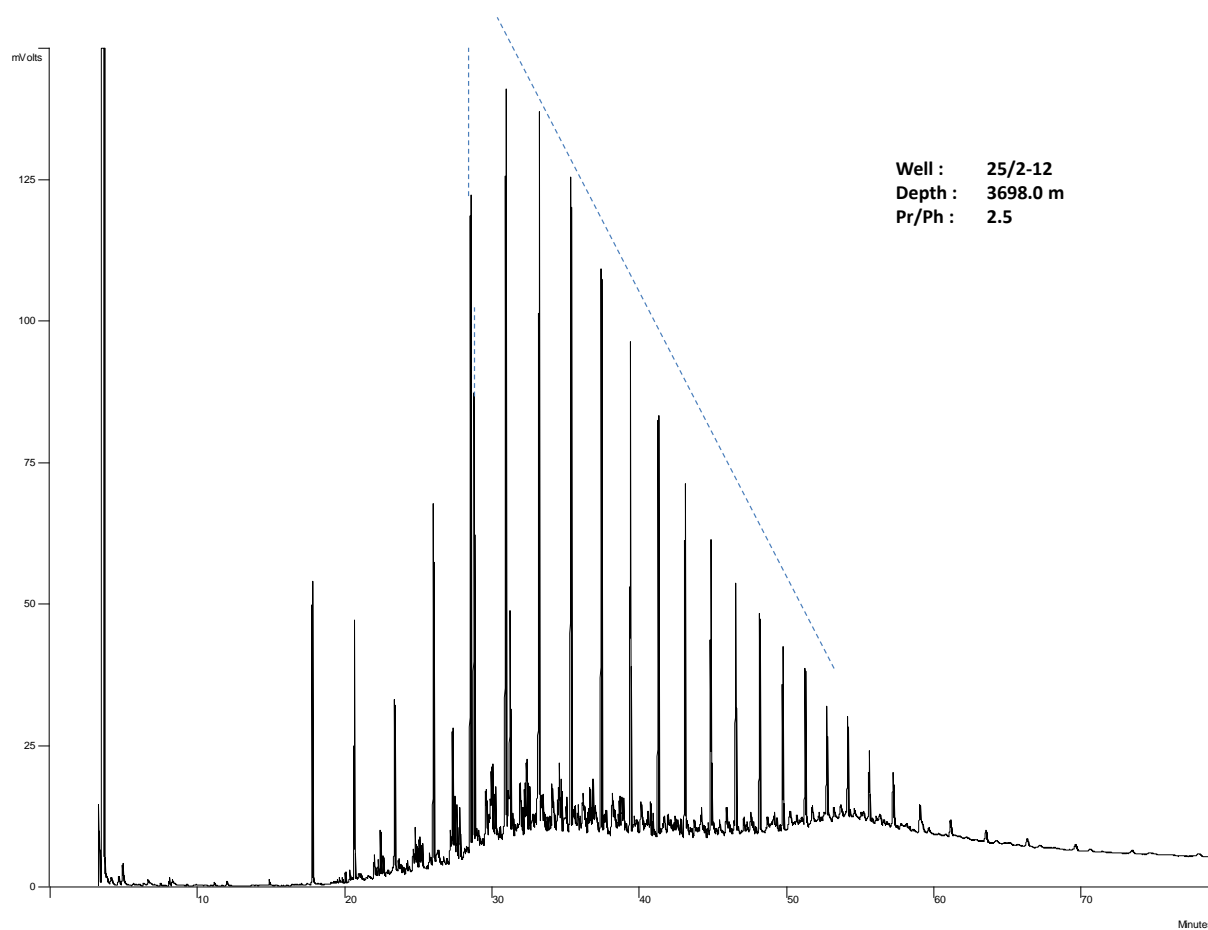


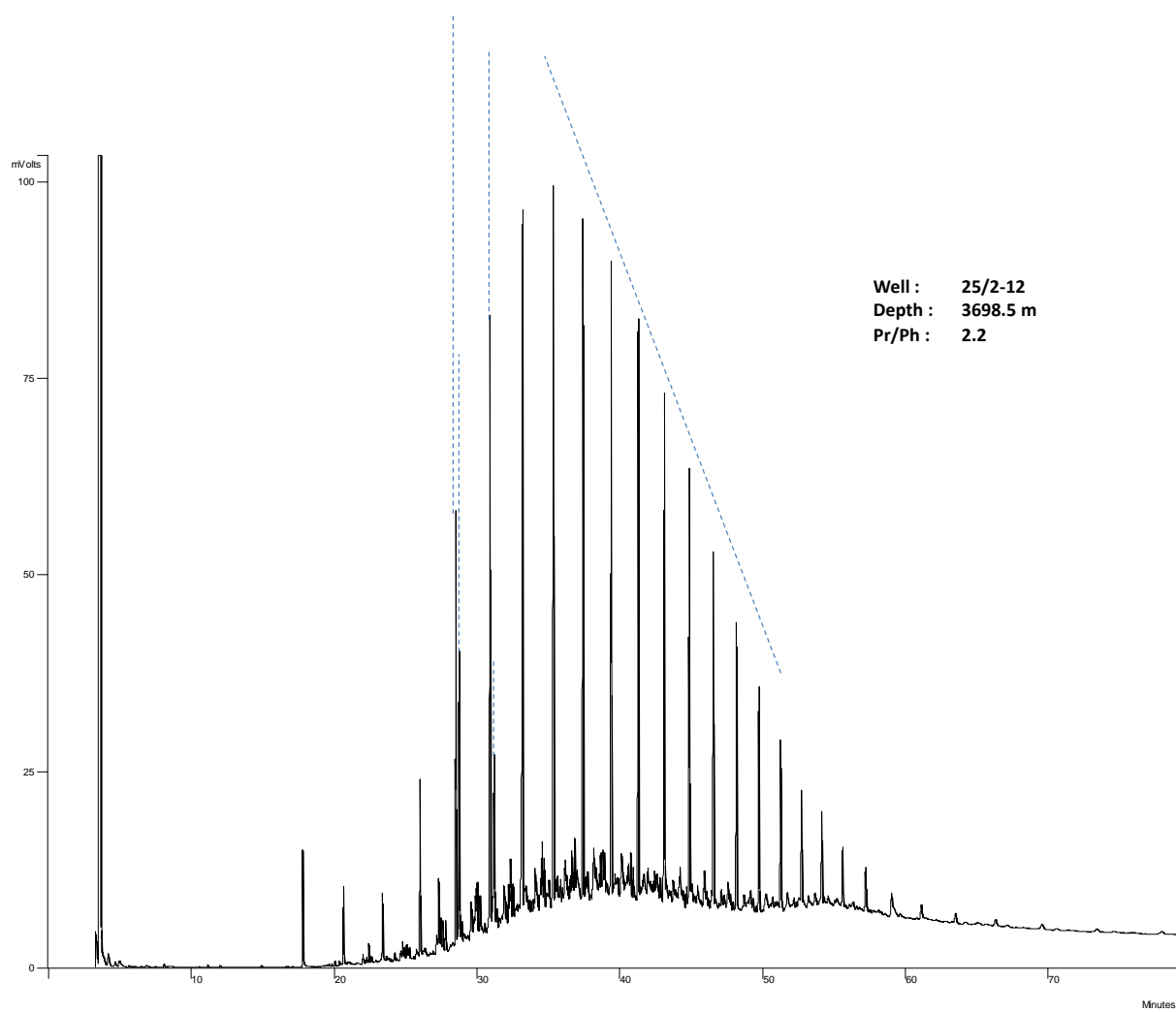
GC-FID Chromatograms for the extrapolated peaks of Isoprenoids and n-alkanes

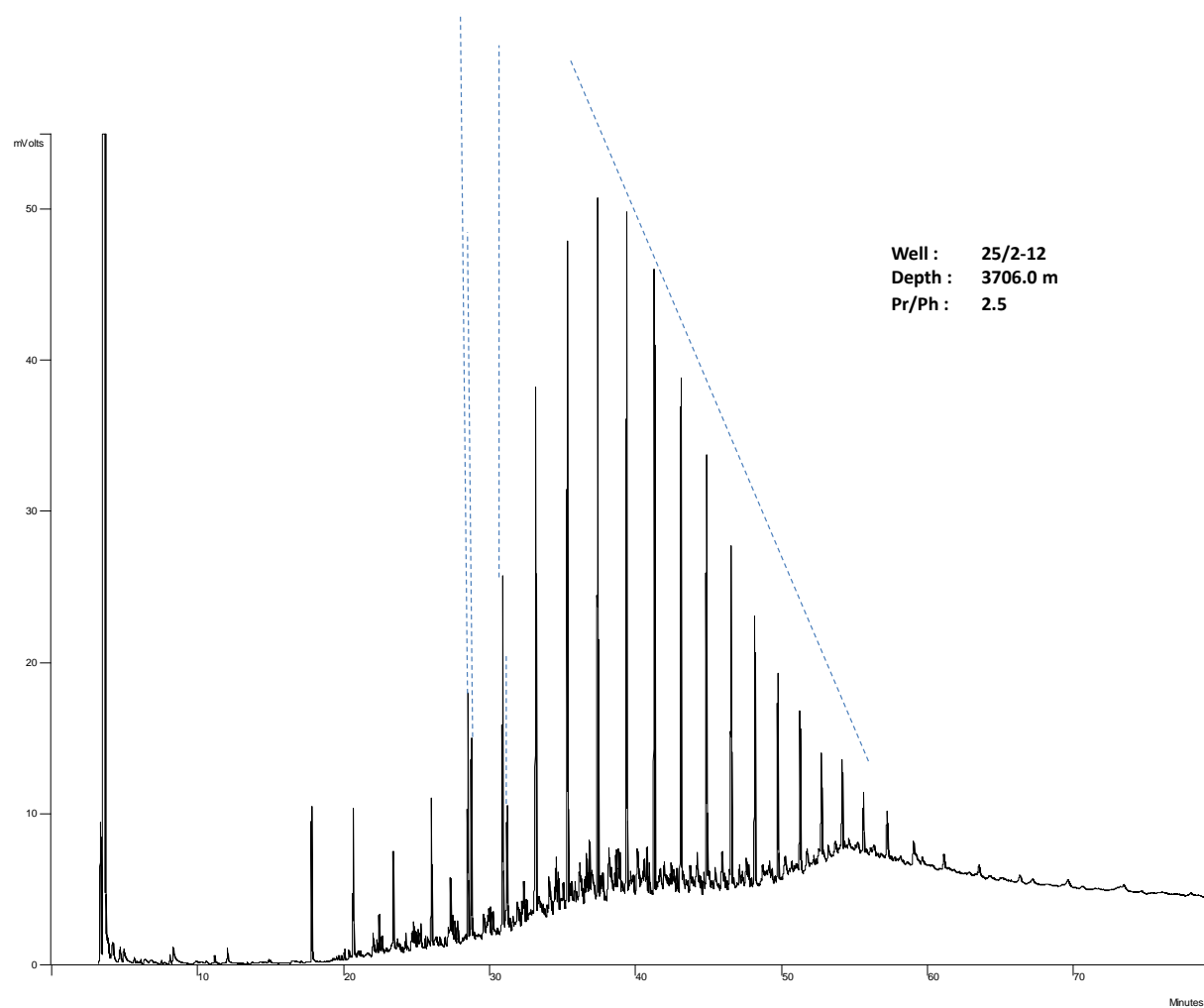


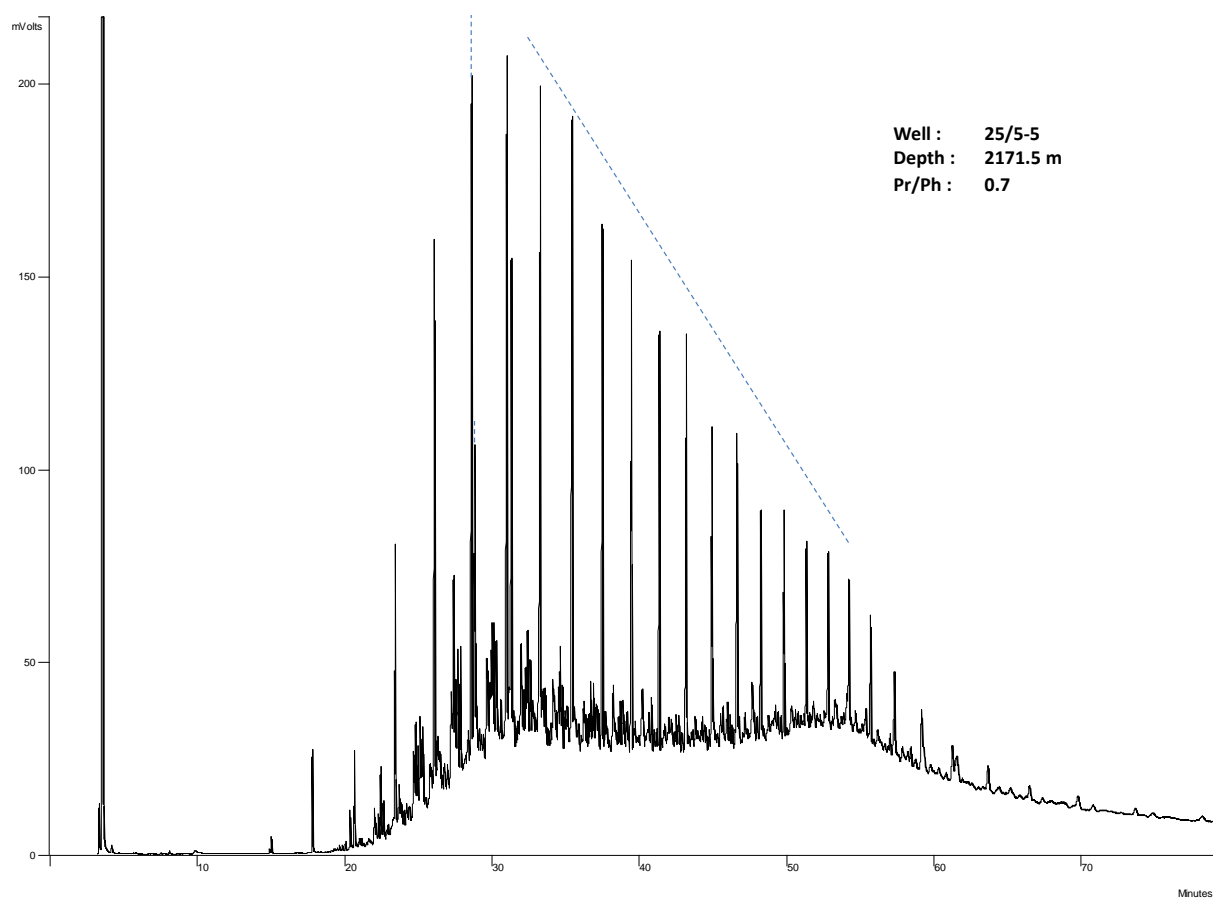


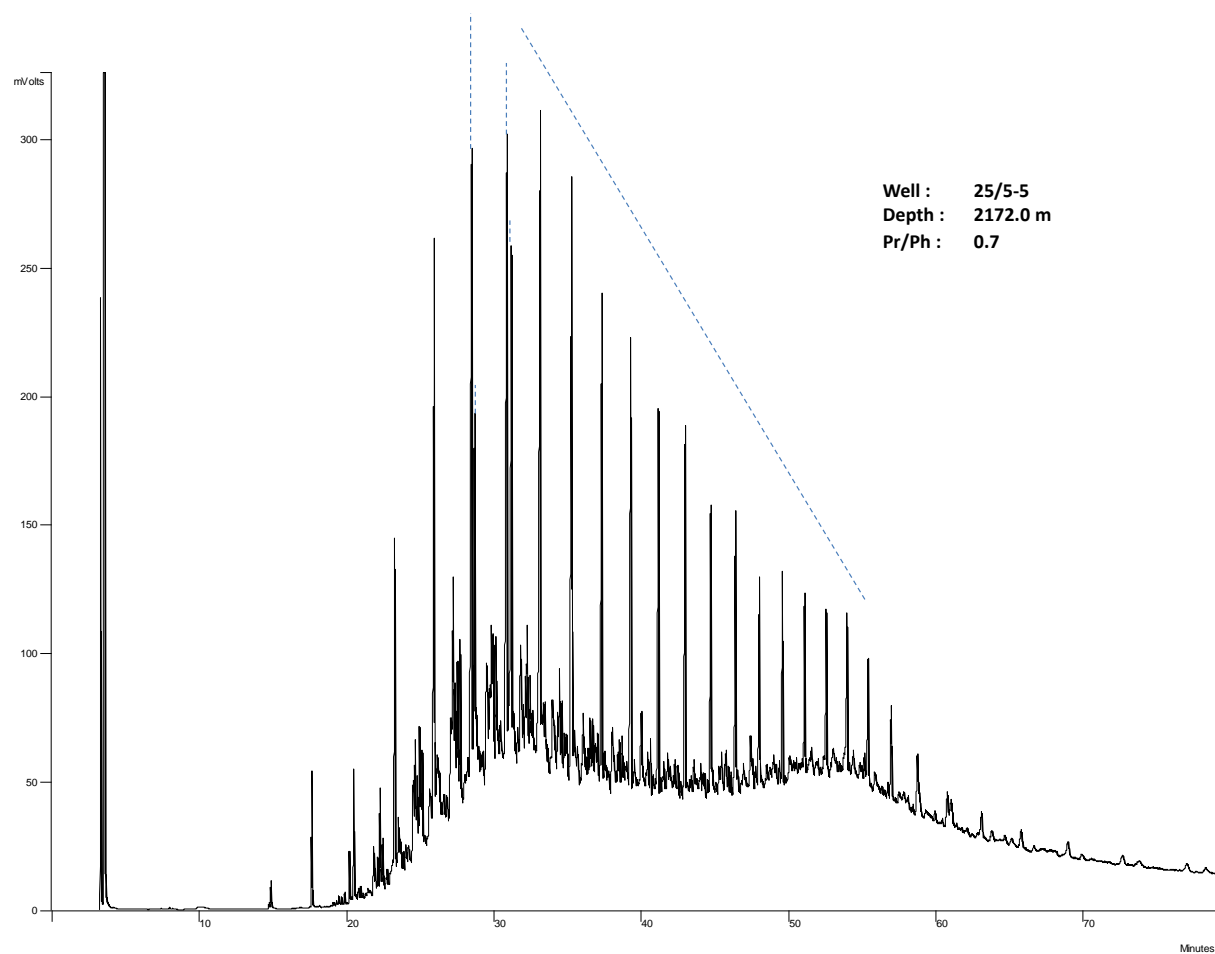


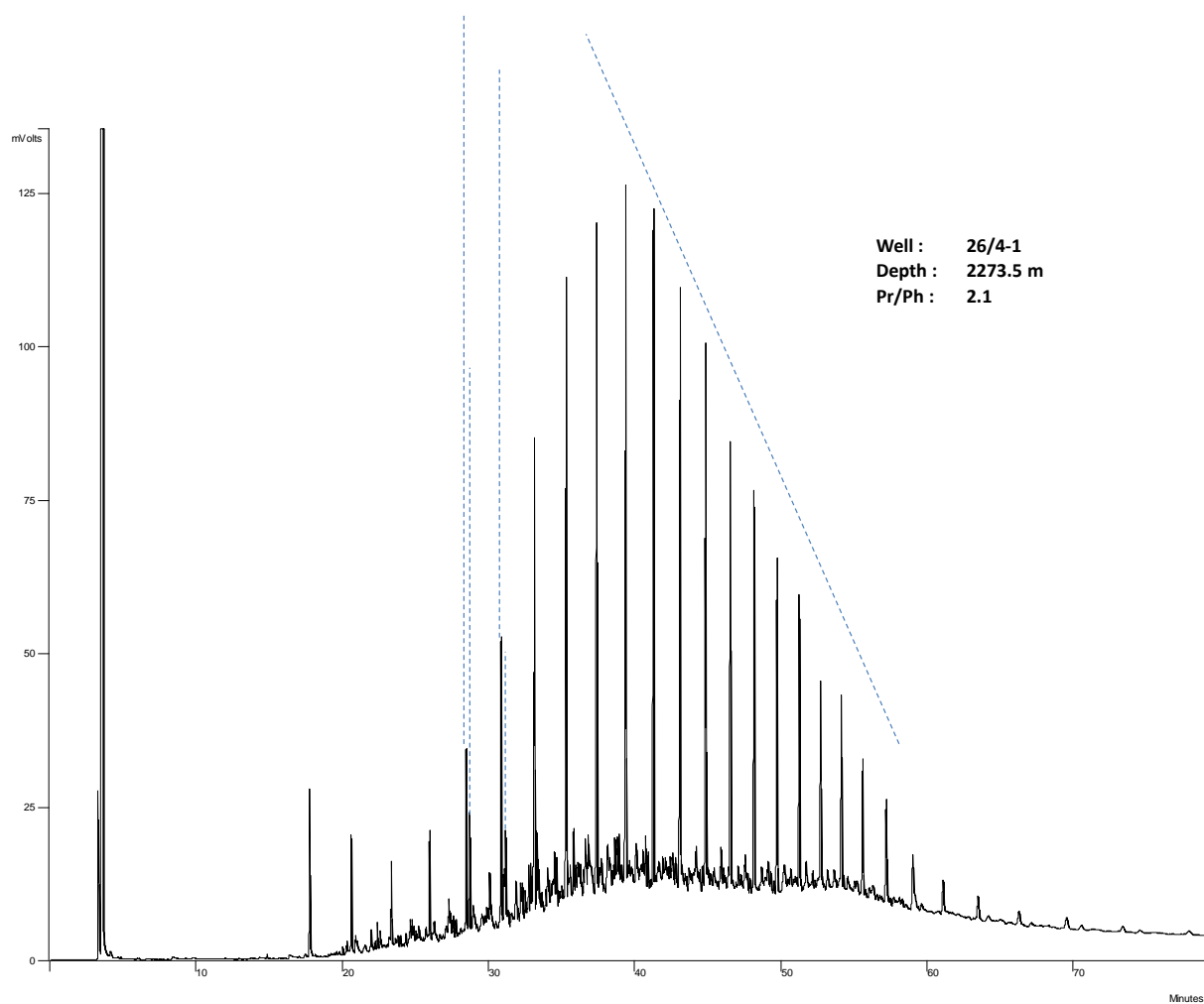


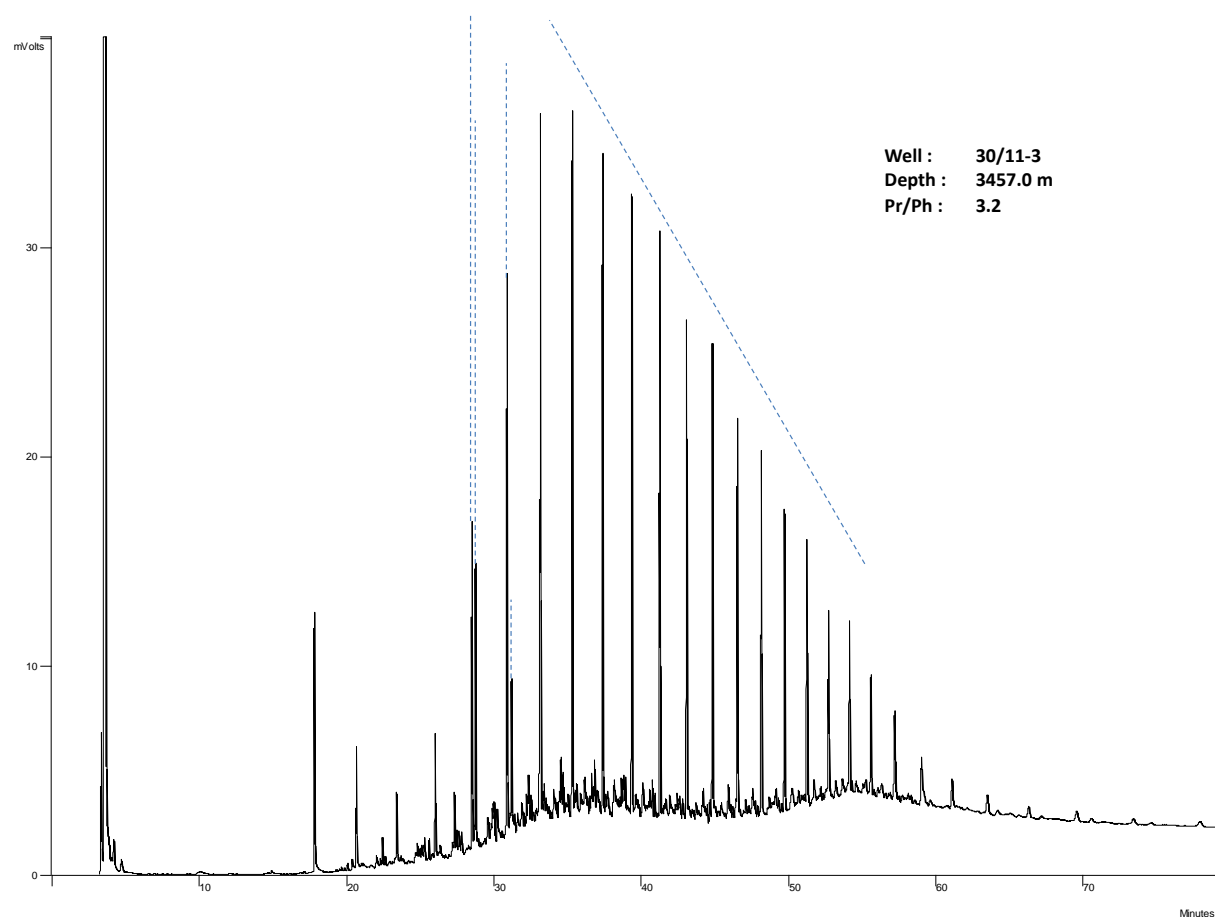


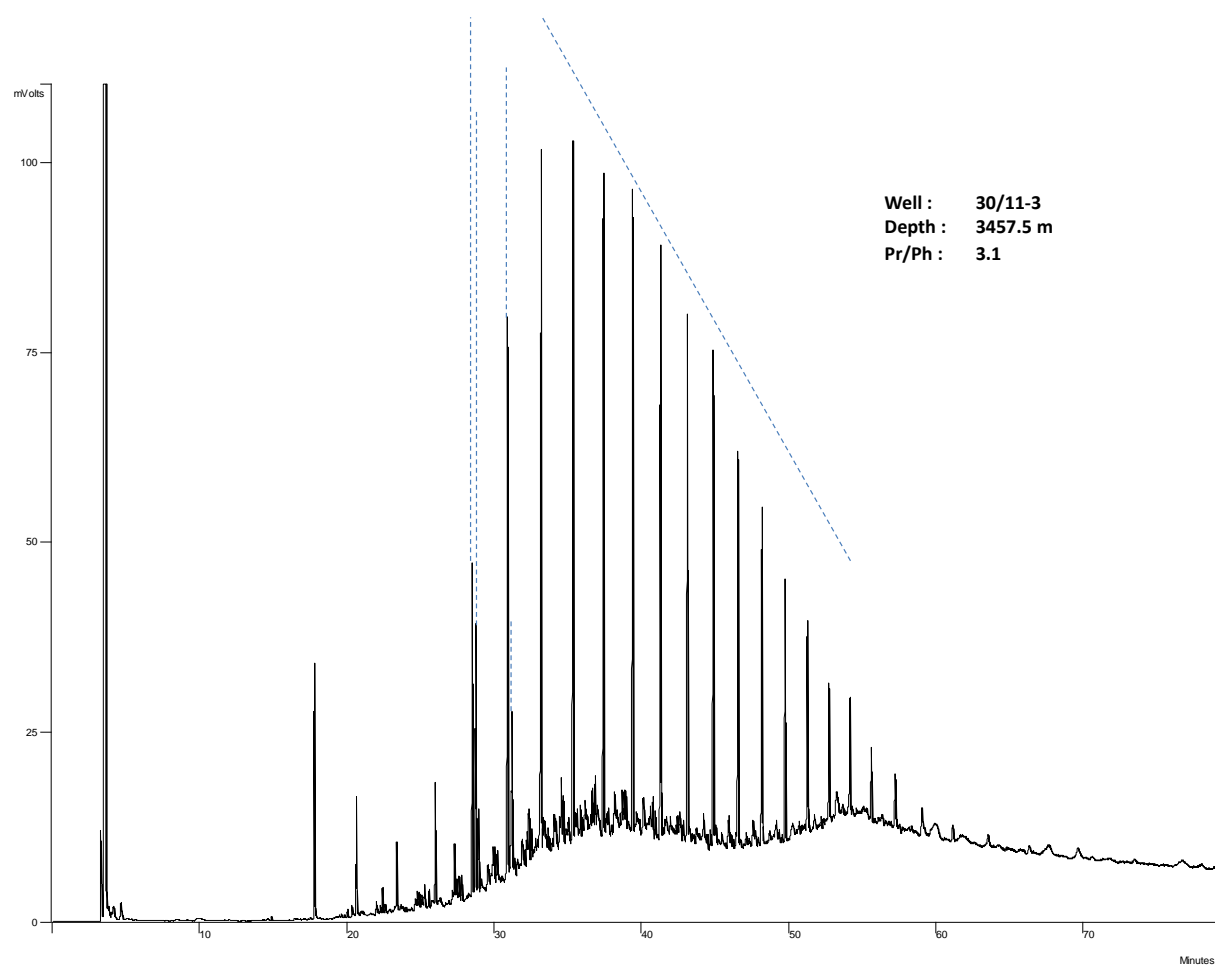


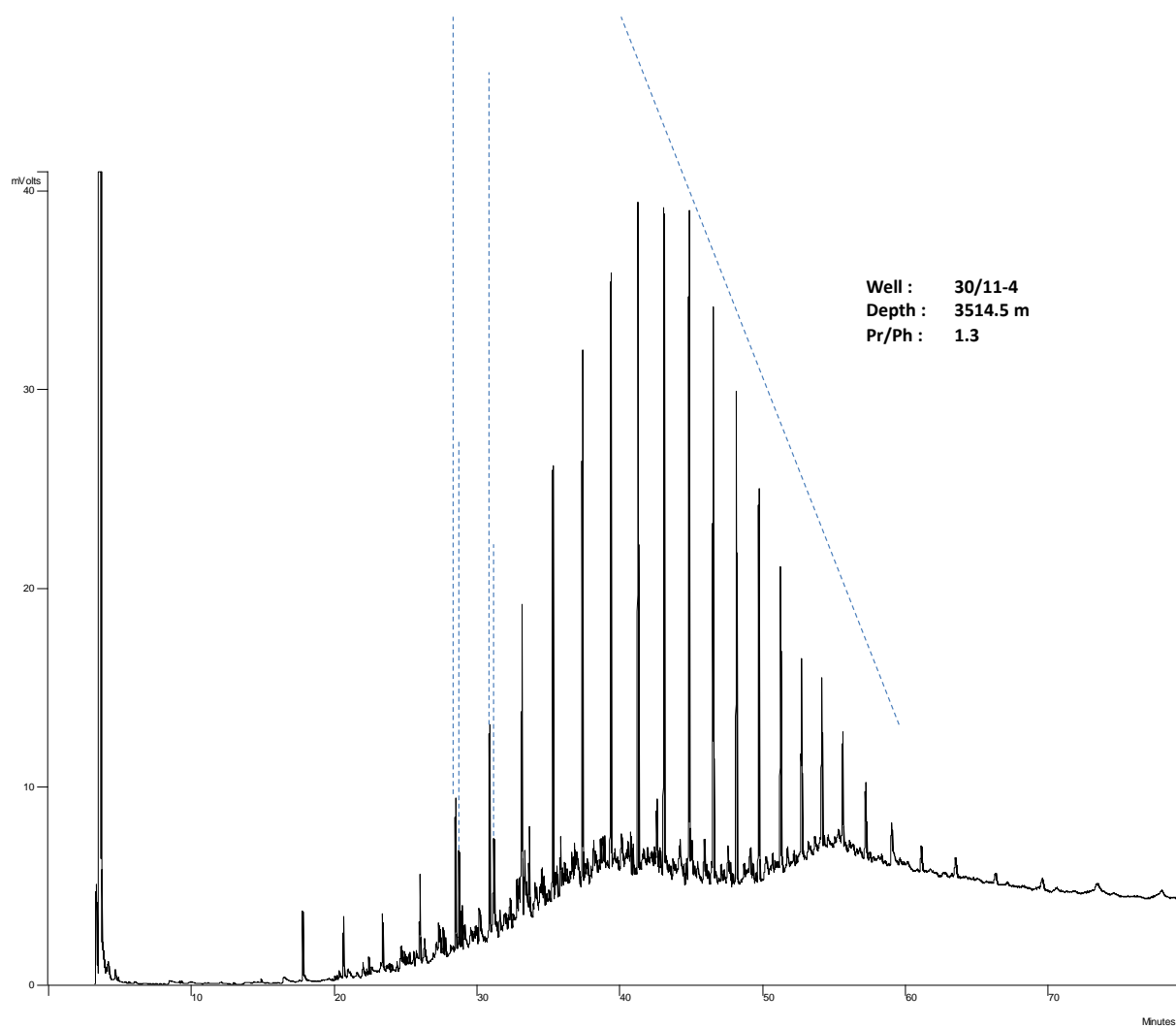


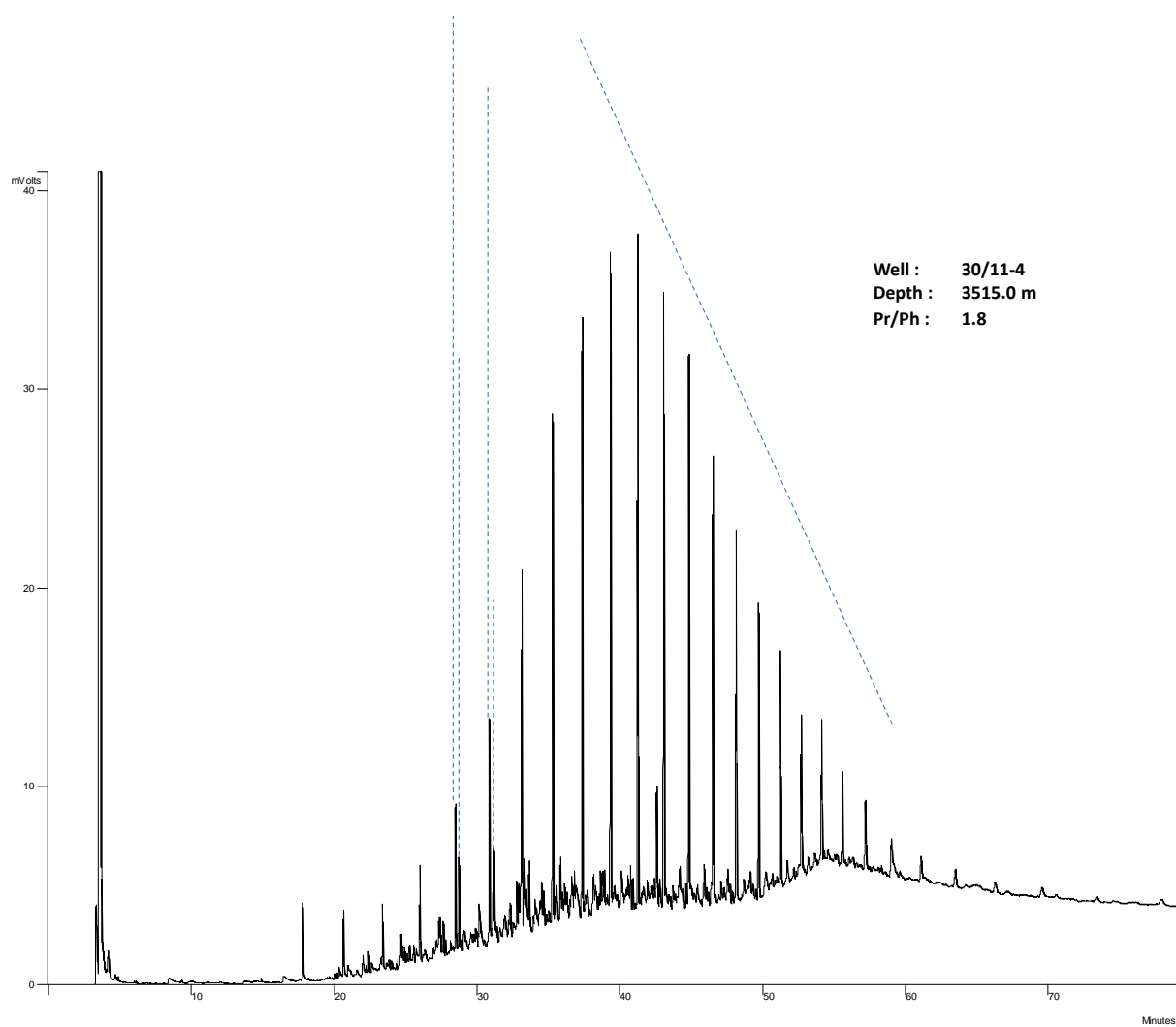


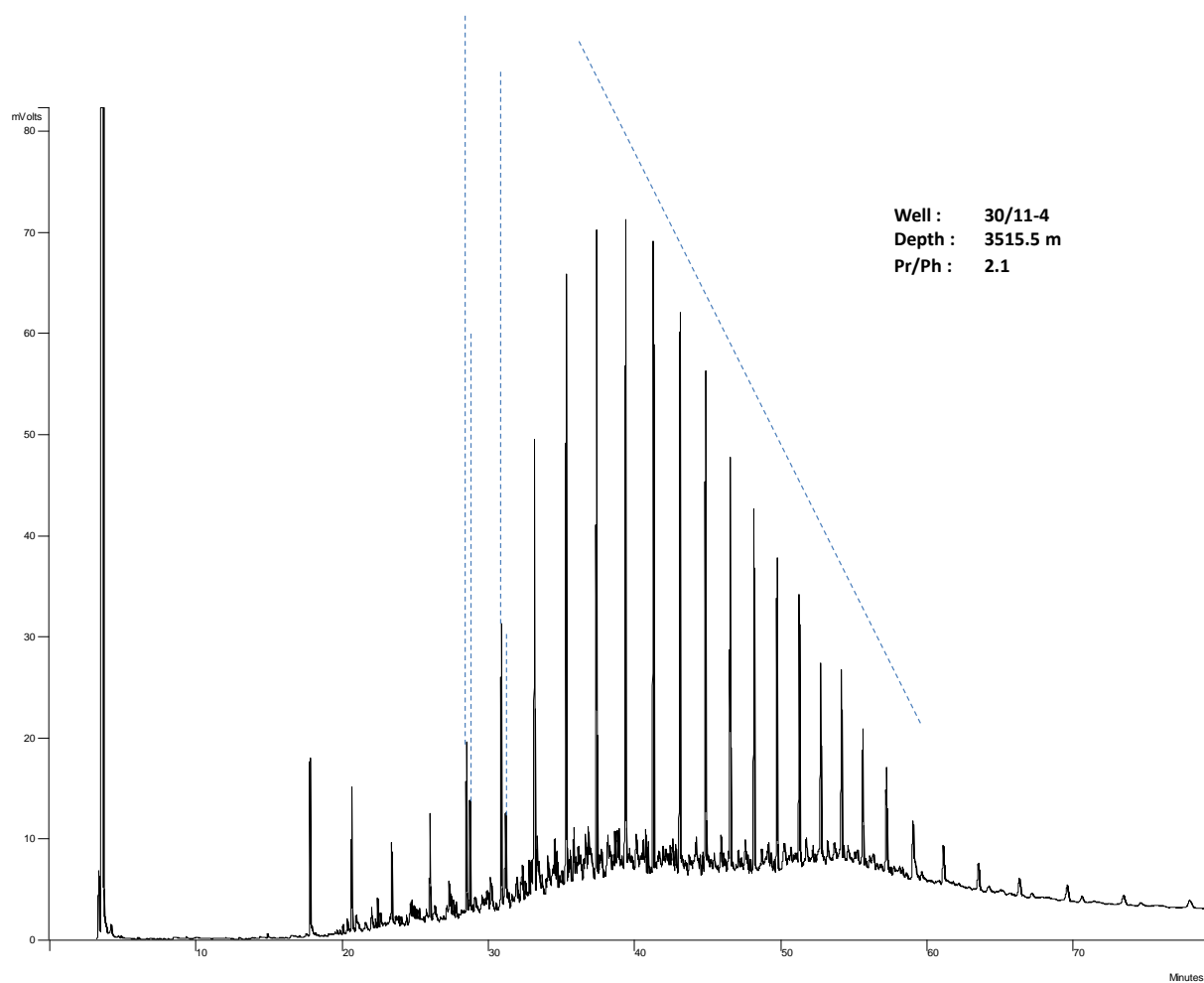


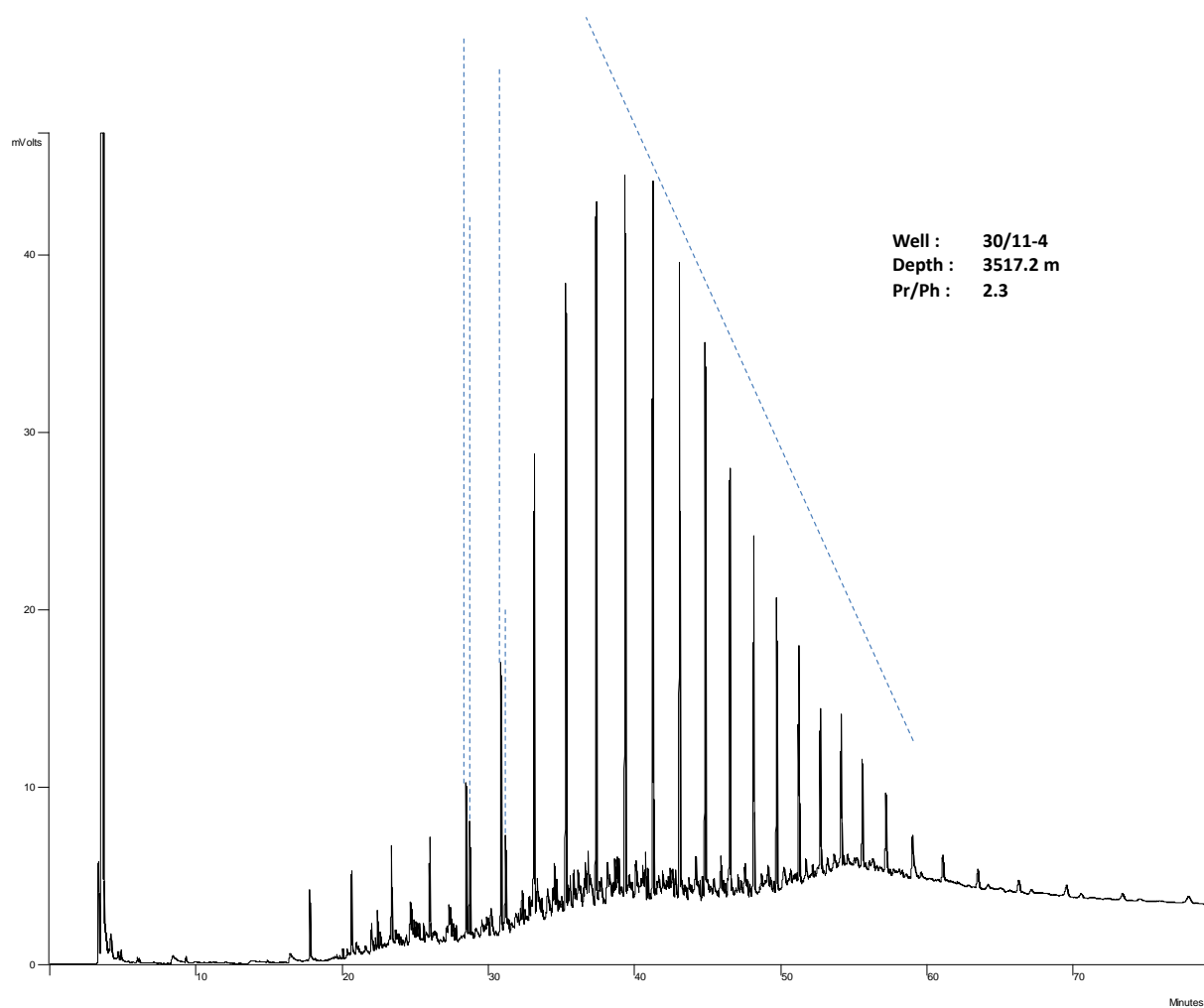




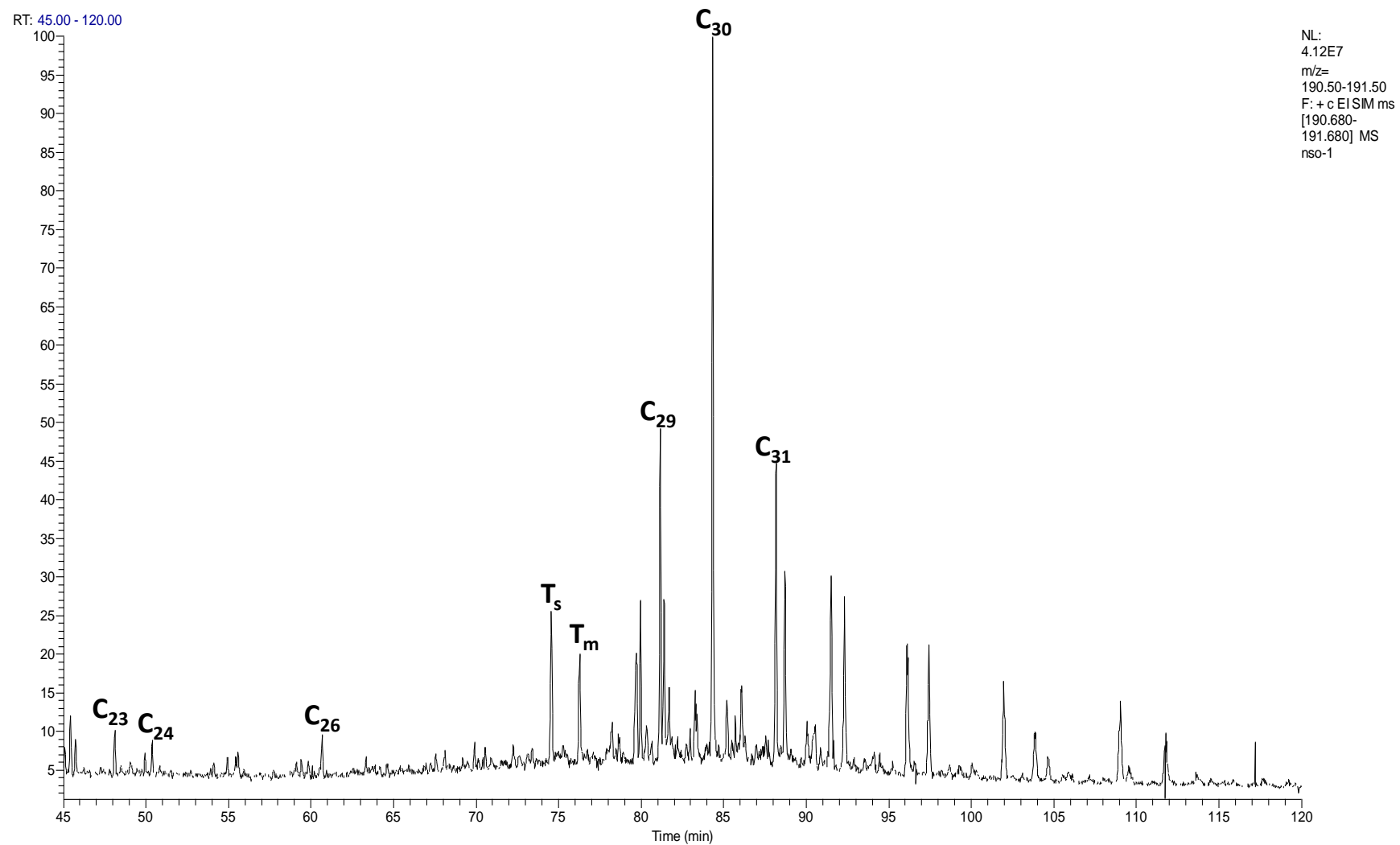


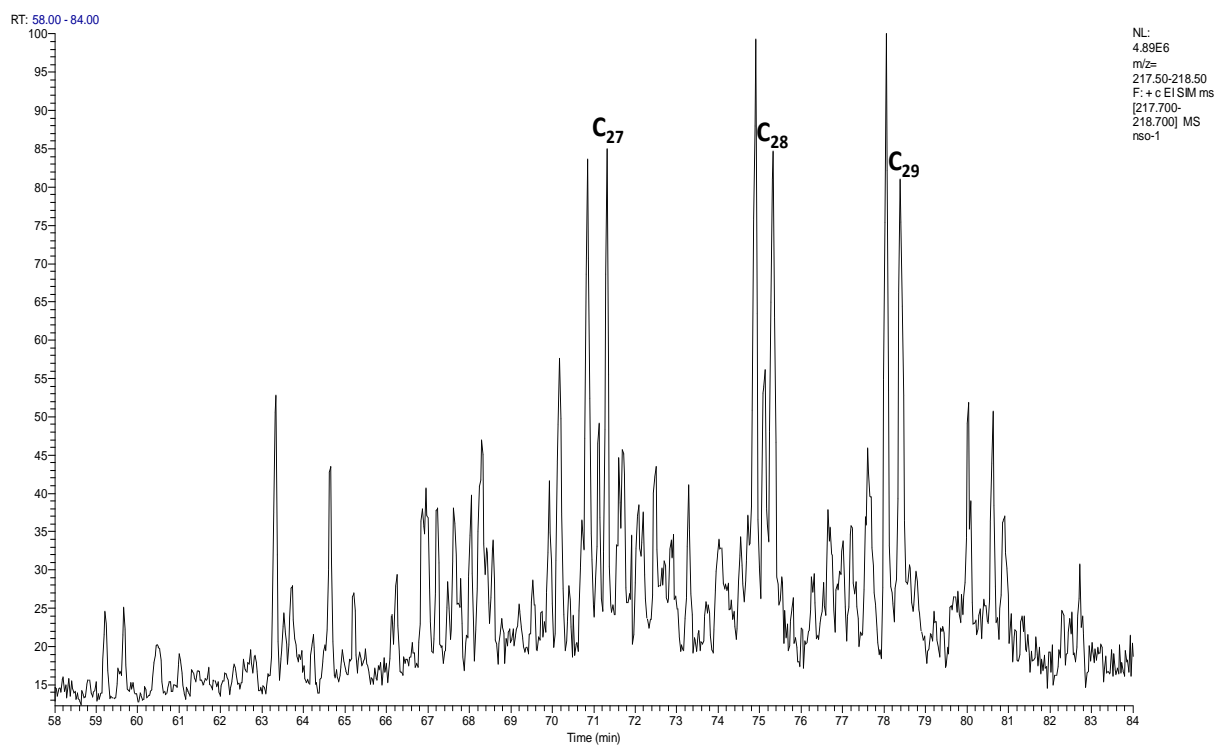
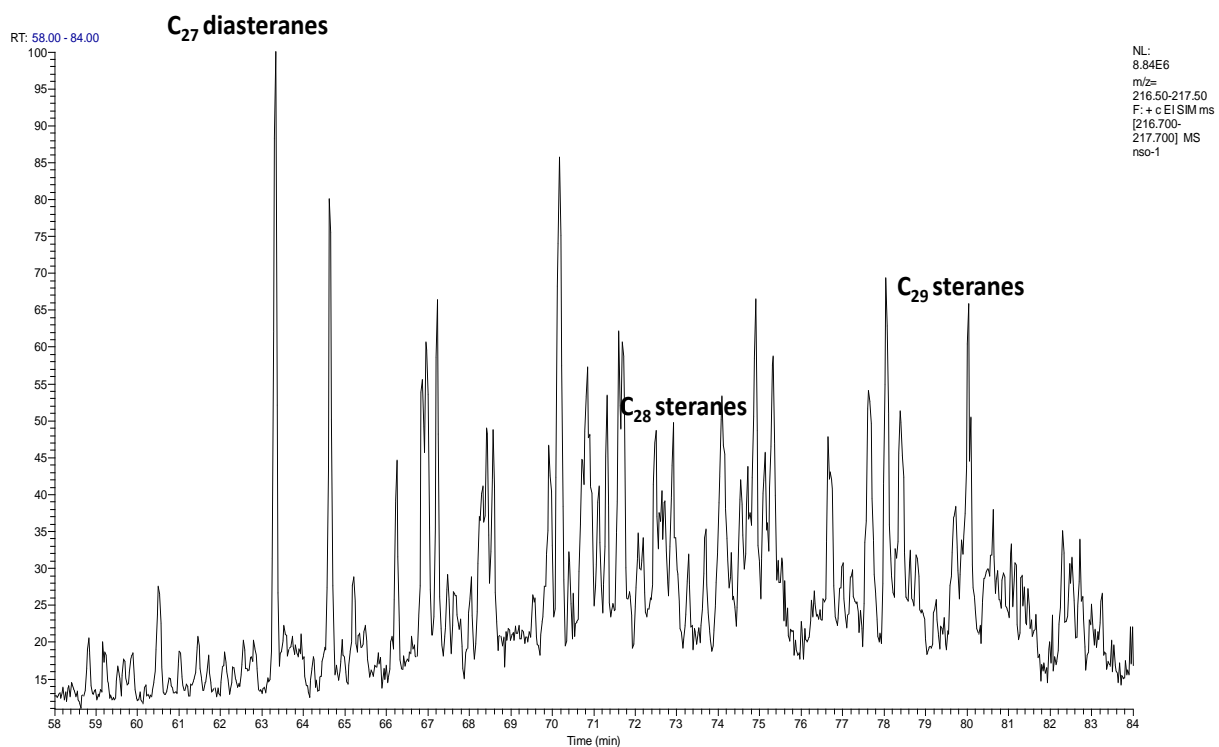


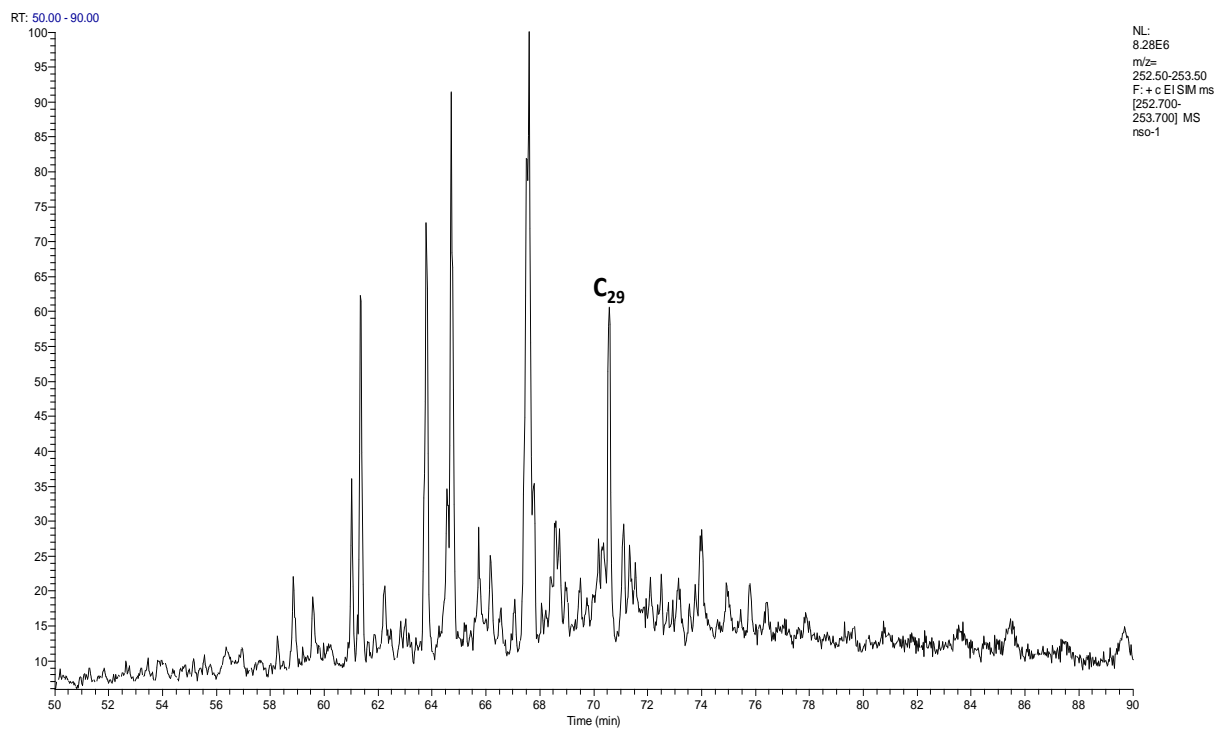
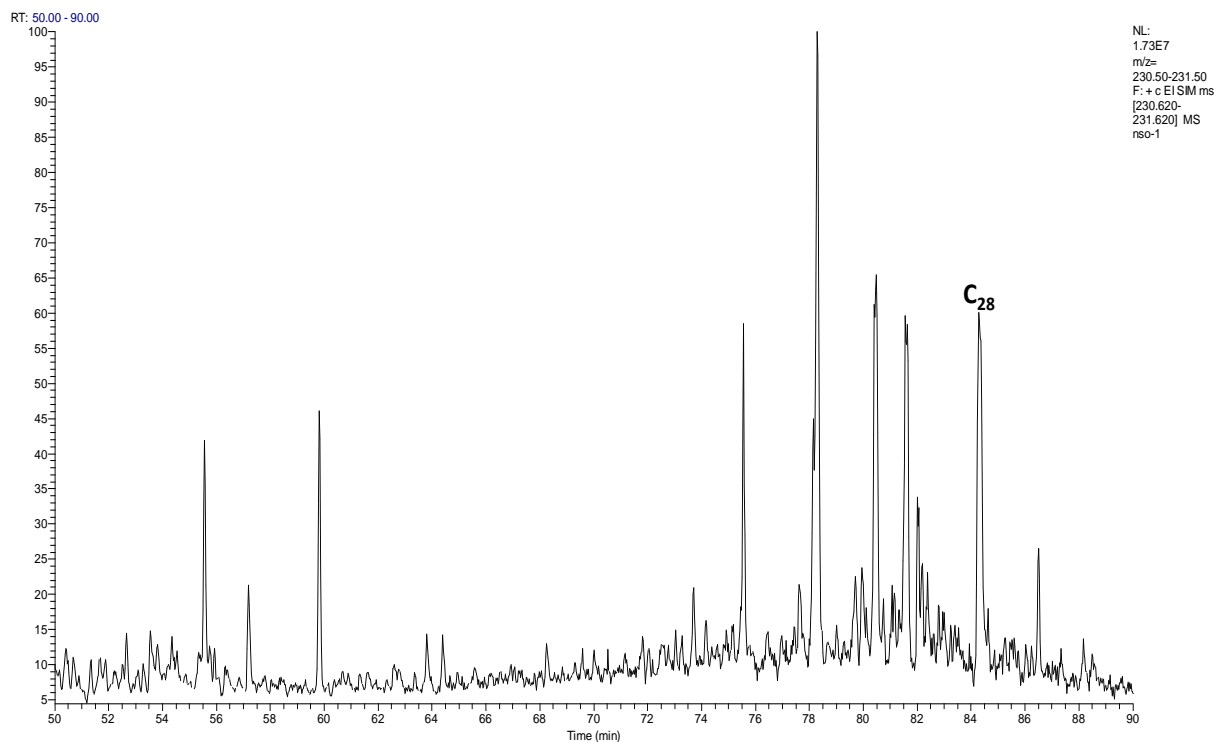


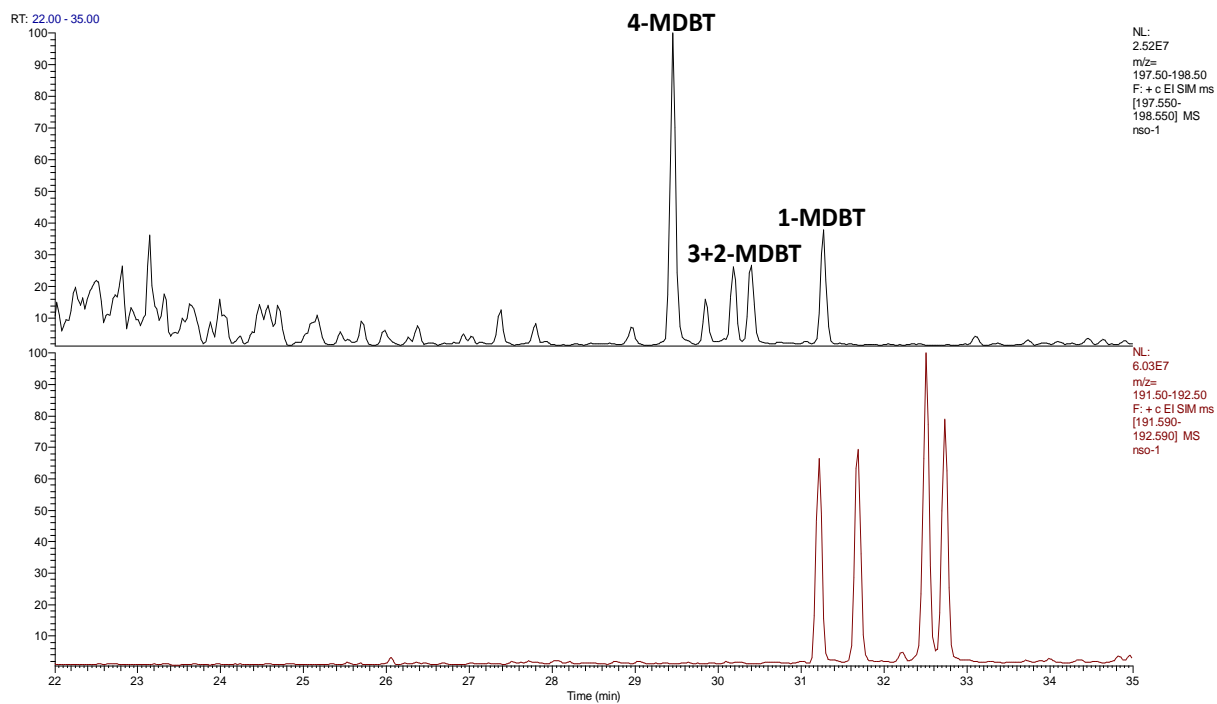
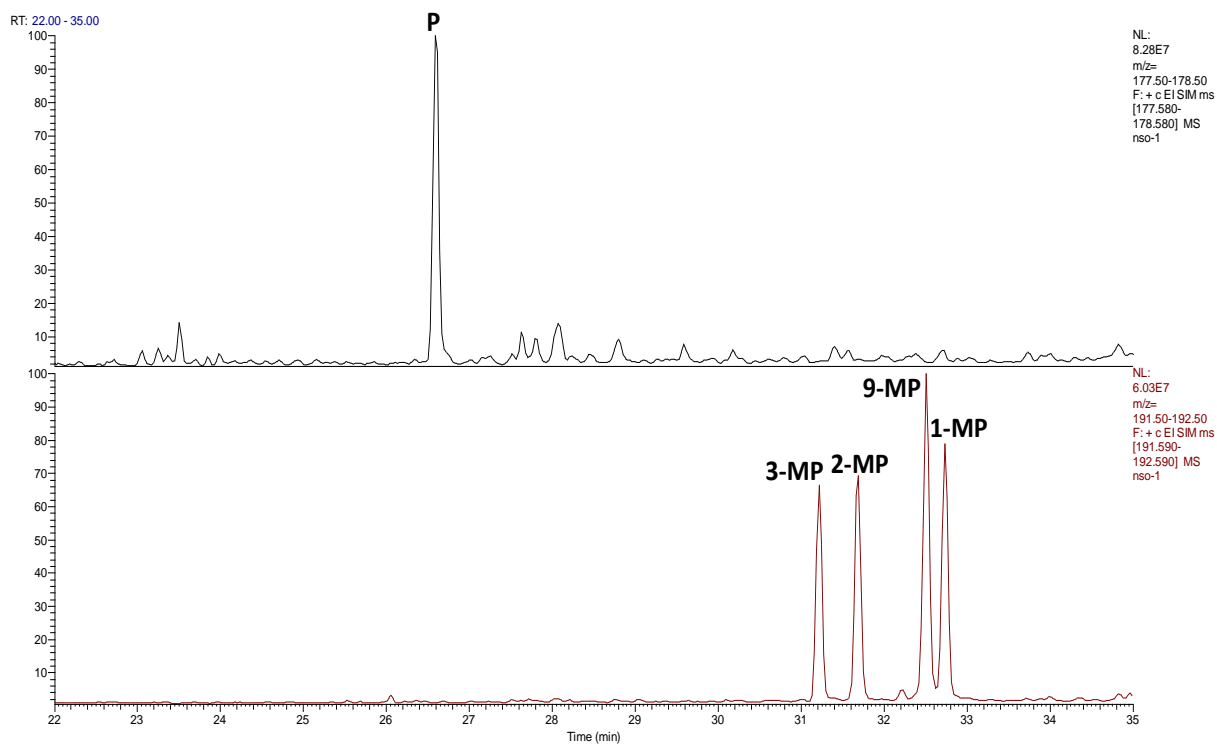


Appendix C (GC-MS Chromatograms)

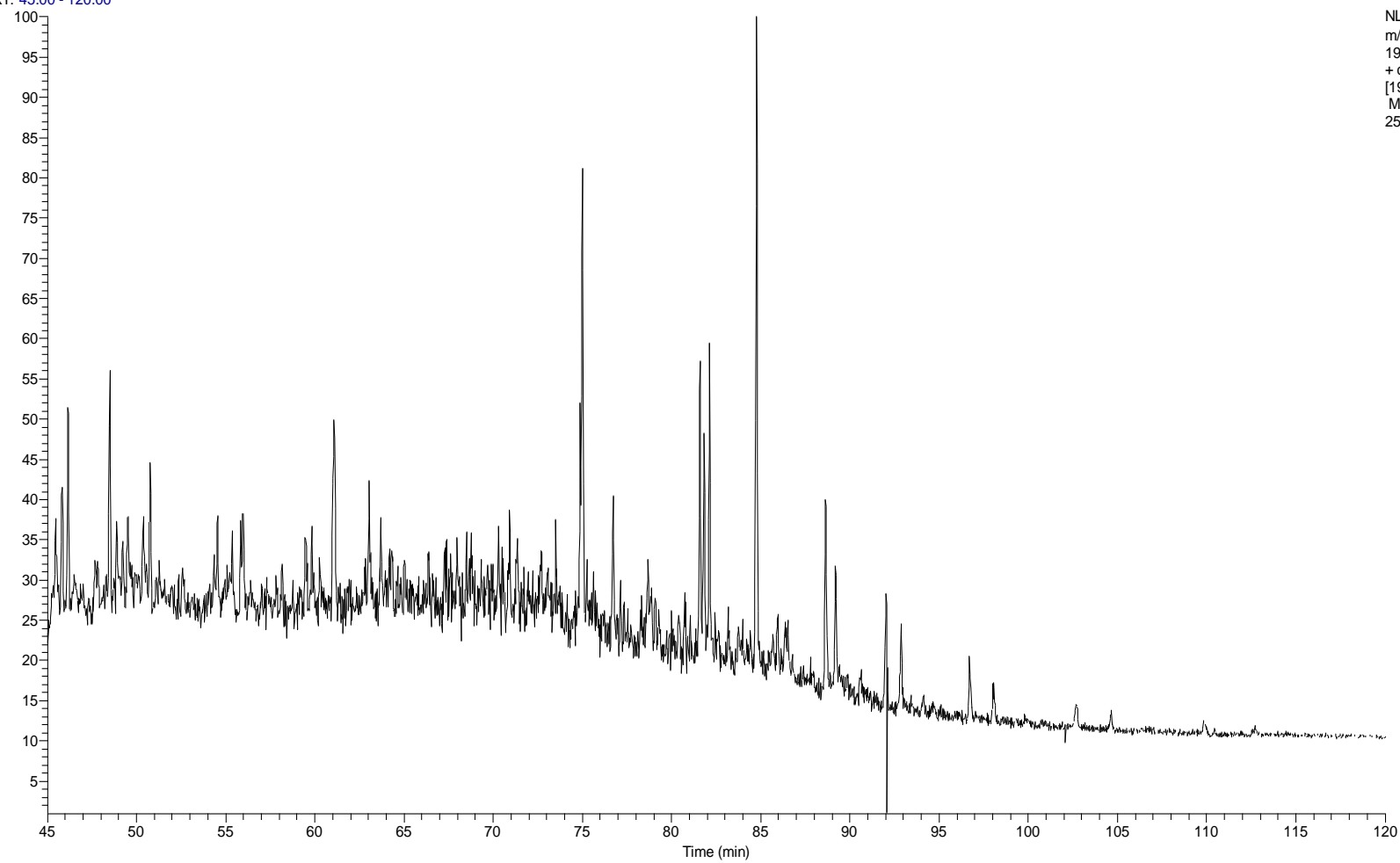




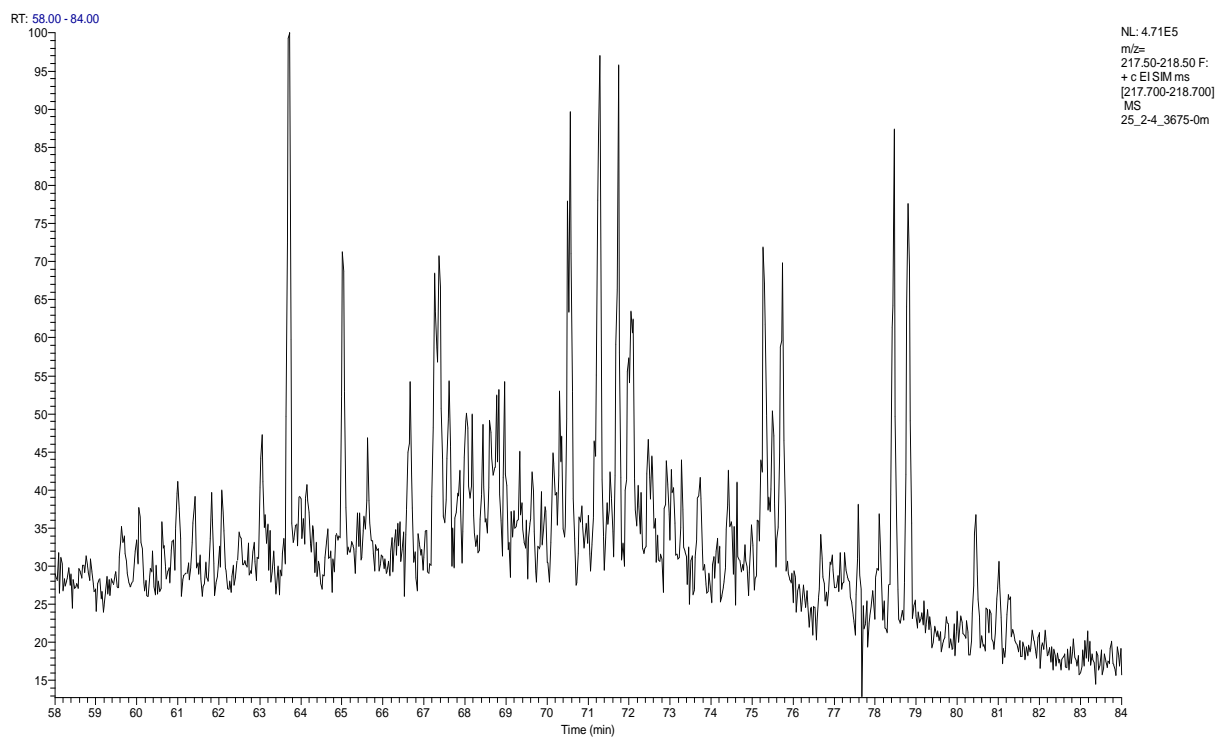
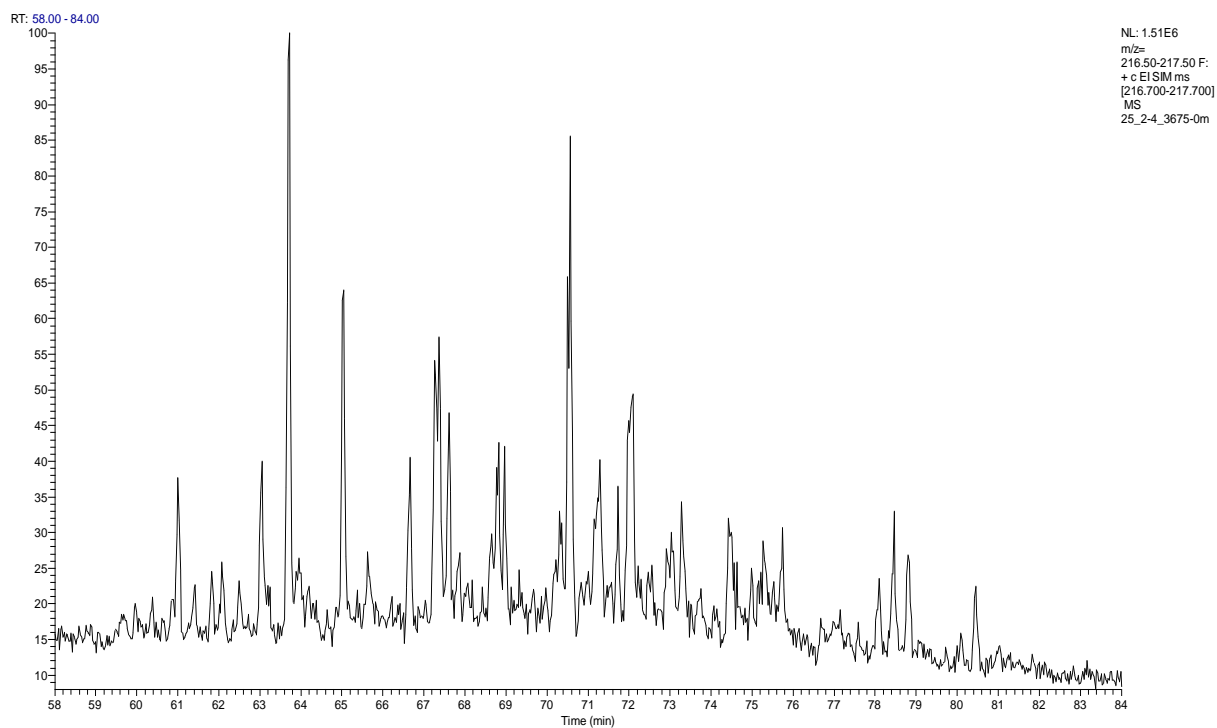


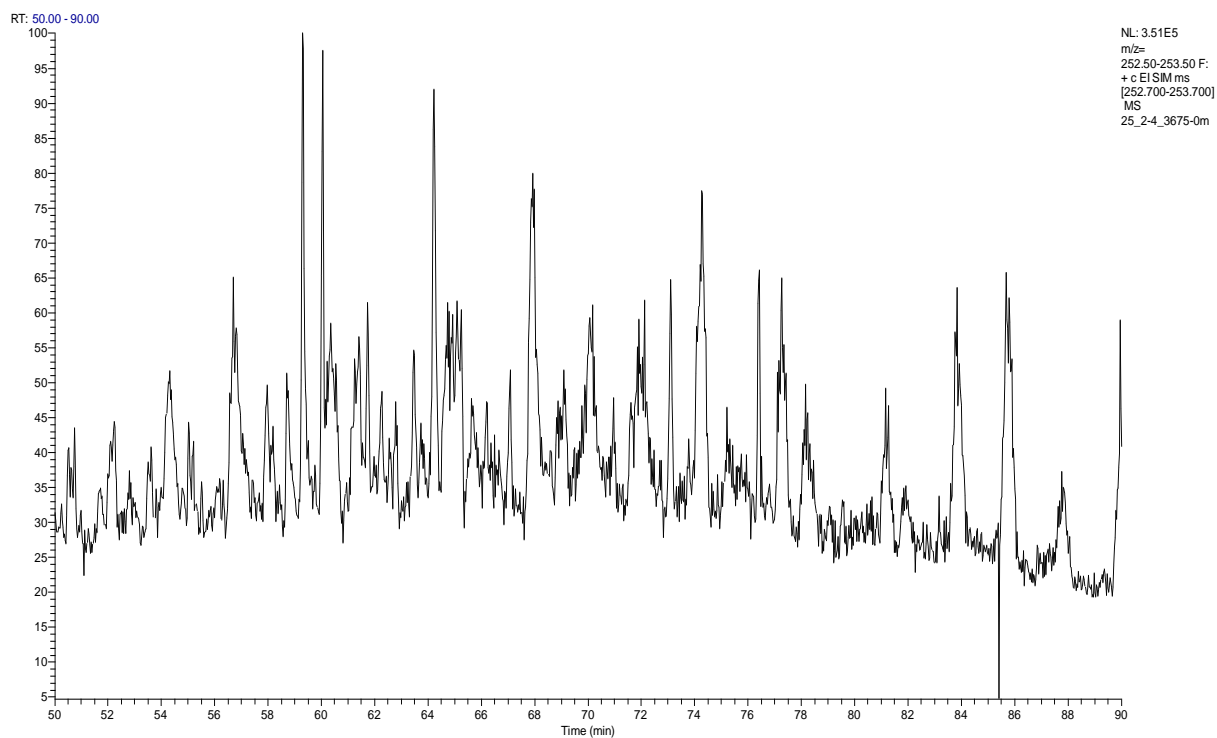
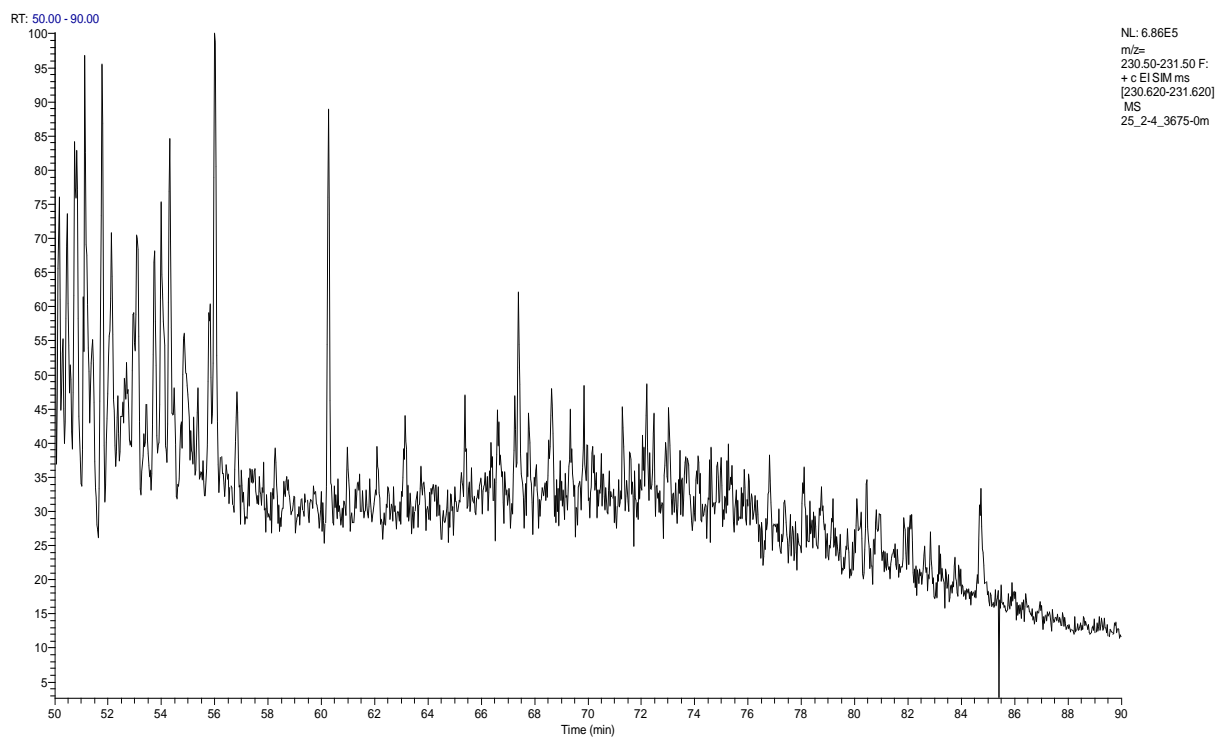


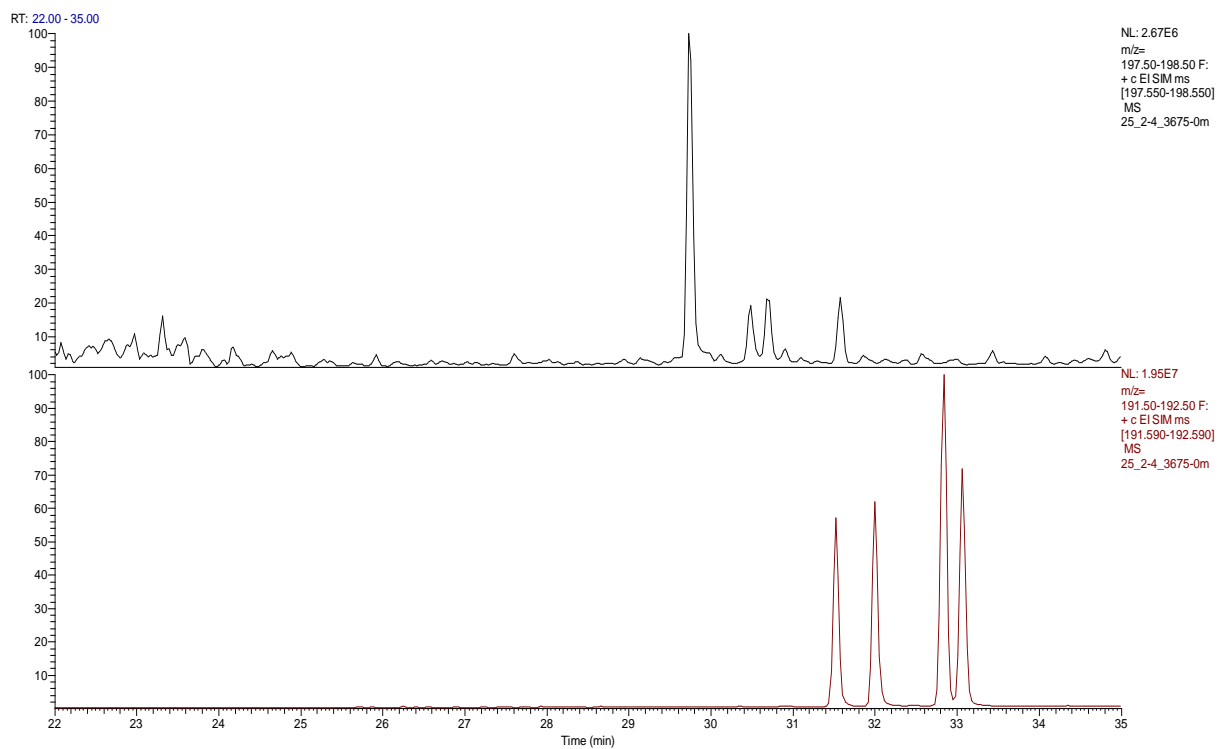
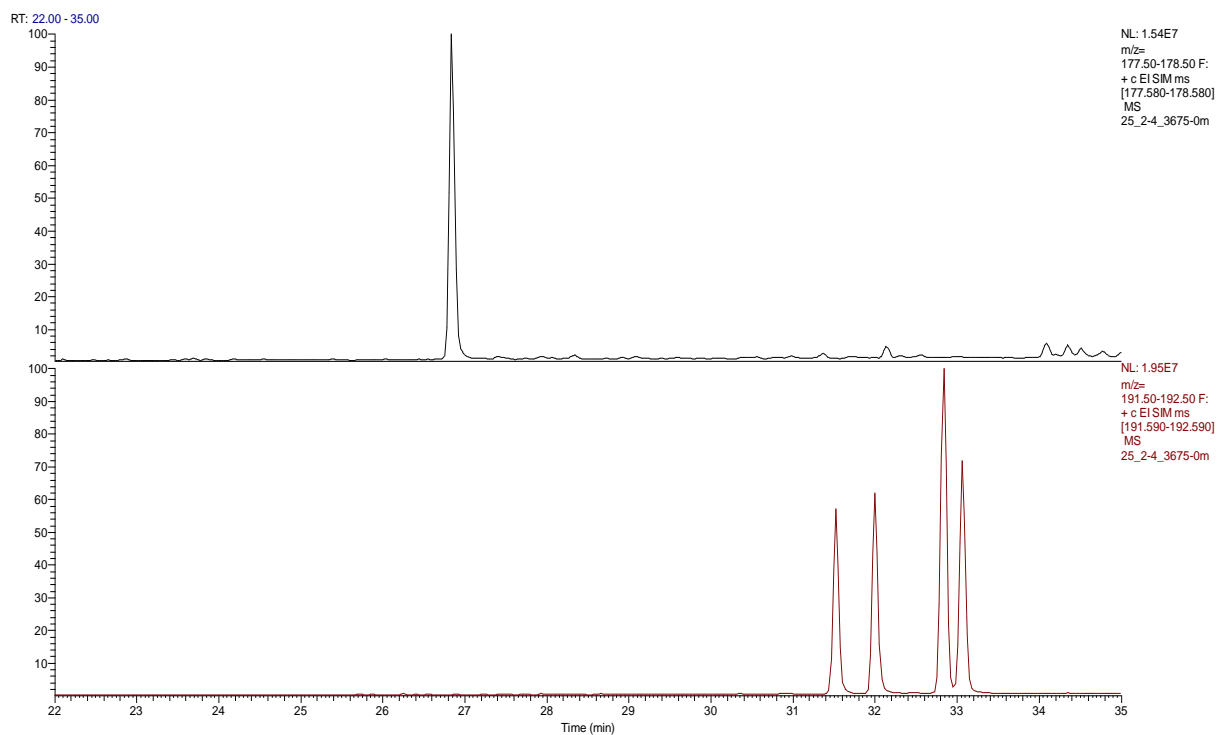
RT: 45.00 - 120.00



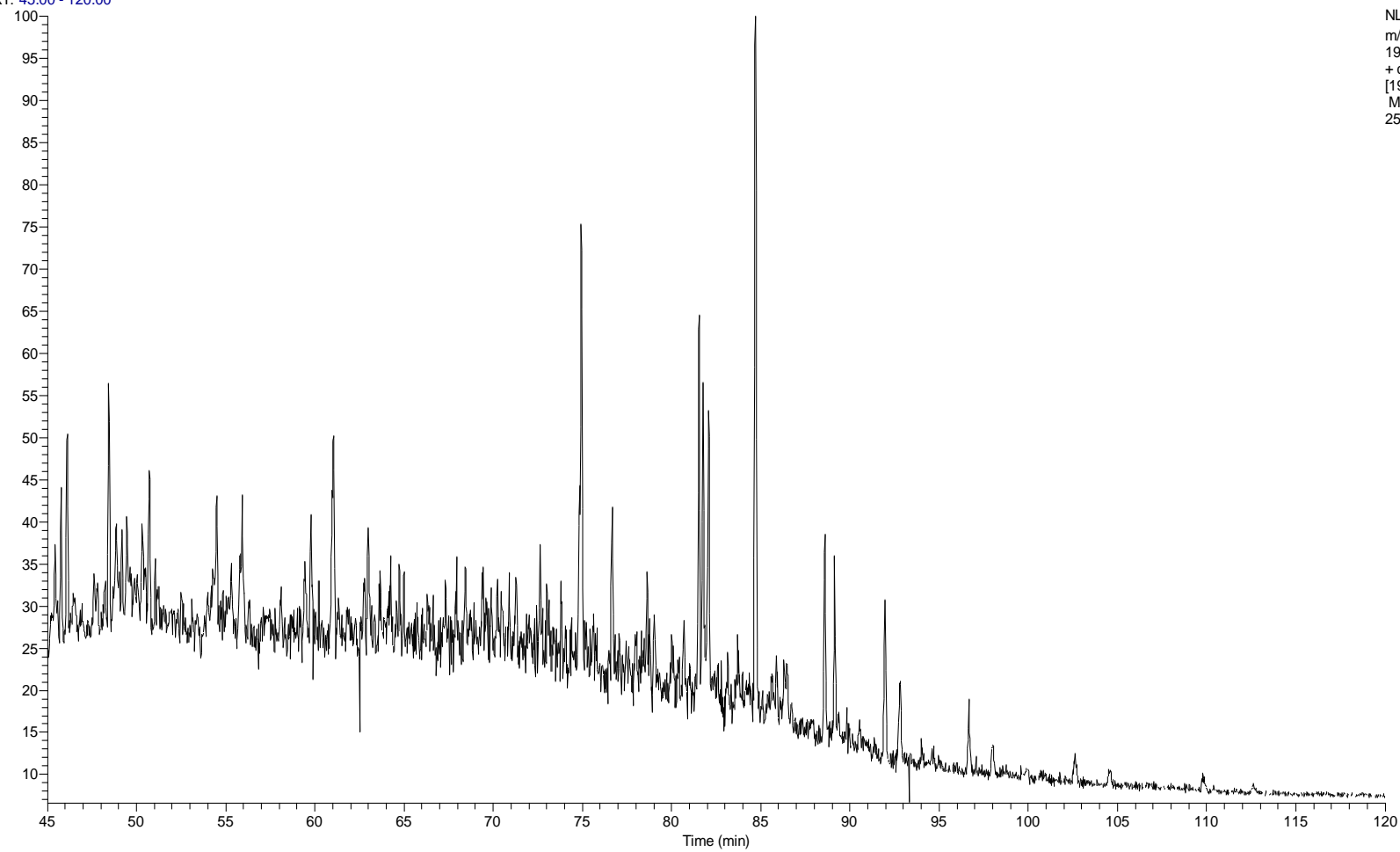
NL: 1.53E6
m/z=
190.50-191.50 F:
+ c EI SIM ms
[190.680-191.680]
MS
25_2-4_3675-0m



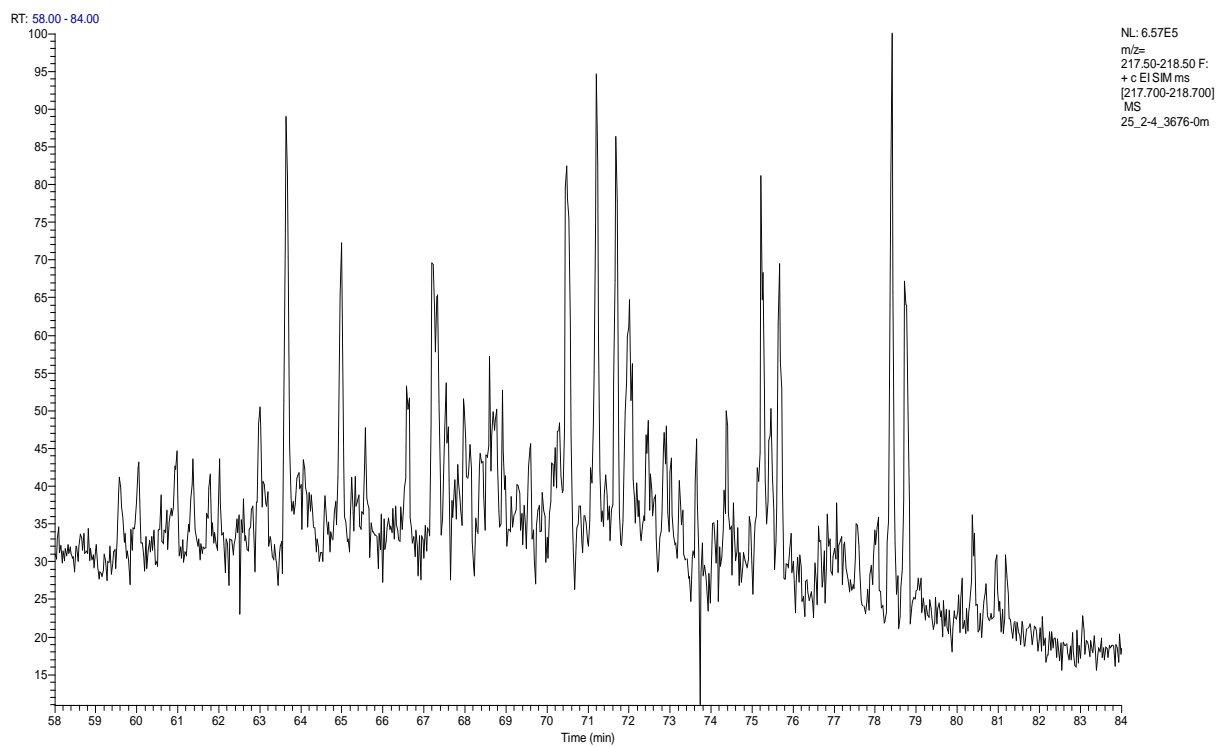
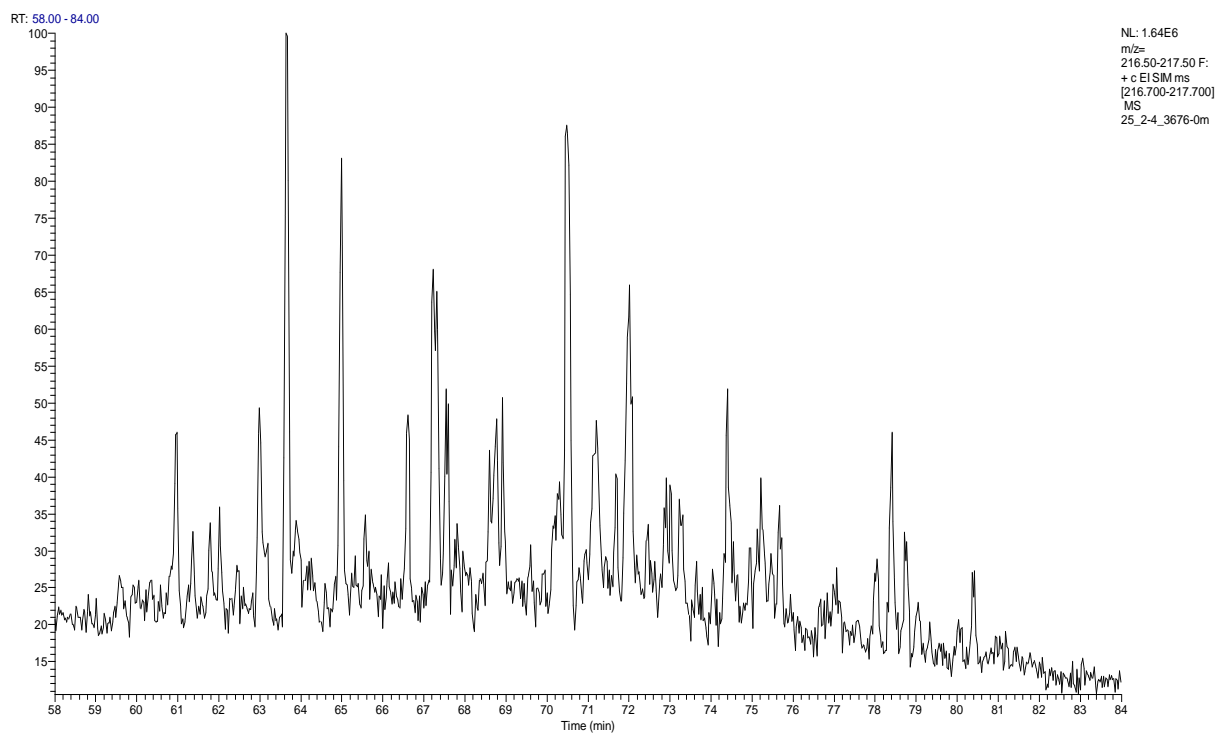


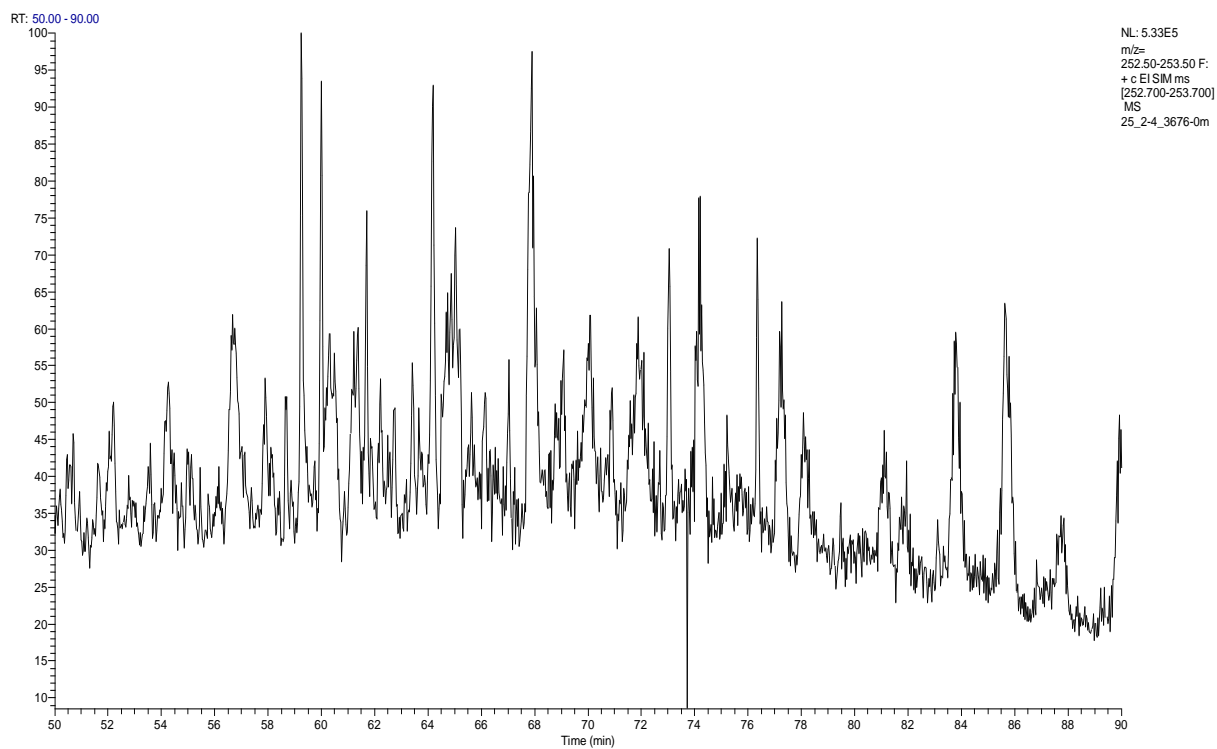
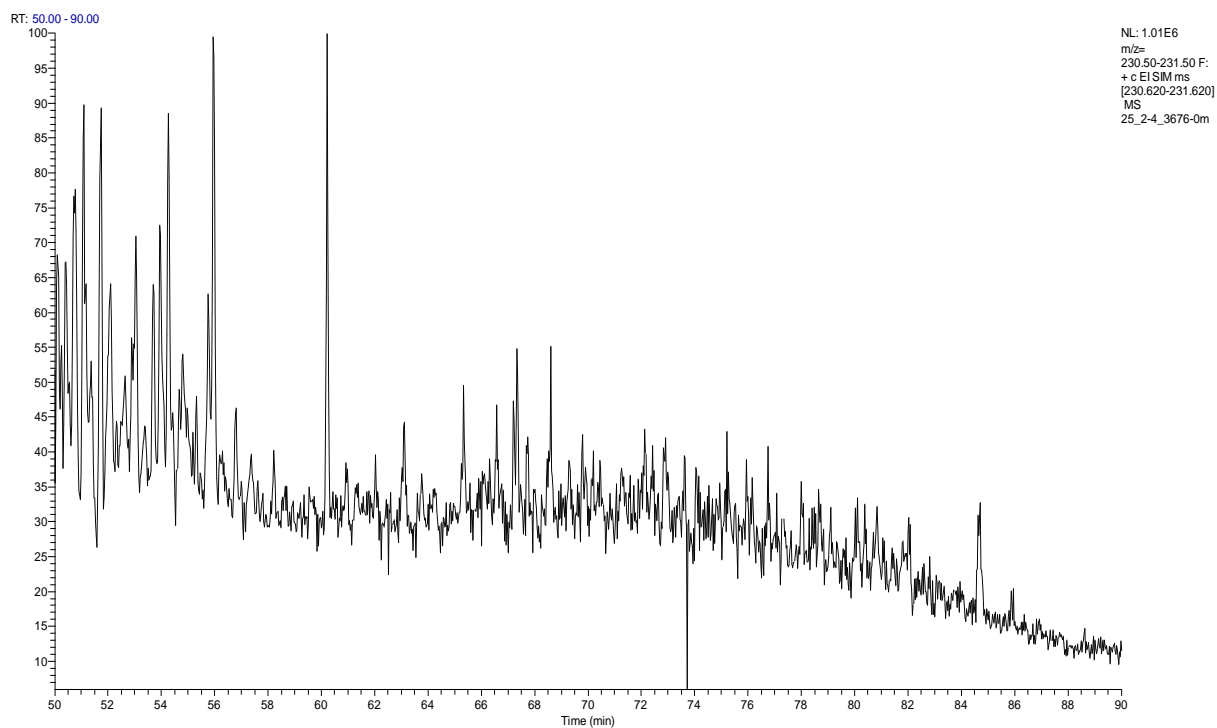


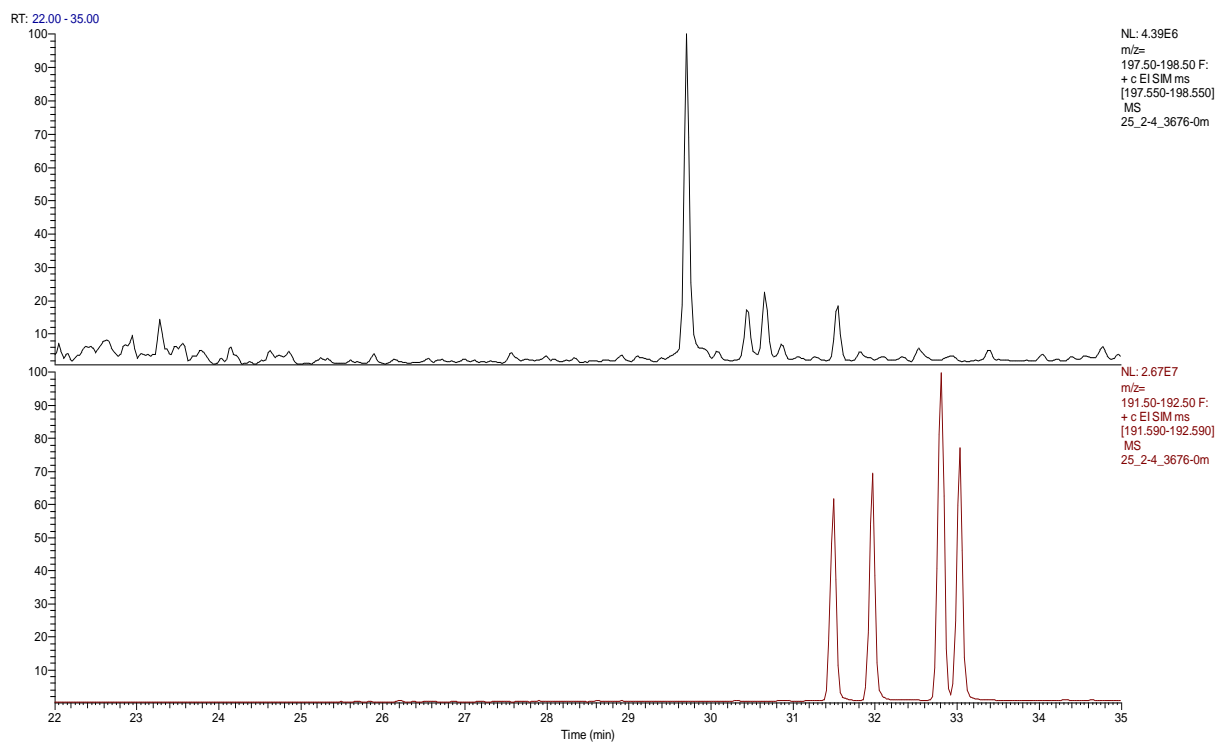
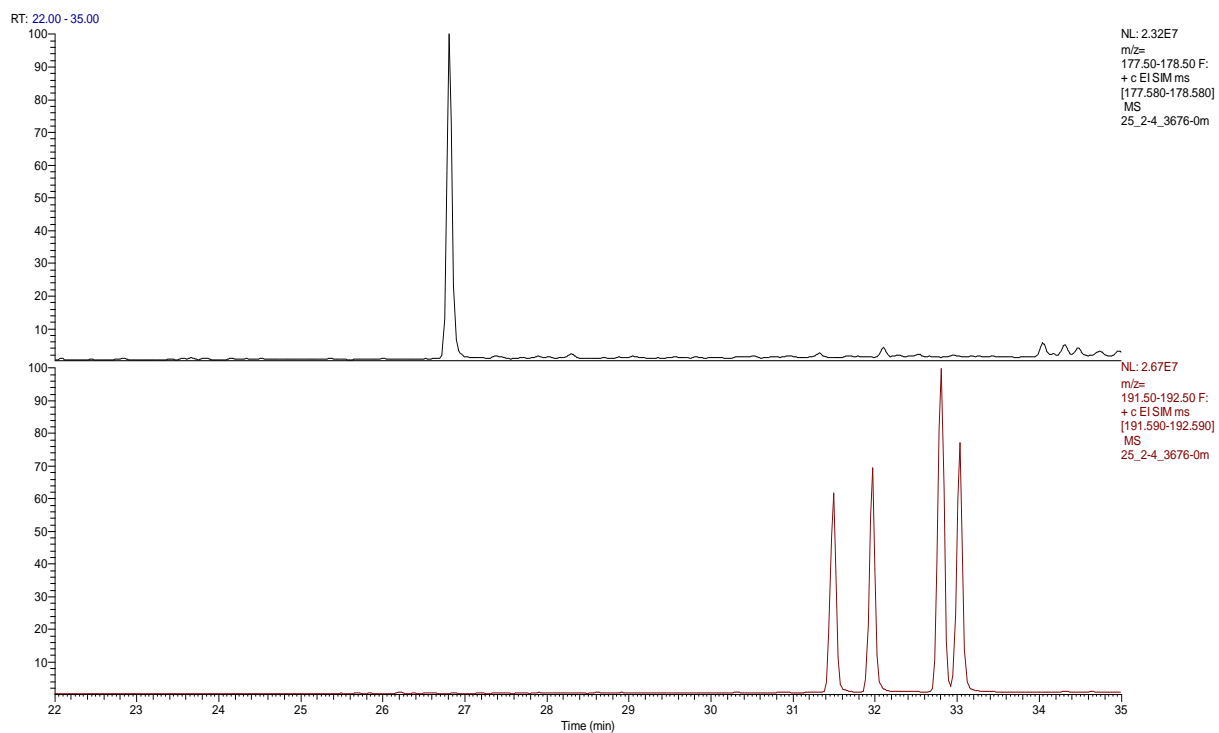
RT: 45.00 - 120.00



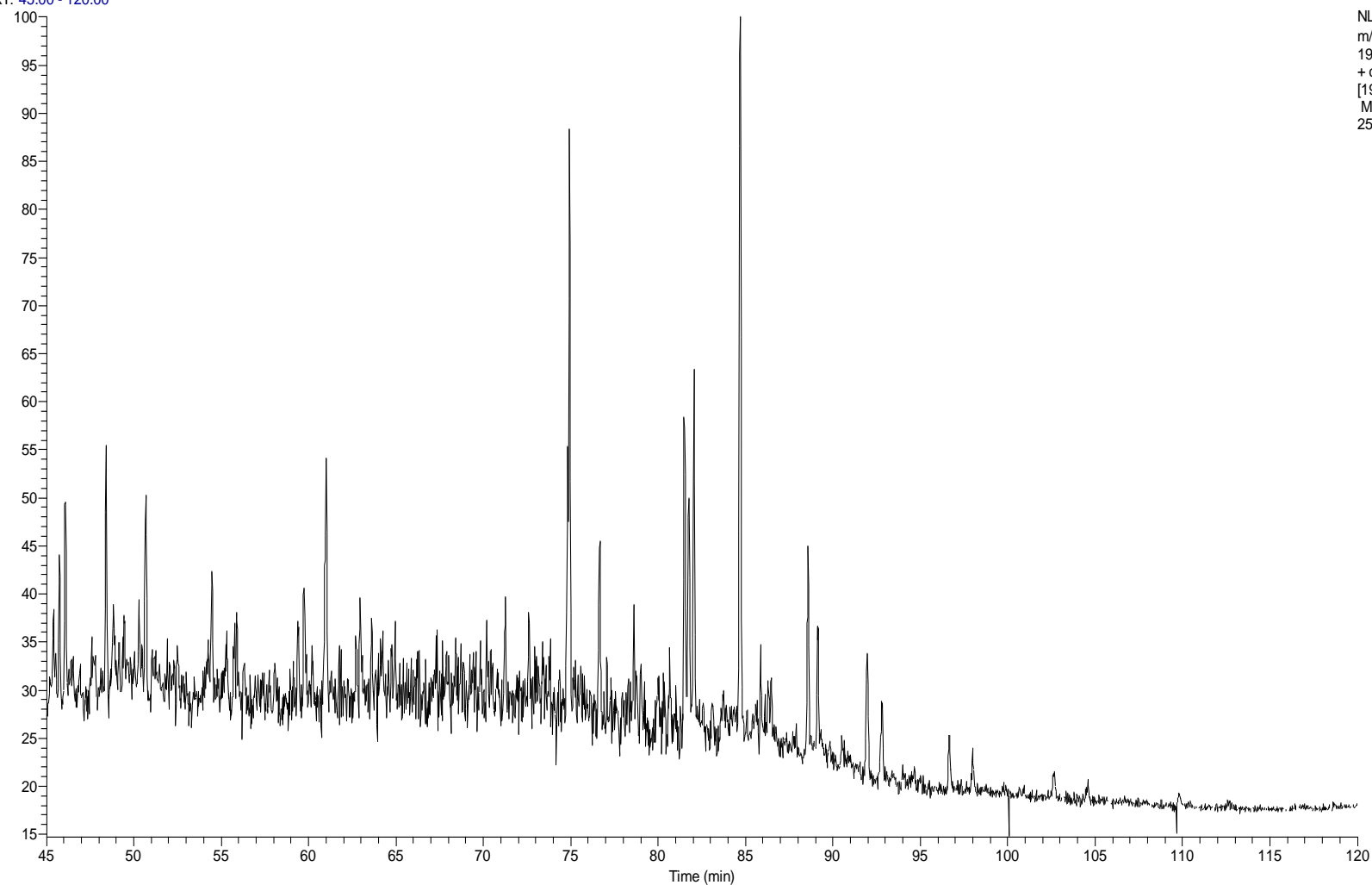
NL: 2.21E6
m/z=
190.50-191.50 F:
+ c EISIM ms
[190.680-191.680]
MS
25_2-4_3676-0m



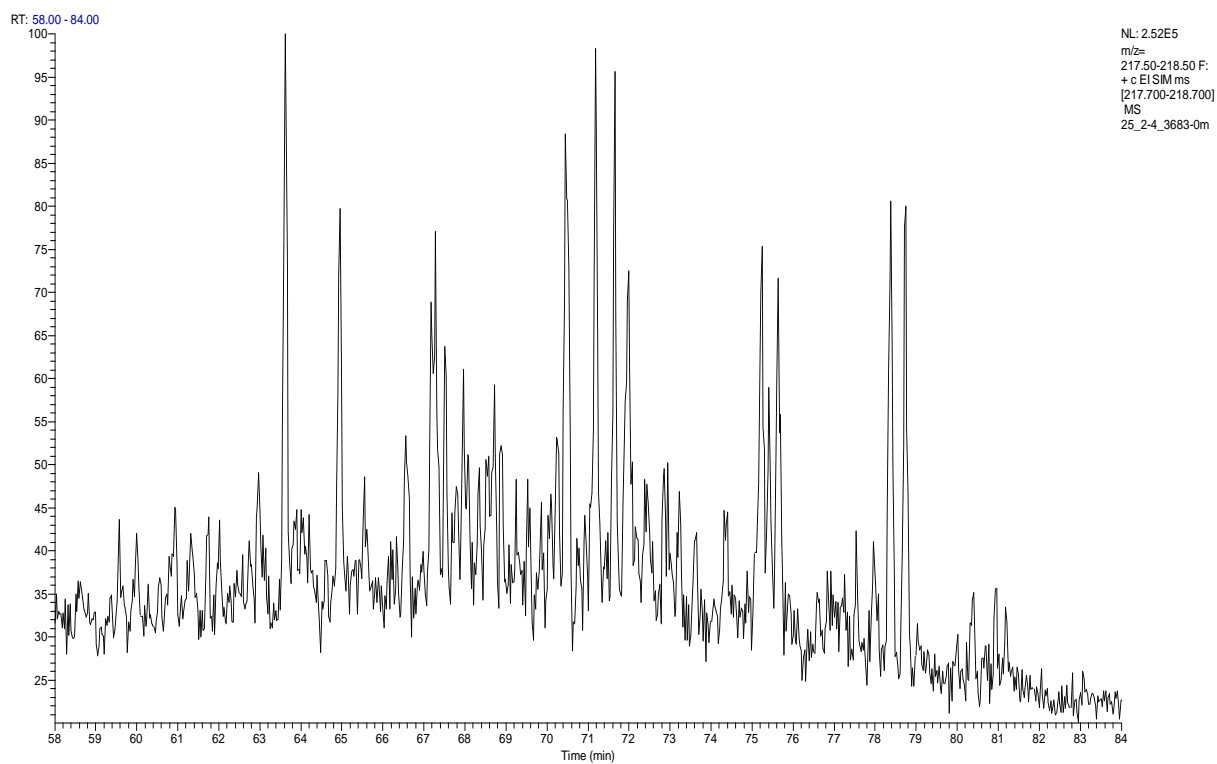
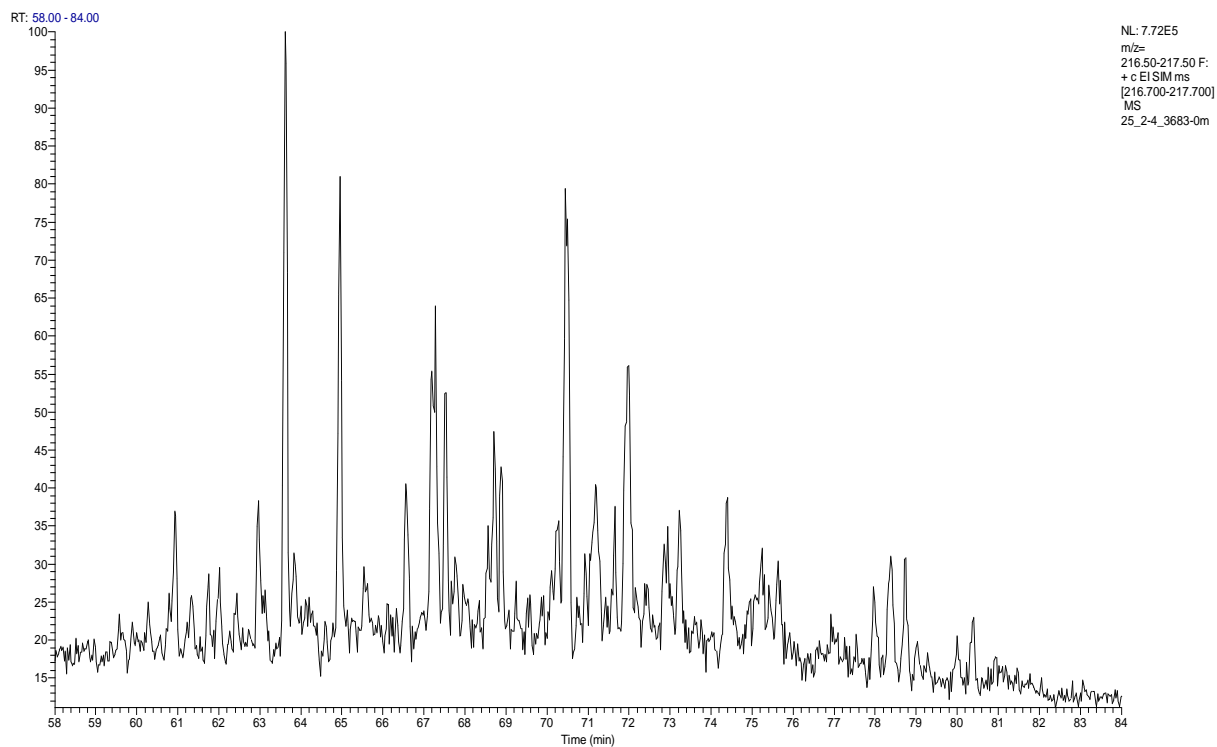


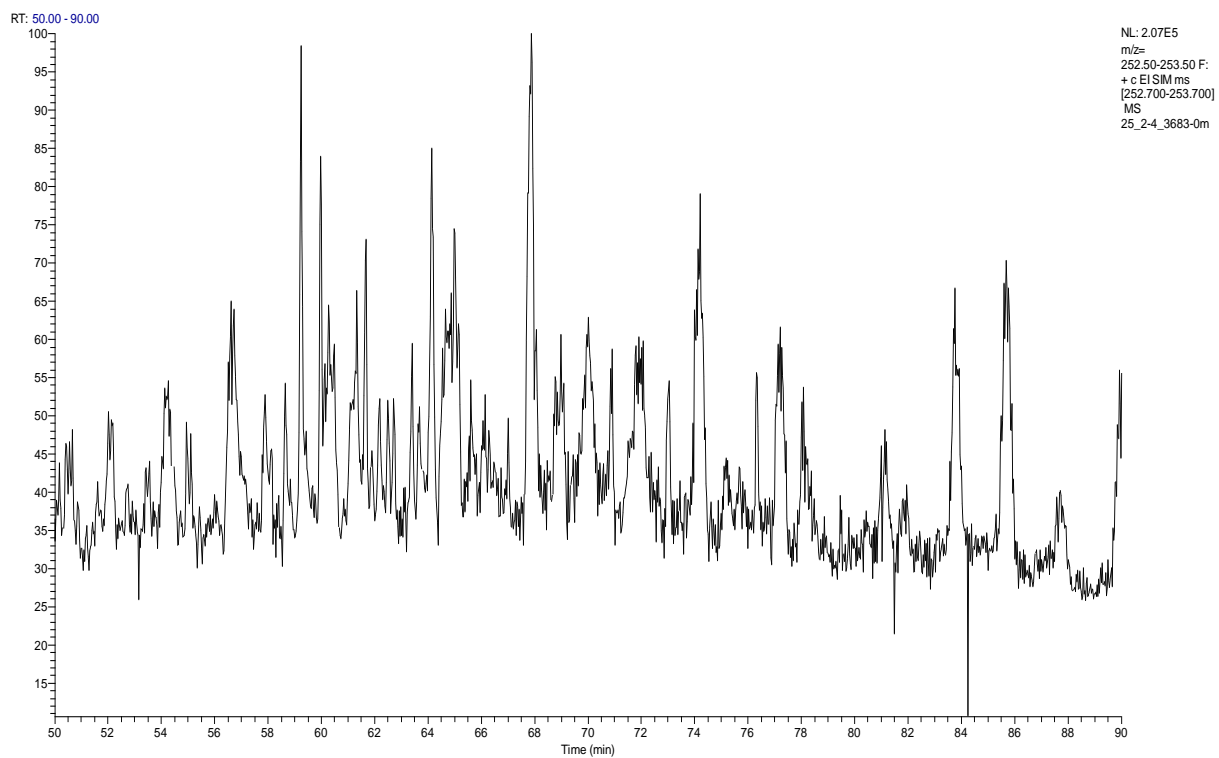
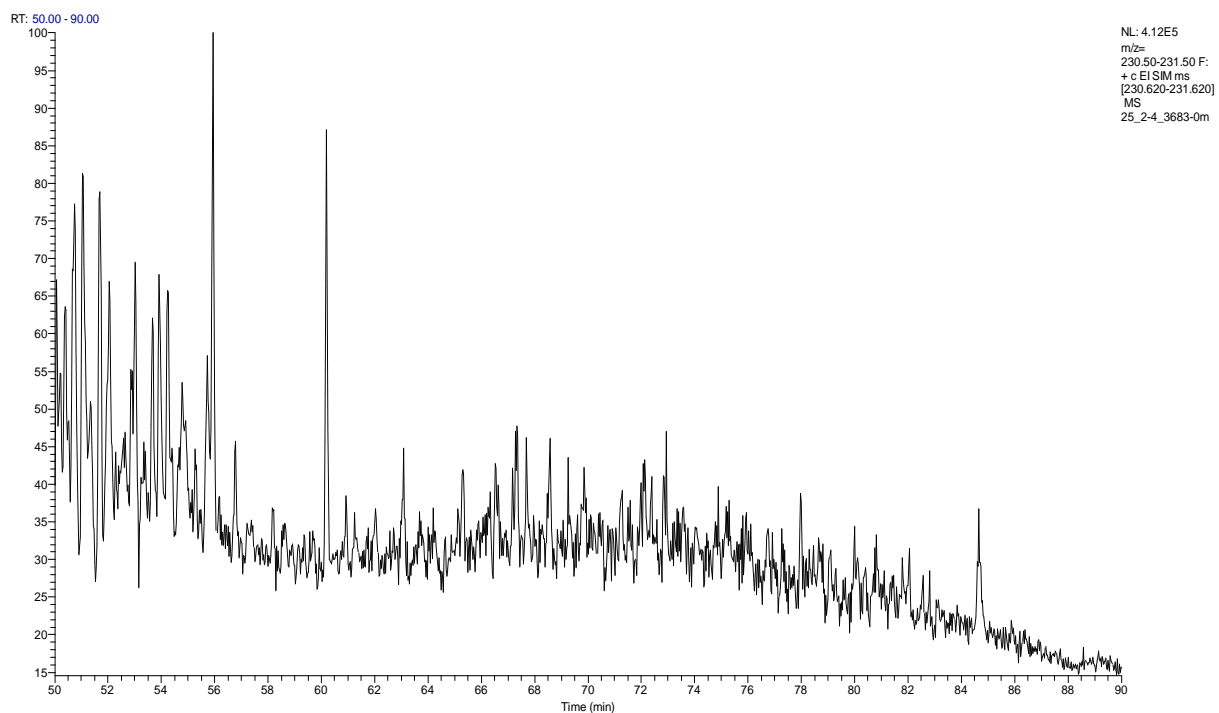


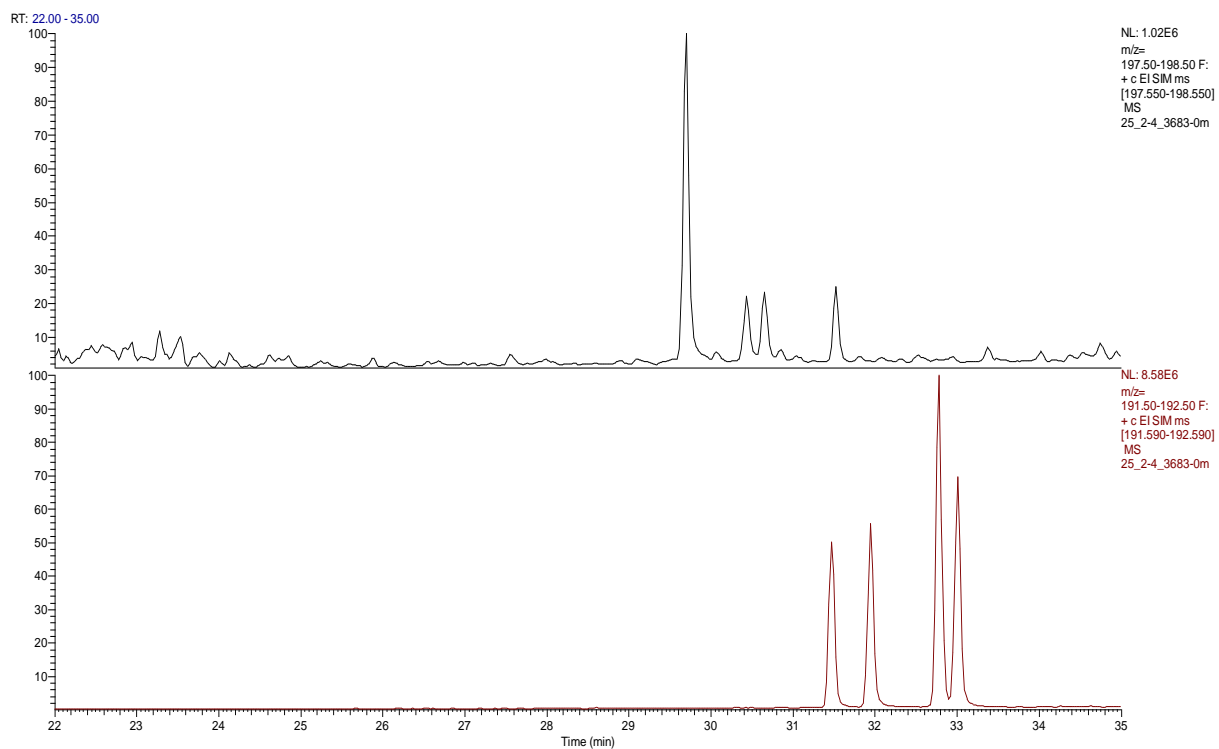
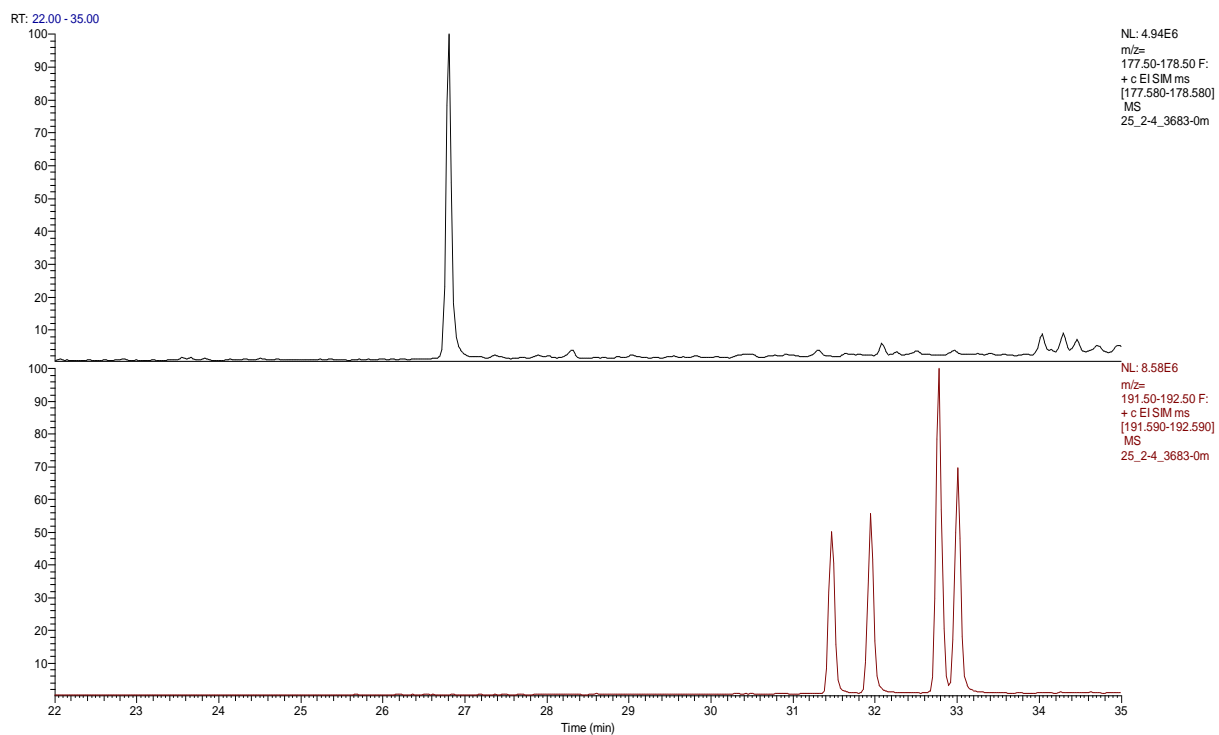
RT: 45.00 - 120.00



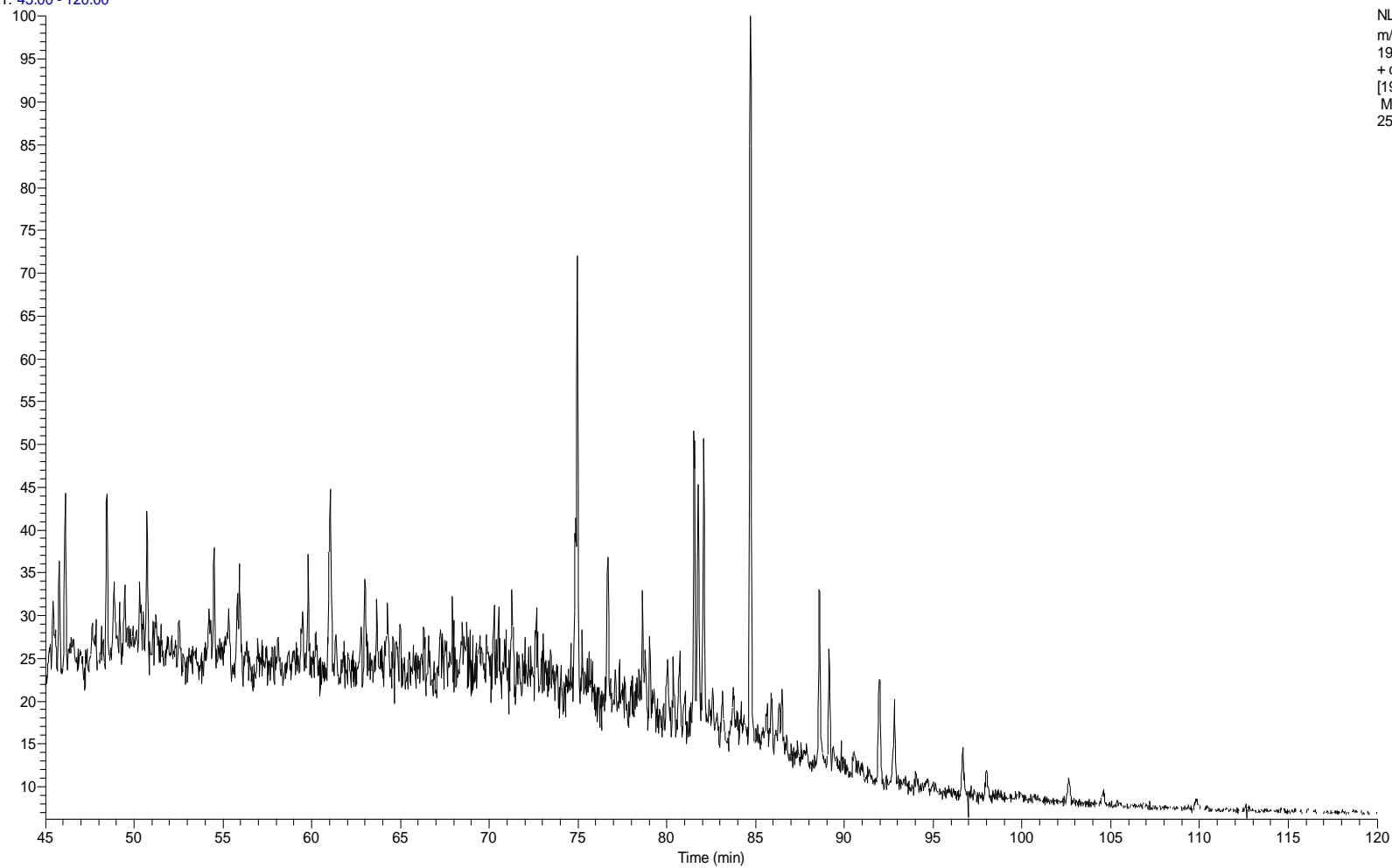
NL: 8.83E5
m/z=
190.50-191.50 F:
+ c EI SIM ms
[190.680-191.680]
MS
25_2-4_3683-0m



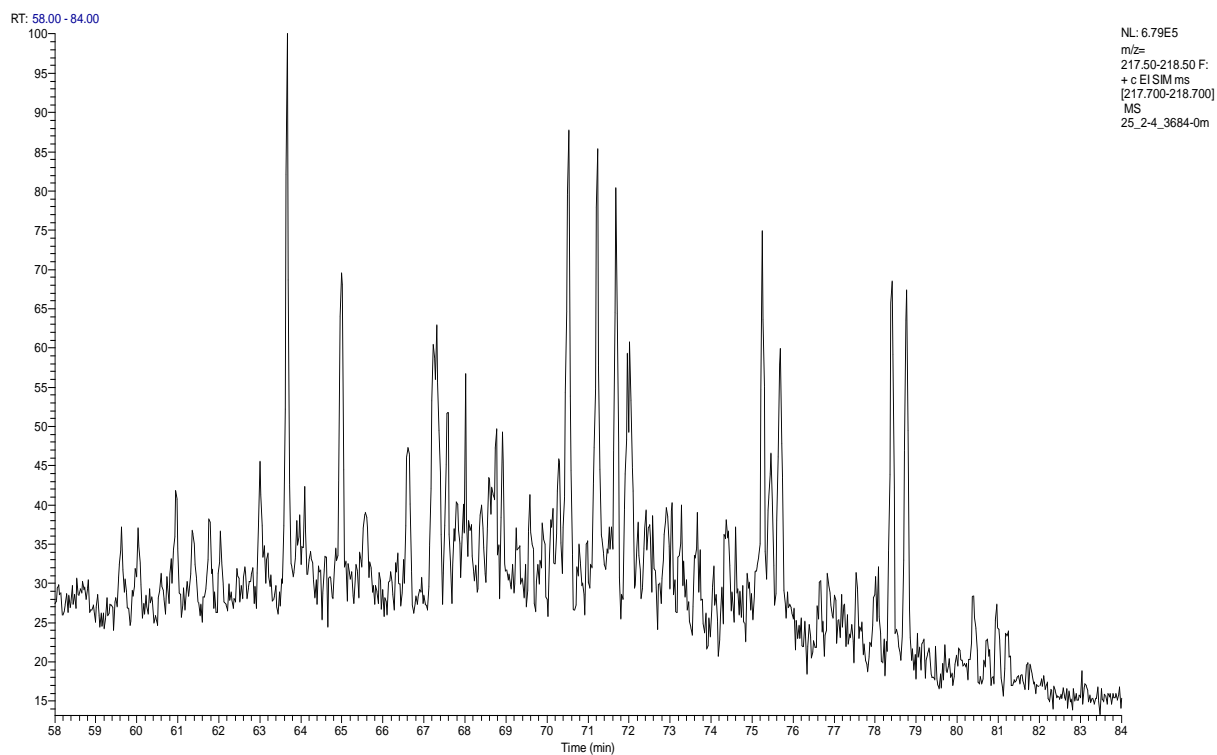
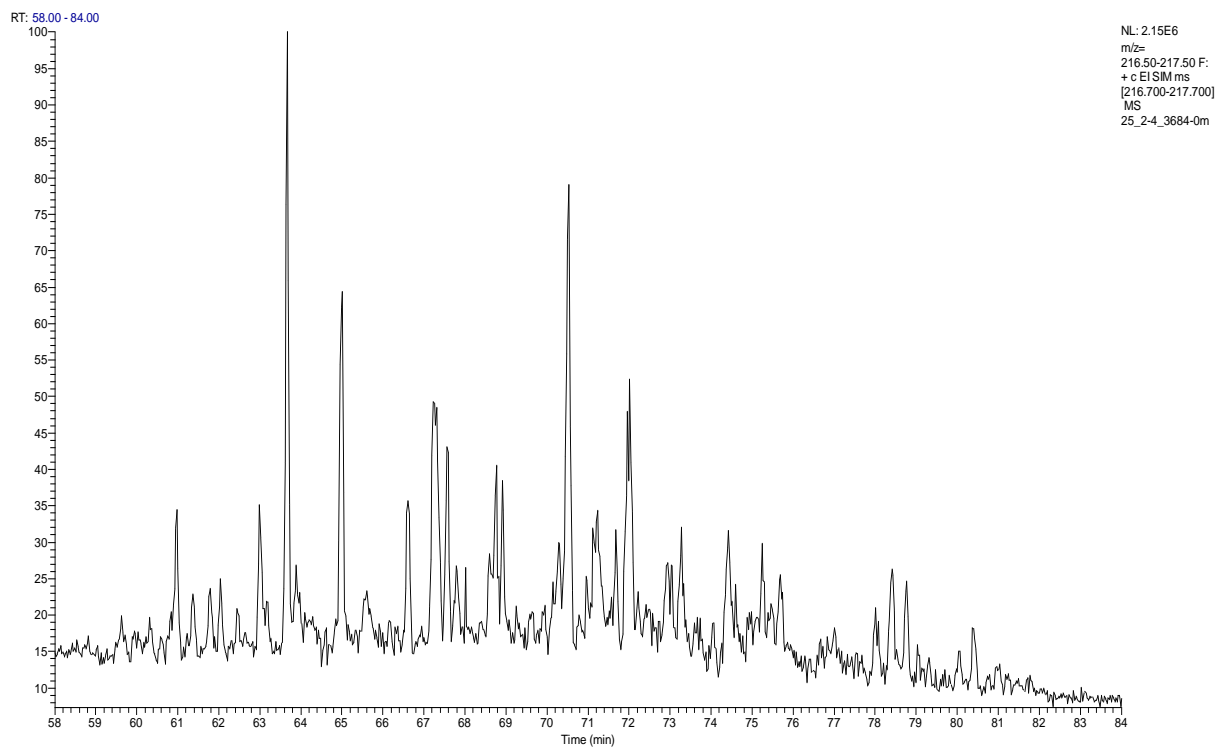


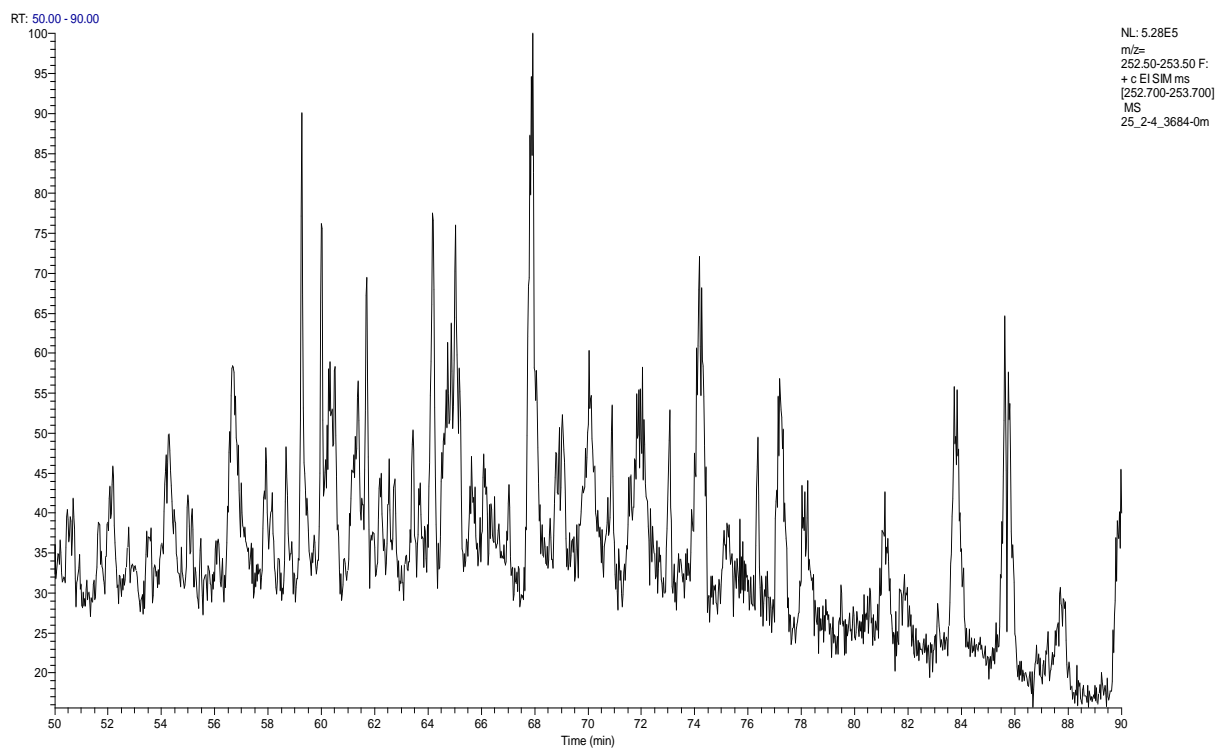
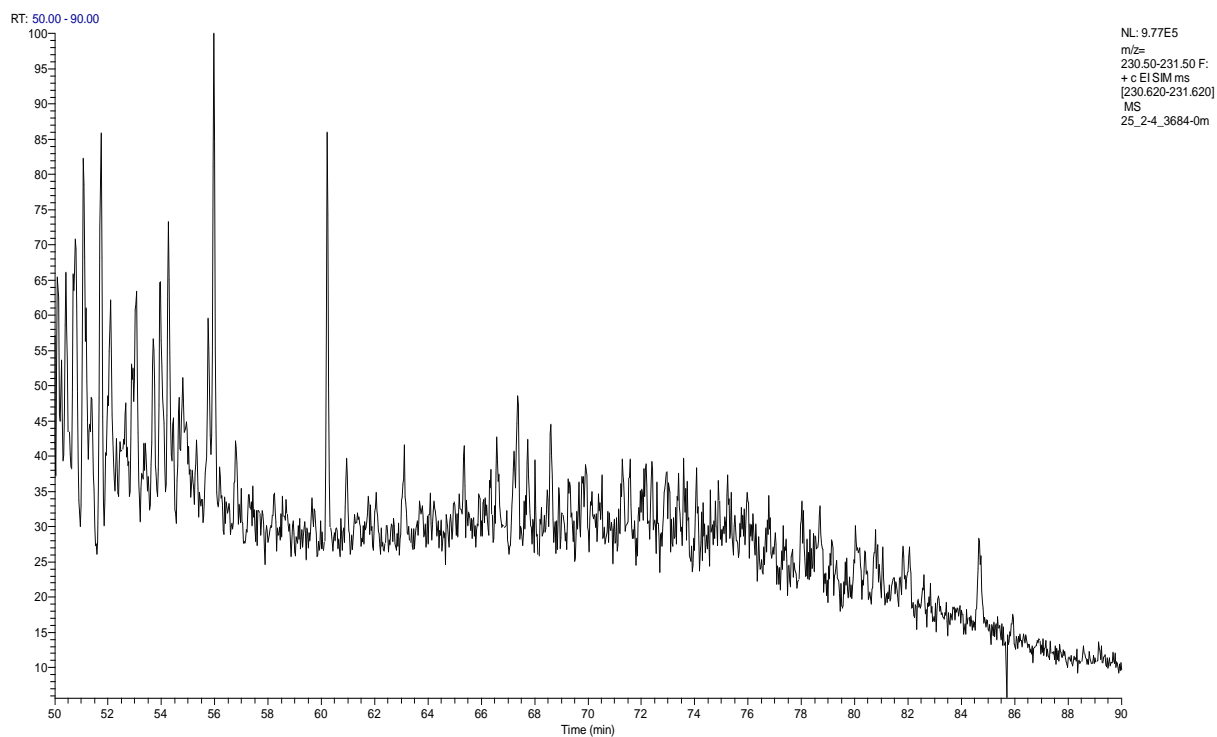


RT: 45.00 - 120.00

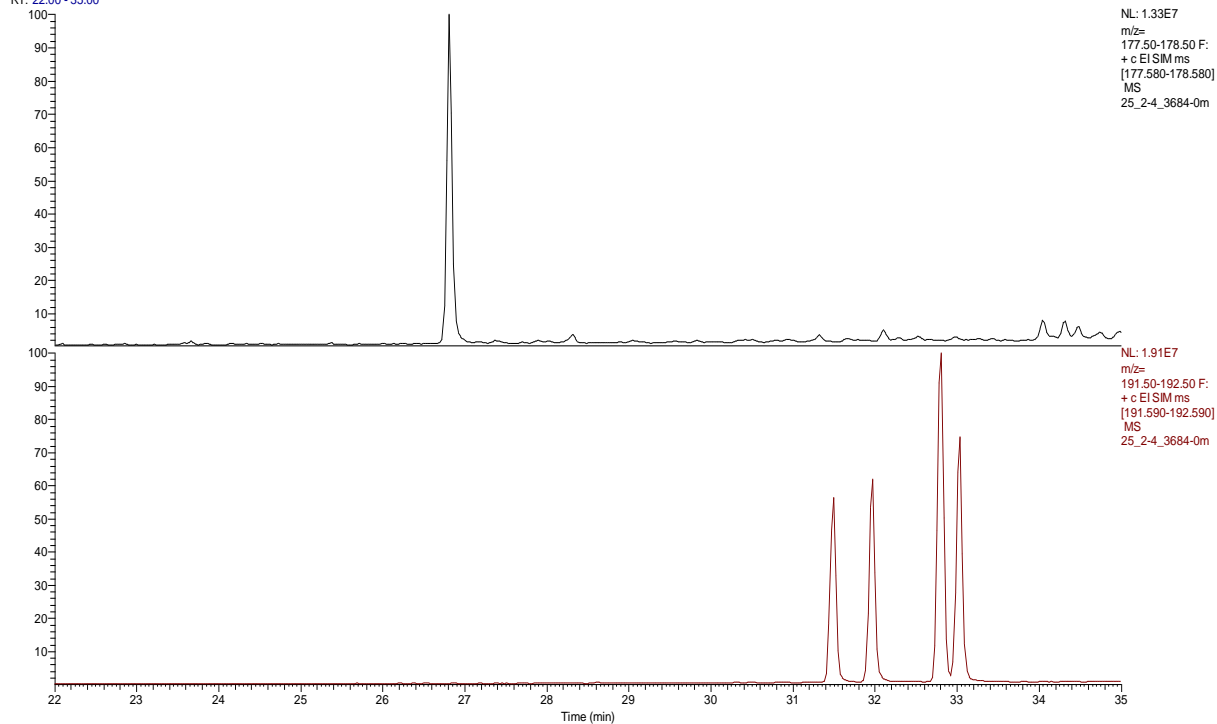


NL: 2.34E6
m/z=
190.50-191.50 F:
+ c EISIM ms
[190.680-191.680]
MS
25_2-4_3684-0m

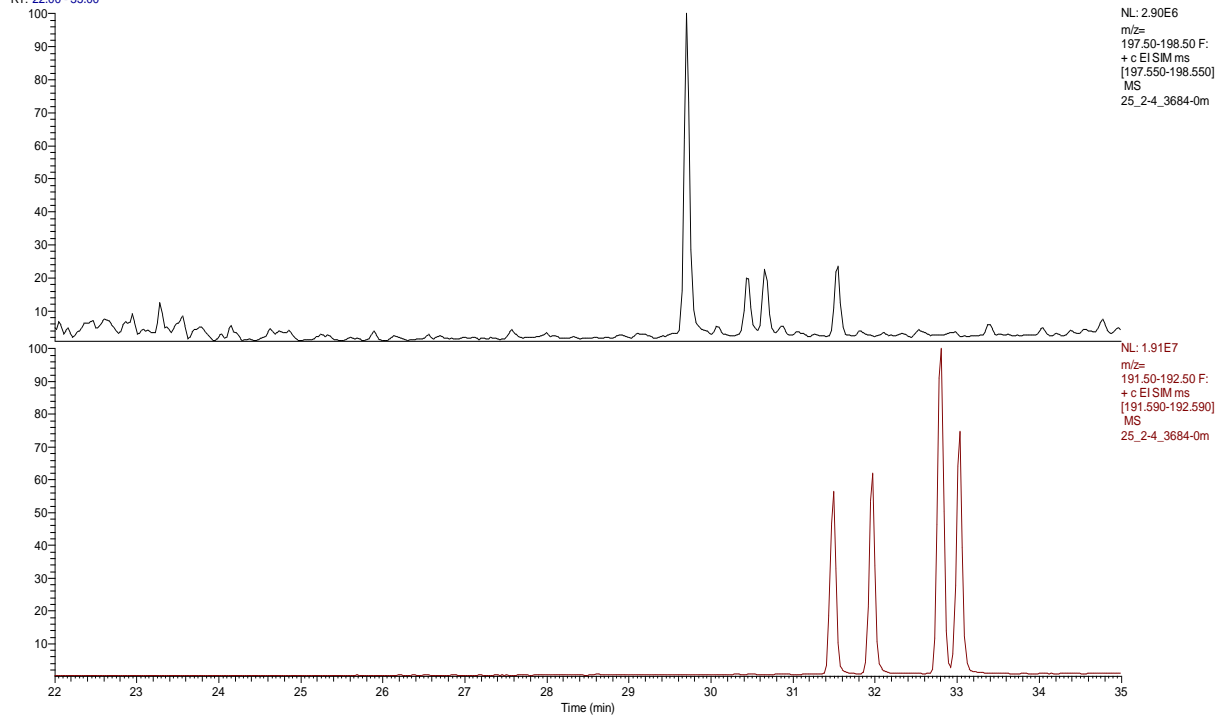




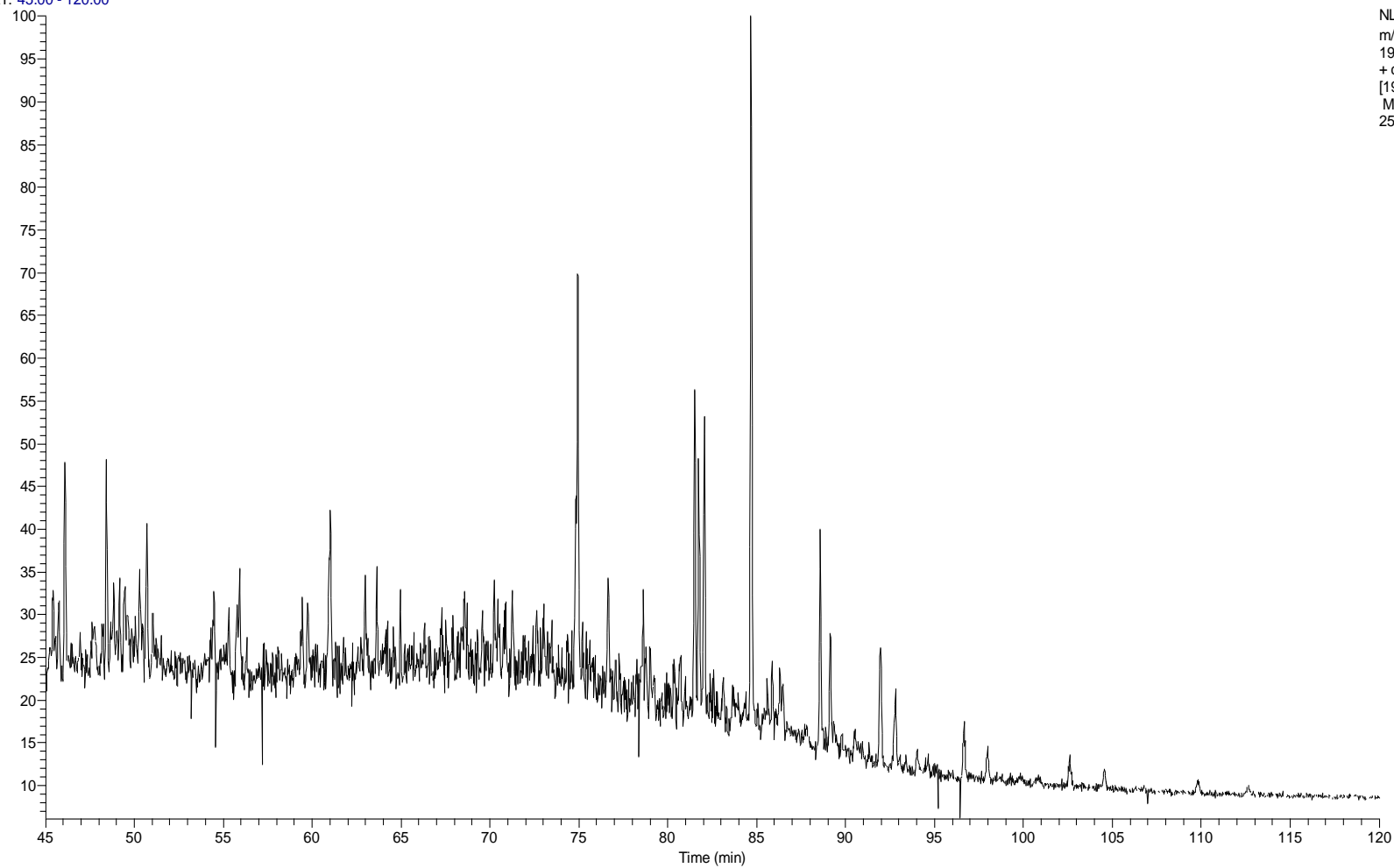
RT: 22.00 - 35.00



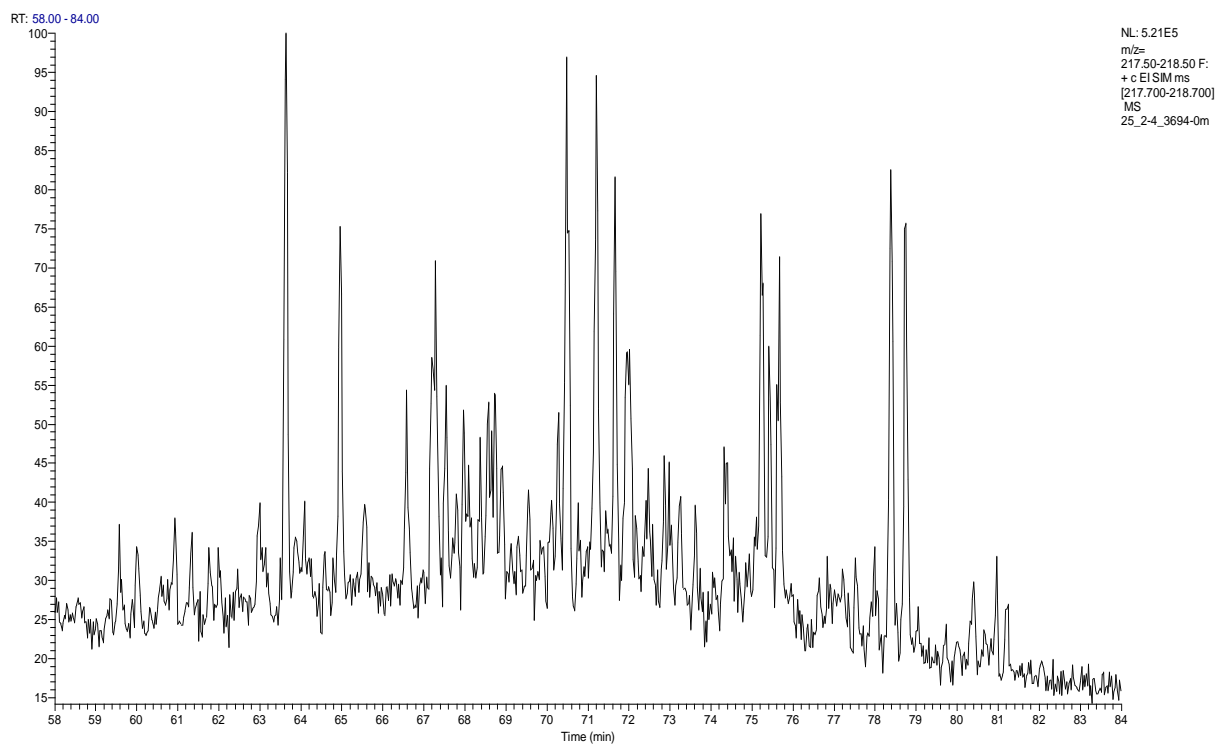
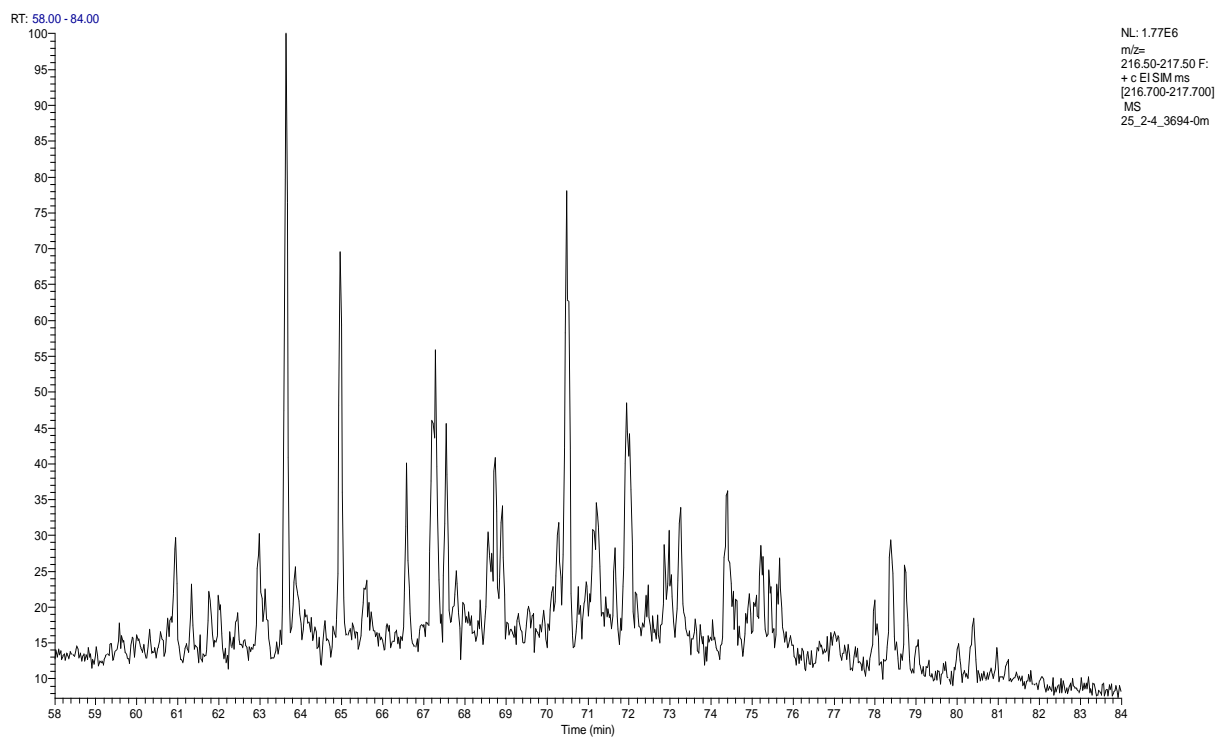
RT: 22.00 - 35.00

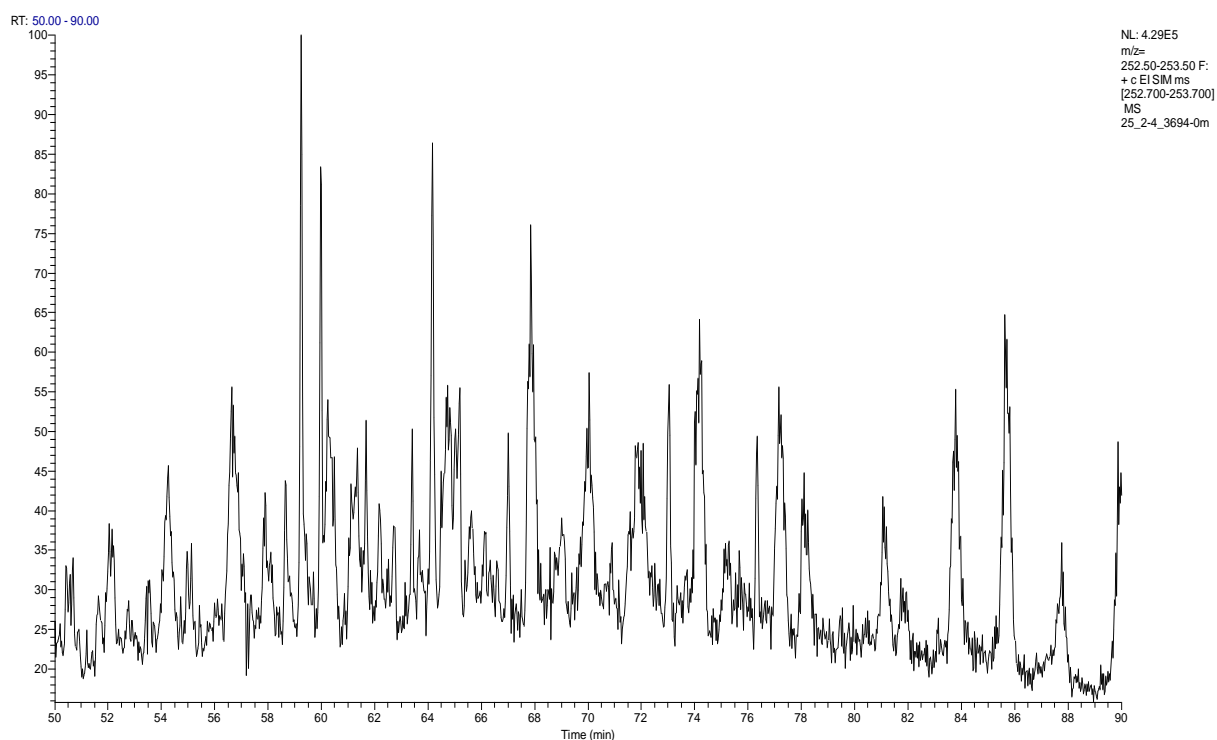
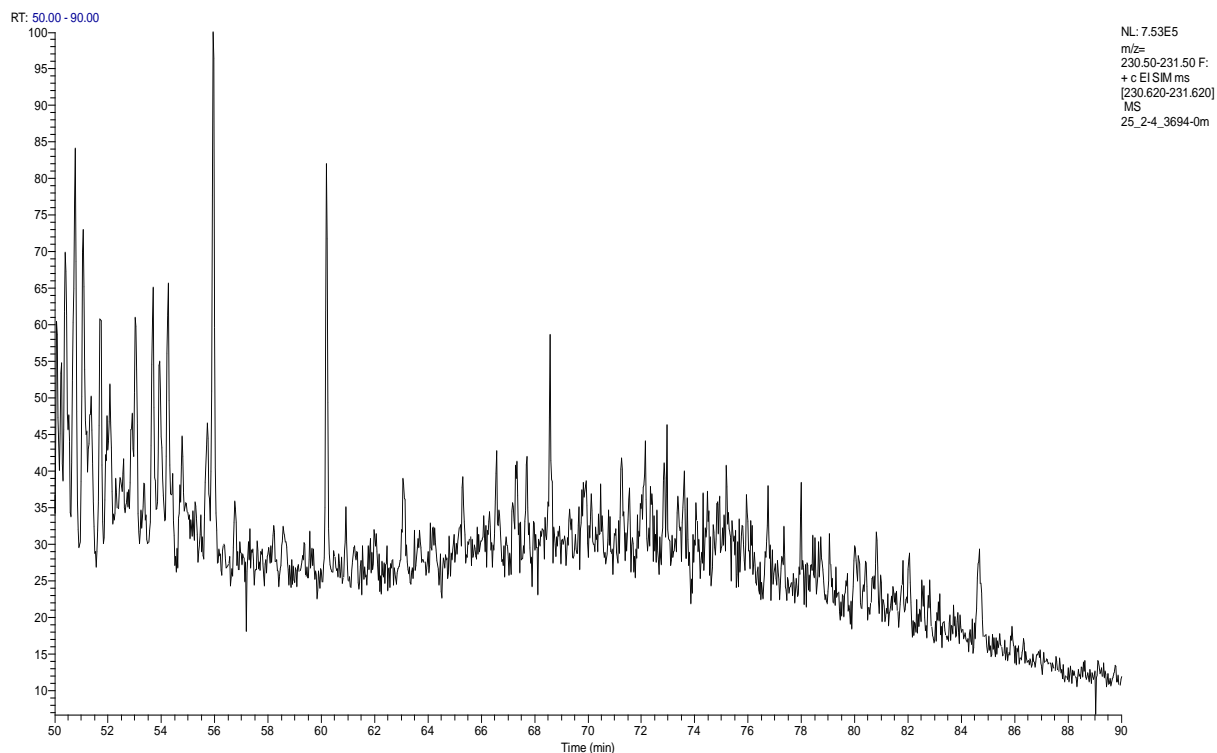


RT: 45.00 - 120.00

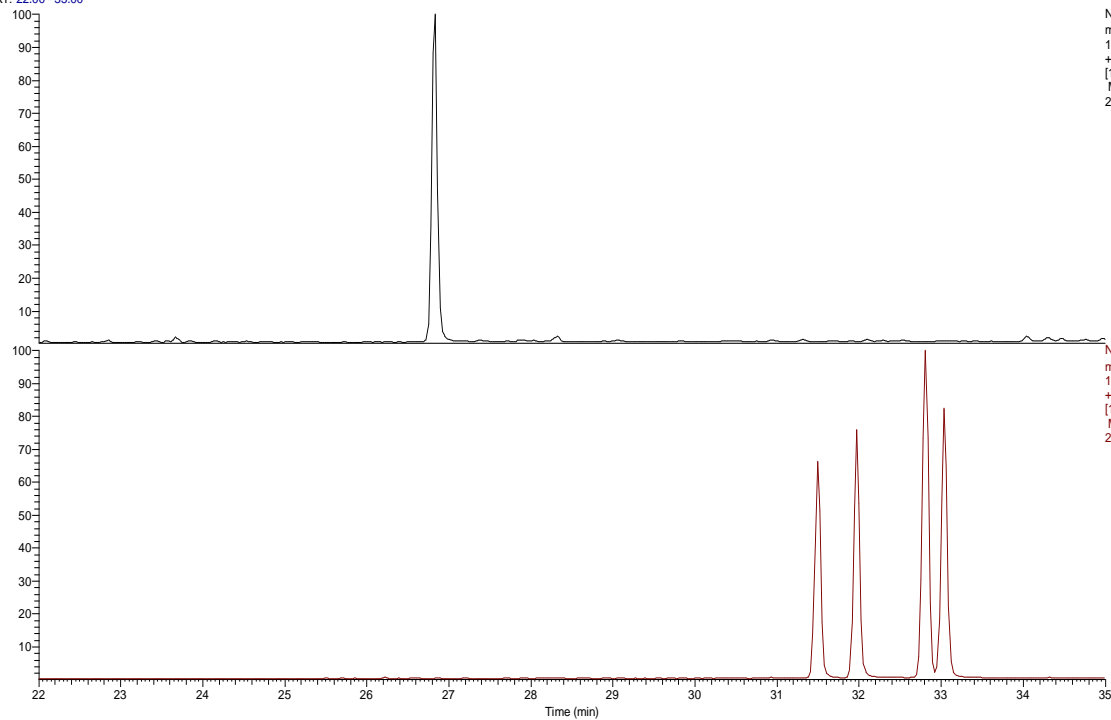


NL: 1.81E6
m/z=
190.50-191.50 F:
+ c EISIM ms
[190.680-191.680]
MS
25_2-4_3694-0m



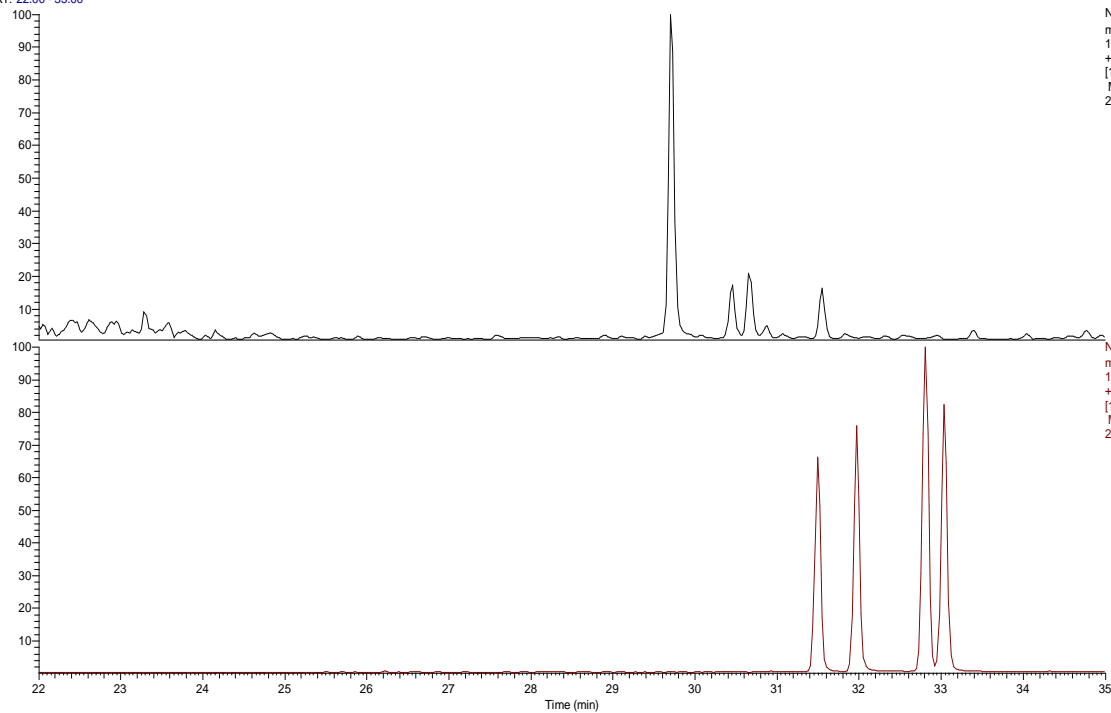


RT: 22.00 - 35.00



NL: 3.91E7
m/z=
177.50-178.50 F:
+ c EI SIM ms
[177.580-178.580]
MS
25_2-4_3694-0m

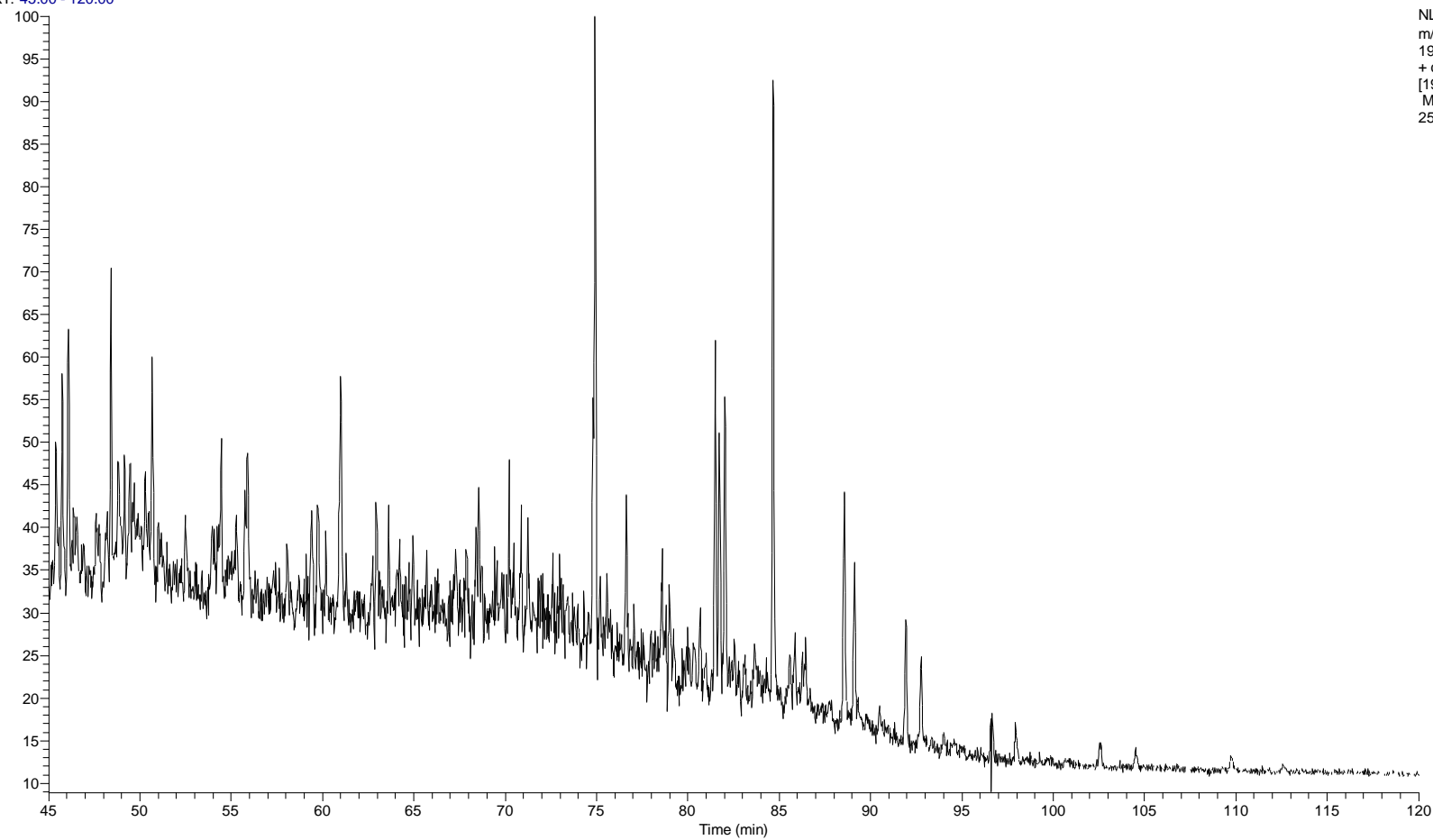
RT: 22.00 - 35.00



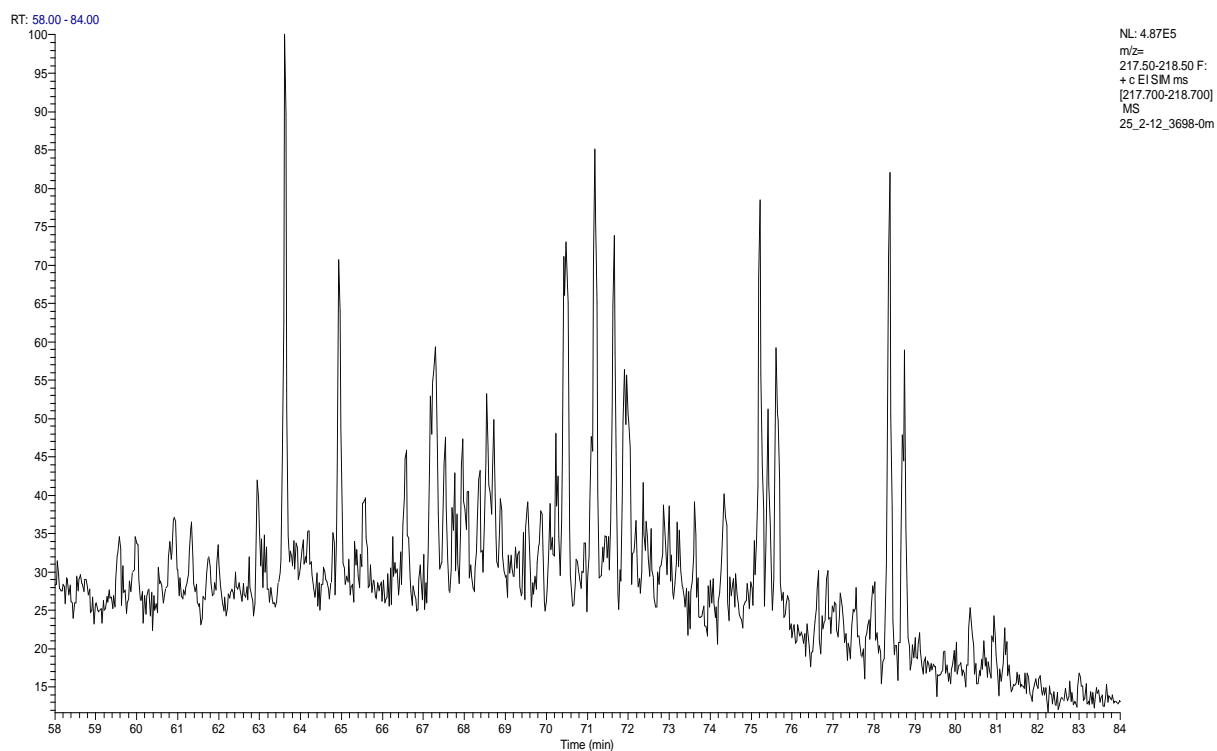
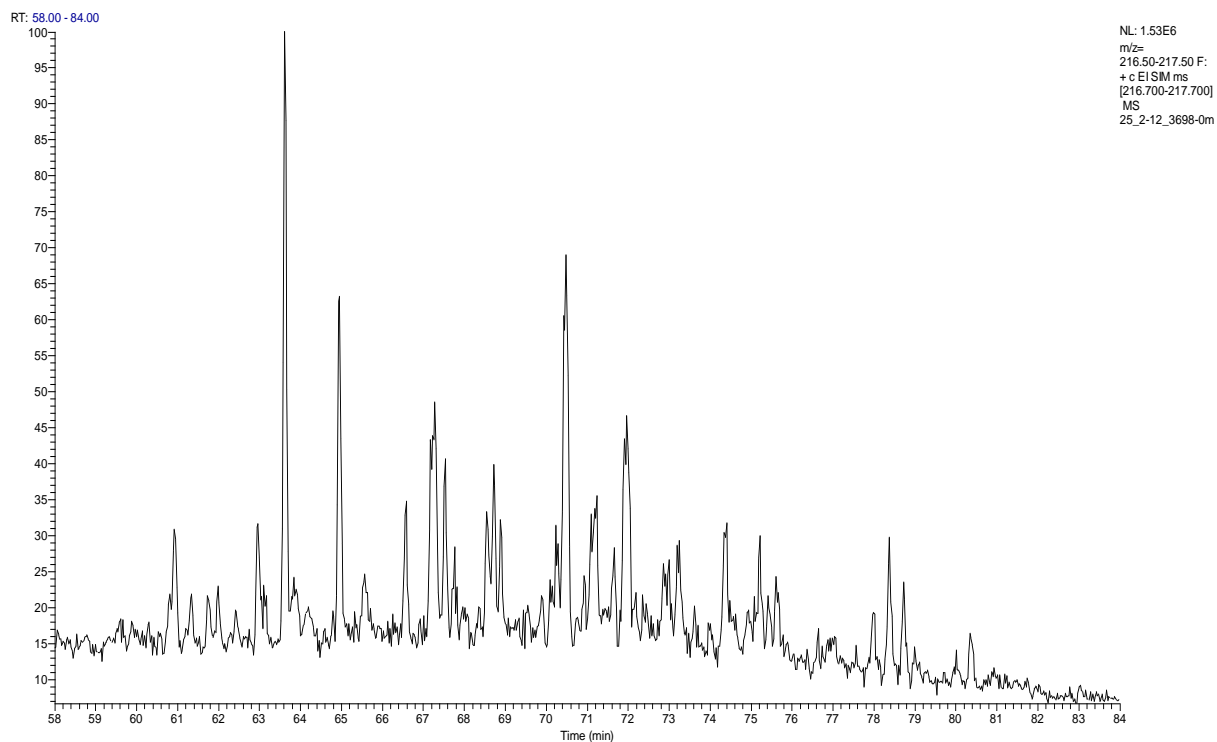
NL: 7.00E6
m/z=
197.50-198.50 F:
+ c EI SIM ms
[197.550-198.550]
MS
25_2-4_3694-0m

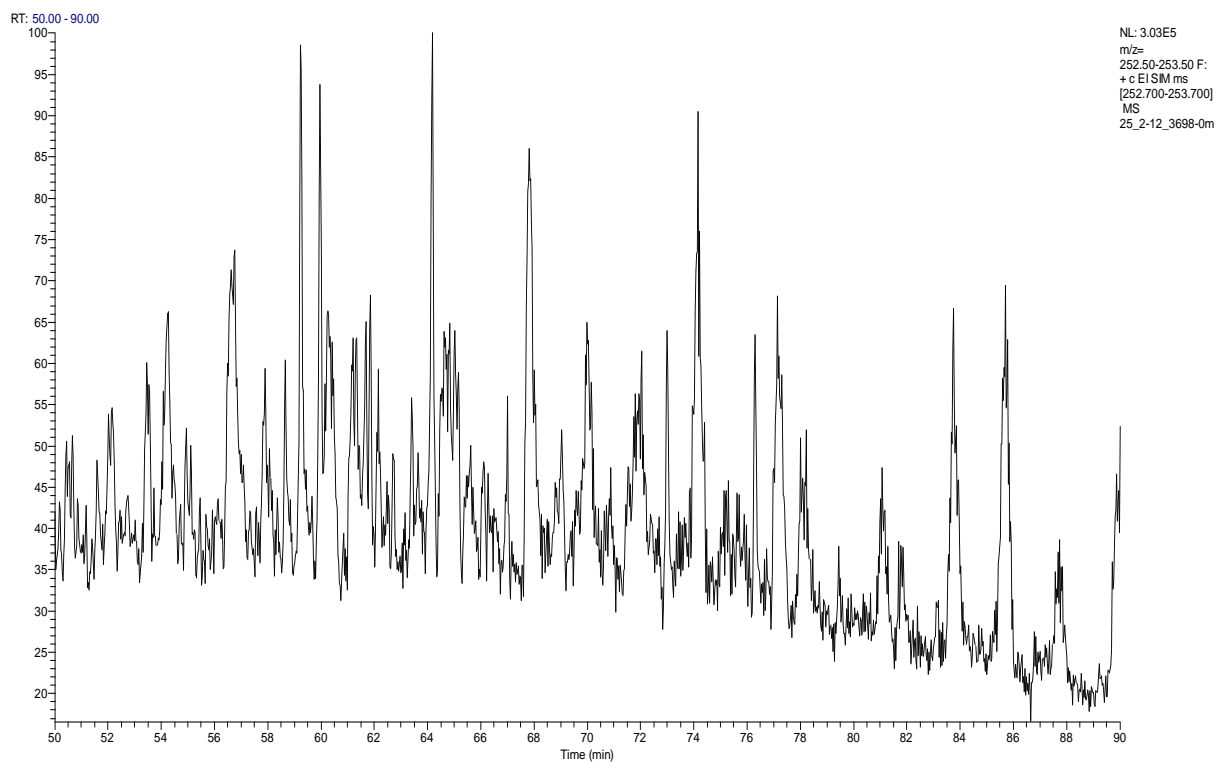
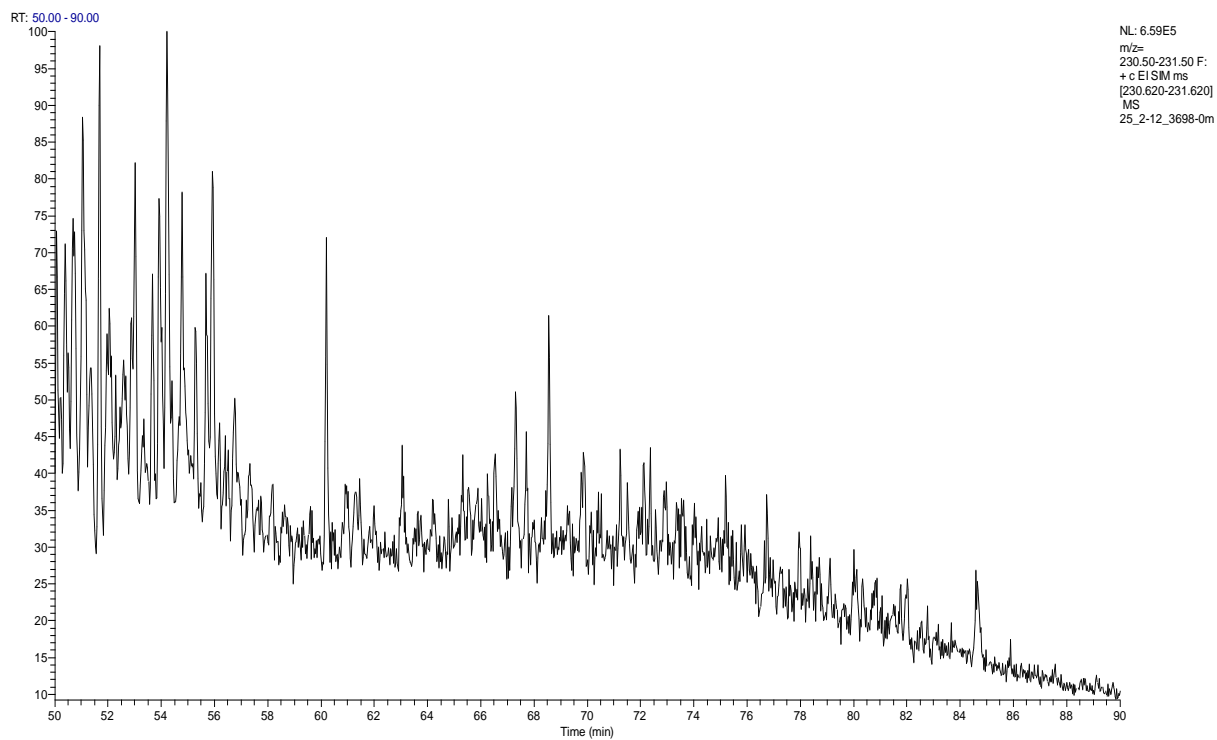
NL: 3.41E7
m/z=
191.50-192.50 F:
+ c EI SIM ms
[191.590-192.590]
MS
25_2-4_3694-0m

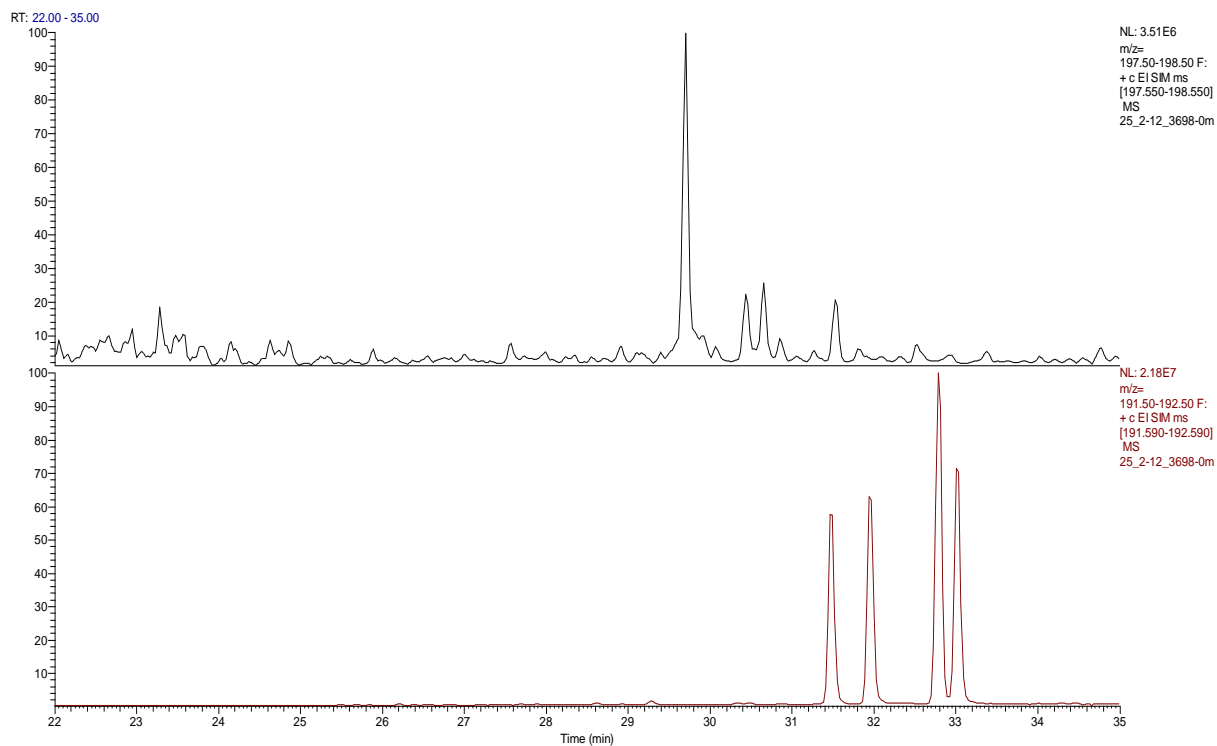
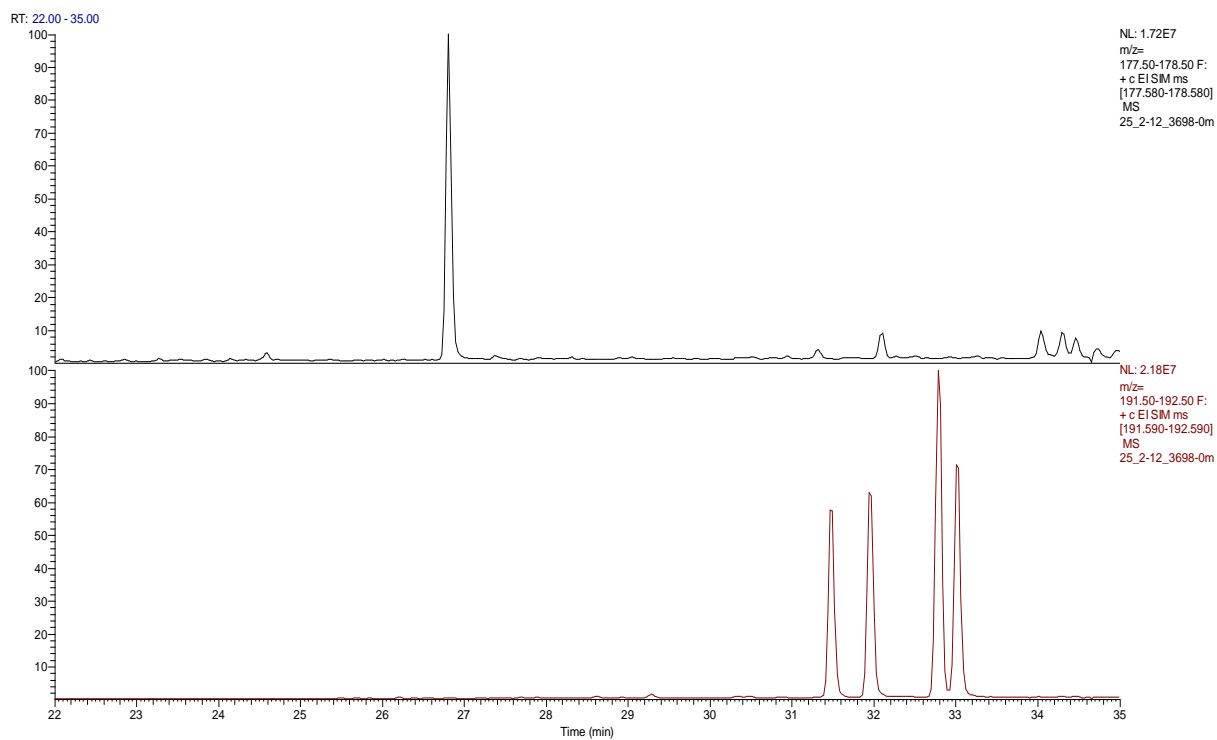
RT: 45.00 - 120.00



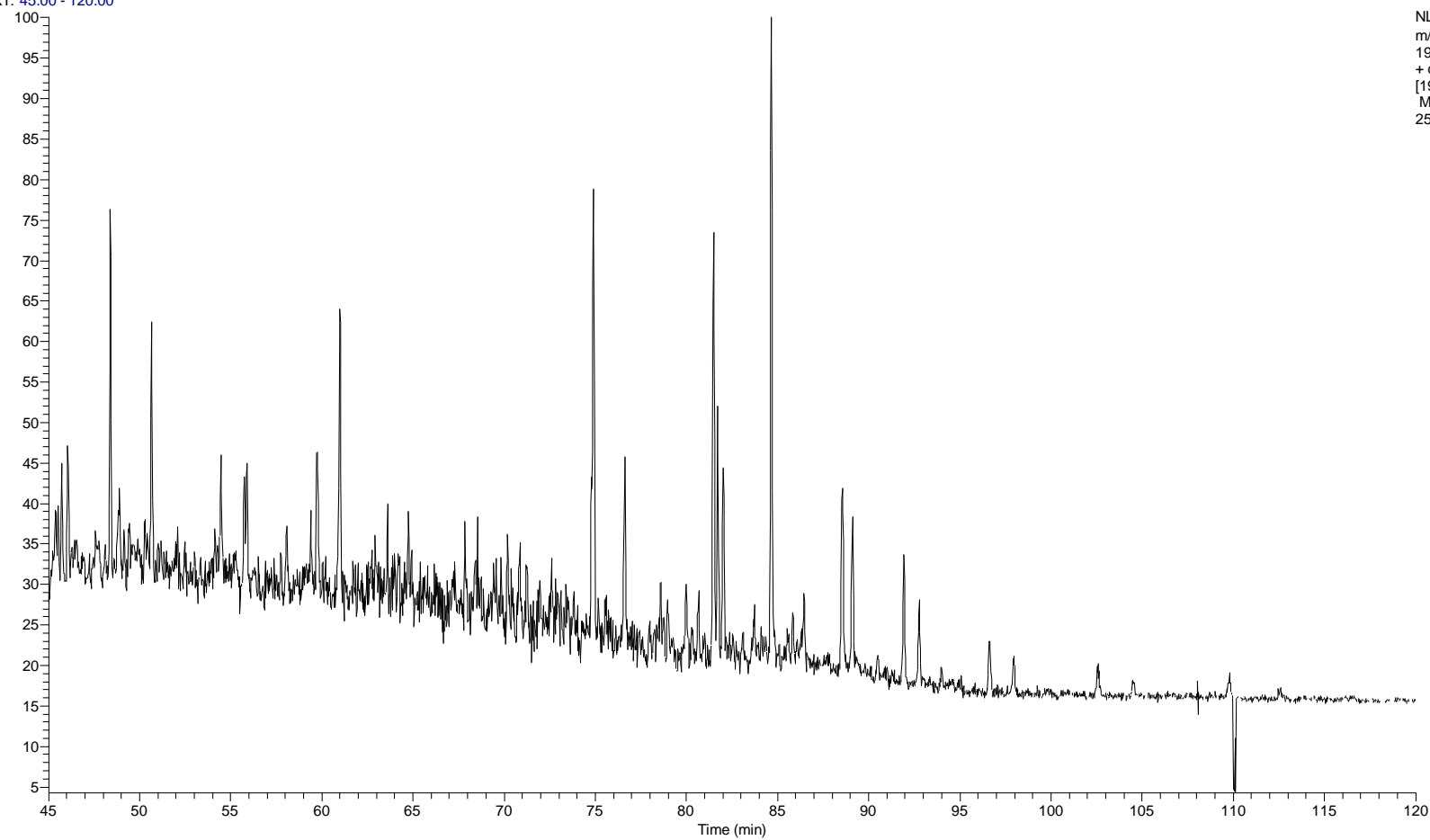
NL: 1.26E6
m/z=
190.50-191.50 F:
+ c EI SIM ms
[190.680-191.680]
MS
25_2-12_3698-0m



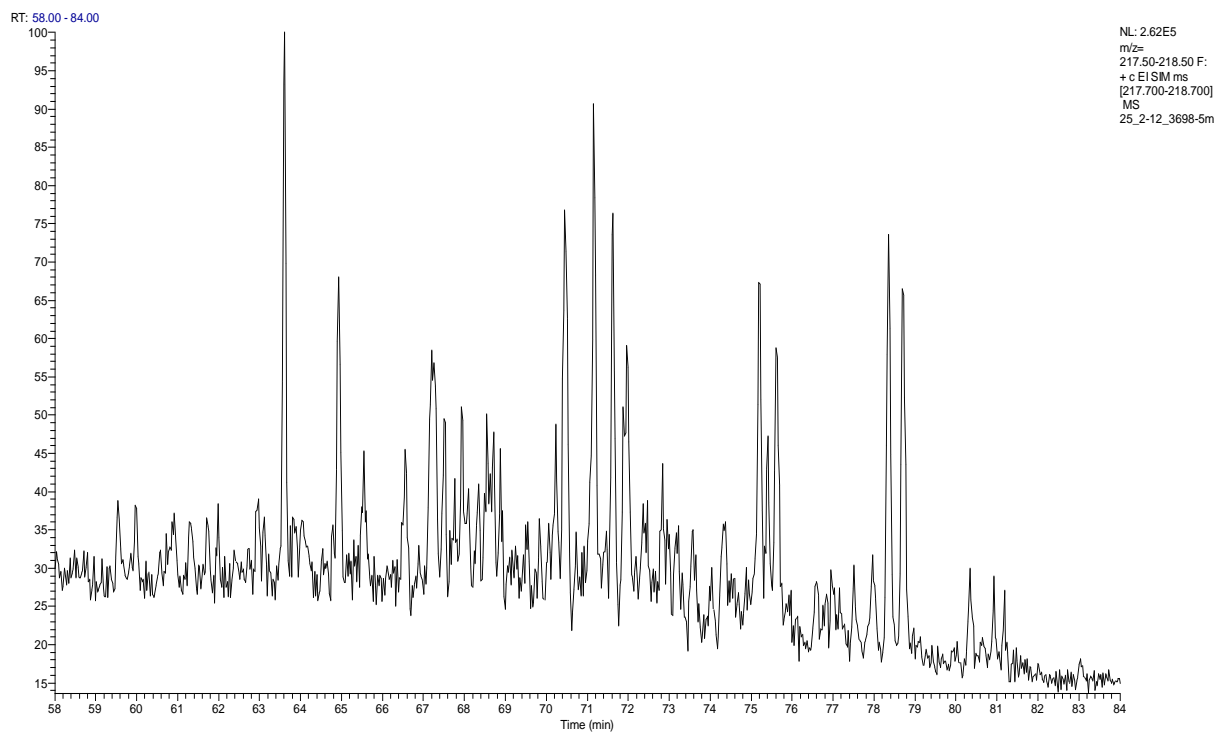
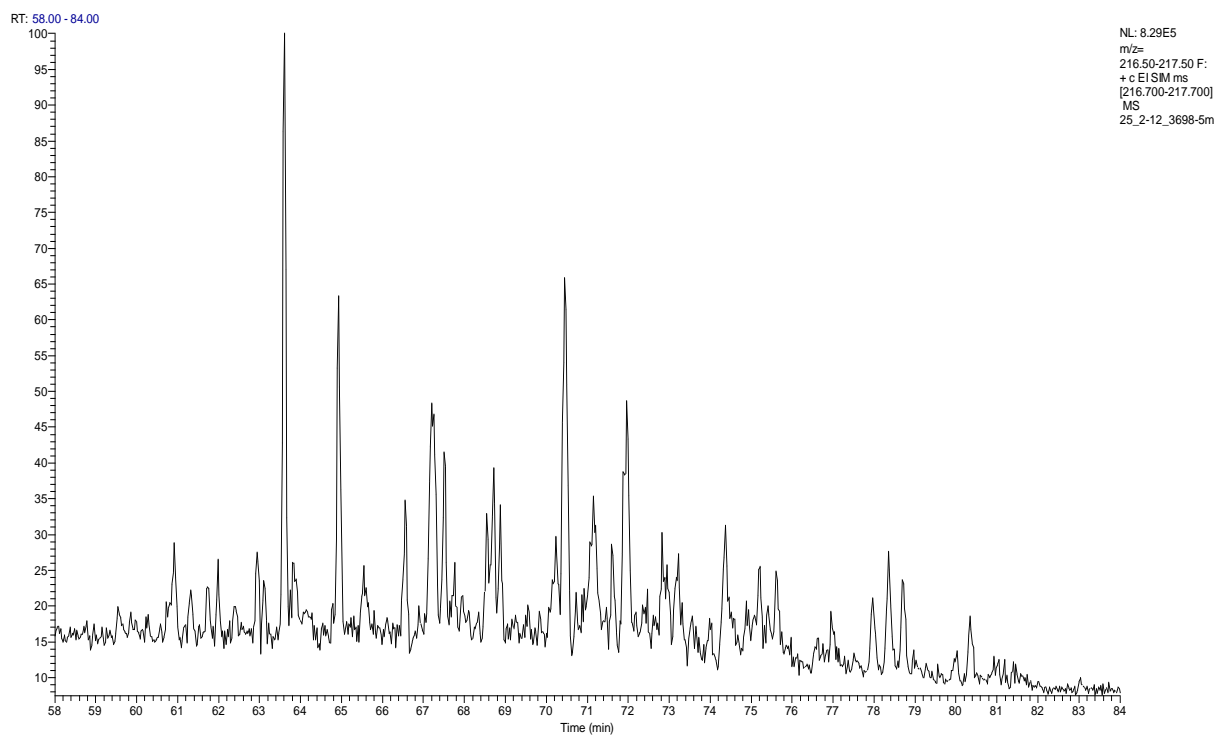


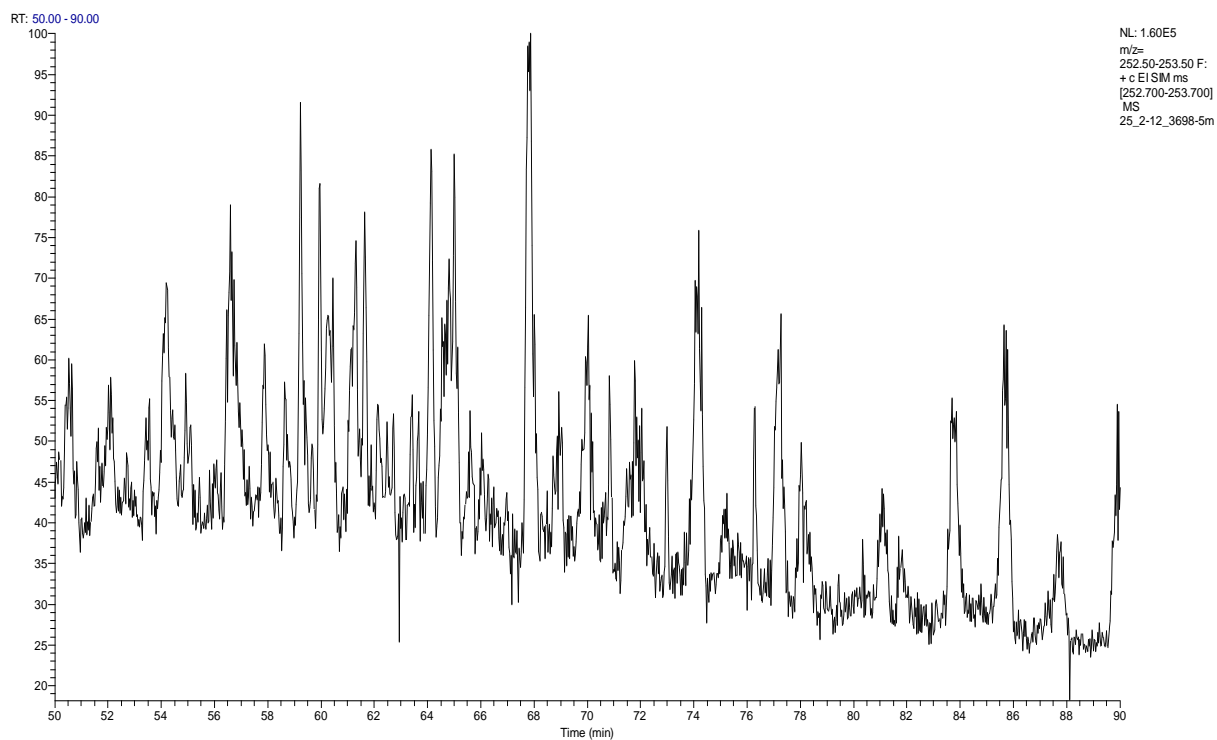
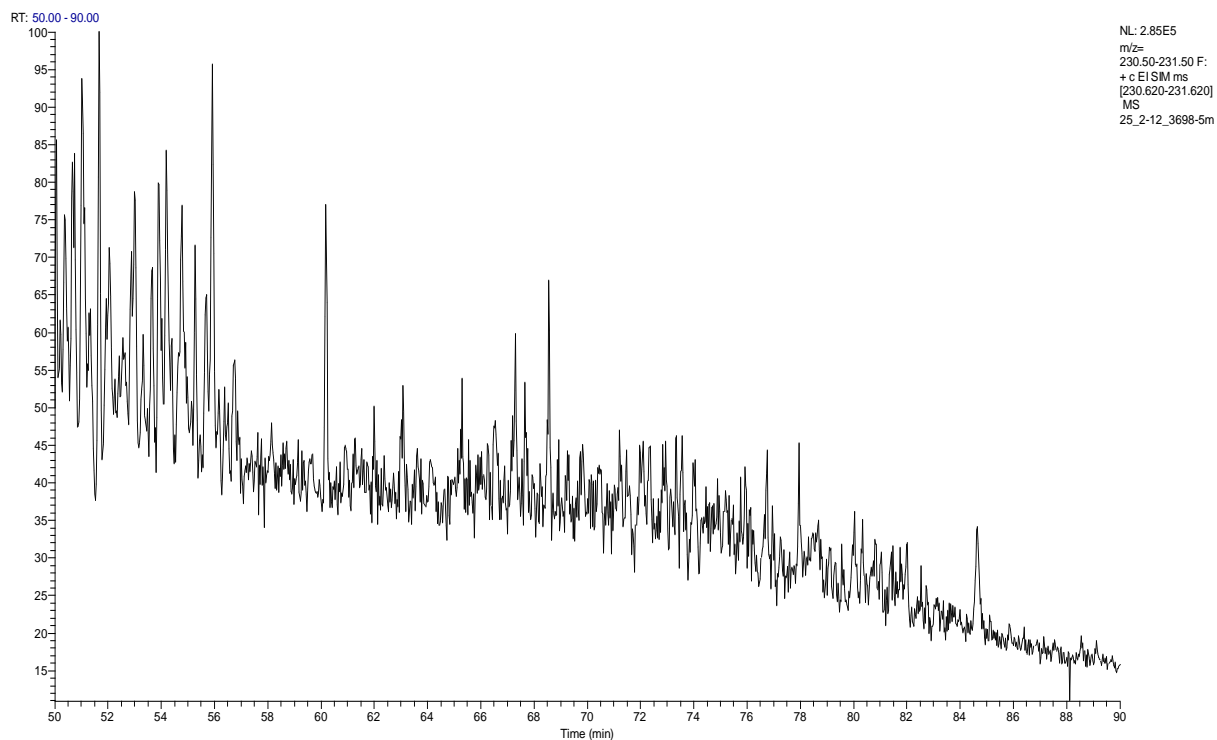


RT: 45.00 - 120.00

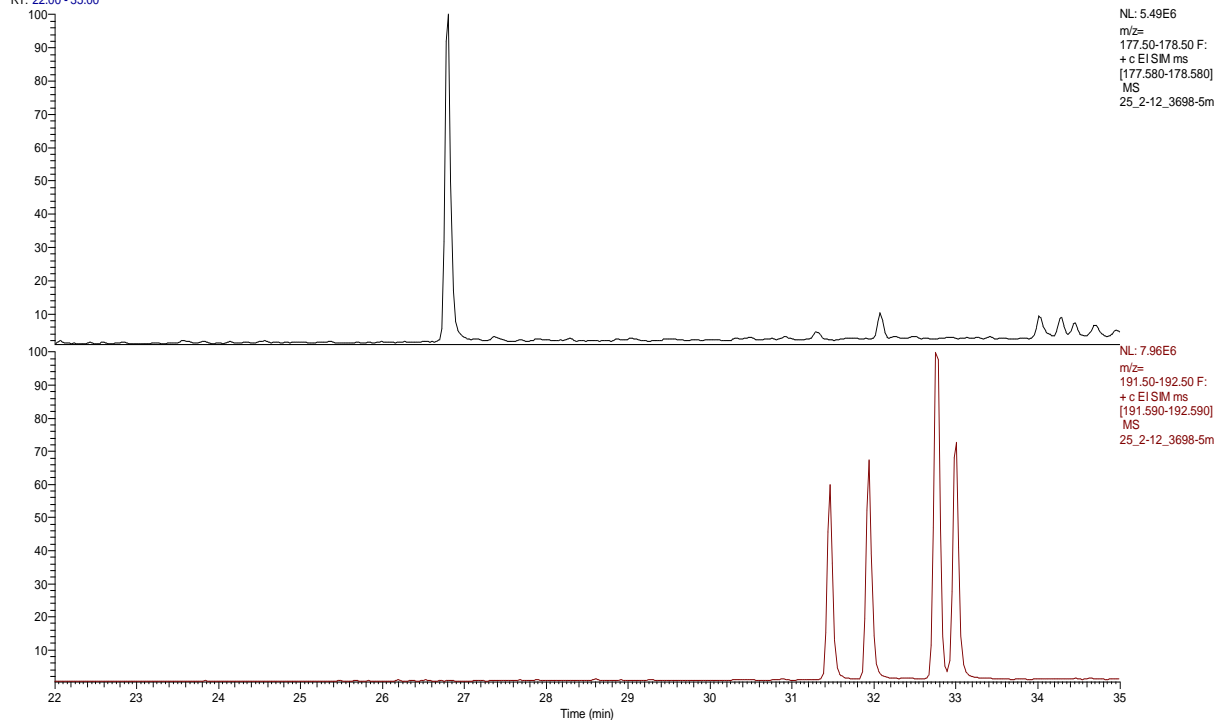


NL: 8.69E5
m/z=
190.50-191.50 F:
+ c EI SIM ms
[190.680-191.680]
MS
25_2-12_3698-5m

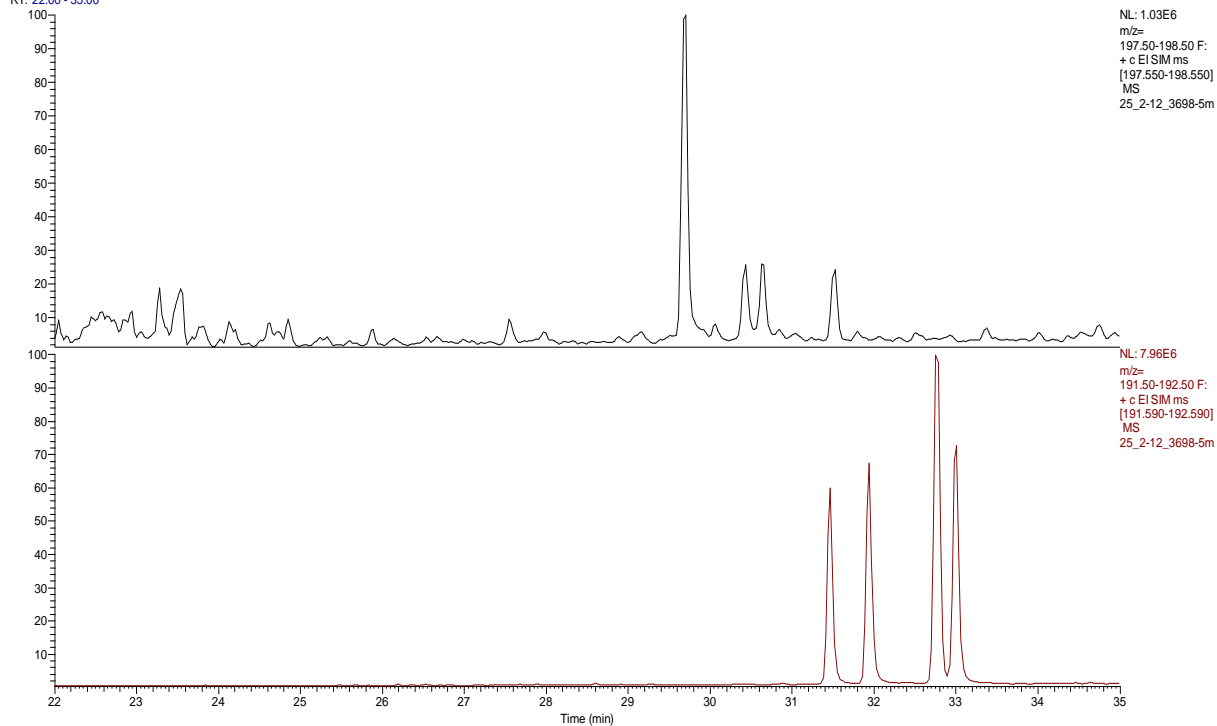




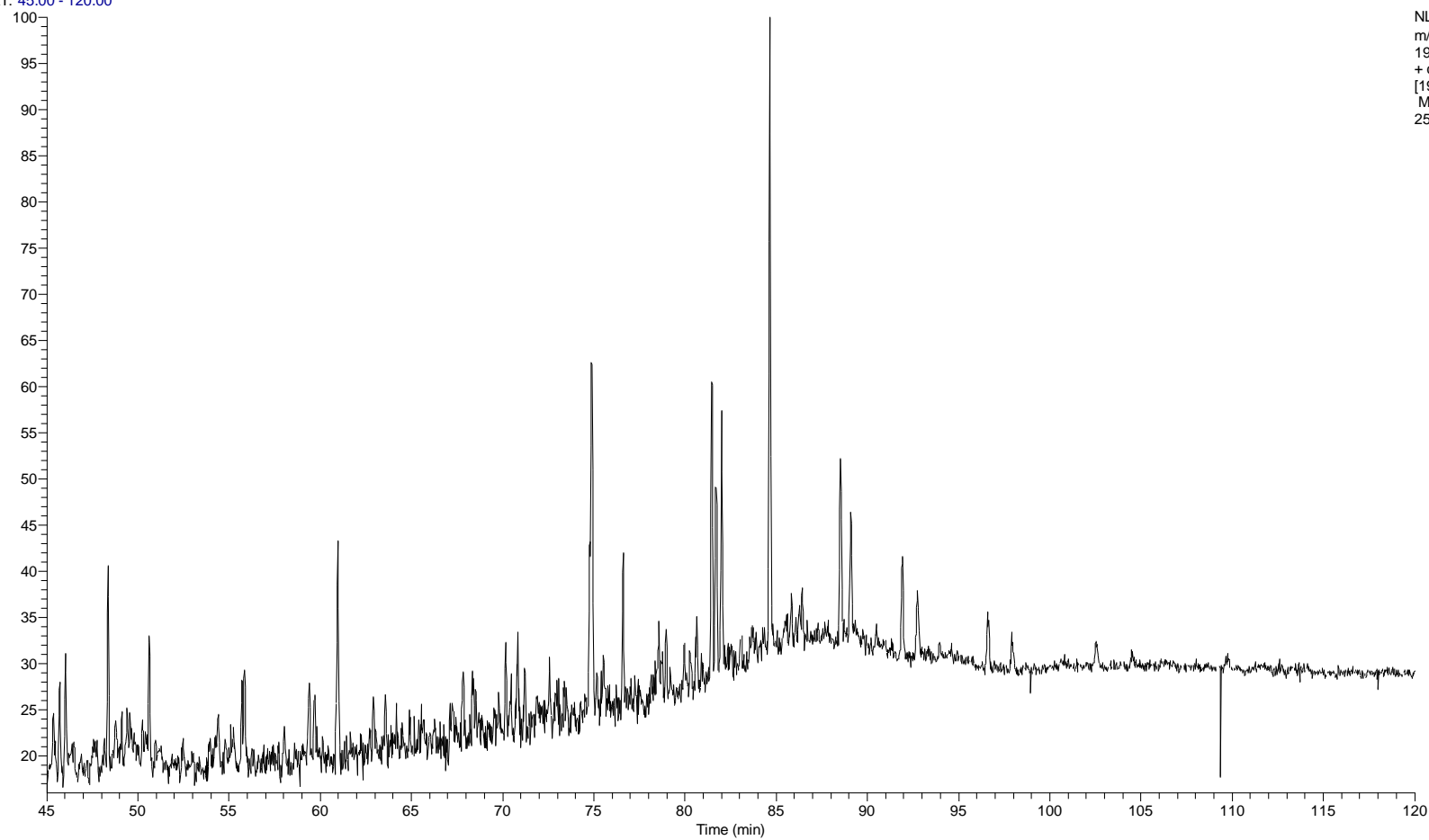
RT: 22.00 - 35.00



RT: 22.00 - 35.00

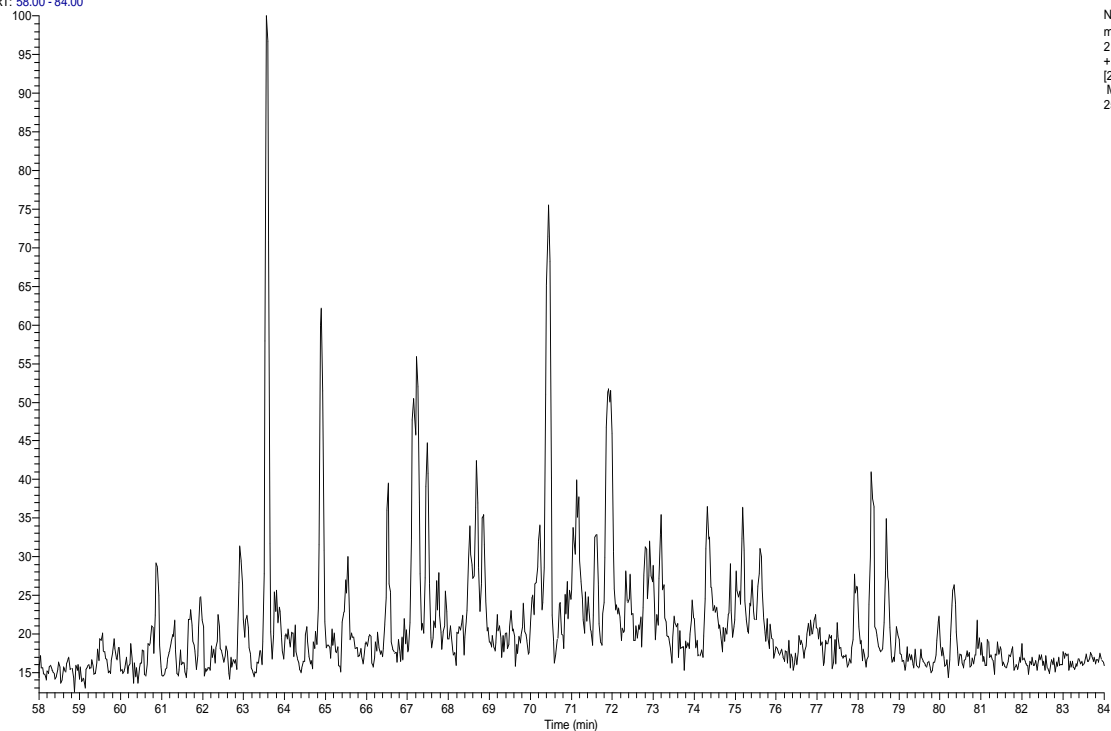


RT: 45.00 - 120.00



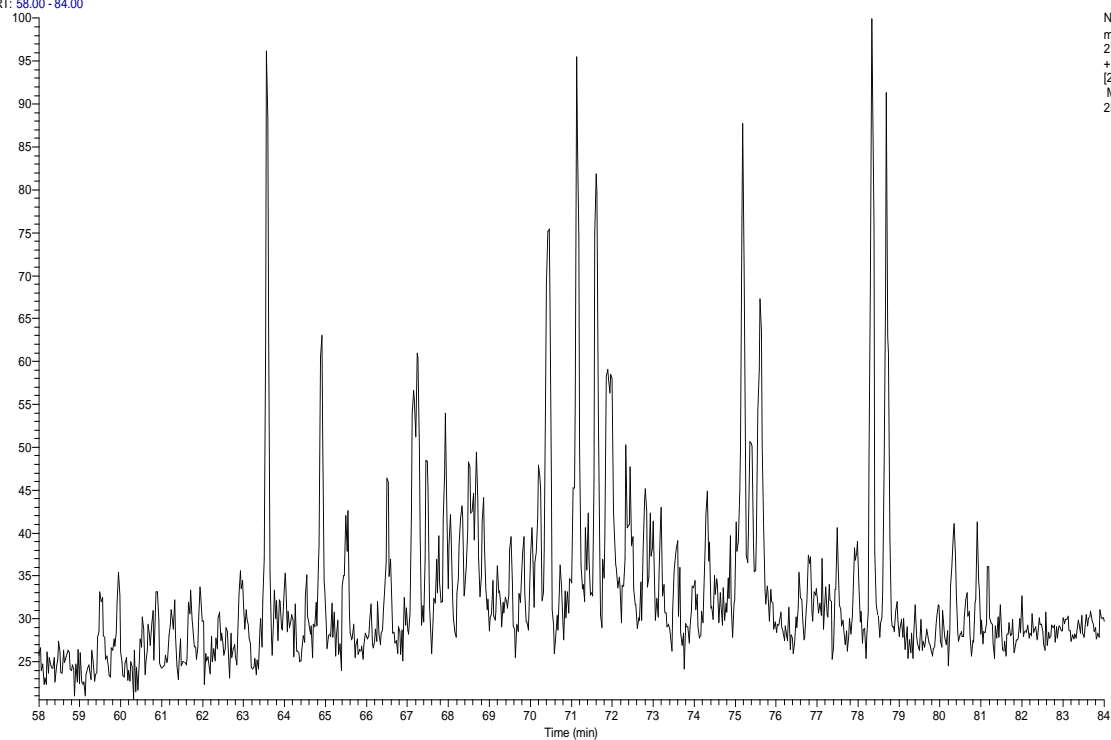
NL: 4.47E5
m/z=
190.50-191.50 F:
+ c EI SIM ms
[190.680-191.680]
MS
25_2-12_3711-0m

RT: 58.00 - 84.00

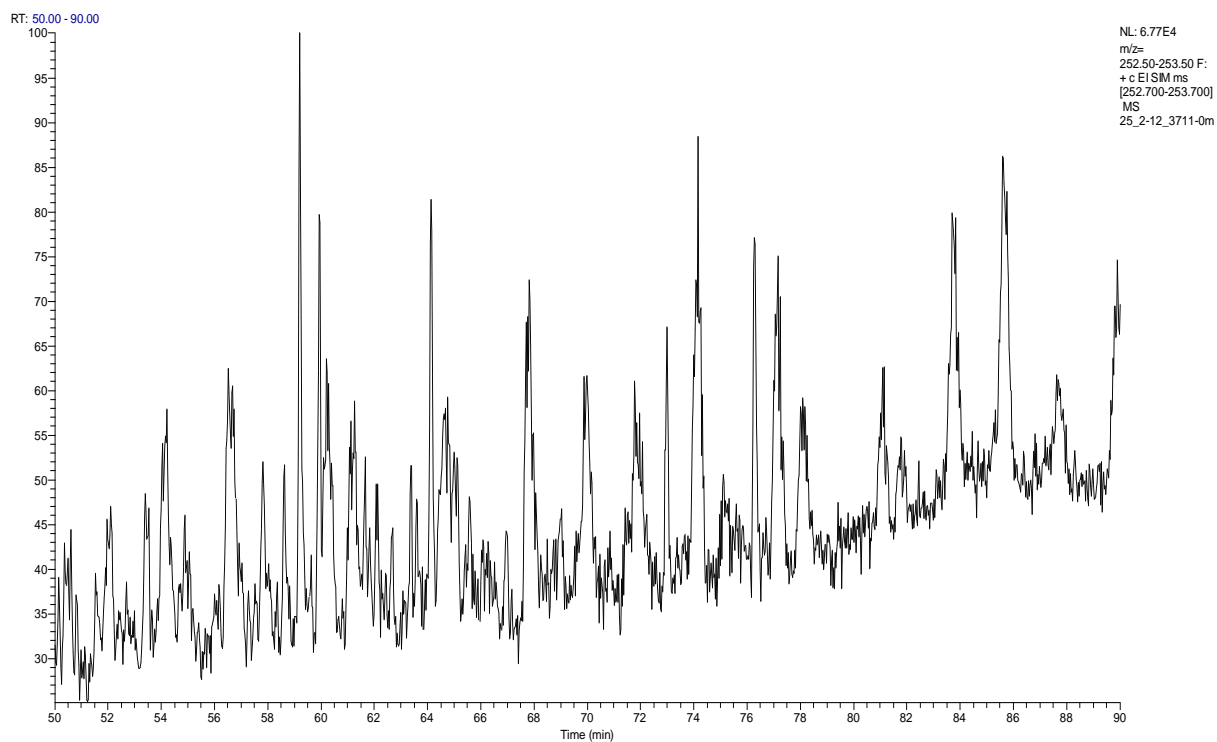
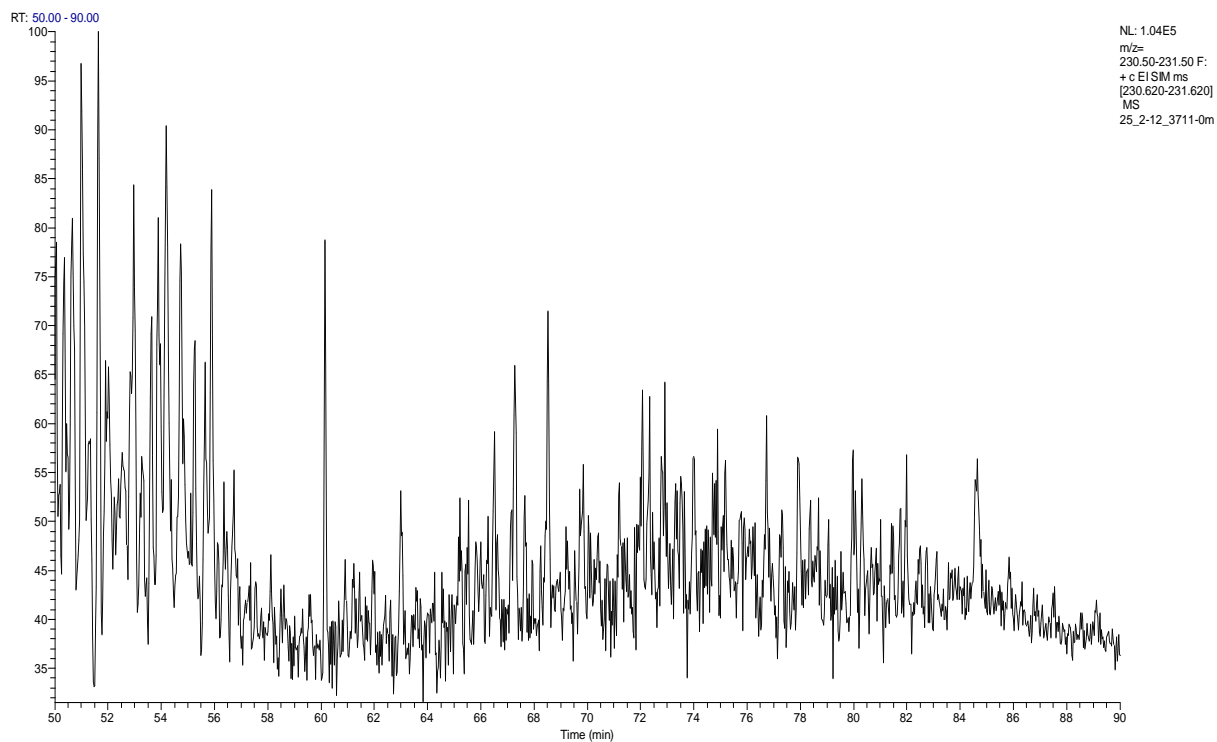


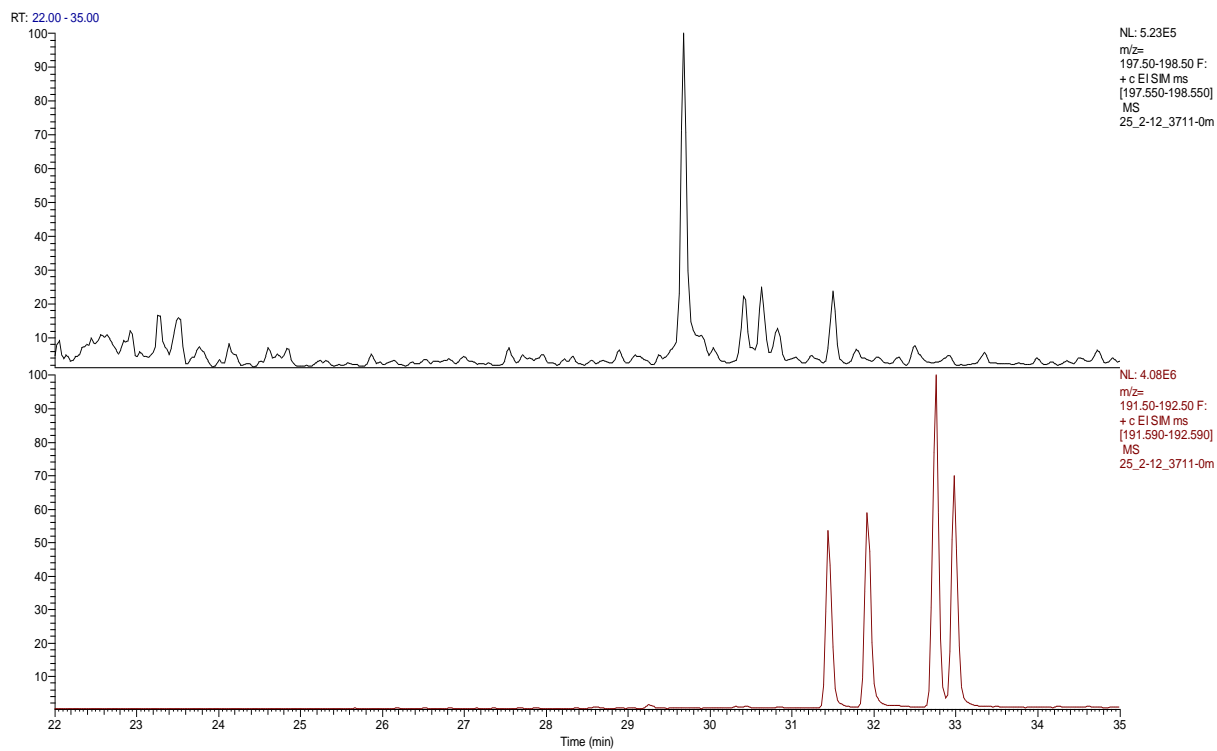
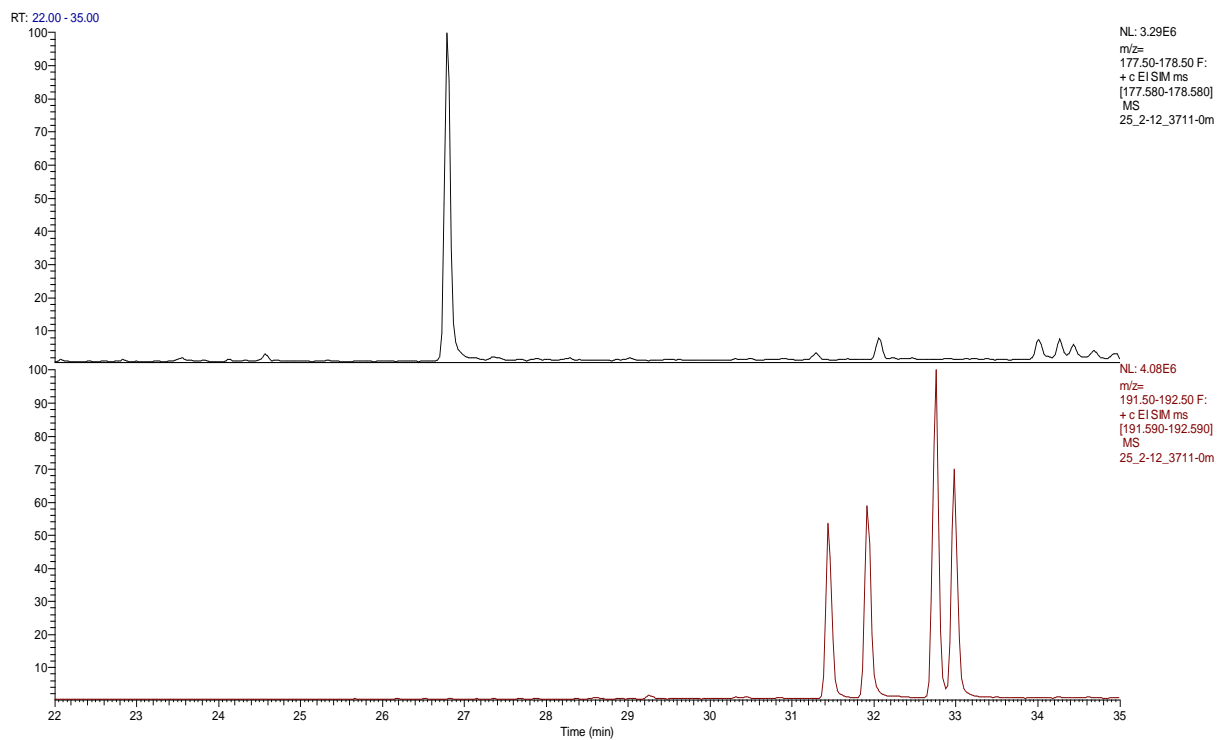
NL: 2.87E5
m/z=
216.50-217.50 F:
+ c EI SIM ms
[216.700-217.700]
MS
25_2-12_3711-0m

RT: 58.00 - 84.00

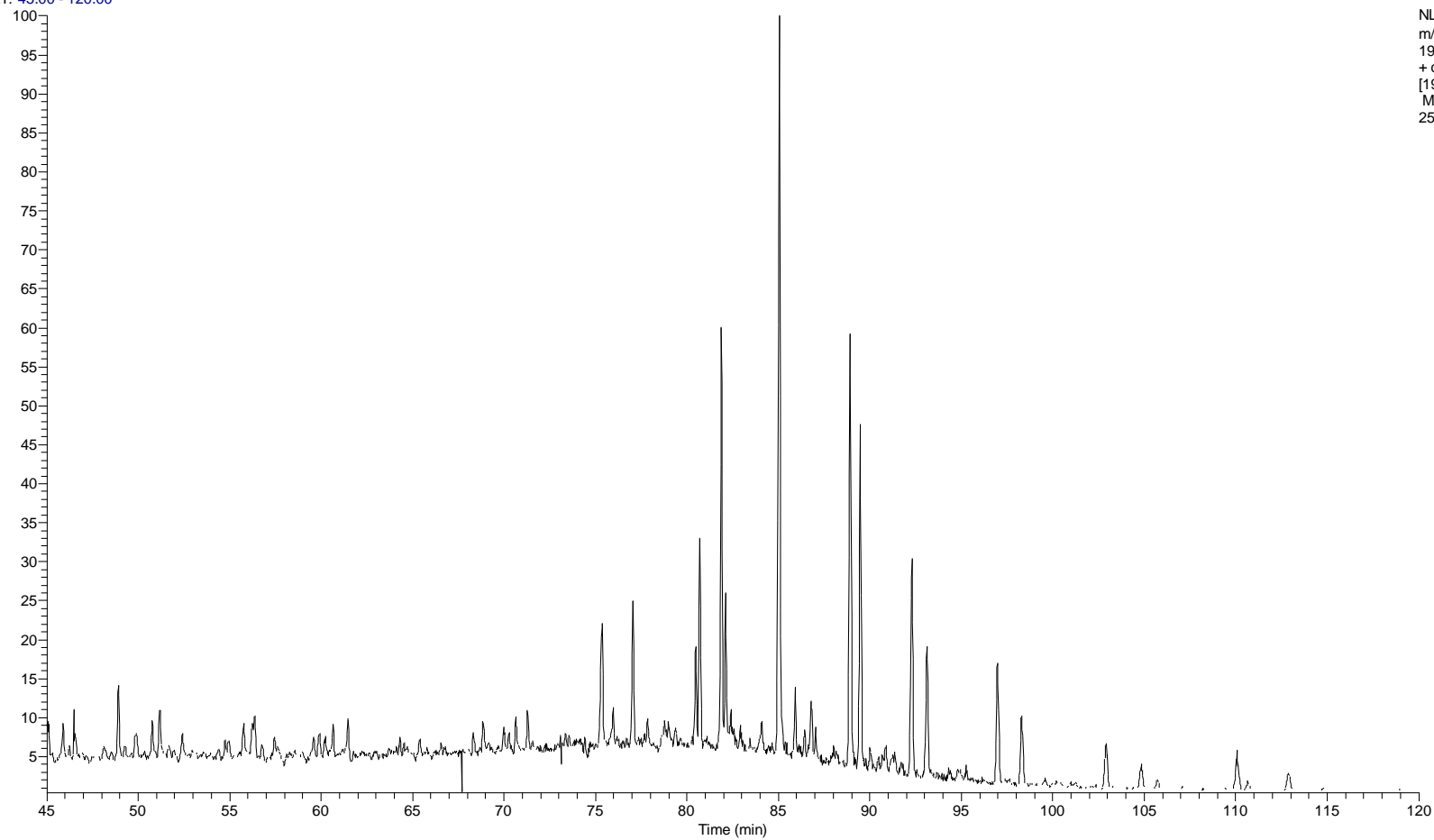


NL: 1.01E5
m/z=
217.50-218.50 F:
+ c EI SIM ms
[217.700-218.700]
MS
25_2-12_3711-0m

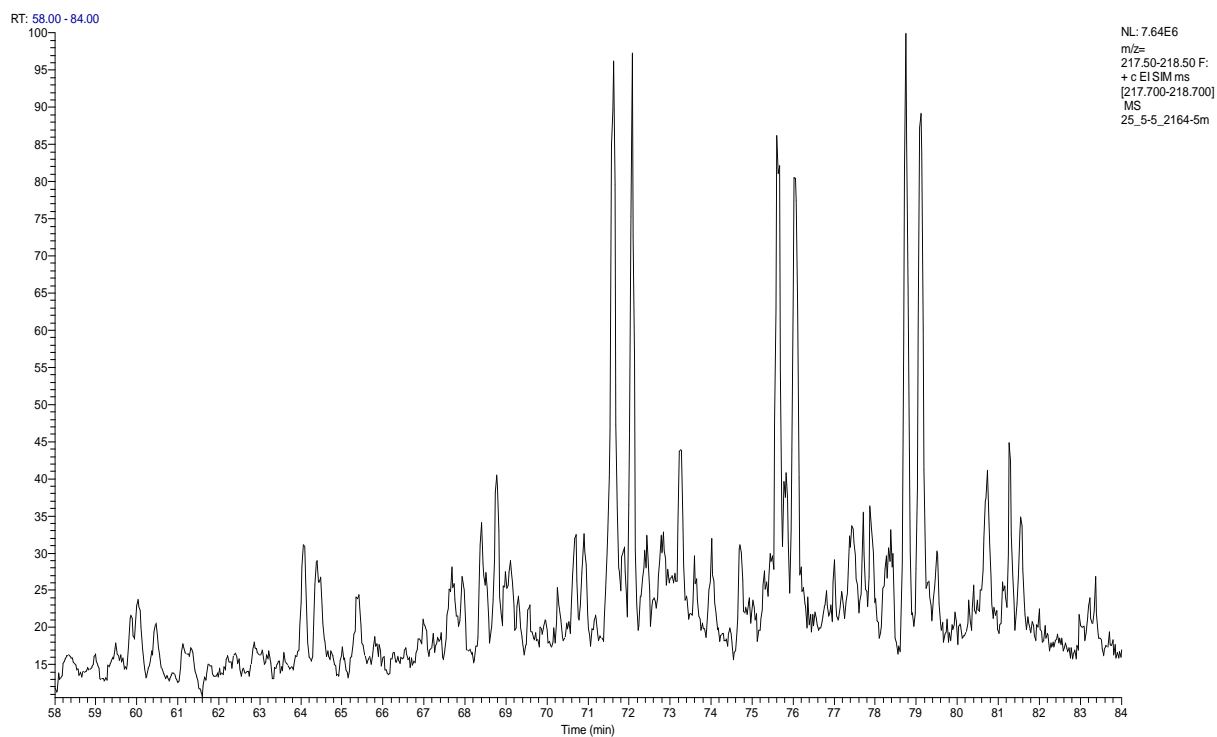
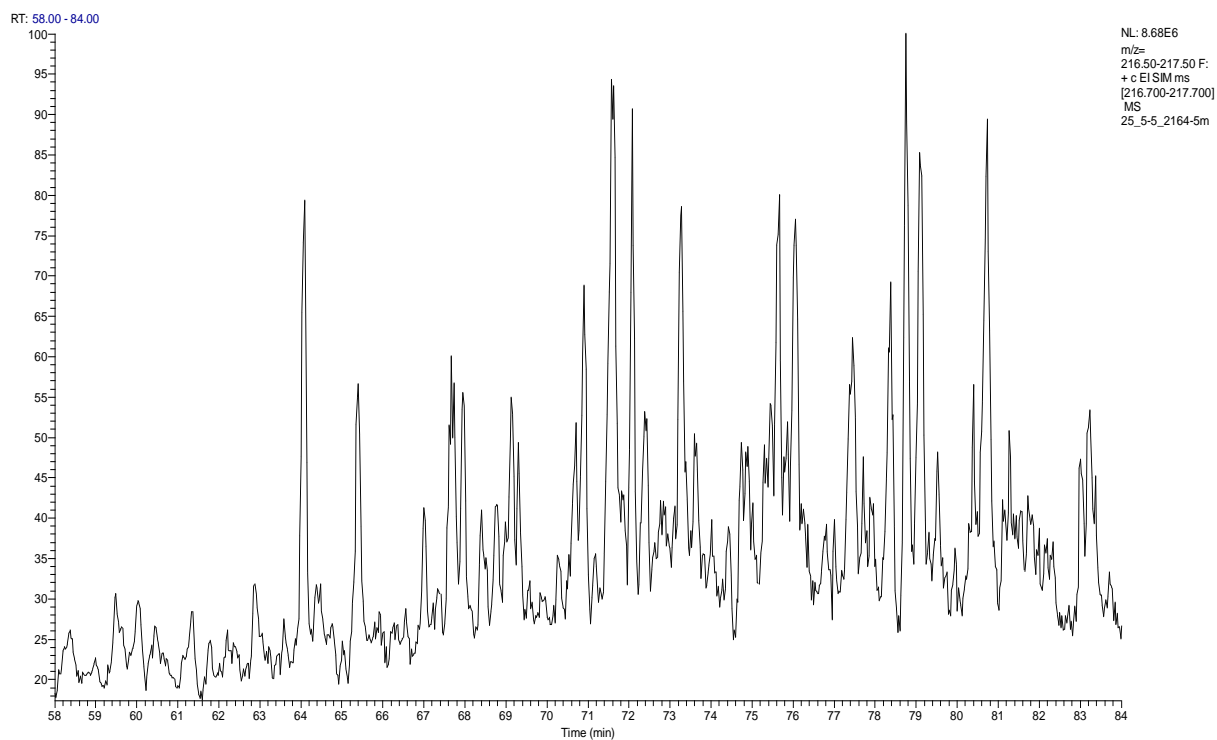




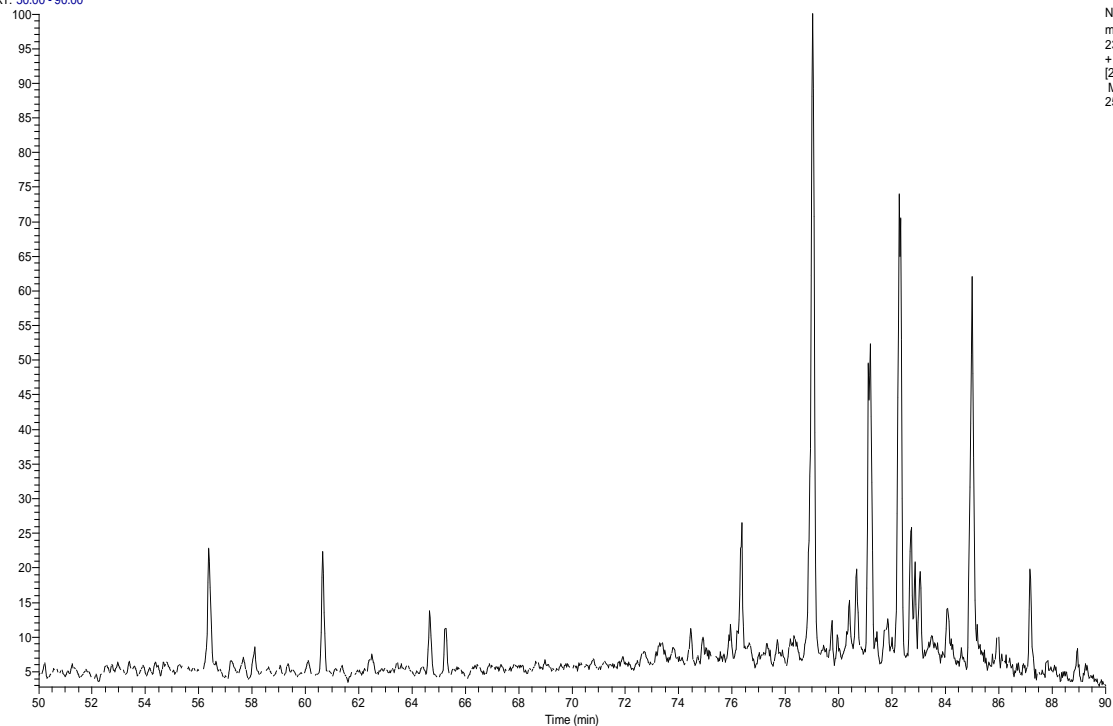
RT: 45.00 - 120.00



NL: 3.92E7
m/z=
190.50-191.50 F:
+ c EISIM ms
[190.680-191.680]
MS
25_5-5_2164-5m

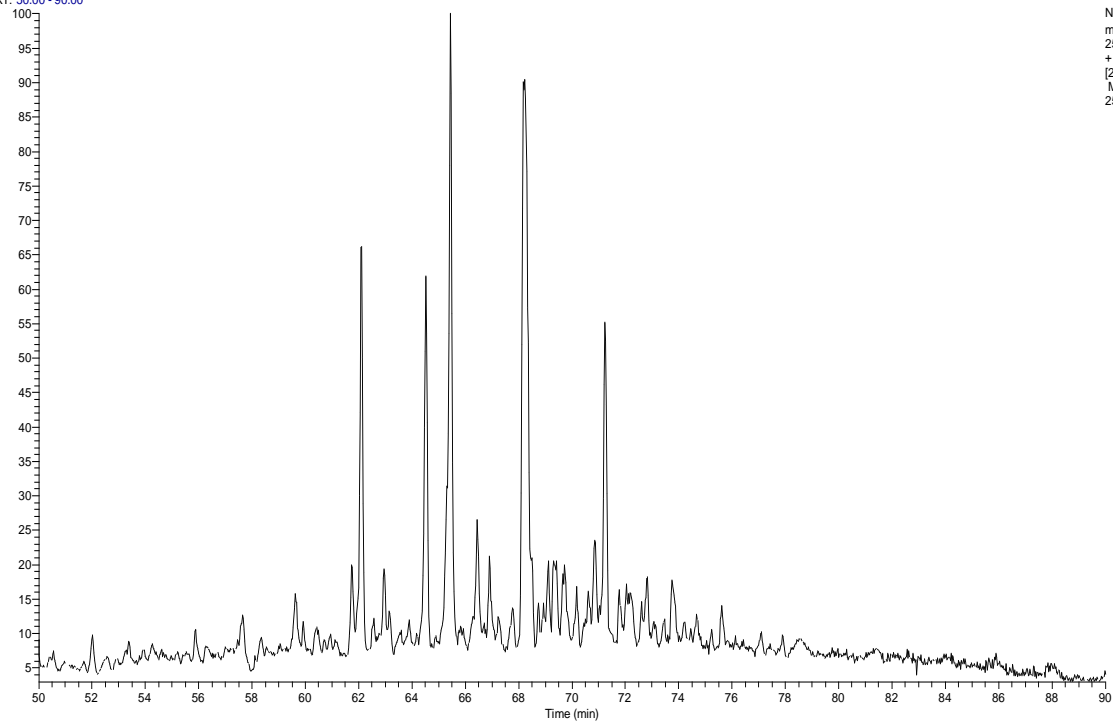


RT: 50.00 - 90.00



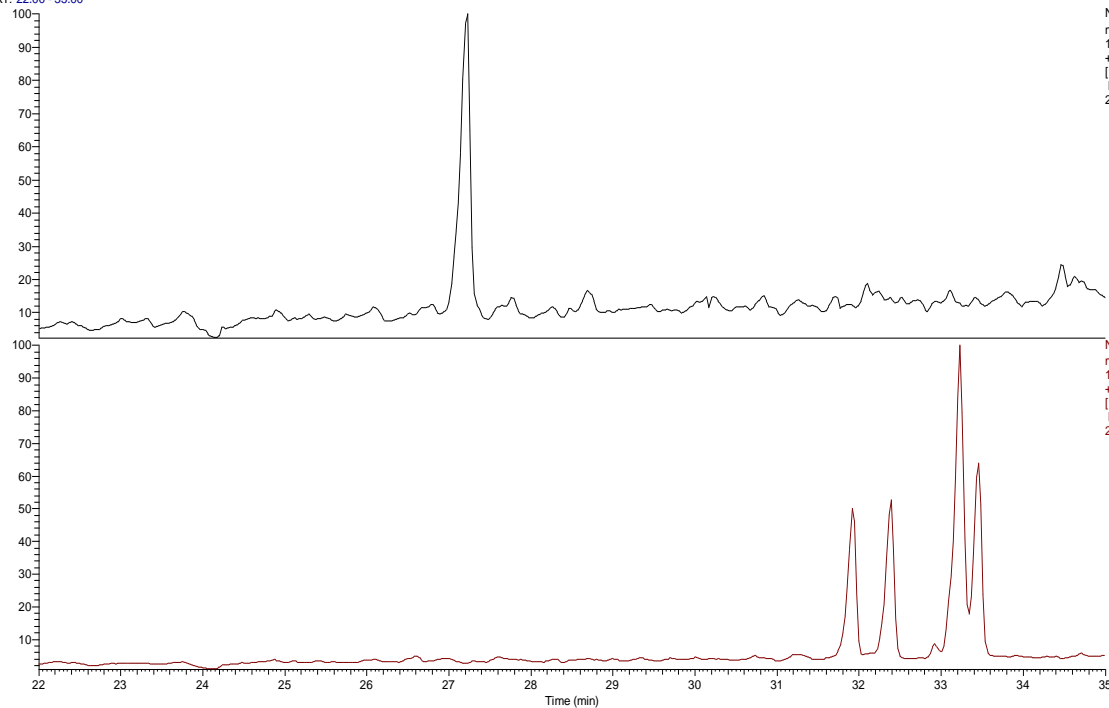
NL: 3.48E7
m/z=
230.50-231.50 F:
+ c E1 SIM ms
[230.620-231.620]
MS
25_5-5_2164-5m

RT: 50.00 - 90.00

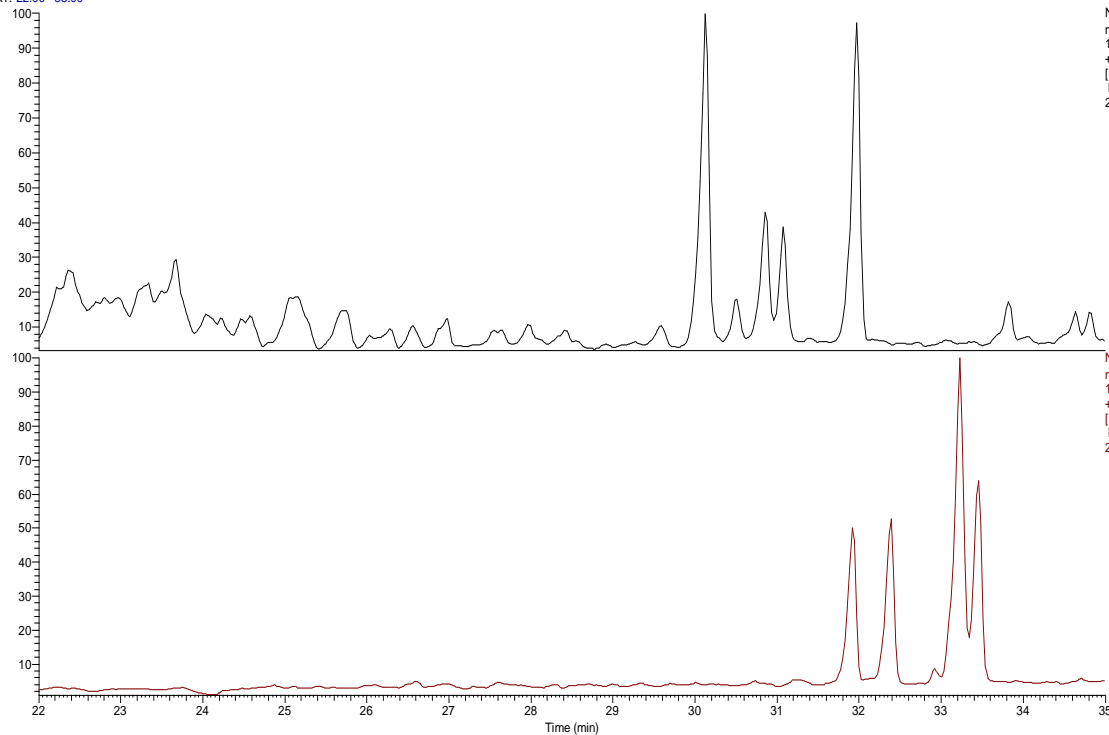


NL: 2.44E7
m/z=
252.50-253.50 F:
+ c E1 SIM ms
[252.700-253.700]
MS
25_5-5_2164-5m

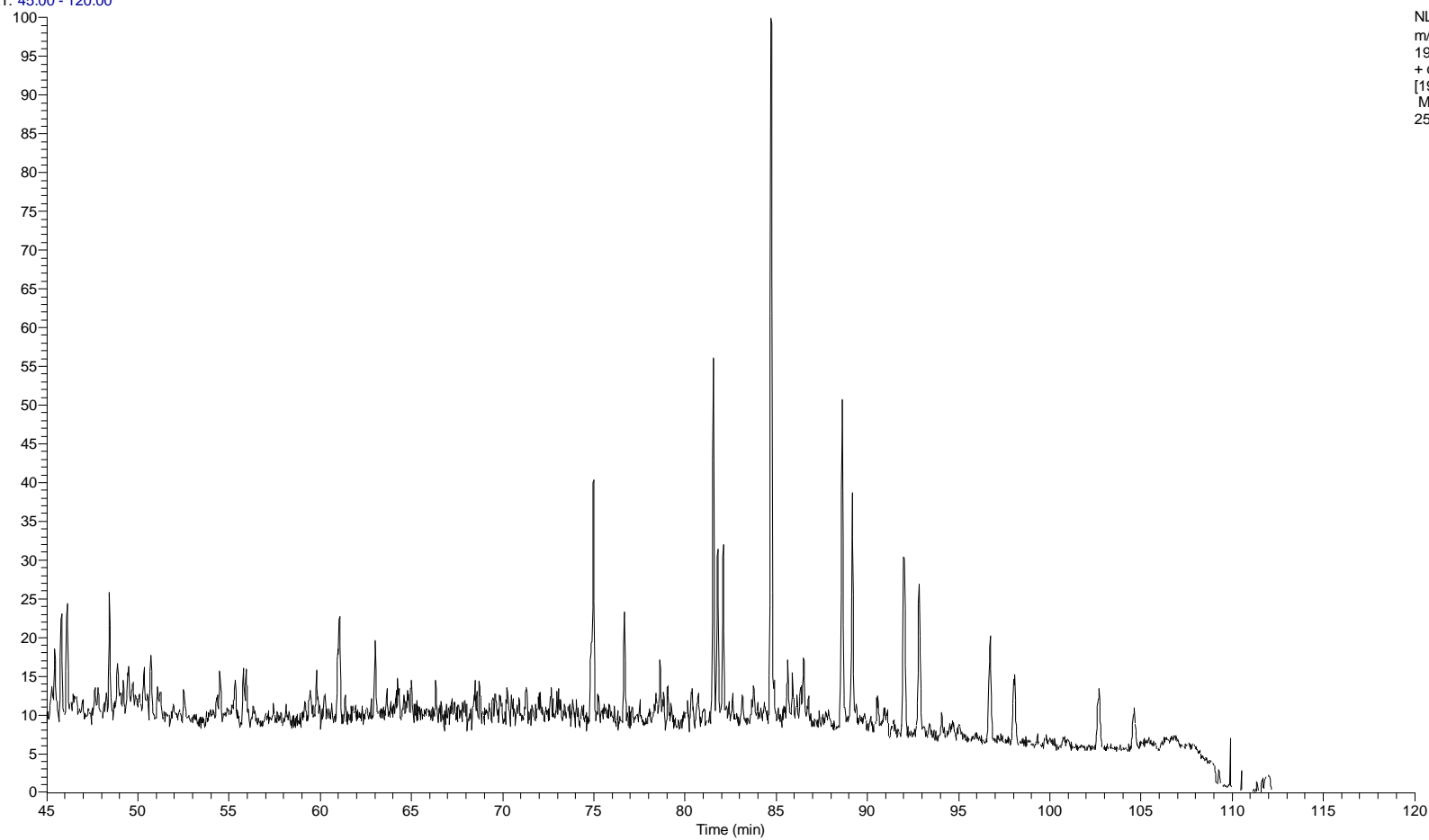
RT: 22.00 - 35.00



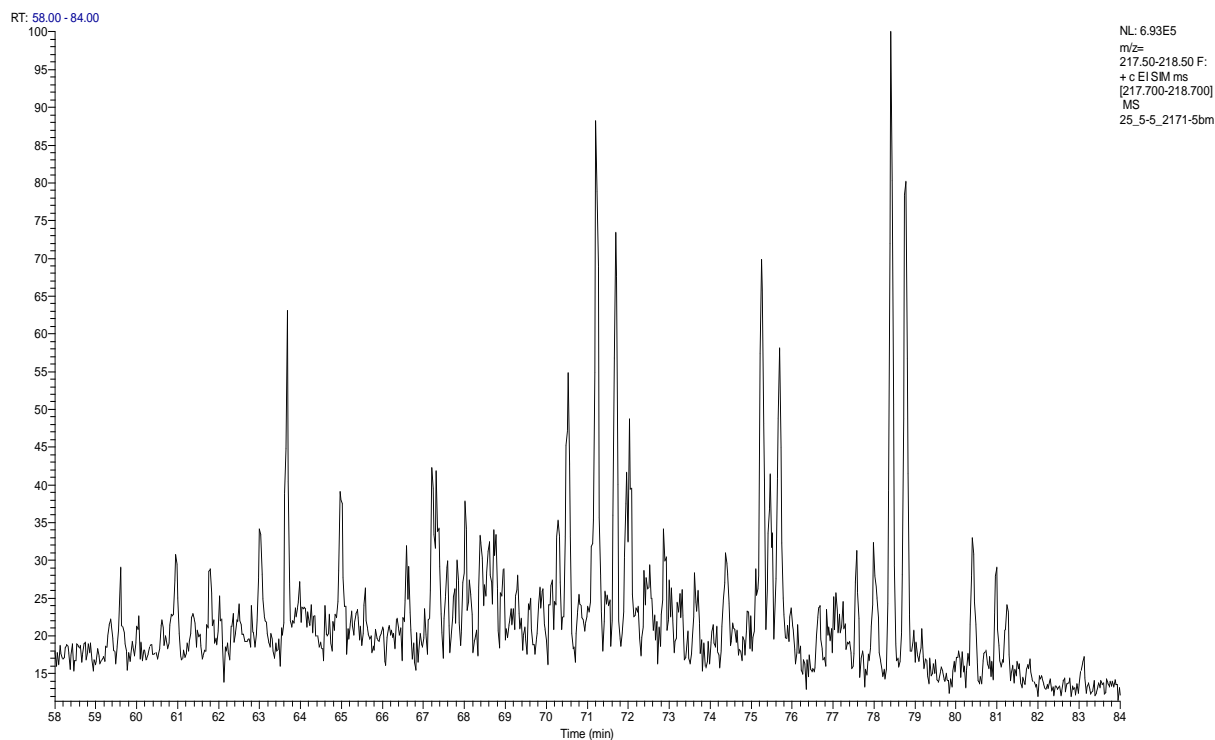
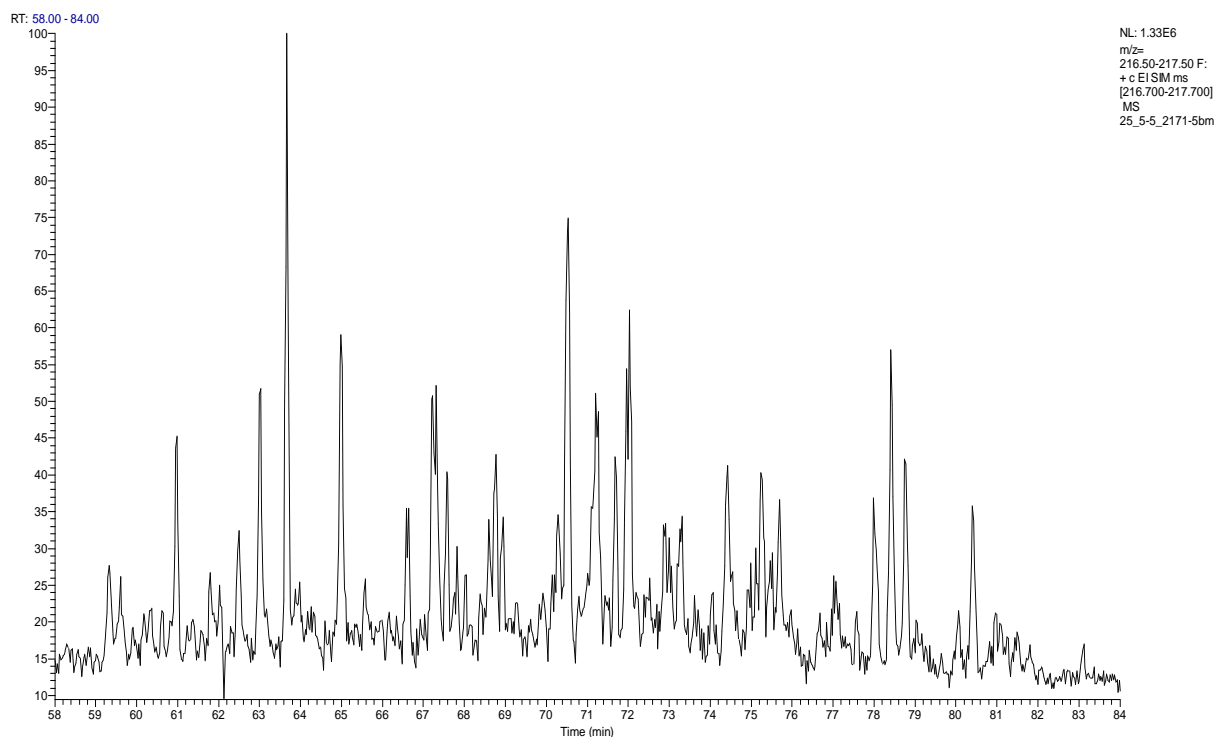
RT: 22.00 - 35.00

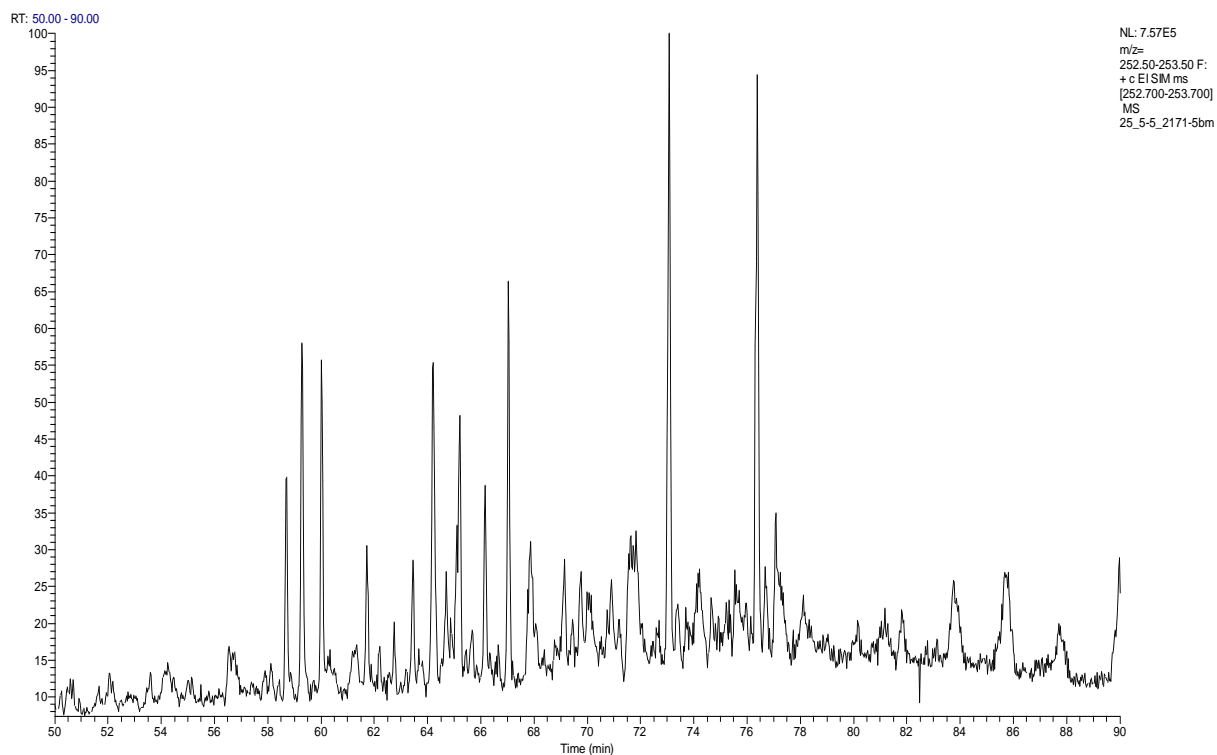
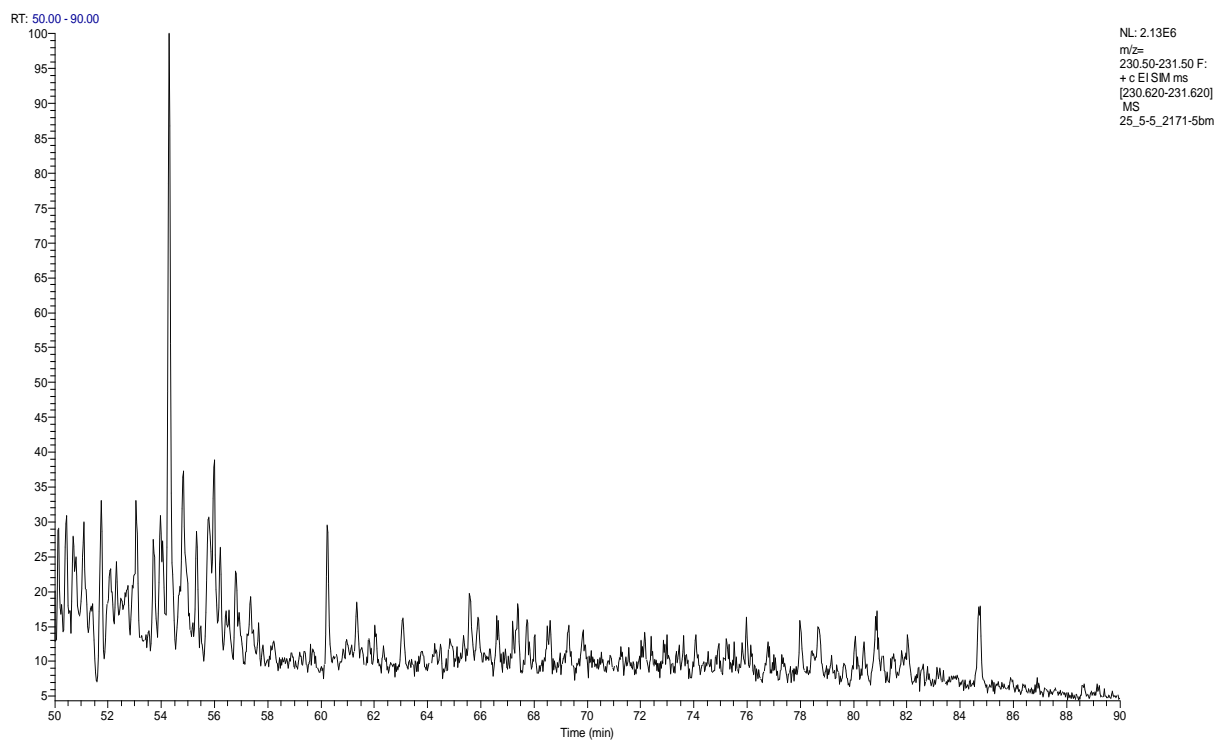


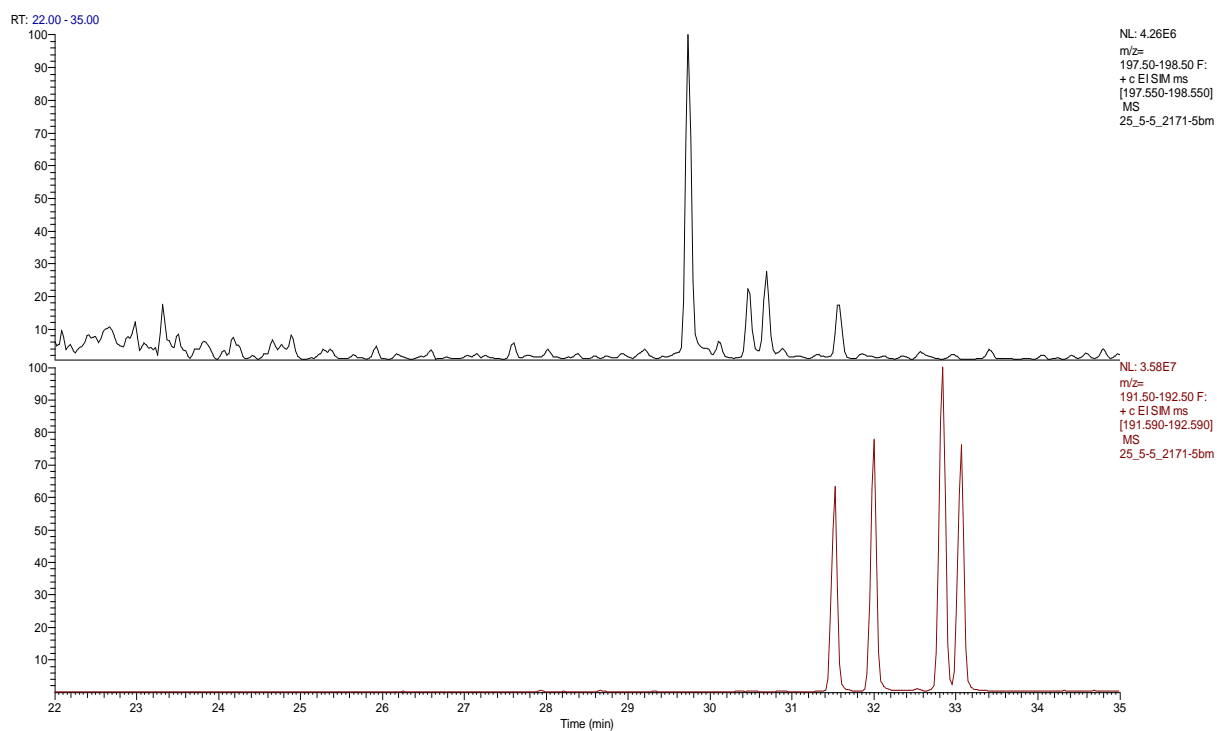
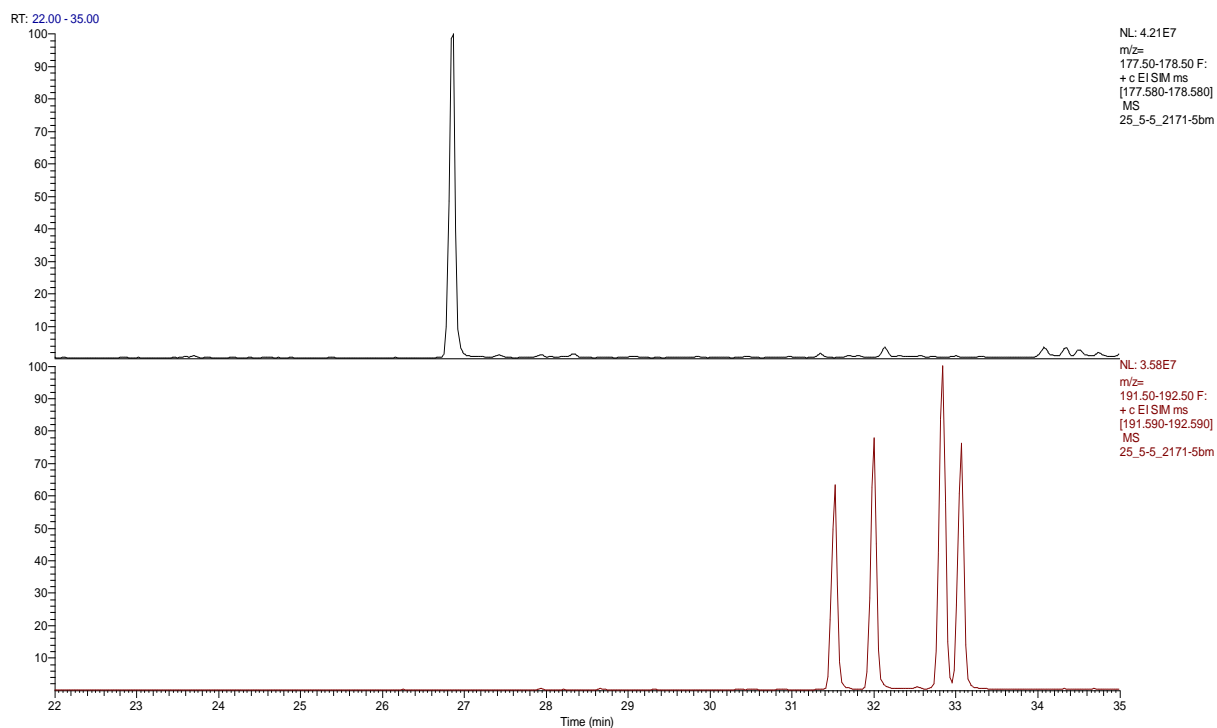
RT: 45.00 - 120.00



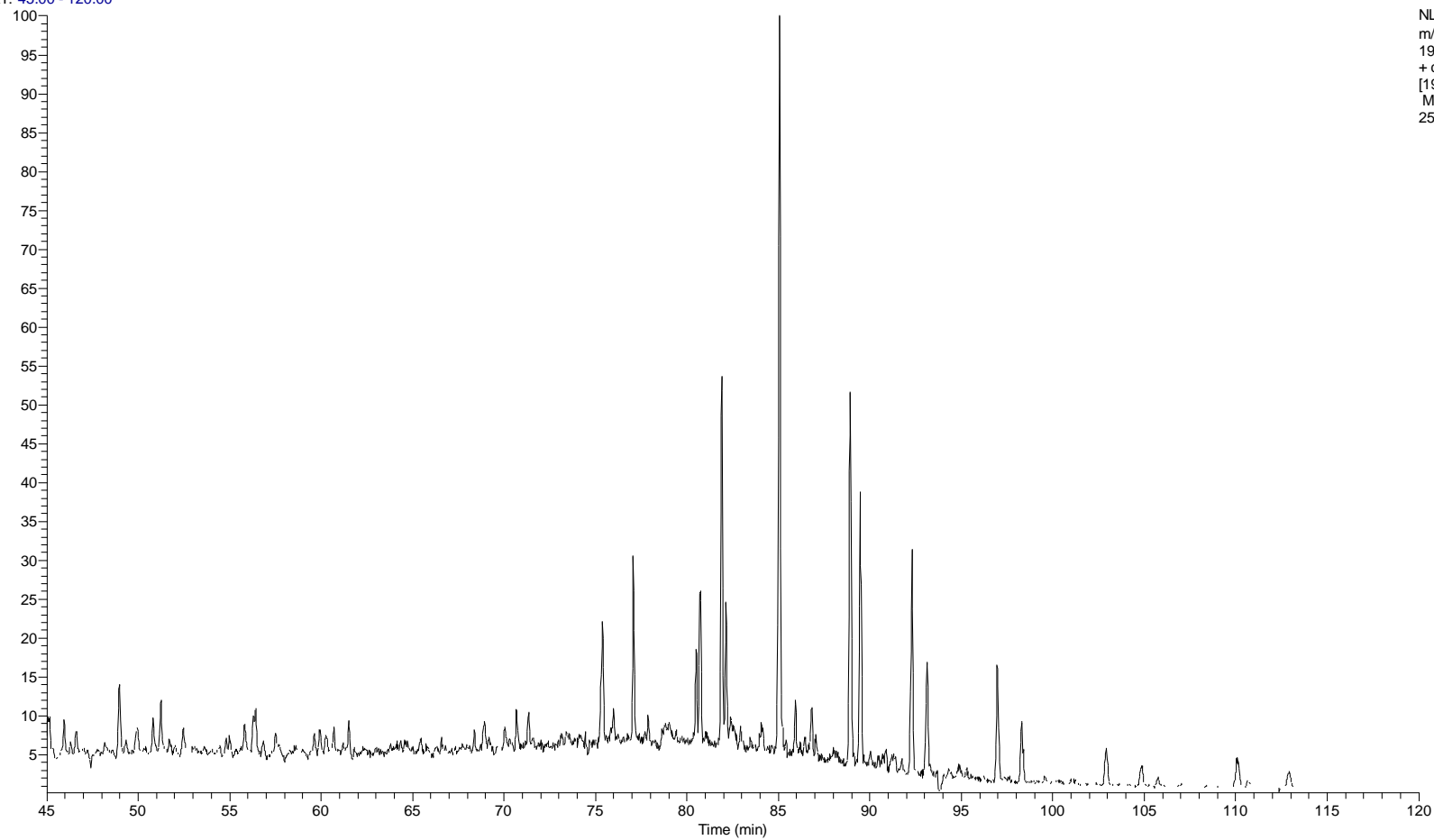
NL: 3.42E6
m/z=
190.50-191.50 F:
+ c EISIM ms
[190.680-191.680]
MS
25_5-5_2171-5bm



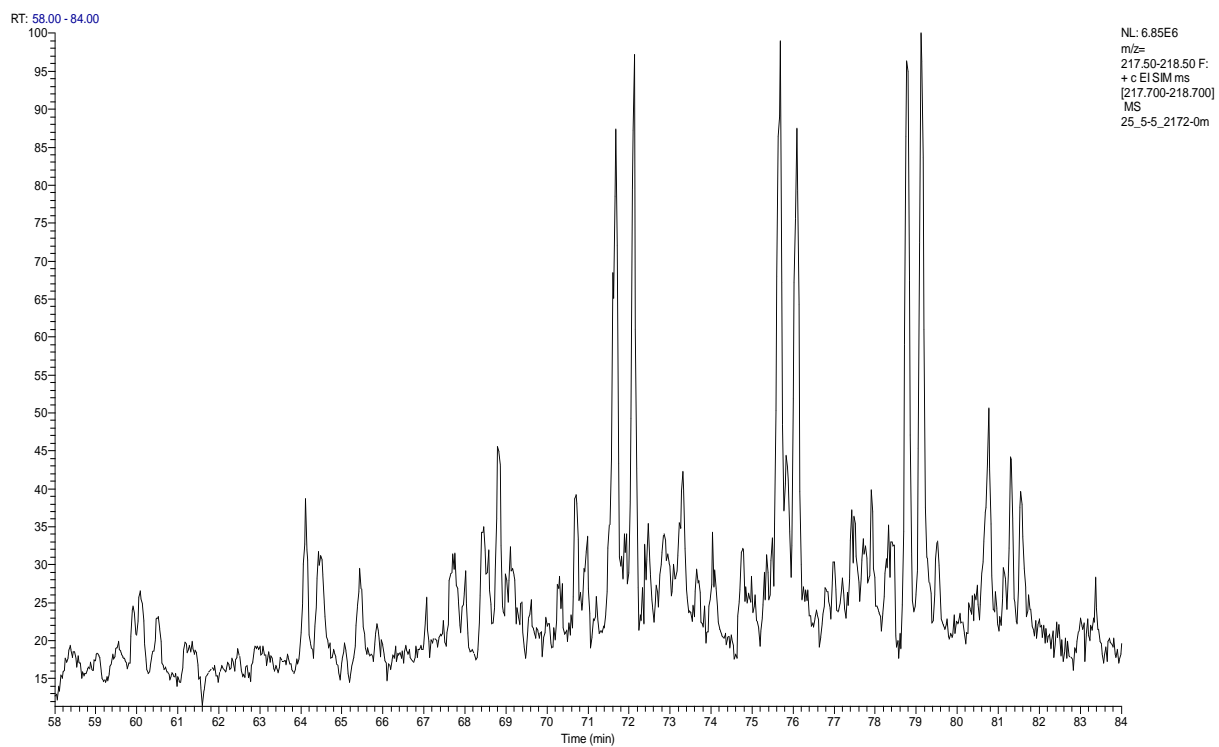
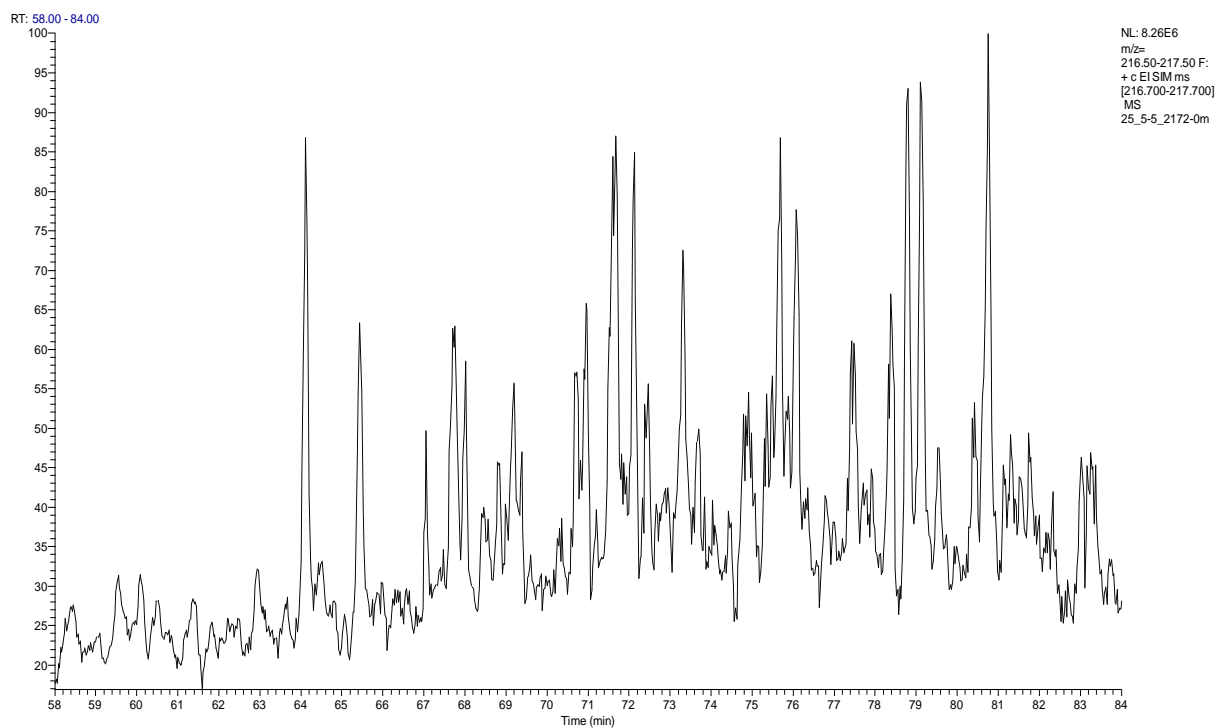


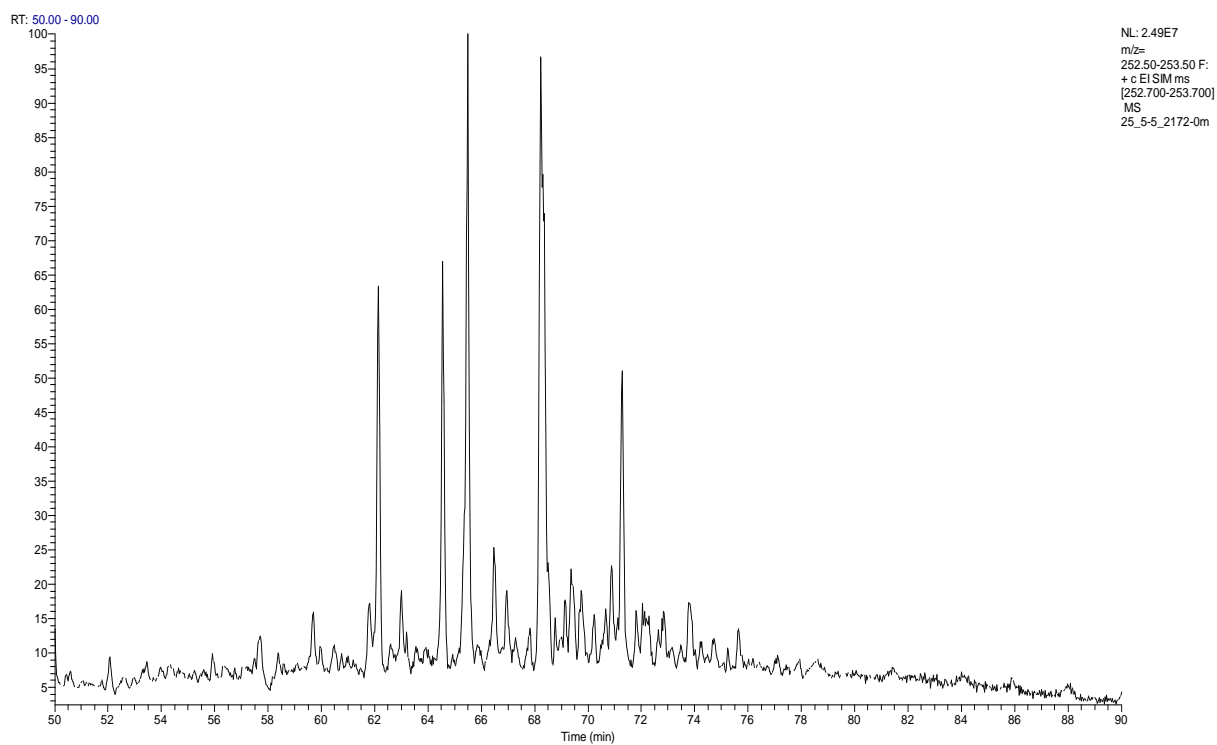
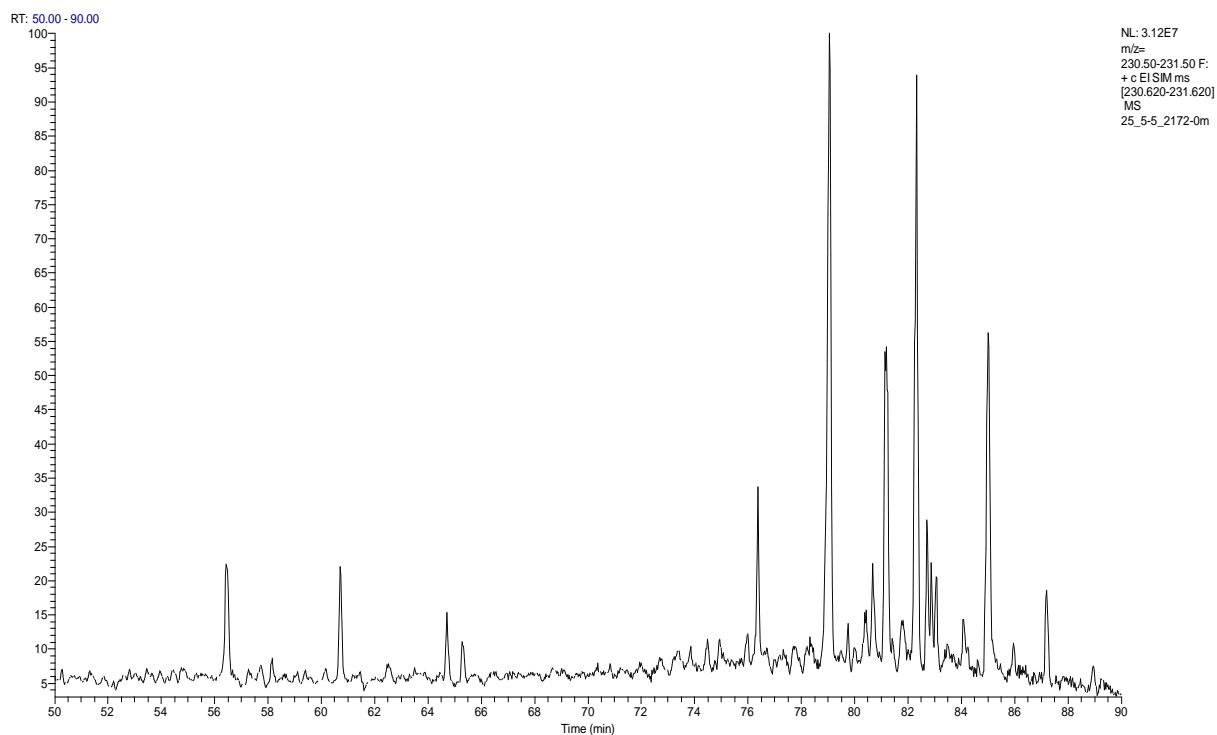


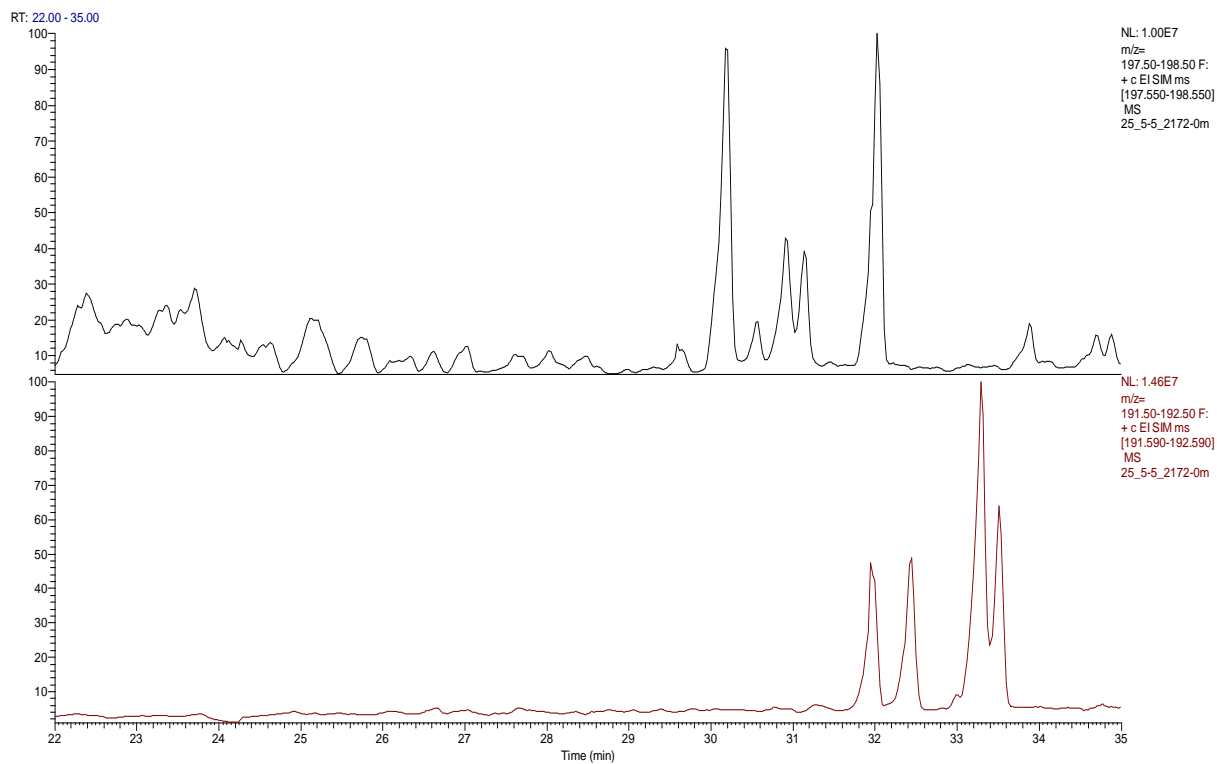
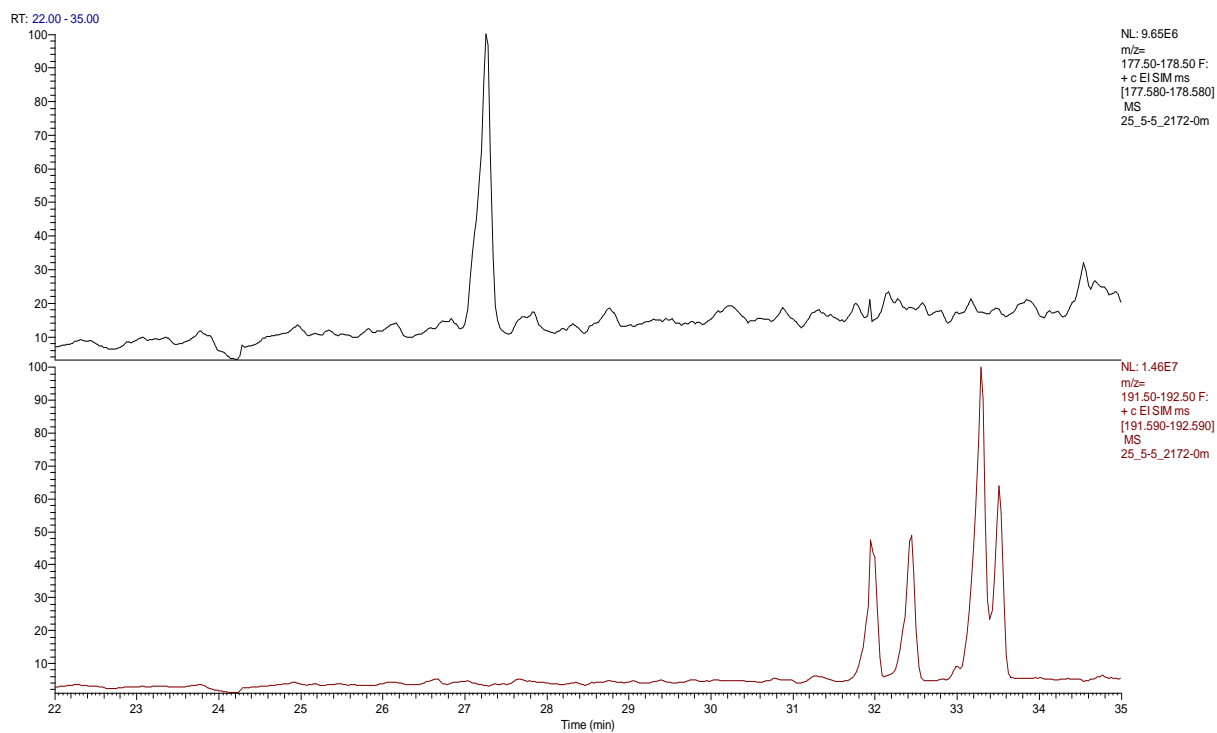
RT: 45.00 - 120.00



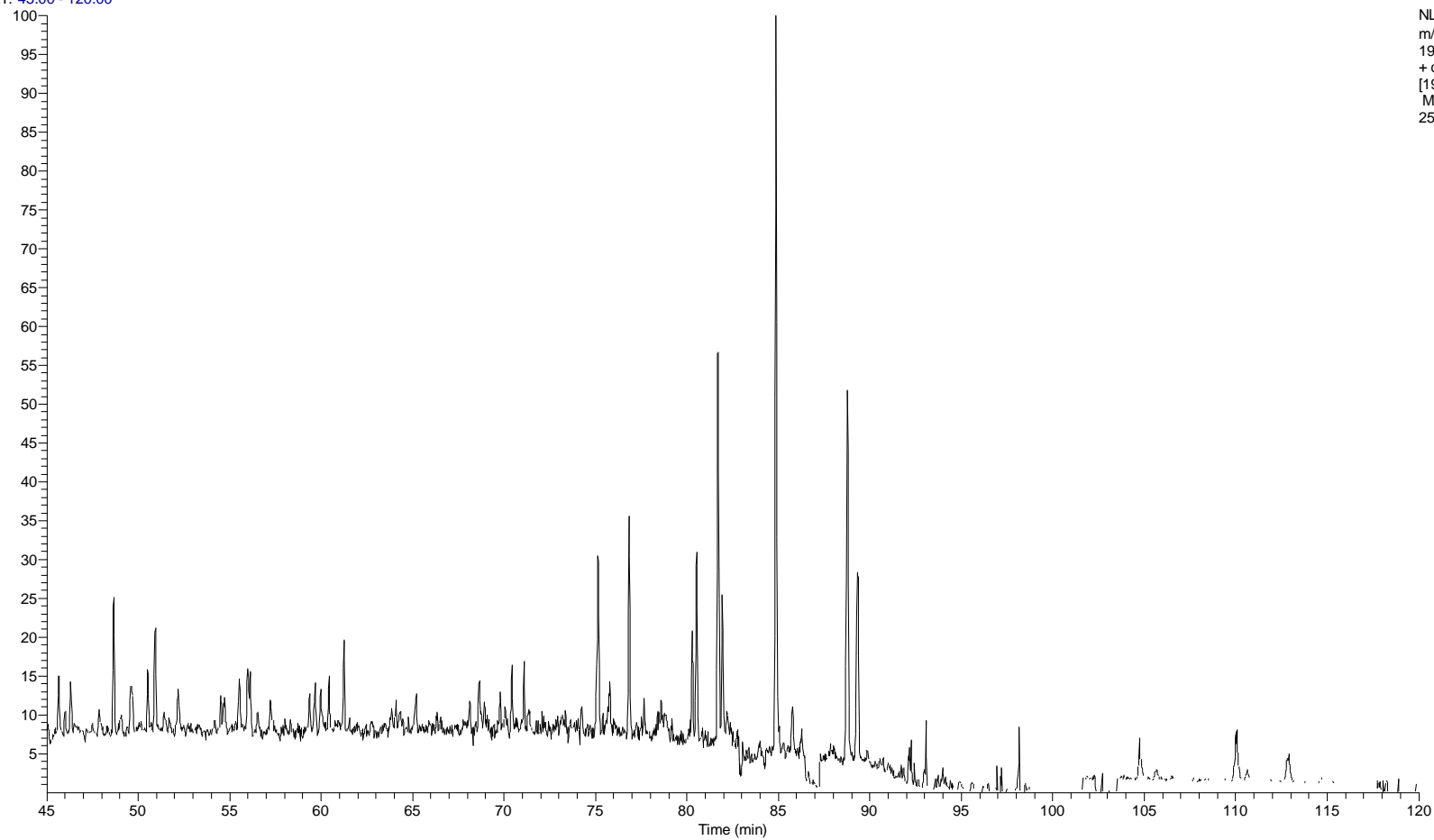
NL: 3.86E7
m/z=
190.50-191.50 F:
+ c EISIM ms
[190.680-191.680]
MS
25_5-5_2172-0m



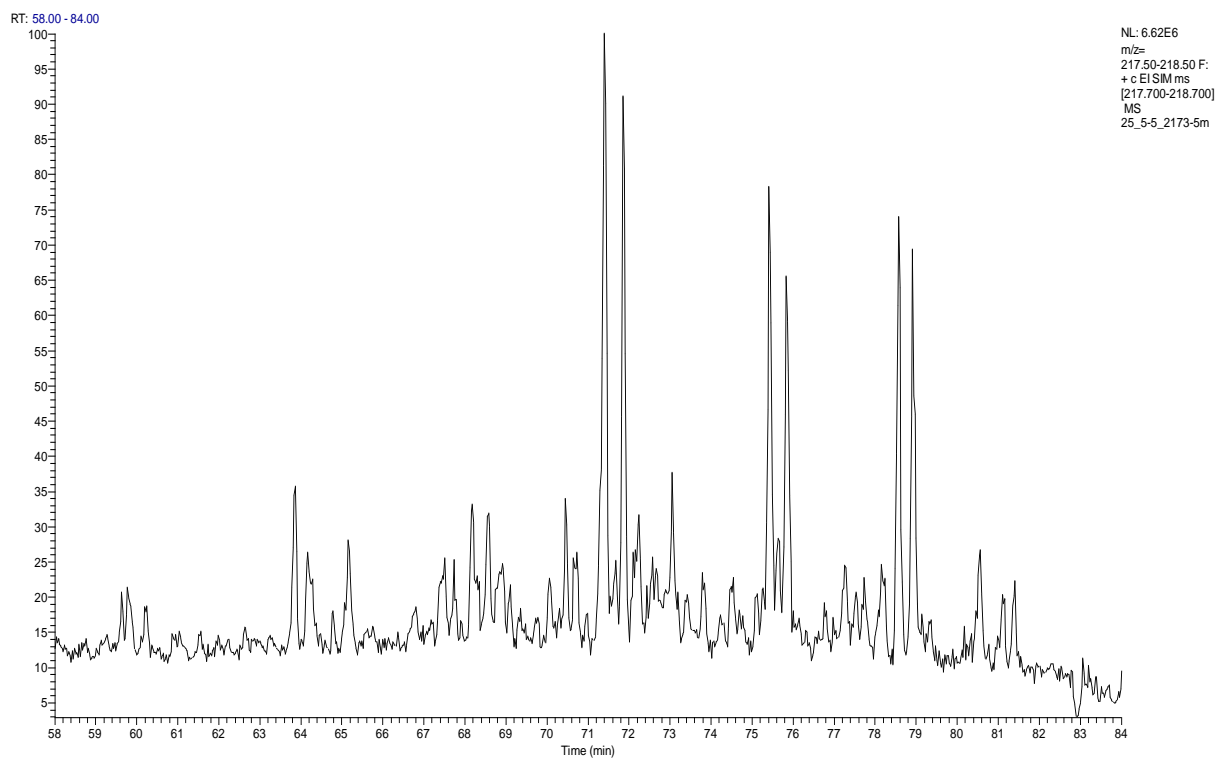
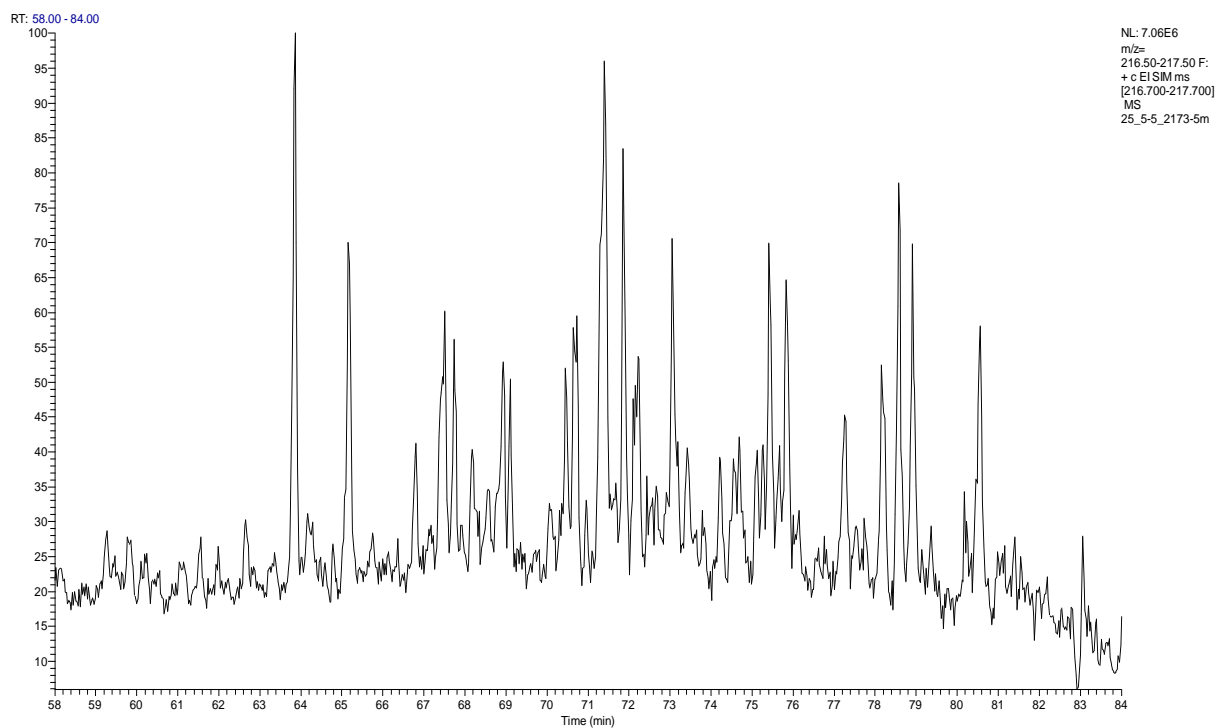


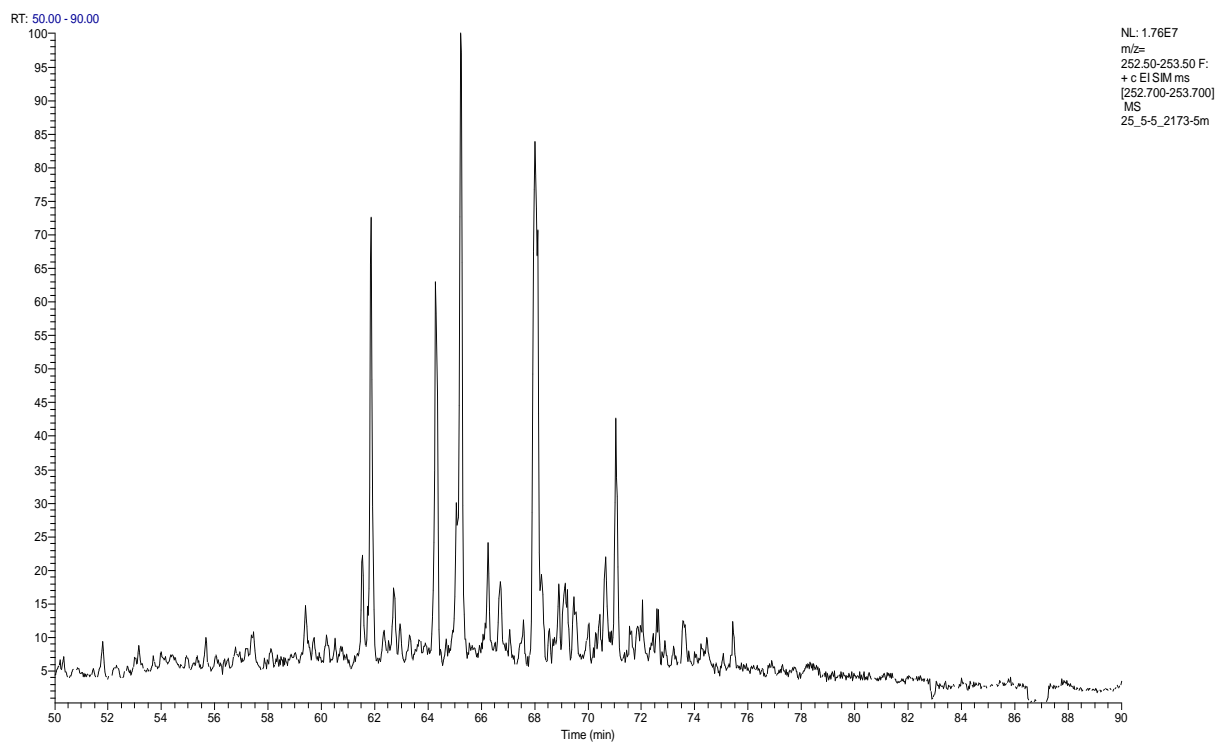
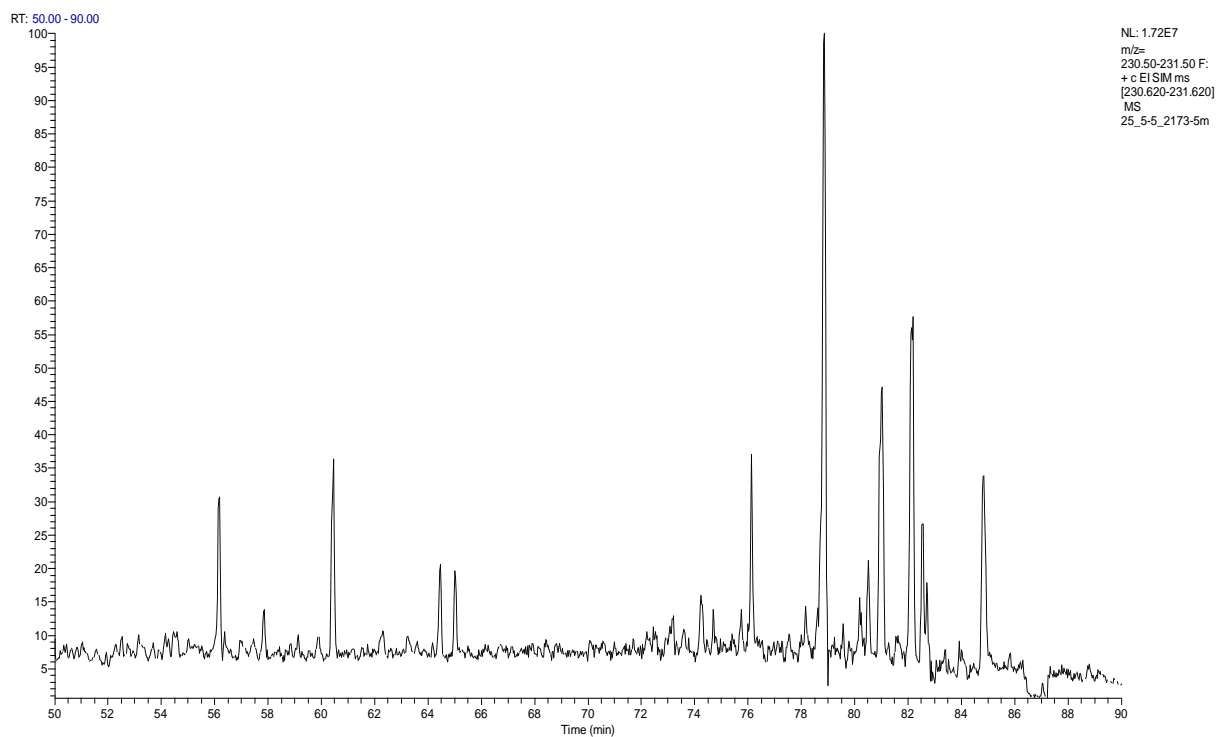


RT: 45.00 - 120.00

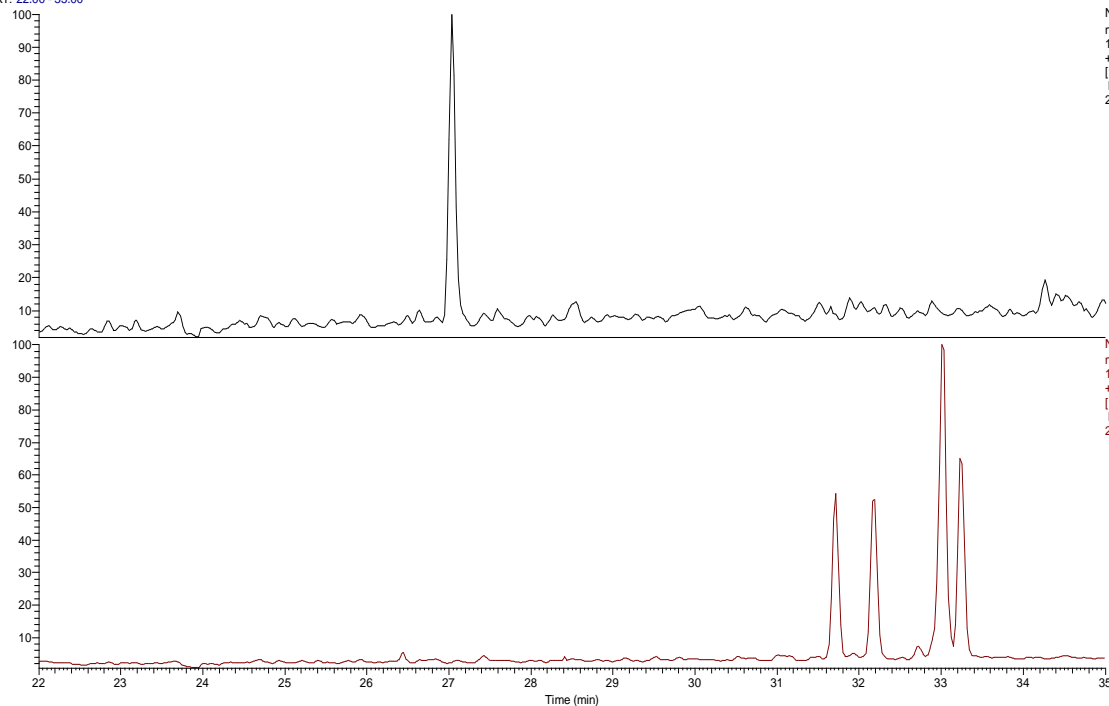


NL: 1.90E7
m/z=
190.50-191.50 F:
+ c EISIM ms
[190.680-191.680]
MS
25_5-5_2173-5m

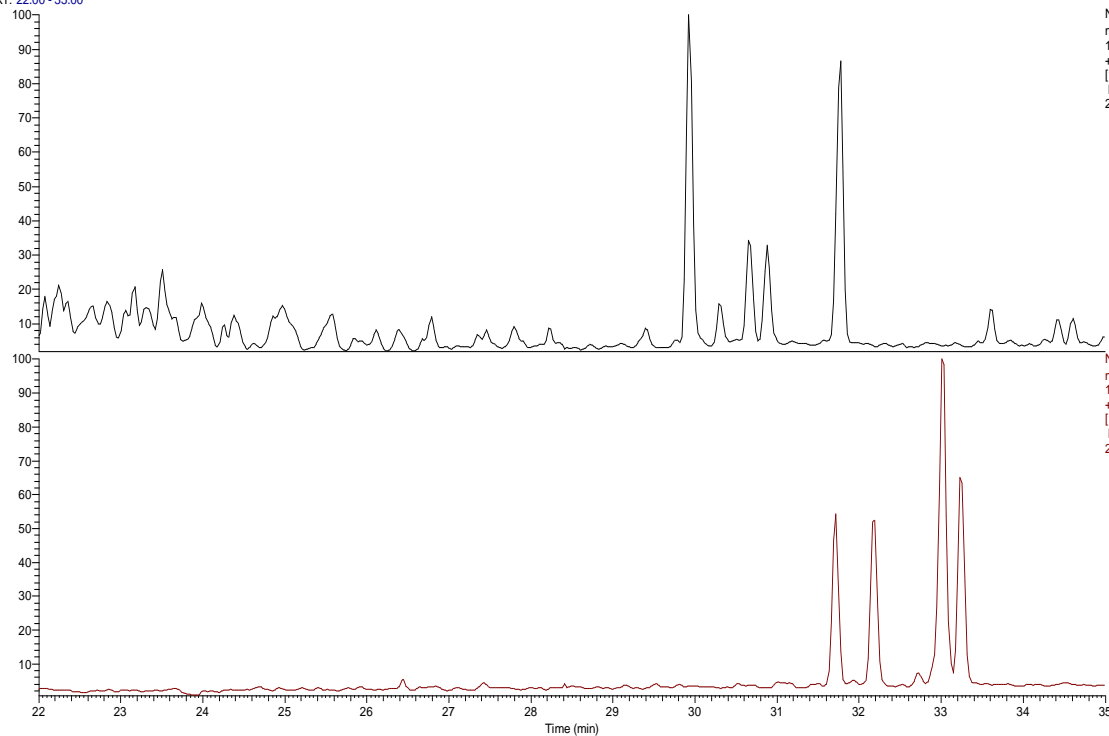




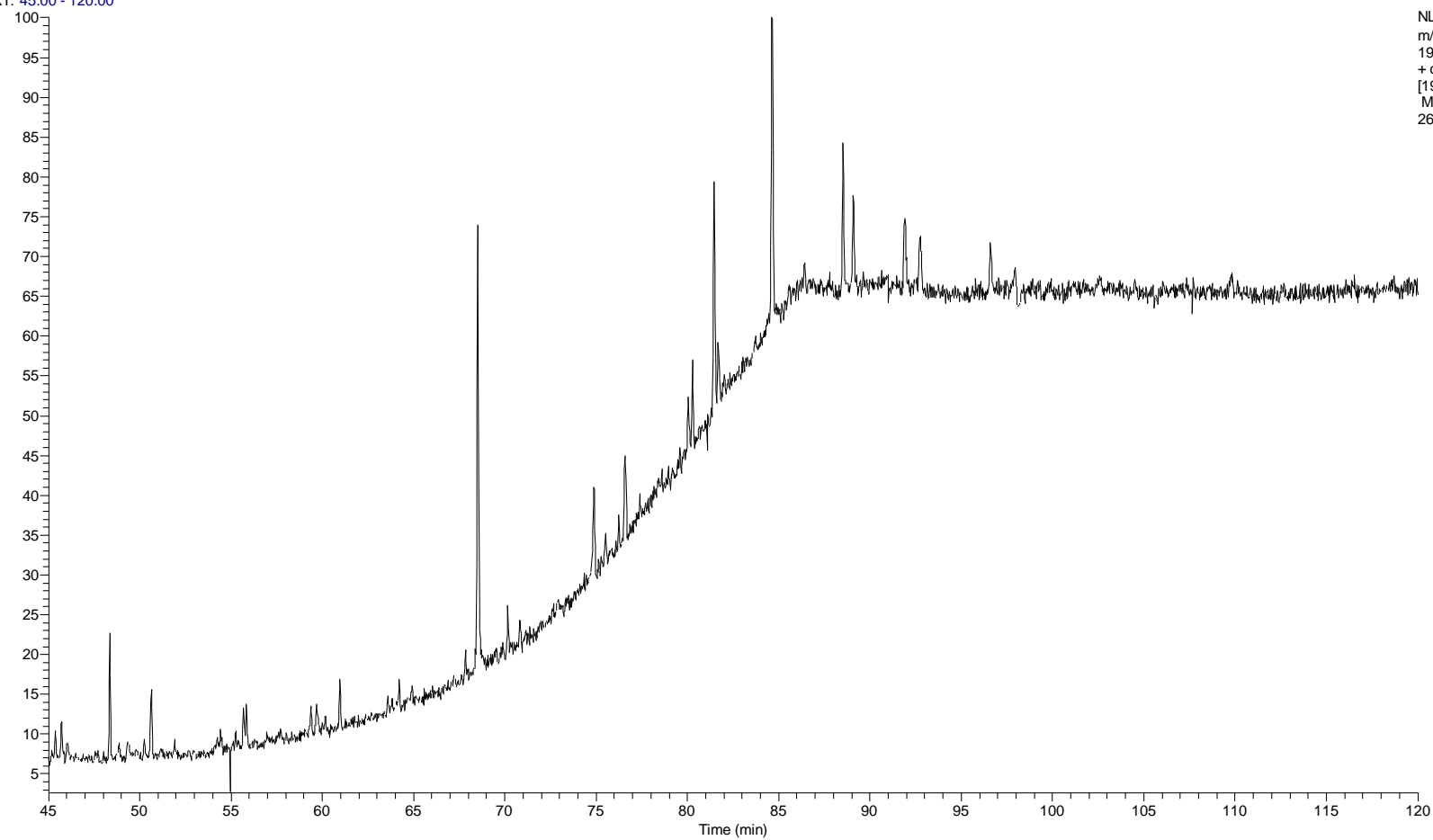
RT: 22.00 - 35.00



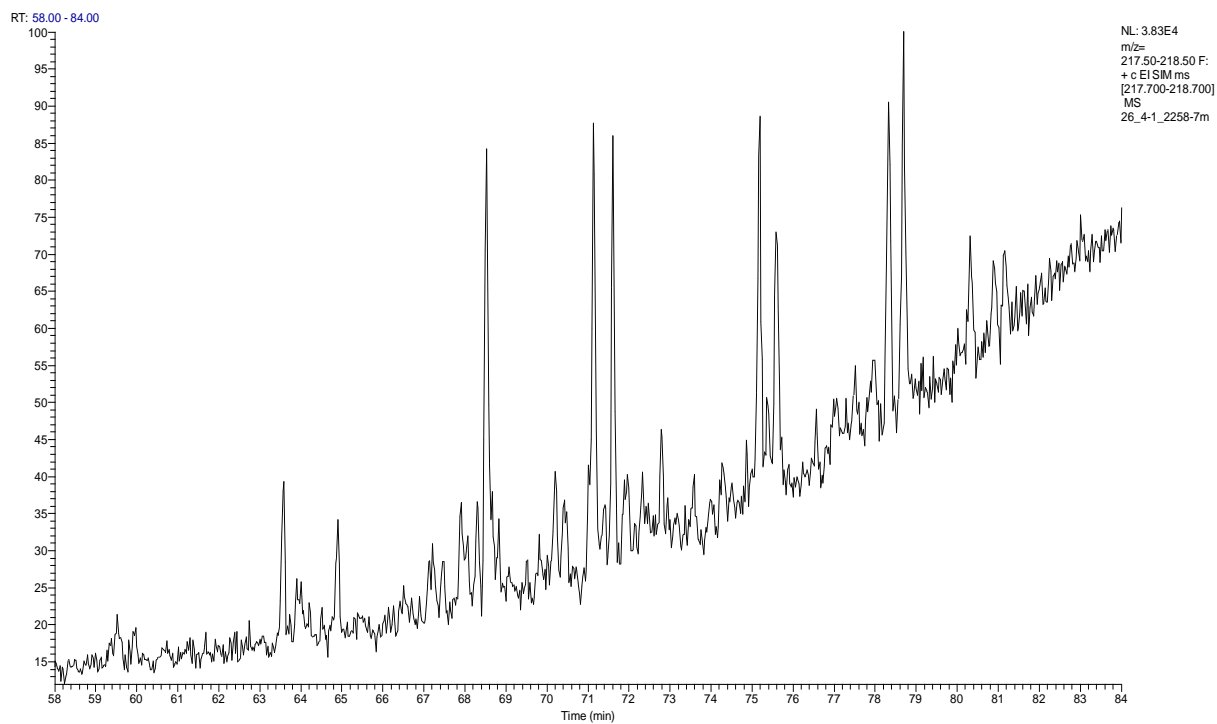
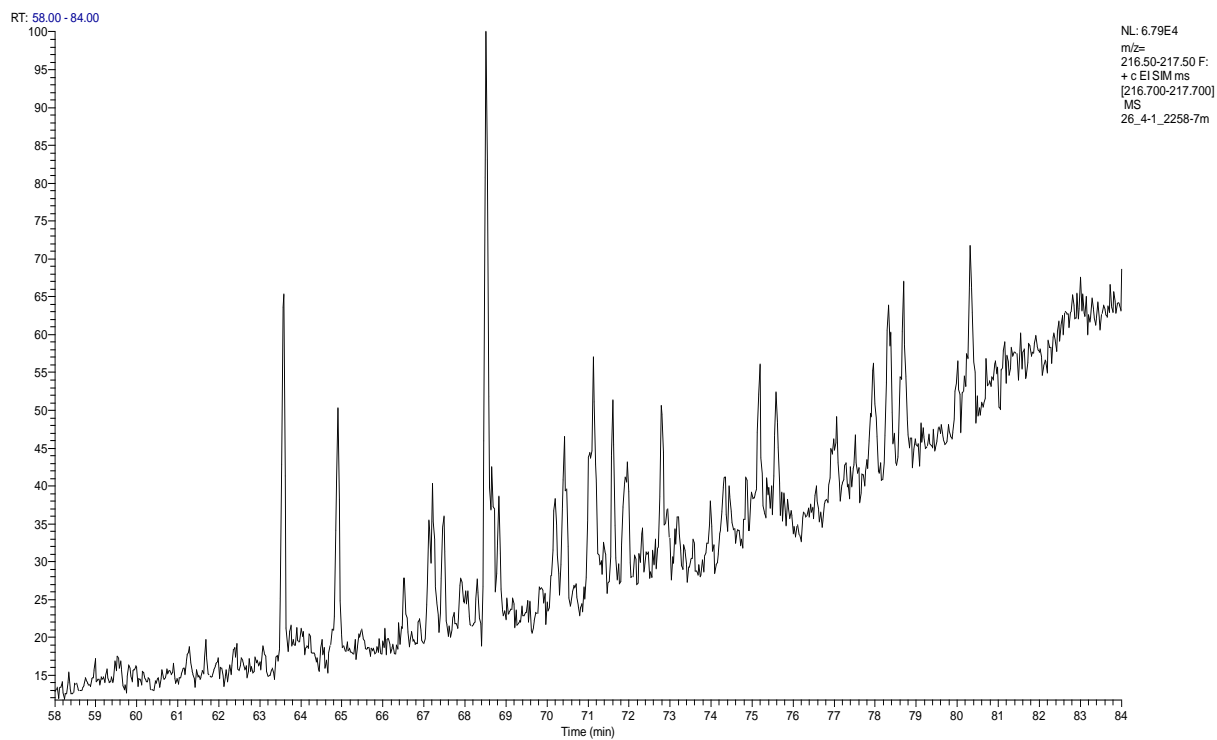
RT: 22.00 - 35.00

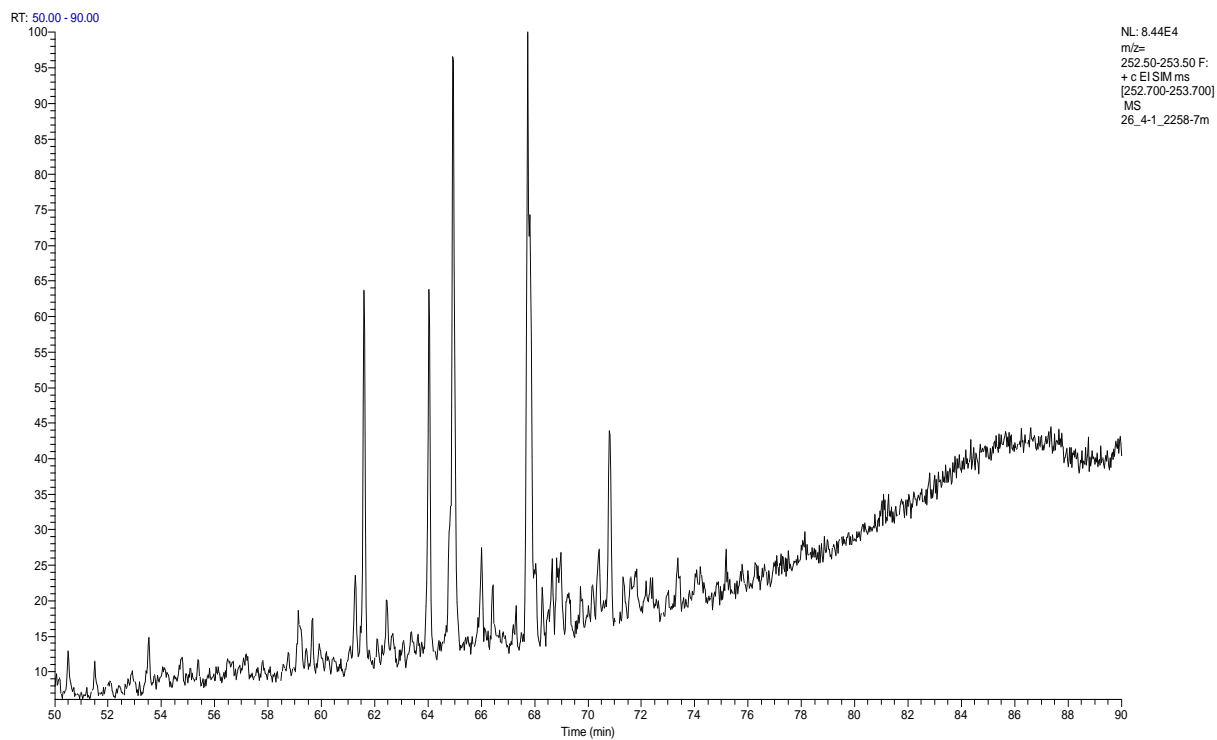
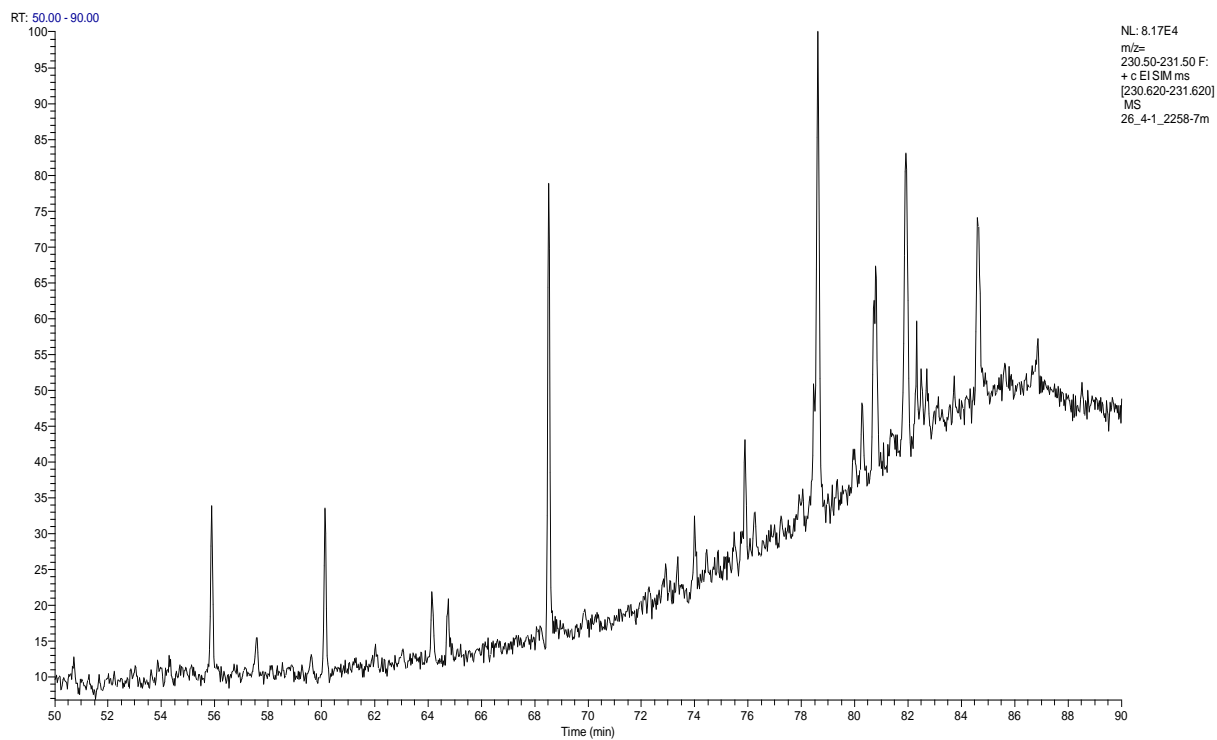


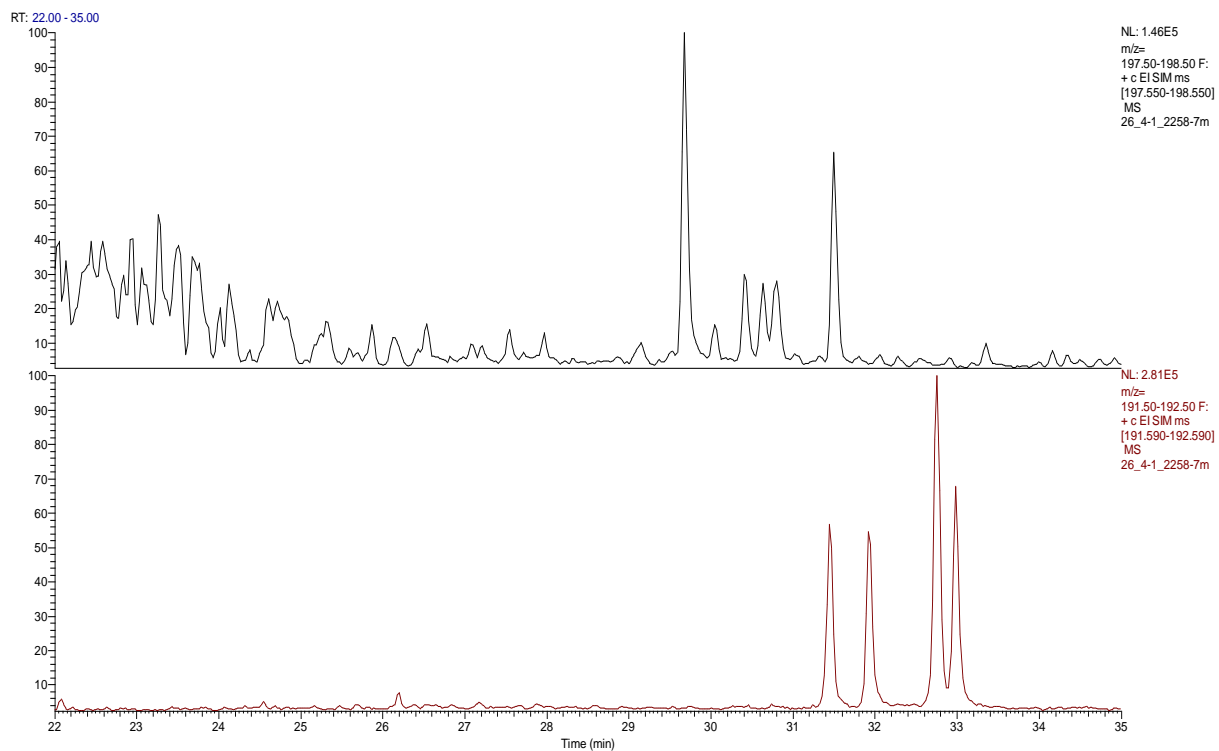
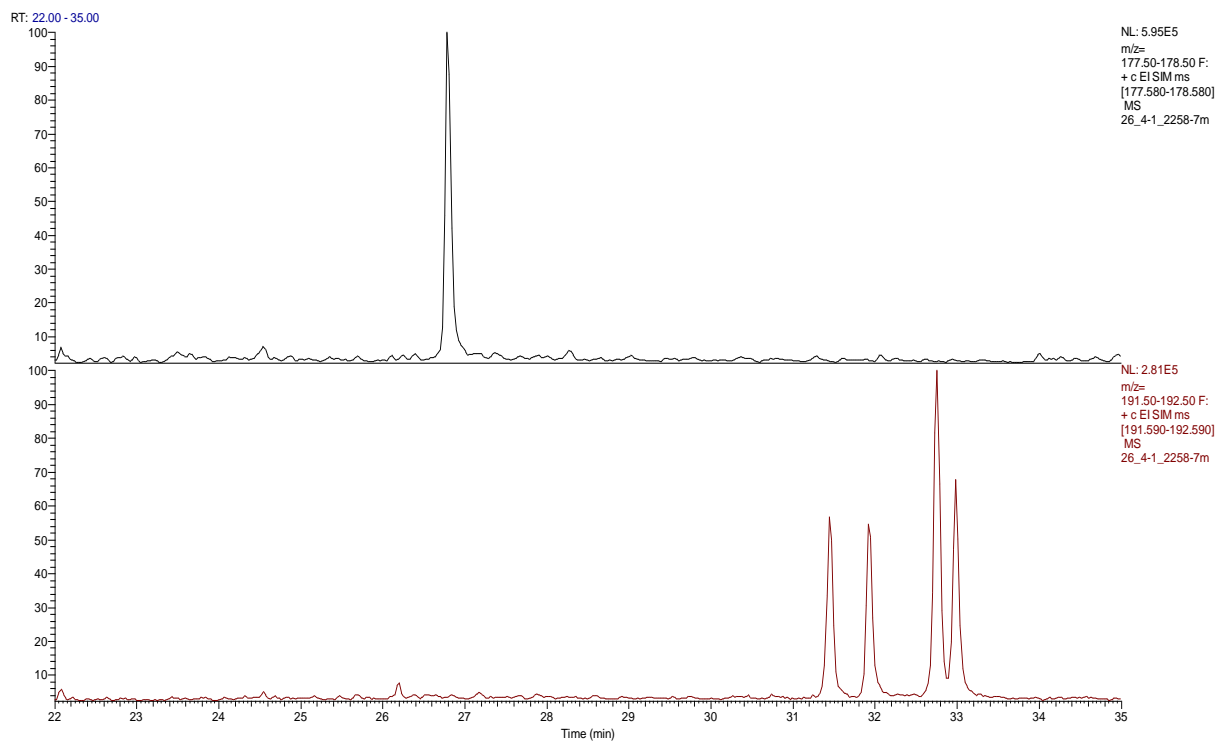
RT: 45.00 - 120.00



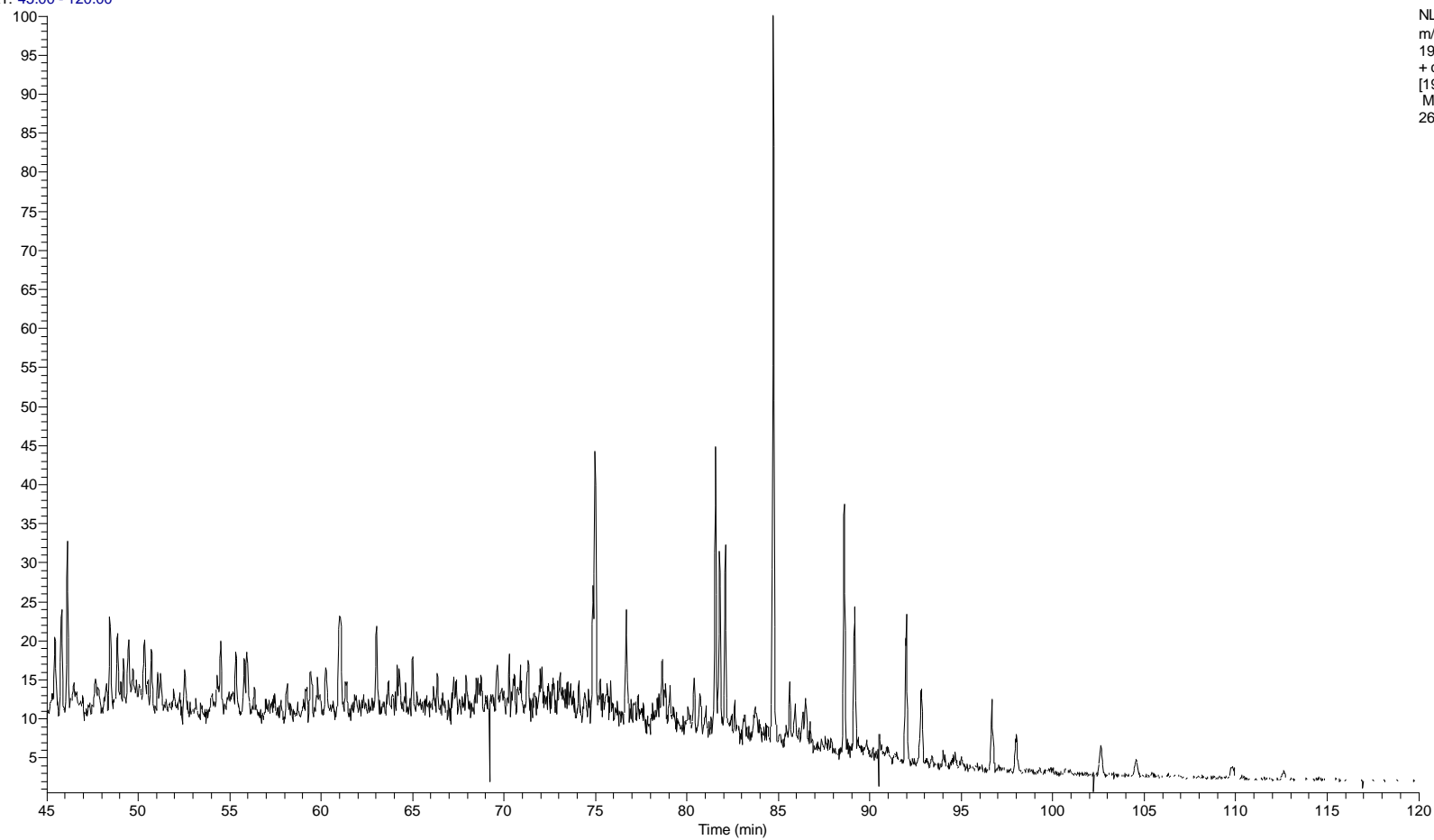
NL: 2.18E5
m/z=
190.50-191.50 F:
+ c EISIM ms
[190.680-191.680]
MS
26_4-1_2258-7m



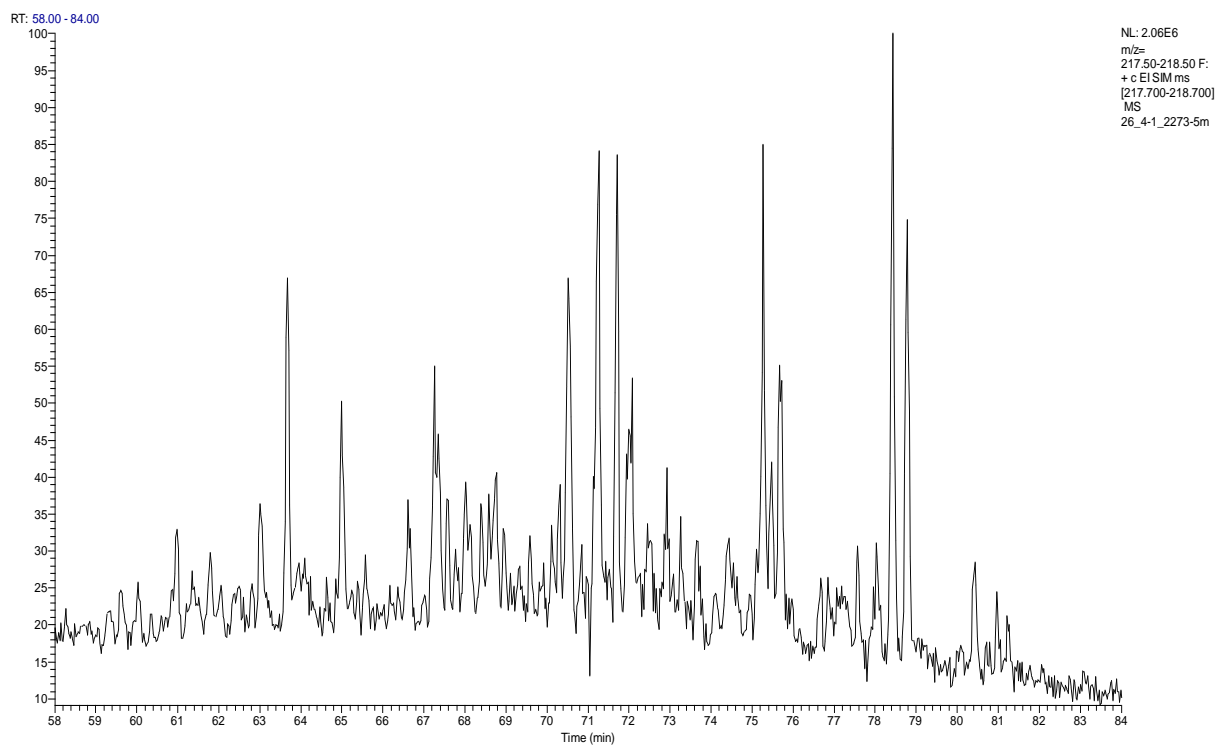
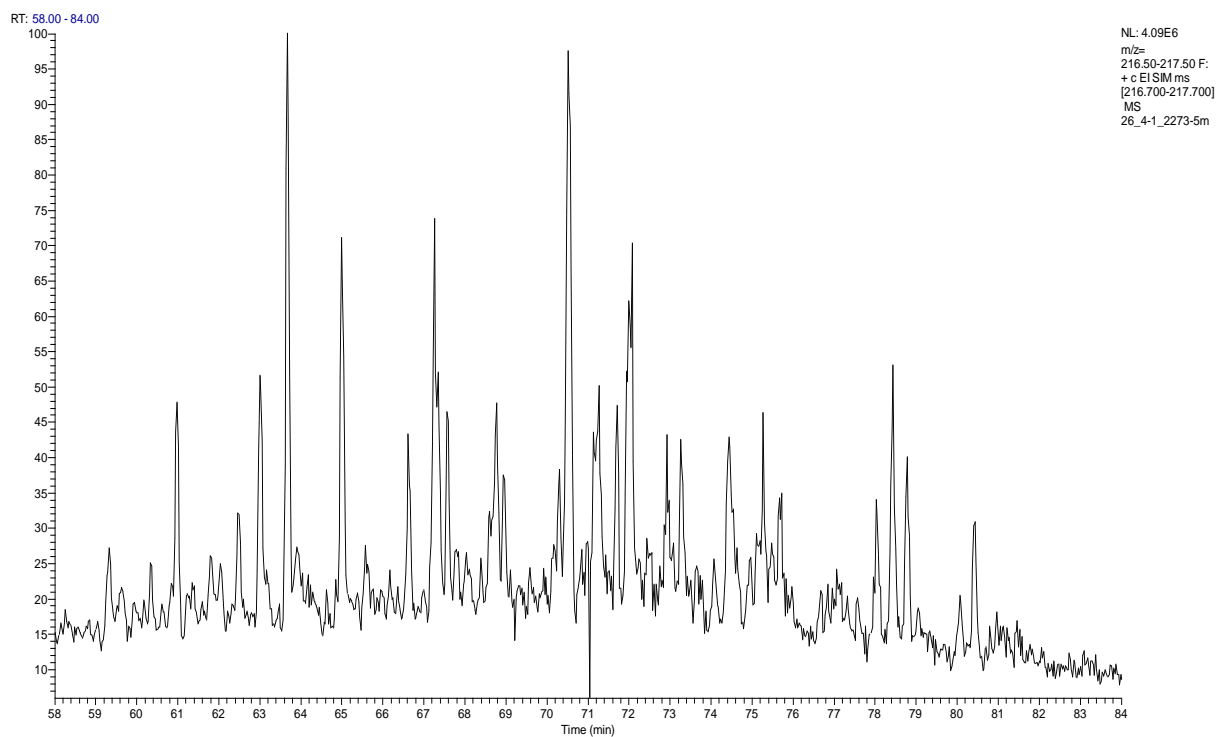


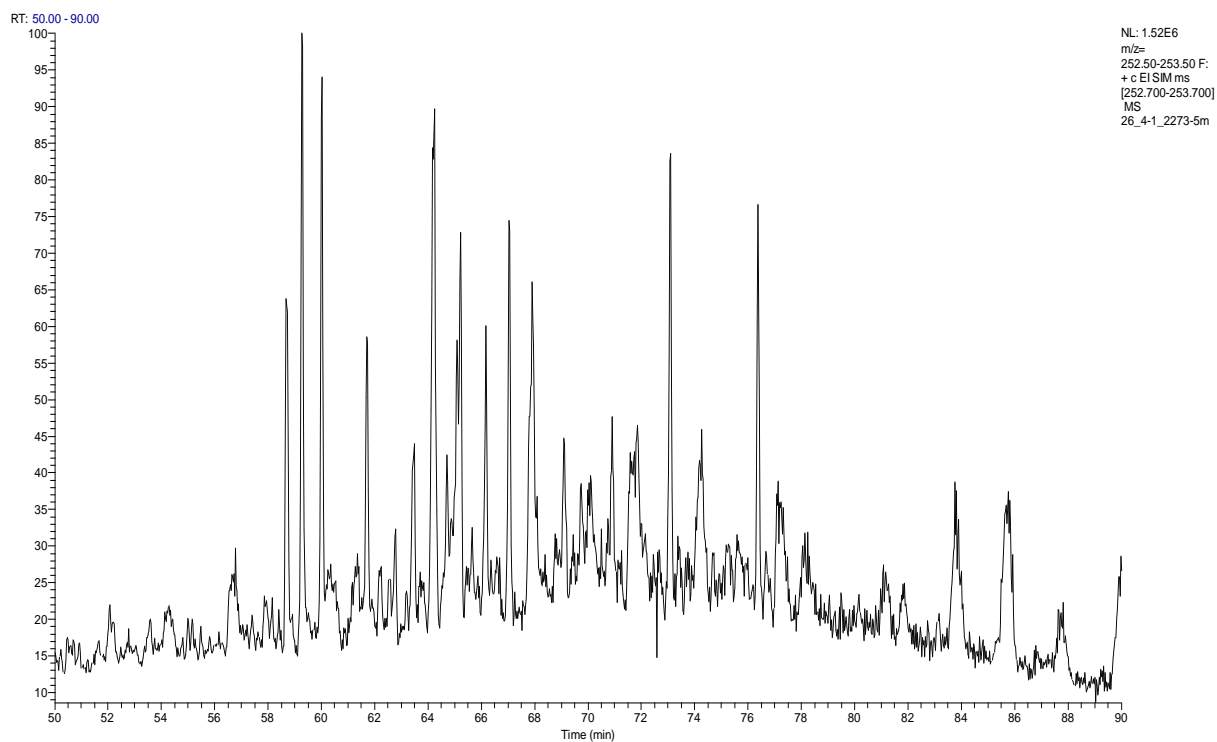
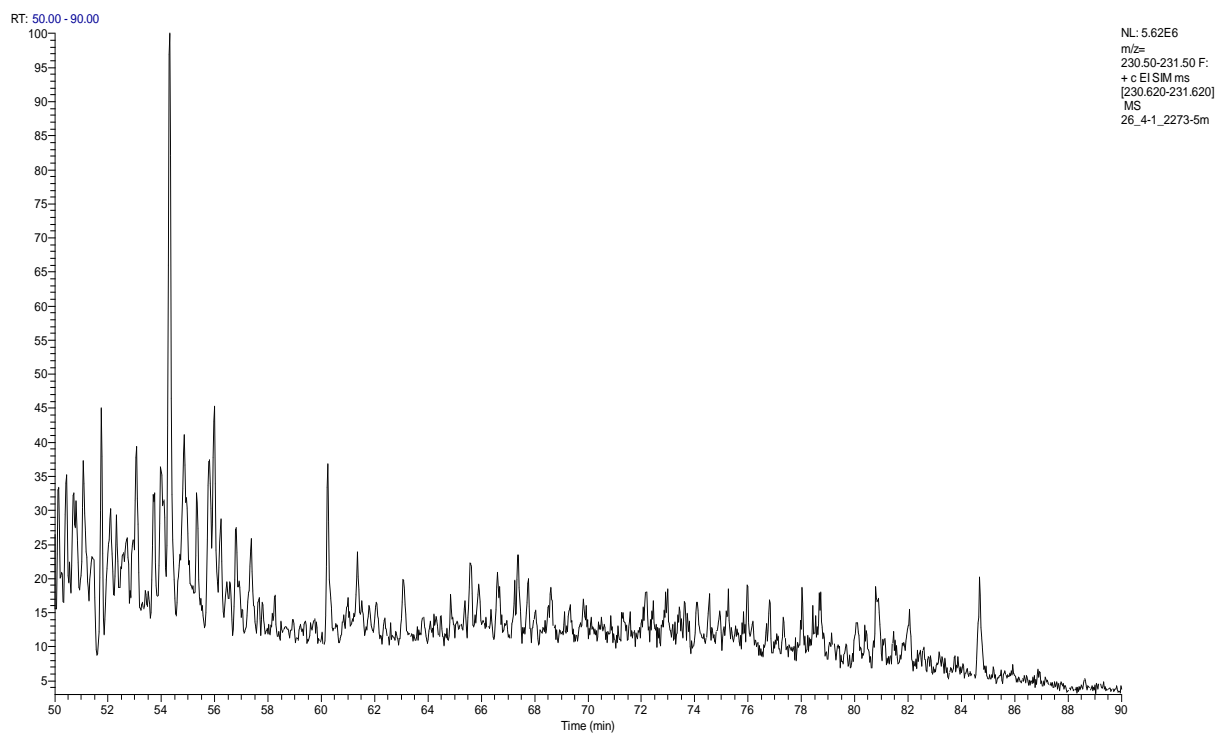


RT: 45.00 - 120.00

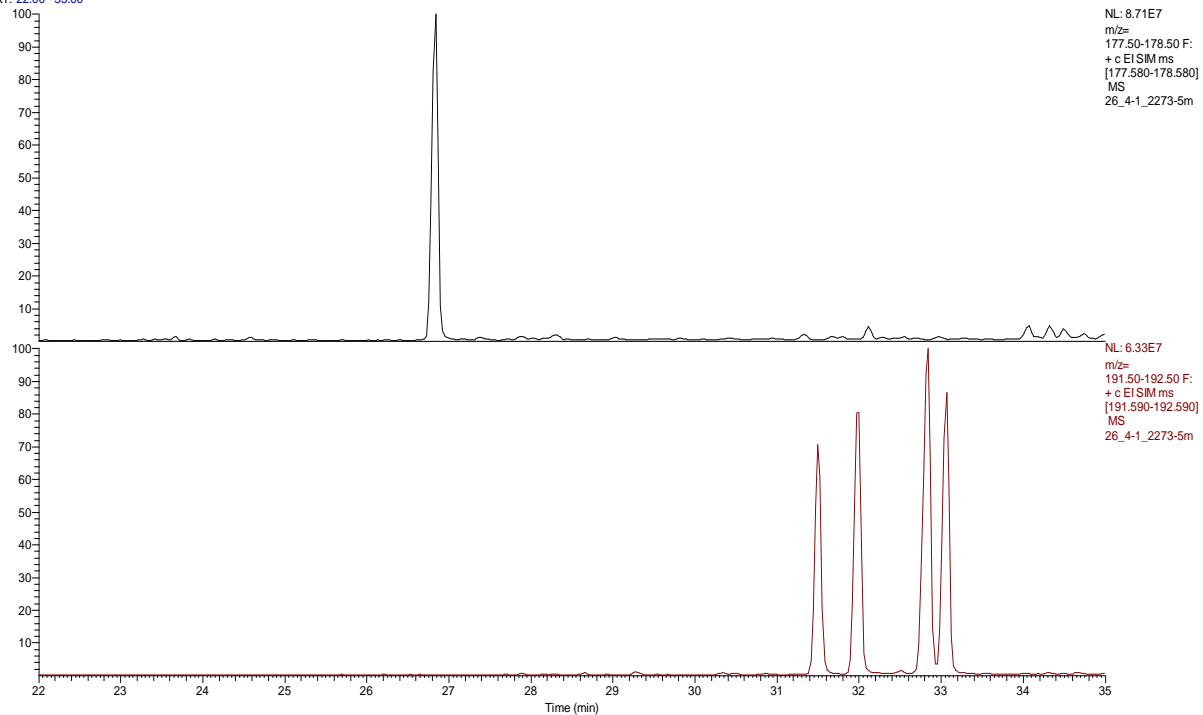


NL: 8.41E6
m/z=
190.50-191.50 F:
+ c EISIM ms
[190.680-191.680]
MS
26_4-1_2273-5m

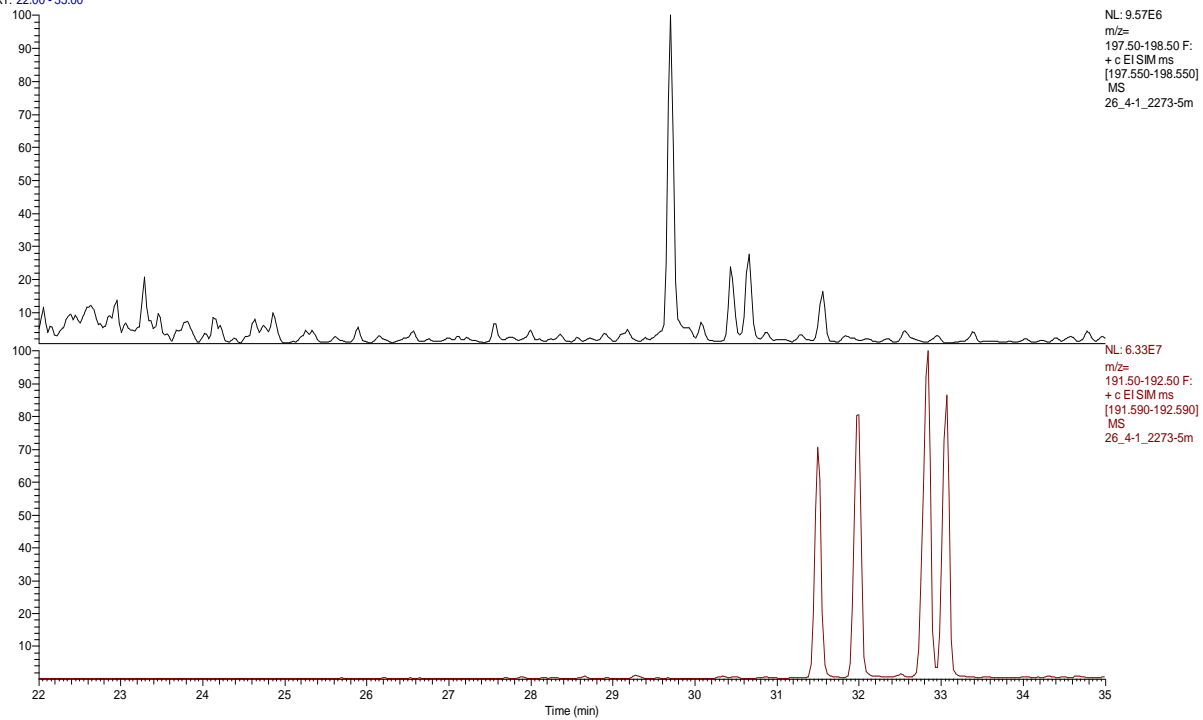


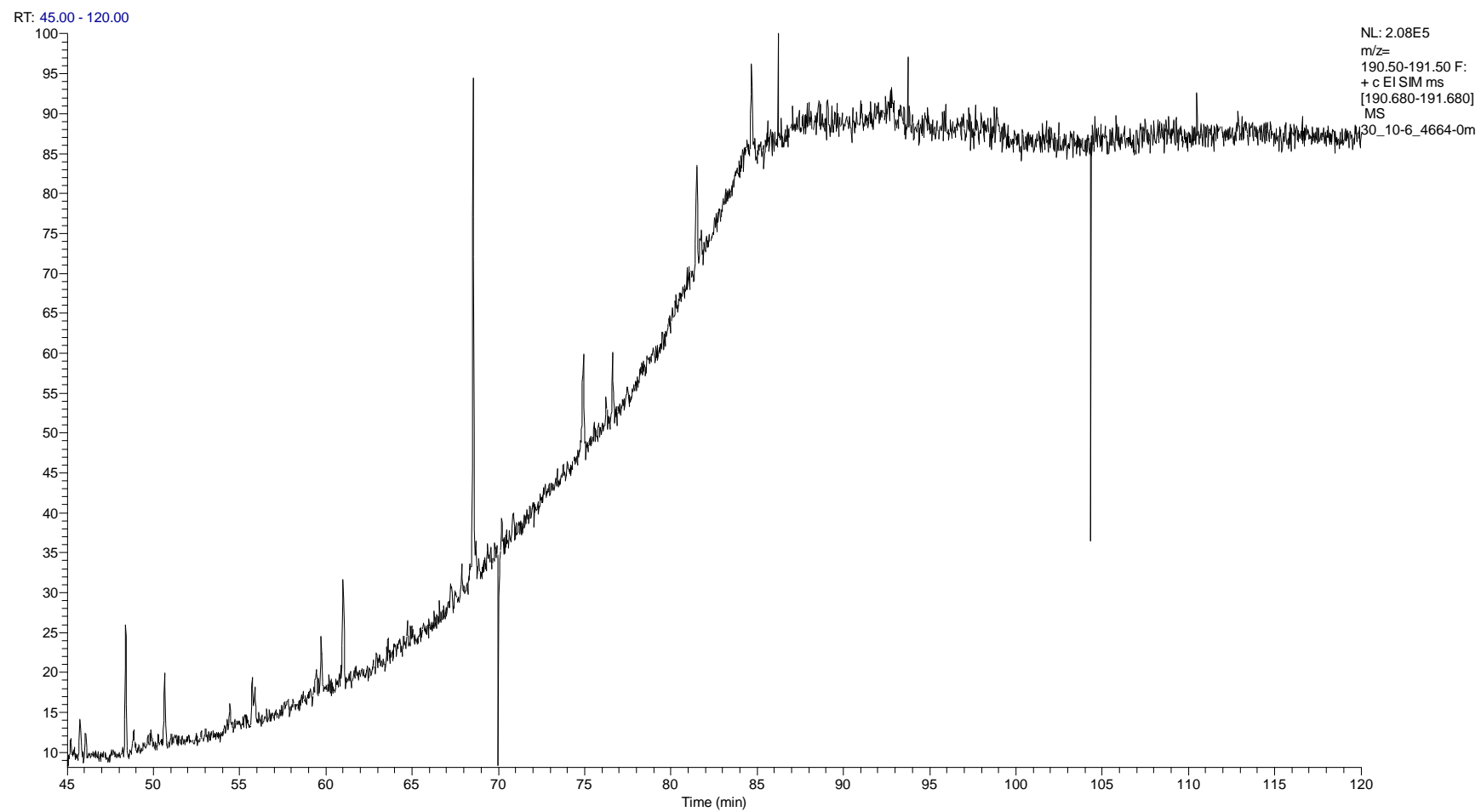


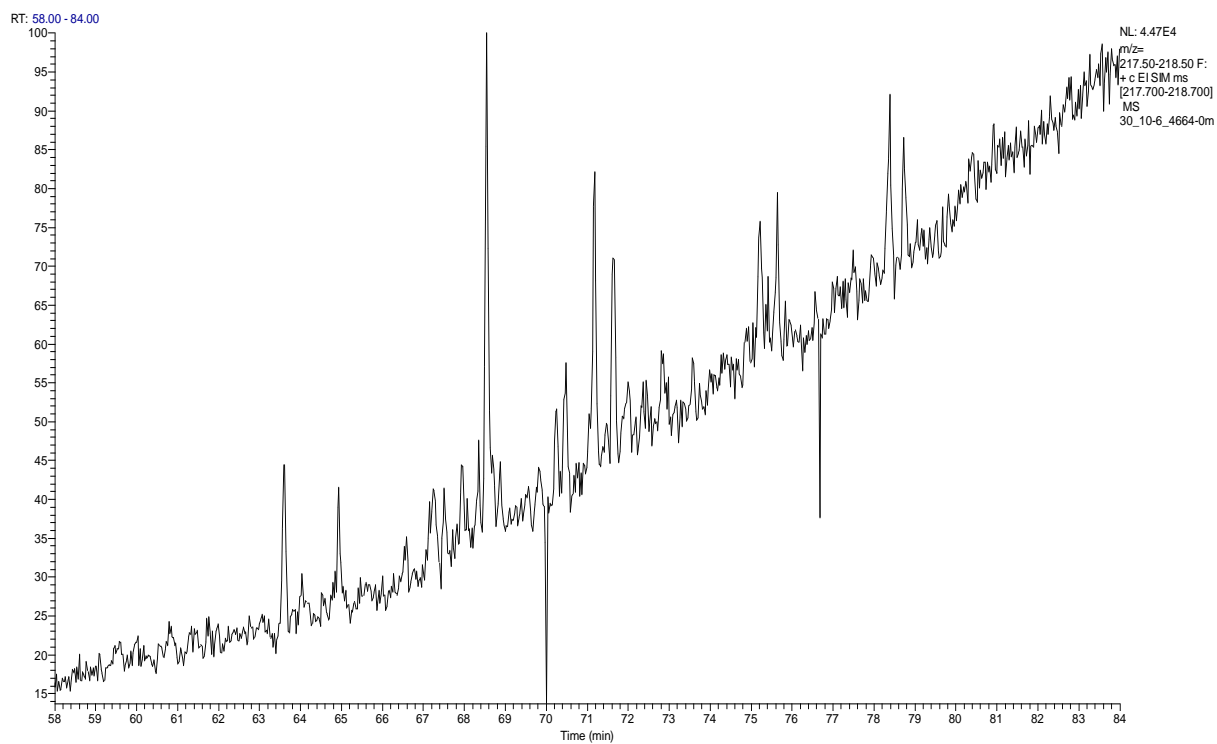
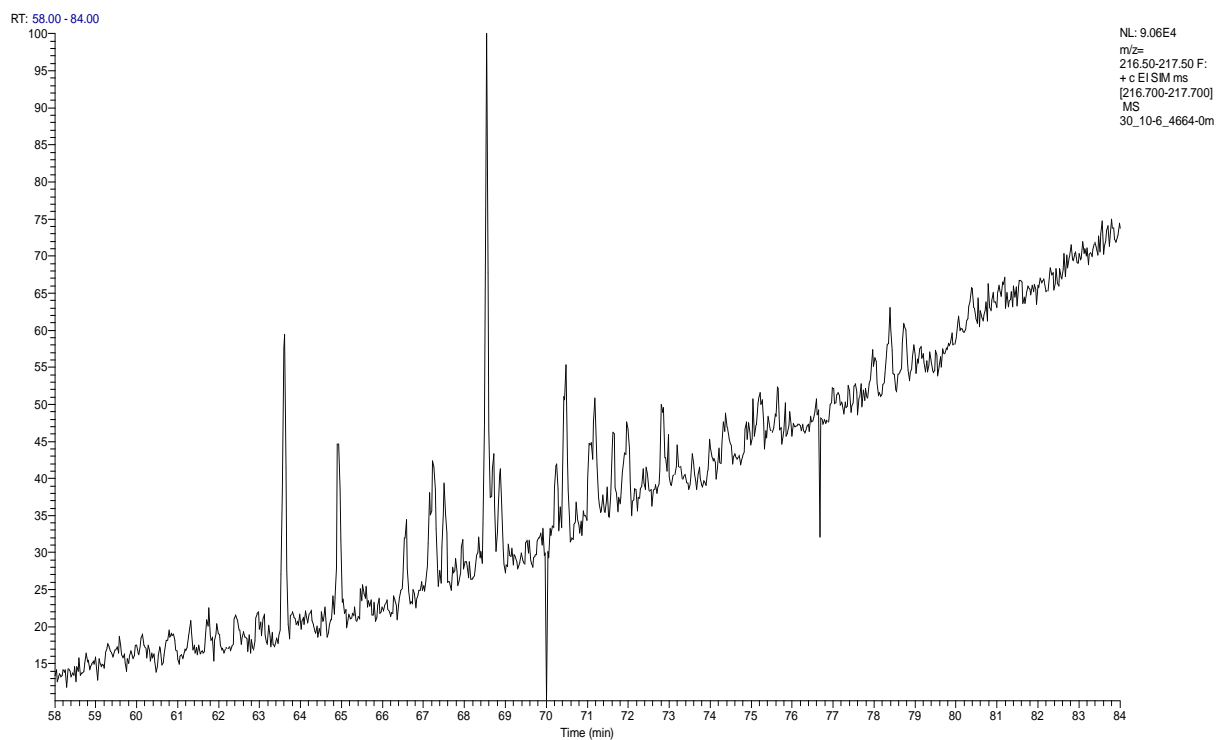
RT: 22.00 - 35.00

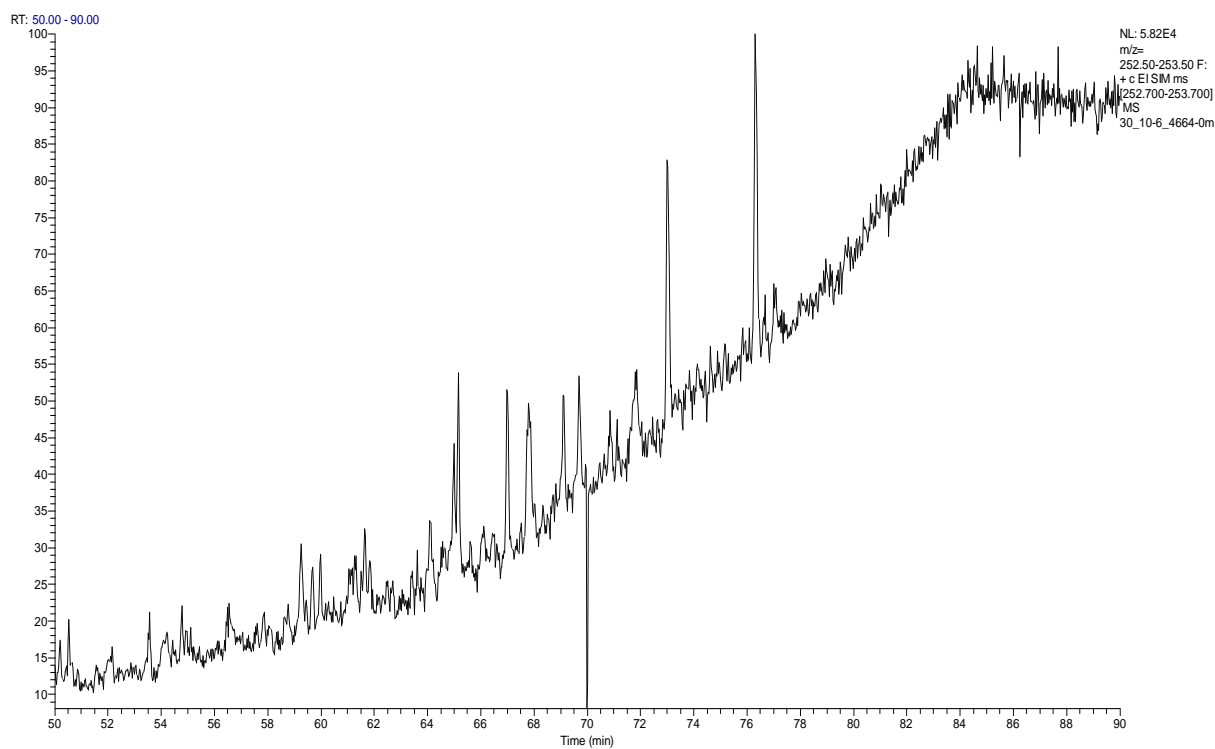
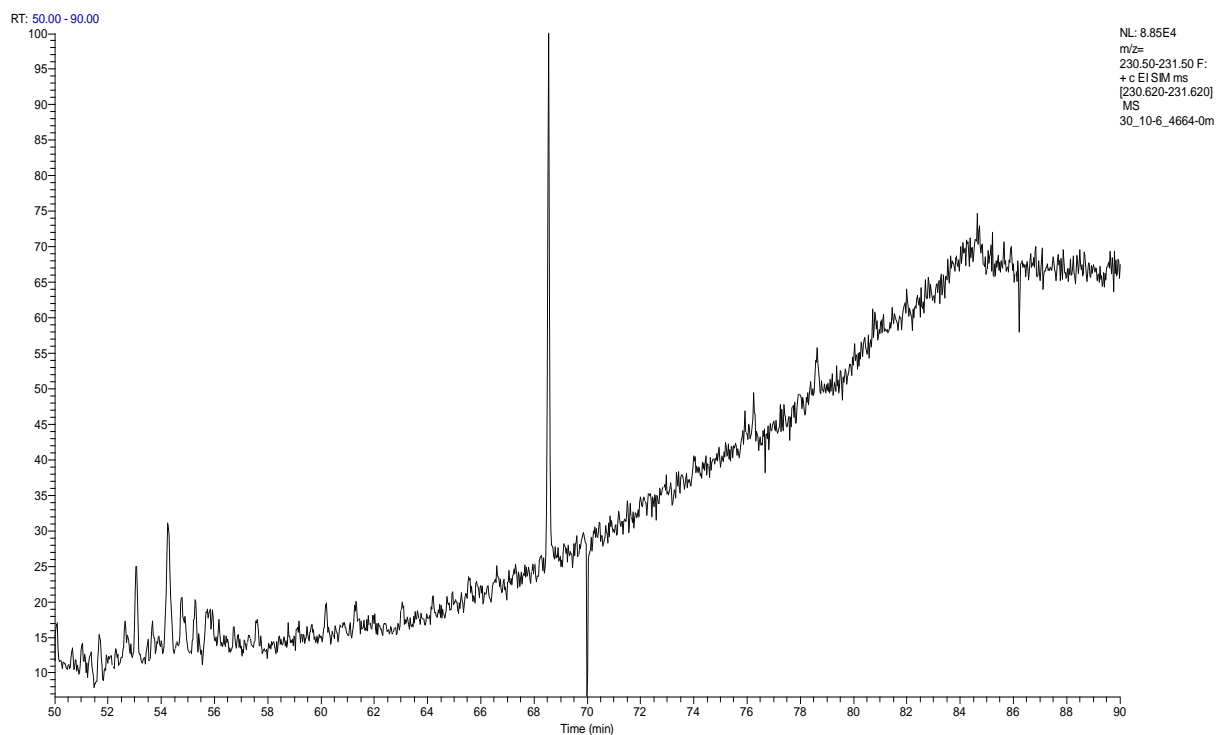


RT: 22.00 - 35.00

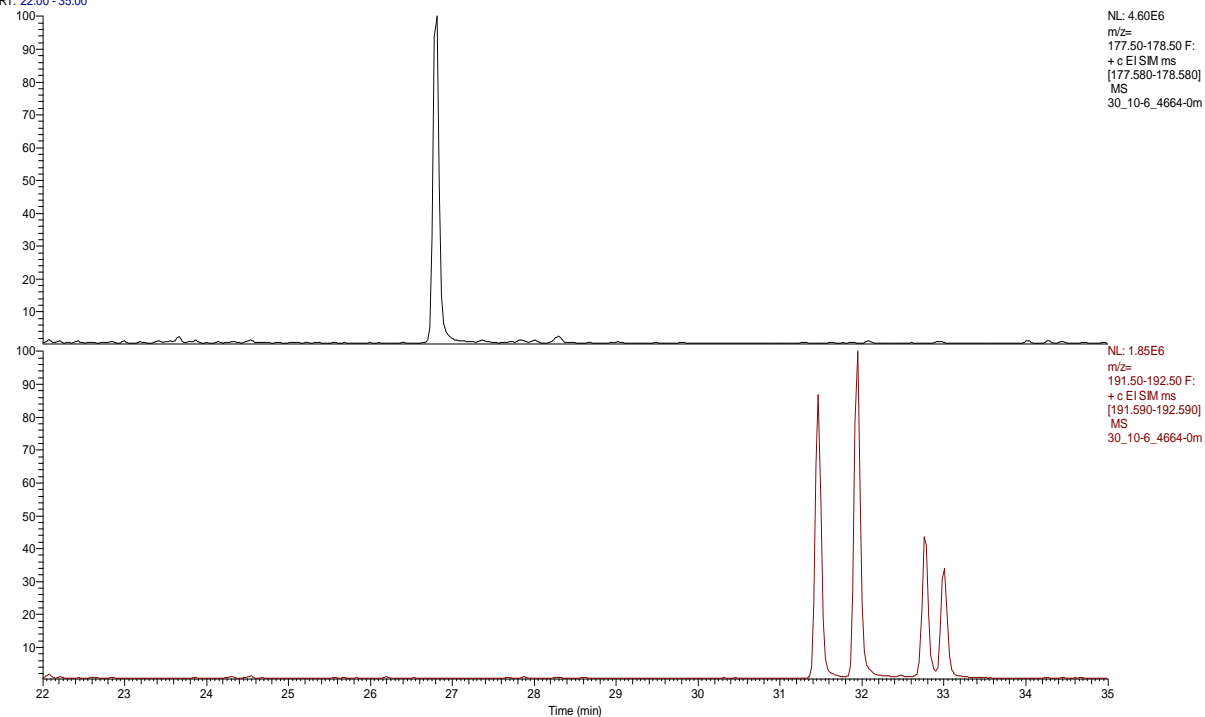




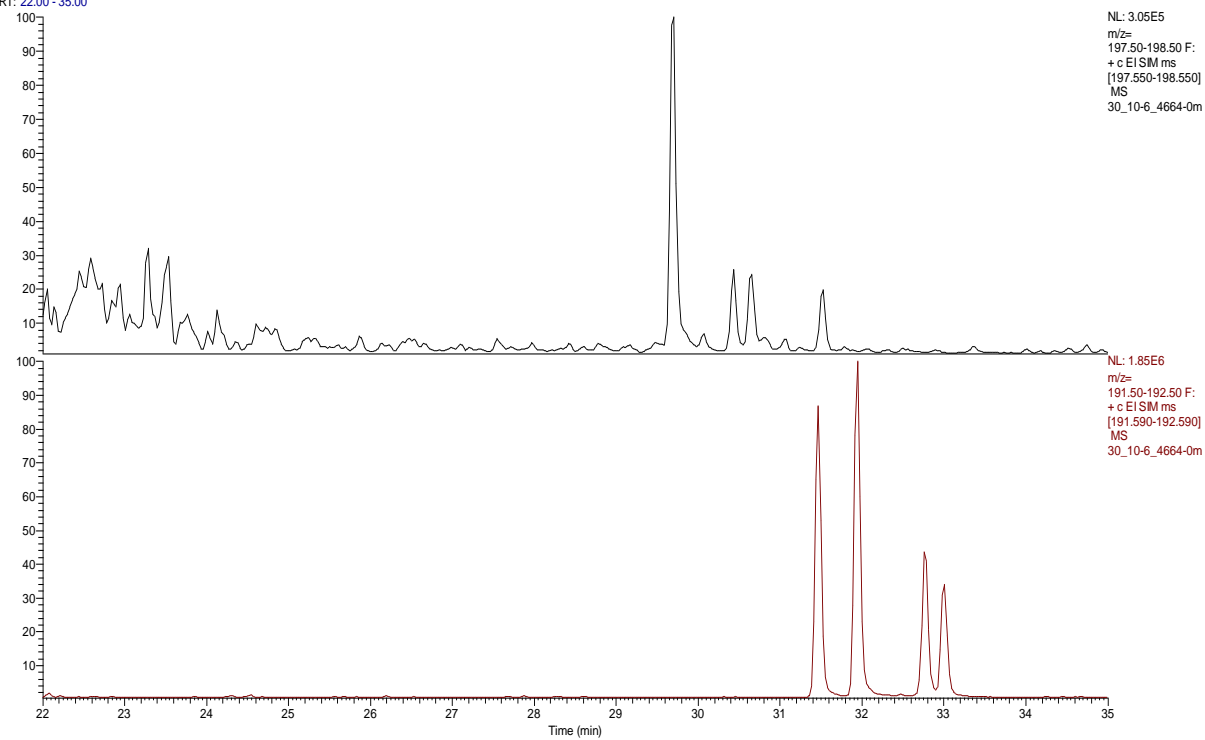




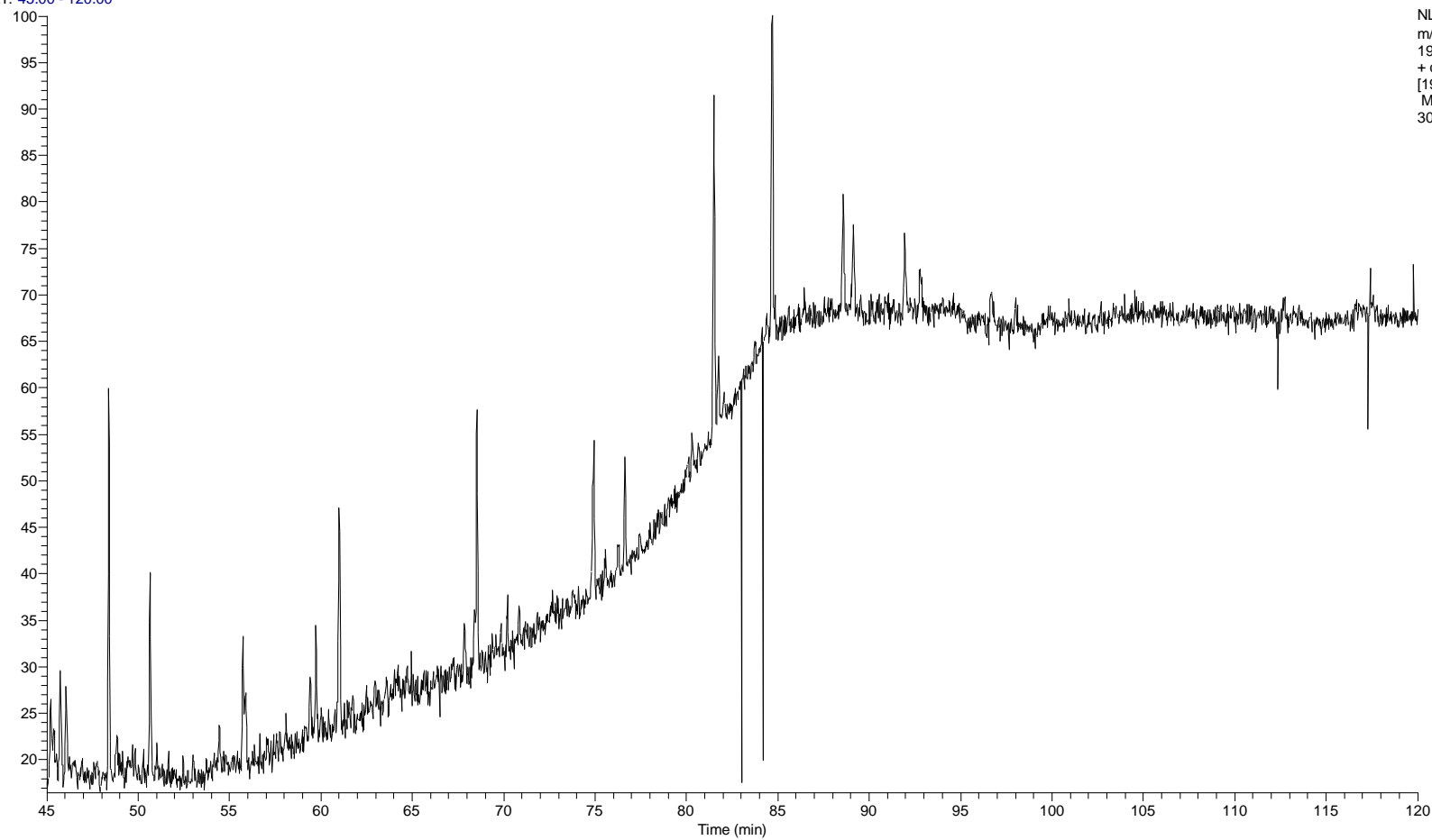
RT: 22.00 - 35.00



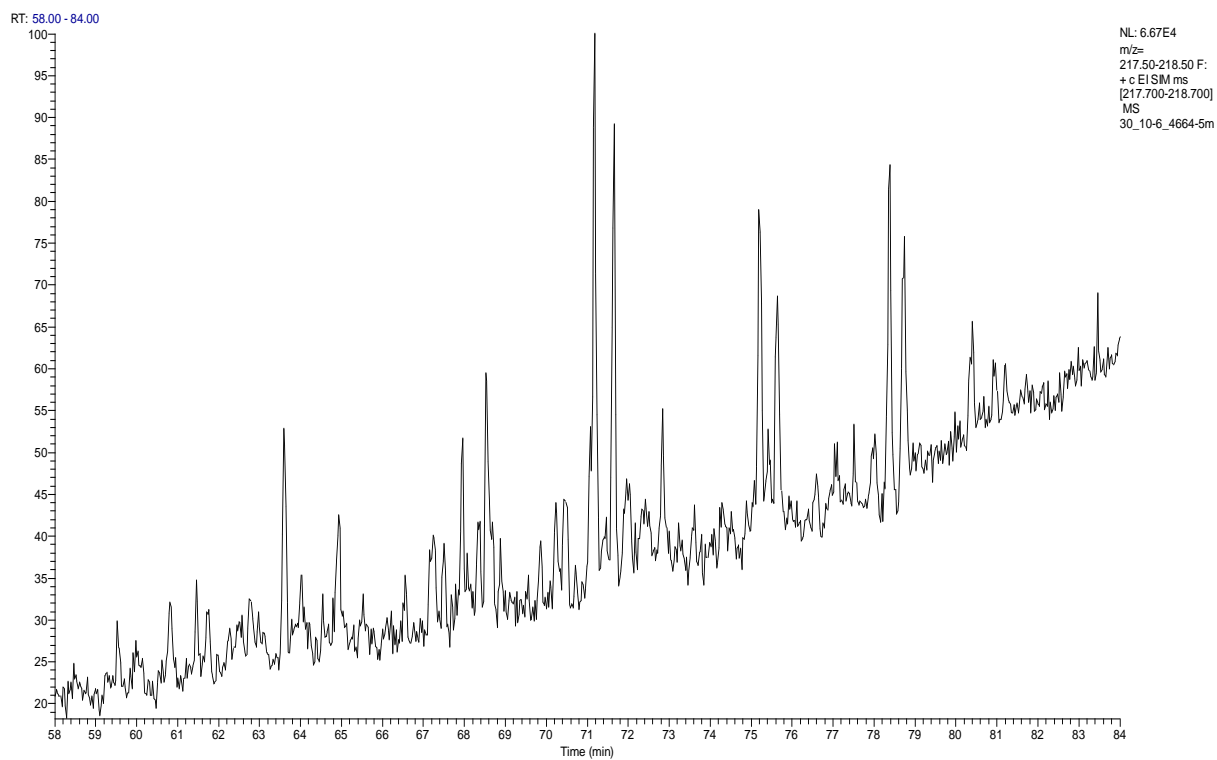
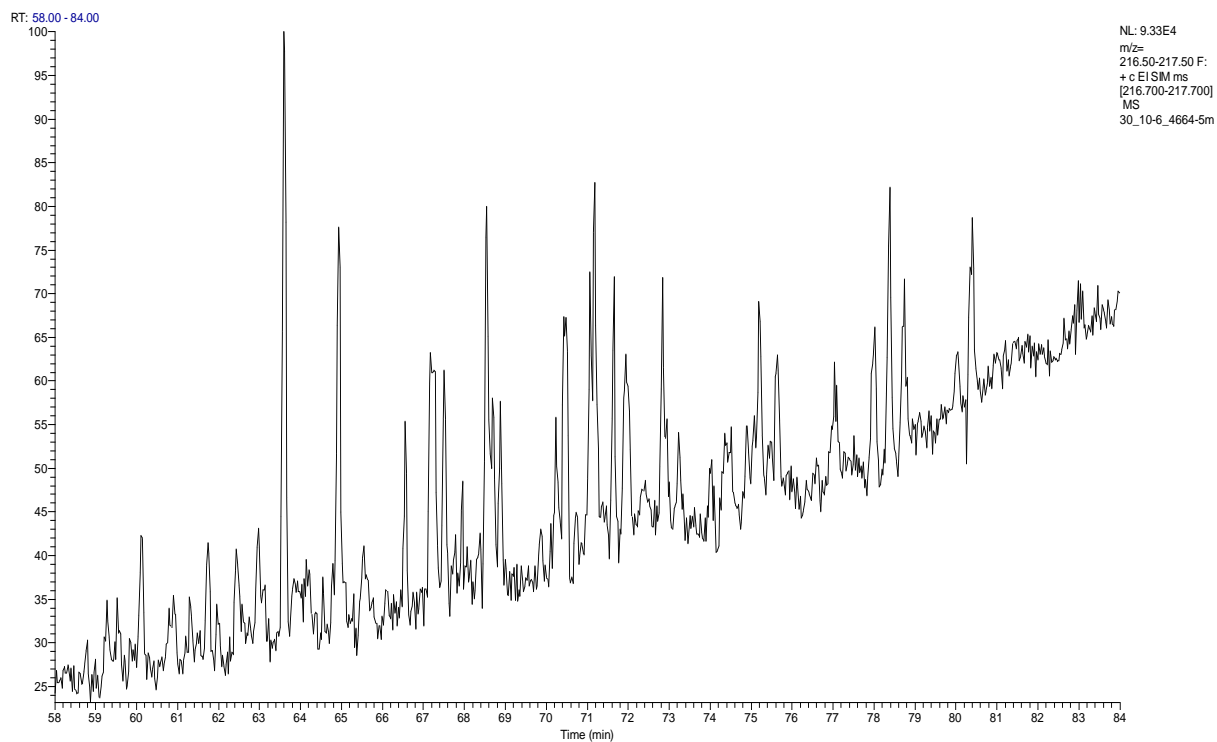
RT: 22.00 - 35.00

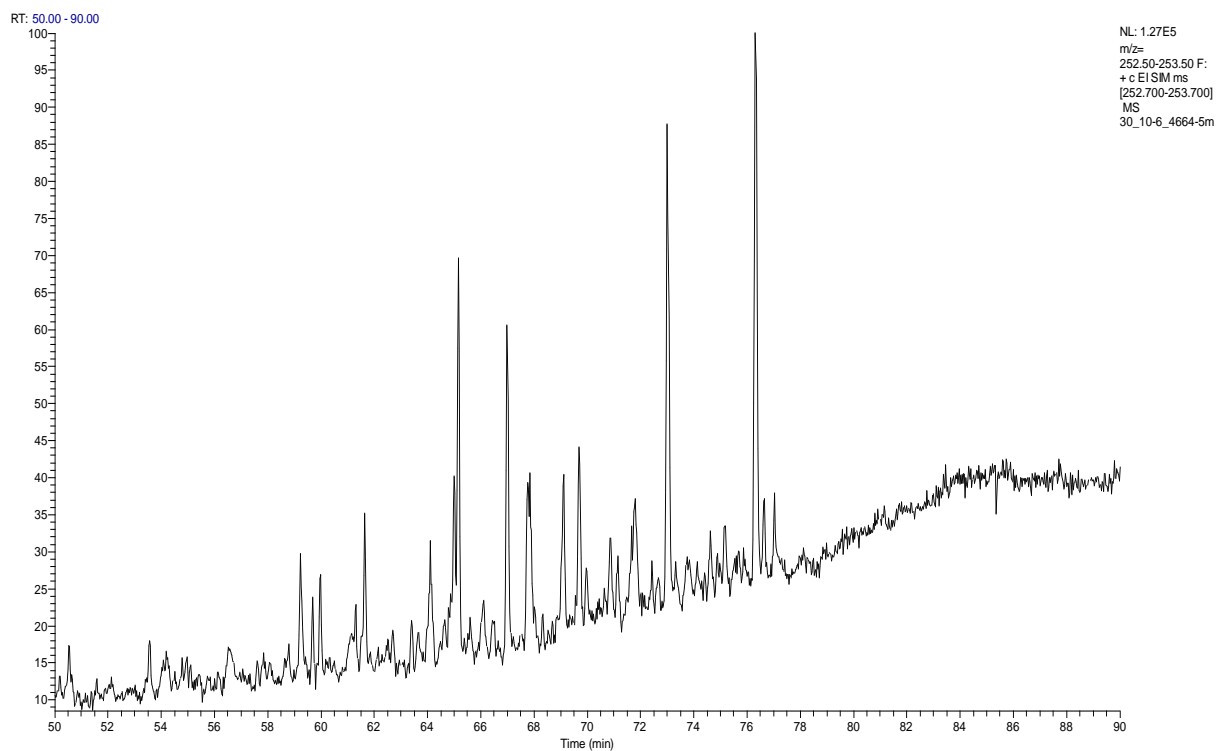
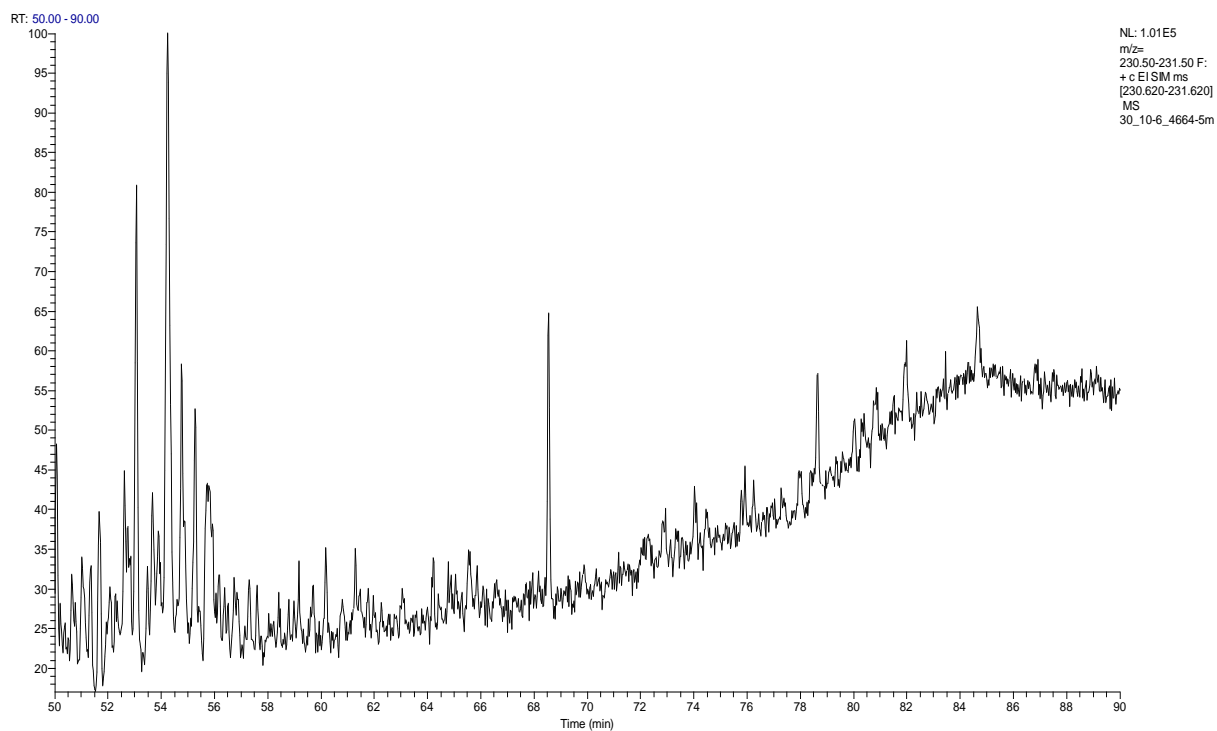


RT: 45.00 - 120.00

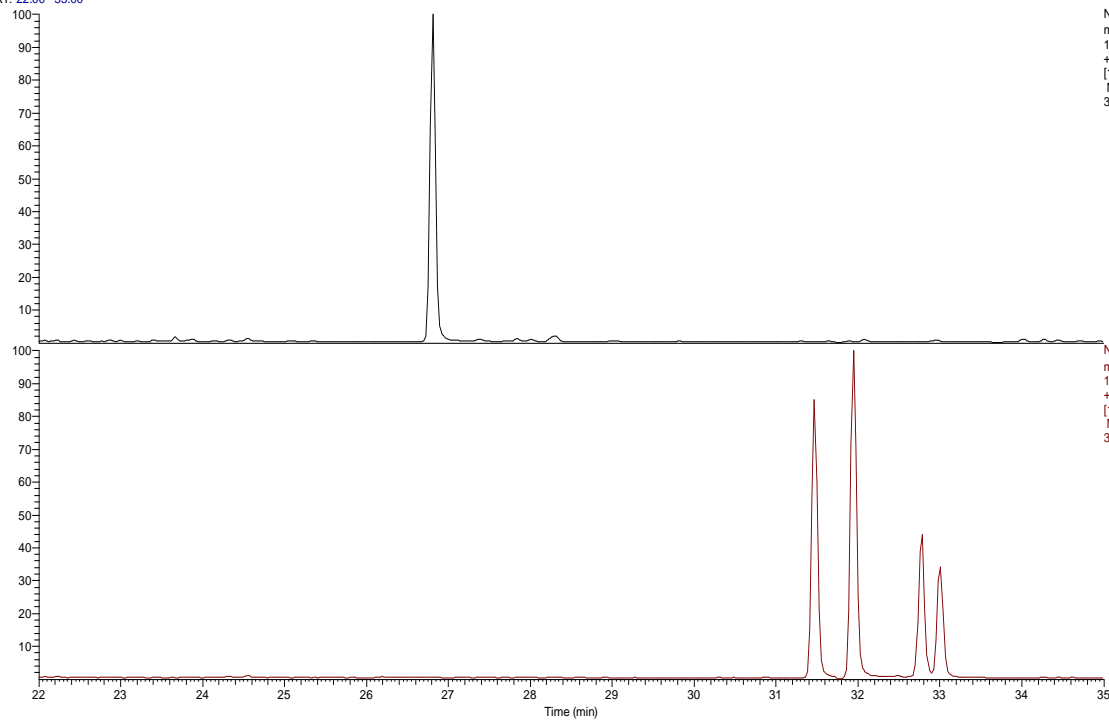


NL: 2.63E5
m/z=
190.50-191.50 F:
+ c EI SIM ms
[190.680-191.680]
MS
30_10-6_4664-5m





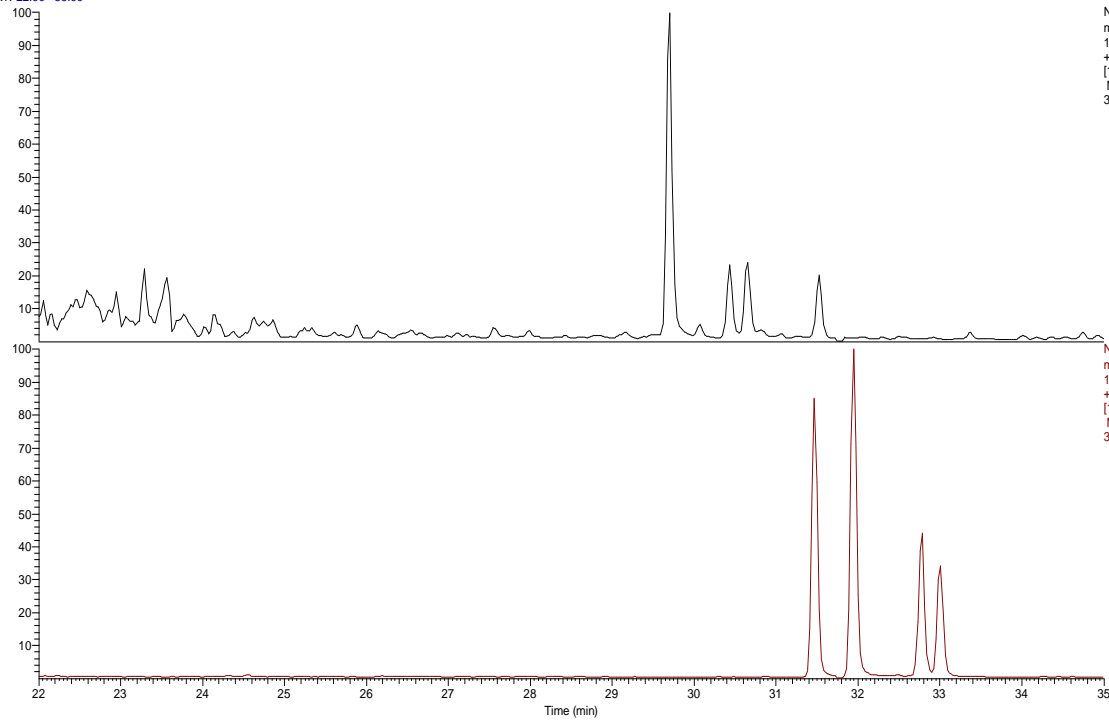
RT: 22.00 - 35.00



NL: 2.36E7
m/z=
177.50-178.50 F:
+ c EI SIM ms
[177.580-178.580]
MS
30_10-6_4664-5m

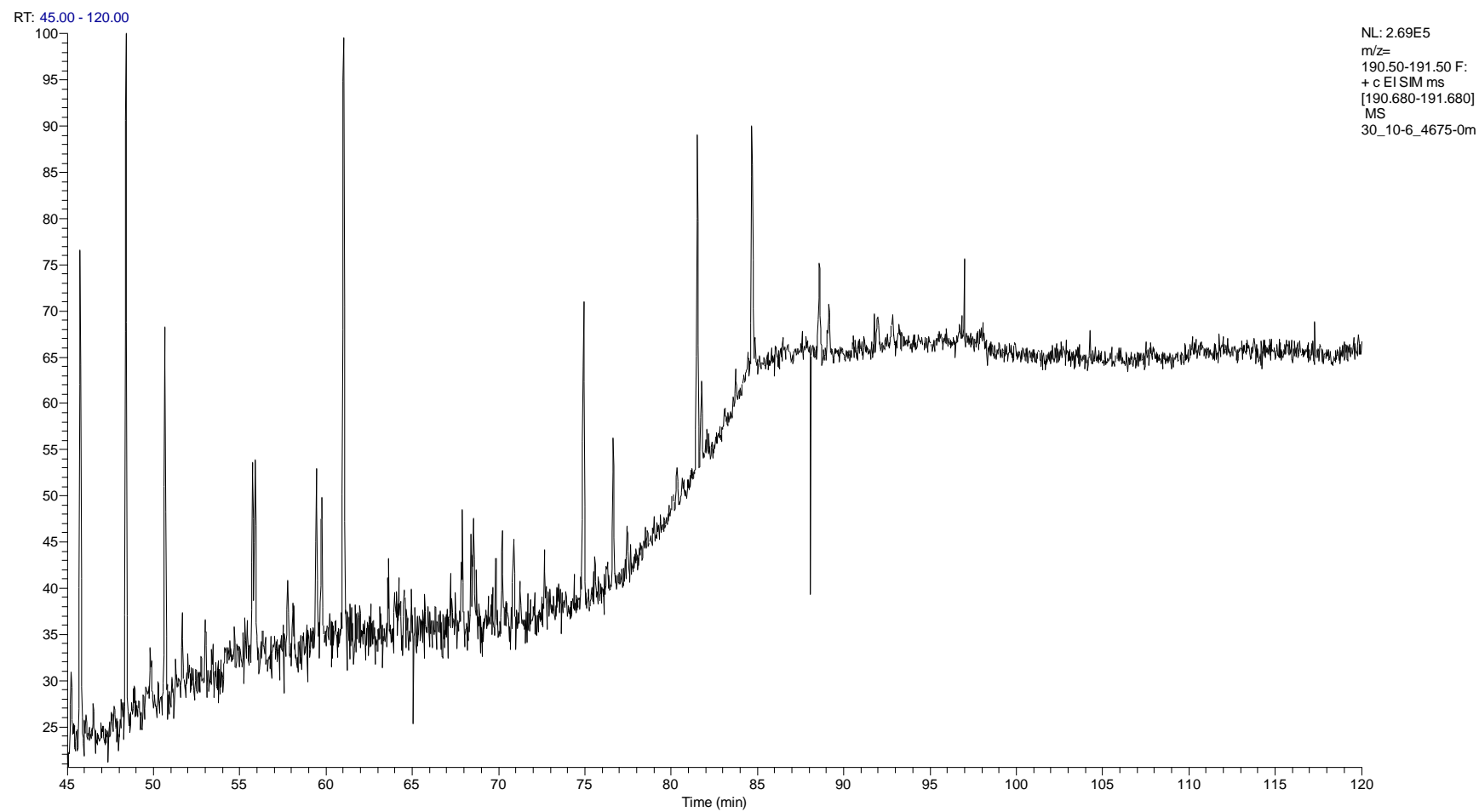
NL: 9.97E6
m/z=
191.50-192.50 F:
+ c EI SIM ms
[191.590-192.590]
MS
30_10-6_4664-5m

RT: 22.00 - 35.00

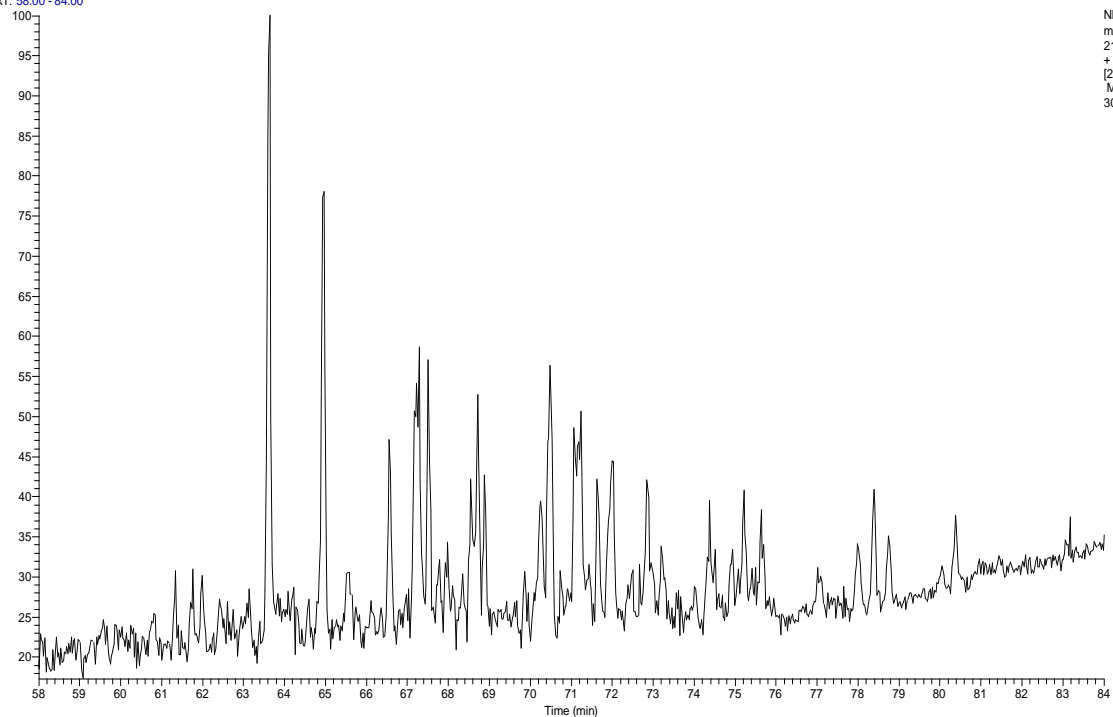


NL: 1.79E6
m/z=
197.50-198.50 F:
+ c EI SIM ms
[197.550-198.550]
MS
30_10-6_4664-5m

NL: 9.97E6
m/z=
191.50-192.50 F:
+ c EI SIM ms
[191.590-192.590]
MS
30_10-6_4664-5m

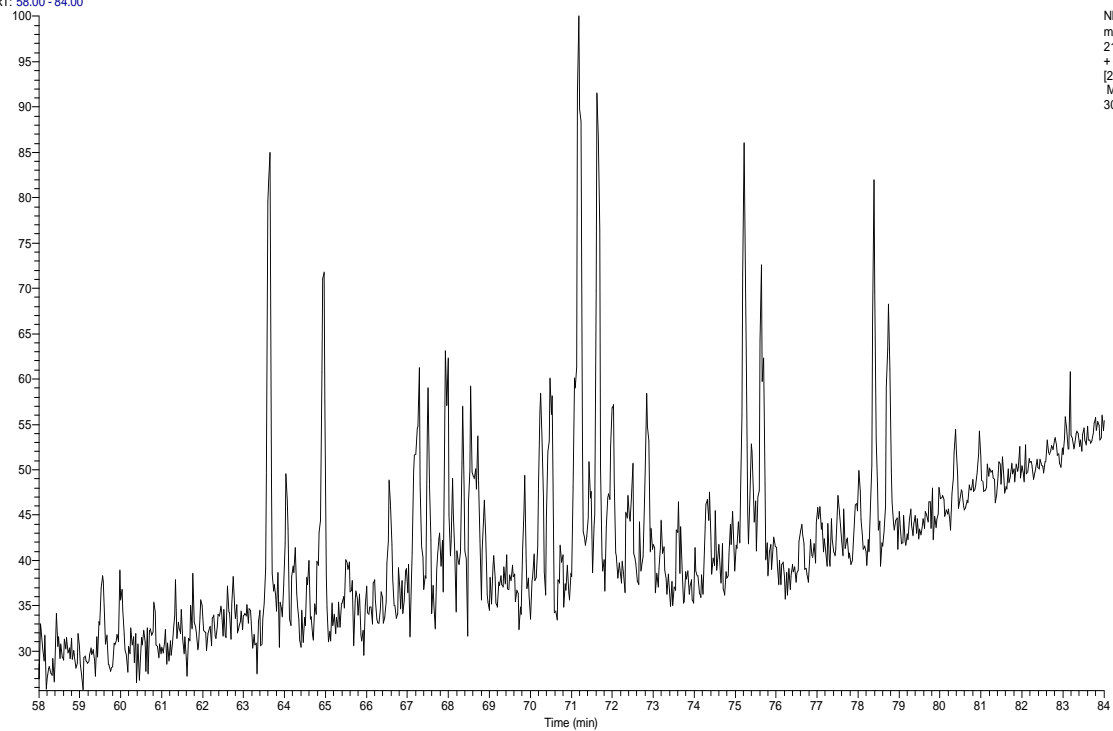


RT: 58.00 - 84.00

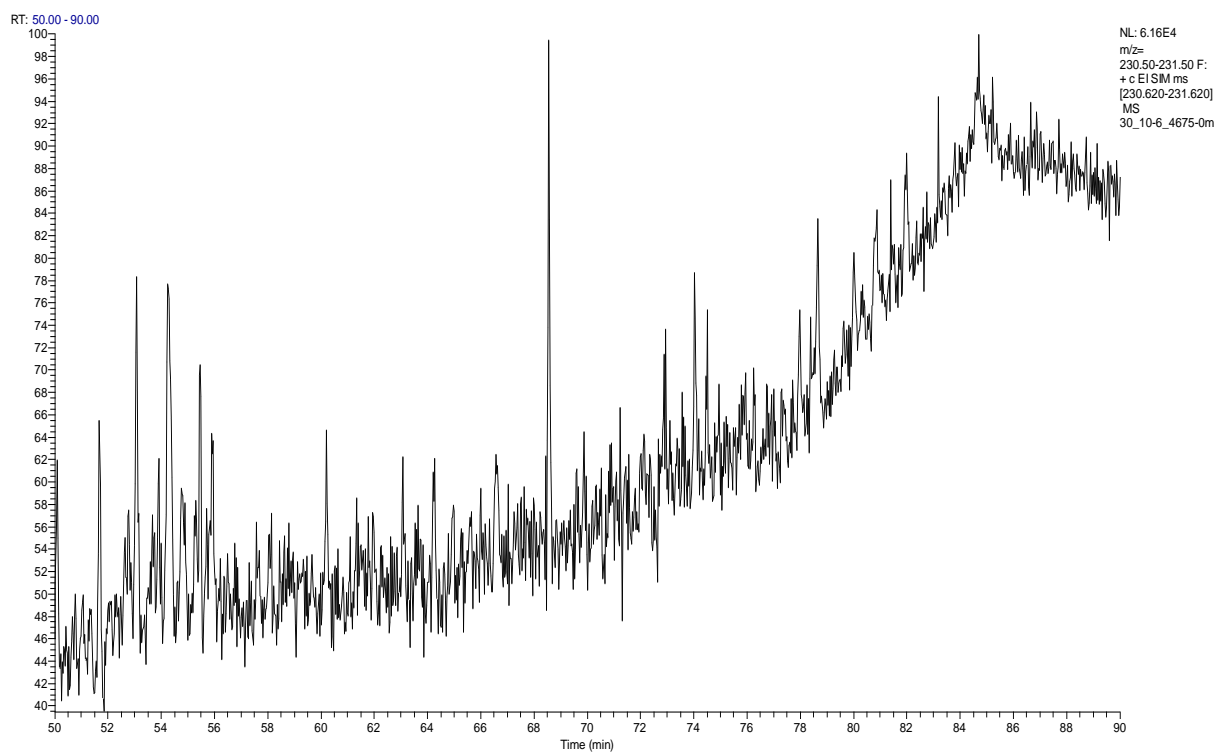
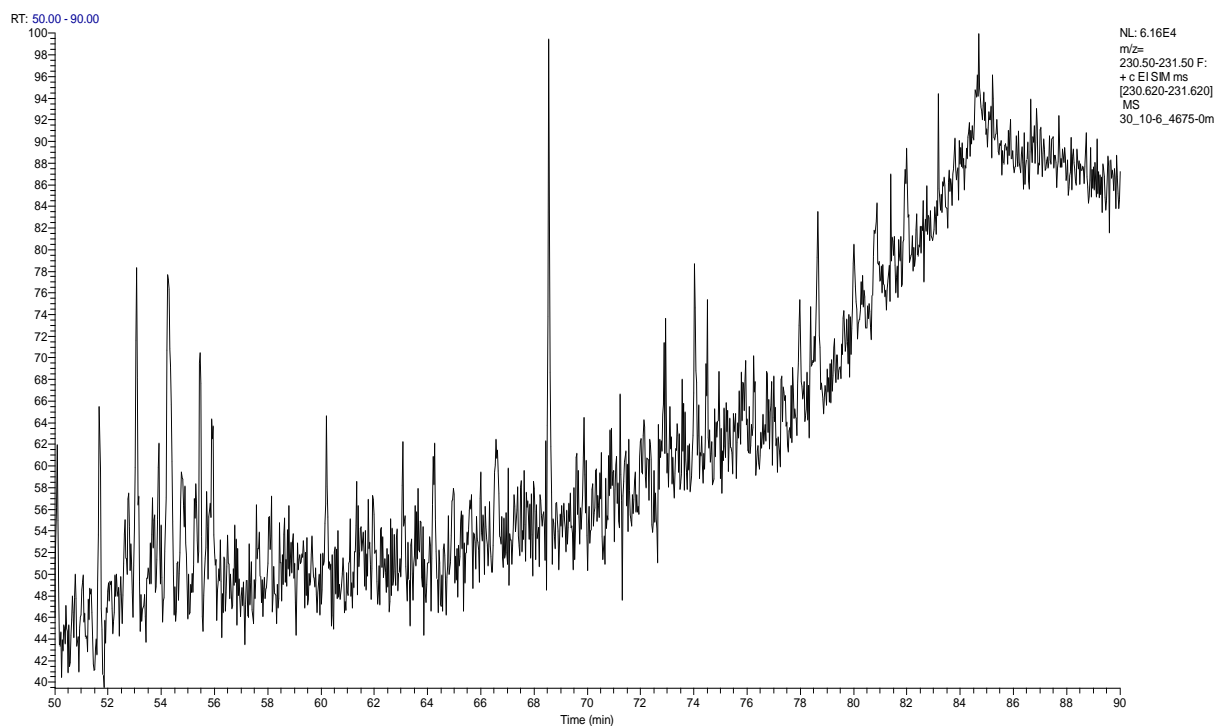


NL: 1.78E5
m/z=
216.50-217.50 F:
+ c EI SIM ms
[216.700-217.700]
MS
30_10-6_4675-0m

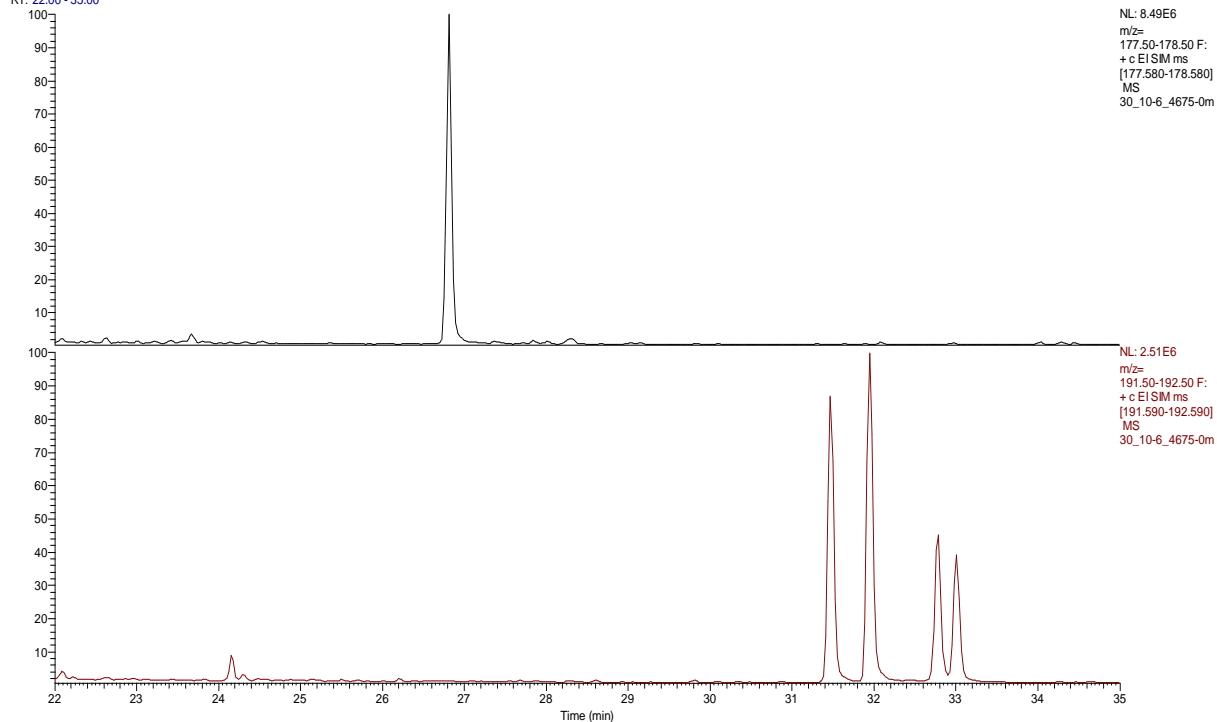
RT: 58.00 - 84.00



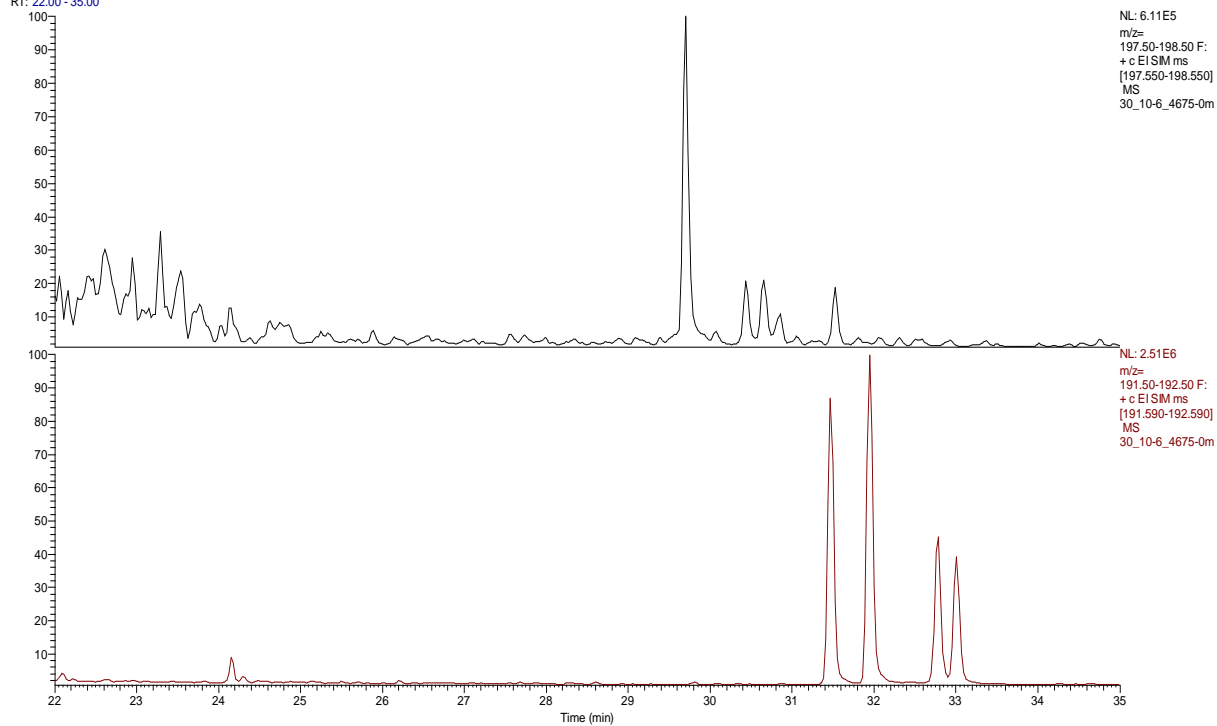
NL: 7.15E4
m/z=
217.50-218.50 F:
+ c EI SIM ms
[217.700-218.700]
MS
30_10-6_4675-0m



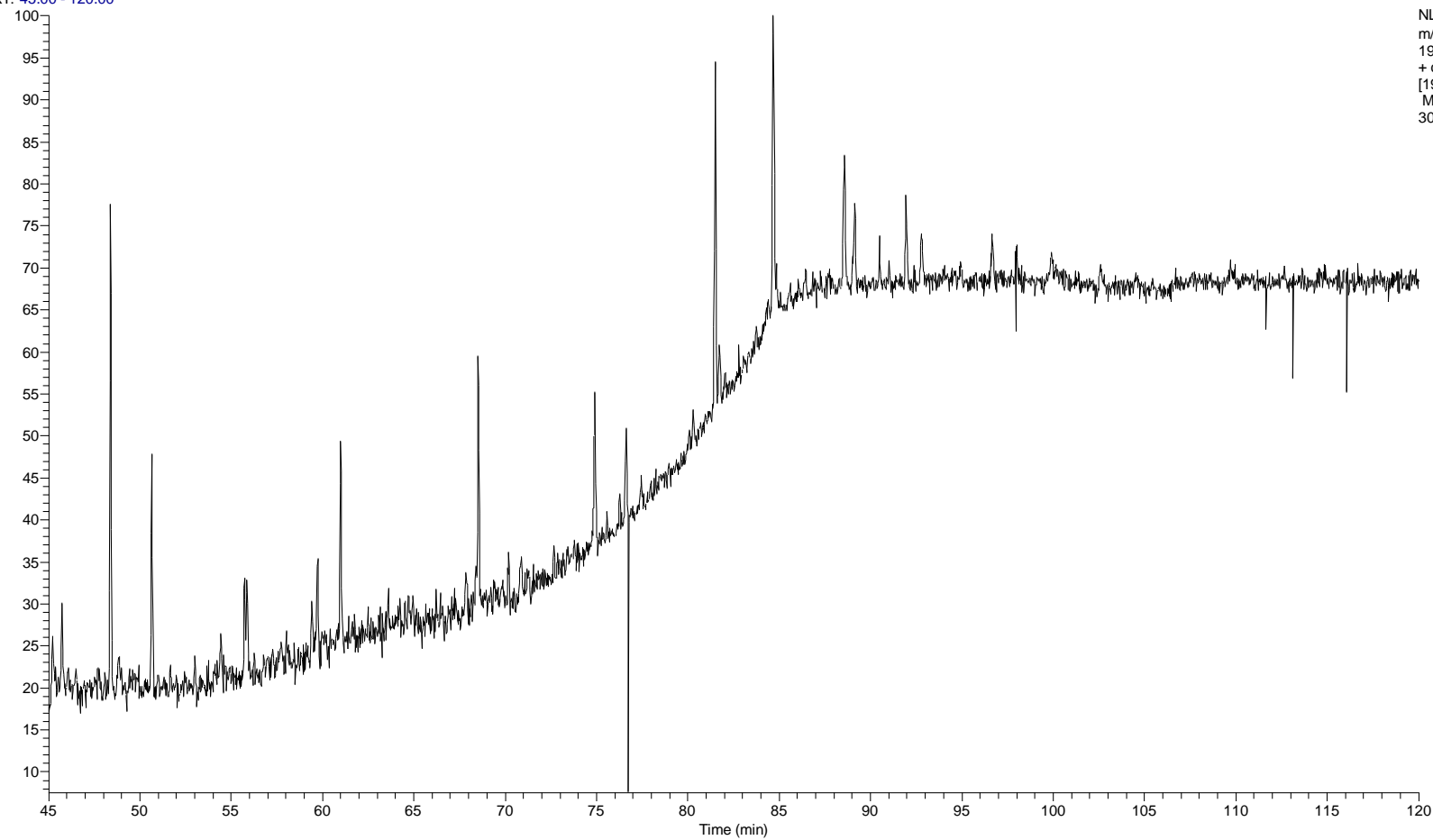
RT: 22.00 - 35.00

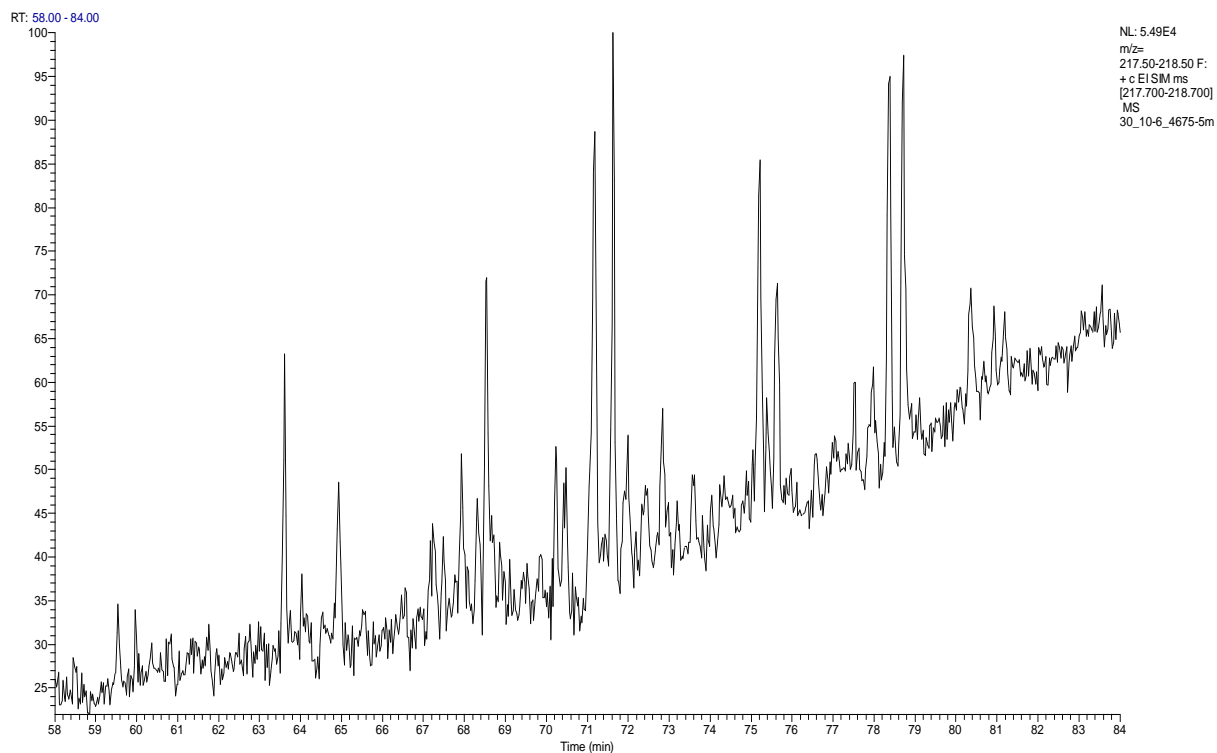
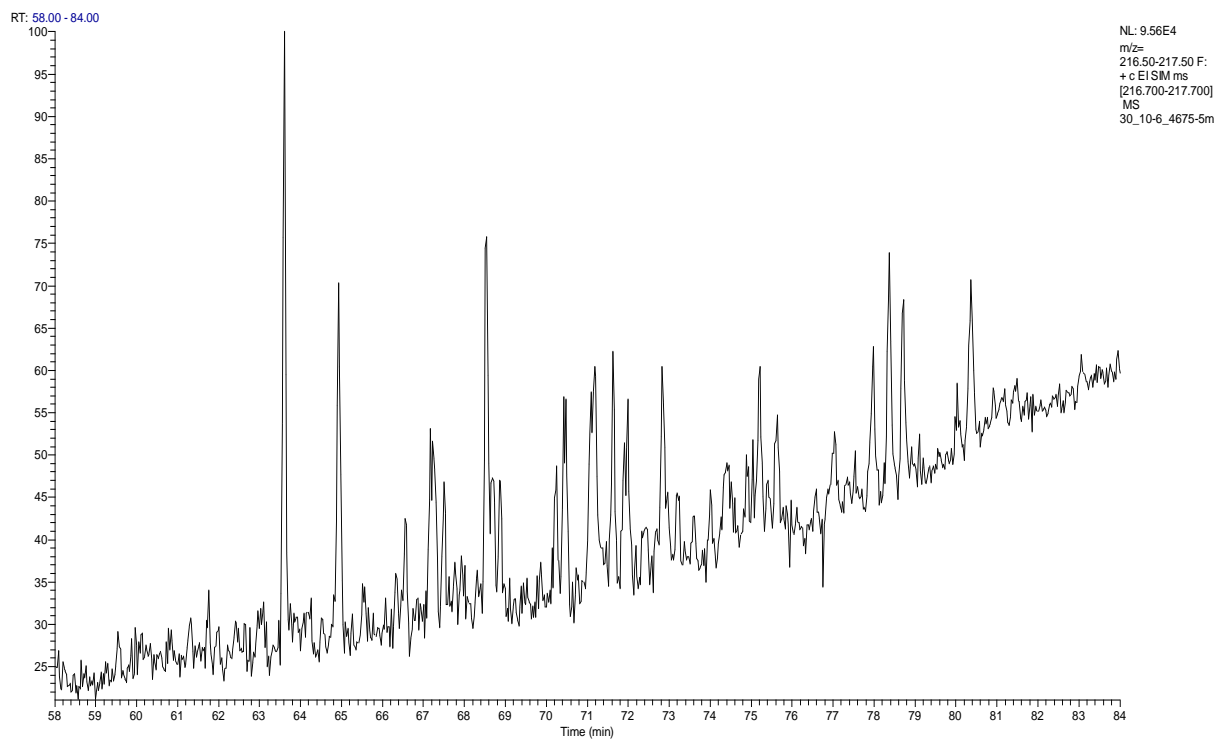


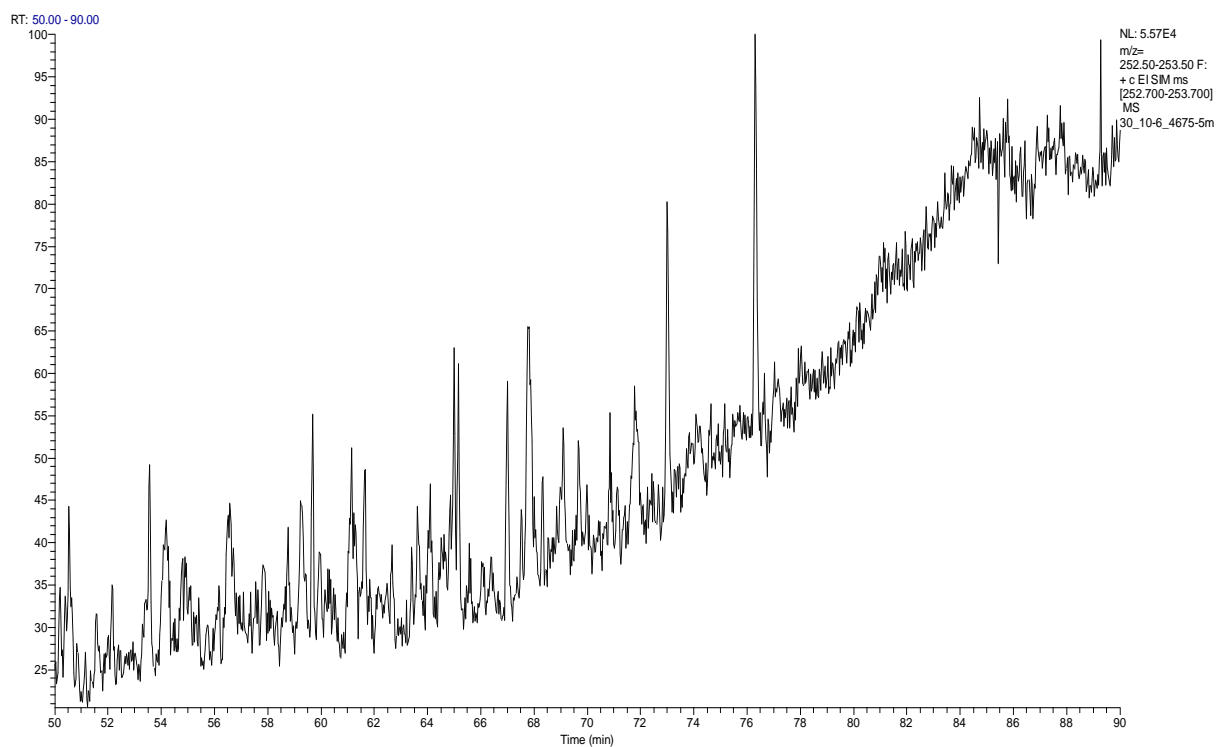
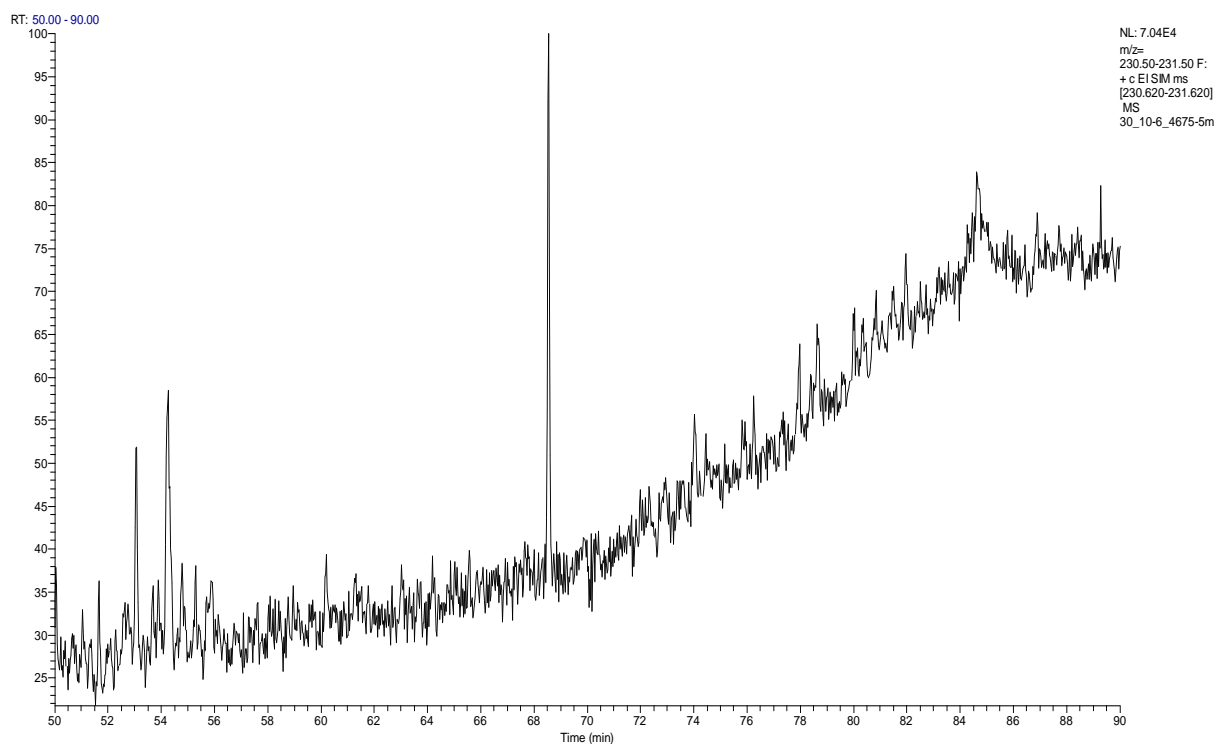
RT: 22.00 - 35.00



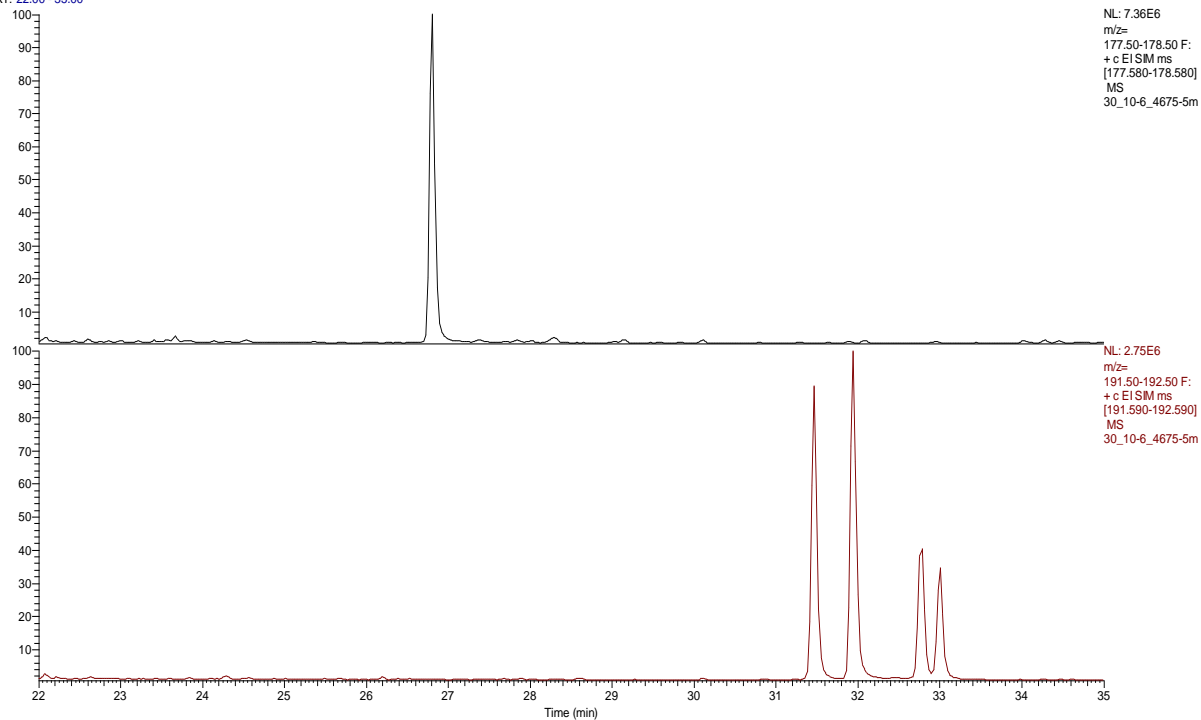
RT: 45.00 - 120.00



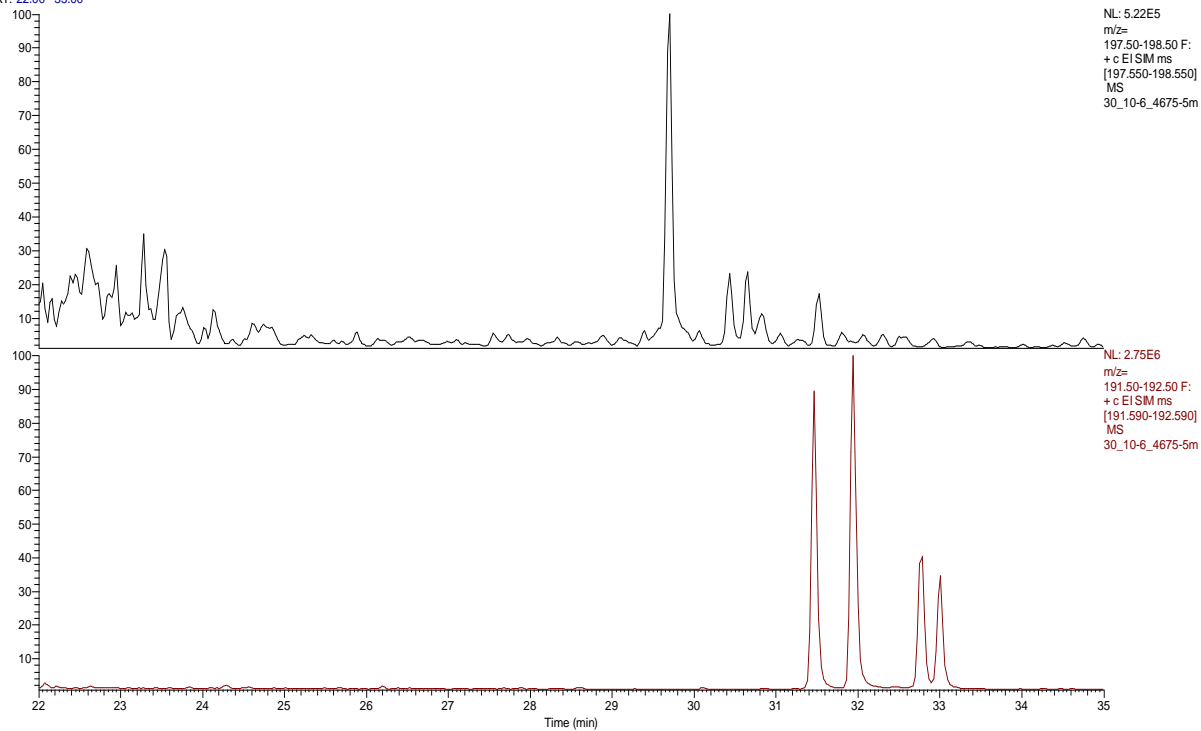




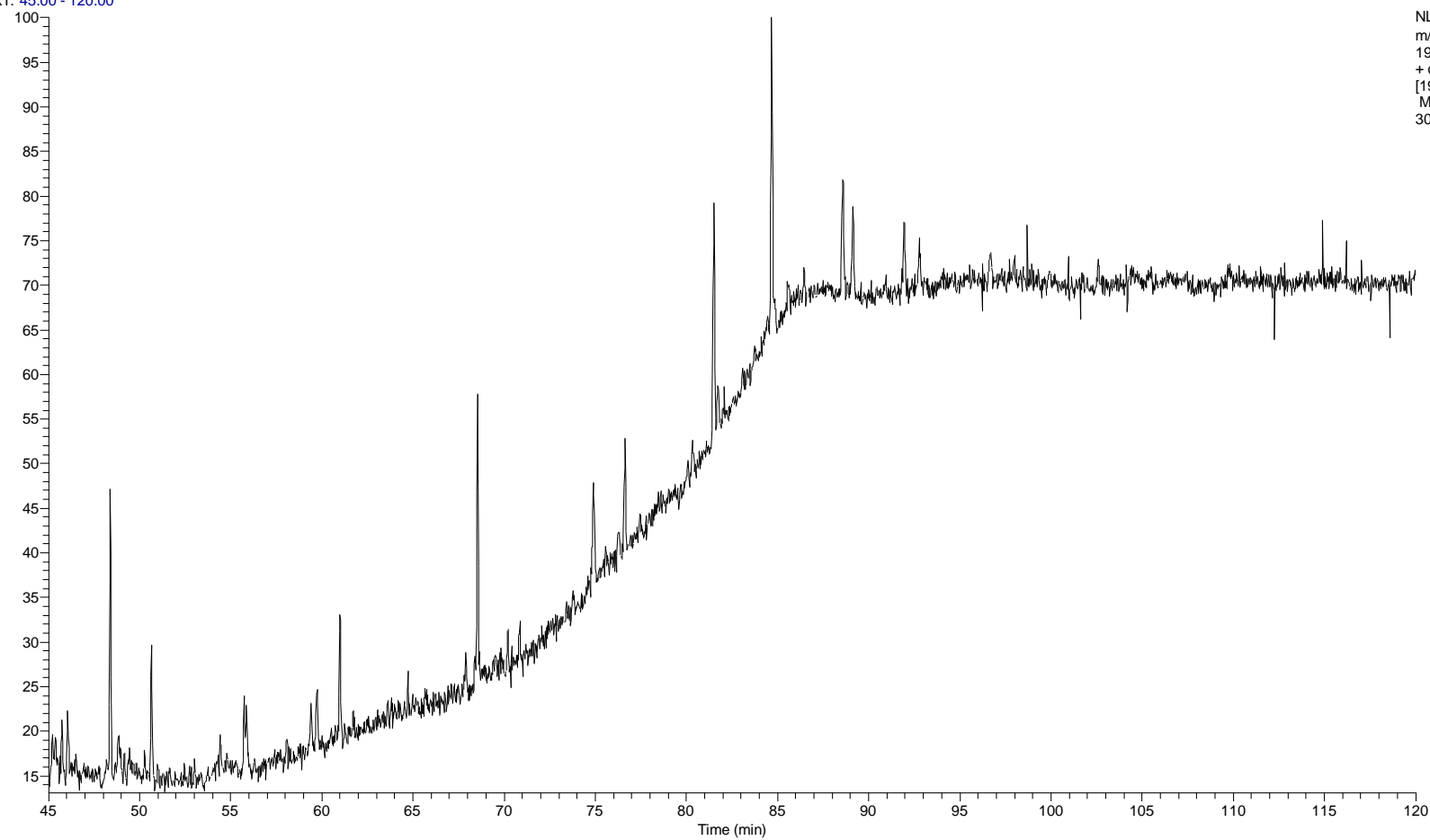
RT: 22.00 - 35.00



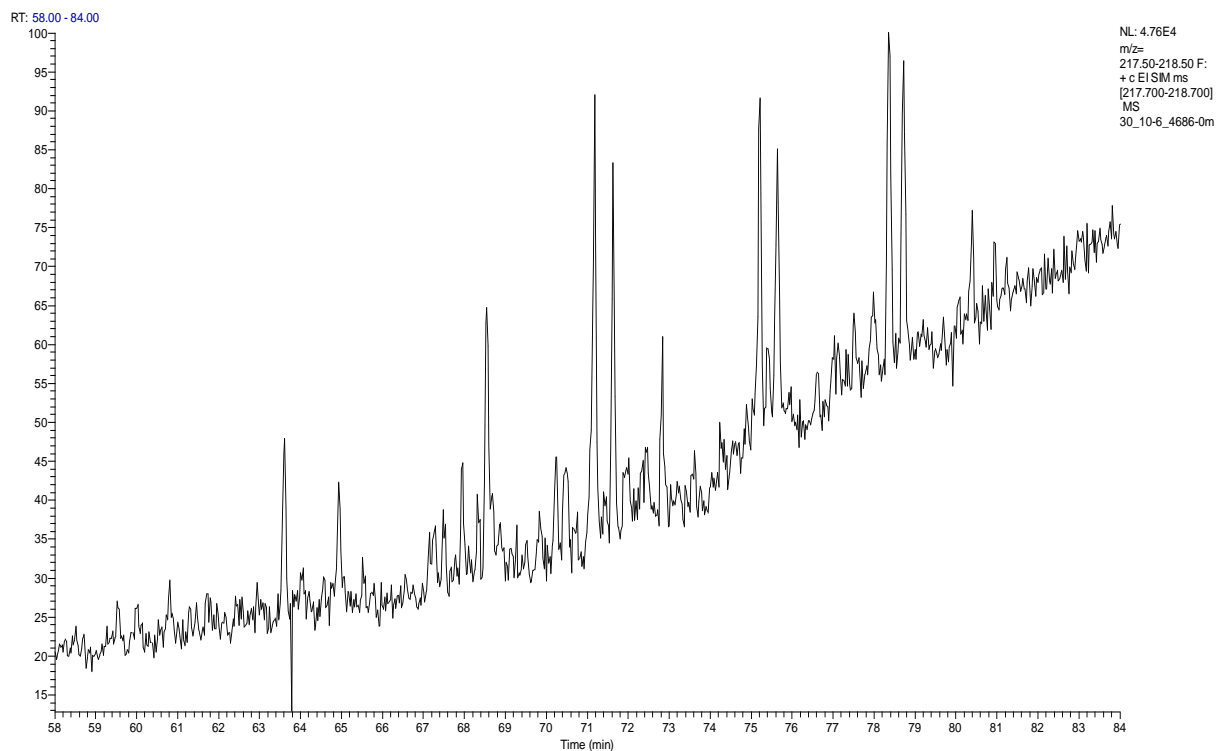
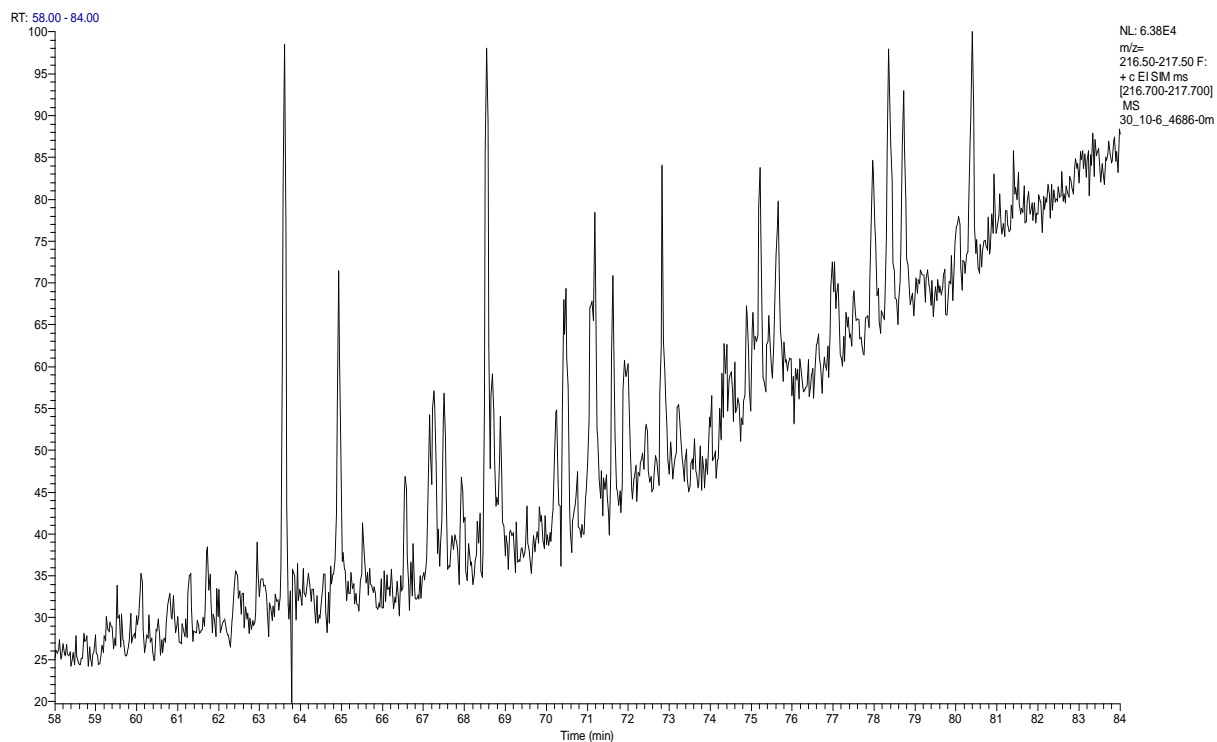
RT: 22.00 - 35.00

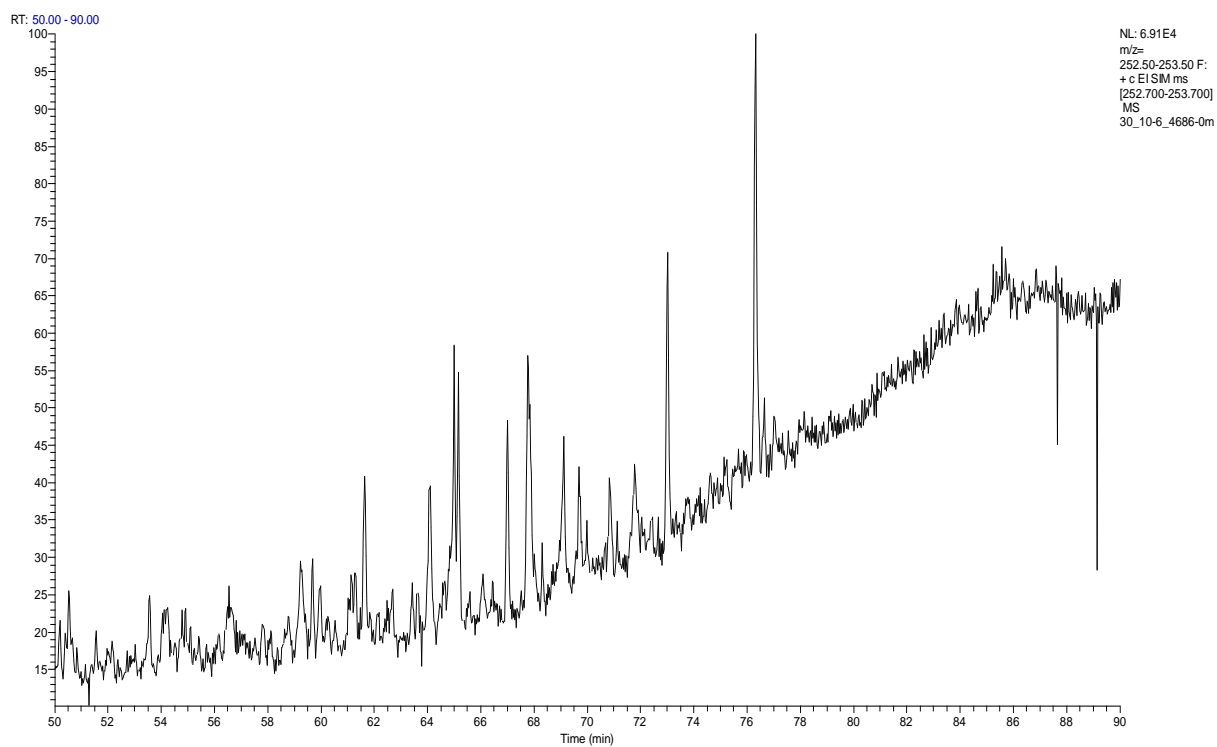
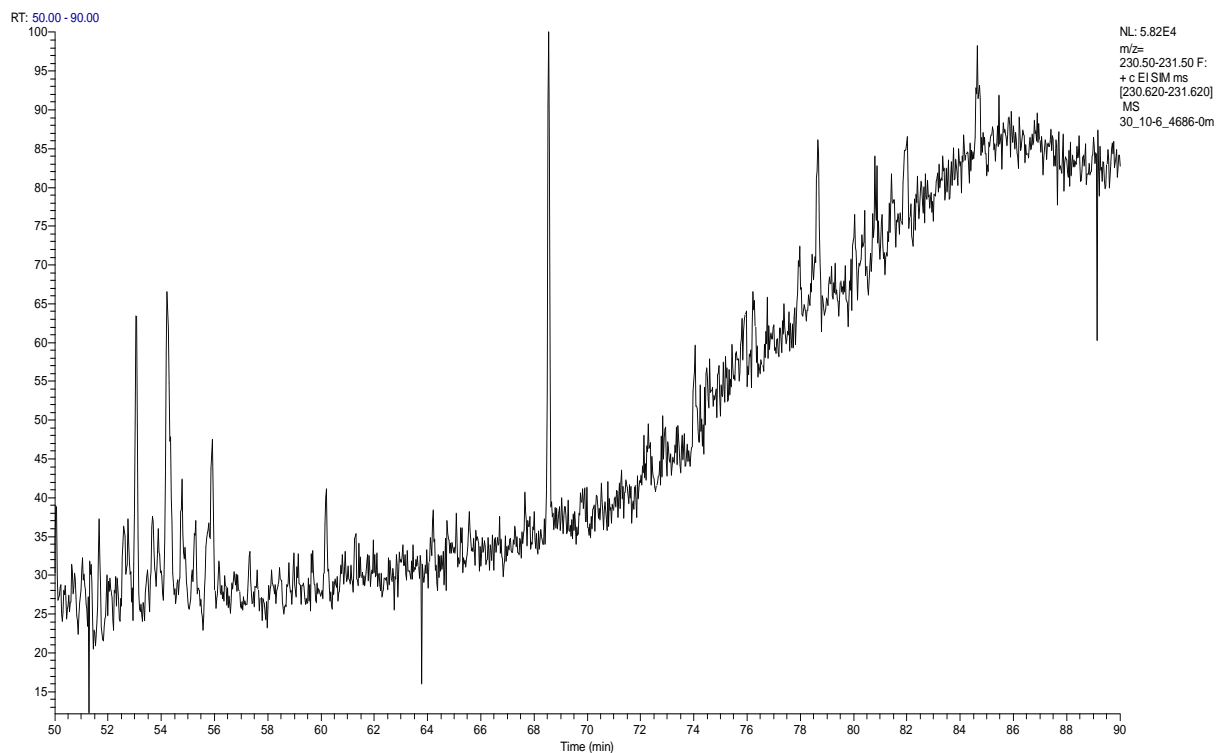


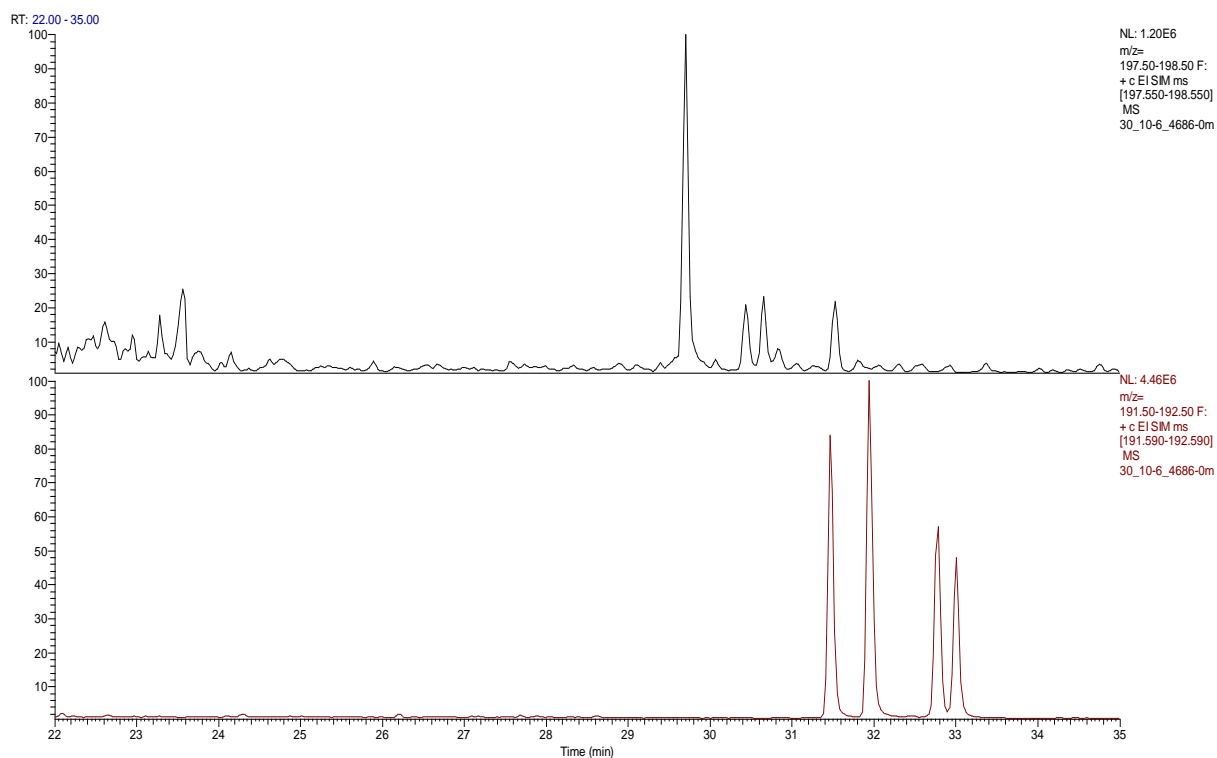
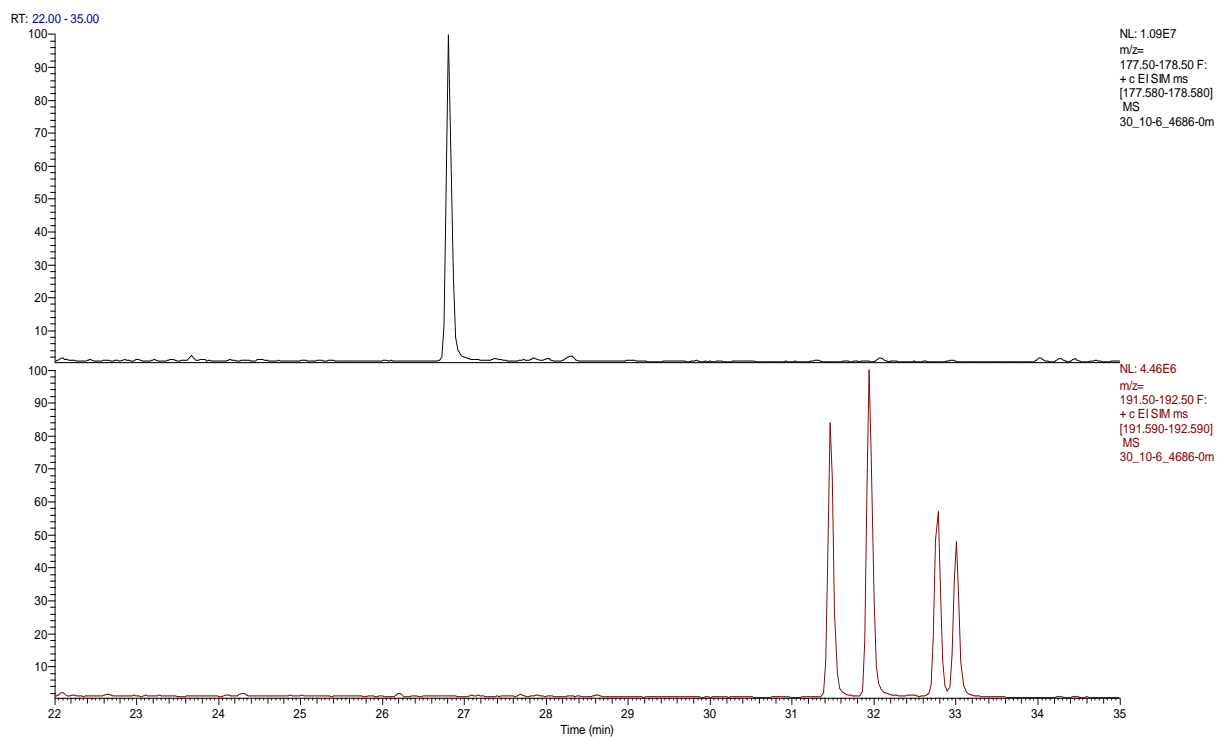
RT: 45.00 - 120.00



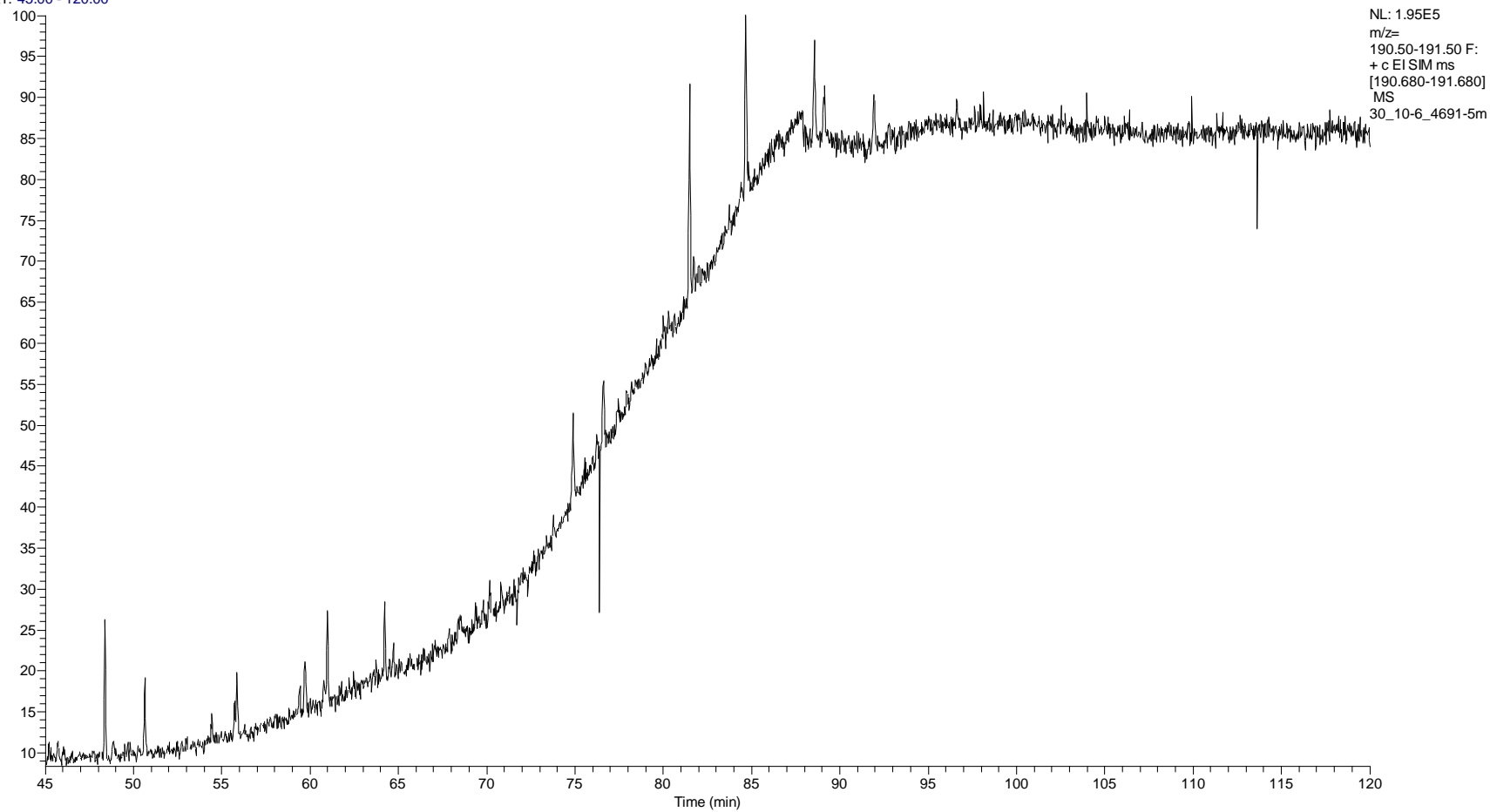
NL: 2.43E5
m/z=
190.50-191.50 F:
+ c EI SIM ms
[190.680-191.680]
MS
30_10-6_4686-0m

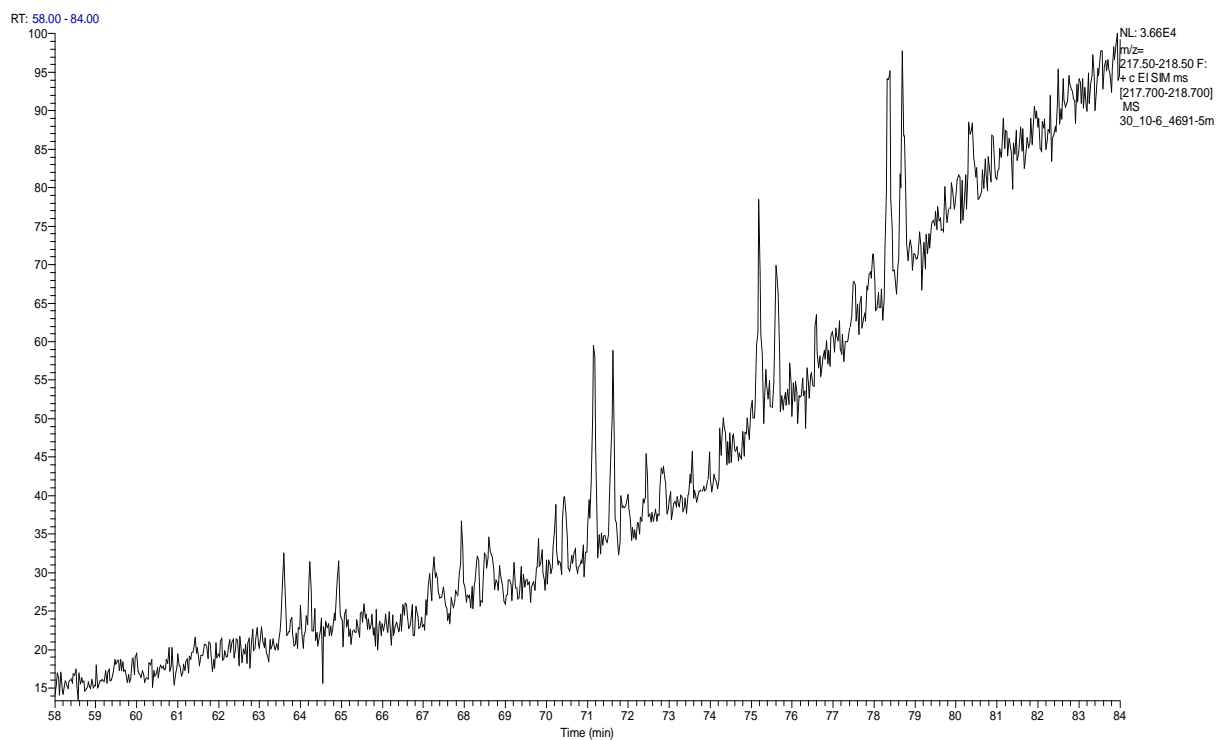
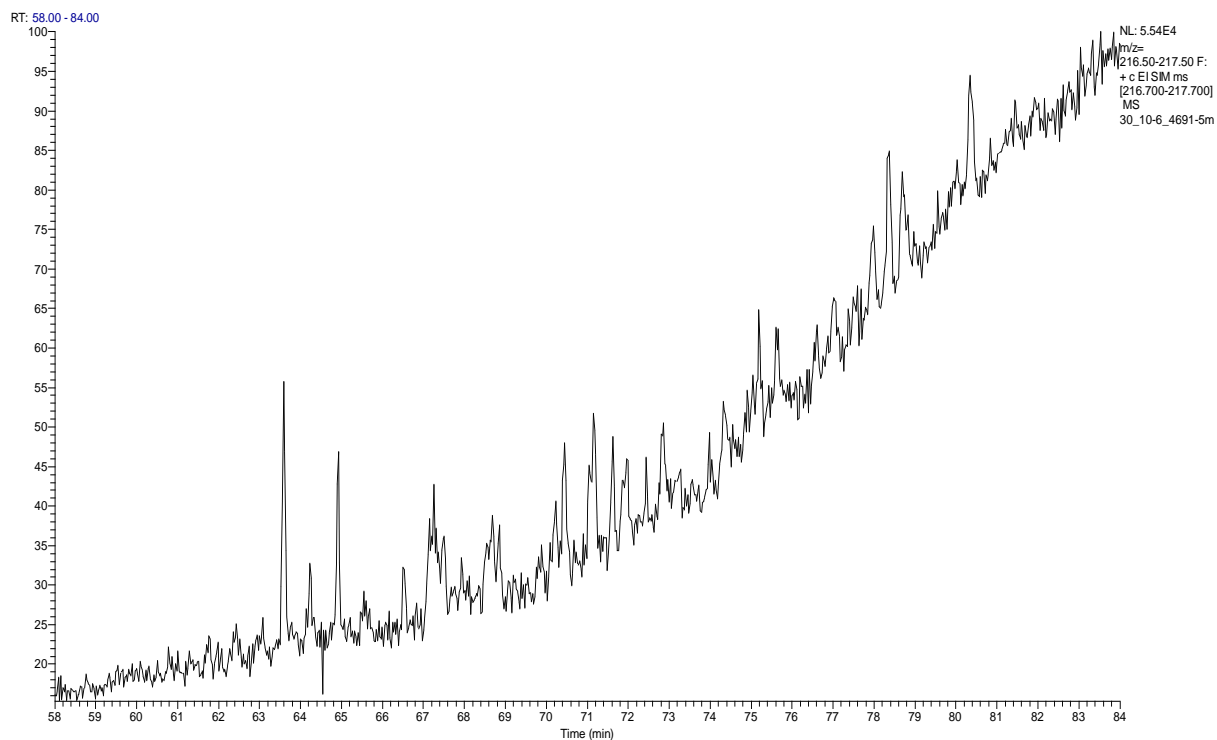


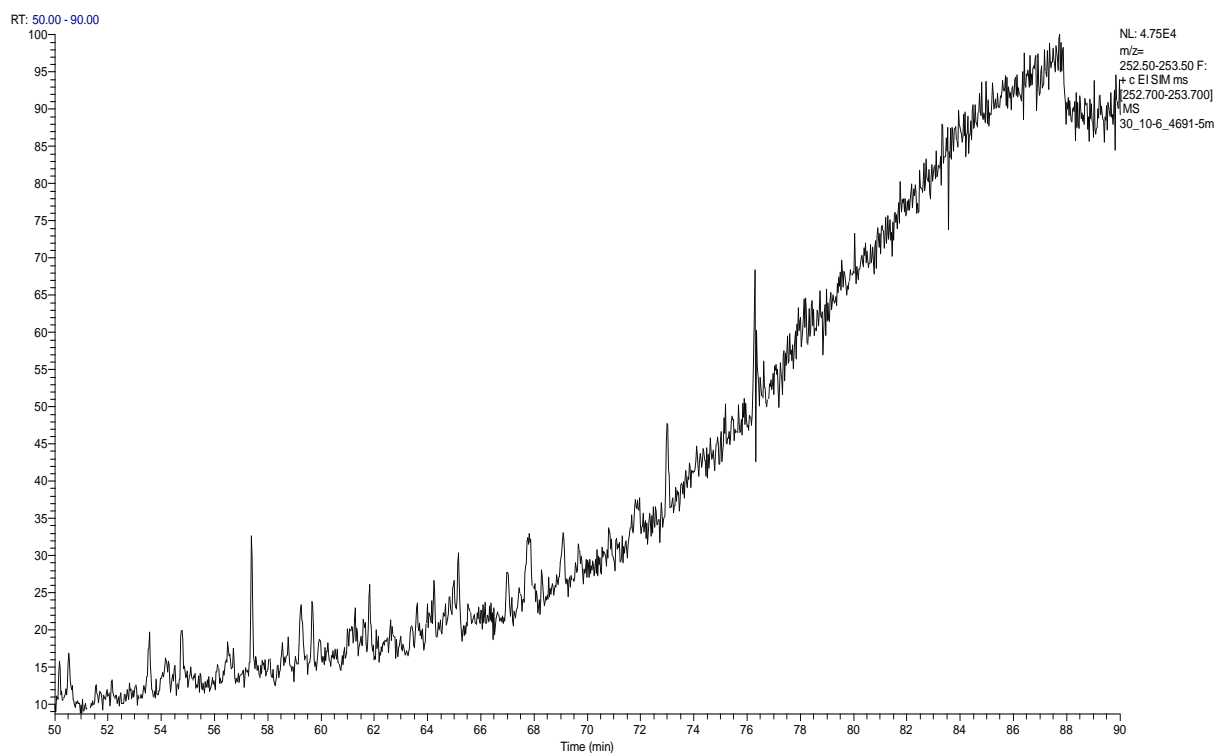
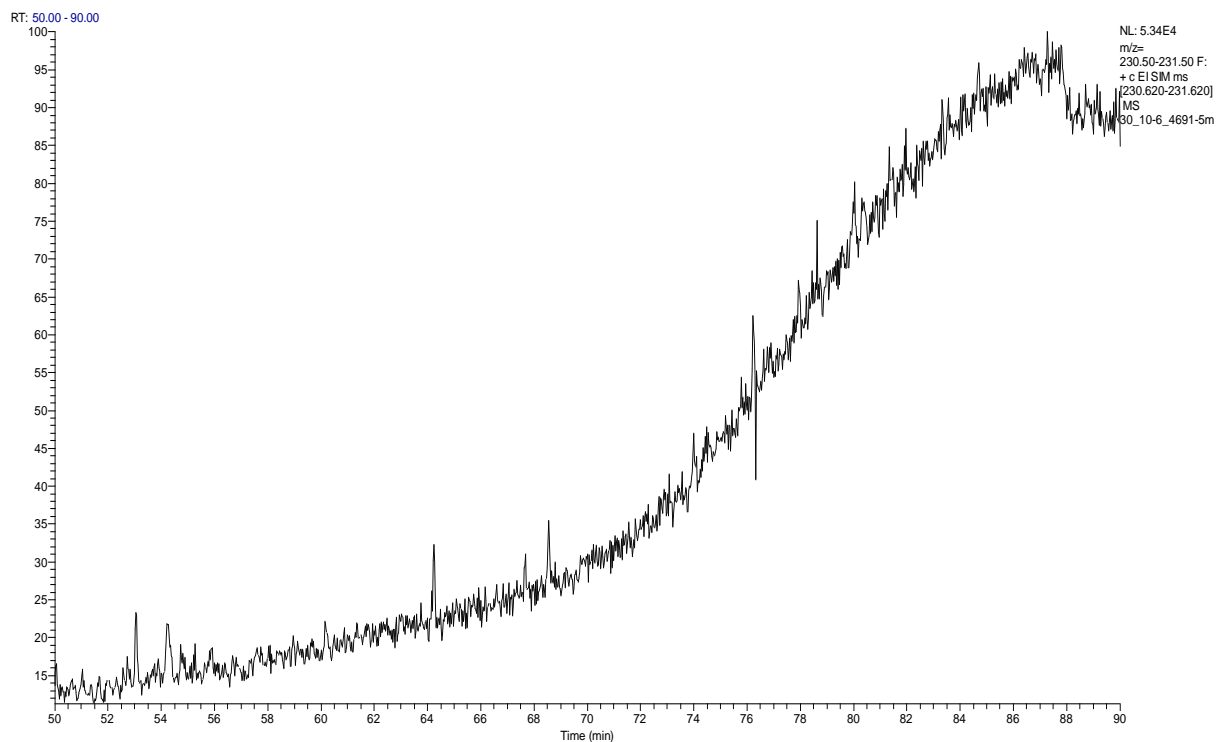




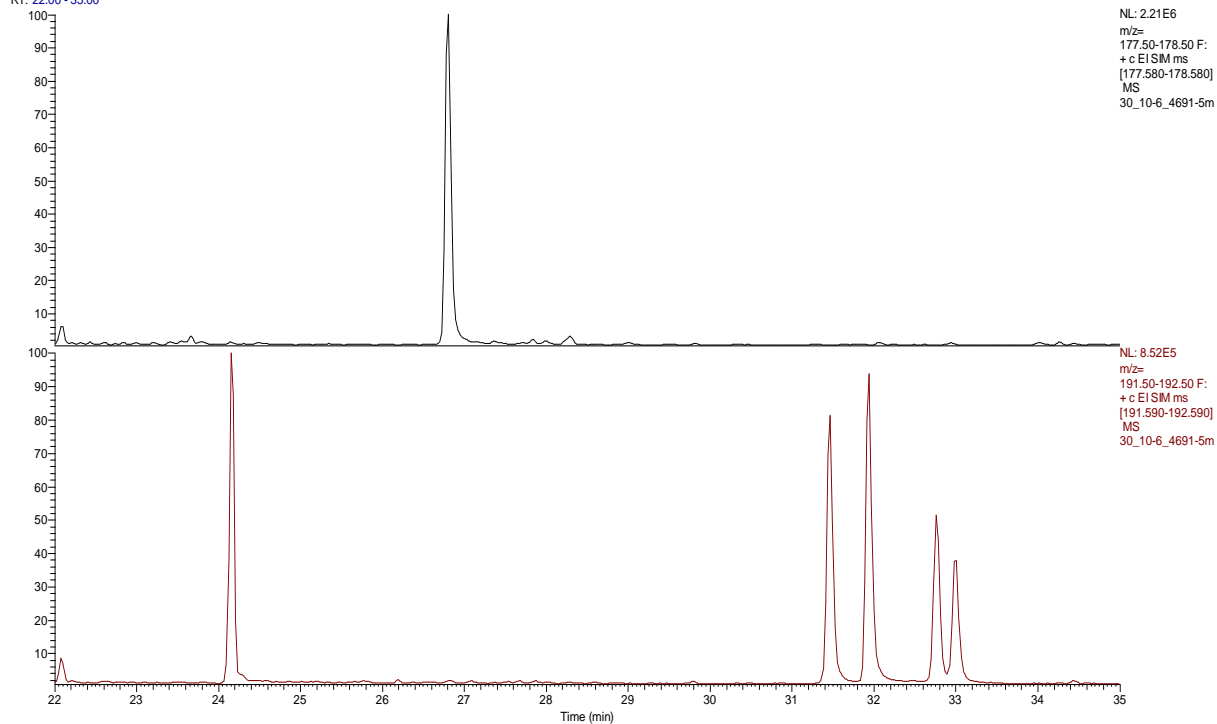
RT: 45.00 - 120.00



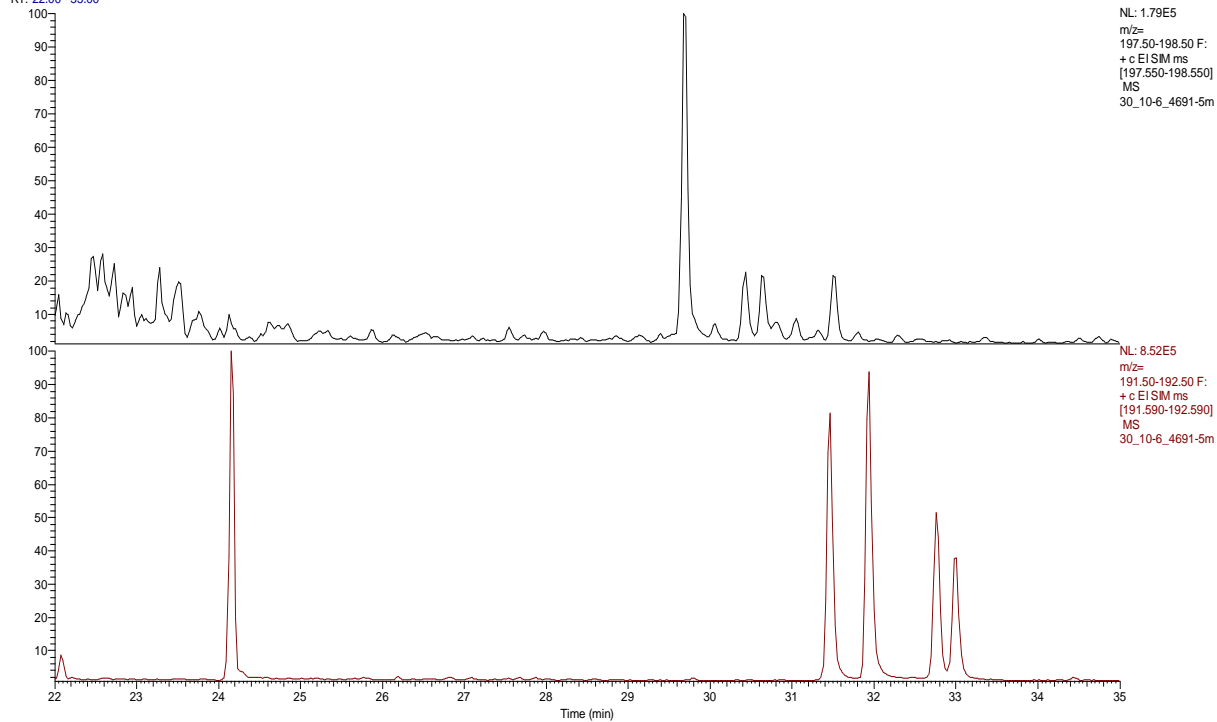




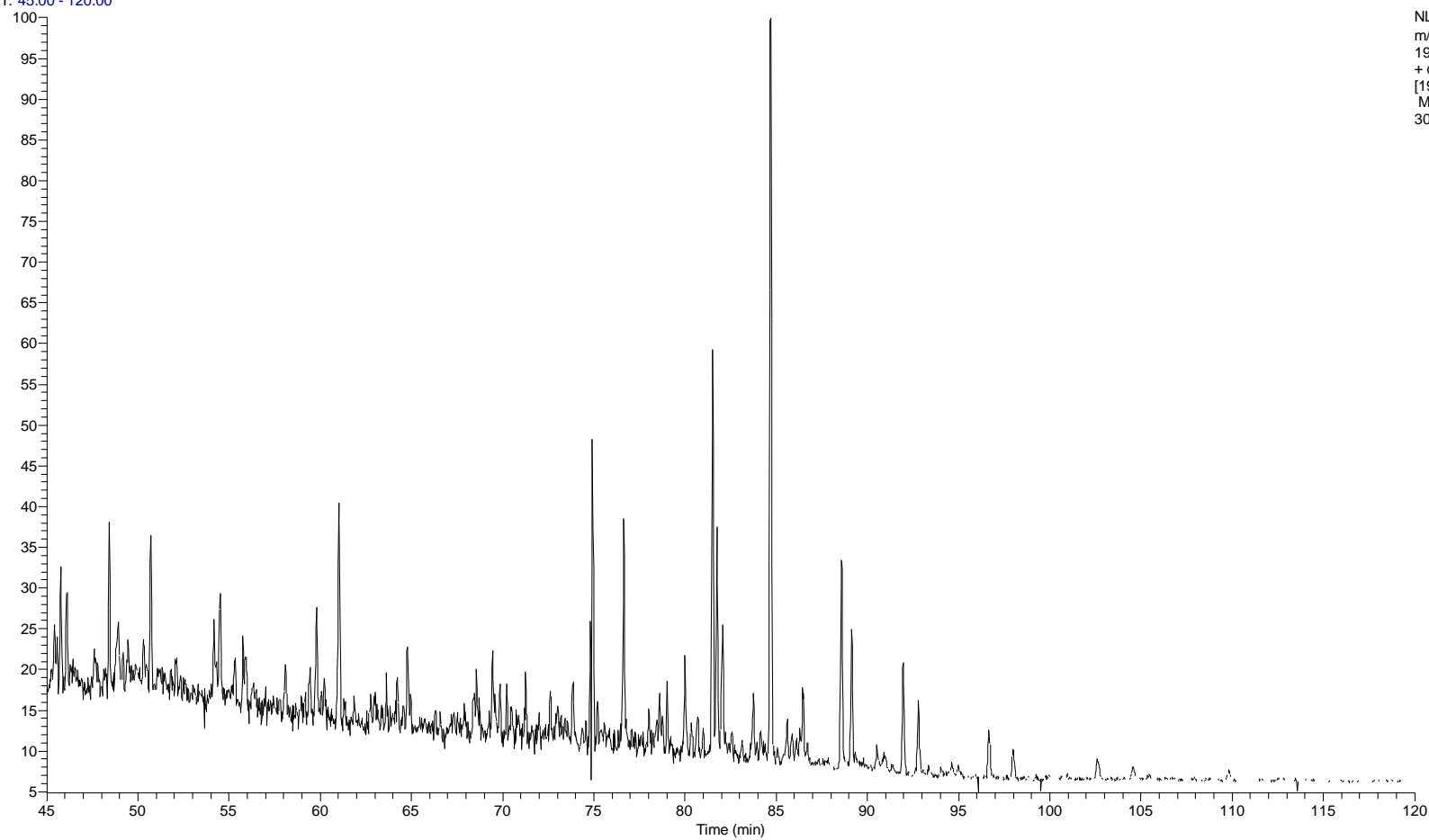
RT: 22.00 - 35.00



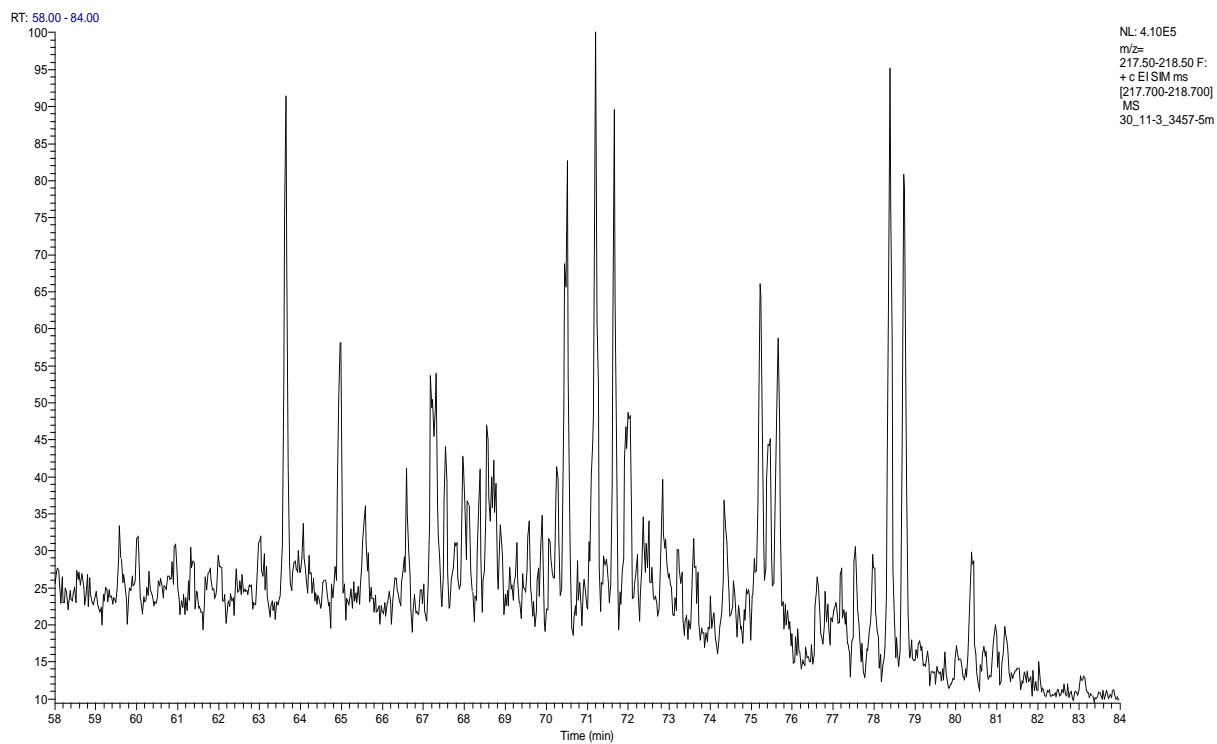
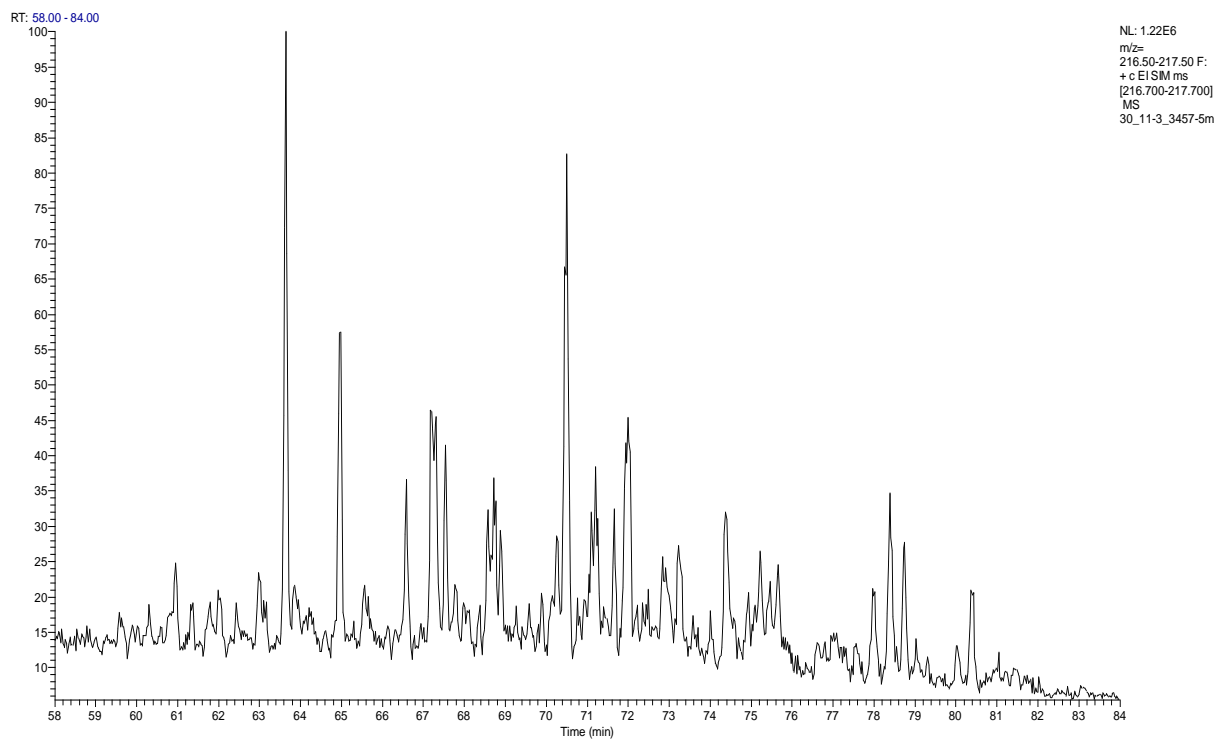
RT: 22.00 - 35.00

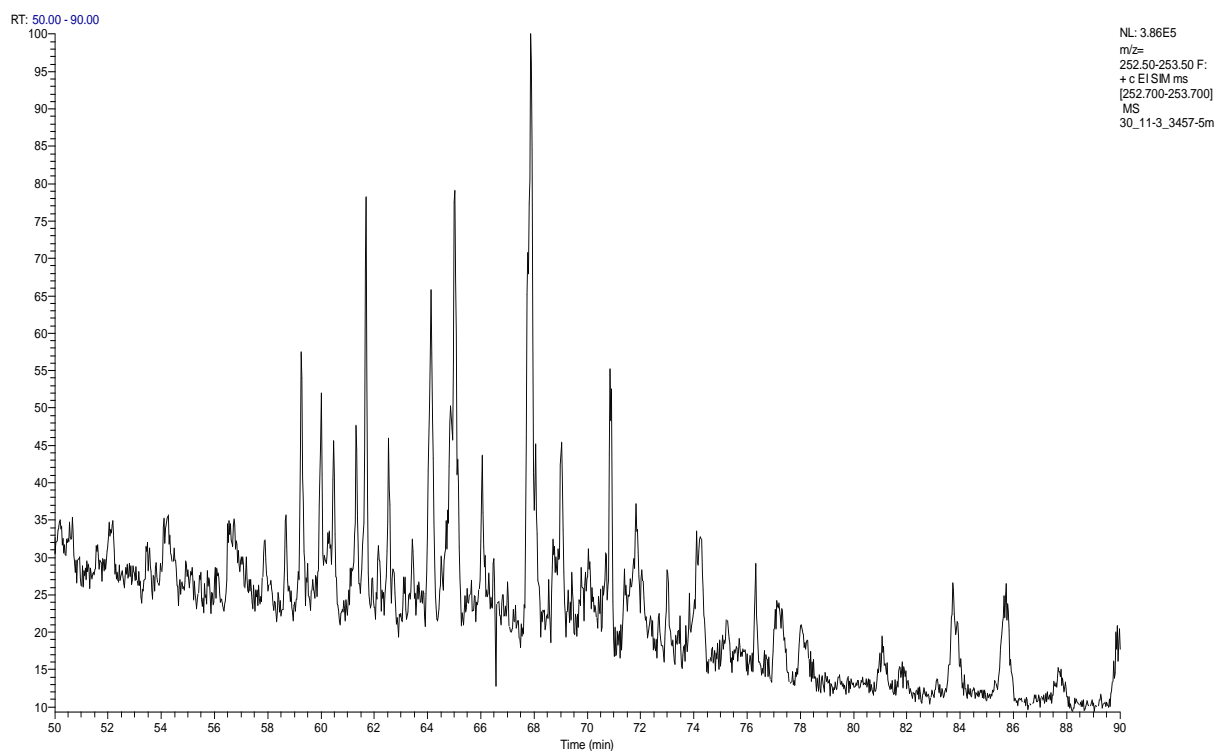
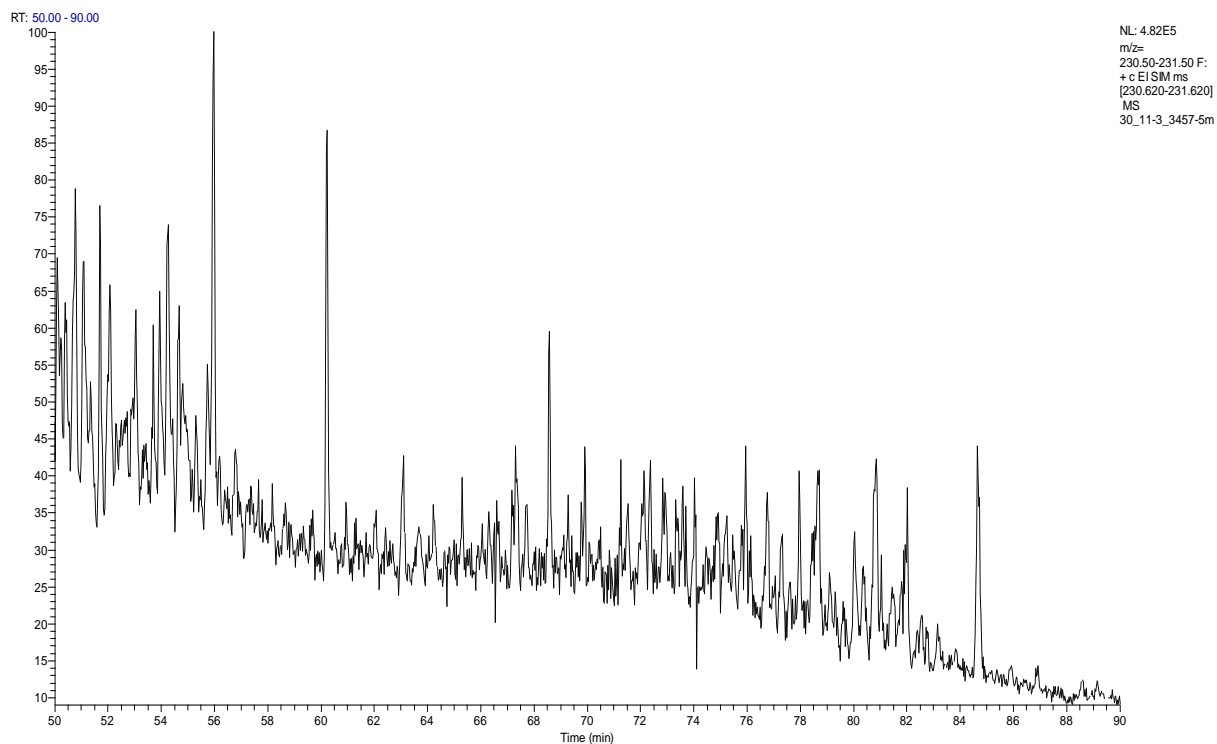


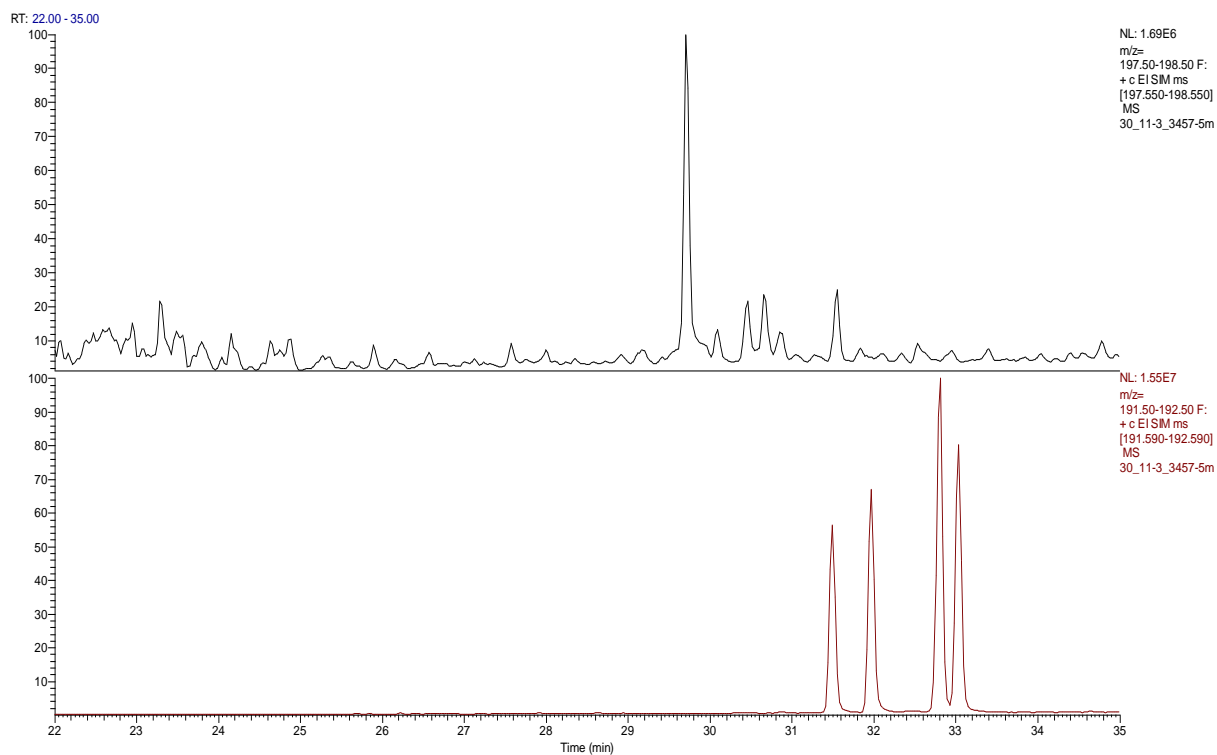
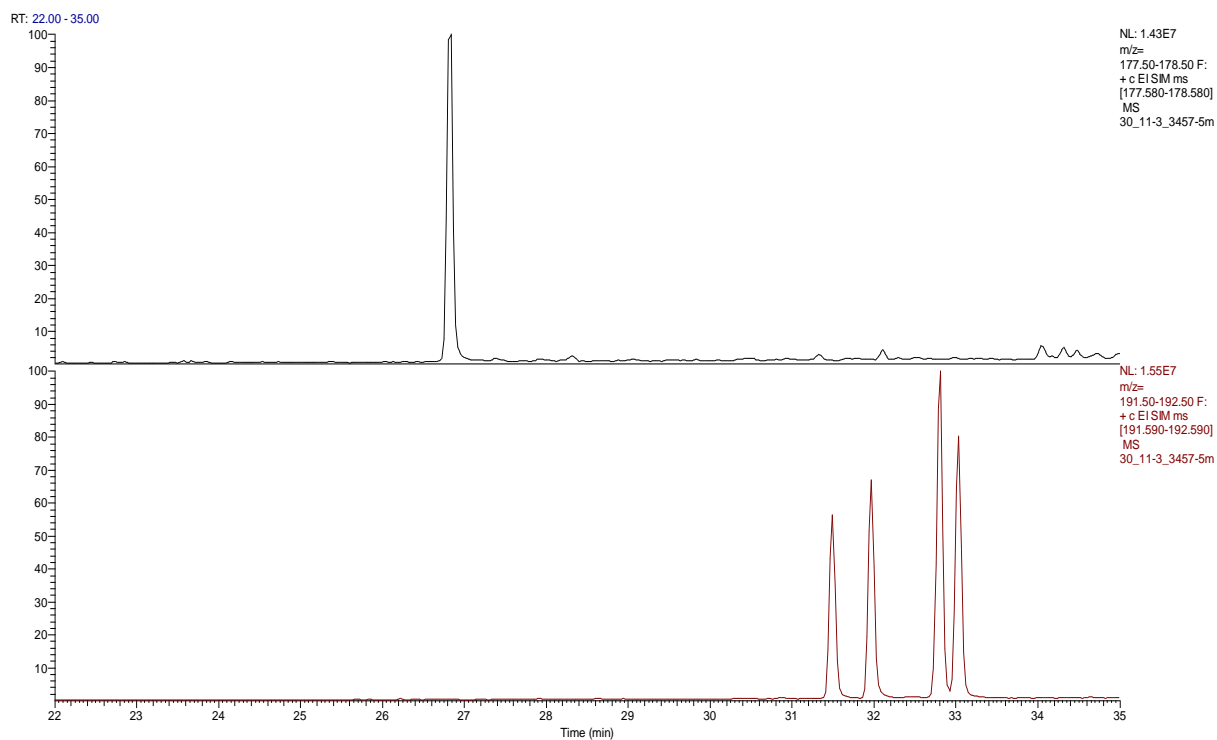
RT: 45.00 - 120.00



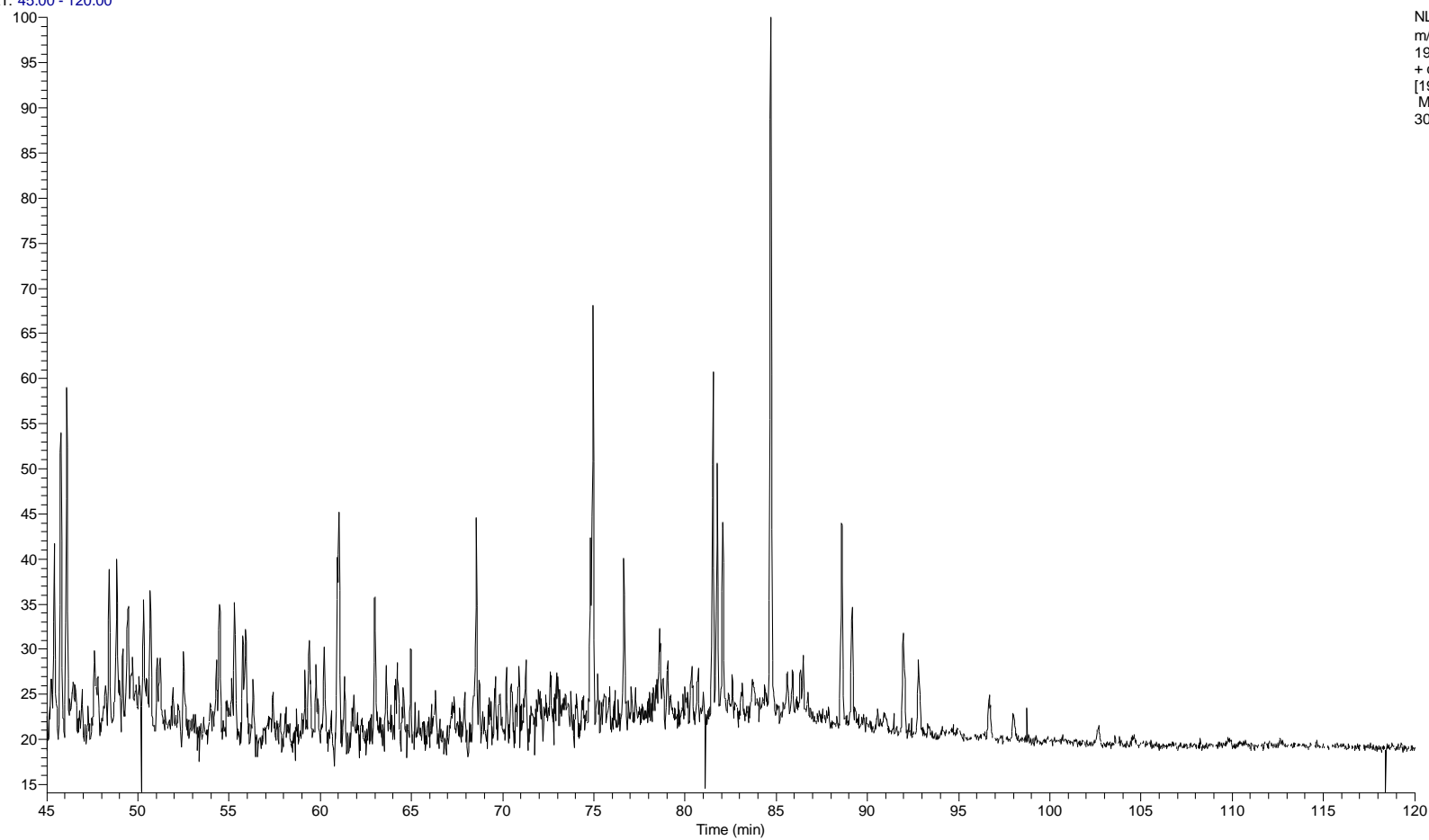
NL: 2.04E6
m/z=
190.50-191.50 F:
+ c EI SIM ms
[190.680-191.680]
MS
30_11-3_3457-5m





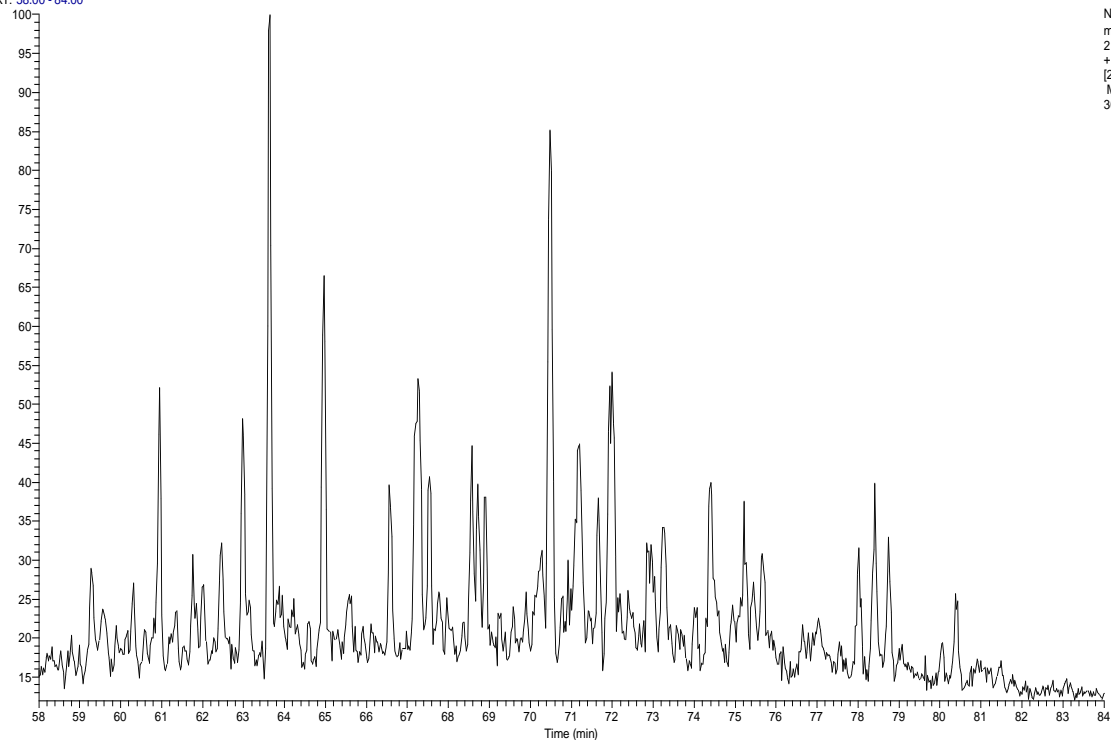


RT: 45.00 - 120.00



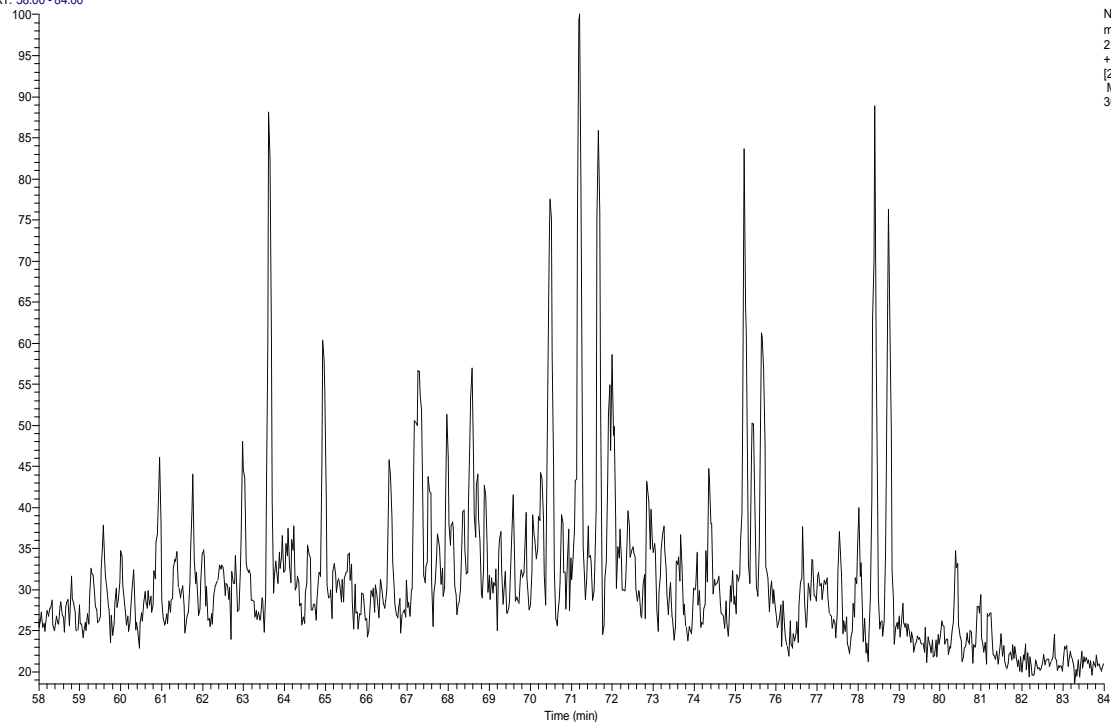
NL: 1.02E6
m/z=
190.50-191.50 F:
+ c EI SIM ms
[190.680-191.680]
MS
30_11-4_3515-5m

RT: 58.00 - 84.00

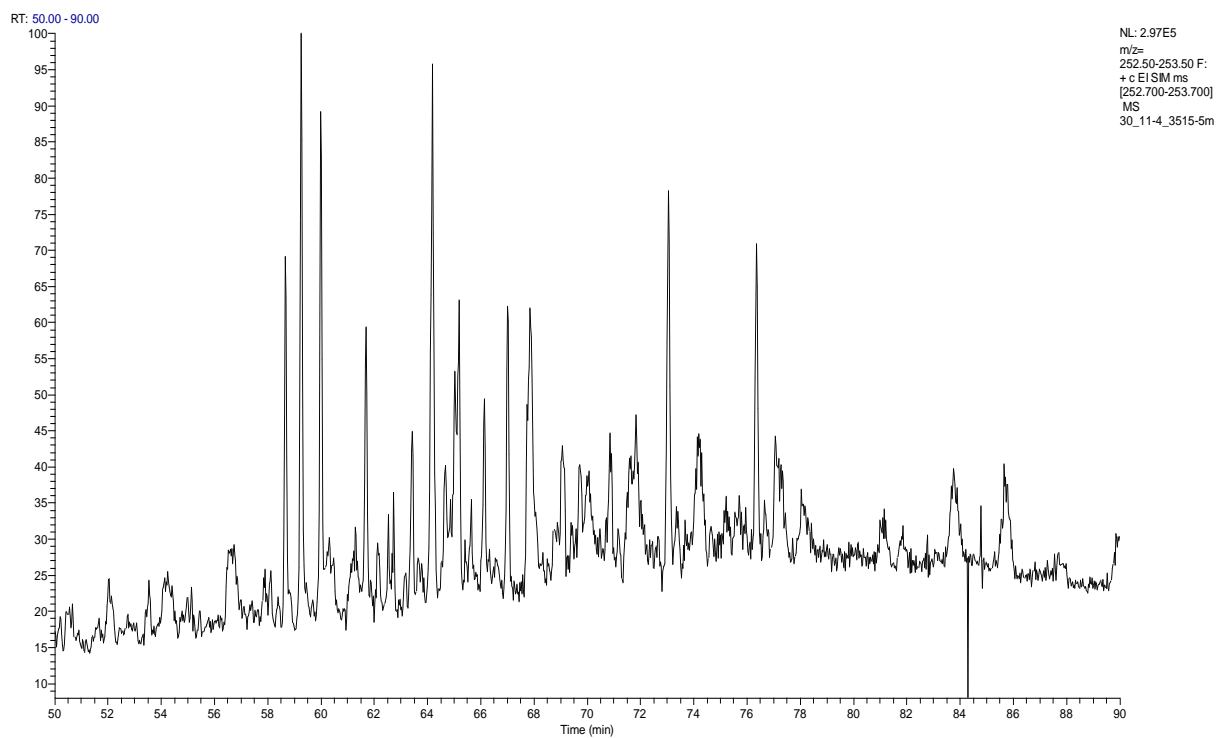
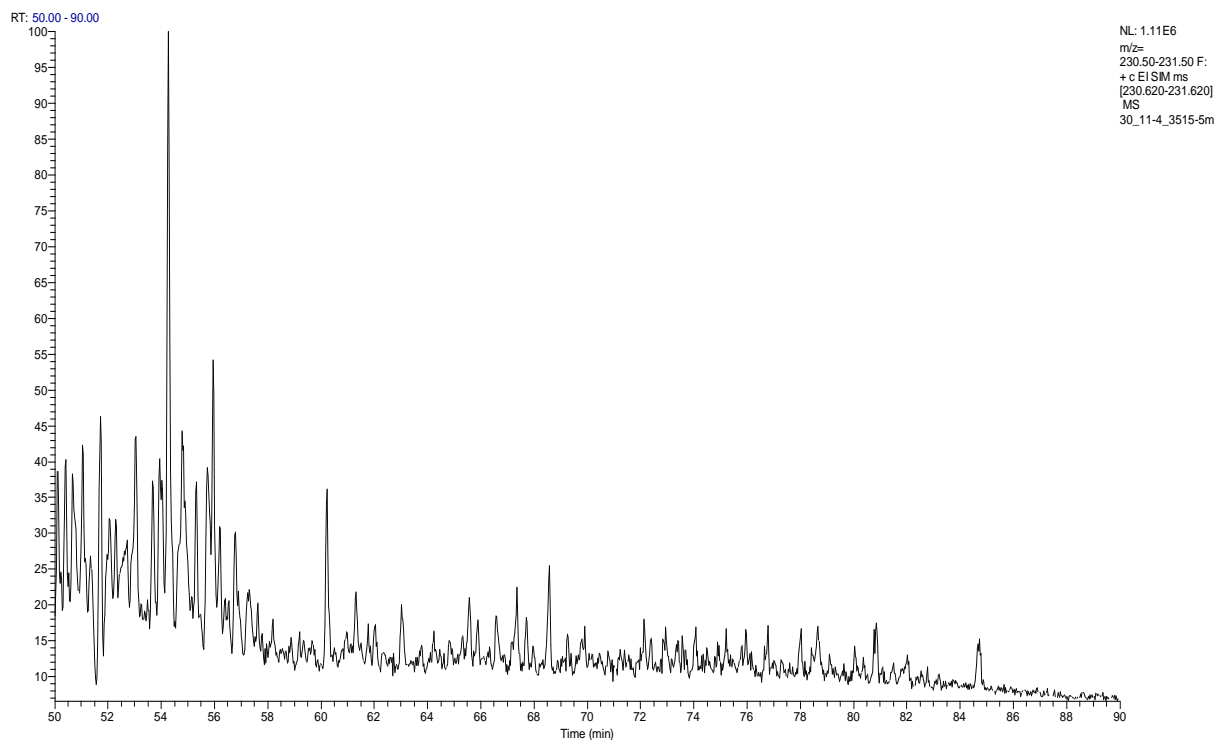


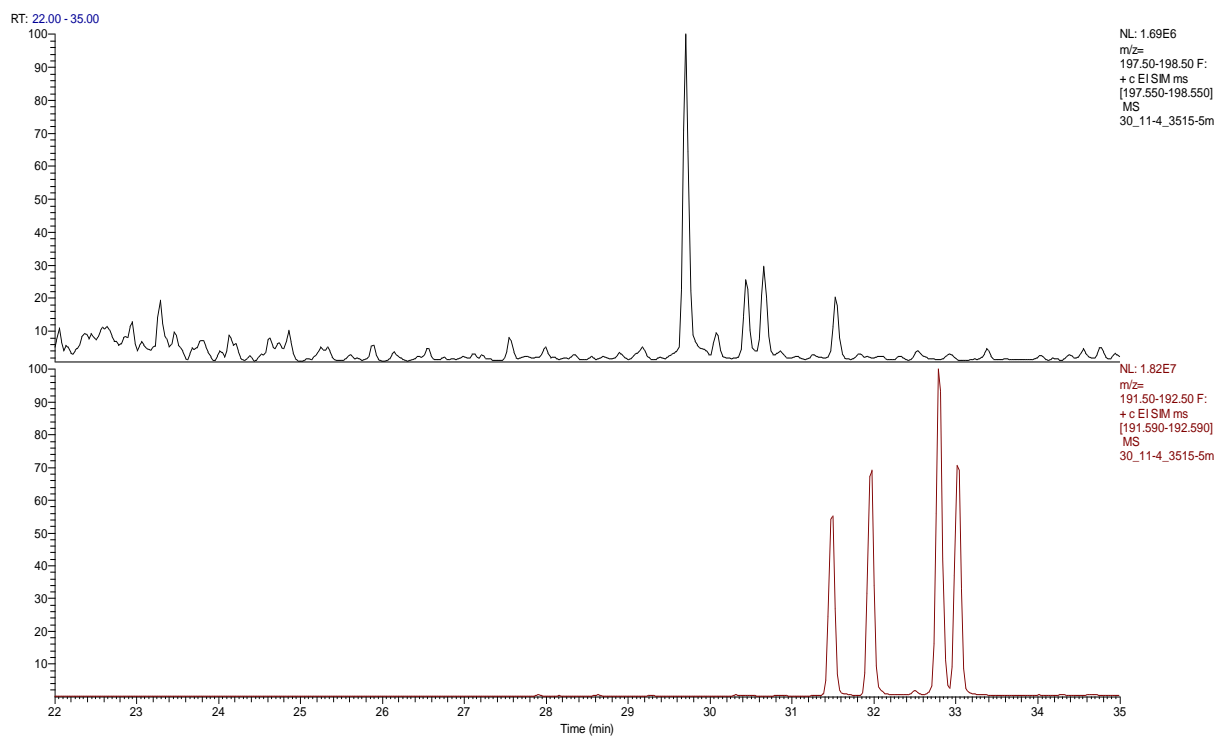
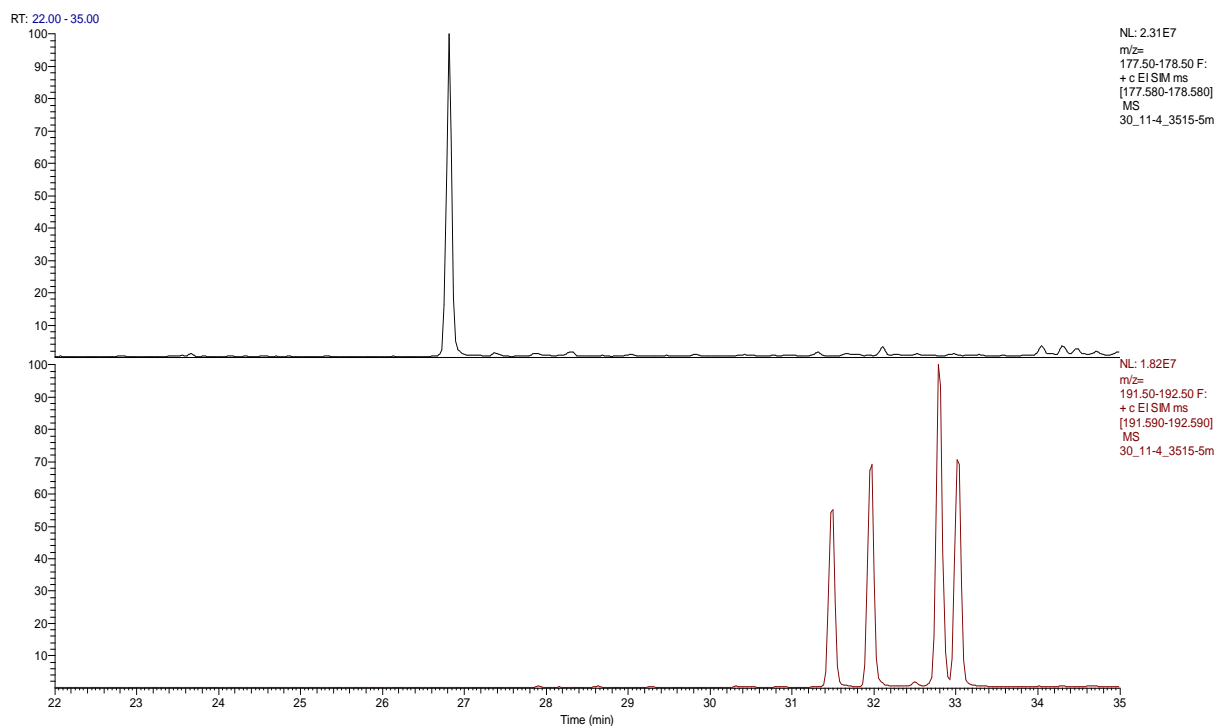
NL: 8.21E5
m/z=
216.50-217.50 F:
+ c E1 SIM ms
[216.700-217.700]
MS
30_11-4_3515-5m

RT: 58.00 - 84.00

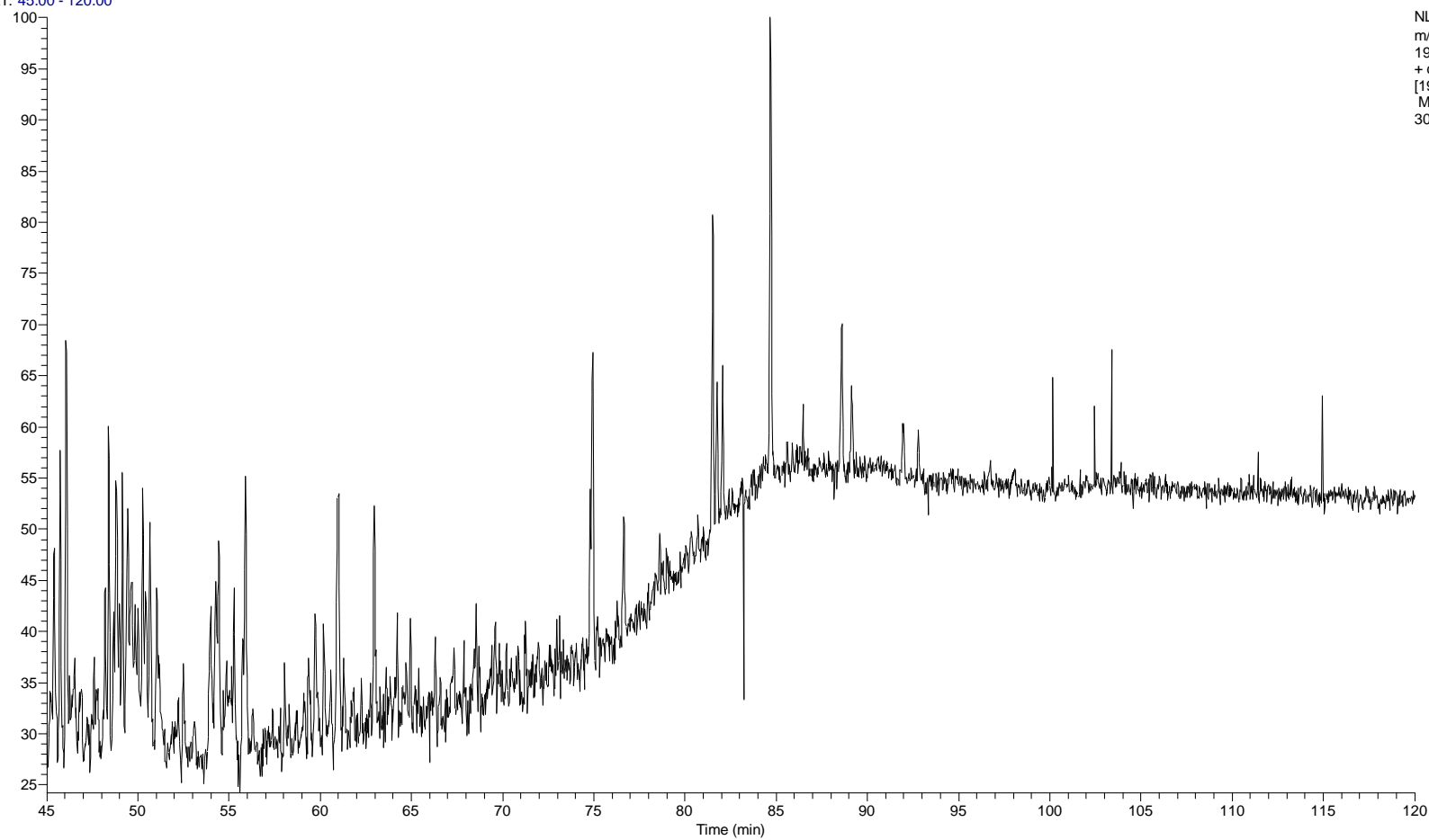


NL: 3.13E5
m/z=
217.50-218.50 F:
+ c E1 SIM ms
[217.700-218.700]
MS
30_11-4_3515-5m





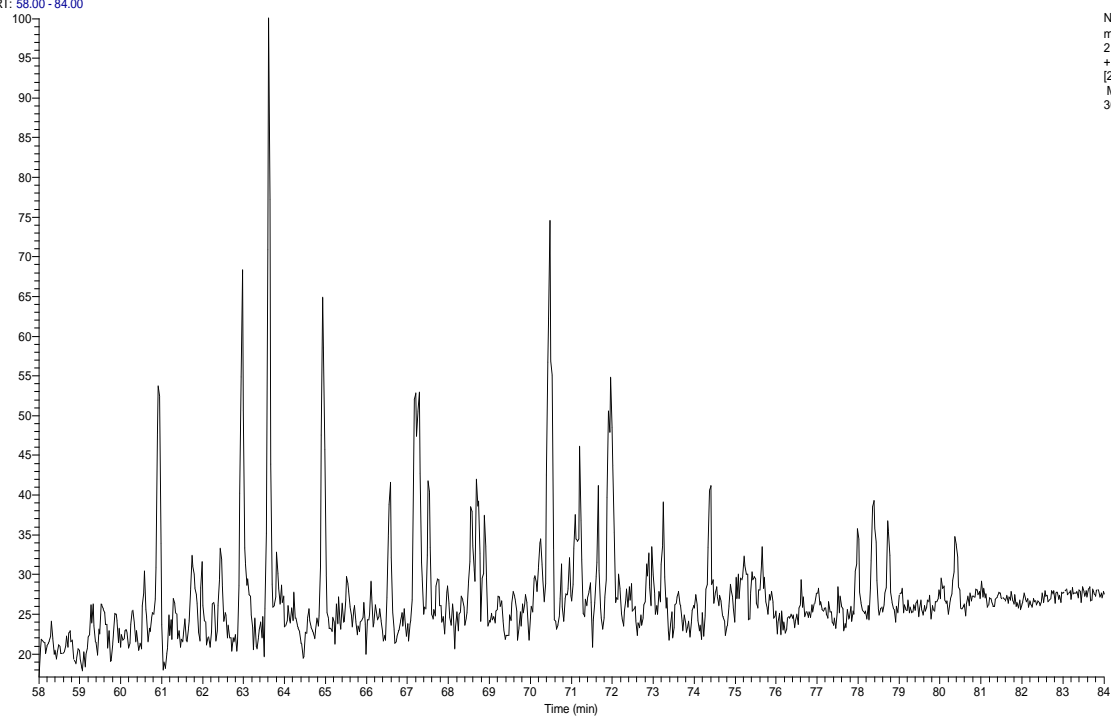
RT: 45.00 - 120.00



NL: 3.45E5
m/z=
190.50-191.50 F:
+ c EI SIM ms
[190.680-191.680]
MS
30_11-4_3526-8m

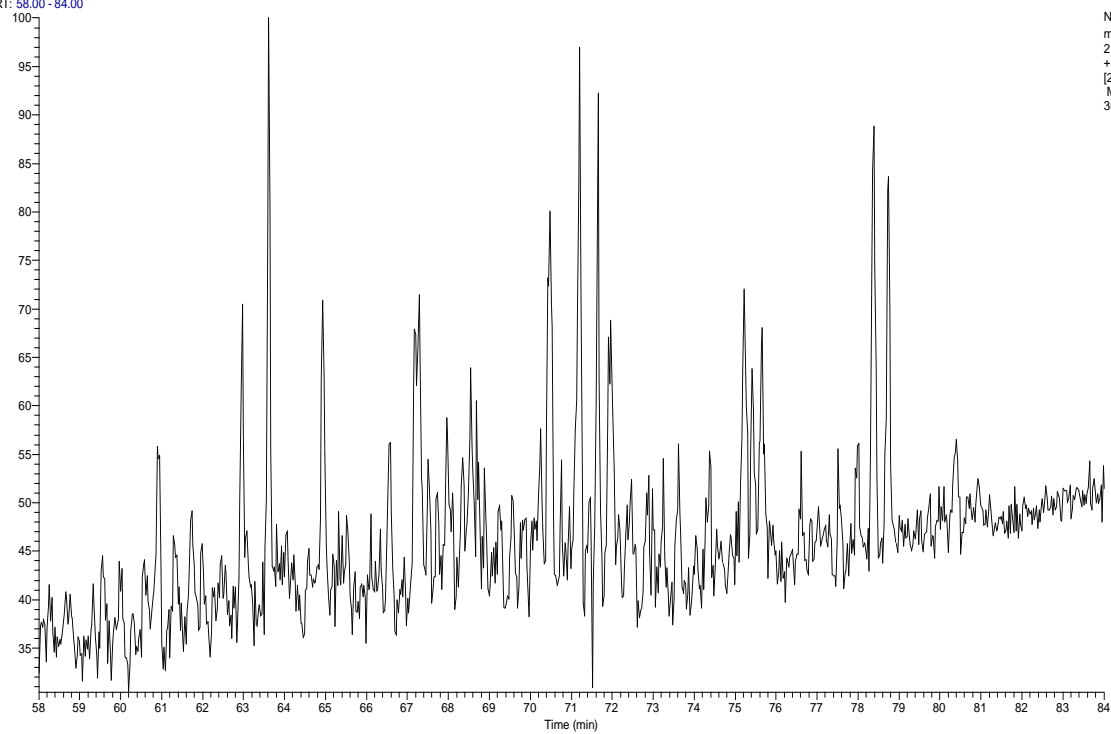
Appendix

RT: 58.00 - 84.00

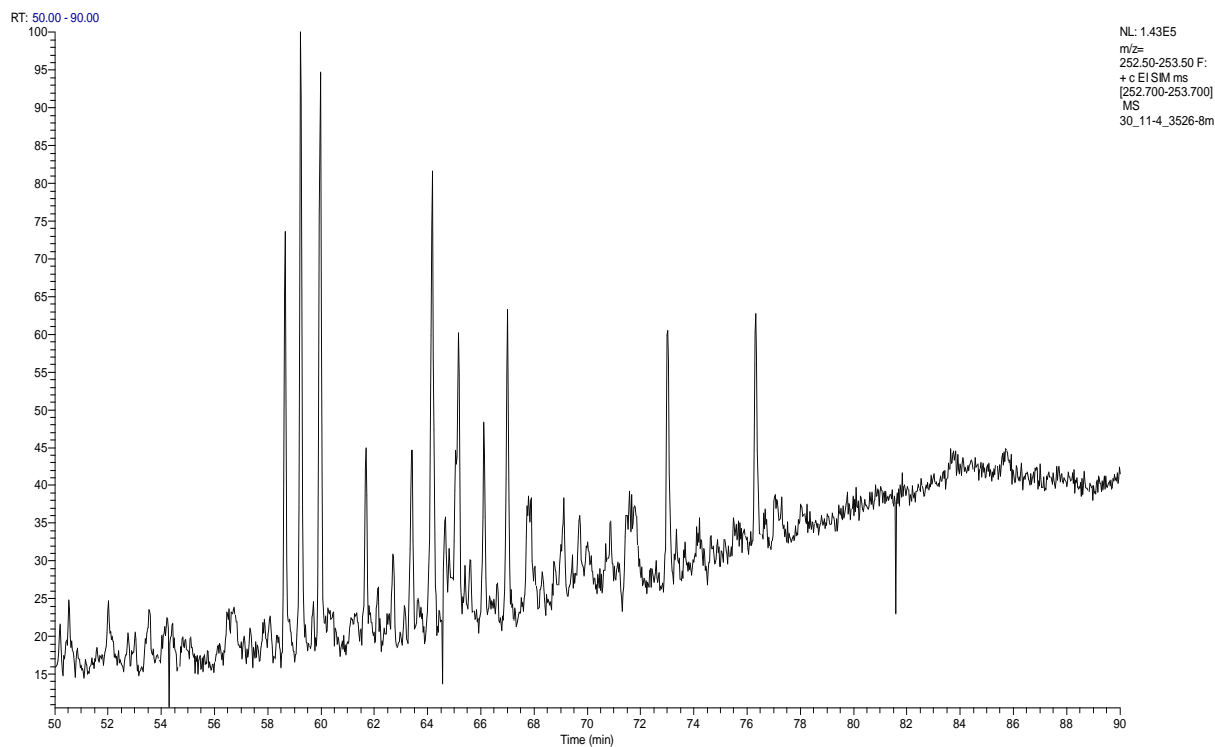
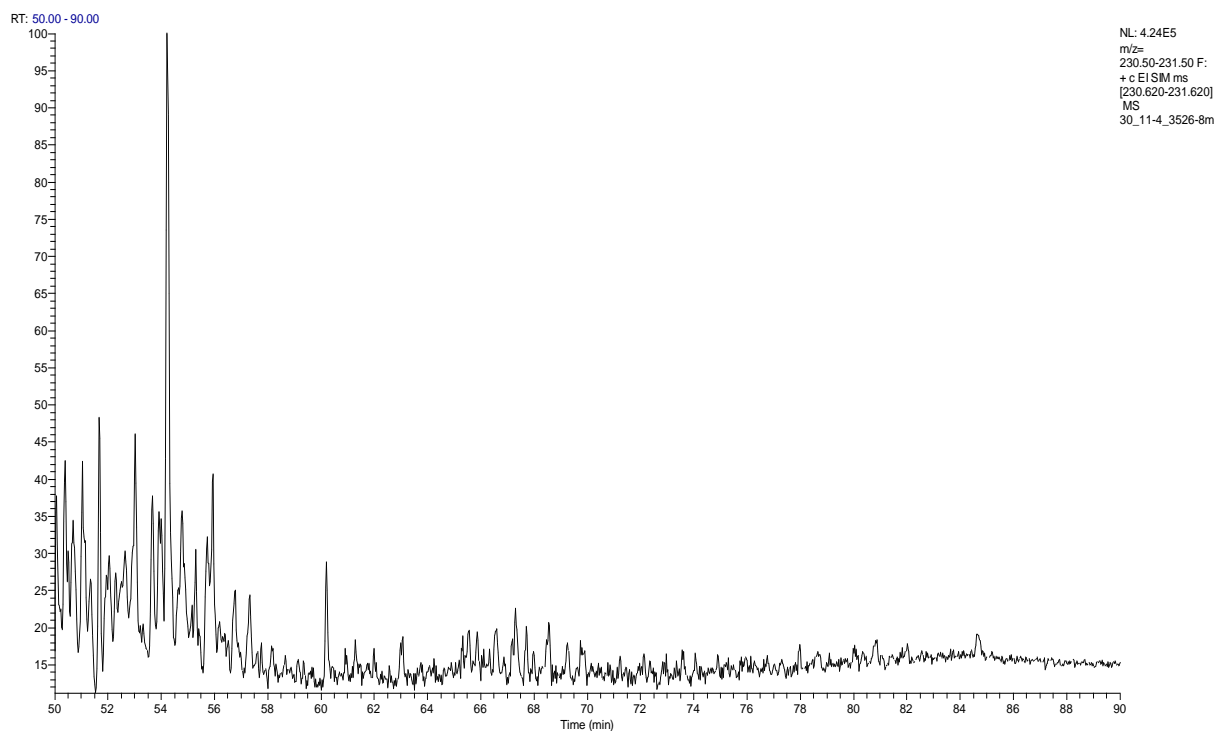


NL: 2.74E5
m/z= 216.50-217.50 F:
+ c E1 SIM ms
[216.700-217.700]
MS
30_11-4_3526-8m

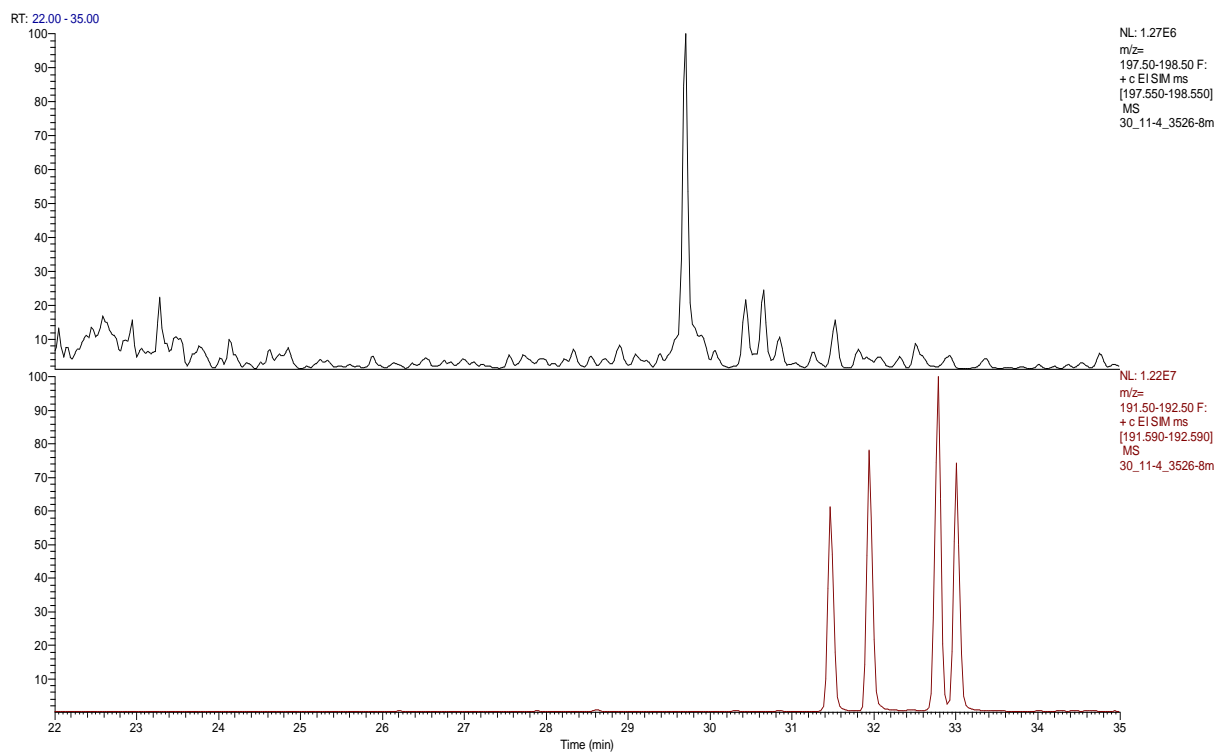
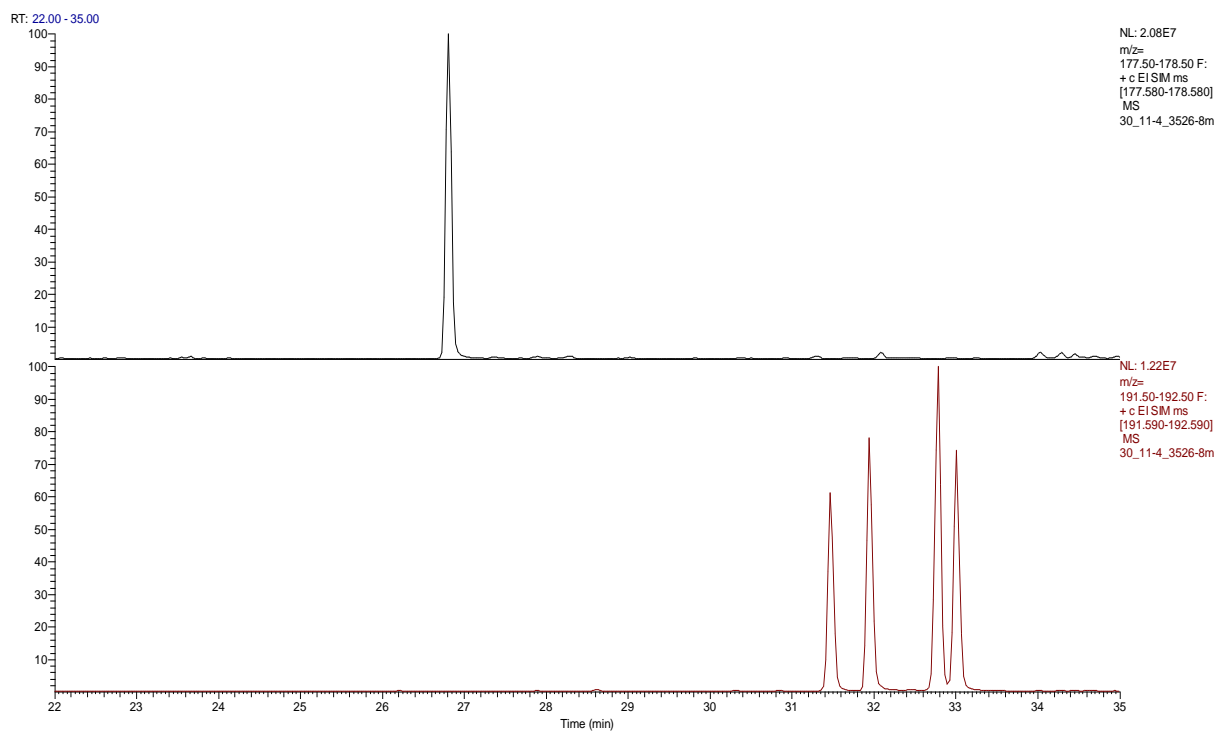
RT: 58.00 - 84.00



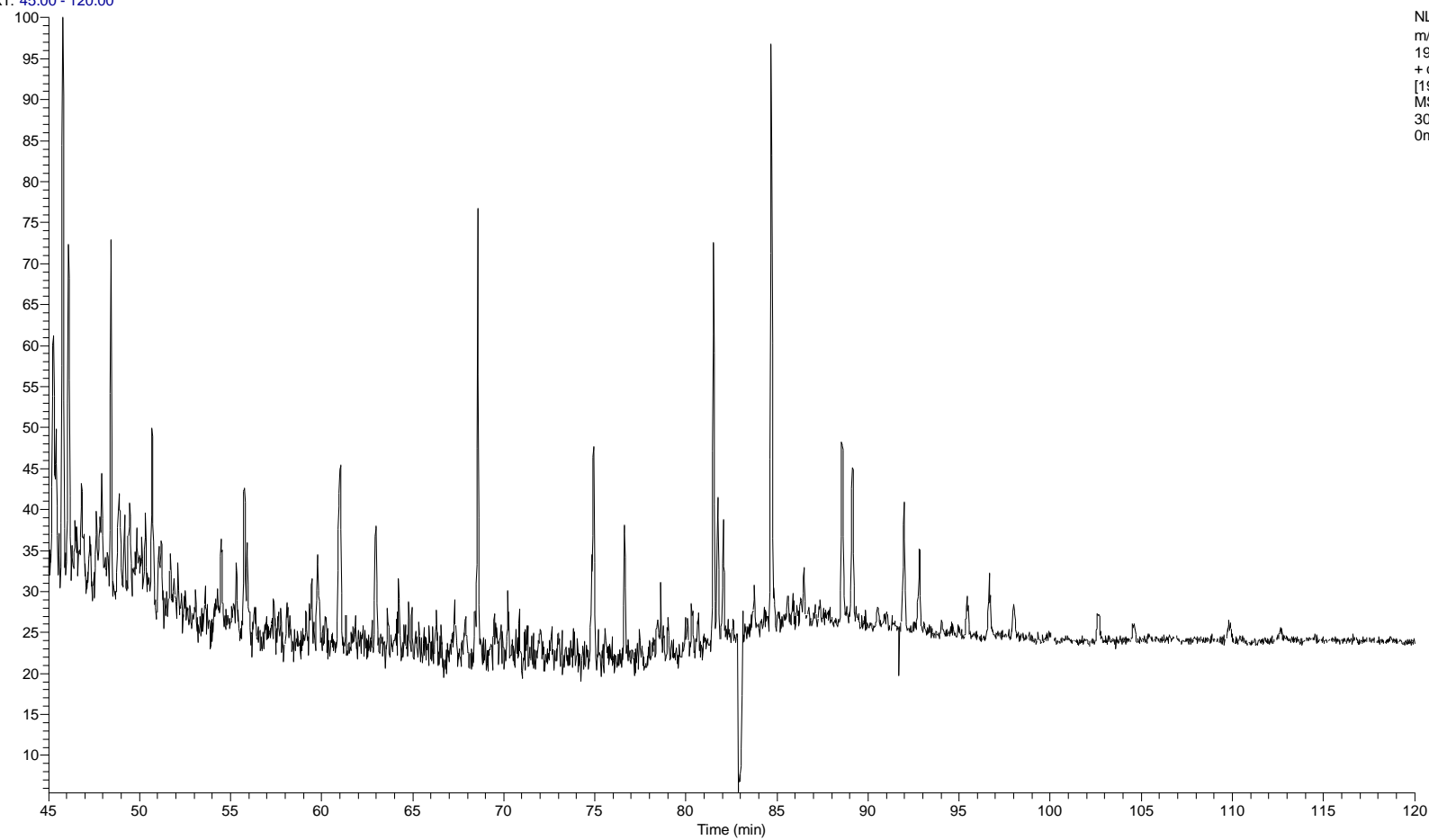
NL: 9.52E4
m/z= 217.50-218.50 F:
+ c E1 SIM ms
[217.700-218.700]
MS
30_11-4_3526-8m



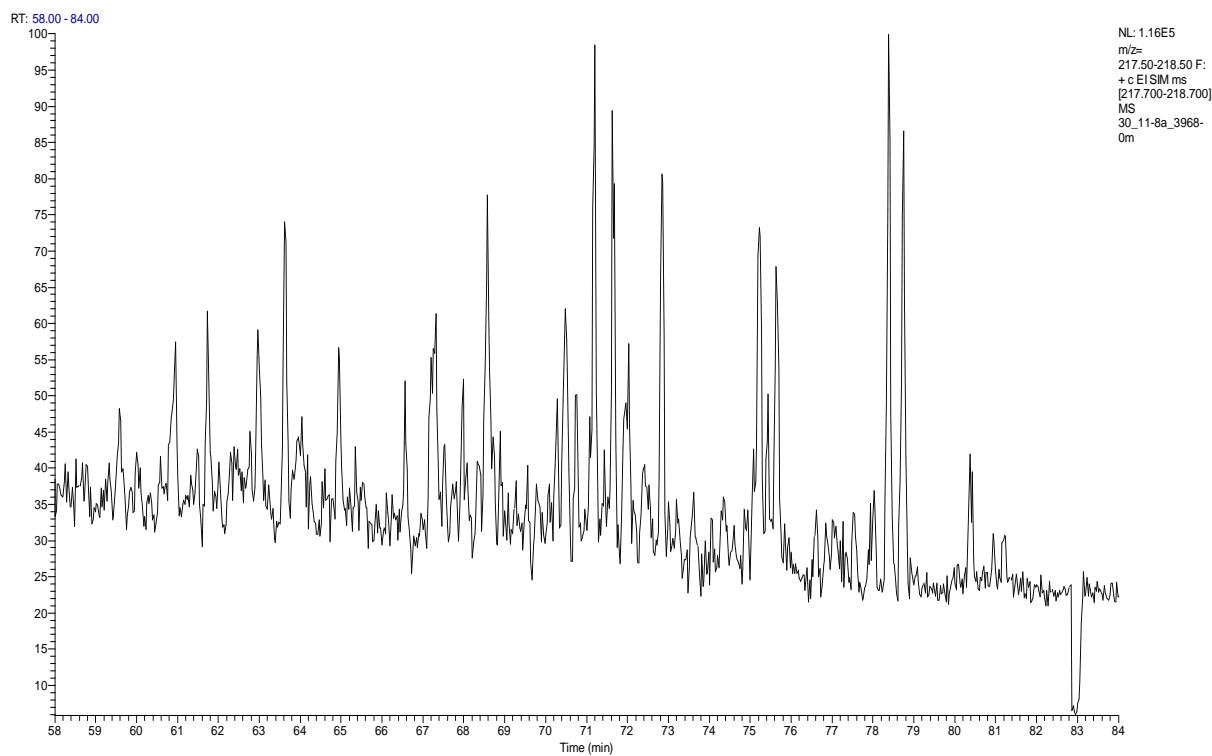
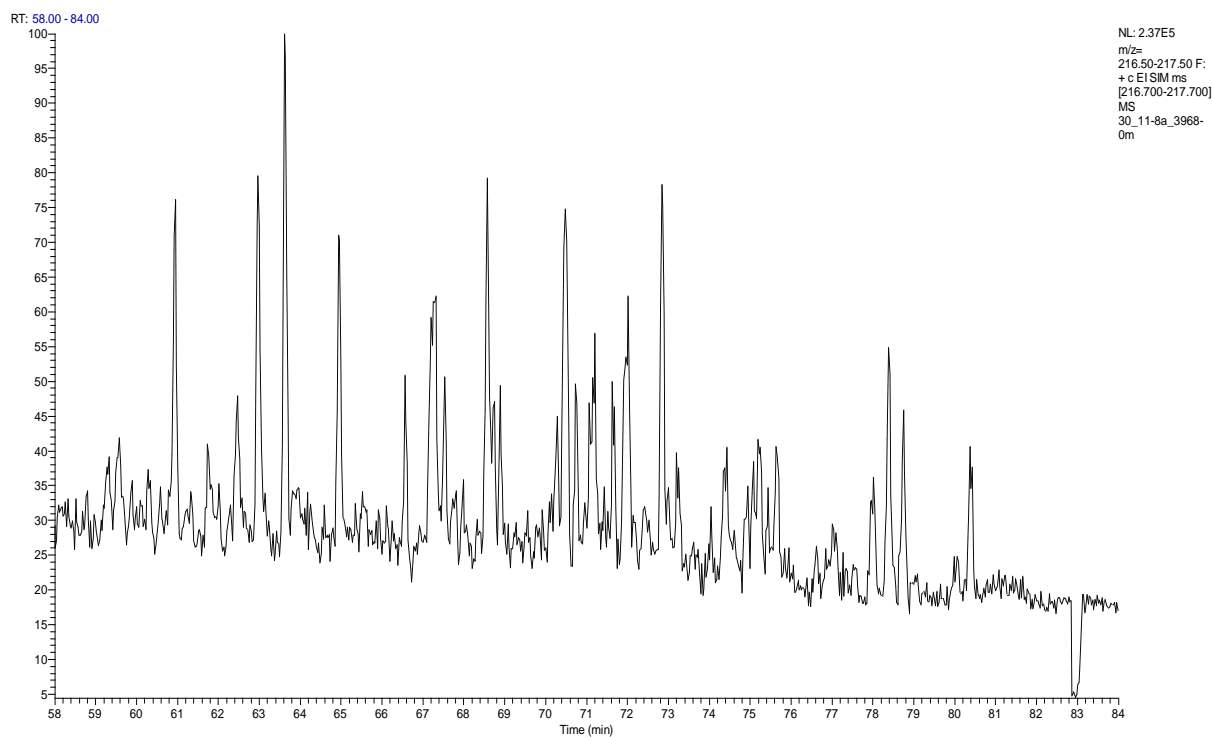
Appendix

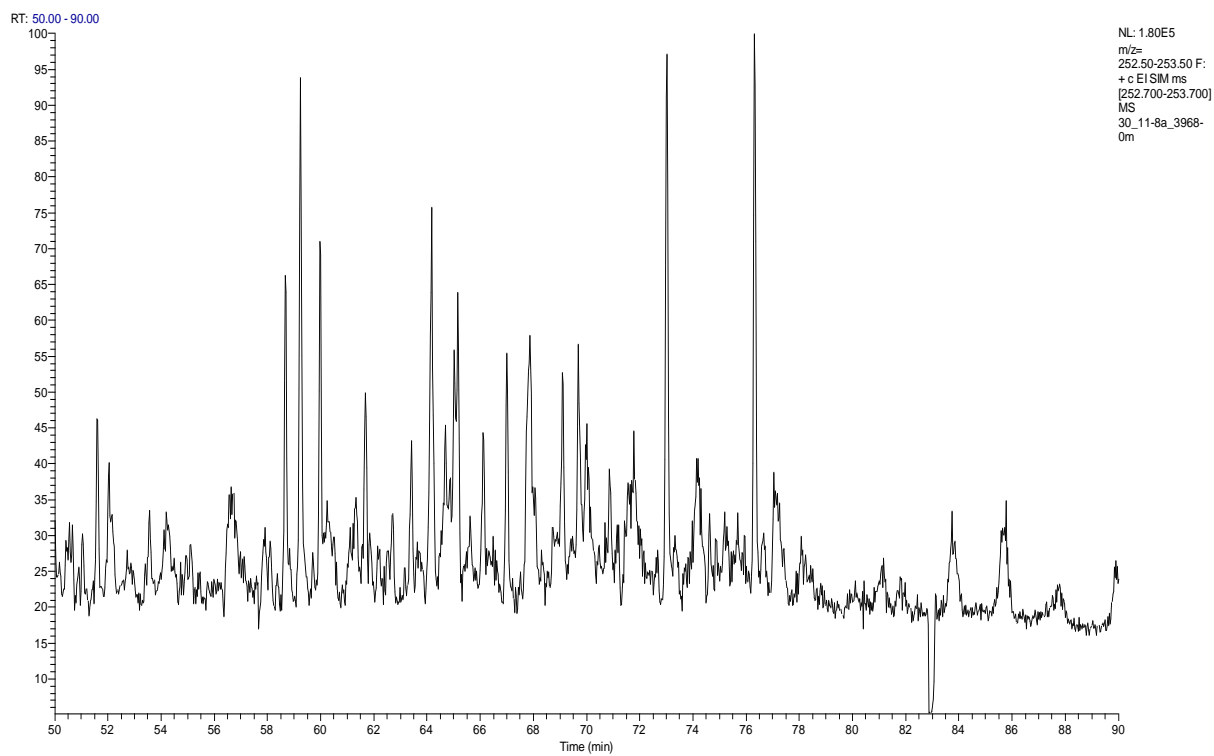
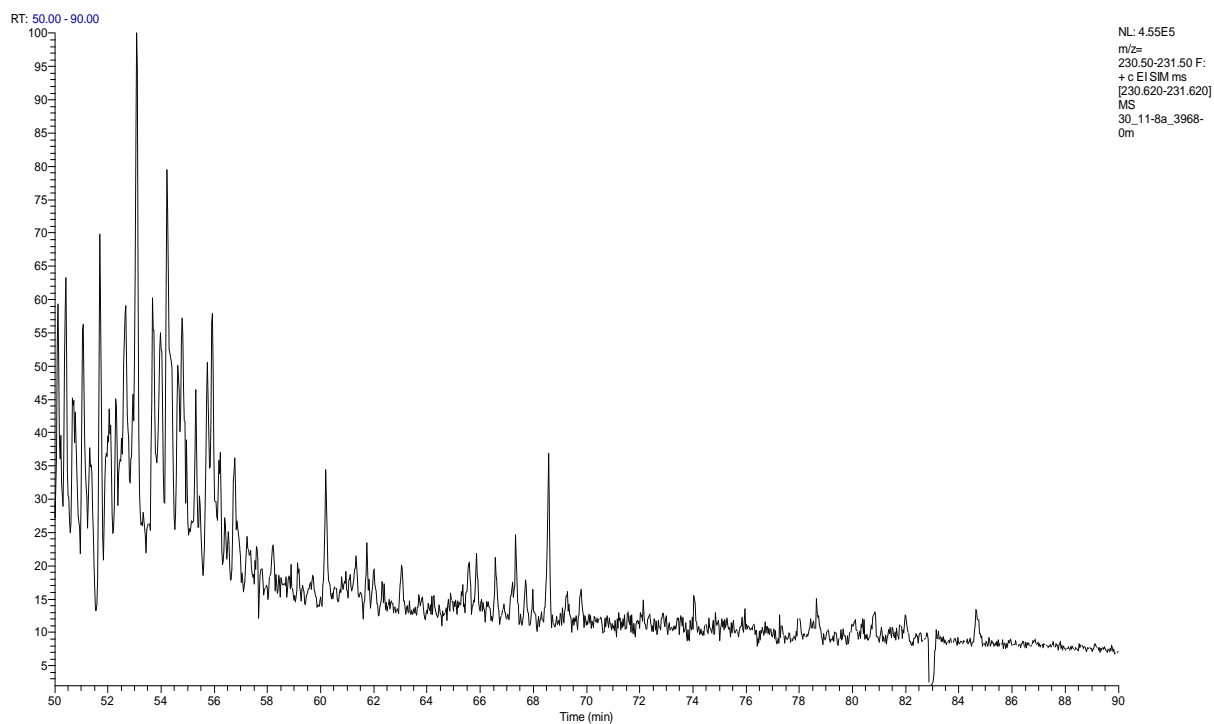


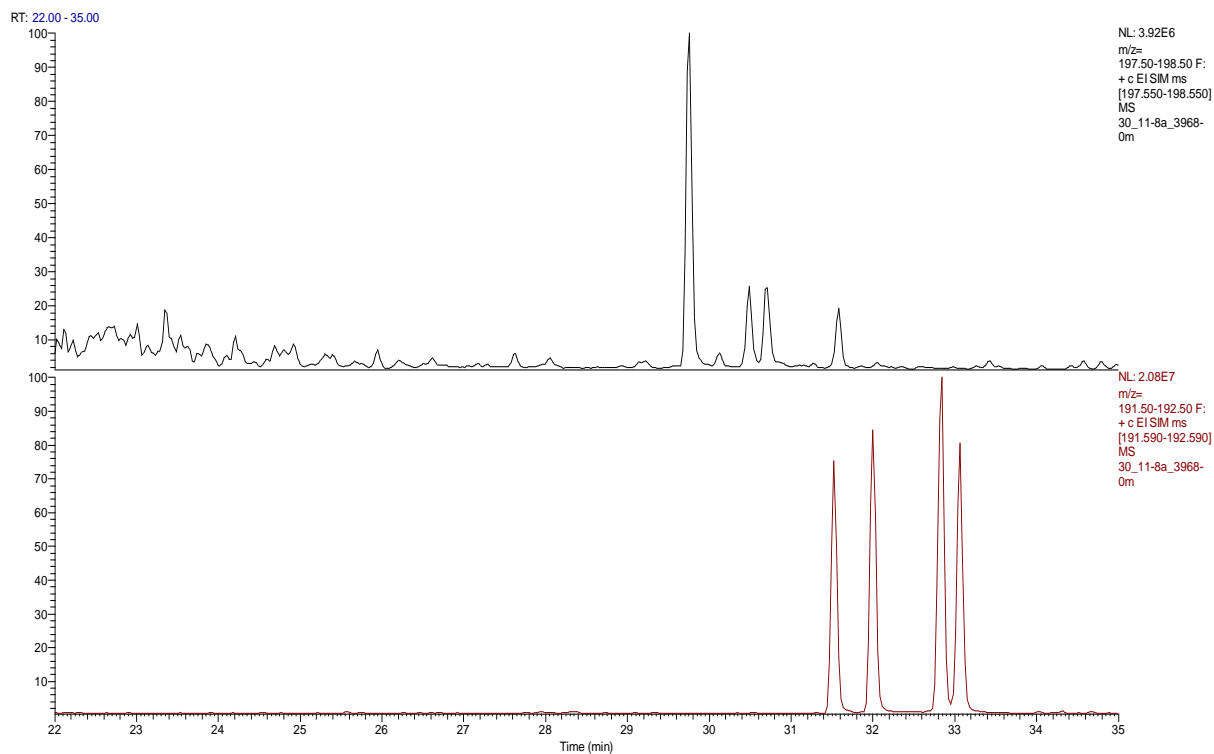
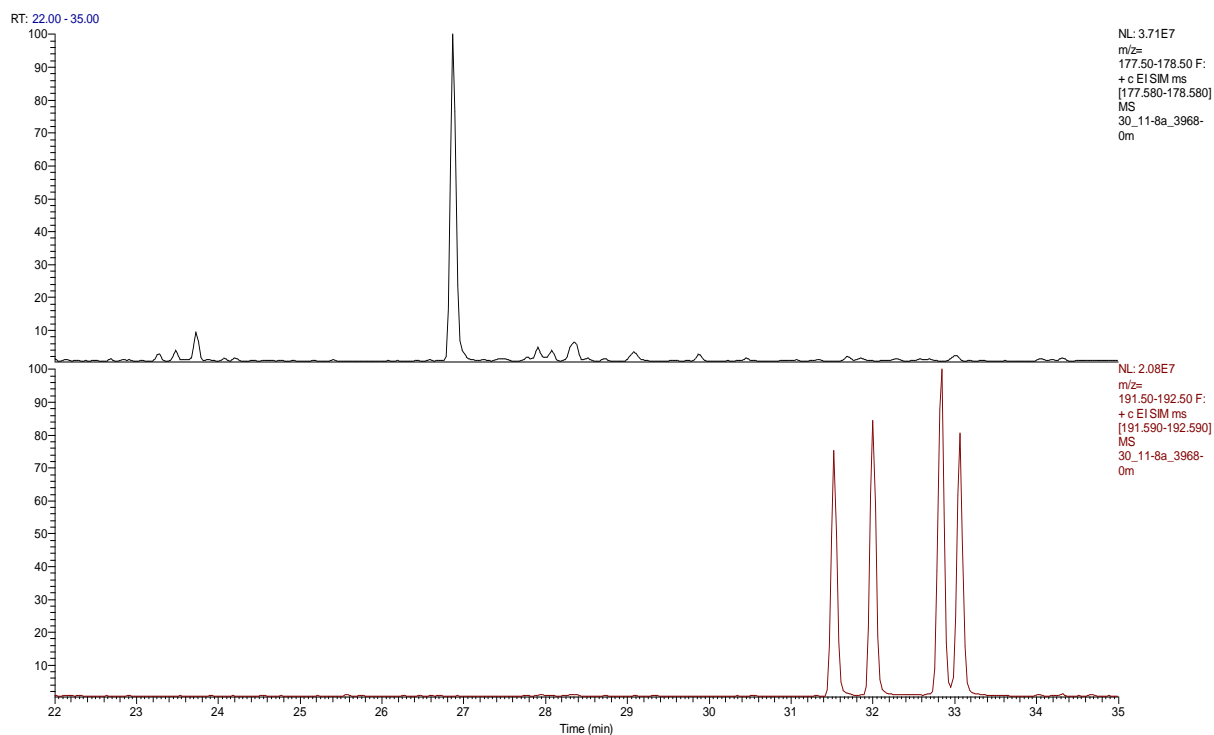
RT: 45.00 - 120.00



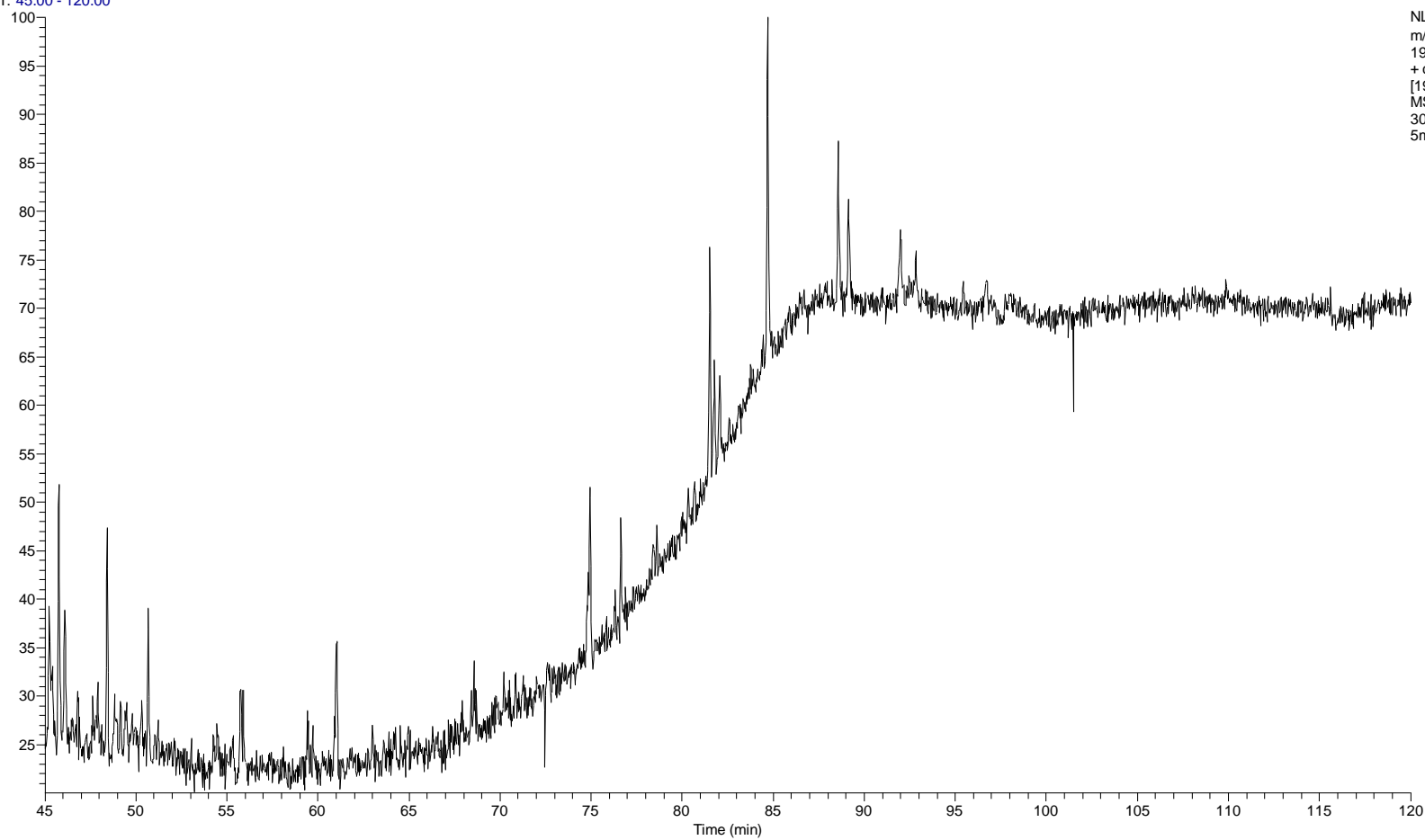
NL: 4.94E5
m/z=
190.50-191.50 F:
+ c E!SIM ms
[190.680-191.680]
MS
30_11-8a_3968-
0m



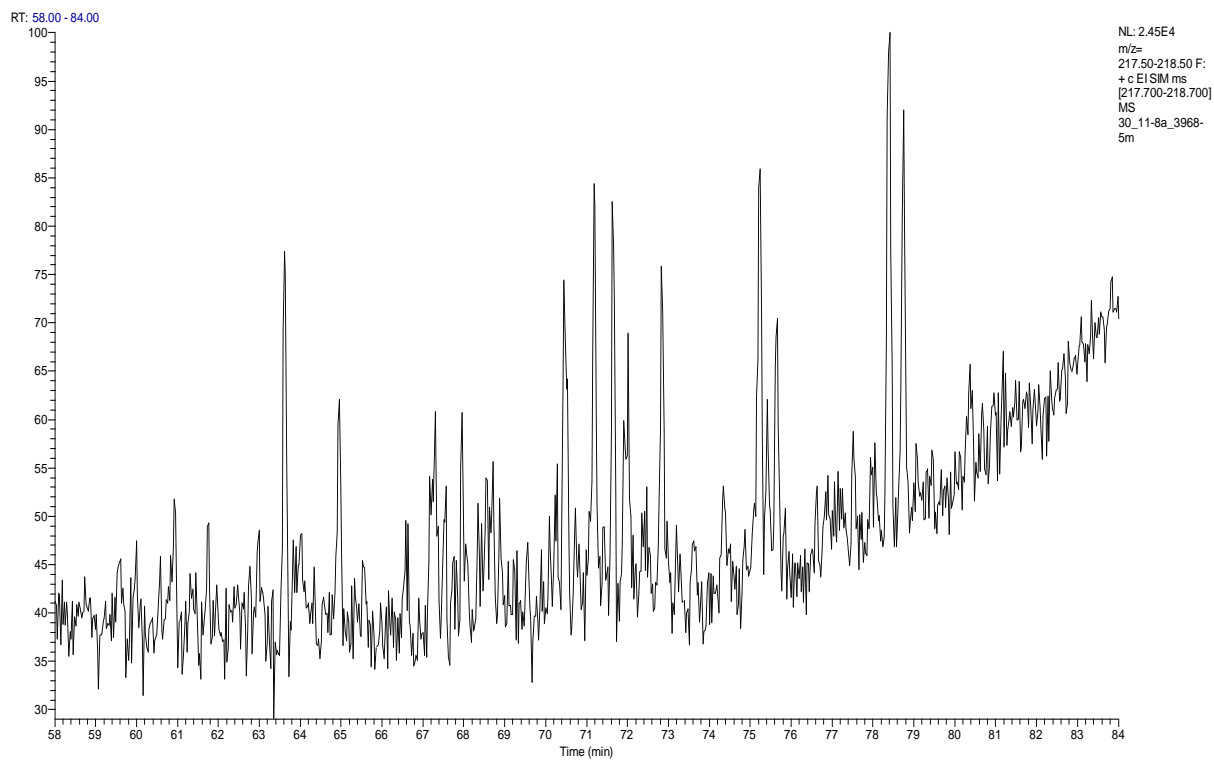
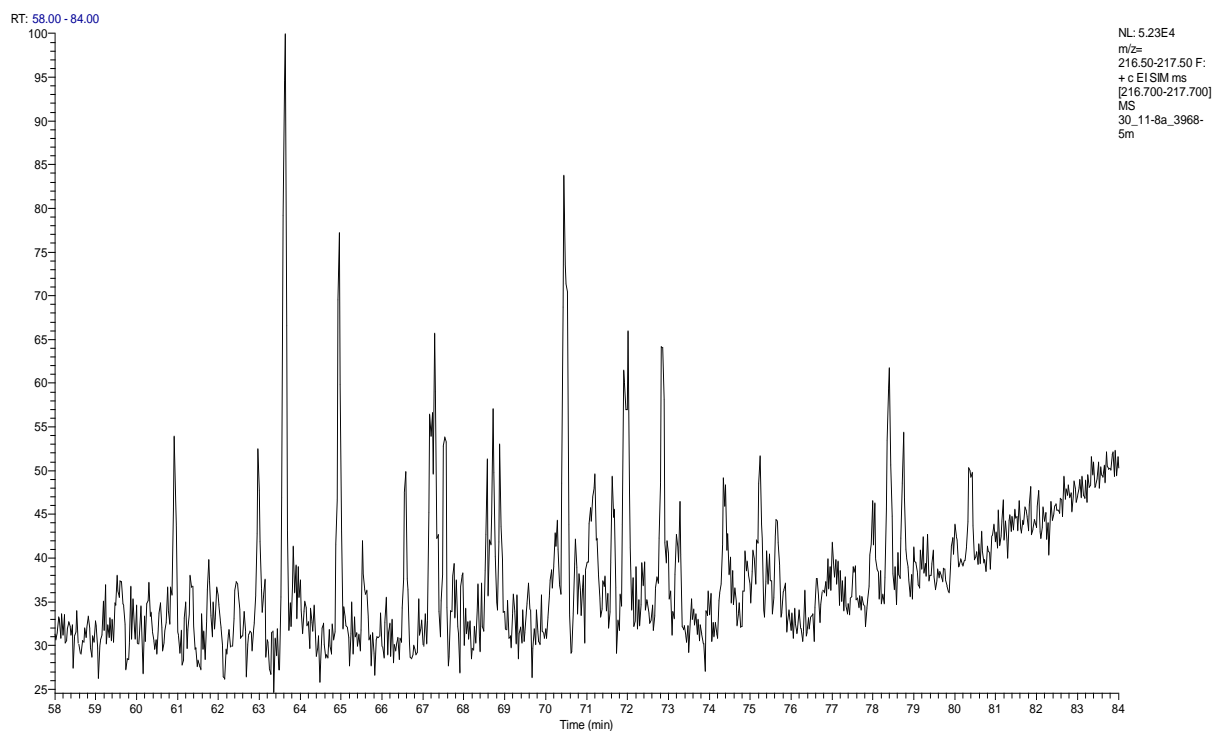


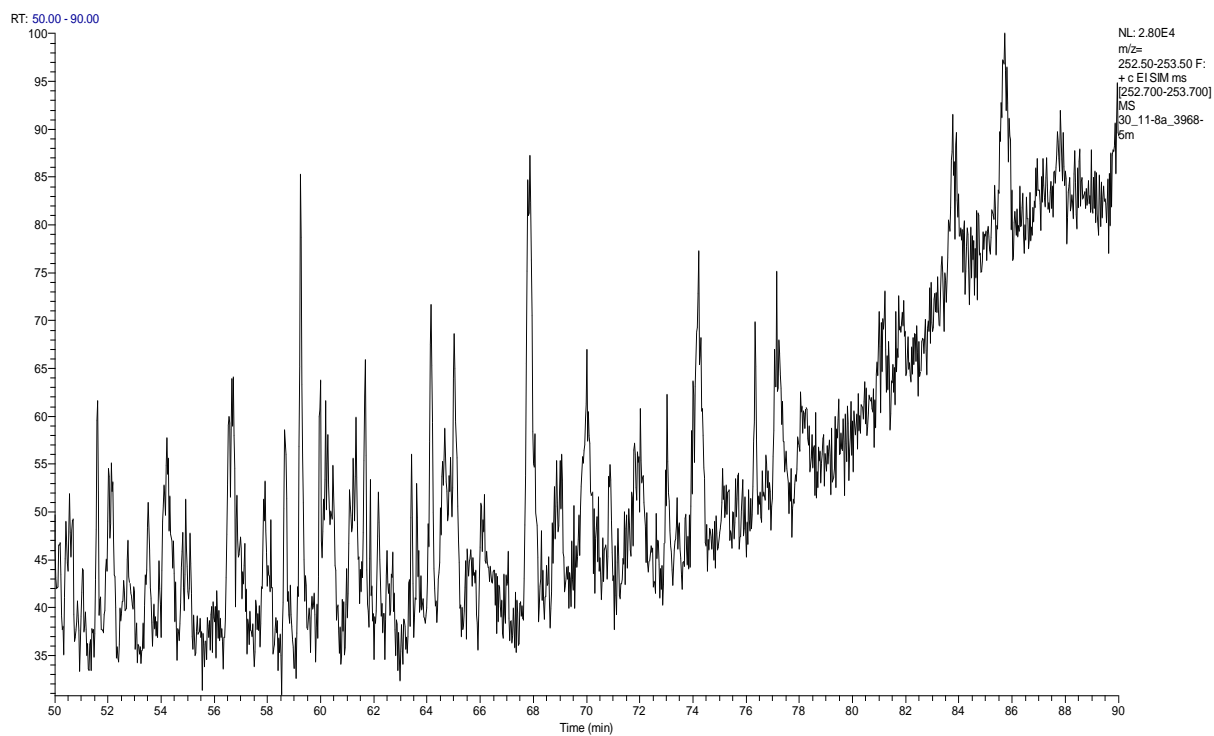
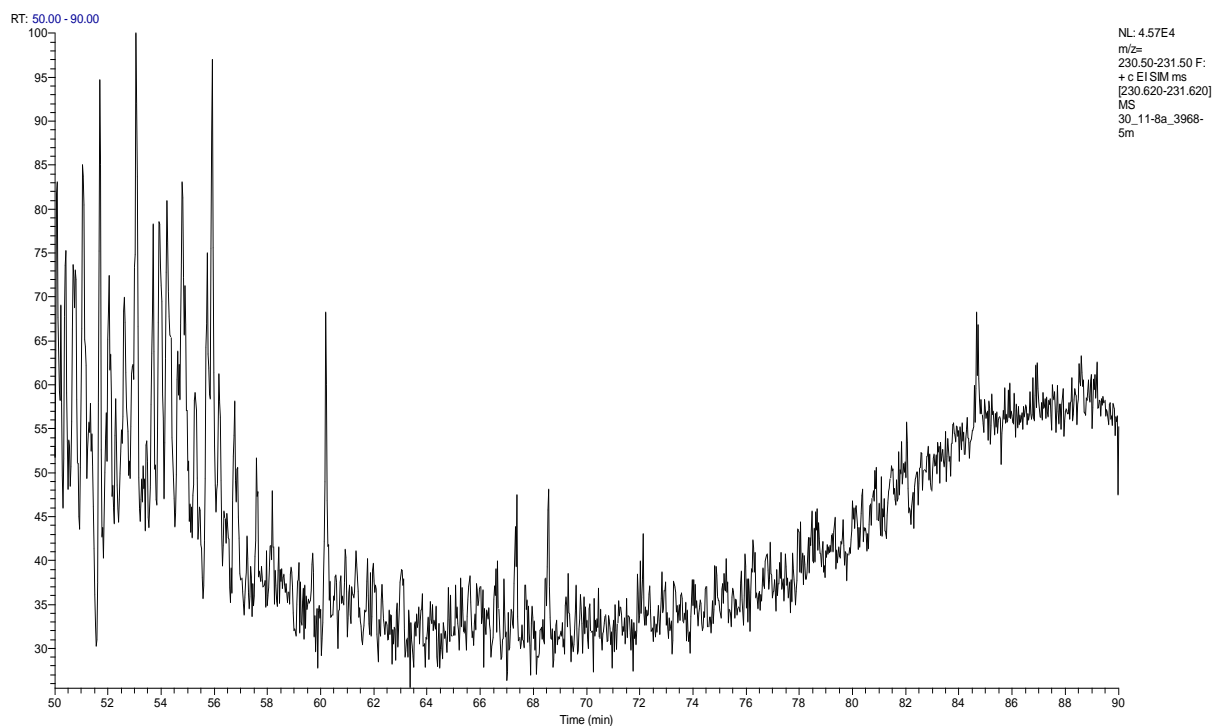


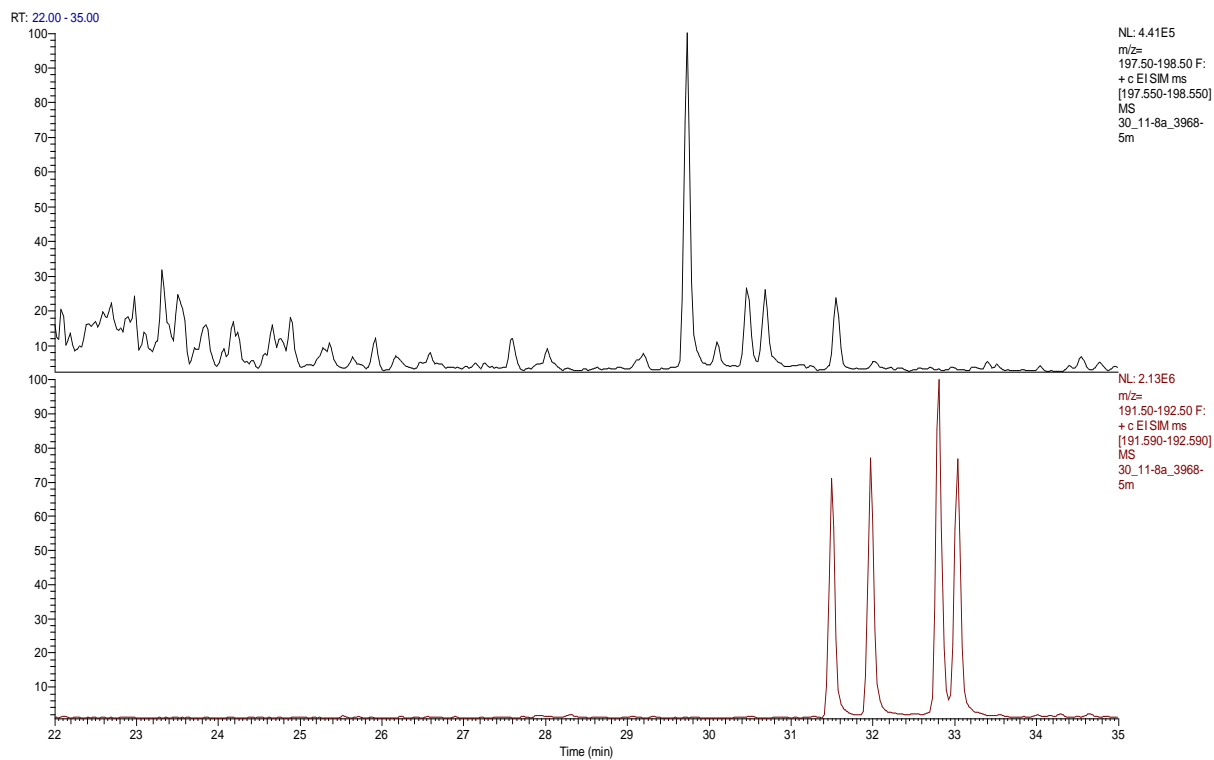
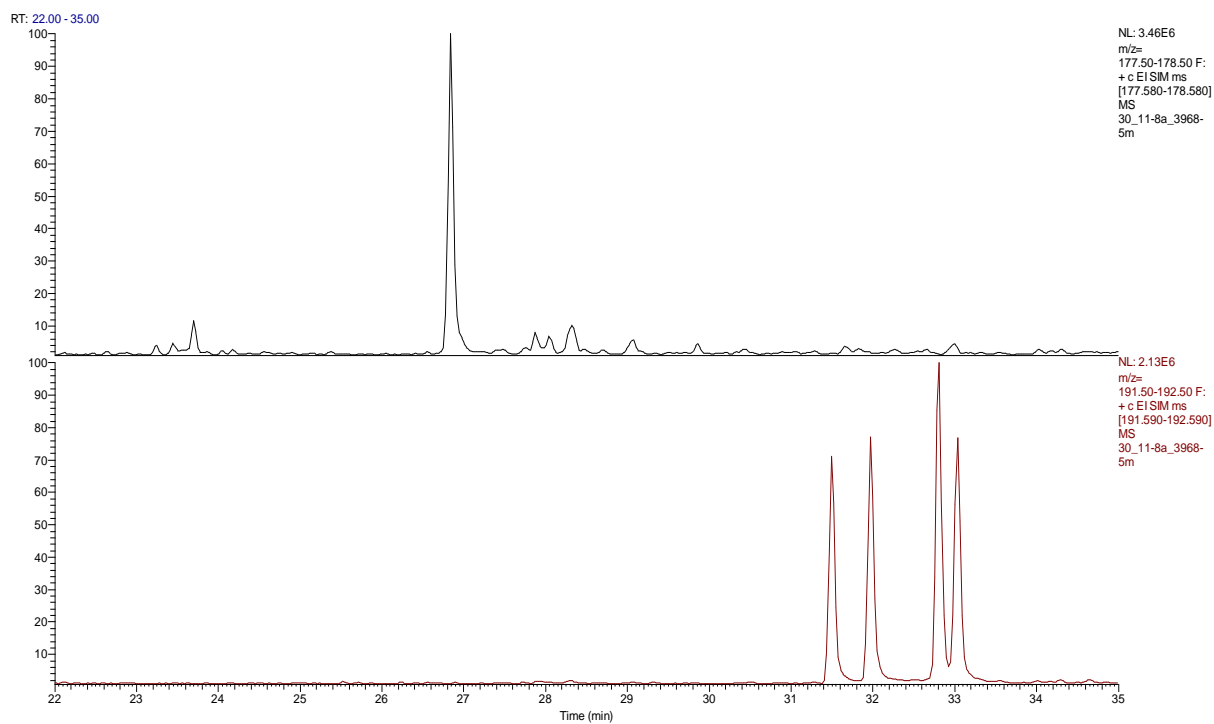
RT: 45.00 - 120.00



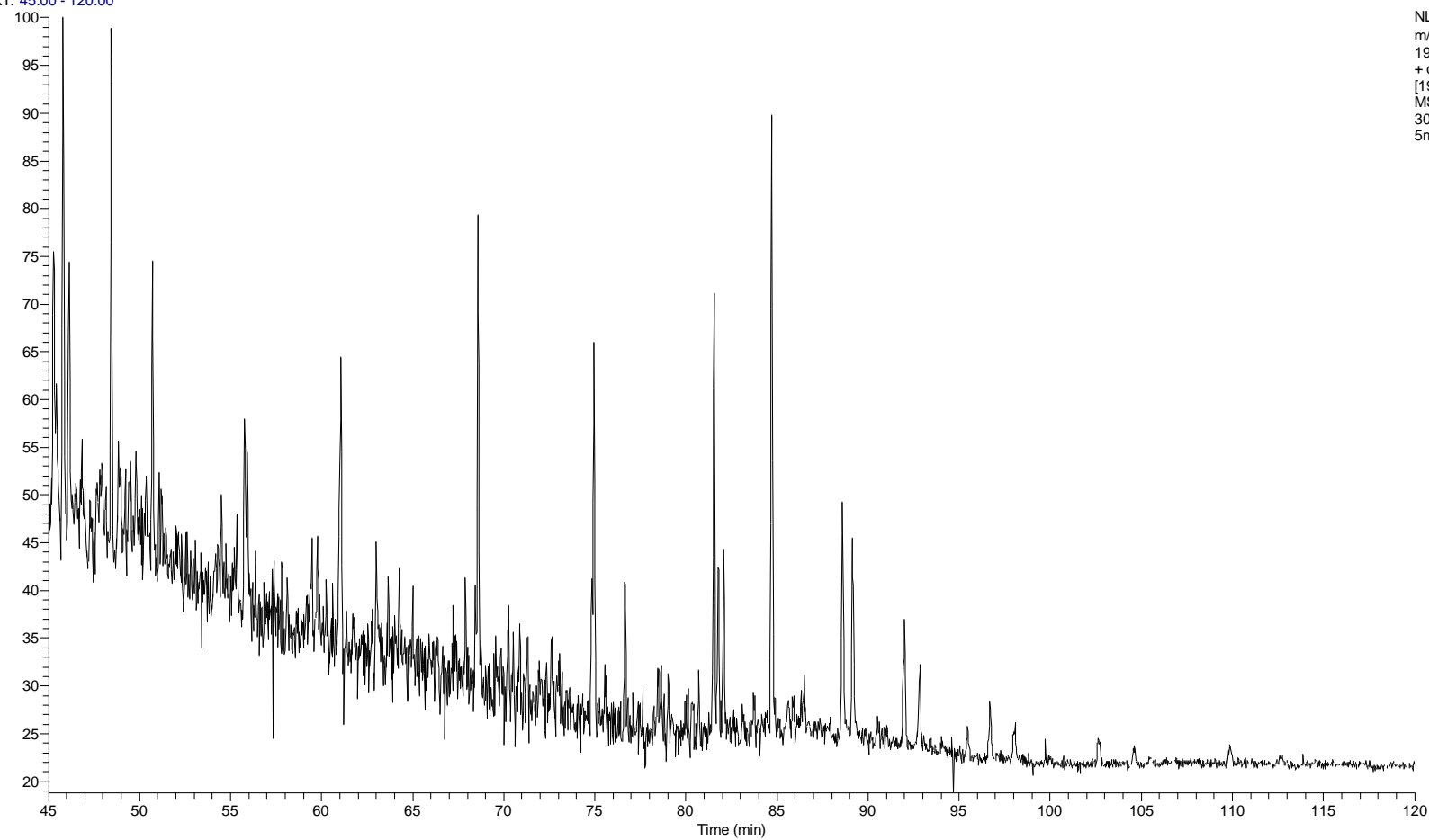
NL: 1.64E5
m/z=
190.50-191.50 F:
+ c E! SIM ms
[190.680-191.680]
MS
30_11-8a_3968-
5m





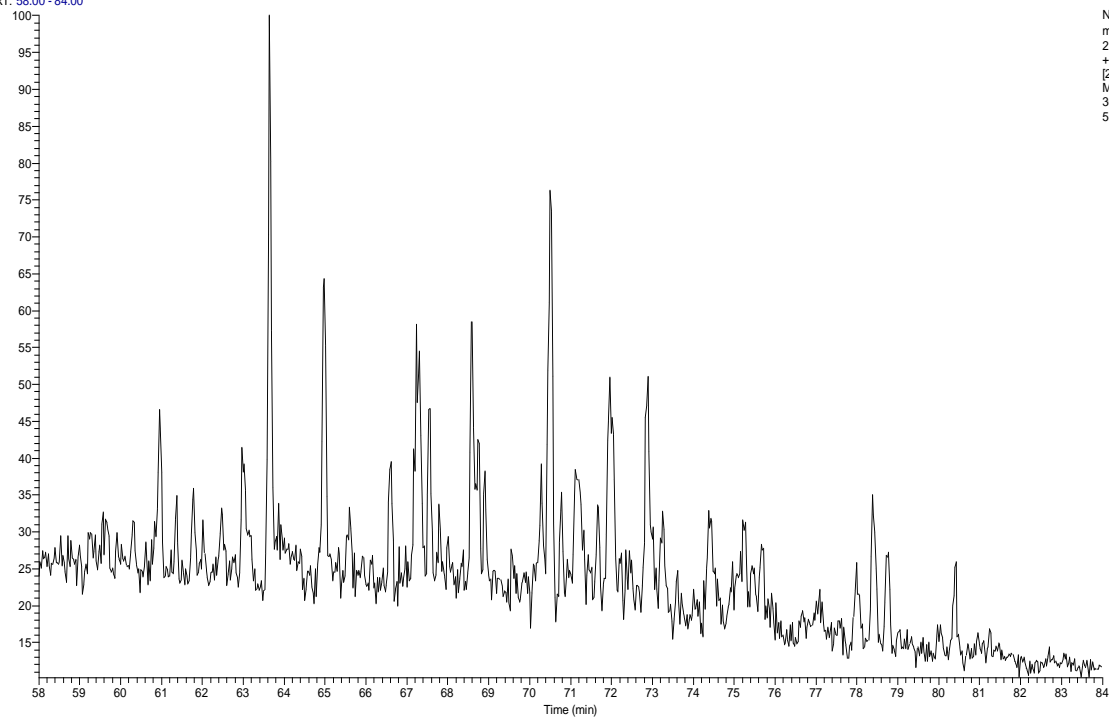


RT: 45.00 - 120.00

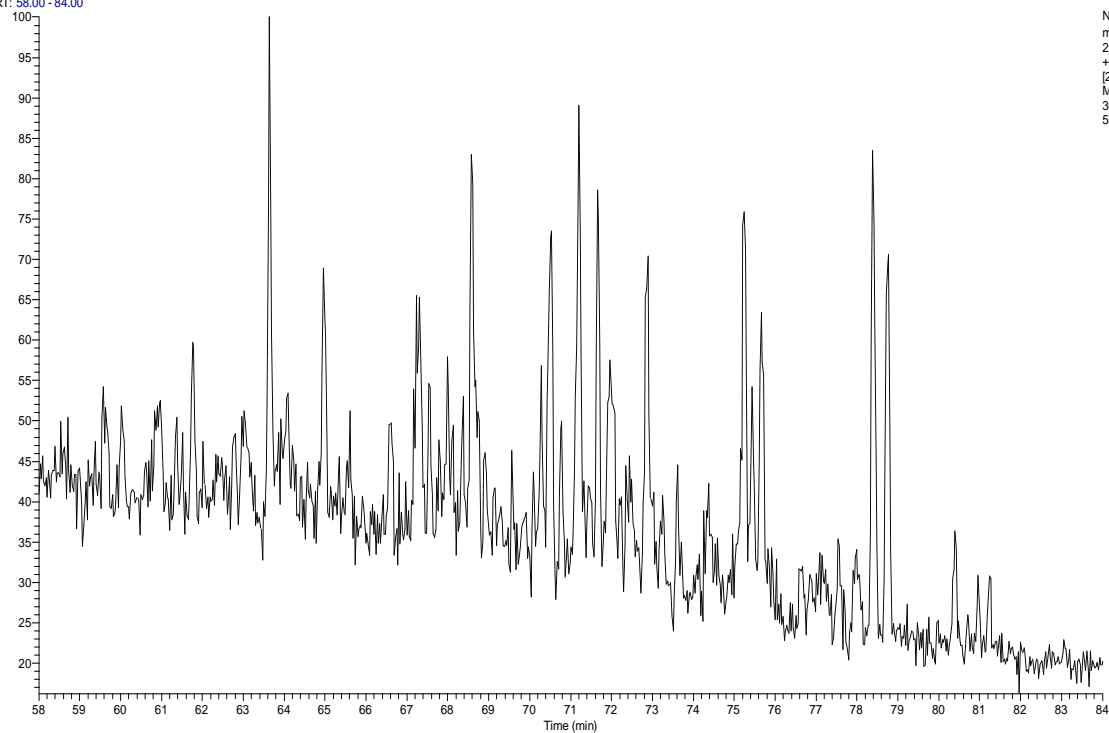


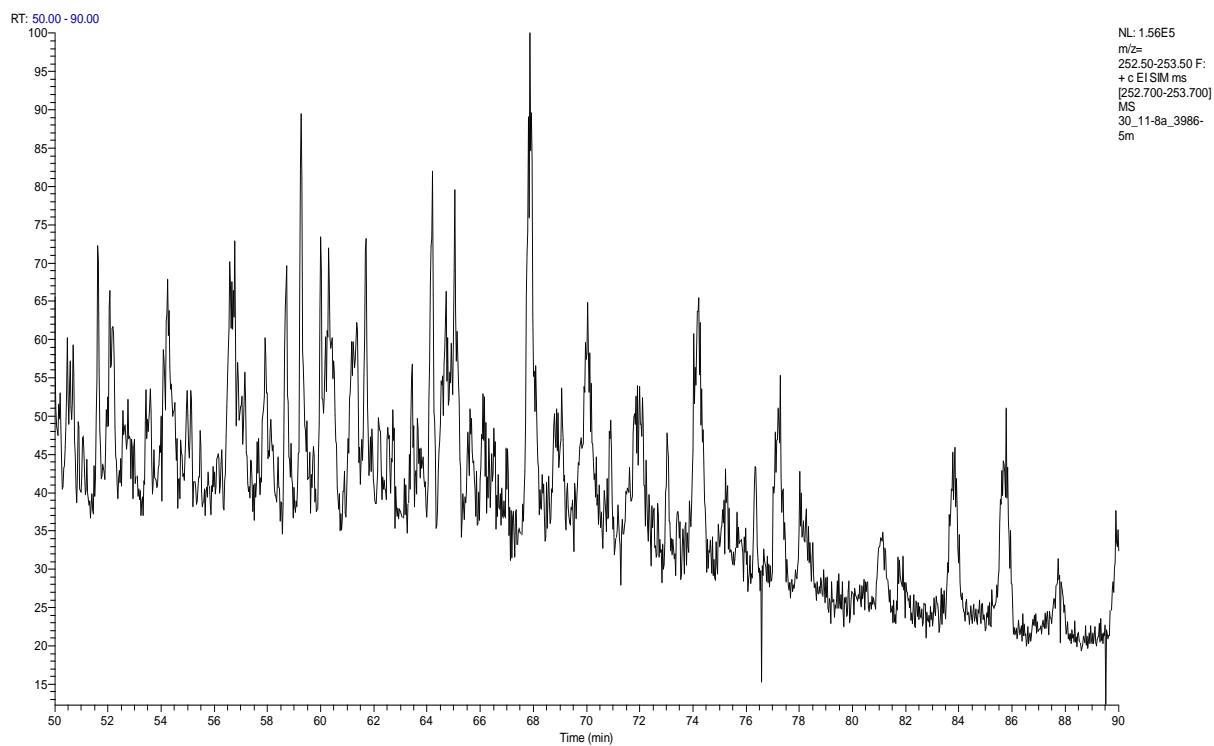
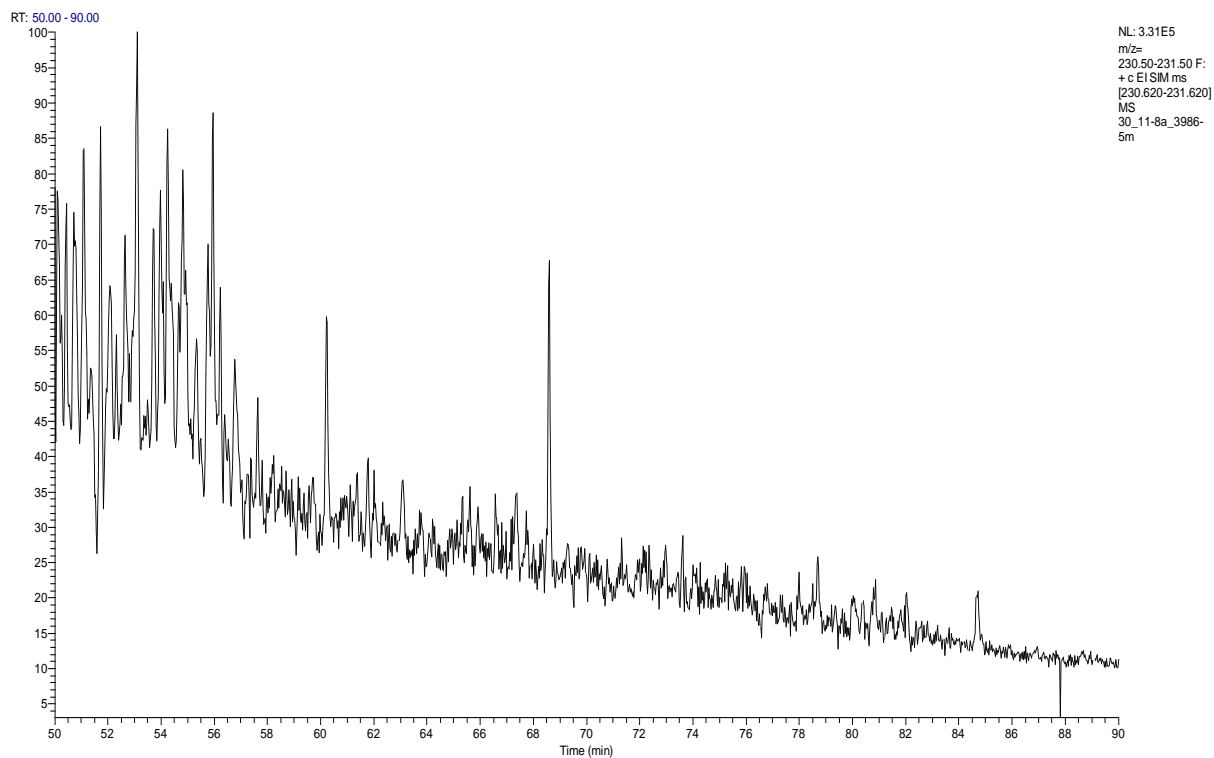
NL: 5.35E5
m/z=
190.50-191.50 F:
+ c E!SIM ms
[190.680-191.680]
MS
30_11-8a_3986-
5m

RT: 58.00 - 84.00

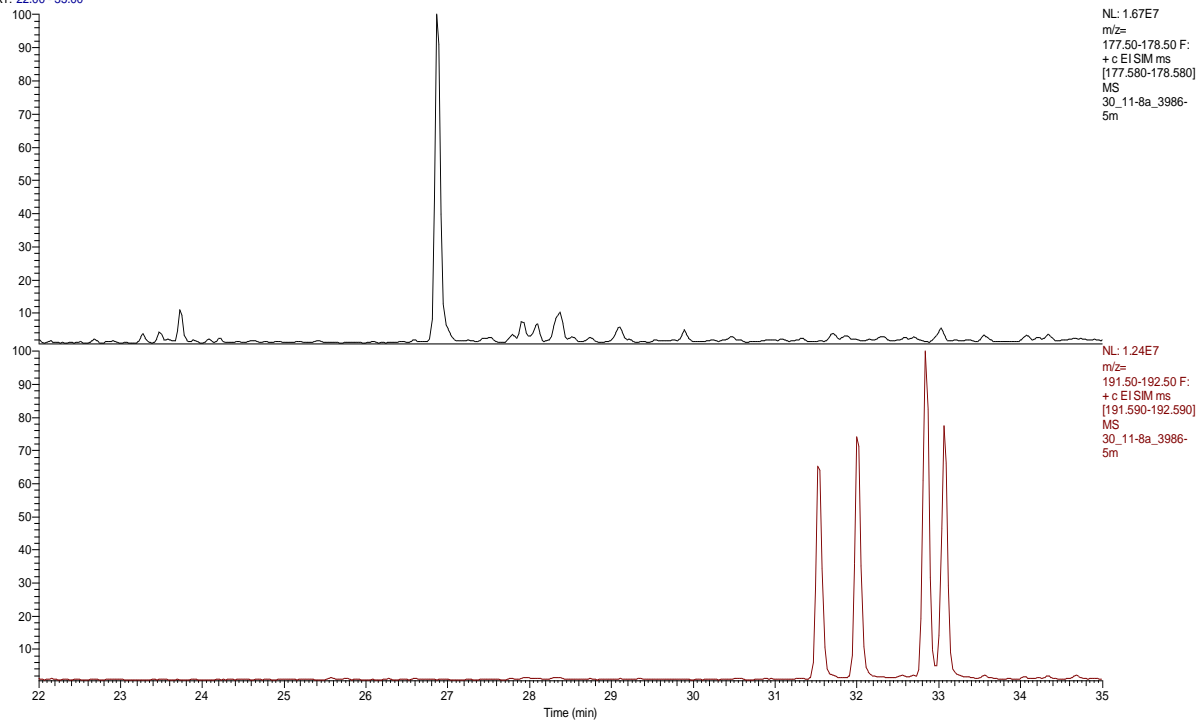


RT: 58.00 - 84.00

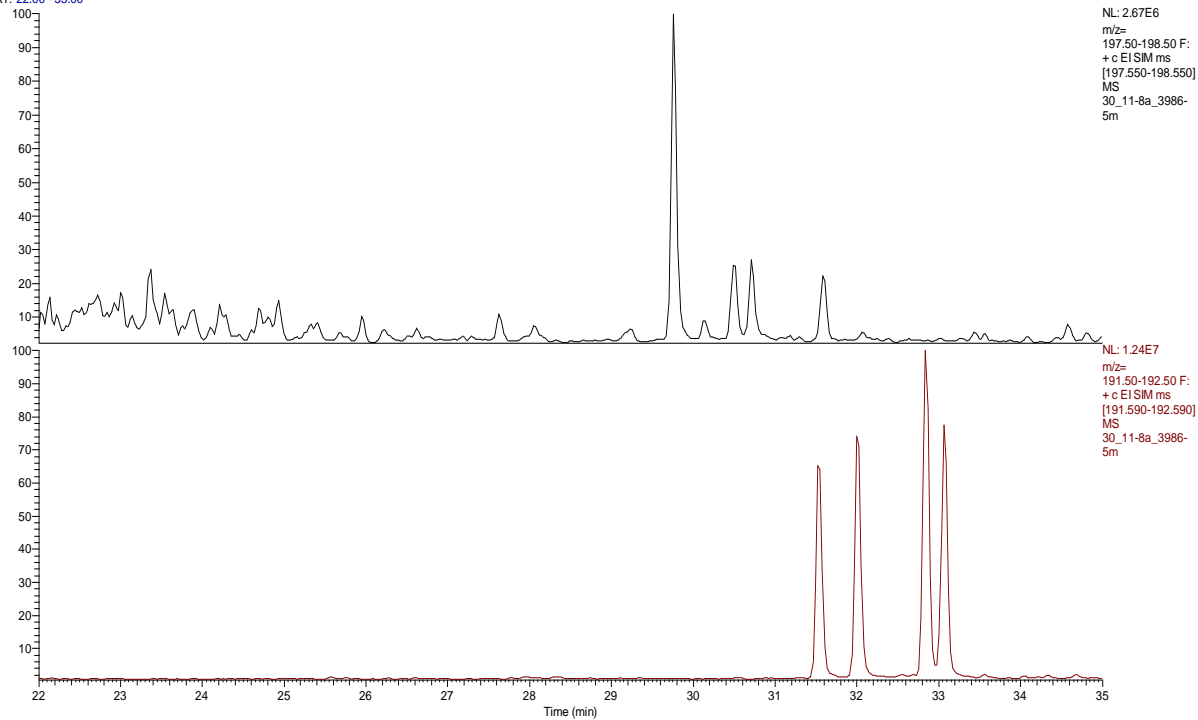




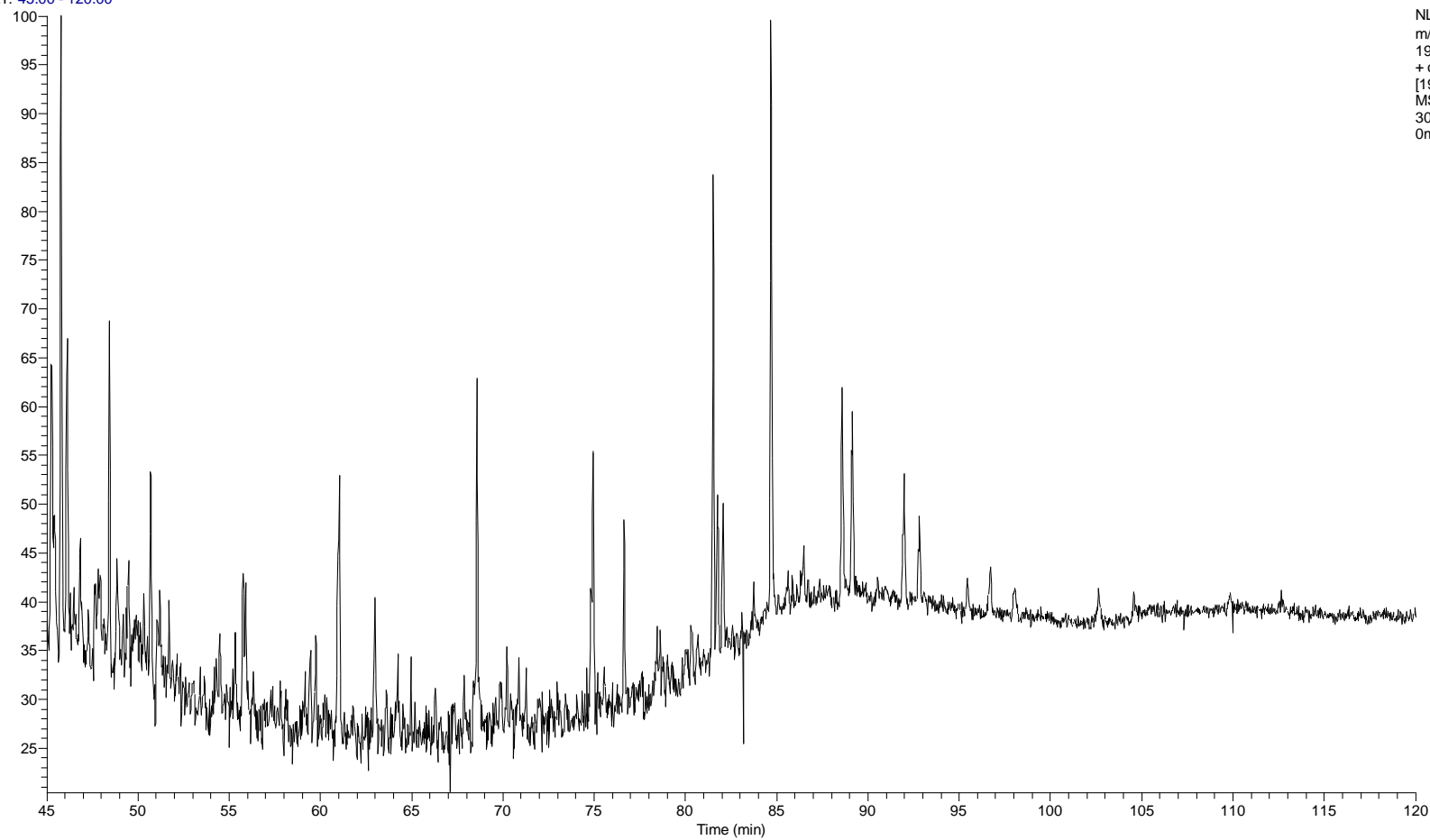
RT: 22.00 - 35.00



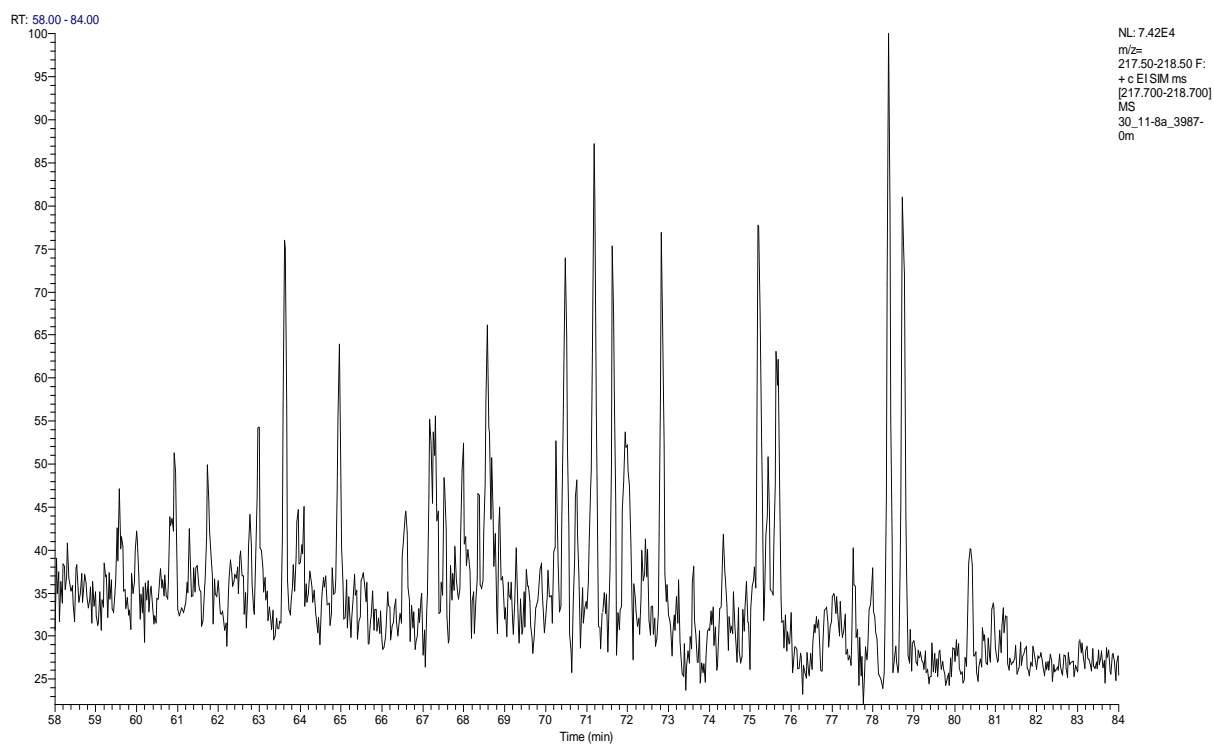
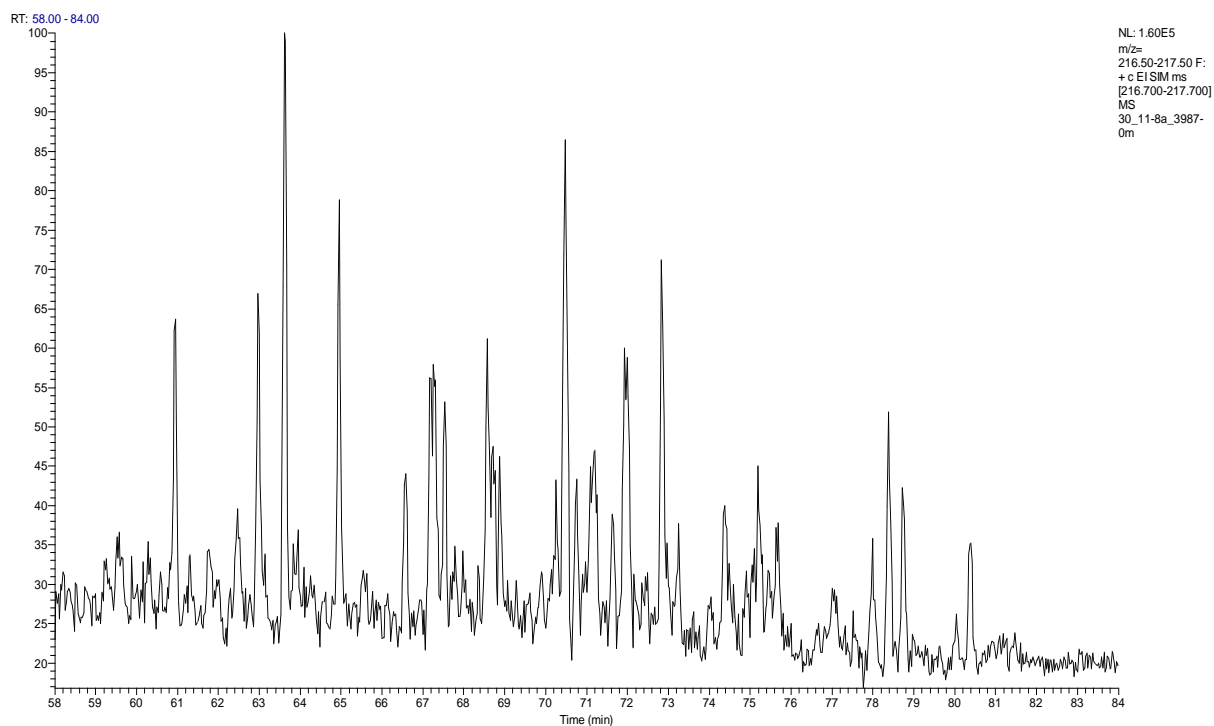
RT: 22.00 - 35.00

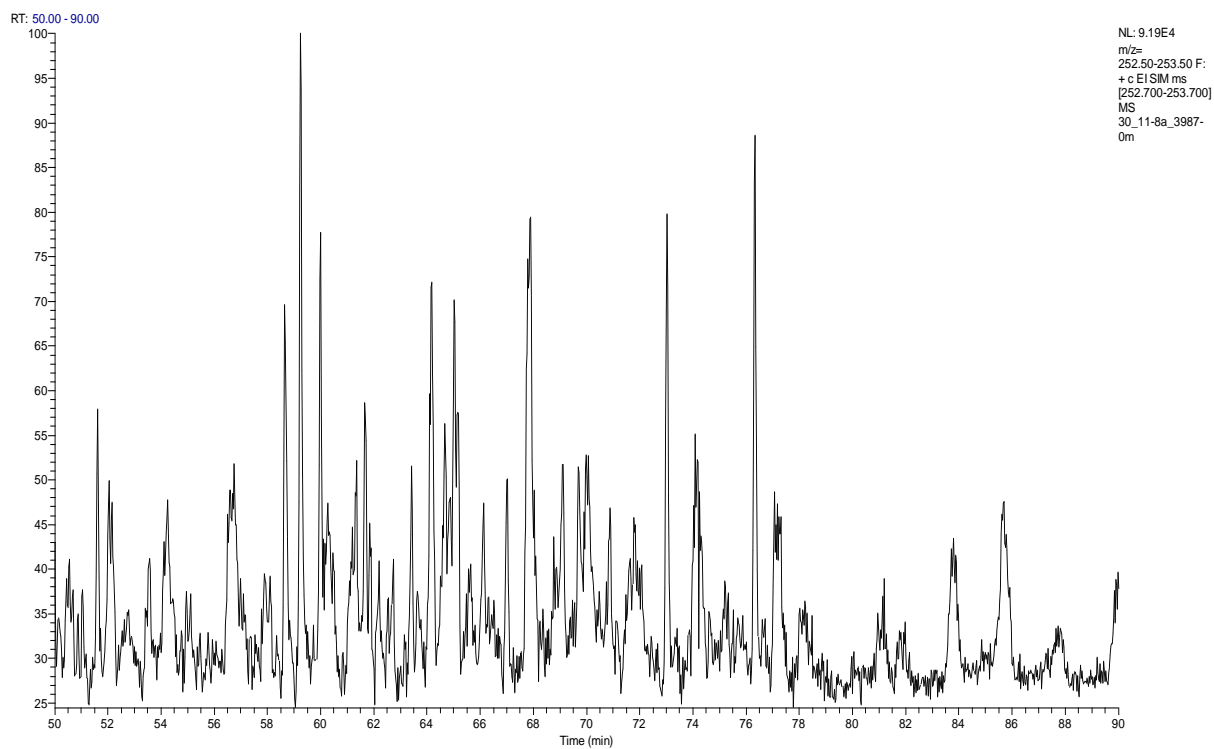
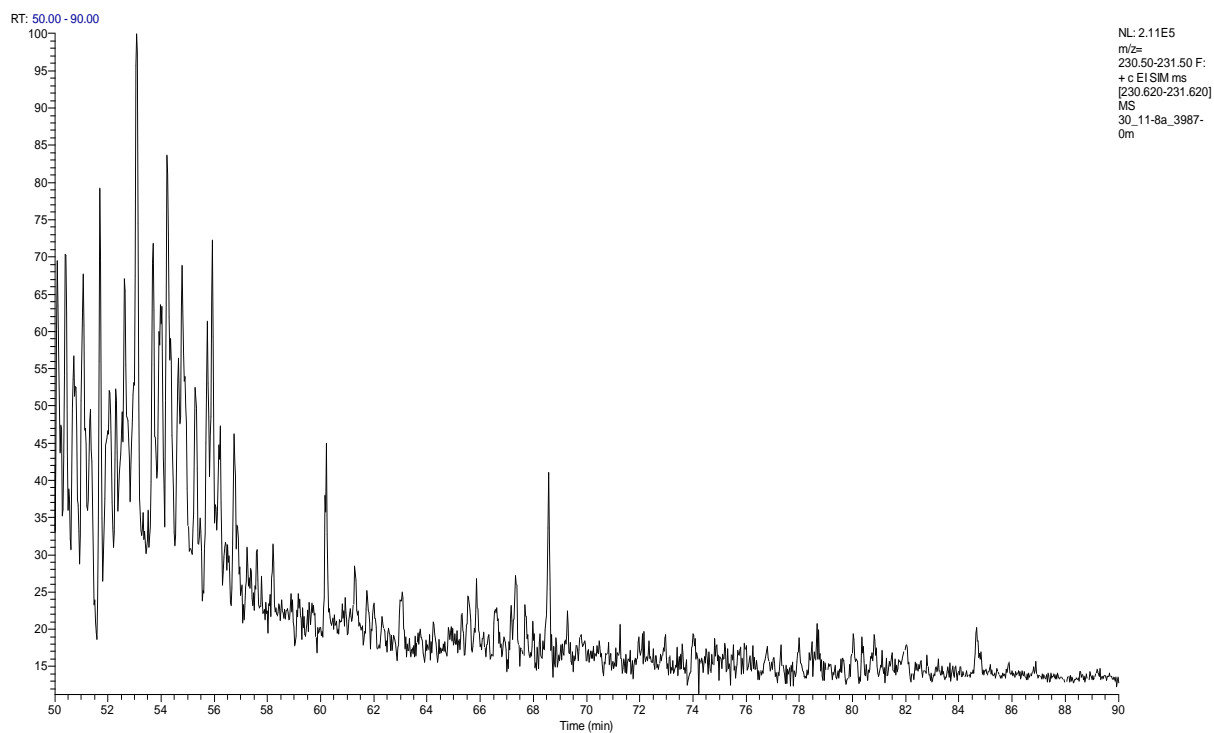


RT: 45.00 - 120.00

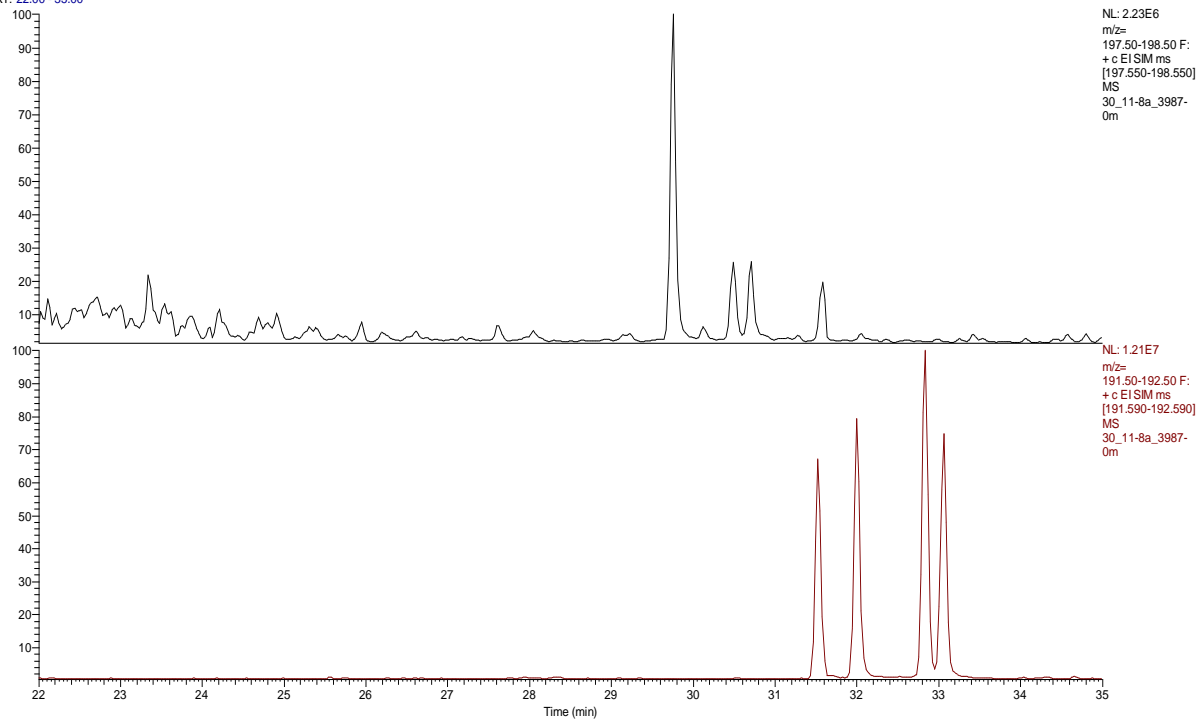


NL: 2.92E5
m/z=
190.50-191.50 F:
+ c ELSIM ms
[190.680-191.680]
MS
30_11-8a_3987-
0m

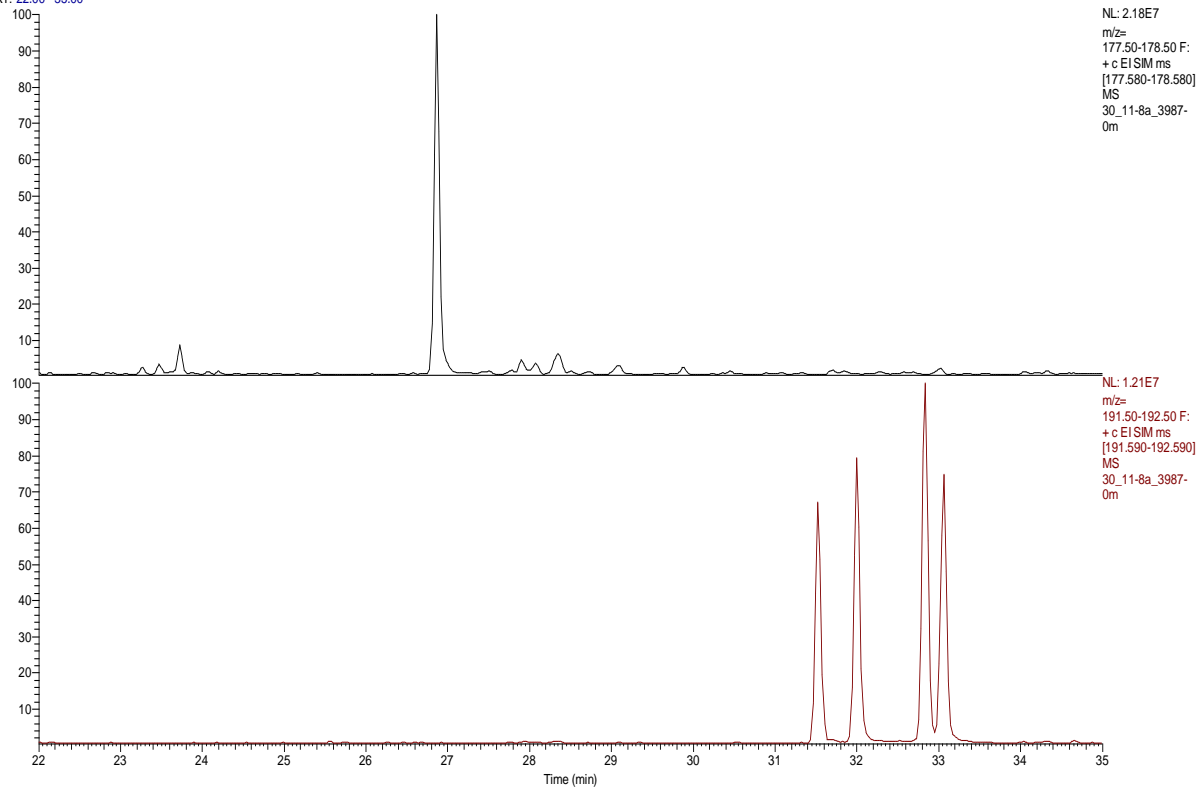




RT: 22.00 - 35.00



RT: 22.00 - 35.00



Appendix D (Iatroscan TLC-FID Chromatograms)

Sample Identifier: 25_2-4_3675.0

Data Processing Parameters

Injected on: 27.03.2014

Injected at: 20:45

Slice Width (ms): 50

Noise (µV/s): undefined

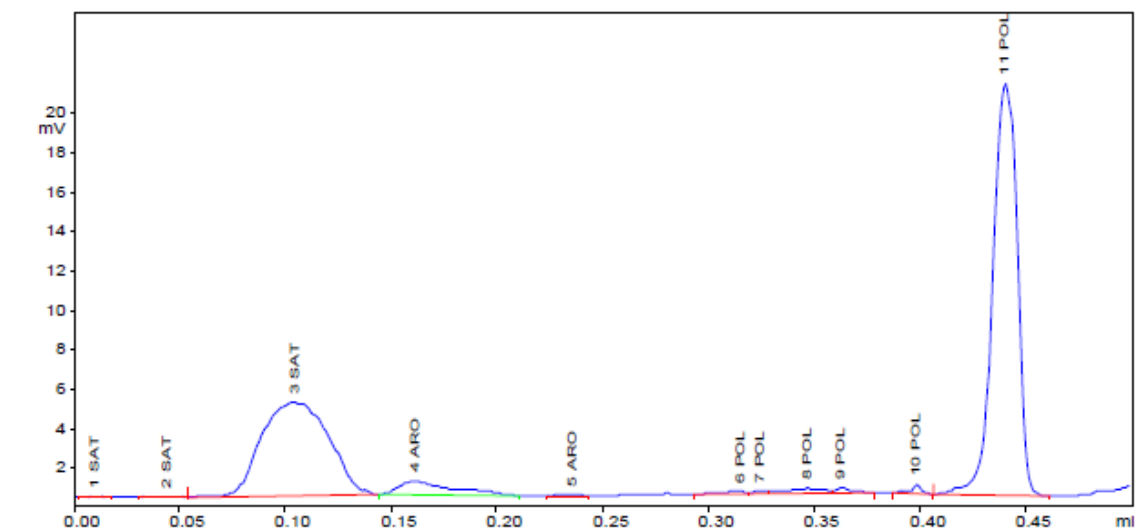
Threshold (mV): 0

Skim Ratio: 0

Parameter Files:

Data Handling File: Iatrosc1

Calculation-File: ~atrosc10007



Calculation Method : Percent

Peak No	Win No.	Ret.Time (min)	Area	Resp.- Fact.	Area%	Name
1	1	0.011	18	1.000	0.116	SAT
2	1	0.045	19	1.000	0.126	SAT
3	1	0.105	5451	1.000	35.786	SAT
4	2	0.162	620	1.000	4.070	ARO
5	2	0.237	22	1.000	0.144	ARO
6	3	0.316	55	1.000	0.364	POL
7	3	0.325	33	1.000	0.217	POL
8	3	0.347	141	1.000	0.923	POL
9	3	0.363	53	1.000	0.349	POL
10	3	0.398	60	1.000	0.396	POL
11	3	0.441	8760	1.000	57.509	POL

15232

100.000

Sample Identifier: 25_2-4_3676.0

Data Processing Parameters

Injected on: 27.03.2014

Injected at: 20:41

Slice Width (ms): 50

Noise (µV/s): undefined

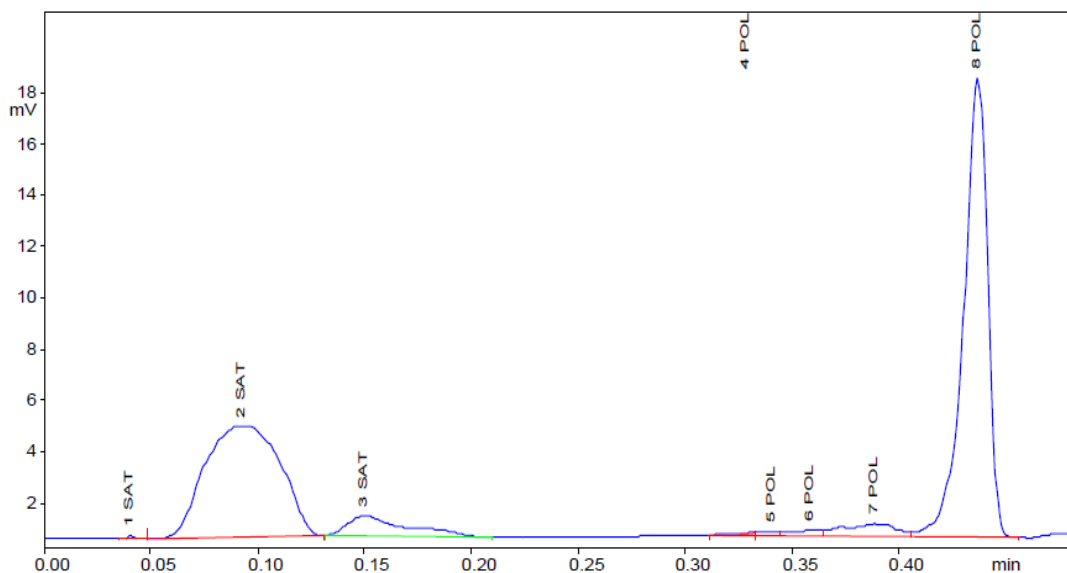
Threshold (mV): 0

Skim Ratio: 0

Parameter Files:

Data Handling File: Iatroscl

Calculation-File: ~atroscl0002



Calculation Method : Percent

Peak No	Win No	Ret.Time (min)	Area	Resp.- Fact.	Area%	Name
1	1	0.040	18	1.000	0.124	SAT
2	1	0.093	5609	1.000	38.692	SAT
3	1	0.150	810	1.000	5.590	SAT
4	2	0.328	16	1.000	0.110	POL
5	2	0.340	70	1.000	0.483	POL
6	2	0.358	120	1.000	0.830	POL
7	2	0.388	457	1.000	3.153	POL
8	2	0.437	7396	1.000	51.019	POL

14498

100.000

Sample Identifier:25_2-4_3683.0

Data Processing Parameters

Injected on: 27.03.2014

Injected at: 20:42

Slice Width (ms): 50

Noise ($\mu\text{V/s}$): 50

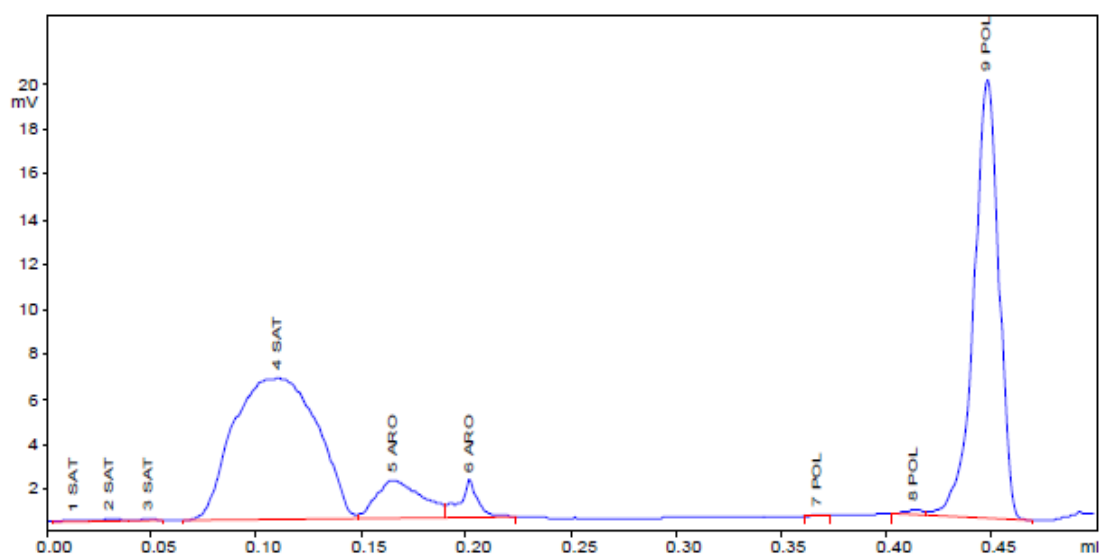
Threshold (mV): 10

Skim Ratio: 3

Parameter Files:

Data Handling File:Iatroscl

Calculation-File:Iatroscl



Calculation Method : Percent

Peak No	Win No.	Ret.Time (min)	Area	Resp.- Fact.	Area%	Name
1	1	0.013	40	1.000	0.203	SAT
2	1	0.031	41	1.000	0.209	SAT
3	1	0.049	22	1.000	0.113	SAT
4	1	0.111	9121	1.000	46.456	SAT
5	2	0.166	1315	1.000	6.698	ARO
6	2	0.203	503	1.000	2.559	ARO
7	3	0.368	8	1.000	0.041	POL
8	3	0.413	75	1.000	0.384	POL
9	3	0.448	8508	1.000	43.336	POL

19633

100.000

Sample Identifier: 25_2-4_3684.0

Data Processing Parameters

Injected on: 27.03.2014

Injected at: 20:43

Slice Width (ms): 50

Noise ($\mu\text{V/s}$): 50

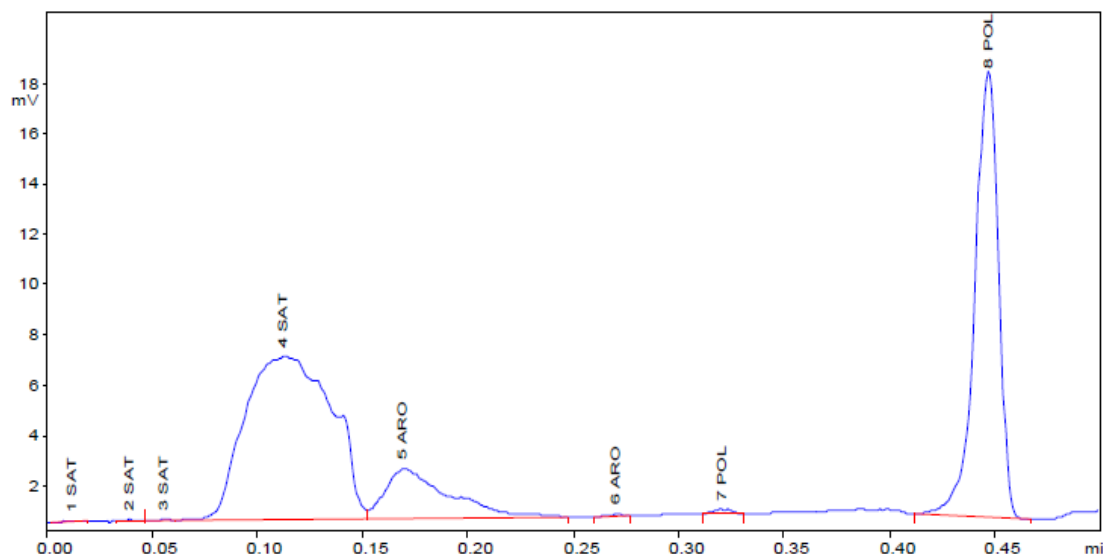
Threshold (mV): 10

Skim Ratio: 3

Parameter Files:

Data Handling File: Iatroscl

Calculation-File: Iatroscl



Calculation Method : Percent

Peak No	Win No.	Ret.Time (min)	Area	Resp.- Fact.	Area%	Name
1	1	0.013	19	1.000	0.099	SAT
2	1	0.040	10	1.000	0.053	SAT
3	1	0.057	18	1.000	0.095	SAT
4	1	0.113	9860	1.000	50.629	SAT
5	2	0.170	2193	1.000	11.260	ARO
6	2	0.271	16	1.000	0.084	ARO
7	3	0.321	46	1.000	0.237	POL
8	3	0.447	7311	1.000	37.543	POL

19475

100.000

Sample Identifier: 25_2-4_3693.0

Data Processing Parameters

Injected on: 27.03.2014

Injected at: 20:43

Slice Width (ms): 50

Noise ($\mu\text{V/s}$): undefined

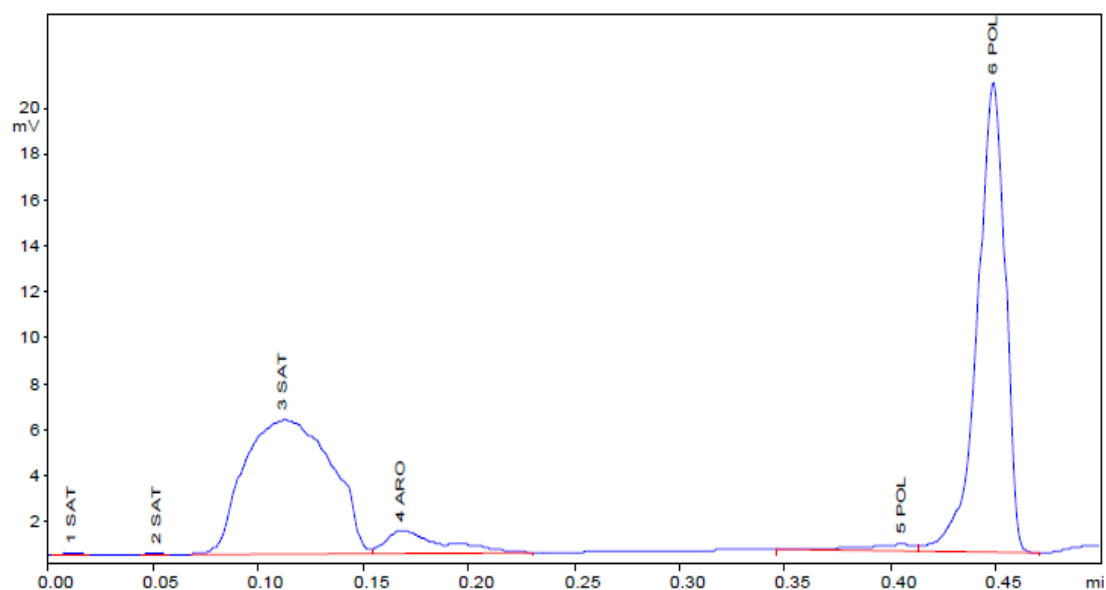
Threshold (mV): 0

Skim Ratio: 0

Parameter Files:

Data Handling File: Iatroscl

Calculation-File: ~atroscl0005



Calculation Method : Percent

Peak No	Win No.	Ret.Time (min)	Area	Resp.- Fact.	Area%	Name
1	1	0.012	20	1.000	0.100	SAT
2	1	0.052	6	1.000	0.031	SAT
3	1	0.112	8803	1.000	44.138	SAT
4	2	0.168	938	1.000	4.704	ARO
5	3	0.406	267	1.000	1.341	POL
6	3	0.449	9910	1.000	49.686	POL

19945

100.000

Sample Identifier: 25_2-4_3694.0

Data Processing Parameters

Injected on: 27.03.2014

Injected at: 20:44

Slice Width (ms): 50

Noise ($\mu\text{V/s}$): undefined

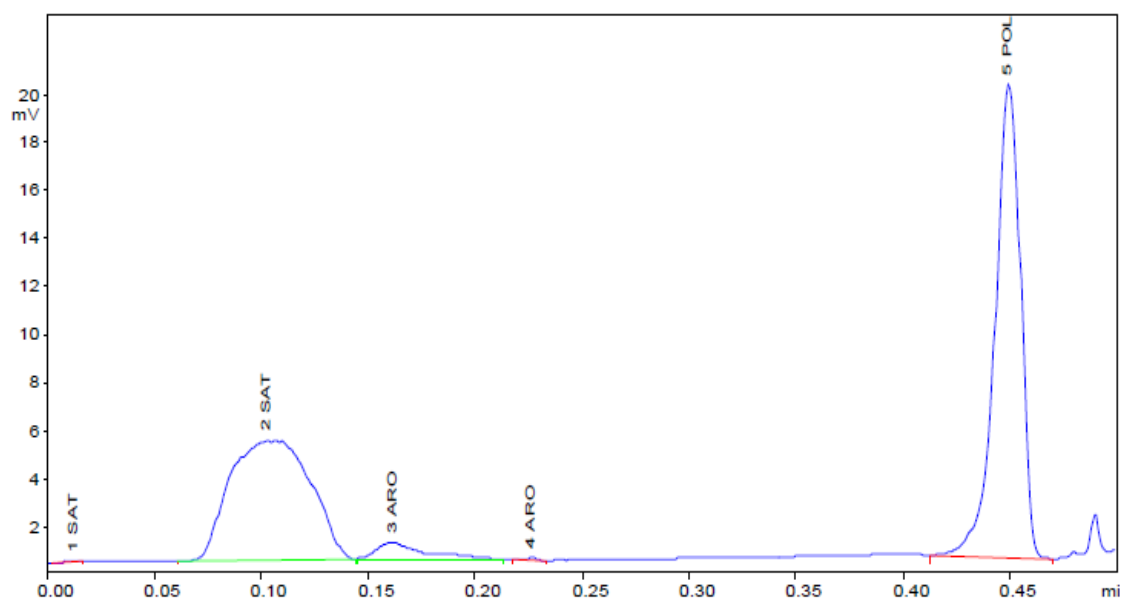
Threshold (mV): 0

Skim Ratio: 0

Parameter Files:

Data Handling File: Iatroscl

Calculation-File: ~atroscl0006



Calculation Method : Percent

Peak No	Win No.	Ret.Time (min)	Area	Resp.- Fact.	Area%	Name
1	1	0.013	14	1.000	0.088	SAT
2	1	0.102	6866	1.000	42.741	SAT
3	2	0.162	555	1.000	3.458	ARO
4	2	0.227	19	1.000	0.116	ARO
5	3	0.449	8610	1.000	53.598	POL

16065

100.000

Sample Identifier: 25_2-12_3698.0

Data Processing Parameters

Injected on: 27.03.2014

Injected at: 20:46

Slice Width (ms): 50

Noise ($\mu\text{V/s}$): undefined

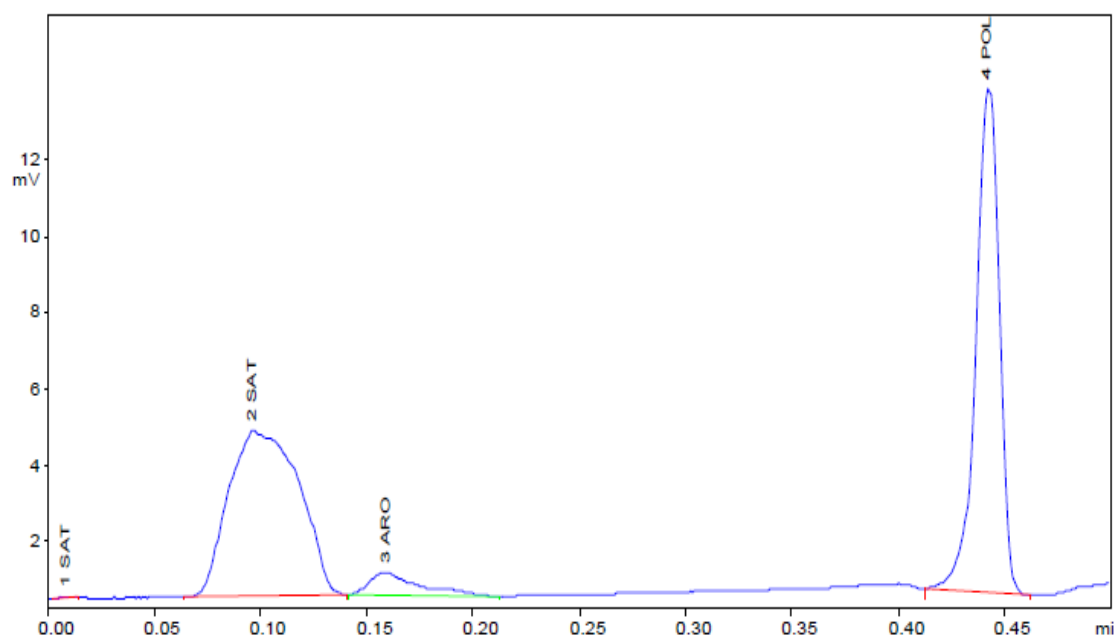
Threshold (mV): 0

Skim Ratio: 0

Parameter Files:

Data Handling File: Iatroscl

Calculation-File: ~atroscl0008



Calculation Method : Percent

Peak No	Win No.	Ret.Time (min)	Area	Resp.- Fact.	Area%	Name
1	1	0.009	9	1.000	0.080	SAT
2	1	0.097	5241	1.000	47.412	SAT
3	2	0.159	501	1.000	4.530	ARO
4	3	0.442	5303	1.000	47.978	POL
			11054	100.000		

Sample Identifier: 25_2-12_3698.5

Data Processing Parameters

Injected on: 27.03.2014

Injected at: 20:46

Slice Width (ms): 50

Noise ($\mu\text{V/s}$): undefined

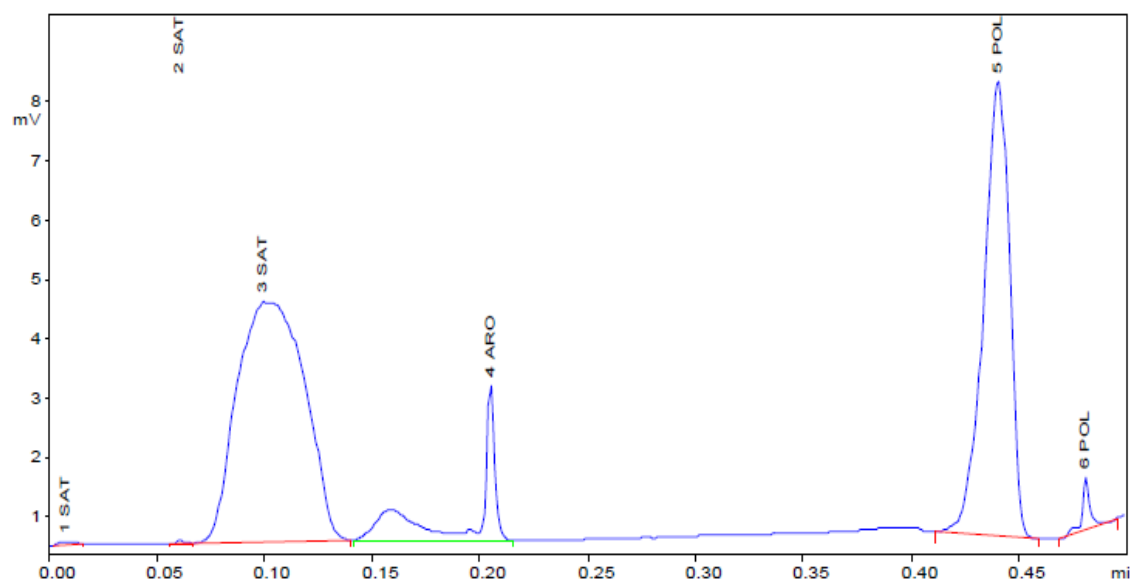
Threshold (mV): 0

Skim Ratio: 0

Parameter Files:

Data Handling File: Iatrosc1

Calculation-File: ~atrosc10009



Calculation Method : Percent

Peak No	Win No.	Ret.Time (min)	Area	Resp.- Fact.	Area%	Name
1	1	0.008	12	1.000	0.139	SAT
2	1	0.061	8	1.000	0.086	SAT
3	1	0.100	4619	1.000	51.991	SAT
4	2	0.205	746	1.000	8.402	ARO
5	3	0.441	3380	1.000	38.044	POL
6	3	0.481	119	1.000	1.338	POL
			8884	100.000		

Sample Identifier: 25_2-12_3706.0

Data Processing Parameters

Injected on: 27.03.2014

Injected at: 20:47

Slice Width (ms): 50

Noise ($\mu\text{V/s}$): 50

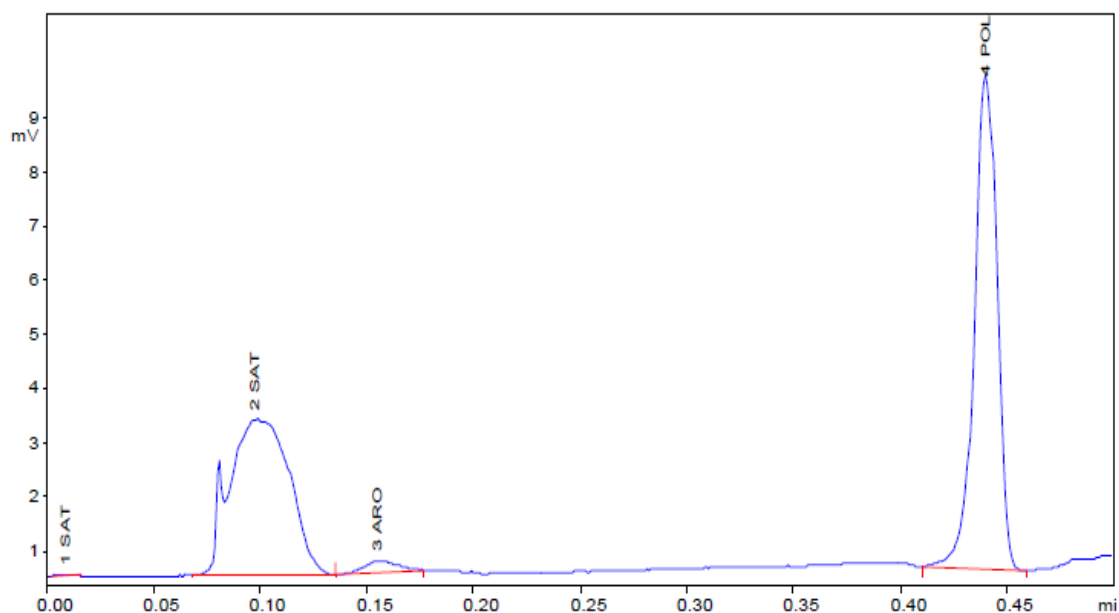
Threshold (mV): 10

Skim Ratio: 3

Parameter Files:

Data Handling File: Iatroscl

Calculation-File: Iatroscl



Calculation Method : Percent

Peak No	Win No.	Ret.Time (min)	Area	Resp.- Fact.	Area%	Name
1	1	0.010	9	1.000	0.141	SAT
2	1	0.098	2922	1.000	44.323	SAT
3	2	0.156	114	1.000	1.722	ARO
4	3	0.441	3547	1.000	53.813	POL
			6592	100.000		

Sample Identifier: 25_2-12_3710.0

Data Processing Parameters

Injected on: 27.03.2014

Injected at: 22:07

Slice Width (ms): 50

Noise (µV/s): 50

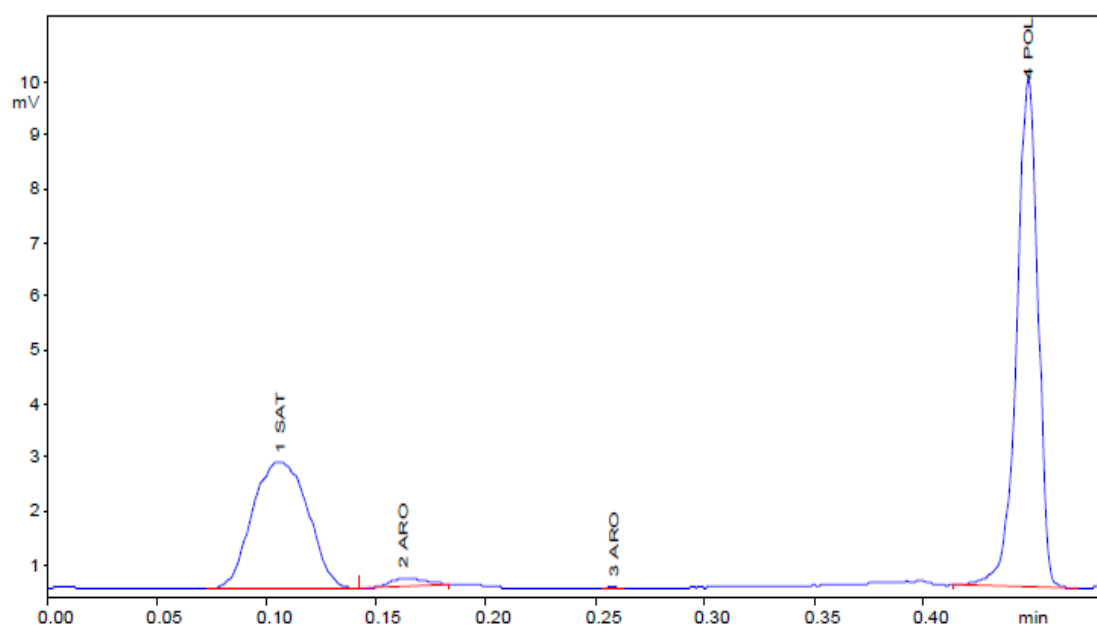
Threshold (mV): 10

Skim Ratio: 3

Parameter Files:

Data Handling File: Iatroscl

Calculation-File: Iatroscl



Calculation Method : Percent

Peak No	Win No.	Ret.Time (min)	Area	Resp.- Fact.	Area%	Name
1	1	0.107	2177	1.000	38.629	SAT
2	2	0.163	85	1.000	1.501	ARO
3	2	0.259	5	1.000	0.084	ARO
4	3	0.448	3370	1.000	59.786	POL
			5637		100.000	

Sample Identifier: 25_2-12_3711.0

Data Processing Parameters

Injected on: 27.03.2014

Injected at: 22:08

Slice Width (ms): 50

Noise ($\mu\text{V/s}$): 50

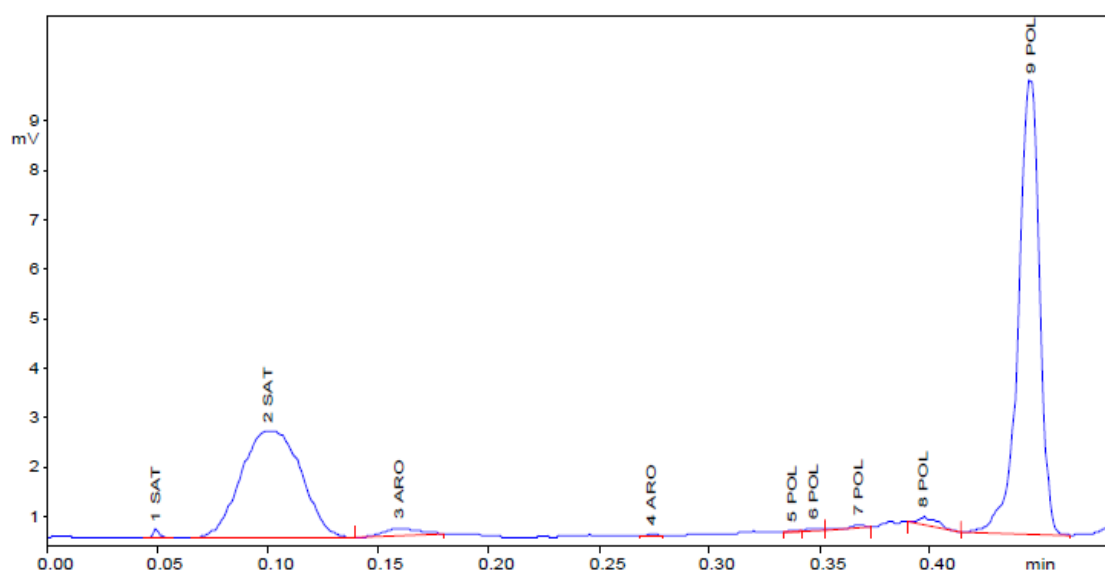
Threshold (mV): 10

Skim Ratio: 3

Parameter Files:

Data Handling File:Iatroscl

Calculation-File:Iatroscl



Calculation Method : Percent

Peak No	Win No.	Ret.Time (min)	Area	Resp.- Fact.	Area%	Name
1	1	0.050	20	1.000	0.360	SAT
2	1	0.101	2135	1.000	38.726	SAT
3	2	0.160	80	1.000	1.449	ARO
4	2	0.274	4	1.000	0.069	ARO
5	3	0.338	6	1.000	0.106	POL
6	3	0.347	16	1.000	0.281	POL
7	3	0.368	8	1.000	0.146	POL
8	3	0.398	50	1.000	0.910	POL
9	3	0.446	3195	1.000	57.953	POL

5514

100.000

Sample Identifier: 26_4-1_2258.7

Data Processing Parameters

Injected on: 26.03.2014

Injected at: 22:16

Slice Width (ms): 50

Noise ($\mu\text{V/s}$): 50

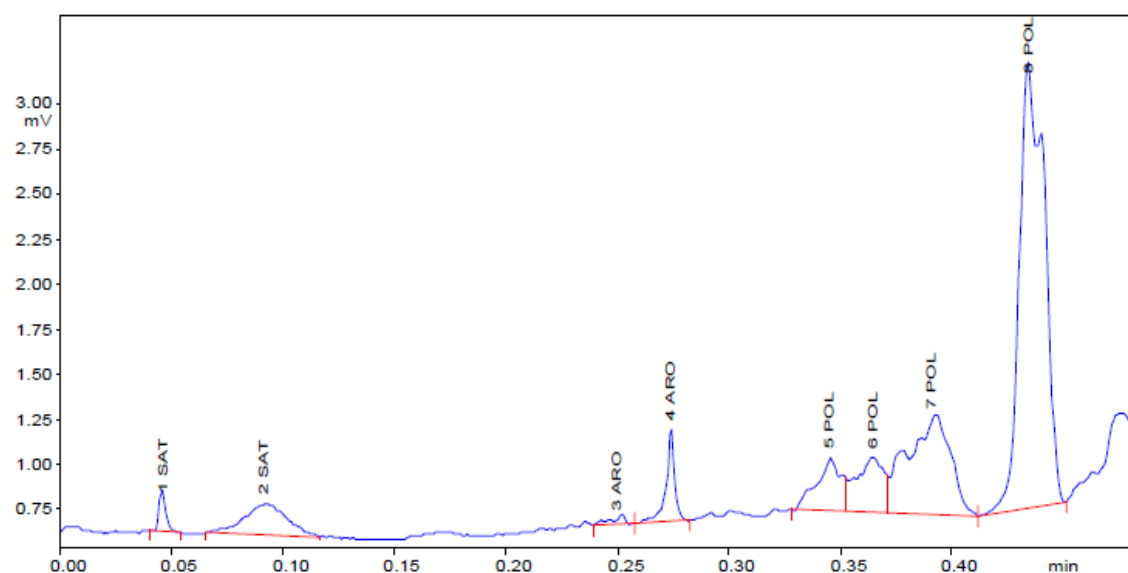
Threshold (mV): 10

Skim Ratio: 3

Parameter Files:

Data Handling File:Iatroscl

Calculation-File:Iatroscl



Calculation Method : Percent

Peak No	Win No.	Ret.Time (min)	Area	Resp.- Fact.	Area%	Name
1	1	0.047	24	1.000	1.267	SAT
2	1	0.092	119	1.000	6.333	SAT
3	2	0.250	12	1.000	0.626	ARO
4	2	0.274	72	1.000	3.849	ARO
5	3	0.346	118	1.000	6.287	POL
6	3	0.365	135	1.000	7.178	POL
7	3	0.392	381	1.000	20.346	POL
8	3	0.435	1014	1.000	54.114	POL

1875

100.000

Sample Identifier: 26_4-1_2273.5

Data Processing Parameters

Injected on: 26.03.2014

Injected at: 22:17

Slice Width (ms): 50

Noise ($\mu\text{V/s}$): 50

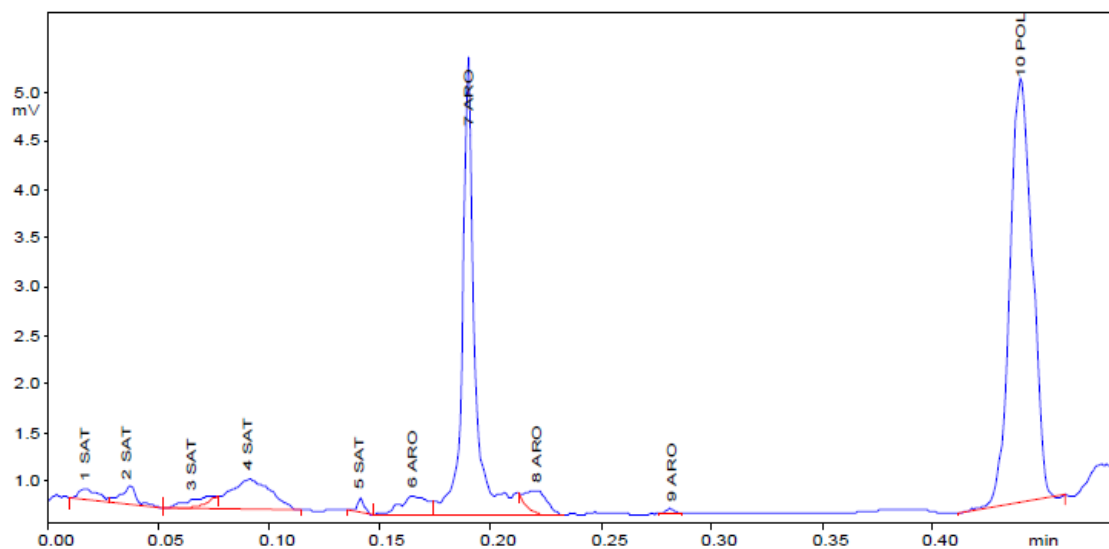
Threshold (mV): 10

Skim Ratio: 3

Parameter Files:

Data Handling File:Iatroscl

Calculation-File:Iatroscl



Calculation Method : Percent

Peak No	Win No.	Ret.Time (min)	Area	Resp.- Fact.	Area%	Name
1	1	0.018	40	1.000	1.256	SAT
2	1	0.037	47	1.000	1.503	SAT
3	1	0.066	34	1.000	1.079	SAT
4	1	0.091	261	1.000	8.250	SAT
5	1	0.142	16	1.000	0.506	SAT
6	2	0.166	95	1.000	3.008	ARO
7	2	0.191	974	1.000	30.827	ARO
8	2	0.222	78	1.000	2.471	ARO
9	2	0.282	6	1.000	0.176	ARO
10	3	0.440	1609	1.000	50.924	POL
			3159		100.000	

Sample Identifier: 26_4-1_2274.0

Data Processing Parameters

Injected on: 26.03.2014

Injected at: 22:18

Slice Width (ms): 50

Noise ($\mu\text{V/s}$): 50

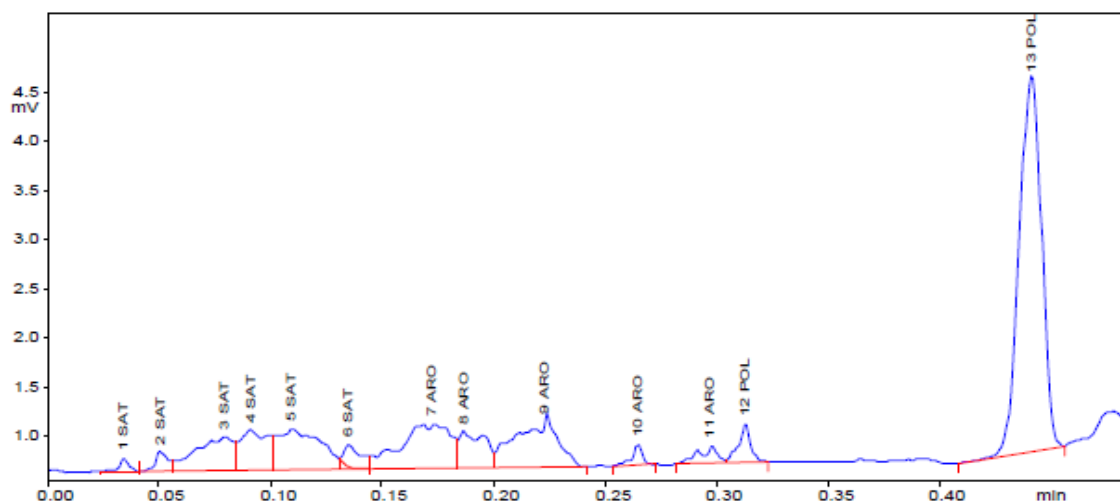
Threshold (mV): 10

Skim Ratio: 3

Parameter Files:

Data Handling File:Iatroscl

Calculation-File:Iatroscl



Calculation Method : Percent

Peak No	Win No.	Ret.Time (min)	Area	Resp.- Fact.	Area%	Name
1	1	0.035	21	1.000	0.652	SAT
2	1	0.052	42	1.000	1.315	SAT
3	1	0.080	203	1.000	6.311	SAT
4	1	0.092	190	1.000	5.893	SAT
5	1	0.110	289	1.000	8.957	SAT
6	1	0.136	60	1.000	1.867	SAT
7	2	0.173	364	1.000	11.292	ARO
8	2	0.188	156	1.000	4.856	ARO
9	2	0.223	327	1.000	10.156	ARO
10	2	0.265	32	1.000	0.992	ARO
11	2	0.298	53	1.000	1.645	ARO
12	3	0.313	78	1.000	2.431	POL
13	3	0.442	1406	1.000	43.631	POL

3222

100.000

Sample Identifier: 26_4-1_2274.8

Data Processing Parameters

Injected on: 26.03.2014

Injected at: 22:18

Slice Width (ms): 50

Noise (µV/s): 50

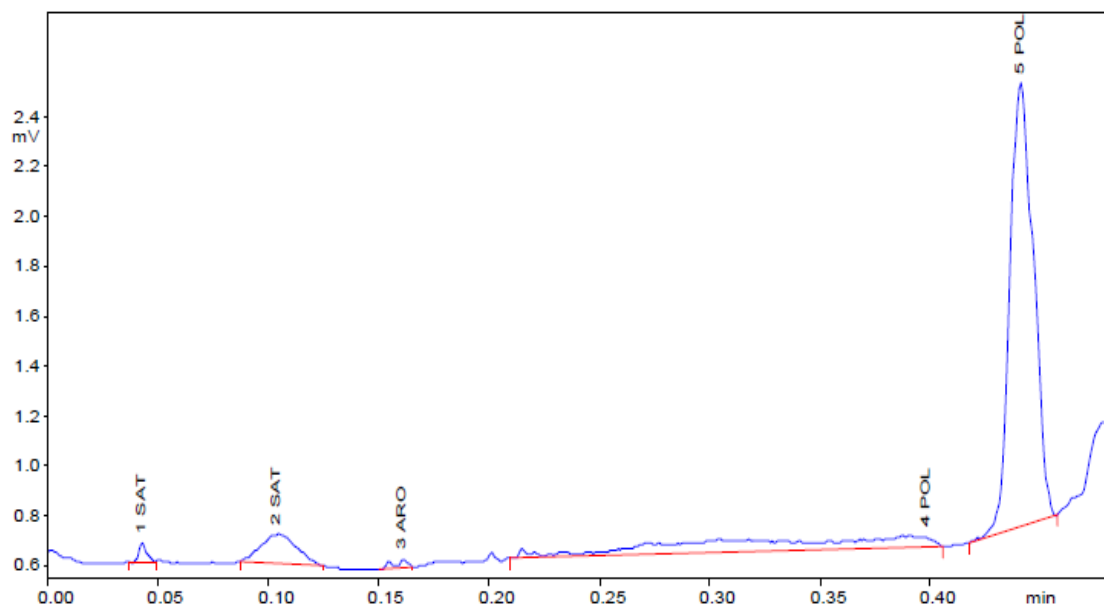
Threshold (mV): 10

Skim Ratio: 3

Parameter Files:

Data Handling File:Iatroscl

Calculation-File:Iatroscl



Calculation Method : Percent

Peak No	Win No.	Ret.Time (min)	Area	Resp.- Fact.	Area%	Name
1	1	0.043	9	1.000	0.958	SAT
2	1	0.104	67	1.000	6.927	SAT
3	2	0.161	8	1.000	0.812	ARO
4	3	0.398	193	1.000	19.922	POL
5	3	0.441	692	1.000	71.382	POL
			970	100.000		

Sample Identifier: 26_4-1_2289.2

Data Processing Parameters

Injected on: 26.03.2014

Injected at: 22:19

Slice Width (ms): 50

Noise ($\mu\text{V/s}$): 50

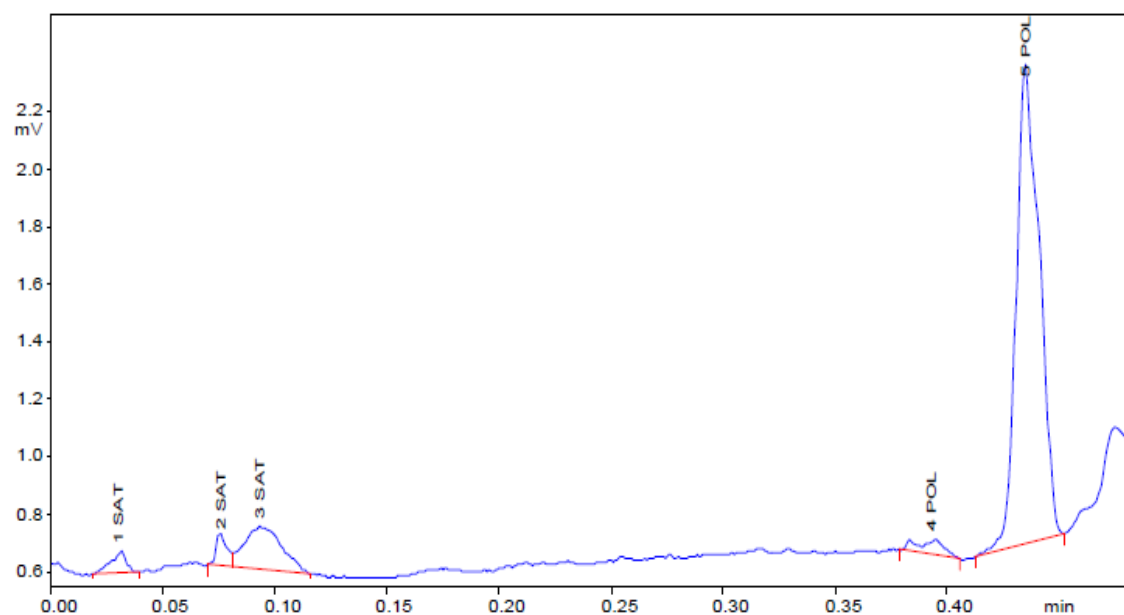
Threshold (mV): 10

Skim Ratio: 3

Parameter Files:

Data Handling File:Iatroscl

Calculation-File:Iatroscl



Calculation Method : Percent

Peak No	Win No.	Ret.Time (min)	Area	Resp.- Fact.	Area%	Name
1	1	0.031	19	1.000	2.462	SAT
2	1	0.077	21	1.000	2.656	SAT
3	1	0.094	89	1.000	11.454	SAT
4	2	0.393	22	1.000	2.752	POL
5	2	0.436	630	1.000	80.674	POL
			781	100.000		

Sample Identifier: 26_4-1_2290.5

Data Processing Parameters

Injected on: 26.03.2014

Injected at: 22:20

Slice Width (ms): 50

Noise ($\mu\text{V/s}$): undefined

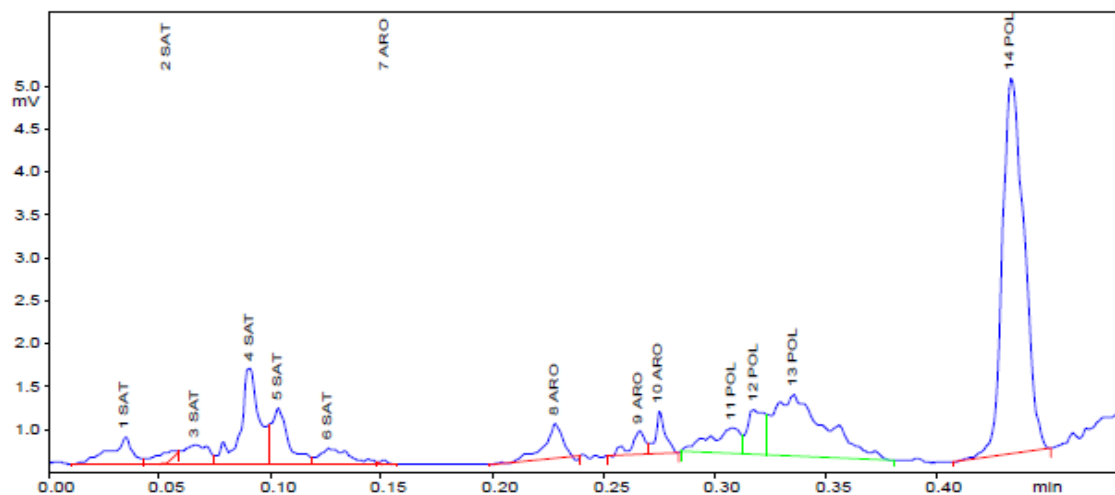
Threshold (mV): 0

Skim Ratio: 0

Parameter Files:

Data Handling File:Iatroscl

Calculation-File:~atroscl0017



Calculation Method : Percent

Peak No	Win No.	Ret.Time (min)	Area	Resp.- Fact.	Area%	Name
1	1	0.035	130	1.000	3.530	SAT
2	1	0.053	47	1.000	1.275	SAT
3	1	0.067	112	1.000	3.047	SAT
4	1	0.091	354	1.000	9.611	SAT
5	1	0.104	191	1.000	5.184	SAT
6	1	0.127	104	1.000	2.834	SAT
7	2	0.152	7	1.000	0.194	ARO
8	2	0.228	127	1.000	3.447	ARO
9	2	0.266	62	1.000	1.685	ARO
10	2	0.275	75	1.000	2.047	ARO
11	3	0.308	152	1.000	4.135	POL
12	3	0.317	160	1.000	4.338	POL
13	3	0.336	597	1.000	16.206	POL
14	3	0.433	1565	1.000	42.467	POL
			3686		100.000	

Sample Identifier: 30_10-6_4664.0

Data Processing Parameters

Injected on: 25.03.2014

Injected at: 19:30

Slice Width (ms): 50

Noise ($\mu\text{V/s}$): 50

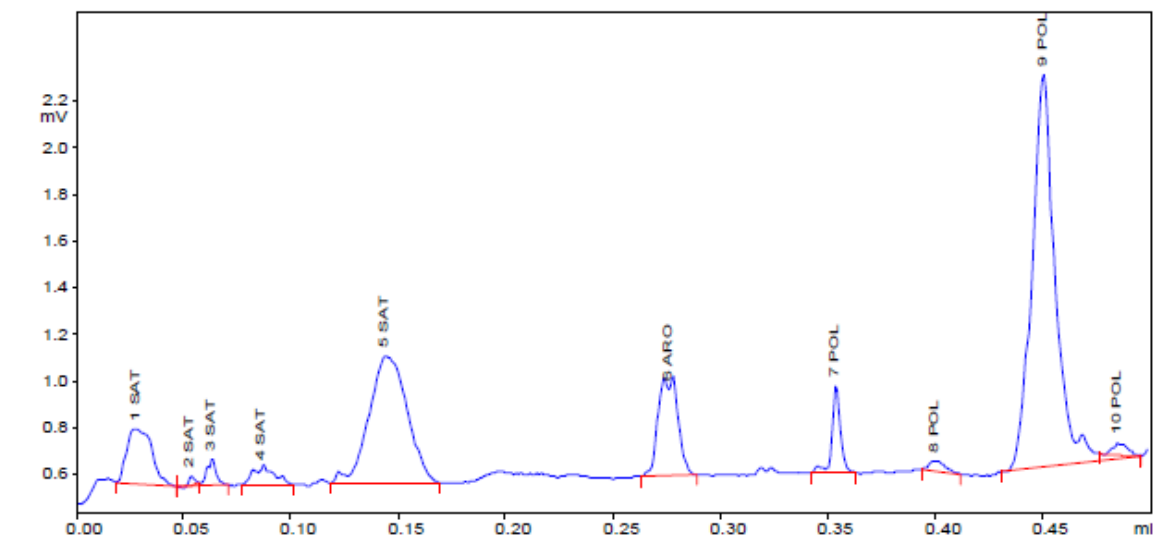
Threshold (mV): 10

Skim Ratio: 3

Parameter Files:

Data Handling File:Iatroscl

Calculation-File:Iatroscl



Calculation Method : Percent

Peak No	Win No.	Ret.Time (min)	Area	Resp.- Fact.	Area%	Name
1	1	0.028	98	1.000	7.094	SAT
2	1	0.054	4	1.000	0.299	SAT
3	1	0.063	24	1.000	1.751	SAT
4	1	0.087	30	1.000	2.163	SAT
5	1	0.144	352	1.000	25.470	SAT
6	2	0.276	141	1.000	10.202	ARO
7	3	0.353	52	1.000	3.767	POL
8	3	0.400	12	1.000	0.875	POL
9	3	0.451	655	1.000	47.447	POL
10	3	0.485	13	1.000	0.932	POL

1381

100.000

Sample Identifier: 30_10-6_4664.5

Data Processing Parameters

Injected on: 25.03.2014

Injected at: 19:30

Slice Width (ms): 50

Noise ($\mu\text{V/s}$): 50

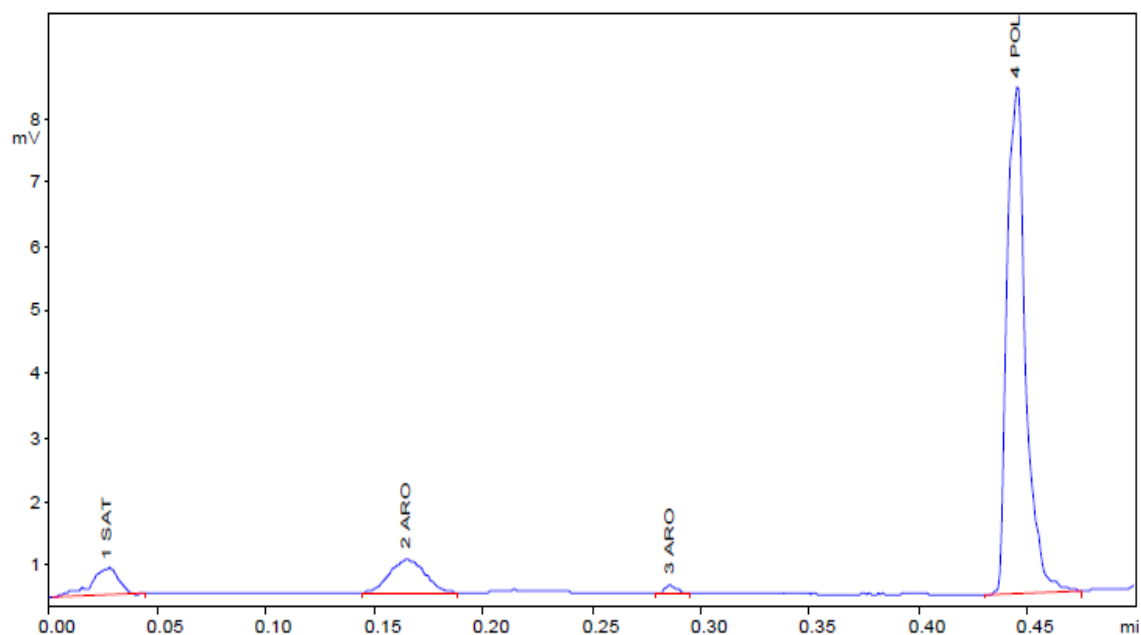
Threshold (mV): 10

Skim Ratio: 3

Parameter Files:

Data Handling File: Iatroscl

Calculation-File: Iatroscl



Calculation Method : Percent

Peak No	Win No.	Ret.Time (min)	Area	Resp.- Fact.	Area%	Name
1	1	0.027	190	1.000	6.470	SAT
2	2	0.165	298	1.000	10.130	ARO
3	2	0.286	23	1.000	0.793	ARO
4	3	0.445	2431	1.000	82.606	POL
			2943		100.000	

Sample Identifier: 30_10-6_4675.0

Data Processing Parameters

Injected on: 25.03.2014

Injected at: 19:31

Slice Width (ms): 50

Noise (µV/s): 50

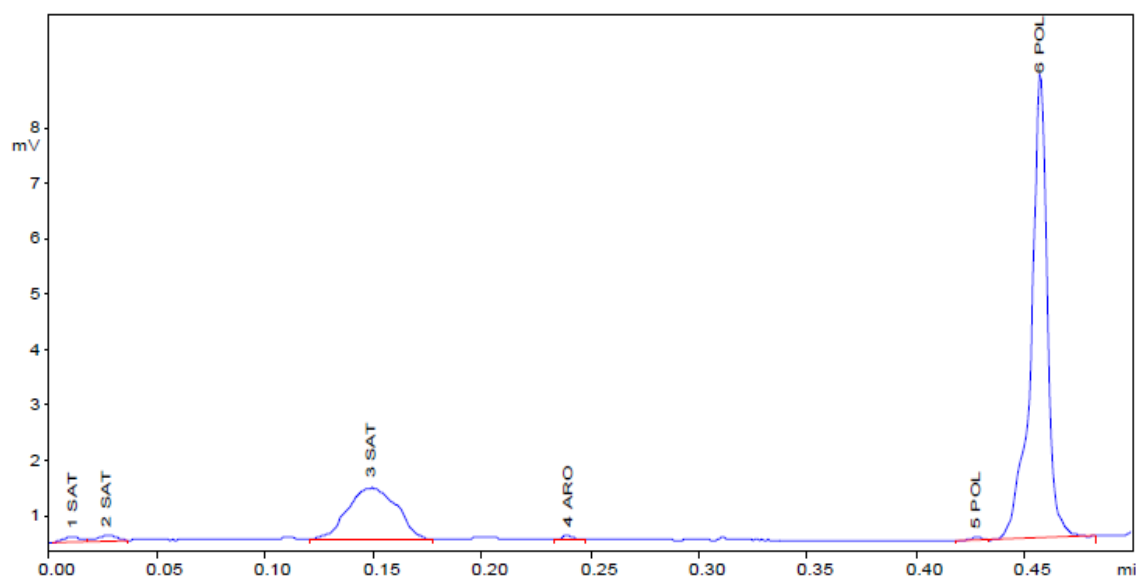
Threshold (mV): 10

Skim Ratio: 3

Parameter Files:

Data Handling File: Iatroscl

Calculation-File: Iatroscl



Calculation Method : Percent

Peak No	Win No.	Ret.Time (min)	Area	Resp.- Fact.	Area%	Name
1	1	0.012	28	1.000	0.891	SAT
2	1	0.027	33	1.000	1.038	SAT
3	1	0.149	753	1.000	23.916	SAT
4	2	0.240	12	1.000	0.378	ARO
5	3	0.428	14	1.000	0.442	POL
6	3	0.458	2310	1.000	73.335	POL

3149

100.000

Sample Identifier: 30_10-6_4675.5

Data Processing Parameters

Injected on: 25.03.2014

Injected at: 19:32

Slice Width (ms): 50

Noise ($\mu\text{V/s}$): 50

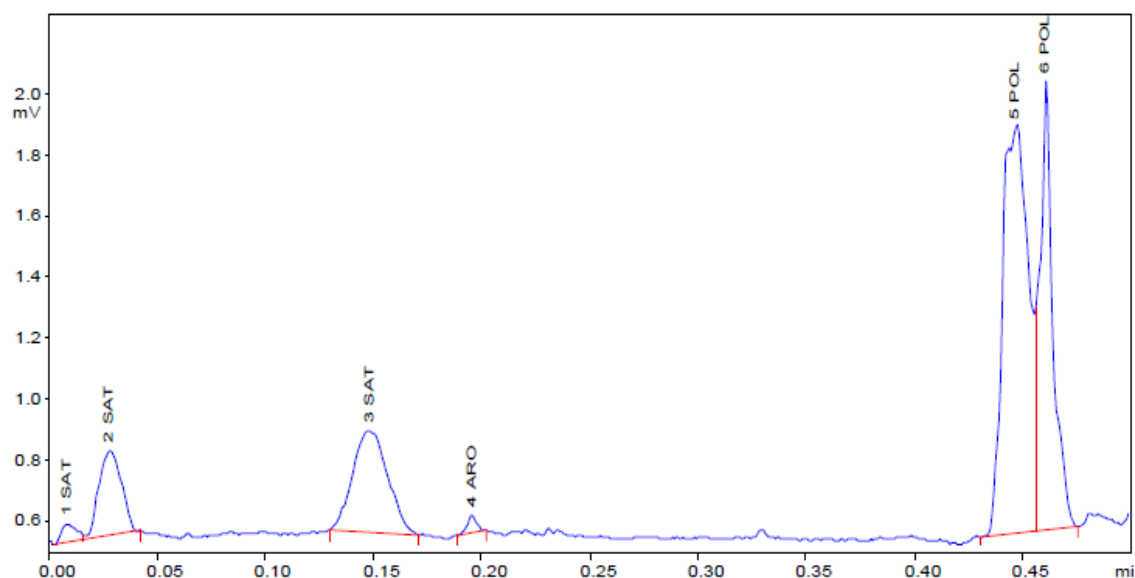
Threshold (mV): 10

Skim Ratio: 3

Parameter Files:

Data Handling File:Iatroscl

Calculation-File:Iatroscl



Calculation Method : Percent

Peak No	Win No.	Ret.Time (min)	Area	Resp.- Fact.	Area%	Name
1	1	0.009	15	1.000	1.210	SAT
2	1	0.028	105	1.000	8.509	SAT
3	1	0.148	194	1.000	15.703	SAT
4	2	0.196	9	1.000	0.763	ARO
5	3	0.447	584	1.000	47.235	POL
6	3	0.461	329	1.000	26.581	POL

1237

100.000

Sample Identifier: 30_10-6_4686.0

Data Processing Parameters

Injected on: 25.03.2014

Injected at: 19:33

Slice Width (ms): 50

Noise ($\mu\text{V/s}$): undefined

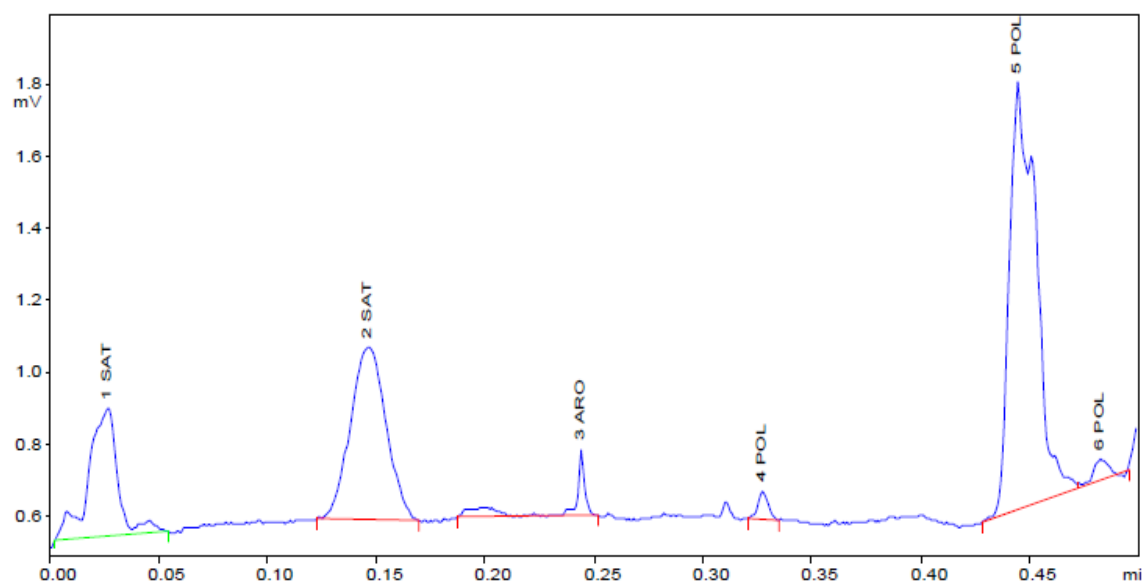
Threshold (mV): 0

Skim Ratio: 0

Parameter Files:

Data Handling File: Iatroscl

Calculation-File: ~atroscl0008



Calculation Method : Percent

Peak No	Win No.	Ret.Time (min)	Area	Resp.- Fact.	Area%	Name
1	1	0.027	173	1.000	16.538	SAT
2	1	0.147	286	1.000	27.362	SAT
3	2	0.244	38	1.000	3.645	ARO
4	3	0.327	13	1.000	1.218	POL
5	3	0.444	522	1.000	49.917	POL
6	3	0.482	14	1.000	1.320	POL

1045

100.000

Sample Identifier: 30_10-6_4686.5

Data Processing Parameters

Injected on: 25.03.2014

Injected at: 19:33

Slice Width (ms): 50

Noise ($\mu\text{V/s}$): 50

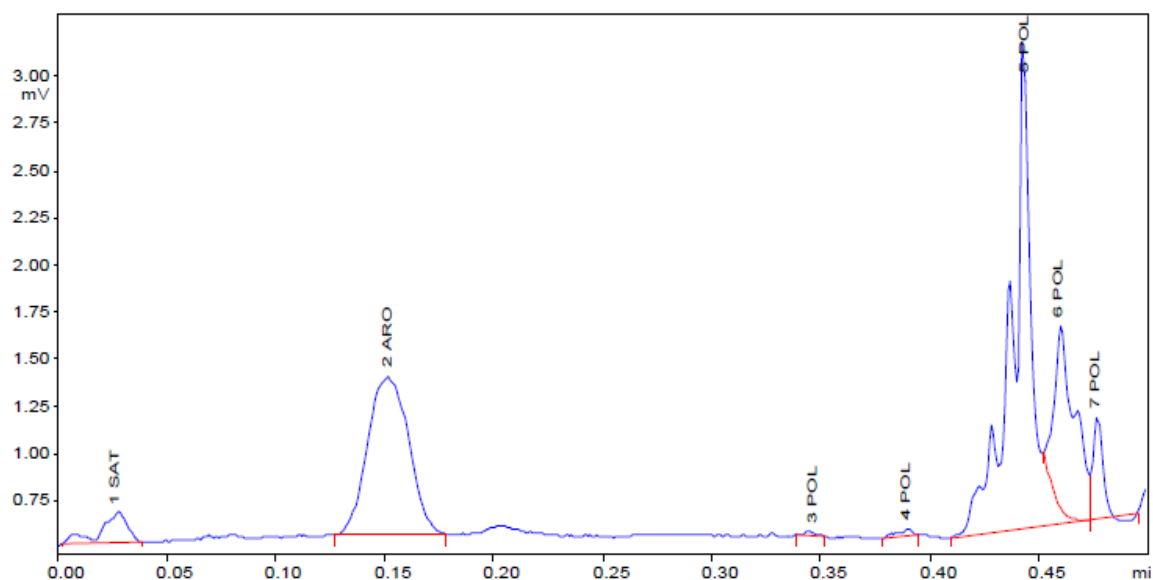
Threshold (mV): 10

Skim Ratio: 3

Parameter Files:

Data Handling File: Iatroscl

Calculation-File: Iatroscl



Calculation Method : Percent

Peak No	Win No.	Ret.Time (min)	Area	Resp.- Fact.	Area%	Name
1	1	0.027	66	1.000	3.406	SAT
2	2	0.152	574	1.000	29.519	ARO
3	3	0.347	4	1.000	0.221	POL
4	3	0.389	8	1.000	0.434	POL
5	3	0.443	867	1.000	44.577	POL
6	3	0.460	343	1.000	17.609	POL
7	3	0.477	82	1.000	4.234	POL

1946

100.000

Sample Identifier: 30_10-6_4691.0

Data Processing Parameters

Injected on: 25.03.2014

Injected at: 19:34

Slice Width (ms): 50

Noise (µV/s): 50

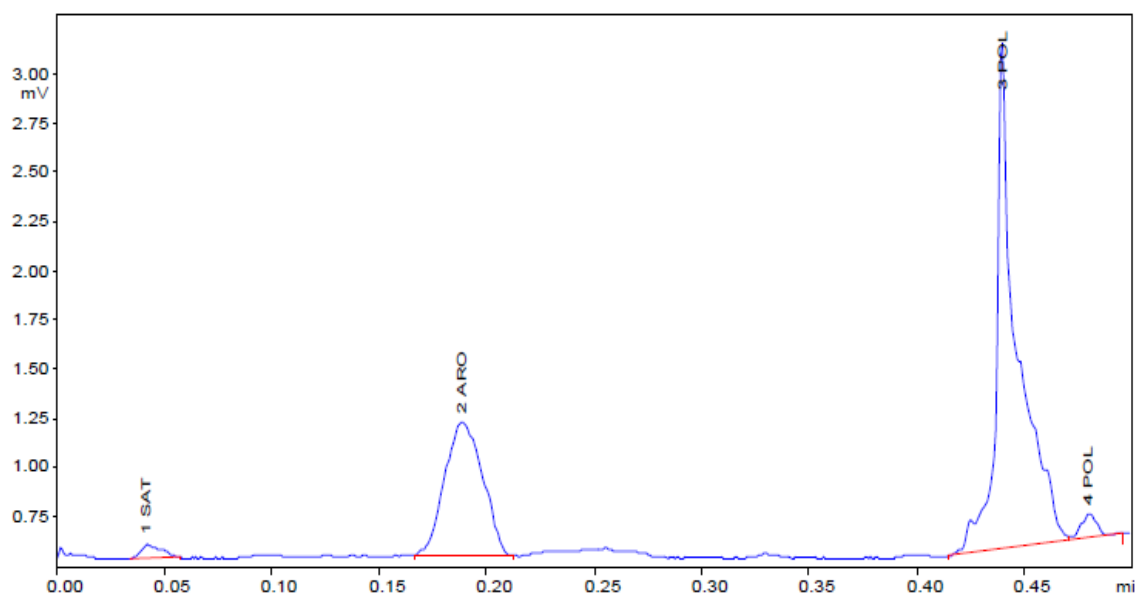
Threshold (mV): 10

Skim Ratio: 3

Parameter Files:

Data Handling File:Iatroscl

Calculation-File:Iatroscl



Calculation Method : Percent

Peak No	Win No.	Ret.Time (min)	Area	Resp.- Fact.	Area%	Name
1	1	0.043	24	1.000	1.727	SAT
2	2	0.189	435	1.000	30.660	ARO
3	3	0.441	928	1.000	65.445	POL
4	3	0.480	31	1.000	2.168	POL
			1418	100.000		

Sample Identifier: 30_10-6_4691.5

Data Processing Parameters

Injected on: 26.03.2014

Injected at: 20:18

Slice Width (ms): 50

Noise ($\mu\text{V/s}$): 50

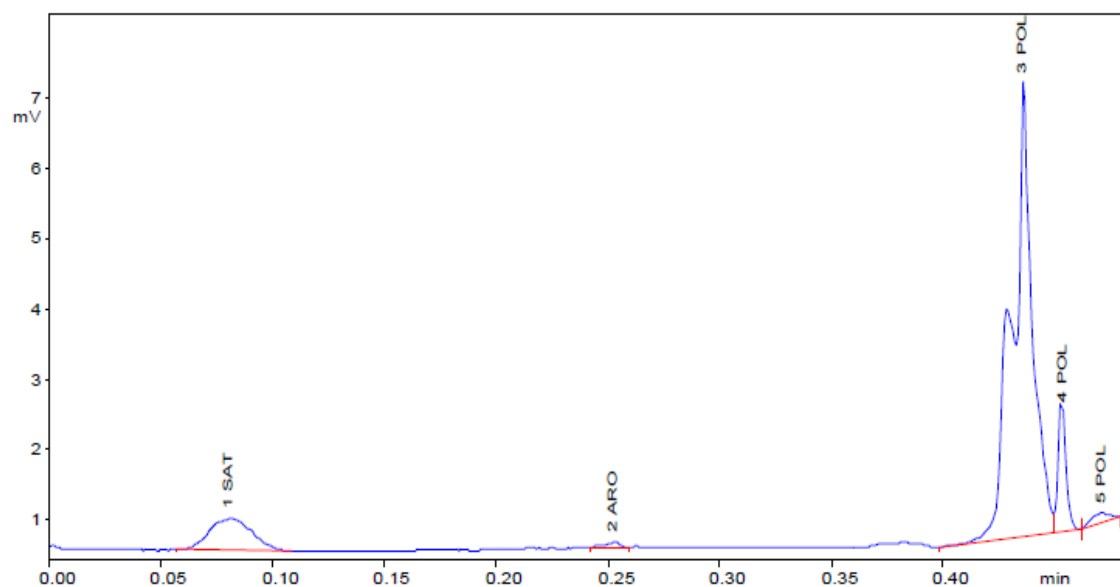
Threshold (mV): 10

Skim Ratio: 3

Parameter Files:

Data Handling File:Iatroscl

Calculation-File:Iatroscl



Calculation Method : Percent

Peak No	Win No.	Ret.Time (min)	Area	Resp.- Fact.	Area%	Name
1	1	0.081	315	1.000	11.597	SAT
2	2	0.252	18	1.000	0.677	ARO
3	3	0.436	2123	1.000	78.219	POL
4	3	0.453	220	1.000	8.094	POL
5	3	0.471	38	1.000	1.412	POL

2715

100.000

Sample Identifier: 30_10-6_4702.0

Data Processing Parameters

Injected on: 26.03.2014

Injected at: 20:19

Slice Width (ms): 50

Noise ($\mu\text{V/s}$): 50

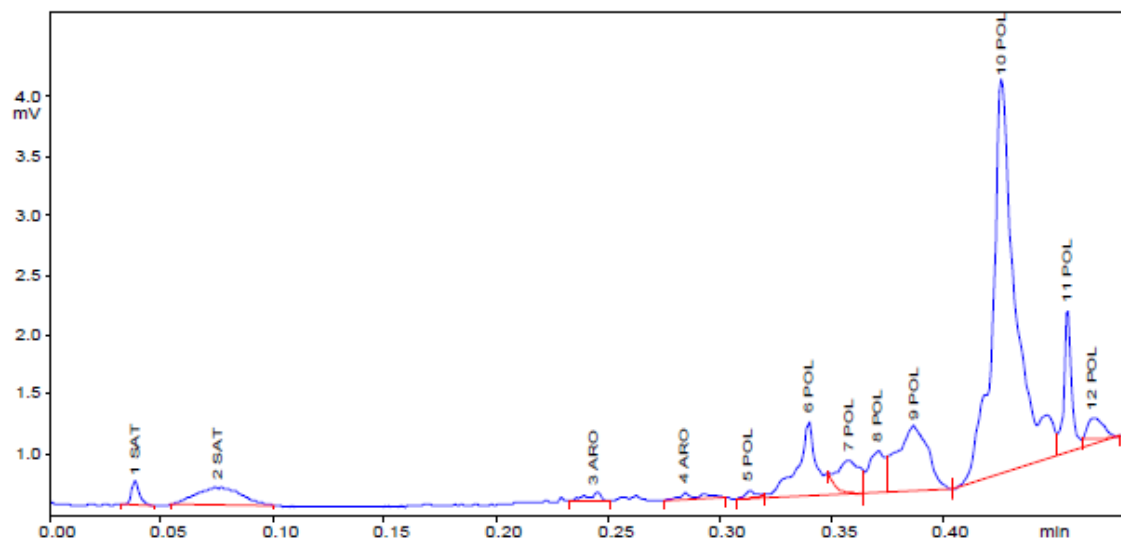
Threshold (mV): 10

Skim Ratio: 3

Parameter Files:

Data Handling File:Iatroscl

Calculation-File:Iatroscl



Calculation Method : Percent

Peak No	Win No.	Ret.Time (min)	Area	Resp.- Fact.	Area%	Name
1	1	0.039	23	1.000	0.974	SAT
2	1	0.076	110	1.000	4.730	SAT
3	2	0.244	17	1.000	0.714	ARO
4	2	0.285	19	1.000	0.815	ARO
5	3	0.313	9	1.000	0.405	POL
6	3	0.340	211	1.000	9.073	POL
7	3	0.358	93	1.000	4.021	POL
8	3	0.371	98	1.000	4.197	POL
9	3	0.387	271	1.000	11.658	POL
10	3	0.427	1281	1.000	55.076	POL
11	3	0.456	159	1.000	6.846	POL
12	3	0.468	35	1.000	1.491	POL
			2325	100.000		

Sample Identifier: 30_10-6_4702.5

Data Processing Parameters

Injected on: 26.03.2014

Injected at: 20:20

Slice Width (ms): 50

Noise (µV/s): undefined

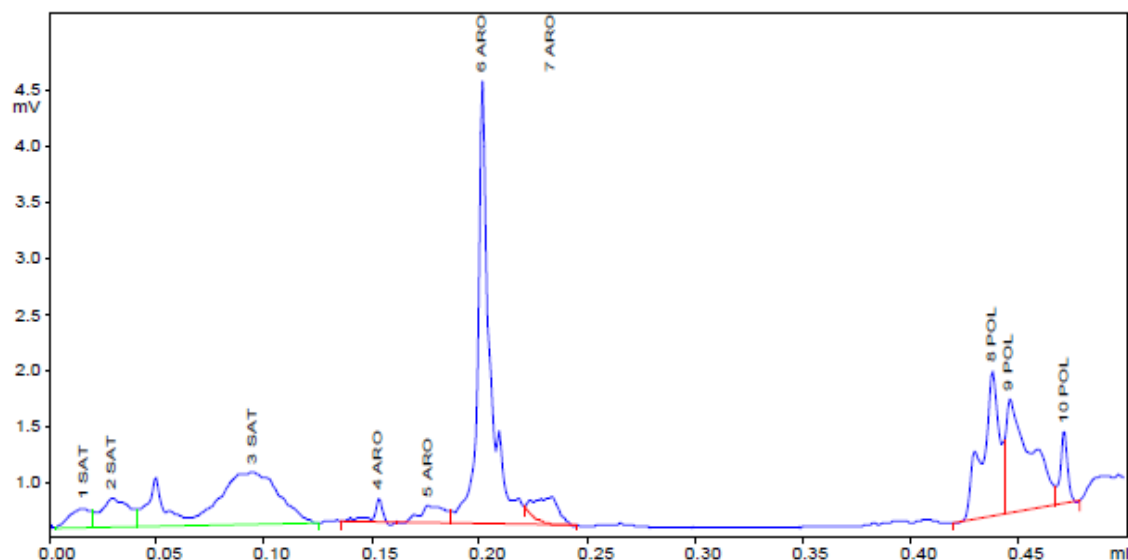
Threshold (mV): 0

Skim Ratio: 0

Parameter Files:

Data Handling File: Iatroscl

Calculation-File: ~atroscl0003



Calculation Method : Percent

Peak No	Win No.	Ret.Time (min)	Area	Resp.- Fact.	Area%	Name
1	1	0.017	61	1.000	2.248	SAT
2	1	0.030	118	1.000	4.368	SAT
3	1	0.095	577	1.000	21.385	SAT
4	2	0.153	32	1.000	1.197	ARO
5	2	0.177	65	1.000	2.398	ARO
6	2	0.202	853	1.000	31.616	ARO
7	2	0.233	95	1.000	3.513	ARO
8	3	0.438	387	1.000	14.345	POL
9	3	0.446	427	1.000	15.820	POL
10	3	0.472	84	1.000	3.111	POL

2697

100.000

Sample Identifier: 30_10-6_4714.7

Data Processing Parameters

Injected on: 26.03.2014

Injected at: 20:21

Slice Width (ms): 50

Noise ($\mu\text{V/s}$): undefined

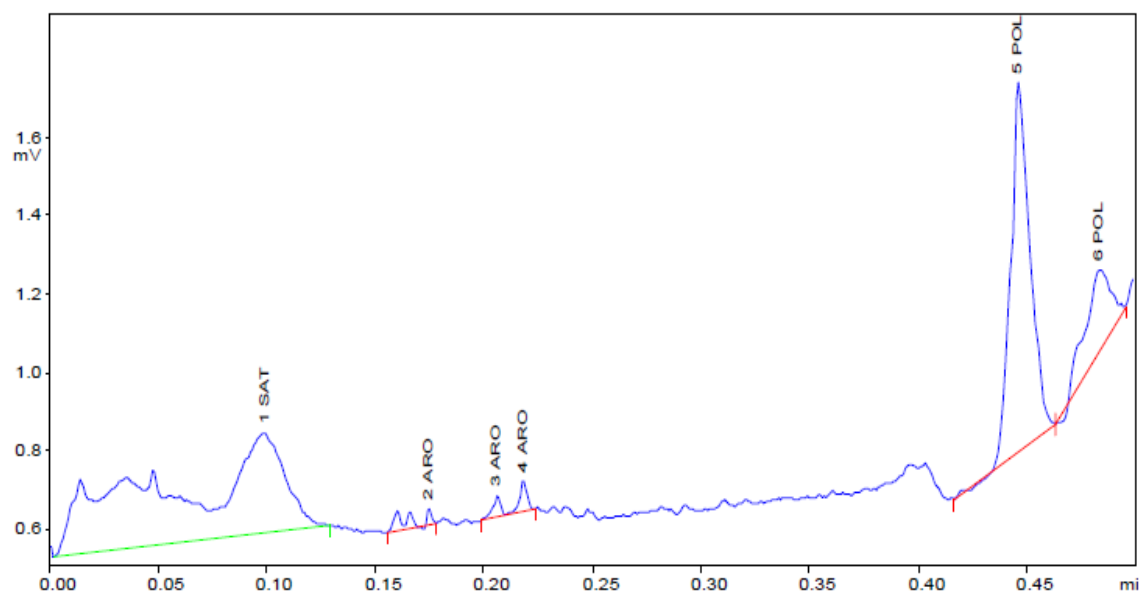
Threshold (mV): 0

Skim Ratio: 0

Parameter Files:

Data Handling File: Iatroscl

Calculation-File: ~atroscl0005



Calculation Method : Percent

Peak No	Win No.	Ret.Time (min)	Area	Resp.- Fact.	Area%	Name
1	1	0.100	504	1.000	53.758	SAT
2	2	0.175	13	1.000	1.408	ARO
3	2	0.206	7	1.000	0.768	ARO
4	2	0.218	10	1.000	1.036	ARO
5	3	0.446	309	1.000	32.935	POL
6	3	0.483	95	1.000	10.096	POL
			938	100.000		

Sample Identifier: 30_10-6_4962.3

Data Processing Parameters

Injected on: 26.03.2014

Injected at: 20:22

Slice Width (ms): 50

Noise ($\mu\text{V/s}$): undefined

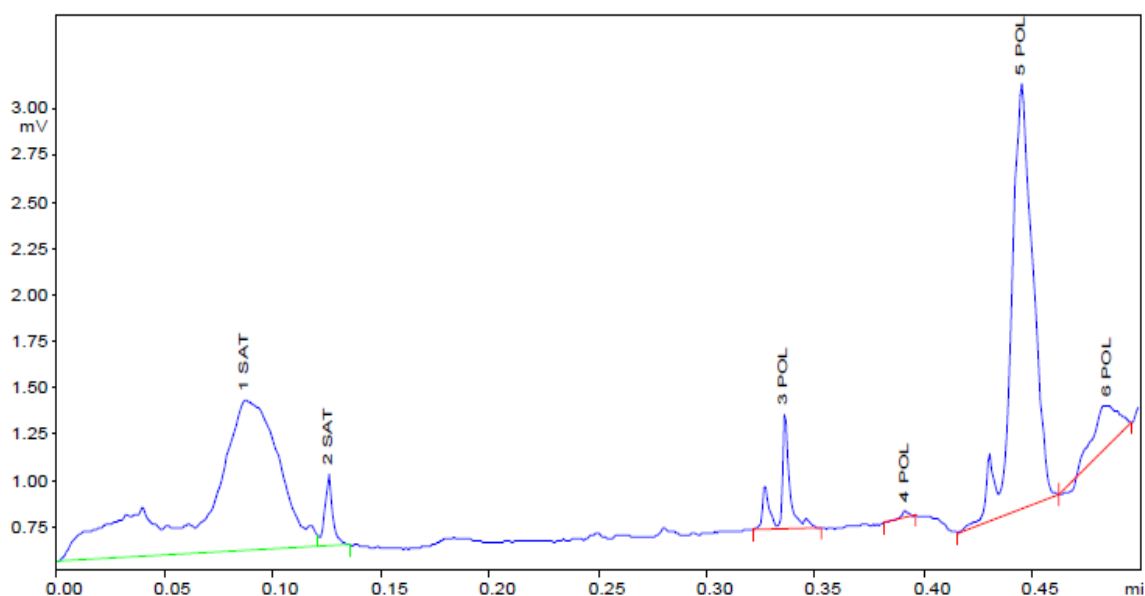
Threshold (mV): 0

Skim Ratio: 0

Parameter Files:

Data Handling File: Iatroscl

Calculation-File: ~atroscl0006



Calculation Method : Percent

Peak No	Win No.	Ret.Time (min)	Area	Resp.- Fact.	Area%	Name
1	1	0.087	1082	1.000	50.019	SAT
2	1	0.126	49	1.000	2.249	SAT
3	2	0.336	101	1.000	4.669	POL
4	2	0.392	5	1.000	0.245	POL
5	2	0.445	827	1.000	38.218	POL
6	2	0.485	100	1.000	4.600	POL

2163

100.000

Sample Identifier: 30_11-3_3450.5

Data Processing Parameters

Injected on: 27.03.2014

Injected at: 18:42

Slice Width (ms): 50

Noise (µV/s): 50

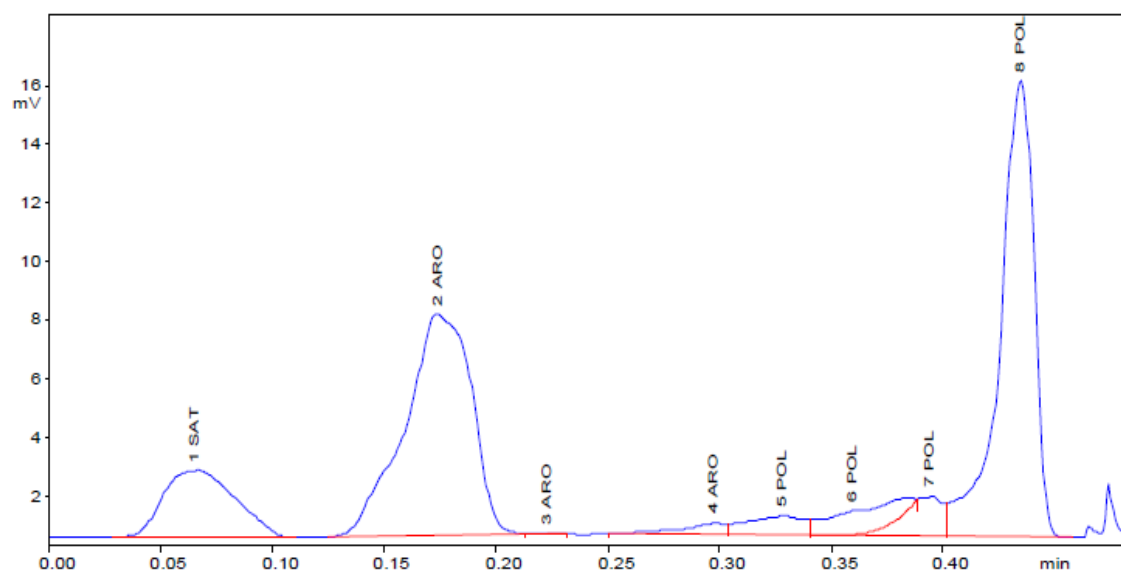
Threshold (mV): 10

Skim Ratio: 3

Parameter Files:

Data Handling File: Iatroscl

Calculation-File: Iatroscl



Calculation Method : Percent

Peak No	Win No.	Ret.Time (min)	Area	Resp.- Fact.	Area%	Name
1	1	0.066	2676	1.000	11.386	SAT
2	2	0.174	8277	1.000	35.221	ARO
3	2	0.223	17	1.000	0.072	ARO
4	2	0.298	295	1.000	1.253	ARO
5	3	0.328	617	1.000	2.627	POL
6	3	0.360	992	1.000	4.220	POL
7	3	0.394	1929	1.000	8.209	POL
8	3	0.435	8698	1.000	37.013	POL

23501

100.000

Sample Identifier: 30_11-3_3457.0

Data Processing Parameters

Injected on: 27.03.2014

Injected at: 18:43

Slice Width (ms): 50

Noise ($\mu\text{V/s}$): undefined

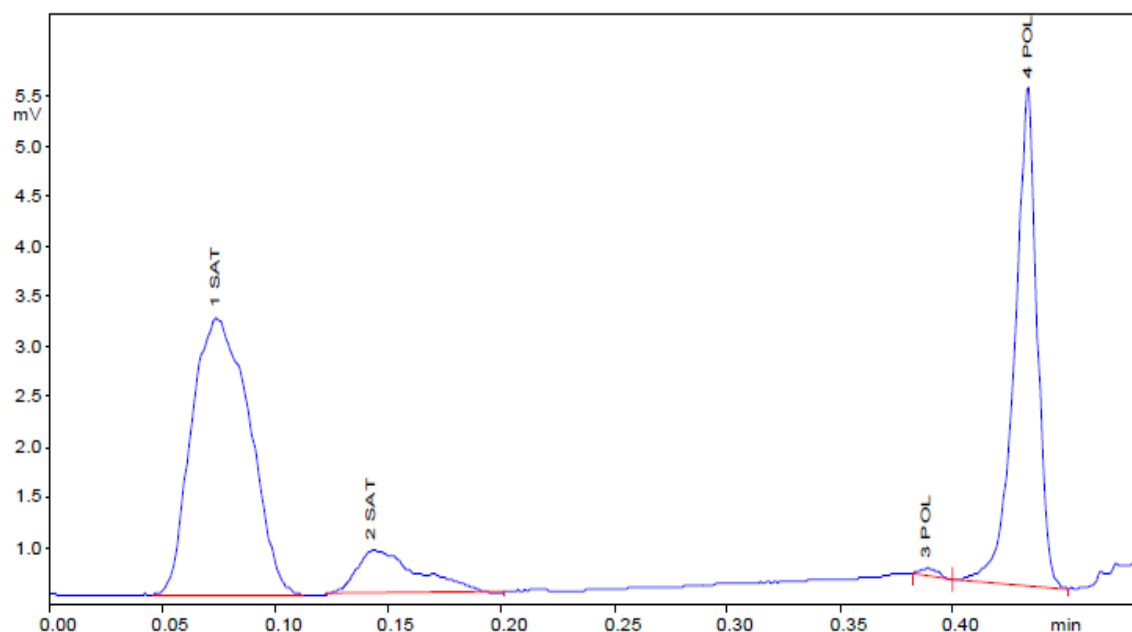
Threshold (mV): 0

Skim Ratio: 0

Parameter Files:

Data Handling File: Iatroscl

Calculation-File: ~atroscl0009



Calculation Method : Percent

Peak No	Win No.	Ret.Time (min)	Area	Resp.- Fact.	Area%	Name
1	1	0.074	2552	1.000	53.268	SAT
2	1	0.143	427	1.000	8.907	SAT
3	2	0.388	19	1.000	0.398	POL
4	2	0.433	1793	1.000	37.427	POL
			4791		100.000	

Sample Identifier: 30_11-3_3457.5

Data Processing Parameters

Injected on: 27.03.2014

Injected at: 18:44

Slice Width (ms): 50

Noise ($\mu\text{V/s}$): undefined

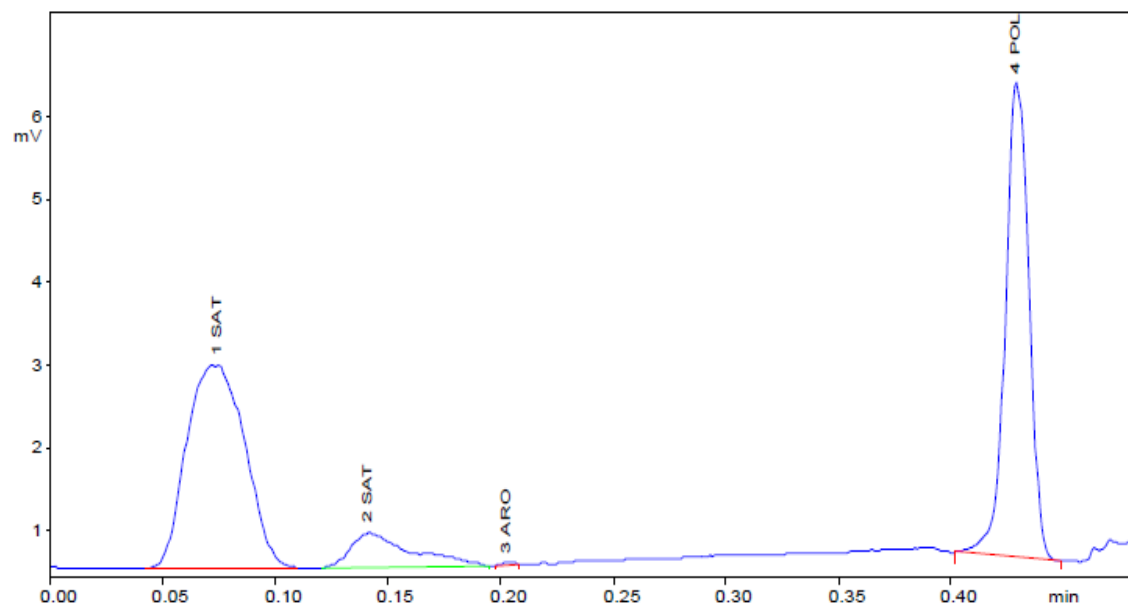
Threshold (mV): 0

Skim Ratio: 0

Parameter Files:

Data Handling File: Iatroscl

Calculation-File: ~atroscl0010



Calculation Method : Percent

Peak No	Win No.	Ret.Time (min)	Area	Resp.- Fact.	Area%	Name
1	1	0.075	2307	1.000	46.872	SAT
2	1	0.142	407	1.000	8.268	SAT
3	2	0.203	5	1.000	0.109	ARO
4	3	0.429	2203	1.000	44.751	POL
			4922		100.000	

Sample Identifier:30_11-3_3468.3

Data Processing Parameters

Injected on: 27.03.2014

Injected at: 20:40

Slice Width (ms): 50

Noise ($\mu\text{V/s}$): 50

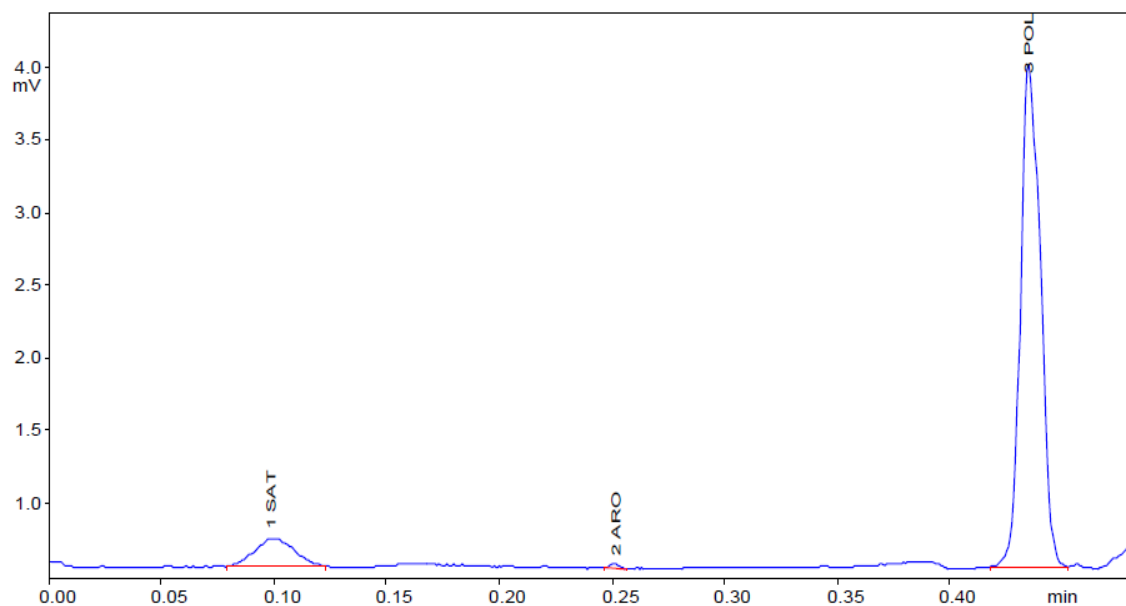
Threshold (mV): 10

Skim Ratio: 3

Parameter Files:

Data Handling File:Iatroscl

Calculation-File:Iatroscl



Calculation Method : Percent

Peak No	Win No.	Ret.Time (min)	Area	Resp.- Fact.	Area%	Name
1	1	0.099	117	1.000	9.357	SAT
2	2	0.252	4	1.000	0.344	ARO
3	3	0.436	1126	1.000	90.299	POL
			1247		100.000	

Sample Identifier: 30_11-4_3514.5

Data Processing Parameters

Injected on: 27.03.2014

Injected at: 18:38

Slice Width (ms): 50

Noise (µV/s): undefined

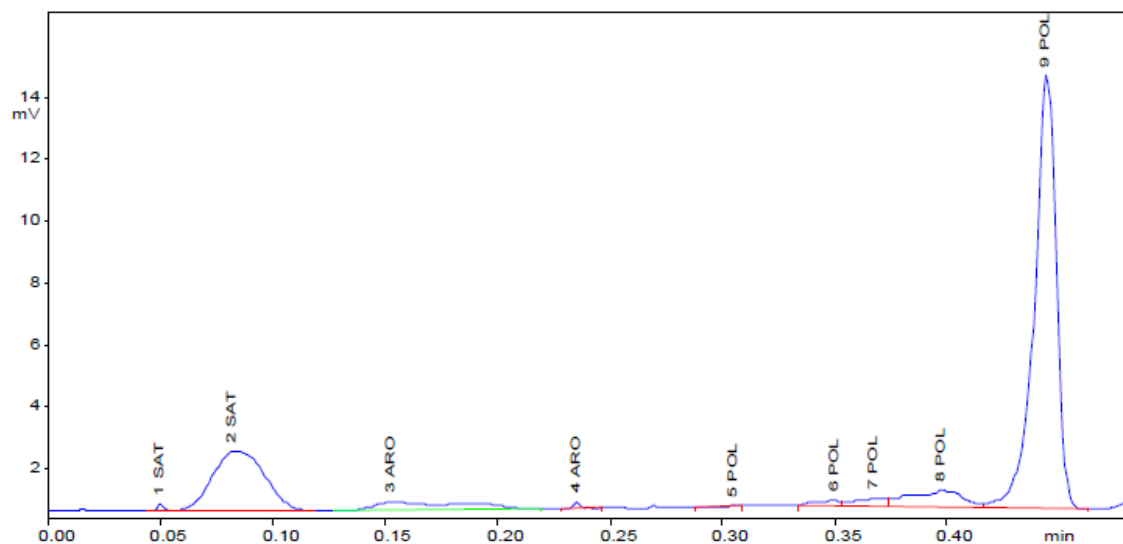
Threshold (mV): 0

Skim Ratio: 0

Parameter Files:

Data Handling File: Iatroscl

Calculation-File: ~atroscl0002



Calculation Method : Percent

Peak No	Win No.	Ret.Time (min)	Area	Resp.- Fact.	Area%	Name
1	1	0.050	25	1.000	0.321	SAT
2	1	0.083	1625	1.000	21.104	SAT
3	2	0.153	416	1.000	5.406	ARO
4	2	0.235	13	1.000	0.174	ARO
5	3	0.305	3	1.000	0.043	POL
6	3	0.350	59	1.000	0.769	POL
7	3	0.368	124	1.000	1.604	POL
8	3	0.398	447	1.000	5.806	POL
9	3	0.444	4988	1.000	64.771	POL
			7701	100.000		

Sample Identifier: 30_11-4_3515.0

Data Processing Parameters

Injected on: 27.03.2014

Injected at: 18:38

Slice Width (ms): 50

Noise (µV/s): 50

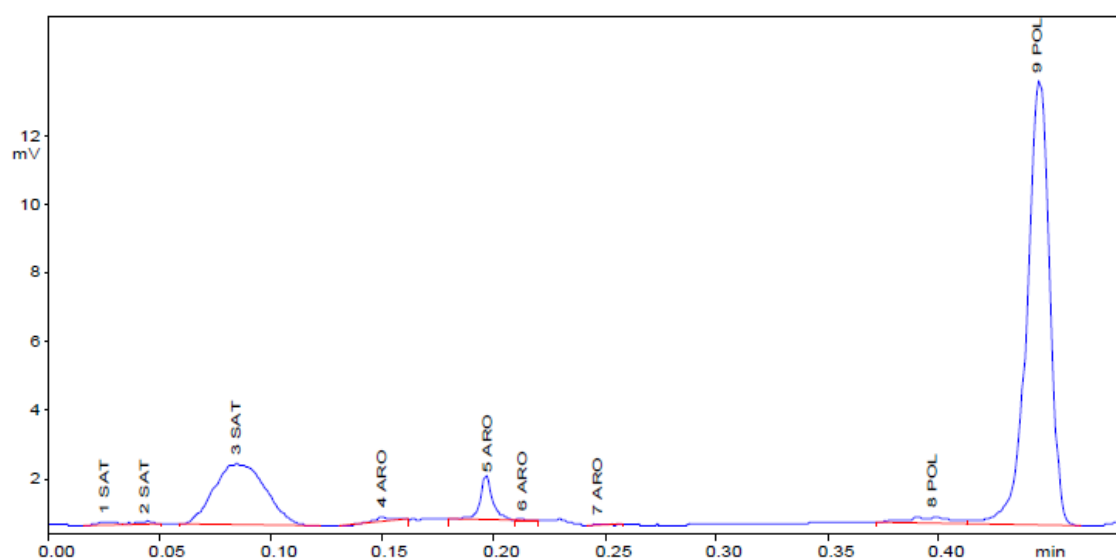
Threshold (mV): 10

Skim Ratio: 3

Parameter Files:

Data Handling File: Iatroscl

Calculation-File: Iatroscl



Calculation Method : Percent

Peak No	Win No.	Ret.Time (min)	Area	Resp.- Fact.	Area%	Name
1	1	0.026	26	1.000	0.388	SAT
2	1	0.044	24	1.000	0.353	SAT
3	1	0.085	1512	1.000	22.346	SAT
4	2	0.151	47	1.000	0.688	ARO
5	2	0.198	247	1.000	3.650	ARO
6	2	0.213	3	1.000	0.038	ARO
7	2	0.248	7	1.000	0.096	ARO
8	3	0.398	114	1.000	1.692	POL
9	3	0.445	4788	1.000	70.749	POL
			6767	100.000		

Sample Identifier: 30_11-4_3515.5

Data Processing Parameters

Injected on: 27.03.2014

Injected at: 18:39

Slice Width (ms): 50

Noise ($\mu\text{V/s}$): 50

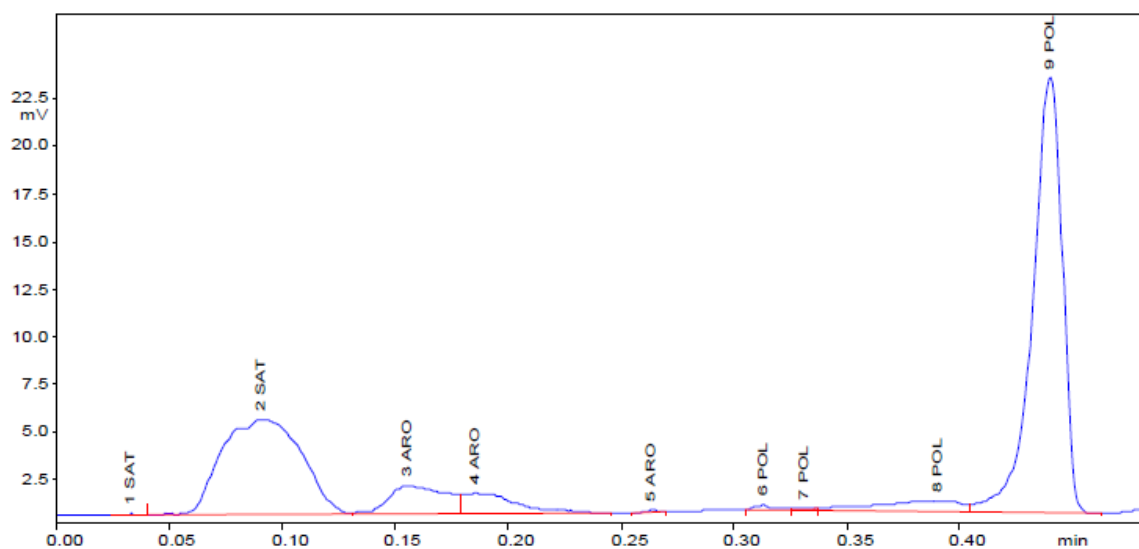
Threshold (mV): 10

Skim Ratio: 3

Parameter Files:

Data Handling File: Iatroscl

Calculation-File: Iatroscl



Calculation Method : Percent

Peak No	Win No.	Ret.Time (min)	Area	Resp.- Fact.	Area%	Name
1	1	0.033	15	1.000	0.072	SAT
2	1	0.091	6490	1.000	31.231	SAT
3	2	0.156	1392	1.000	6.698	ARO
4	2	0.186	900	1.000	4.329	ARO
5	2	0.264	20	1.000	0.095	ARO
6	3	0.313	74	1.000	0.358	POL
7	3	0.332	29	1.000	0.138	POL
8	3	0.391	824	1.000	3.965	POL
9	3	0.440	11037	1.000	53.114	POL

20780

100.000

Sample Identifier: 30_11-4_3516.0

Data Processing Parameters

Injected on: 27.03.2014

Injected at: 18:40

Slice Width (ms): 50

Noise ($\mu\text{V/s}$): 50

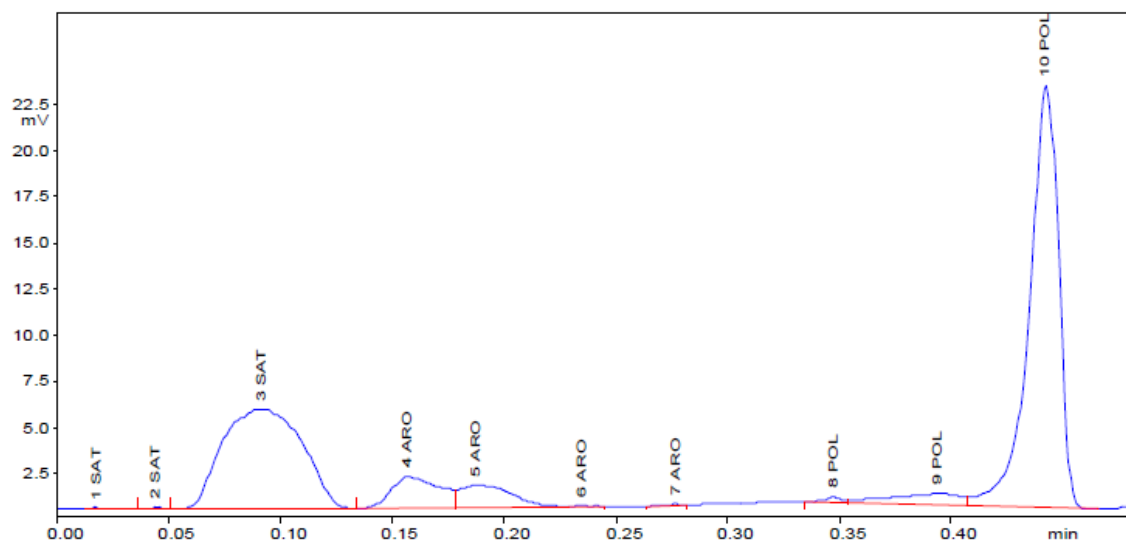
Threshold (mV): 10

Skim Ratio: 3

Parameter Files:

Data Handling File:Iatroscl

Calculation-File:Iatroscl



Calculation Method : Percent

Peak No	Win No.	Ret.Time (min)	Area	Resp.- Fact.	Area%	Name
1	1	0.018	19	1.000	0.091	SAT
2	1	0.045	15	1.000	0.073	SAT
3	1	0.092	7019	1.000	33.074	SAT
4	2	0.157	1356	1.000	6.391	ARO
5	2	0.188	1017	1.000	4.791	ARO
6	2	0.235	19	1.000	0.088	ARO
7	2	0.278	9	1.000	0.040	ARO
8	3	0.347	82	1.000	0.385	POL
9	3	0.394	689	1.000	3.247	POL
10	3	0.442	10997	1.000	51.820	POL

21221

100.000

Sample Identifier: 30_11-4_3517.2

Data Processing Parameters

Injected on: 27.03.2014

Injected at: 18:41

Slice Width (ms): 50

Noise ($\mu\text{V/s}$): 50

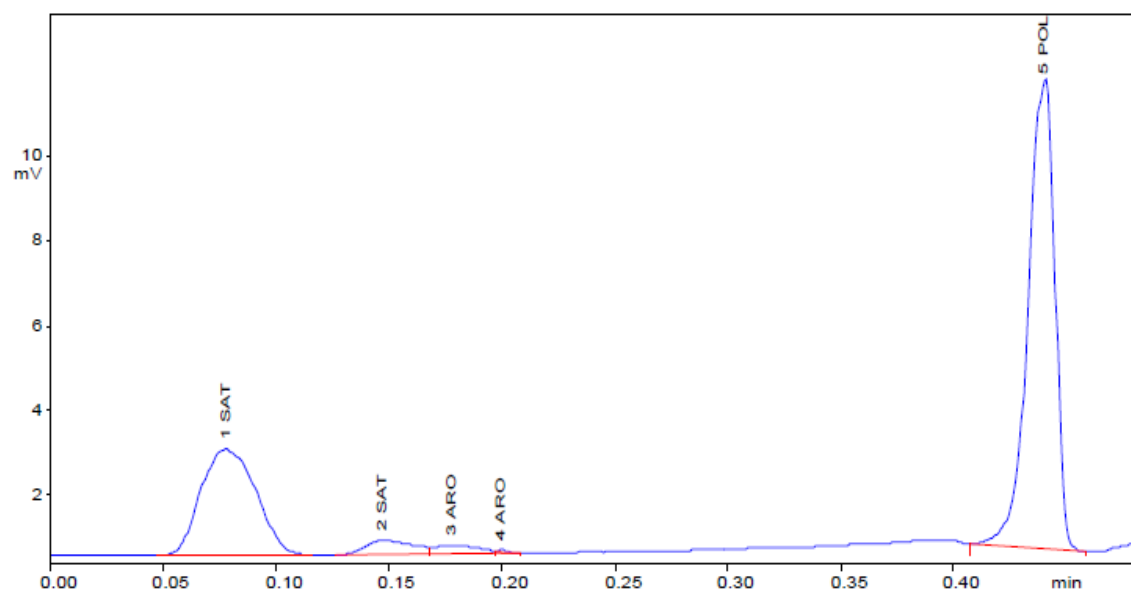
Threshold (mV): 10

Skim Ratio: 3

Parameter Files:

Data Handling File: Iatroscl

Calculation-File: Iatroscl



Calculation Method : Percent

Peak No	Win No.	Ret.Time (min)	Area	Resp.- Fact.	Area%	Name
1	1	0.078	2228	1.000	29.861	SAT
2	1	0.147	263	1.000	3.527	SAT
3	2	0.178	146	1.000	1.961	ARO
4	2	0.200	9	1.000	0.122	ARO
5	3	0.440	4815	1.000	64.530	POL
			7461		100.000	

Sample Identifier: 30_11-4_3526.8

Data Processing Parameters

Injected on: 27.03.2014

Injected at: 18:41

Slice Width (ms): 50

Noise ($\mu\text{V/s}$): 50

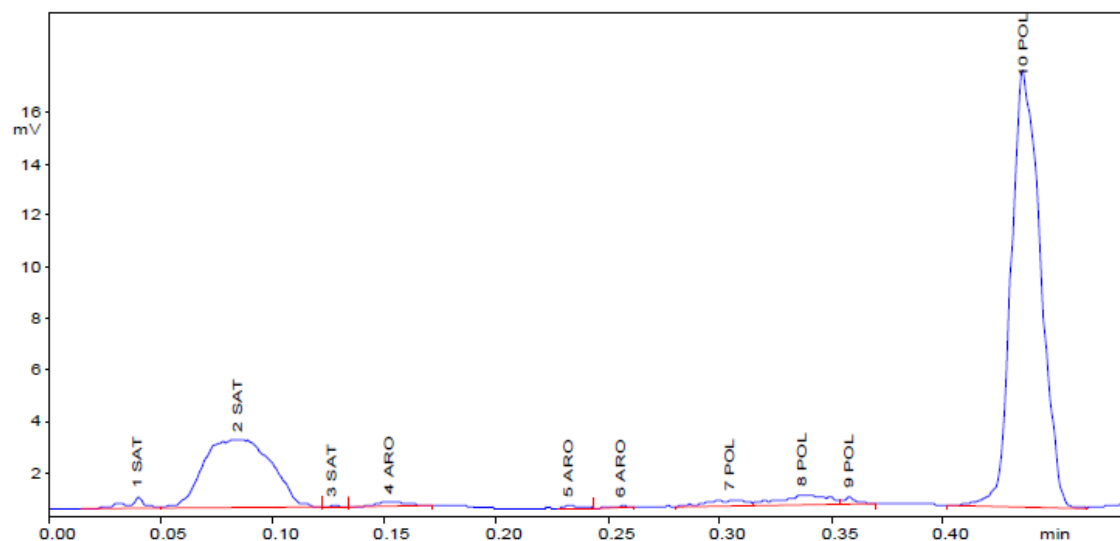
Threshold (mV): 10

Skim Ratio: 3

Parameter Files:

Data Handling File:Iatroscl

Calculation-File:Iatroscl



Calculation Method : Percent

Peak No	Win No.	Ret.Time (min)	Area	Resp.- Fact.	Area%	Name
1	1	0.040	147	1.000	1.243	SAT
2	1	0.085	2997	1.000	25.322	SAT
3	1	0.127	15	1.000	0.125	SAT
4	2	0.153	87	1.000	0.734	ARO
5	2	0.233	19	1.000	0.164	ARO
6	2	0.257	7	1.000	0.061	ARO
7	3	0.305	136	1.000	1.145	POL
8	3	0.338	286	1.000	2.413	POL
9	3	0.358	49	1.000	0.418	POL
10	3	0.437	8093	1.000	68.375	POL

11836

100.000

Sample Identifier: 30_11-8A_3968.0

Data Processing Parameters

Injected on: 26.03.2014

Injected at: 20:23

Slice Width (ms): 50

Noise ($\mu\text{V/s}$): 50

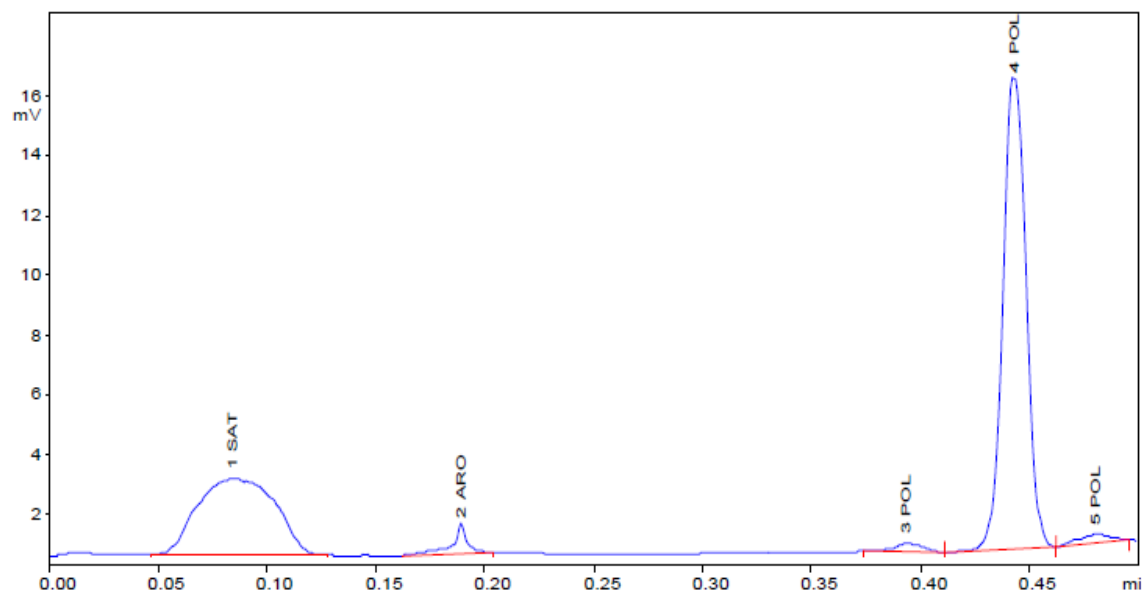
Threshold (mV): 10

Skim Ratio: 3

Parameter Files:

Data Handling File:Iatroscl

Calculation-File:Iatroscl



Calculation Method : Percent

Peak No	Win No.	Ret.Time (min)	Area	Resp.- Fact.	Area%	Name
1	1	0.085	3295	1.000	33.291	SAT
2	2	0.190	242	1.000	2.440	ARO
3	3	0.394	133	1.000	1.345	POL
4	3	0.443	6080	1.000	61.418	POL
5	3	0.481	149	1.000	1.506	POL

9899

100.000

Sample Identifier: 30_11-8A_3968.5

Data Processing Parameters

Injected on: 26.03.2014

Injected at: 20:24

Slice Width (ms): 50

Noise ($\mu\text{V/s}$): 50

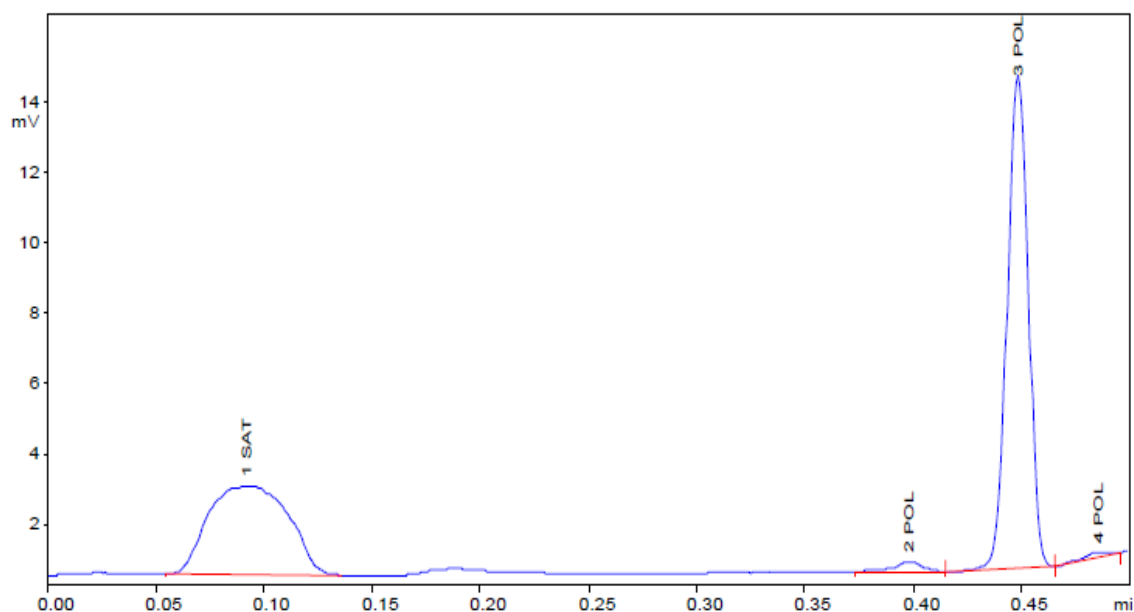
Threshold (mV): 10

Skim Ratio: 3

Parameter Files:

Data Handling File: Iatroscl

Calculation-File: Iatroscl



Calculation Method : Percent

Peak No	Win No.	Ret.Time (min)	Area	Resp.- Fact.	Area%	Name
1	1	0.093	3359	1.000	39.086	SAT
2	2	0.398	140	1.000	1.632	POL
3	2	0.449	5023	1.000	58.450	POL
4	2	0.487	71	1.000	0.831	POL

8594

100.000

Sample Identifier: 30_11-8A_3986.5

Data Processing Parameters

Injected on: 26.03.2014

Injected at: 20:25

Slice Width (ms): 50

Noise ($\mu\text{V/s}$): 50

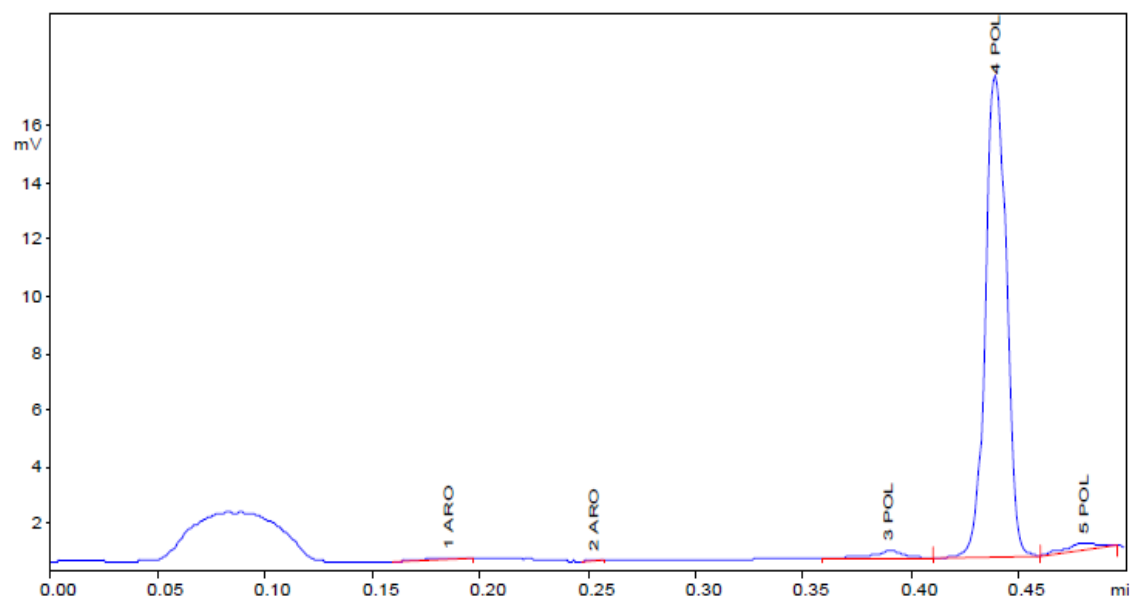
Threshold (mV): 10

Skim Ratio: 3

Parameter Files:

Data Handling File:Iatroscl

Calculation-File:Iatroscl



Calculation Method : Percent

Peak No	Win No.	Ret.Time (min)	Area	Resp.-Fact.	Area%	Name
1	1	0.186	60	1.000	0.938	ARO
2	1	0.253	4	1.000	0.063	ARO
3	2	0.390	158	1.000	2.464	POL
4	2	0.440	6058	1.000	94.756	POL
5	2	0.481	114	1.000	1.779	POL

6394

100.000

Sample Identifier: 30_11-8A_3987.0

Data Processing Parameters

Injected on: 26.03.2014

Injected at: 22:15

Slice Width (ms): 50

Noise (µV/s): 50

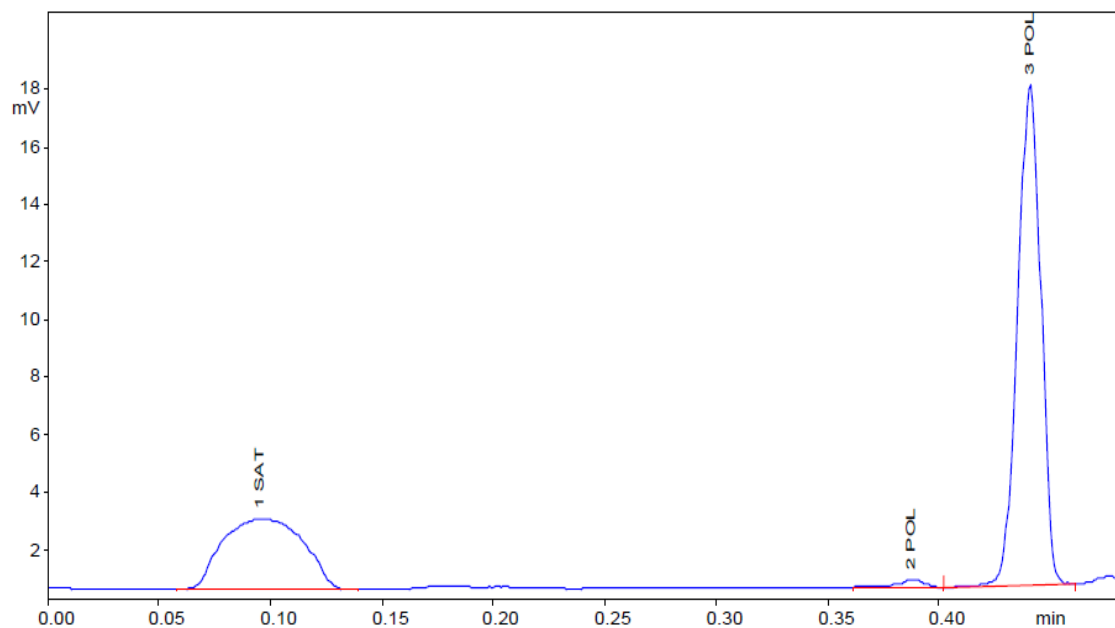
Threshold (mV): 10

Skim Ratio: 3

Parameter Files:

Data Handling File:Iatroscl

Calculation-File:Iatroscl



Calculation Method : Percent

Peak No	Win No.	Ret.Time (min)	Area	Resp.- Fact.	Area%	Name
1	1	0.096	3276	1.000	32.721	SAT
2	2	0.387	113	1.000	1.127	POL
3	2	0.441	6622	1.000	66.152	POL

10011

100.000

Iatroscan TLC-FID Chromatograms with drilling mud contamination

Sample Identifier:25_5-5_2164.5

Data Processing Parameters

Injected on: 26.03.2014

Injected at: 22:21

Slice Width (ms): 50

Noise ($\mu\text{V/s}$): 50

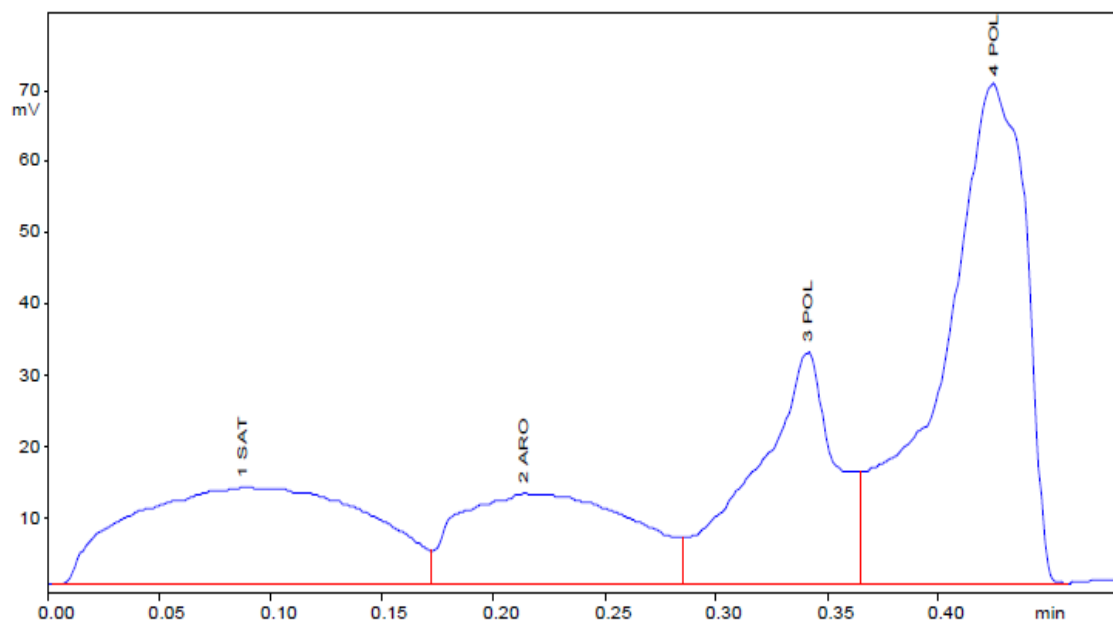
Threshold (mV): 10

Skim Ratio: 3

Parameter Files:

Data Handling File:Iatroscl

Calculation-File:Iatroscl



Calculation Method : Percent

Peak No	Win No.	Ret.Time (min)	Area	Resp.- Fact.	Area%	Name
1	1	0.088	53461	1.000	23.406	SAT
2	2	0.214	36110	1.000	15.810	ARO
3	3	0.342	42682	1.000	18.687	POL
4	3	0.425	96151	1.000	42.097	POL
			228403		100.000	

Sample Identifier: 25_5-5_2171.5

Data Processing Parameters

Injected on: 26.03.2014

Injected at: 22:22

Slice Width (ms): 50

Noise ($\mu\text{V/s}$): 50

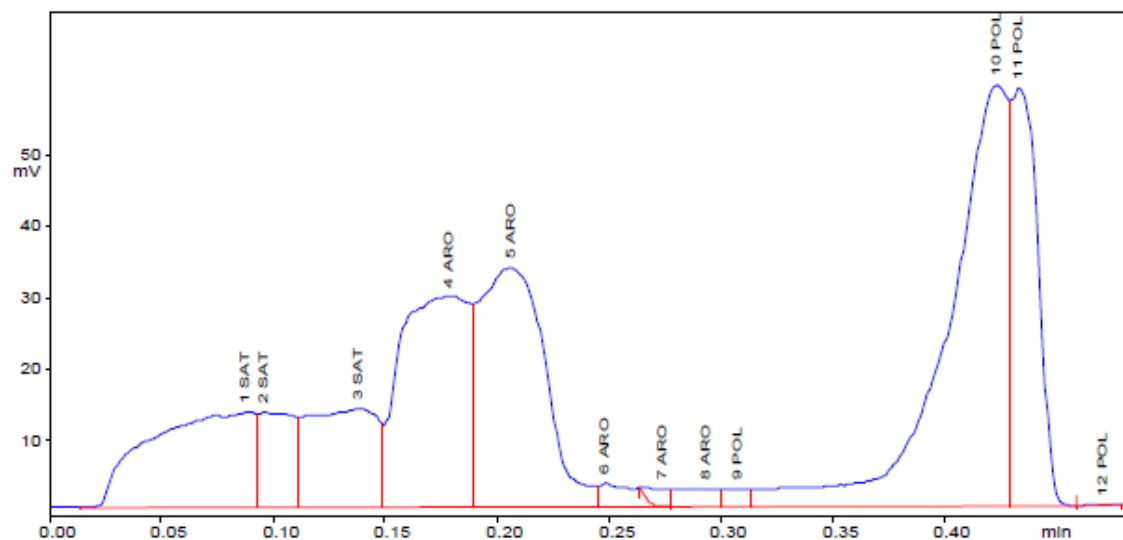
Threshold (mV): 10

Skim Ratio: 3

Parameter Files:

Data Handling File:Iatroscl

Calculation-File:Iatroscl



Calculation Method : Percent

Peak No	Win No.	Ret.Time (min)	Area	Resp.-Fact.	Area%	Name
1	1	0.088	23088	1.000	11.416	SAT
2	1	0.097	7562	1.000	3.739	SAT
3	1	0.138	15472	1.000	7.651	SAT
4	2	0.179	32887	1.000	16.261	ARO
5	2	0.207	35541	1.000	17.574	ARO
6	2	0.249	1887	1.000	0.933	ARO
7	2	0.274	923	1.000	0.456	ARO
8	2	0.294	1713	1.000	0.847	ARO
9	3	0.308	953	1.000	0.471	POL
10	3	0.423	57695	1.000	28.528	POL
11	3	0.433	24470	1.000	12.099	POL
12	3	0.471	49	1.000	0.024	POL

202240

100.000

Sample Identifier: 25_5-5_2172.0

Data Processing Parameters

Injected on: 26.03.2014

Injected at: 22:22

Slice Width (ms): 50

Noise ($\mu\text{V/s}$): 50

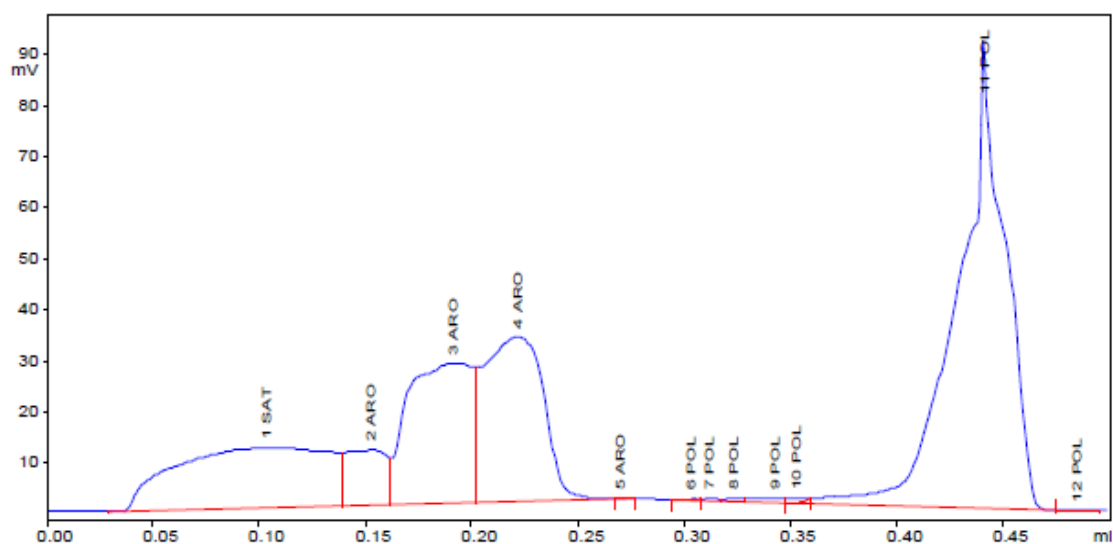
Threshold (mV): 10

Skim Ratio: 3

Parameter Files:

Data Handling File:Iatroscl

Calculation-File:Iatroscl



Calculation Method : Percent

Peak No	Win No.	Ret.Time (min)	Area	Resp.- Fact.	Area%	Name
1	1	0.104	31516	1.000	17.844	SAT
2	2	0.153	7449	1.000	4.218	ARO
3	2	0.192	30691	1.000	17.377	ARO
4	2	0.222	32360	1.000	18.322	ARO
5	2	0.271	3	1.000	0.002	ARO
6	3	0.304	12	1.000	0.007	POL
7	3	0.313	156	1.000	0.088	POL
8	3	0.324	169	1.000	0.095	POL
9	3	0.343	406	1.000	0.230	POL
10	3	0.353	298	1.000	0.169	POL
11	3	0.442	73523	1.000	41.628	POL
12	3	0.486	35	1.000	0.020	POL

176617

100.000

Sample Identifier: 25_5-5_2173.5

Data Processing Parameters

Injected on: 27.03.2014

Injected at: 18:37

Slice Width (ms): 50

Noise ($\mu\text{V/s}$): 50

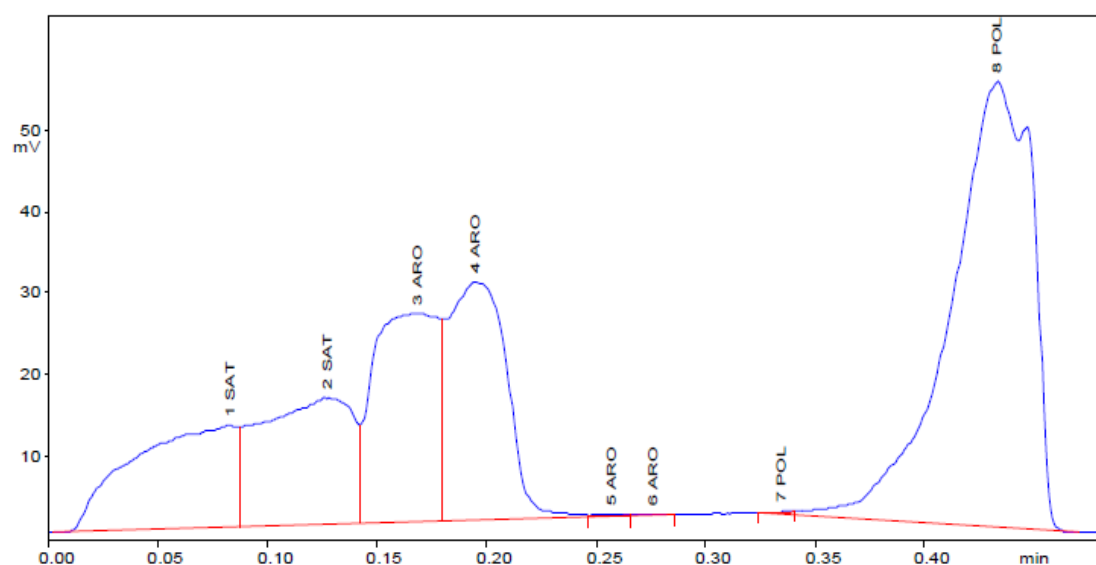
Threshold (mV): 10

Skim Ratio: 3

Parameter Files:

Data Handling File: Iatroscl

Calculation-File: Iatroscl



Calculation Method : Percent

Peak No	Win No.	Ret.Time (min)	Area	Resp.- Fact.	Area%	Name
1	1	0.083	21959	1.000	12.448	SAT
2	1	0.128	24028	1.000	13.620	SAT
3	2	0.169	27717	1.000	15.711	ARO
4	2	0.196	27947	1.000	15.842	ARO
5	2	0.257	87	1.000	0.050	ARO
6	2	0.277	59	1.000	0.034	ARO
7	3	0.335	43	1.000	0.024	POL
8	3	0.433	74572	1.000	42.272	POL

176412

100.000

Sample Identifier: 30_11-7_3987.5

Data Processing Parameters

Injected on: 25.03.2014

Injected at: 16:36

Slice Width (ms): 50

Noise ($\mu\text{V/s}$): 50

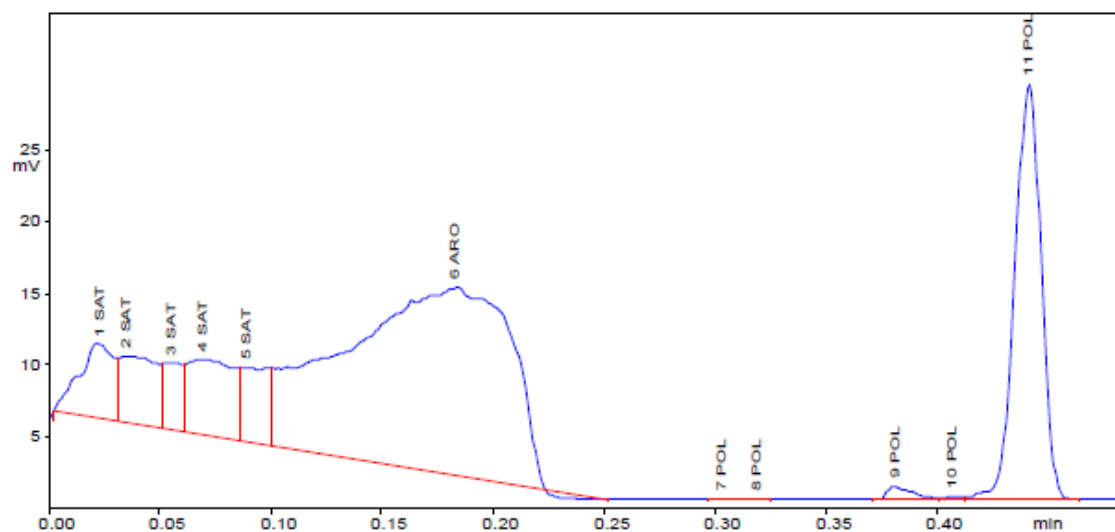
Threshold (mV): 10

Skim Ratio: 3

Parameter Files:

Data Handling File: Iatroscl

Calculation-File: Iatroscl



Calculation Method : Percent

Peak No	Win No.	Ret.Time (min)	Area	Resp.- Fact.	Area%	Name
1	1	0.023	3010	1.000	4.849	SAT
2	1	0.036	2870	1.000	4.622	SAT
3	1	0.056	1337	1.000	2.153	SAT
4	1	0.070	4135	1.000	6.661	SAT
5	1	0.090	2195	1.000	3.536	SAT
6	2	0.183	35358	1.000	56.951	ARO
7	3	0.303	10	1.000	0.017	POL
8	3	0.319	5	1.000	0.008	POL
9	3	0.382	429	1.000	0.692	POL
10	3	0.408	71	1.000	0.114	POL
11	3	0.442	12665	1.000	20.399	POL
			62086	100.000		

Sample Identifier: 30_11-7_3988.0

Data Processing Parameters

Injected on: 25.03.2014

Injected at: 16:36

Slice Width (ms): 50

Noise ($\mu\text{V/s}$): 50

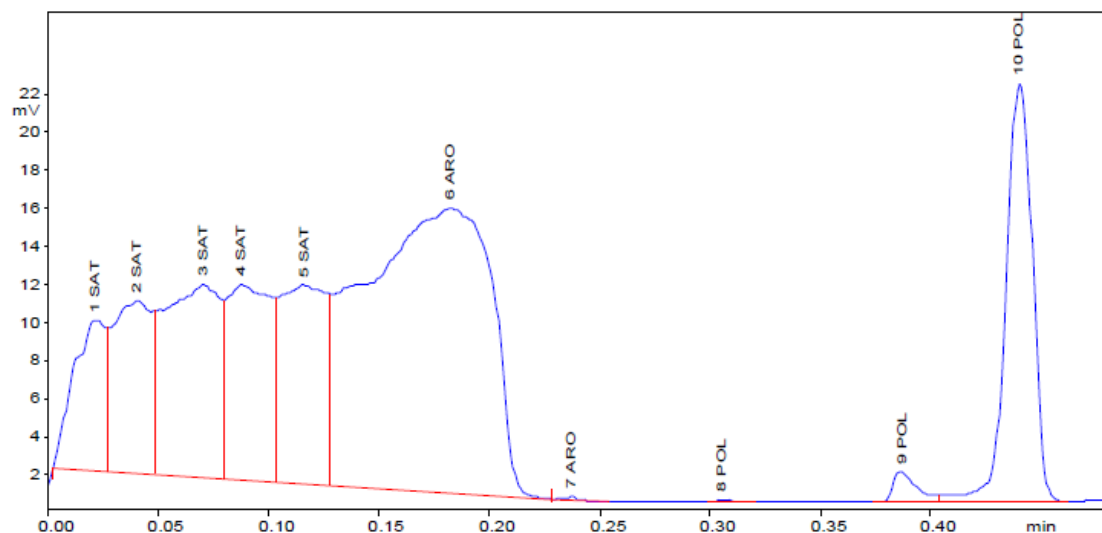
Threshold (mV): 10

Skim Ratio: 3

Parameter Files:

Data Handling File: Iatroscl

Calculation-File: Iatroscl



Calculation Method : Percent

Peak No	Win No.	Ret.Time (min)	Area	Resp.- Fact.	Area%	Name
1	1	0.023	4316	1.000	5.684	SAT
2	1	0.041	5589	1.000	7.360	SAT
3	1	0.071	9345	1.000	12.306	SAT
4	1	0.088	7255	1.000	9.553	SAT
5	1	0.117	7980	1.000	10.509	SAT
6	2	0.183	31153	1.000	41.025	ARO
7	2	0.237	28	1.000	0.037	ARO
8	3	0.306	28	1.000	0.037	POL
9	3	0.387	606	1.000	0.797	POL
10	3	0.440	9637	1.000	12.691	POL
			75937	100.000		

Sample Identifier: 30_11-7_3988.5

Data Processing Parameters

Injected on: 25.03.2014

Injected at: 16:37

Slice Width (ms): 50

Noise ($\mu\text{V/s}$): 50

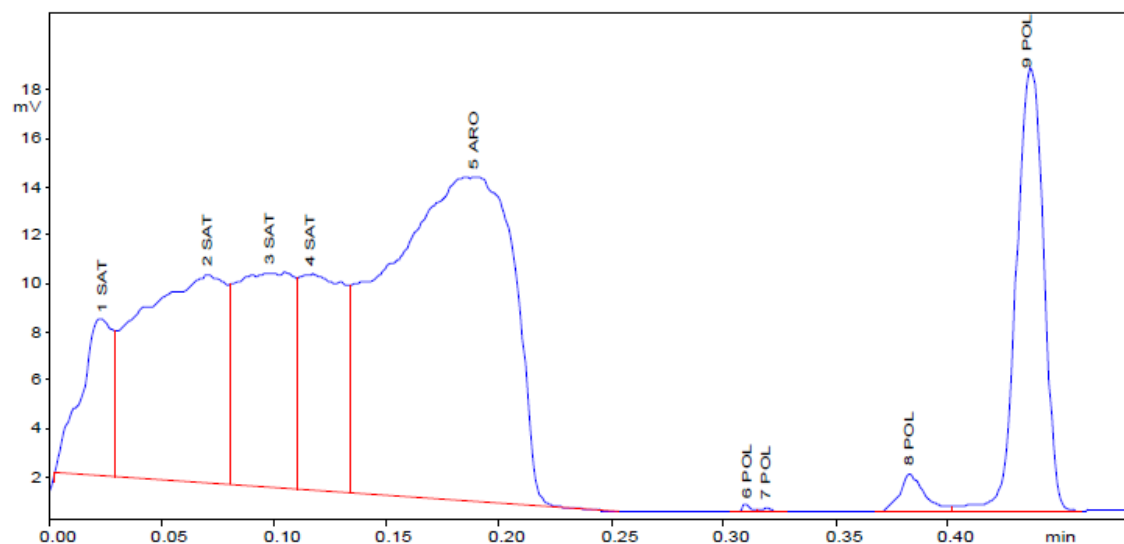
Threshold (mV): 10

Skim Ratio: 3

Parameter Files:

Data Handling File:Iatroscl

Calculation-File:Iatroscl



Calculation Method : Percent

Peak No	Win No.	Ret.Time (min)	Area	Resp.- Fact.	Area%	Name
1	1	0.024	3556	1.000	5.332	SAT
2	1	0.071	12202	1.000	18.297	SAT
3	1	0.098	8218	1.000	12.323	SAT
4	1	0.117	6423	1.000	9.631	SAT
5	2	0.189	27491	1.000	41.224	ARO
6	3	0.311	45	1.000	0.068	POL
7	3	0.319	24	1.000	0.036	POL
8	3	0.383	626	1.000	0.938	POL
9	3	0.436	8103	1.000	12.150	POL

66687

100.000

Sample Identifier: 30_11-7_3989.2

Data Processing Parameters

Injected on: 25.03.2014

Injected at: 16:38

Slice Width (ms): 50

Noise ($\mu\text{V/s}$): 50

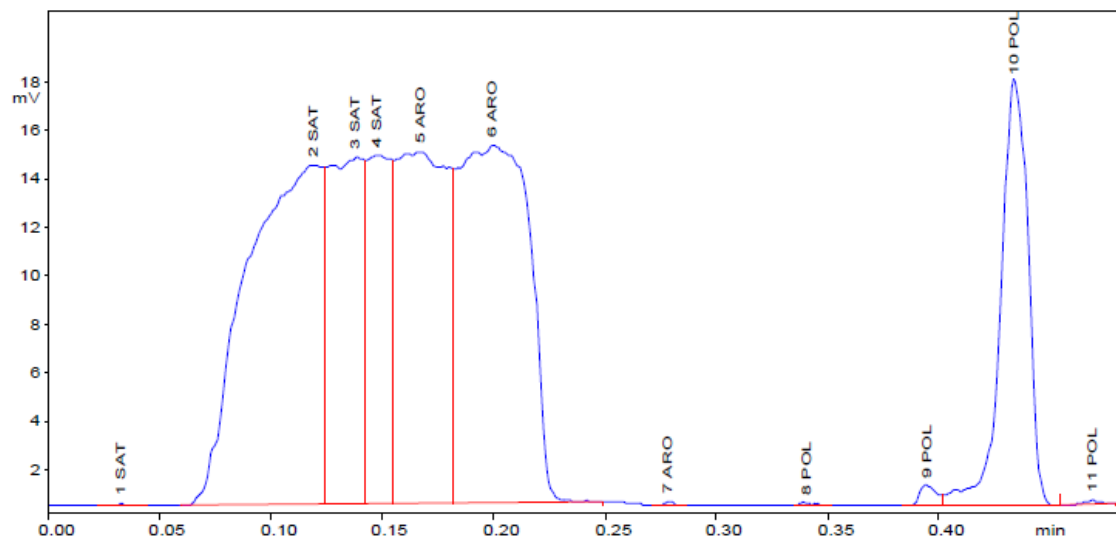
Threshold (mV): 10

Skim Ratio: 3

Parameter Files:

Data Handling File:Iatroscl

Calculation-File:Iatroscl



Calculation Method : Percent

Peak No	Win No.	Ret.Time (min)	Area	Resp.- Fact.	Area%	Name
1	1	0.033	19	1.000	0.028	SAT
2	1	0.120	17270	1.000	25.431	SAT
3	1	0.138	8093	1.000	11.918	SAT
4	1	0.148	5609	1.000	8.260	SAT
5	2	0.168	11874	1.000	17.486	ARO
6	2	0.200	16857	1.000	24.823	ARO
7	2	0.279	20	1.000	0.029	ARO
8	3	0.341	19	1.000	0.029	POL
9	3	0.395	226	1.000	0.333	POL
10	3	0.434	7881	1.000	11.606	POL
11	3	0.469	39	1.000	0.057	POL

67907

100.000

Sample Identifier: 30_11-7_3989.8

Data Processing Parameters

Injected on: 25.03.2014

Injected at: 18:07

Slice Width (ms): 50

Noise ($\mu\text{V/s}$): 50

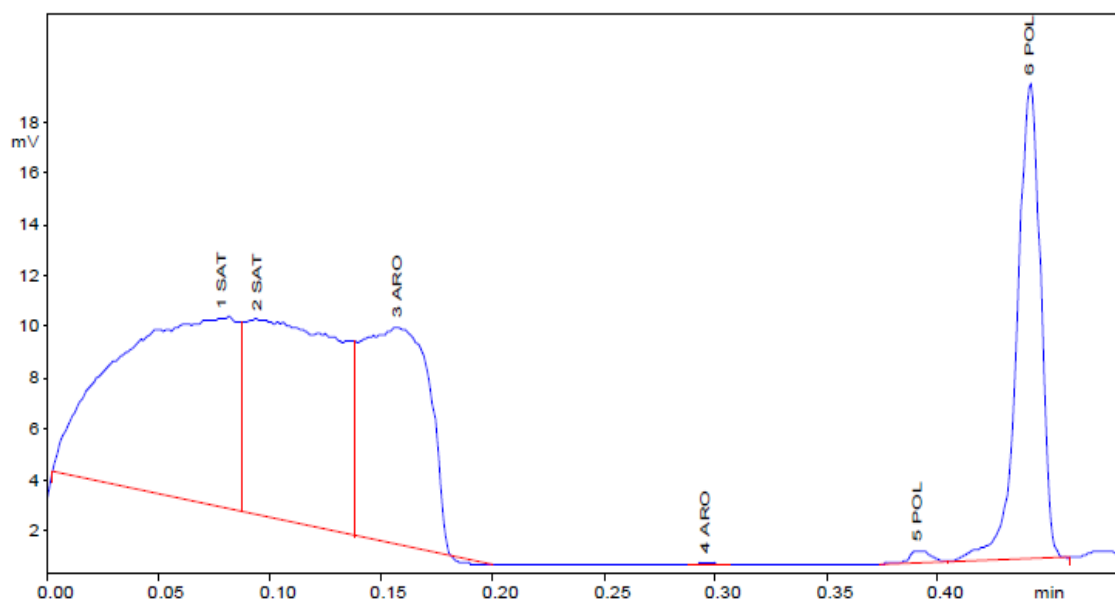
Threshold (mV): 10

Skim Ratio: 3

Parameter Files:

Data Handling File: Iatroscl

Calculation-File: Iatroscl



Calculation Method : Percent

Peak No	Win No.	Ret.Time (min)	Area	Resp.- Fact.	Area%	Name
1	1	0.079	14406	1.000	33.343	SAT
2	1	0.095	12147	1.000	28.114	SAT
3	2	0.158	9262	1.000	21.438	ARO
4	2	0.296	22	1.000	0.050	ARO
5	3	0.392	159	1.000	0.369	POL
6	3	0.442	7210	1.000	16.686	POL

43206 100.000

Sample Identifier: 30_11-7_3990.3

Data Processing Parameters

Injected on: 25.03.2014

Injected at: 18:08

Slice Width (ms): 50

Noise ($\mu\text{V/s}$): 50

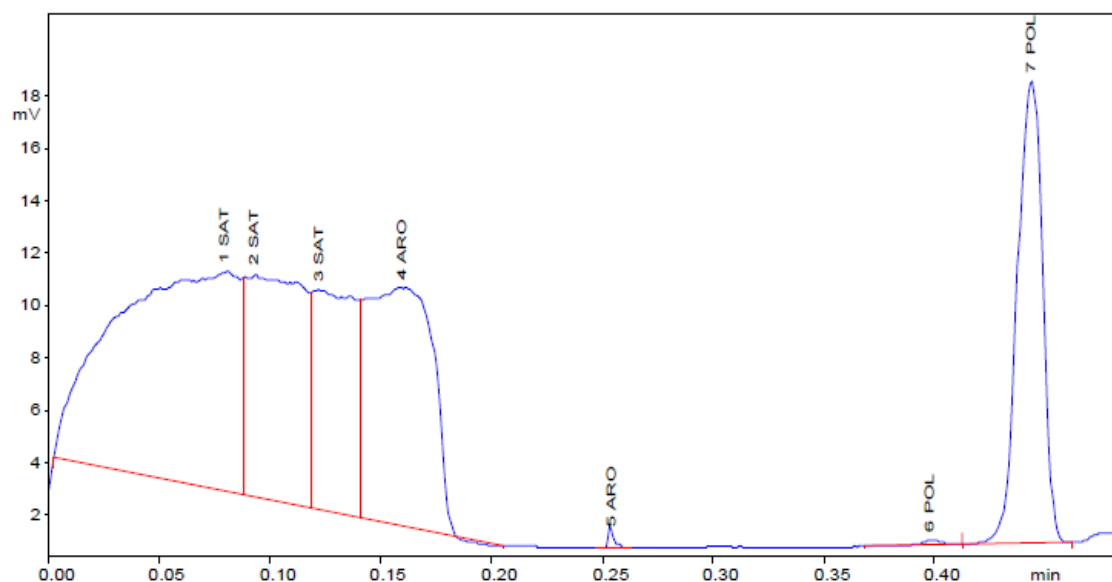
Threshold (mV): 10

Skim Ratio: 3

Parameter Files:

Data Handling File:Iatroscl

Calculation-File:Iatroscl



Calculation Method : Percent

Peak No	Win No.	Ret.Time (min)	Area	Resp.- Fact.	Area%	Name
1	1	0.080	16850	1.000	35.125	SAT
2	1	0.093	8163	1.000	17.016	SAT
3	1	0.123	5679	1.000	11.839	SAT
4	2	0.160	9817	1.000	20.464	ARO
5	2	0.255	86	1.000	0.180	ARO
6	3	0.398	74	1.000	0.155	POL
7	3	0.444	7302	1.000	15.221	POL

47971

100.000